PERFORINS AND CHOLESTEROL-DEPENDENT CYTOLYSINS IN IMMUNITY AND PATHOGENESIS

EDITED BY: George P. Munson, Robert John Crispin Gilbert and Gabriele Pradel

PUBLISHED IN: Frontiers in Immunology, Frontiers in Microbiology and Frontiers in Cellular and Infection Microbiology

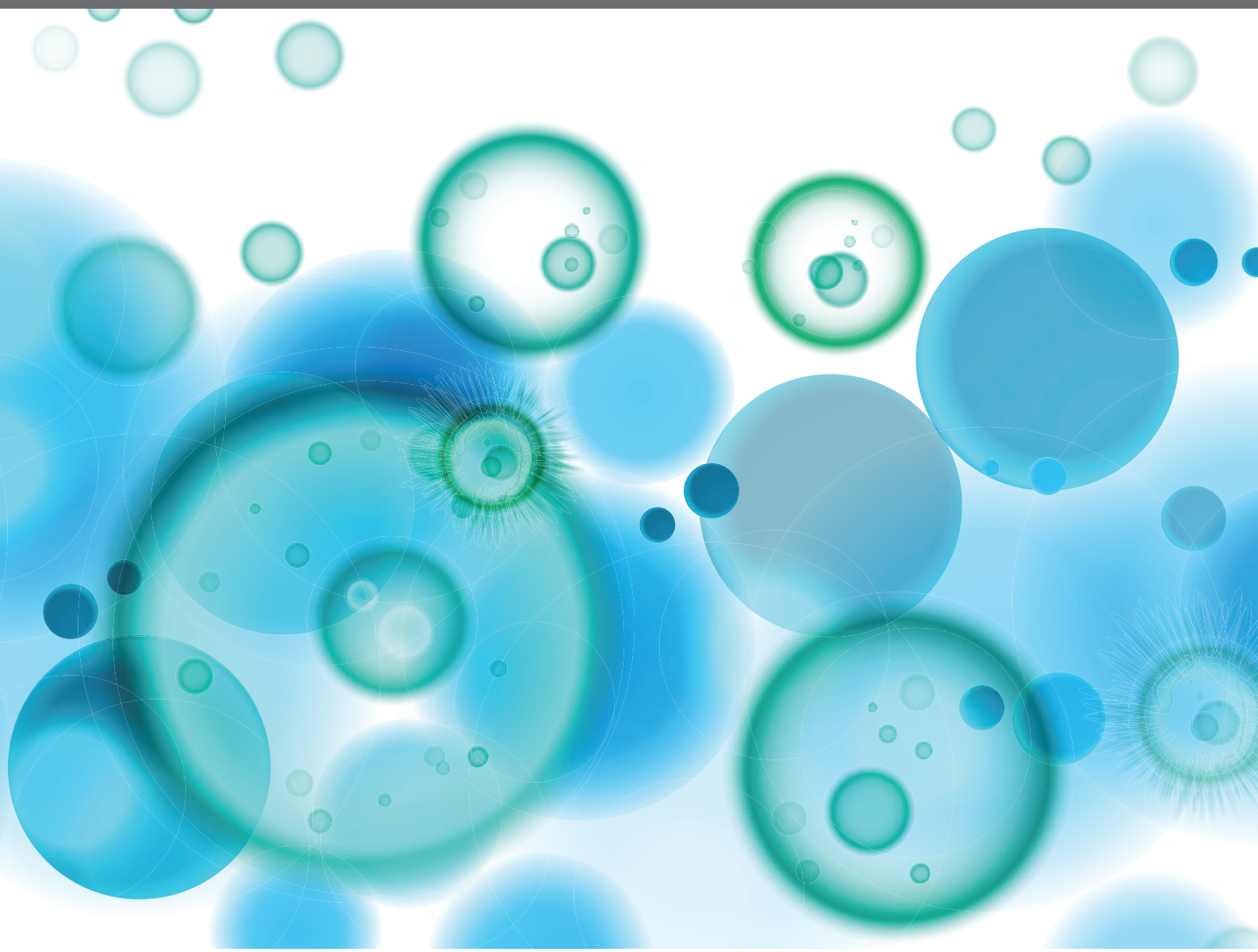

frontiers Research Topics

frontiers

ISSN 1664-8714
ISBN 978-2-88976-217-0
DOI 10.3389/978-2-88976-217-0

About Frontiers

Frontiers is more than just an open-access publisher of scholarly articles: it is a pioneering approach to the world of academia, radically improving the way scholarly research is managed. The grand vision of Frontiers is a world where all people have an equal opportunity to seek, share and generate knowledge. Frontiers provides immediate and permanent online open access to all its publications, but this alone is not enough to realize our grand goals.

Frontiers Journal Series

The Frontiers Journal Series is a multi-tier and interdisciplinary set of open-access, online journals, promising a paradigm shift from the current review, selection and dissemination processes in academic publishing. All Frontiers journals are driven by researchers for researchers; therefore, they constitute a service to the scholarly community. At the same time, the Frontiers Journal Series operates on a revolutionary invention, the tiered publishing system, initially addressing specific communities of scholars, and gradually climbing up to broader public understanding, thus serving the interests of the lay society, too.

Dedication to Quality

Each Frontiers article is a landmark of the highest quality, thanks to genuinely collaborative interactions between authors and review editors, who include some of the world's best academicians. Research must be certified by peers before entering a stream of knowledge that may eventually reach the public - and shape society; therefore, Frontiers only applies the most rigorous and unbiased reviews.
Frontiers revolutionizes research publishing by freely delivering the most outstanding research, evaluated with no bias from both the academic and social point of view. By applying the most advanced information technologies, Frontiers is catapulting scholarly publishing into a new generation.

What are Frontiers Research Topics?

Frontiers Research Topics are very popular trademarks of the Frontiers Journals Series: they are collections of at least ten articles, all centered on a particular subject. With their unique mix of varied contributions from Original Research to Review Articles, Frontiers Research Topics unify the most influential researchers, the latest key findings and historical advances in a hot research area! Find out more on how to host your own Frontiers Research Topic or contribute to one as an author by contacting the Frontiers Editorial Office: frontiersin.org/about/contact

PERFORINS AND CHOLESTEROL-DEPENDENT CYTOLYSINS IN IMMUNITY AND PATHOGENESIS

Topic Editors:
George P. Munson, University of Miami, United States
Robert John Crispin Gilbert, University of Oxford, United Kingdom
Gabriele Pradel, RWTH Aachen University, Germany

Citation: Munson, G. P., Gilbert, R. J. C., Pradel, G., eds. (2022). Perforins and Cholesterol-Dependent Cytolysins in Immunity and Pathogenesis. Lausanne: Frontiers Media SA. doi: 10.3389/978-2-88976-217-0

Table of Contents

05 ***Editorial: Perforins and Cholesterol-Dependent Cytolysins in Immunity and Pathogenesis***
George P. Munson, Robert J. C. Gilbert and Gabriele Pradel

08 ***Impaired B Cell Function in Mice Lacking Perforin-2***
Daniela Frasca, Alain Diaz, Maria Romero, Thomas Vazquez, Natasa Strbo, Laura Romero, Ryan M. McCormack, Eckhard R. Podack and Bonnie B. Blomberg

20 ***Novel Role for Animal Innate Immune Molecules: Enterotoxic Activity of a Snail Egg MACPF-Toxin***
Matías L. Giglio, Santiago Ituarte, Andrés E. Ibañez, Marcos S. Dreon, Eduardo Prieto, Patricia E. Fernández and Horacio Heras

34 ***Plasmodium Perforin-Like Protein Pores on the Host Cell Membrane Contribute in Its Multistage Growth and Erythrocyte Senescence***
Swati Garg, Abhishek Shivappagowdar, Rahul S. Hada, Rajagopal Ayana, Chandramohan Bathula, Subhabrata Sen, Inderjeet Kalia, Soumya Pati, Agam P. Singh and Shailja Singh

50 ***Pneumolysin: Pathogenesis and Therapeutic Target***
Andrew T. Nishimoto, Jason W. Rosch and Elaine I. Tuomanen

60 ***An Ancient Molecular Arms Race:* Chlamydia *vs. Membrane Attack Complex/Perforin (MACPF) Domain Proteins***
Gabrielle Keb and Kenneth A. Fields

69 ***The Complicated Evolutionary Diversification of the Mpeg-1/Perforin-2 Family in Cnidarians***
Brian M. Walters, Michael T. Connelly, Benjamin Young and Nikki Traylor-Knowles

74 ***Contribution of Nlrp3 Inflammasome Activation Mediated by Suilysin to Streptococcal Toxic Shock-like Syndrome***
Liqiong Song, Xianping Li, Yuchun Xiao, Yuanming Huang, Yongqiang Jiang, Guangxun Meng and Zhihong Ren

86 ***Perforins Expression by Cutaneous Gamma Delta T Cells***
Katelyn O'Neill, Irena Pastar, Marjana Tomic-Canic and Natasa Strbo

94 ***Perforin-Like Proteins of Apicomplexan Parasites***
Juliane Sassmannshausen, Gabriele Pradel and Sandra Bennink

101 **Staphylococcus epidermidis *Boosts Innate Immune Response by Activation of Gamma Delta T Cells and Induction of Perforin-2 in Human Skin***
Irena Pastar, Katelyn O'Neill, Laura Padula, Cheyanne R. Head, Jamie L. Burgess, Vivien Chen, Denisse Garcia, Olivera Stojadinovic, Suzanne Hower, Gregory V. Plano, Seth R. Thaller, Marjana Tomic-Canic and Natasa Strbo

113 ***Corrigendum:*** **Staphylococcus epidermidis** ***Boosts Innate Immune Response by Activation of Gamma Delta T Cells and Induction of Perforin-2 in Human Skin***
Irena Pastar, Katelyn O'Neill, Laura Padula, Cheyanne R. Head, Jamie L. Burgess, Vivien Chen, Denisse Garcia, Olivera Stojadinovic, Suzanne Hower, Gregory V. Plano, Seth R. Thaller, Marjana Tomic-Canic and Natasa Strbo

115 ***Ancient but Not Forgotten: New Insights Into MPEG1, a Macrophage Perforin-Like Immune Effector***
Charles Bayly-Jones, Siew Siew Pang, Bradley A. Spicer, James C. Whisstock and Michelle A. Dunstone

132 **Vibrio vulnificus** ***Hemolysin: Biological Activity, Regulation of*** **vvhA** ***Expression, and Role in Pathogenesis***
Yuan Yuan, Zihan Feng and Jinglin Wang

140 ***MPEG1/Perforin-2 Haploinsufficiency Associated Polymicrobial Skin Infections and Considerations for Interferon-γ Therapy***
Leidy C. Merselis, Shirley Y. Jiang, on behalf of Undiagnosed Diseases Network, Stanley F. Nelson, Hane Lee, Kavitha K. Prabaker, Jennifer L. Baker, George P. Munson and Manish J. Butte

147 ***Soluble Membrane Attack Complex: Biochemistry and Immunobiology***
Scott R. Barnum, Doryen Bubeck and Theresa N. Schein

161 ***To Kill But Not Be Killed: Controlling the Activity of Mammalian Pore-Forming Proteins***
Patrycja A. Krawczyk, Marco Laub and Patrycja Kozik

176 ***Breaching the Bacterial Envelope: The Pivotal Role of Perforin-2 (MPEG1) Within Phagocytes***
Leidy C. Merselis, Zachary P. Rivas and George P. Munson

frontiers | Frontiers in Immunology

EDITORIAL
published: 09 June 2022
doi: 10.3389/fimmu.2022.932502

Editorial: Perforins and Cholesterol-Dependent Cytolysins in Immunity and Pathogenesis

George P. Munson[1]*, *Robert J. C. Gilbert*[2] and *Gabriele Pradel*[3]

[1] Department of Microbiology and Immunology, Leonard M. Miller School of Medicine, University of Miami, Miami, FL, United States, [2] Division of Structural Biology, Wellcome Centre for Human Genetics, University of Oxford, Oxford, United Kingdom, [3] Cellular and Applied Infection Biology, RWTH Aachen University, Aachen, Germany

Keywords: perforin-2/MPEG1, membrane attack complex (MAC), pore-forming protein, complement, cholesterol-dependent cytolysins (CDC), plasmodium perforin like proteins (PPLP), pneumolysin (PLY), suilysin (SLY)

Editorial on the Research Topic

Perforins and Cholesterol-Dependent Cytolysins in Immunity and Pathogenesis

In humans and other mammals, the pore-forming proteins C9 and the perforins are important innate immune effectors. C9 forms the membrane attack complex (MAC) in an assemblage with the complement proteins C5b, C6, C7, and C8 that attacks the envelopes of gram-negative bacteria. Perforin is deployed by degranulating killer lymphocytes to destroy virally infected or cancerous cells. The product of macrophage expressed gene 1 (Mpeg1), named perforin-2 by the late Eckhard R. Podack (1943–2015), appears to play a central role in the destruction of phagocytosed bacteria. All three pore-forming proteins contain a membrane attack complex-perforin (MACPF) domain. However, the MACPF domain is not exclusive to mammals. Rather, proteins with MACPF domains are found in a diverse array of taxa including plants, fungi, invertebrates, and a variety of protozoans such as the malaria parasite *Plasmodium falciparum*, or *Toxoplasma gondii*, the causative agent of toxoplasmosis. MACPF domains have also been identified in some prokaryotes including pathogenic species of *Chlamydia*. Pore-forming proteins within the MACPF family share a canonical fold with the cholesterol-dependent cytolysins (CDCs) (1). CDCs are pore-forming proteins that contribute to the virulence of several gram-positive pathogens such as *Clostridium perfringens*, *Listeria monocytogenes*, and group A streptococci. Thus, evolution has produced pore-forming proteins with opposing roles in host defense and pathogenesis that have shared structural features. As previewed below, this article collection highlights the immunological and pathological roles of MACPF/CDC pore-forming proteins.

PERFORIN-2: AN ANCIENT PORE FORMING PROTEIN

Perforin-2 (MPEG1) is the most recently described member of the MACPF family of pore forming proteins. Although newly introduced by researchers in the fields of immunology and structural biology, perforin-2 is an evolutionarily ancient protein that spans taxa from sponges to humans (2). Two reviews focus on perforin-2 and each provides a unique perspective on the topic. Both reviews critically evaluate the current literature and discuss areas that warrant further investigation to resolve discrepancies and uncertainties. The review by Bayly-Jones et al. emphasizes the structural features and molecular

OPEN ACCESS

Edited and reviewed by:
Ian Marriott,
University of North Carolina at Charlotte, United States

***Correspondence:**
George P. Munson
gmunson@miami.edu

Specialty section:
This article was submitted to Microbial Immunology, a section of the journal Frontiers in Immunology

Received: *29 April 2022*
Accepted: *26 May 2022*
Published: *09 June 2022*

Citation:
Munson GP, Gilbert RJC and Pradel G (2022) Editorial: Perforins and Cholesterol-Dependent Cytolysins in Immunity and Pathogenesis. Front. Immunol. 13:932502. doi: 10.3389/fimmu.2022.932502

mechanisms of pore formation by mammalian perforin-2). Although mammalian perforin-2 is also discussed in the review by Merselis et al., the authors also evaluate studies of perforin-2 in invertebrates and bony fish. The discussion of invertebrate perforin-2 is complemented by a perspective by Walters et al. that covers the evolution and possible roles of perforin-2 in corals, sea anemones and other Cnidarians.

The research article by Pastar et al. investigates a connection between a commensal skin microbe and perforin-2. The investigators find that *Staphylococcus epidermidis* activates gamma delta T cells and increases the expression of perforin-2 in gamma delta T cells, keratinocytes, and fibroblasts. Interestingly, this may be beneficial to the host because the induction of perforin-2 enhances the killing of intracellular *Staphylococcus aureus* by skin cells. In a related minireview by O'Neill et al., the authors expand upon the findings of Pastar et al. by reviewing the roles of both perforin and perforin-2 in gamma delta T cells.

Merselis et al. present the first case report of perforin-2 deficiency. They report the case of a female patient with recurrent abscesses and cellulitis of the breast that was refractory to antibiotic treatment and surgical interventions. Whole genome sequencing revealed a nonsense mutation, Tyr430*, in one allele of *mpeg1* resulting in a severely truncated protein. Functional analyses find that the patient's macrophages and neutrophils were less able to kill intracellular bacteria than cells from healthy donors. This case report of perforin-2 haploinsufficiency and the study by Pastar et al. establish the importance of perforin-2 in skin and soft tissues.

Although perforin-2 is primarily thought of as an innate immune effector, the research article by Frasca et al. demonstrates that perforin-2 deficiency also affects adaptive immunity. Specifically, the researchers find that perforin-2 knockout mice have reduced antibody responses to an influenza vaccine compared to wild-type mice. This is due to chronic inflammation of knockout mice caused by their failure to efficiently block the translocation of gut microbes and/or microbial products to extra-intestinal sites. Systemic, but low-grade, inflammation causes intrinsic B cell inflammation and reduces their ability to produce antibodies in response to antigens. Thus, the researchers demonstrate a previously unknown connection between perforin-2 and a properly functioning adaptive immune response.

SOLUBLE COMPLEXES OF MACPFS AND THE PREVENTION OF OFF-TARGET EFFECTS

The MAC of the complement system has been extensively characterized at immunological, mechanistic, and molecular levels. In contrast, the soluble MAC (sMAC) is much less understood. Both are assemblages of the complement proteins C5b, C6, C7, C8, and C9, but the stoichiometry of complement proteins in MAC and sMAC are radically different. For example, sMAC may also contain clusterin and/or vitronectin, and unlike MAC are not pore forming complexes. These and other differences are reviewed by Barnum et al. The authors also discuss sMAC as a long standing enigma in the field of immunology. Nevertheless, the authors provide a compelling case for the utility of sMACs as biomarkers of disease.

Although the pore forming proteins MAC, perforin, perforin-2, and gasdermins have important defensive and immunological functions, their capacity to form pores in lipid bilayers poses a risk of self-inflicted harm to the host. This biological conundrum is addressed in the review by Krawczyk et al. Their review covers the "where and when" of pore-forming protein expression, processing, subcellular storage, and molecular mechanisms that prevent the attack of off-target membranes.

PERFORIN-LIKE PROTEINS IN PROTOZOAN PARASITES

Perforin-like proteins were also identified in apicomplexan parasites, intracellularly-living protists that actively invade their host cells. These parasites require a fine-tuned molecular machinery for host cell penetration and egress, but also for crossing epithelial barriers, and some of these functions are mediated by perforins. In their review article, Sassmannshausen et al. highlight the diverse roles of the perforin-like proteins during life-cycle progression of apicomplexan parasites. The authors lay the focus on the two parasites *Plasmodium* and *Toxoplasma*, the causative agents of malaria and toxoplasmosis, for which the perforins are best studied. In these parasites, perforins are used to perforate the membranes of the parasitophorous vacuole and the host cell membrane during exit, but also to overcome epithelial barriers during tissue passage. *Plasmodium* and *Toxoplasma* express five and two variants of perforins, respectively, and these perforins appear to have distinct functions that are specific for both tissue type and life-cycle stage.

In this context, the original research article by Garg et al. reports on the pore-forming activity of the Pan-active MACPF Domain (PMD), a centrally located and highly conserved region of perforin-like proteins of the malaria parasite, and further evaluate the inhibitory potential of specifically designed PMD inhibitors. The authors show that the incubation of erythrocytes with PMD induces senescence in these cells, which may attribute to severe malarial anemia. Anti-PMD inhibitors effectively prevent the parasites from invasion of, and egress from, host erythrocytes, but also block the hepatic stages and transmission stages of the malaria parasite, suggesting that PMDs represent multi-stage, transmission-blocking inhibitors.

CDCs AND MACPFs OF BACTERIAL PATHOGENS

The research article by Song et al. elucidates the contribution of suilysin to the development of streptococcal toxic shock-like syndrome. Suilysin is a CDC produced by *Streptococcus suis*. Although primarily a swine pathogen of significant concern to the agricultural industry, *S. suis* can also cause meningitis and streptococcal toxic shock-like syndrome in humans. Through a combination of *in vitro* and *in vivo* approaches the authors show that suilysin causes the release of IL-1β *via* activation of the NLRP3

inflammasome. Although the mechanism of inflammasome activation is currently unknown, chemical or genetic blockade of the pathway protects mice from suilysin's cytotoxic effects.

Streptococcus pneumoniae is a commensal microbe that commonly colonizes the nasal cavity. Although most colonized individuals are asymptomatic, *S. pneumoniae* is also an opportunistic pathogen capable of causing a wide range of symptoms and disease outcomes. The minireview by Nishimoto et al. discusses the role of pneumolysin in various phases of pneumococcal disease. Pneumolysin is a CDC that is cytolytic to a wide range of host cell types that contributes to both transmission and colonization. The authors conclude with a review of vaccines against the CDC and drugs that limit pneumolysin's cytotoxic effects.

Unlike pneumolysin, the contribution of hemolysin to *Vibrio vulnificus* pathogenicity has been more controversial. *V. vulnificus* infections are typically acquired through the consumption of raw shellfish and in some cases can lead to fatal septicemia. The minireview by Yuan et al. evaluates recent progress towards understanding the biological effects of the *V. vulnificus* CDC and its roles in gastroenteritis and septicemia.

The review by Keb and Fields returns the discussion to MACPFs. *Chlamydia* spp. are obligate intracellular bacteria that parasitize eukaryotic cells. The authors review evidence that suggest *Chlamydia* pathogenicity is little impacted by MAC. They propose that this can be explained by the unique properties of the envelopes of extracellular elementary bodies that likely make them refractory to the deposition of the complement proteins of MAC. Also reviewed are studies indicating that Perforin of natural killer cells and cytotoxic T lymphocytes is not a major mediator of *Chlamydia* infectivity and pathogenicity. In contrast to MAC and Perforin, the authors review evidence that indicates perforin-2 significantly limits chlamydial infection. They conclude with a discussion of chlamydial MACPFs.

PERIVITELLIN-2 ENTEROTOXIN: AN UNUSUAL EVOLUTIONARY ADAPTATION OF A MACPF

Undoubtedly, the most unexpected submission to the collection was the research article by Giglio et al. *Pomacea maculata* is a snail species whose eggs contain a toxin known as perivitellin-2 (PV2). This toxin contains both a lectin binding domain and a MACPF, and the authors show that PV2 is cytotoxic to immune and epithelial cells. The latter are significant because the authors propose that PV2 may have evolved to prevent predation of the eggs. As predicted, PV2 is found on the surface of enterocytes and induces morphological changes in the small intestines of mice orally challenged with PV2. Based on several criteria the authors argue that PV2 meets the definition of an enterotoxin and, as such, it is the first known animal enterotoxin.

CONCLUSIONS

Although unified by the topic of perforins and CDCs, this collection brings together diverse viewpoints from researchers from around the globe. This diversity is reflected by the variety of subject matter in articles that span from mini-reviews to original research articles. Authors represent numerous disciplines and specialties including, but not limited to, structural and evolutionary biology, parasitology, bacterial pathogenesis, and immunology. We thank them for their contributions and participation in this endeavor. Their unique perspectives, experimental approaches, and critical evaluations of the literature have come together in this collection to provide a broad understanding of the field of MACPF/CDCs.

AUTHOR CONTRIBUTIONS

GM and GP composed the first draft of the manuscript. All authors reviewed the document and contributed to editing. All authors contributed to the article and approved the submitted version.

FUNDING

Perforin-2 research in the laboratory of GM is supported by the National Institute of Allergy and Infectious Diseases of the National Institutes of Health under award numbers R01AI110810, R21AI156567, and R21AI159794. The content of this publication is solely the responsibility of the authors and does not necessarily represent the official views of the National Institutes of Health. GP acknowledges funding by the SPP 2225 of the Deutsche Forschungsgemeinschaft (PR905/19-1).

REFERENCES

1. Gilbert R. MACPF/CDC Proteins - Agents of Defence, Attack and Invasion. *Subcell Biochem* (2014) 80:47–62. doi: 10.1007/978-94-017-8881-6_4
2. McCormack R, Podack ER. Perforin-2/Mpeg1 and Other Pore-Forming Proteins Throughout Evolution. *J Leuk Biol* (2015) 98:761–8. doi: 10.1189/jlb.4mr1114-523rr

Conflict of Interest: The authors declare that the research was conducted in the absence of any commercial or financial relationships that could be construed as a potential conflict of interest.

frontiers in Immunology

ORIGINAL RESEARCH
published: 27 February 2020
doi: 10.3389/fimmu.2020.00328

Impaired B Cell Function in Mice Lacking Perforin-2

Daniela Frasca, Alain Diaz, Maria Romero, Thomas Vazquez, Natasa Strbo, Laura Romero, Ryan M. McCormack, Eckhard R. Podack and Bonnie B. Blomberg*

Department of Microbiology and Immunology, University of Miami Miller School of Medicine, Miami, FL, United States

Perforin-2 (P2) is a pore-forming protein with cytotoxic activity against intracellular bacterial pathogens. P2 knockout (P2KO) mice are unable to control infections and die from normally non-lethal bacterial infections. Here we show that P2KO mice as compared to WT mice show significantly higher levels of systemic inflammation, measured by inflammatory markers in serum, due to continuous microbial translocation from the gut which cannot be controlled as these mice lack P2. Systemic inflammation in young and old P2KO mice induces intrinsic B cell inflammation. Systemic and B cell intrinsic inflammation are negatively associated with *in vivo* and *in vitro* antibody responses. Chronic inflammation leads to class switch recombination defects, which are at least in part responsible for the reduced *in vivo* and *in vitro* antibody responses in young and old P2KO vs. WT mice. These defects include the reduced expression of activation-induced cytidine deaminase (AID), the enzyme for class switch recombination, somatic hypermutation and IgG production and of its transcriptional activators E47 and Pax5. Of note, the response of young P2KO mice is not different from the one observed in old WT mice, suggesting that the chronic inflammatory status of mice lacking P2 may accelerate, or be equivalent, to that seen in old mice. The inflammatory status of the splenic B cells is associated with increased frequencies and numbers of the pro-inflammatory B cell subset called Age-associated B Cells (ABCs) in the spleen and the visceral adipose tissue (VAT) of P2KO old mice. We show that B cells differentiate into ABCs in the VAT following interaction with the adipocytes and their products, and this occurs more in the VAT of P2KO mice as compared to WT controls. This is to our knowledge the first study on B cell function and antibody responses in mice lacking P2.

Keywords: splenic B cells, adipose tissue B cells, inflammation, perforin-2, antibody responses

OPEN ACCESS

Edited by:
Gabriele Pradel,
RWTH Aachen University, Germany

Reviewed by:
Masaaki Miyazawa,
Kindai University, Japan
Hong Zan,
The University of Texas Health Science Center at San Antonio, United States

****Correspondence:***
Daniela Frasca
dfrasca@med.miami.edu

Specialty section:
This article was submitted to Microbial Immunology, a section of the journal Frontiers in Immunology

Received: *30 October 2019*
Accepted: *10 February 2020*
Published: *27 February 2020*

Citation:
Frasca D, Diaz A, Romero M, Vazquez T, Strbo N, Romero L, McCormack RM, Podack ER and Blomberg BB (2020) Impaired B Cell Function in Mice Lacking Perforin-2. Front. Immunol. 11:328. doi: 10.3389/fimmu.2020.00328

INTRODUCTION

Perforin-2 (MPEG1, P2) is a pore-forming protein with broad-spectrum activity against infectious bacteria in both mice and humans (1). P2 is constitutively expressed in phagocytes and other immune cells and can be induced in parenchymal, tissue-forming cells (2, 3). *In vitro*, P2 prevents the intracellular replication of bacterial pathogens (3). P2 knockout (P2KO) mice are unable to control the systemic dissemination of bacterial pathogens and die from bacterial infections that are normally not lethal (3). Other bactericidal molecules have been found to be less effective in the absence of P2, suggesting that P2 is essential for the activity of mammalian immune defense mechanisms. It has recently been shown that P2 facilitates the delivery of proteases and other antimicrobial effectors to the sites of bacterial infection leading to effective killing of phagocytosed bacteria (4).

Translocation of bacteria and their products from the gastrointestinal tract to extra-intestinal sites (lymph nodes, liver, spleen, kidney, blood) is a phenomenon that may occur spontaneously in healthy conditions in humans and mice without apparent deleterious consequences (5). Bacterial translocation is increased in different clinical pathological conditions and is certainly involved in the pathophysiological mechanisms of many diseases. Translocation of bacteria and/or their toxic products from the gastro-intestinal tract is strongly suspected to be responsible for the establishment of systemic chronic inflammation. This condition may be exacerbated in P2KO mice.

We have previously shown in mice (6) and humans (7, 8) that B cell function decreases with age and this decrease is associated with chronic low-grade systemic inflammation, called "inflammaging" (9). Higher levels of inflammaging, measured by serum TNF-α, induce higher TNF-α production by B cells from old mice and humans *in vivo* and *in vitro*, leading to significant decreases in their capacity to make protective antibodies in response to antigenic/mitogenic stimulation (6, 7). Serum TNF-α has been shown to up-regulate the expression of its receptors (TNFRI and TNFRII) on B cells, and interaction of TNF-α with its receptors induces NF-kB activation and secretion of TNF-α as well as of other pro-inflammatory cytokines and chemokines (10). Importantly, blocking TNF-α with specific antibodies has been shown to increase B cell function, at least *in vitro*, in both mice (6) and humans (7).

The purpose of this study is to evaluate B cell function in P2KO mice. We hypothesized that P2KO mice are unable to control the translocation of bacteria and/or toxic bacterial products and this would generate a systemic low-grade chronic inflammation which negatively affects B cell function and antibody responses. Our results herein show that this is indeed the case. P2KO mice show significantly higher levels of systemic and intrinsic B cell inflammation which are negatively associated with protective antibody responses to a vaccine. This is to our knowledge the first study evaluating B cell function and antibody responses in mice lacking P2.

MATERIALS AND METHODS

Mice

Male P2KO and wild type (WT) mice, both on a 129/SvJ background, were generated as previously described (3). Mice were young (3–4 months) and old (>18 months), bred at the University of Miami, Miller School of Medicine Transgenic Core Facility. Mice were allowed to freely access food and water and were housed at 23°C on a 12 hr light/dark cycle under specific pathogen-free conditions. All studies adhered to the principles of laboratory animal care guidelines and were IACUC approved (protocols #16-252 and #16-006).

Influenza Vaccine Response

Mice were injected intramuscularly with 4 μg of the quadrivalent influenza vaccine (Fluzone Sanofi Pasteur 2017–2018) in alum (Aluminum Potassium Sulfate Dodecahydrate, SIGMA A-7210). Total volume of injection was 100 μl. Mice were sacrificed 28 days after the injection (peak of the response).

B Cell Enrichment

B cells were isolated from the spleens after 20 min incubation at 4°C using CD19 MicroBeads (Miltenyi Biotec 130-121-301), according to the MiniMACS protocol (20 μl Microbeads + 80 μl PBS, for 10^7 cells). At the end of the purification procedure, cells were 90–95% CD19-positive by cytofluorimetric analysis. They were then maintained in PBS for 3 hrs at 4°C to minimize potential effects of anti-CD19 antibodies on B cell activation. After positive selection, B cells were divided in two aliquots: one aliquot was used for culture stimulation, the other aliquot for RNA extraction after cells were resuspended in TRIzol (ThermoFisher Scientific).

B Cell Culture

Splenic B cells (10^6/ml) were cultured in complete medium (RPMI 1640, supplemented with 10% FCS, 100 U/ml Penicillin-Streptomycin, 2×10^{-5} M 2-ME, and 2 mM L-glutamine). FCS was certified to be endotoxin-free. B cells were stimulated in 24 well culture plates with 1 μg/ml of LPS (from *E. coli*, SIGMA L2880) for 1–7 days. At the end of the stimulation time, B cells were counted in a solution of trypan blue to evaluate viability which was found comparable in cultures of WT and P2KO mice.

Isolation of Epididymal VAT

Epididymal VAT was collected, weighed, washed with 1X Hanks' balanced salt solution (HBSS), resuspended in Dulbecco's modified Eagle Medium (DMEM), minced into small pieces, passed through a 70 μm filter and digested with collagenase type I (SIGMA C-9263) for 1 hr at 37°C in a water bath. Digested cells were passed through a 300 μm filter, centrifuged at 300 g in order to separate the floating adipocytes from the stromal vascular fraction (SVF) containing the immune cells. The cells floating on the top were transferred to a new tube as adipocytes. The cell pellet (SVF) on the bottom was resuspended in a solution of Ammonium Chloride Potassium (ACK) for 3 min at RT (room temperature) to lyse the red blood cells. Both adipocytes and SVF were washed 3 times with DMEM. B cells were isolated from the SVF as indicated immediately below. Adipocytes were sonicated for cell disruption in the presence of TRIzol, and then centrifuged at 1,000 × g at 4°C for 20 min to separate the soluble fraction from the lipids and cell debris. The soluble fraction was then used for RNA isolation.

Cell Staining

Splenic and VAT B cell subsets were identified by the following membrane markers. Follicular (FO): CD19+AA4.1-CD43-CD23+CD21^{int}; Marginal Zone (MZ): CD19+AA4.1-CD43-CD23$^{low/neg}$CD21^{hi}; Age-associated B cells (ABC): CD19+CD43-AA4.1-CD23-CD21-. AA4.1 (CD93) is the marker of transitional B cells. CD43 is the marker of B1 B cells. Both transitional and B1 B cells are excluded by cell sorting to obtain only B2 B cells. Plasma cells were evaluated by membrane expression of CD138 in cultured cells.

B cells were membrane stained for 20 min at rt with Live/Dead detection kit (ThermoFisher) and with the following antibodies:

PacBlue-conjugated anti-CD45 (Biolegend 103125), APC-Cy7-conjugated anti-CD19 (BD 557655), PE-Cy7-conjugated anti-AA4.1 (eBioscience 25-5892-81), APC-conjugated anti-CD43 (BD 560663), FITC-conjugated anti-CD21/CD35 (BD 553818), and PE-conjugated anti-CD23 (BD 553139). To evaluate plasma cell frequencies, splenic B cells were membrane stained with PE-conjugated anti-CD138 antibody (BD 553714). Cells were then fixed with BD Cytofix (BD 554655). Up to 10^5 events in the lymphocyte gate were acquired on an LSR-Fortessa (BD) and analyzed using FlowJo 10.0.6 software.

Cell Sorting

FO B cells were sorted with the Sony SH800 cell sorter. FO B cells were incubated with adipocytes in transwell as detailed below.

RNA Extraction and cDNA Preparation

The mRNA was extracted from LPS-stimulated B cells at day 1 (to evaluate E47, Pax5) and at day 5 (to evaluate AID), using the μMACS mRNA isolation kit (Miltenyi), according to the manufacturer's protocol, eluted into 75 μl of preheated elution buffer, and stored at −80°C until use. Total RNA was extracted from unstimulated VAT B cells, as well as from adipocytes, resuspended in TRIzol, according to the manufacturer's protocol, eluted into 10 μl of preheated H_2O, and stored at −80°C until use. Reverse Transcriptase (RT) reactions were performed in a Mastercycler Eppendorf Thermocycler to obtain cDNA. Briefly, 10 μl of mRNA or 2 μl of RNA at the concentration of 0.5 μg/μl were used as template for cDNA synthesis in the RT reaction. Conditions were: 40 min at 42°C and 5 min at 65°C.

Quantitative PCR (qPCR)

Reactions were conducted in MicroAmp 96-well plates, and run in the ABI 7300 machine. Calculations were made with ABI software. Briefly, we determined the cycle number at which transcripts reached a significant threshold (Ct). A value for the amount of the target gene, relative to GAPDH, was calculated and expressed as ΔCt. Results are expressed as $2^{-\Delta\Delta Ct}$. Reagents and primers for qPCR amplification were from ThermoFisher. Primers were: GAPDH Mm99999915_g1, Tcfe2a/E47 Mm01175588_m1, Pax5 Mm00435501_m1, AID Mm00507774_m1, Prdm1 Mm00476128_m1, TNF-α Mm00443258_m1, IL-6 Mm00446190_m1, CXCL10 Mm00445235_m1, CCL2 Mm00441242_m1, CCL5 Mm01302427.

Enzyme-Linked Immunosorbent Assay (ELISA)

To measure microbial translocation in serum, Lonza QCL-1000 kit was used for the detection of Gram-negative bacterial endotoxin.

To measure influenza vaccine serum IgG and IgA responses, the influenza vaccine was used for coating ELISA plates. The vaccine was used at the concentration of 10 μg/ml. Detection antibodies were HRP-conjugated affinity-purified $F(ab')_2$ of a goat anti-mouse IgG (Jackson IR Labs 115-036-062) and HRP-conjugated goat anti-mouse IgA (ThermoFisher 62-6720).

To measure stool-specific IgG antibodies in serum, we first obtained total protein lysates from stools of WT and P2KO mice that were used for coating ELISA plates. Stool sample collection and processing was performed as described (11). Total protein lysates were obtained using the M-PER mammalian protein extraction reagent (ThermoFiscer 78501), according to the manufacturer's protocol. Protein lysates were used at the concentration of 10 μg/ml. Detection antibody was an HRP-conjugated affinity-purified $F(ab')_2$ of a goat anti-mouse IgG (Jackson IR Labs 115-036-062).

To measure LPS-induced IgG3 in culture supernatants, purified IgG3 subclass-specific antibodies were used for coating (Southern Biotech 1101-01), at the concentration of 2 μg/ml. Detection antibody was the same as above.

Co-culture of Adipocytes and Splenocytes

The ratio between adipocytes and splenic lymphocytes in co-cultures was equal to that which we measured in *ex vivo* isolated VAT (ratio adipocytes:lymphocytes). In the transwells, cells were co-cultured by using inserts with a 0.4 μm porous membrane (Corning) to separate adipocytes and splenic lymphocytes. Cells were left unstimulated. After 72 h, cells in the upper wells (splenic lymphocytes) were harvested, washed and stained to evaluate percentages and numbers of B cell subsets.

Statistical Analyses

To examine differences between 4 groups, two-way ANOVA was used. Group-wise differences were analyzed afterwards with Bonferroni's multiple comparisons test, with $p < 0.05$ set as criterion for significance. To examine differences between 2 groups, Student's *t*-tests (two-tailed) were used. To examine the relationships between variables, bivariate Pearson's correlation analyses were performed, using GraphPad Prism 5 software. Principal Component Analyses (PCA) were generated using RStudio Version 1.1.463.

RESULTS

Increased Microbial Translocation in the Serum of P2KO vs. WT Mice

We first measured microbial translocation by quantifying serum levels of LPS, the major component of Gram-negative bacterial cell walls. LPS in serum indicates microbial translocation (12). Results in **Figure 1A** show increased serum LPS in young and old P2KO mice as compared to WT controls, the highest levels being observed in old P2KO mice. Serum LPS levels in young P2KO mice are comparable to those observed in old WT mice. These results confirm our initial hypothesis that translocation of bacteria and their products from the gastro-intestinal tract occurs in P2KO mice and this may be responsible for the establishment of systemic chronic inflammation. We have also measured bacterial translocation by serum levels of IgG antibodies specific for stool-derived proteins. Results have indicated higher stool-specific IgG in the serum of P2KO as compared to that of WT mice, confirming LPS results (data not shown).

Reduced *in vivo* Influenza Vaccine Antibody Response in P2KO vs. WT Mice

Bacterial translocation affects immune responses by inducing Immune Activation (IA) in circulating immune cells. The

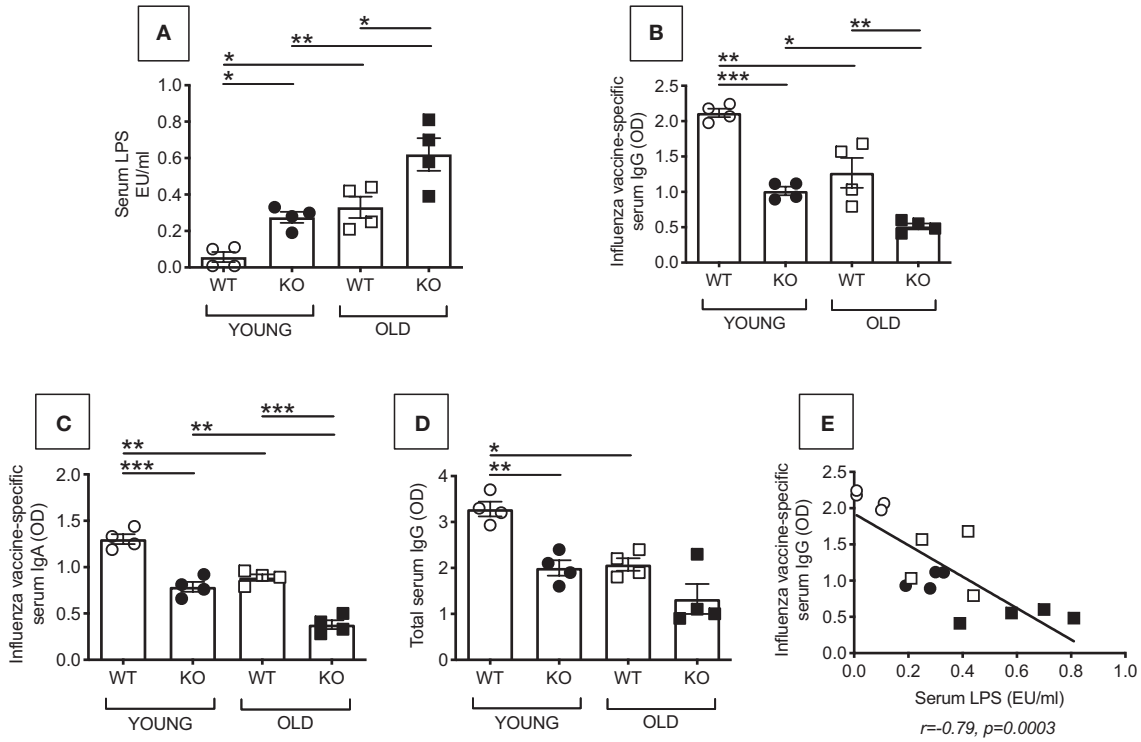

FIGURE 1 | Increased microbial translocation and reduced *in vivo* influenza vaccine antibody response in P2KO vs. WT mice. **(A)** Microbial translocation in serum was measured by ELISA for LPS in young and old WT and P2KO mice (4 mice/group). Mean comparisons between groups were performed by two-way ANOVA. $^{*}p < 0.05$, $^{**}p < 0.01$. **(B)** To measure the influenza vaccine response, mice were immunized intramuscularly with the influenza vaccine. Serum response to the vaccine was evaluated at day 28 post vaccination by ELISA. **(C)** Influenza vaccine-specific IgA responses measured by ELISA at day 28 post vaccination. **(D)** Total serum IgG measured by ELISA. Mean comparisons between groups were performed by two-way ANOVA followed by Bonferroni's multiple comparisons test. $^{*}p < 0.05$, $^{**}p < 0.01$, $^{***}p < 0.001$. **(E)** Correlation of microbial translocation and influenza vaccine response. Pearson's *r* and *p*-values are at the bottom of the figure.

receptor for LPS, TLR4, is one of the several markers of IA so far identified. It is known that there is a negative association between the expression of IA markers in immune cells before stimulation and the response of the same immune cells after *in vivo* or *in vitro* stimulation. Therefore, IA is negatively associated with functional immune cells. This has been shown in chronic inflammatory conditions (aging and age-associated conditions) as well as in chronic infections (HIV, malaria) (7, 13–16). We measured *in vivo* antibody production in young and old WT and P2KO mice by measuring the serum response to the influenza vaccine by ELISA. Results in **Figure 1B** show that P2KO mice of both age groups have significantly decreased *in vivo* responses to the vaccine and make significantly less influenza vaccine-specific IgG antibodies as compared to WT controls. Noteworthily, the response of young P2KO mice is not different from the one observed in old WT mice. Influenza vaccine-specific IgA (**Figure 1C**) and total IgG show a similar pattern (**Figure 1D**). The influenza vaccine response, as expected, was negatively correlated with microbial translocation (**Figure 1E**).

Reduced *in vitro* Class Switch in B Cells From P2KO VS. WT Mice

We then measured *in vitro* class switch, IgG secretion and plasma cell frequencies in LPS-stimulated splenic B cells from young and old WT and P2KO mice. We evaluated E47, Pax5, Prdm1 (Blimp-1), and activation-induced cytidine deaminase (AID) mRNA expression by qPCR. This was done at time points that we found optimal in our previously published work measuring *in vitro* class switch in splenic B cells from young and old C57BL/6 mice. Briefly, we found that E47 mRNA is higher at day 1 and then decreases at days 2–3 after stimulation (17, 18). Pax5 mRNA expression has a kinetic similar to E47 (unpublished). AID mRNA is already detectable at day 3 but peaks at day 5, to decrease later on (17). Prdm1(Blimp-1) is detectable at day 2 and increases at later days, peaking at day 4, and it stays up until day 7 (18).

E47 (19, 20), and Pax5 (21, 22) are transcriptional regulators of AID, the enzyme necessary for class switch recombination, the process leading to the production of secondary, class-switched antibodies, and somatic hypermutation (23–25). AID is a measure of optimal B cell function. Prdm1 (Blimp-1) is the transcription factor for plasma cell differentiation (26). In addition to transcription factors for class switch recombination and plasma cell differentiation, and AID, we also measured IgG3 secretion by ELISA. IgG3 is the Ig subclass secreted in larger amounts in response to LPS alone. In response to LPS and class switch cytokines or B lymphocyte stimulator (BlyS), a key survival factor for B cells also known to induce class switch (27),

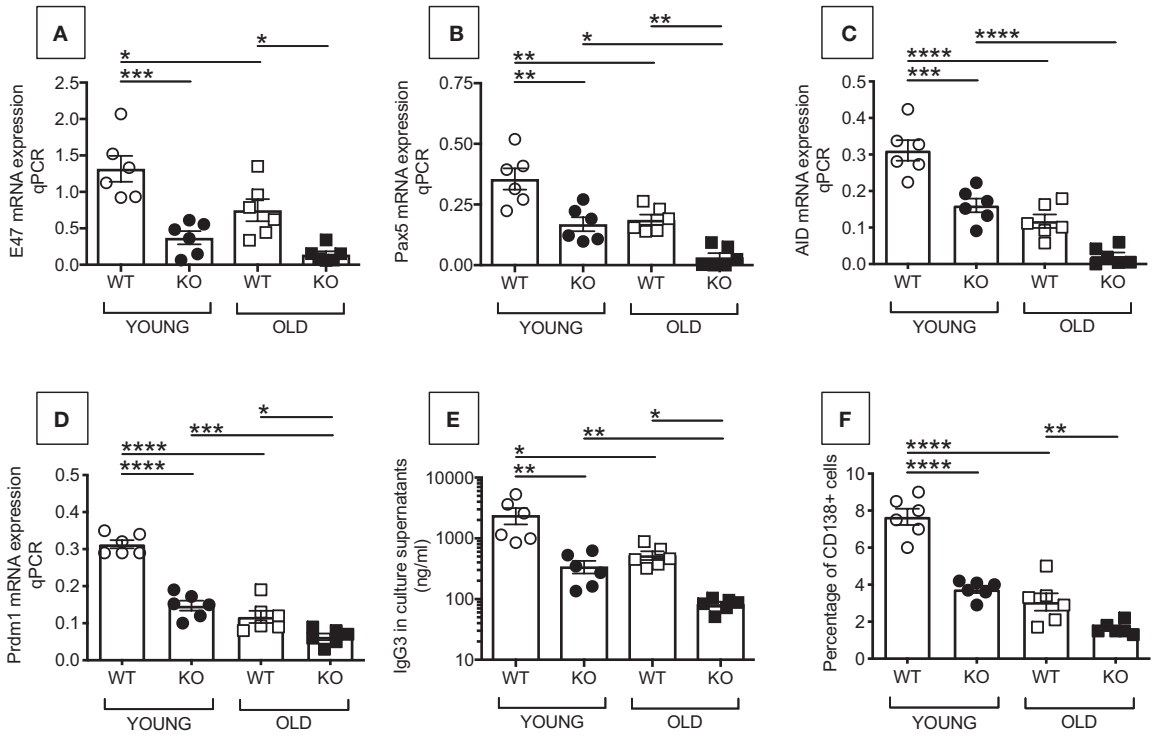

FIGURE 2 | Reduced *in vitro* class switch in B cells from P2KO vs. WT mice. B cells were isolated from the spleens of young and old WT and P2KO mice (6 mice/group) by magnetic sorting. B cells (10^6/ml) were stimulated for 1–7 days with 1 μg/ml of LPS, then mRNA was extracted and qPCR performed to evaluate mRNA expression of E47 **(A)** and Pax5 **(B)** (at day 1), AID **(C)** (at day 5), and Prdm1 (Blimp-1) **(D)** (at day 4). Results show qPCR values ($2^{-\Delta\Delta Ct}$). At day 5, cells are harvested to evaluate frequencies of CD138+ cells by flow cytometry **(F)**. At day 7, supernatants were collected to measure IgG3 secretion by ELISA **(E)**. Mean comparisons between groups were performed by two-way ANOVA followed by Bonferroni's multiple comparisons test. $^*p < 0.05$, $^{**}p < 0.01$, $^{***}p < 0.001$, $^{****}p < 0.0001$.

splenic B cells from 129/SvJ mice make predominantly IgG1 followed by IgG2b (28). Frequencies of plasma cells by flow cytometry were also evaluated in LPS-stimulated splenic B cells from young and old WT and P2KO mice.

Results in **Figure 2** show that B cells from P2KO mice, both young and old, express significantly less mRNA for E47 (A), Pax5 (B), AID (C), and Prdm1 (Blimp-1) (D) and secrete significantly less IgG3 antibodies (E), as compared to WT controls. Also the frequencies of plasma cells are less in cultured B cells from P2KO as compared to those from WT mice (F). Again, the response of young P2KO mice is not different from the one observed in old WT mice.

Increased Intrinsic Inflammation in Splenic B Cells From P2KO vs. WT Mice

We have previously shown in both mice (6) and humans (7) that high TNF-α mRNA levels in resting B cells negatively correlate with the response of the same B cells when stimulated *in vivo* or *in vitro* with mitogens and/or vaccines, clearly demonstrating that the inflammatory status of the B cells impacts their own function. We therefore measured mRNA expression of the pro-inflammatory cytokines TNF-α and IL-6 in unstimulated splenic B cells from young and old WT and P2KO mice. Results in **Figure 3** show that TNF-α (top) and IL-6 (bottom) mRNA expression in unstimulated B cells from from P2KO mice are significantly higher as compared to those in B cells from WT mice (A). Moreover, TNF-α (top) and IL-6 (bottom) mRNA expression in unstimulated B cells are negatively associated with the *in vivo* influenza vaccine response (B) and with the *in vitro* AID mRNA expression (C). These results altogether confirm and extend our previous findings that higher mRNA expression of the inflammatory cytokines TNF-α and IL-6 in B cells, prior to any stimulation, renders the same B cells incapable of being optimally stimulated by vaccines or mitogens.

Increased Frequencies and Numbers of Pro-inflammatory B Cells in the Spleen of P2KO vs. WT Mice

The above results, showing higher inflammation (TNF-α and IL-6 mRNA expression) in unstimulated B cells from P2KO mice, as compared to WT controls, are supported by the findings of higher frequencies of pro-inflammatory B cell subsets in the spleens of P2KO vs. WT mice, as shown in **Figure 4**. We previously showed in mice (29) and humans (7) conditions and pro-inflammatory B cell subsets contributing to reduced function in the aged. We measured by flow cytometry the percentages of FO, ABC and MZ B cell subsets in the spleens of WT and P2KO old mice (the ones with the highest levels of inflammation). Results

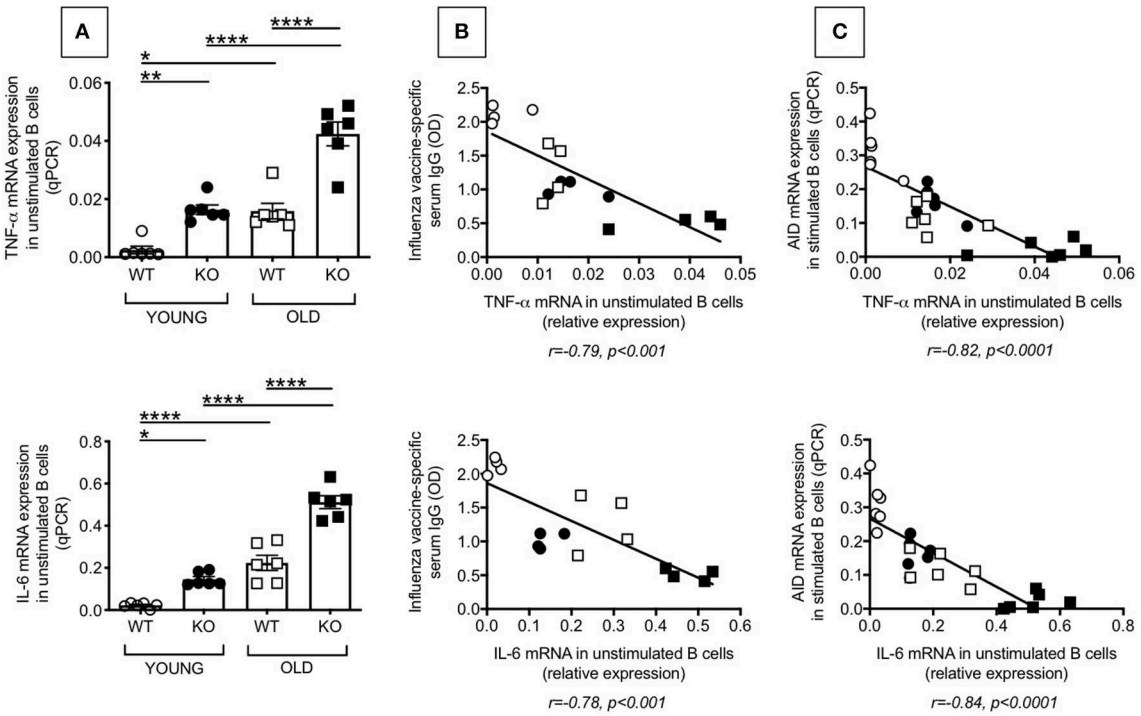

FIGURE 3 | Increased intrinsic inflammation in splenic B cells from P2KO vs. WT mice. **(A)** B cells isolated from the spleens of young and old WT and P2KO mice (6 mice/group) by magnetic sorting were left unstimulated. The mRNA was extracted from the unstimulated B cells and qPCR performed to evaluate mRNA expression of TNF-α and IL-6. Results show qPCR values ($2^{-\Delta\Delta Ct}$). Mean comparisons between groups were performed by two-way ANOVA followed by Bonferroni's multiple comparisons test $^{*}p < 0.05$, $^{**}p < 0.01$, $^{***}p < 0.001$, $^{****}p < 0.0001$. **(B)** Correlation of TNF-α (top) and IL-6 (bottom) mRNA expression with *in vivo* influenza vaccine antibody response. Pearson's *r* and *p*-values are at the bottom of the figure. **(C)** Correlation of TNF-α (top) and IL-6 (bottom) expression with *in vitro* class switch measured by mRNA expression of AID after 5 day stimulation with LPS. Pearson's *r* and *p*-values are at the bottom of the figure.

show significantly reduced frequencies (A) and numbers (B) of the anti-inflammatory FO subset, and significantly increased frequencies and numbers of the pro-inflammatory ABC subset, in the spleens of old P2KO vs. WT mice. No differences in frequencies and numbers of MZ B cells were observed between WT and P2KO mice.

No Difference Between WT and P2KO Mice in Fat Measures but Increased Frequencies of ABCs in the VAT of P2KO vs. WT Mice

Fat mass increases with age in mice (30) and humans (30, 31). The increase in fat mass with age is responsible for increased local and systemic levels of pro-inflammatory mediators that are markers of inflammaging (9). Higher fat mass also induces pro-inflammatory B cells and impairs B cell function in old mice (29) and humans (32, 33). Therefore, obesity may be considered a mechanism of aging.

We analyzed the VAT to identify contributors to the phenotypic and functional changes observed in splenic B cells from old P2KO mice as compared to WT controls. Results in **Figure 5** show that both mouse weight (A) and epididymal VAT weight (B) are comparable in WT and P2KO mice. The 2 measures are positively correlated (C). Additionally, mouse weight is negatively associated with *in vitro* class switch, measured by AID mRNA expression in stimulated splenic B cells (D).

To explain the results in D and identify mechanisms responsible for the VAT-driven inflammation leading to the down-regulation of AID, we compared frequencies of ABCs in the VAT of P2KO vs. WT old mice. Results in **Figure 6** show that FO B cells significantly decrease in frequencies and numbers, while ABCs significantly increase, in the VAT of old P2KO mice as compared to age-matched WT controls. These results demonstrate that although no significant differences were observed in mouse weight and epididymal VAT weight between P2KO and WT mice, frequencies and numbers of ABCs, the most pro-inflammatory B cell subset, are increased in the VAT of P2KO mice and they contribute to local and systemic inflammation which negatively impacts B cell function.

Increased Differentiation of ABCs in the VAT of P2KO vs. WT Mice

To understand if ABC frequencies in the VAT of P2KO mice increase as a consequence of increased differentiation of ABCs, we performed the following experiment in which we evaluated the ability of adipocytes to induce ABCs. We co-cultured in transwells adipocytes from the VAT of WT or P2KO old mice with splenic B cells from WT mice. These experiments were

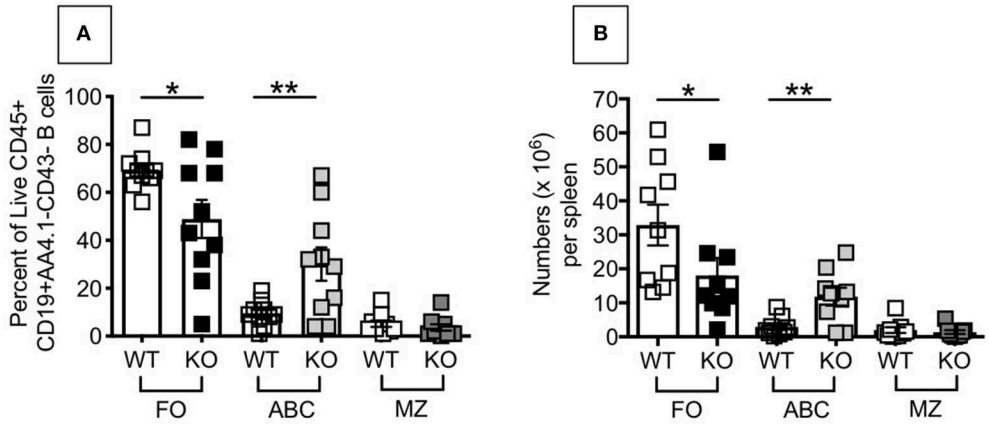

FIGURE 4 | Increased frequencies and numbers of ABCs/pro-inflammatory B cells in the spleen of P2KO vs. WT mice. The spleens of old WT and P2KO mice (10 mice/group) were stained to evaluate frequencies **(A)** and numbers **(B)** of FO, ABC and MZ B cell subsets. Results are gated on Live CD45+CD19+AA4.1-CD43- cells to exclude transitional (AA4.1+) and B1 (CD43+) B cells. Mean comparisons between groups were performed by two-way ANOVA followed by Bonferroni's multiple comparisons test. $^{*}p < 0.05$, $^{**}p < 0.01$.

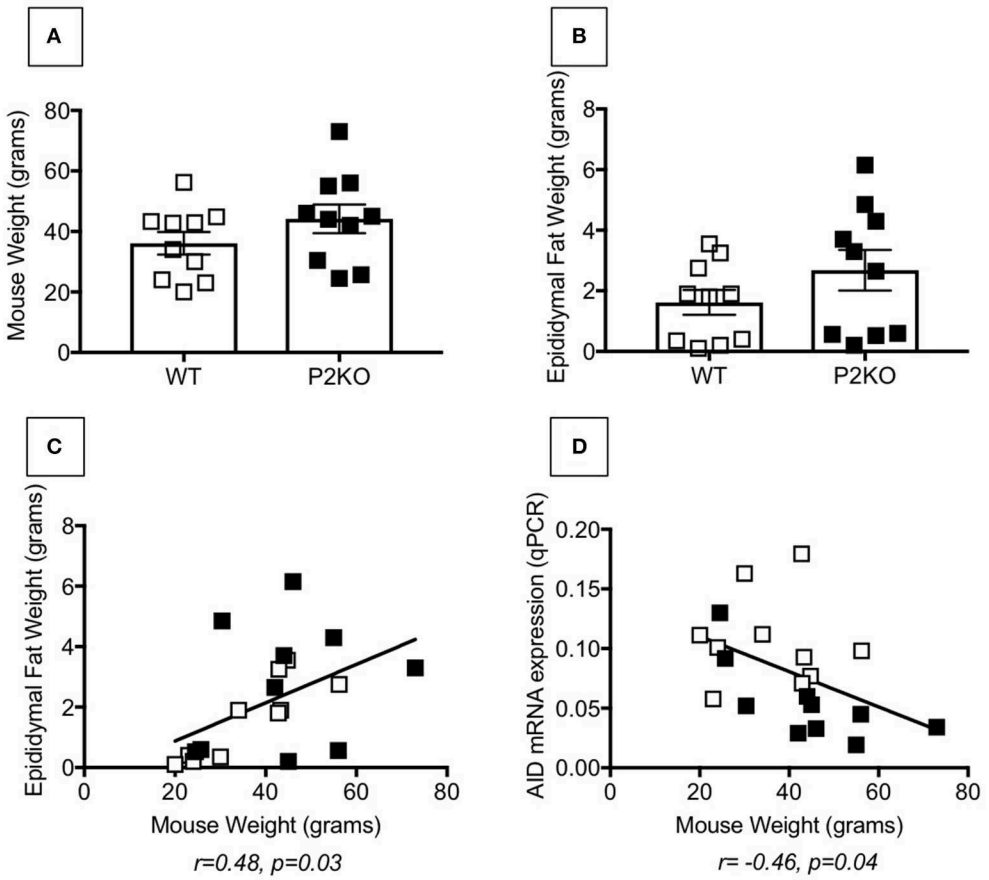

FIGURE 5 | Comparable fat measures in P2KO vs. WT mice. Ten pairs of old WT and P2KO mice were sacrificed. Mouse weight and epididymal VAT weight are shown in **(A,B)**, respectively. **(C)** Correlation between mouse weight and epididymal VAT weight. Pearson's *r* and *p*-values are at the bottom of the figure. **(D)** Correlation between mouse weight and mRNA expression of AID in stimulated splenic B cells after 5 day stimulation with LPS. Pearson's *r* and *p*-values are at the bottom of the figure.

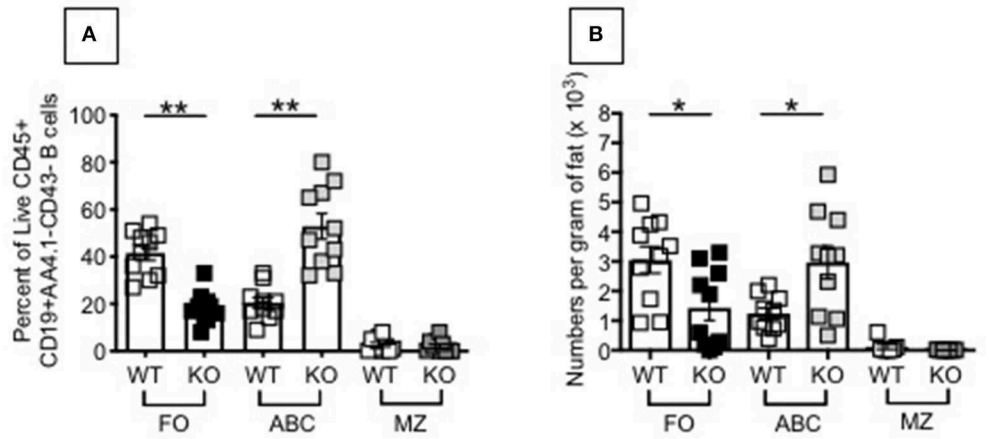

FIGURE 6 | Increased frequencies and numbers of ABCs/pro-inflammatory B cell subsets in the SVF of P2KO vs. WT mice. The SVF from the VAT of old WT and P2KO mice (10 mice/group) were stained to evaluate frequencies **(A)** and numbers **(B)** of FO, ABC, and MZ B cell subsets. Results are gated as in **Figure 4**. Mean comparisons between groups were performed by two-way ANOVA followed by Bonferroni's multiple comparisons test. $^{*}p < 0.05$, $^{**}p < 0.01$.

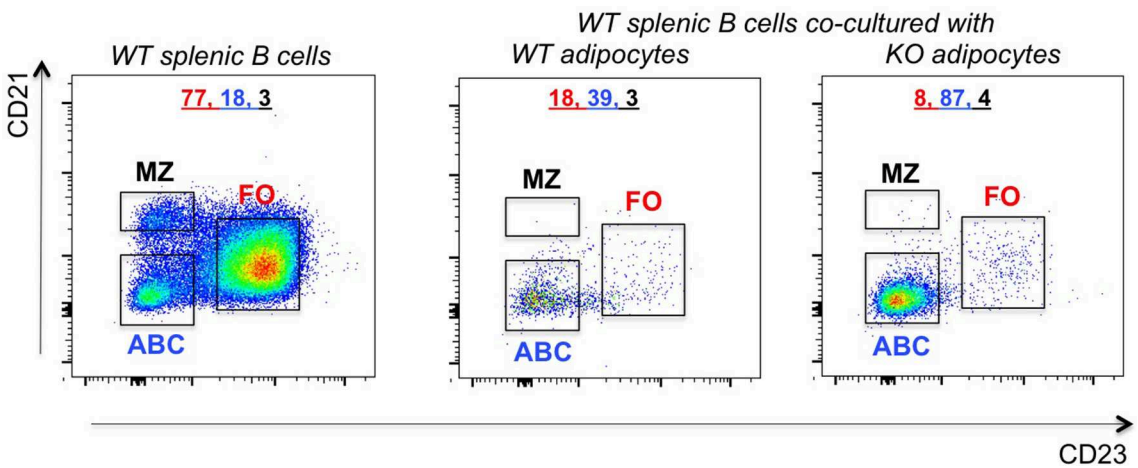

FIGURE 7 | Increased frequencies of ABCs in the VAT of P2KO vs. WT mice. B cells from the spleen of old WT mice were stained as in **Figure 4** and frequencies of FO, ABC, MZ were evaluated. Adipocytes were isolated from the VAT of WT and P2KO old mice and cultured for 72 h in transwells with the splenic B cells of old WT mice. After this time, B cells were stained as indicated above and the frequencies of B cell subsets measured by flow cytometry. Results are representative of four independent experiments.

performed in the absence of any exogenous stimulation. Results in **Figure 7** show that co-culture of 72 hrs significantly changed the relative percentages of the B cell subsets, leading to a significant increase in ABC percentages, similar to what we have observed in the VAT (**Figure 6**). The reason why the co-culture of WT adipocytes and splenic B cells also changes the relative proportions of FO and ABC (reducing FO and increasing ABC percentages) is because WT adipocytes are also inflammatory, although not as much as P2KO adipocytes.

To further confirm that FO do not decrease because they die but because they differentiate into ABCs, as we have previously shown in C57BL/6 mice (29), we co-cultured adipocytes from P2KO old mice with sorted splenic FO B cells from the same mice and we compared gene expression profiles of these FO B cells before and after 72 h in transwell. We measured Prdm1 (Blimp-1), a marker up-regulated in ABCs vs. FO, as we (29) and others (34) have previously shown. Results in **Figure 8** show that the co-culture with adipocytes induced differentiation of FO B cells into ABCs, as splenic FO B cells acquired markers typical of ABCs. It is relevant to note that adipocyte-driven ABC differentiation occurred in the absence of any exogenous (antigen/mitogen) stimulation. This culture condition is different from that in which FO are stimulated with antigens/mitogens *in vitro* to generate Prdm1 (Blimp-1) expressing plasma cells.

Adipocytes From P2KO Mice Are More Inflammatory Than Those From WT Mice

We then compared the inflammatory profile of adipocytes from the VAT of WT and P2KO mice, which is responsible for the recruitment of inflammatory B cell subsets to the VAT and for

their differentiation. We measured in particular RNA expression of pro-inflammatory cytokines (TNF-α, IL-6) and chemokines (CXCL10, CCL2, CCL5). Results in **Figure 9** show significantly higher expression levels of the RNA for pro-inflammatory cytokines (A) and chemokines (B) in adipocytes from P2KO mice as compared to WT controls. In the PCA analysis (C) we show distinct clustering of the 2 groups of adipocytes.

DISCUSSION

The mouse and human gastrointestinal tracts are colonized by a huge number of microorganisms. Although the gut provides a functional barrier between these microorganisms and the host, translocation of bacteria and/or their products is still occurring even in normal, healthy conditions. Our study is based on the hypothesis that these events of microbial translocation are strongly suspected to lead to the establishment of systemic chronic inflammation, intrinsic B cell inflammation and dysfunctional antibody responses. P2KO mice, lacking the mechanisms to control the proliferation and dissemination of the different microbes, are characterized by higher intrinsic B cell inflammation and more dysfunctional antibody responses as compared to WT controls. This is clearly shown by increased microbial translocation in the serum of P2KO mice as compared to WT controls, which is negatively associated with a protective response against the influenza vaccine. This is to our knowledge the first study evaluating B cell function and antibody responses in mice lacking P2.

Studies in mice have clearly demonstrated that intestinal components also regulate the VAT [reviewed in Tilg and Kaser (35)] and results have shown that gut permeability is increased in obesity (36, 37) leading to the release of LPS in the circulation. LPS, as well as other intestinal antigens, has been shown to be absorbed in the VAT through lipid-driven mechanisms (38, 39).

Based on our previous data in aged mice and humans, we know that the inflammatory status of the individual and of B cells themselves impacts B cell function. Here we show that the ability to generate an *in vivo* specific antibody response to the influenza vaccine is reduced in P2KO mice as compared to WT controls. The class switch recombination defects at least in part responsible for the reduced *in vivo* and *in vitro* antibody responses include the reduced expression of AID and of its transcriptional activators E47 and Pax5. Moreover, splenic unstimulated B cells from P2KO mice make higher levels of TNF-α and IL-6 mRNA than those from WT mice and these negatively correlate with B cell function, measured *in vivo* by the response to the influenza vaccine and *in vitro* by AID mRNA expression in stimulated B cell cultures. These results confirm and extend our previously published results showing a negative impact of systemic chronic inflammation on B cell function and antibody production *in vivo* and *in vitro*.

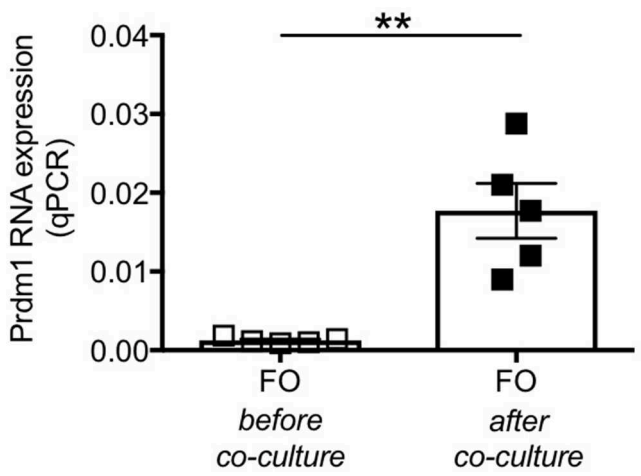

FIGURE 8 | Splenic FO B cells co-cultured with P2KO adipocytes show markers of ABCs. FO B cells sorted from the spleen of P2KO old mice were co-cultured with adipocytes from the same old mice. RNA was extracted before and after 72 h in transwell and expression of Prdm1 was evaluated by qPCR. Results show qPCR values ($2^{-\Delta\Delta Ct}$). Mean comparisons between groups were performed by paired Student's *t*-test (two-tailed). $^{**}p < 0.01$.

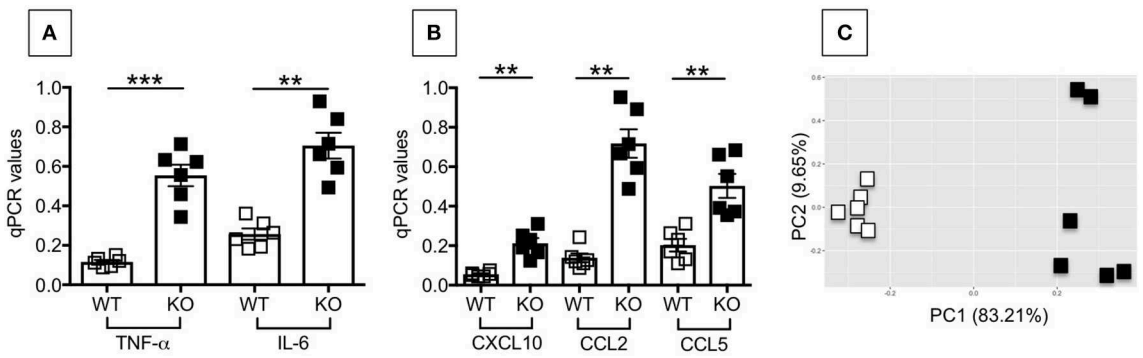

FIGURE 9 | Adipocytes from P2KO mice are more inflammatory than those from WT mice. Adipocytes were isolated from the VAT of WT and P2KO old mice, sonicated for cell disruption in the presence of TRIzol to separate the soluble fraction from lipids and cell debris. Results show qPCR values ($2^{-\Delta\Delta Ct}$) of TNF-α and IL-6 **(A)**, CXCL10, CCL2, and CCL5 **(B)** RNA expression. Mean comparisons between groups were performed by Student's *t*-test (two-tailed). $^{**}p < 0.01$, $^{***}p < 0.001$. **(C)** PCA analysis with the axes showing the percentage of variation explained by PC1 and PC2. Each symbol corresponds to one mouse.

This inflammatory status of the splenic B cells is associated with increased frequencies and numbers of the pro-inflammatory B cell subset called ABCs. These cells have been reported to increase in aging and in age-associated inflammatory conditions in both mice (29, 34, 40, 41) and humans (42–46). These cells have a unique transcriptomic phenotype (34) and are characterized by a senescence-associated secretory phenotype responsible for the secretion of several pro-inflammatory markers, including chemokines, cytokines, growth factors and matrix metalloproteinases (47).

ABCs not only increase in the spleens but also in the SVF of the VAT of P2KO mice, despite a lack of increase in mouse weight and fat mass. The reason for us to evaluate the VAT is because with aging the VAT undergoes significant changes in abundance, distribution, cellular composition, endocrine signaling and it has been shown to affect the function of other systems including the immune system. ABCs differentiate in the VAT following interaction with the adipocytes and this occurs more in the VAT of P2KO mice as compared to WT controls. Differentiation of ABCs in the VAT is accompanied by the acquisition of markers typical of this B cell subset and expressed at almost indiscernible levels in FO B cells. We measured Prdm1, the gene coding for Blimp-1, the transcription factor for plasma cells, among others, as the RNA expression of this marker was found 10-fold higher in unstimulated splenic ABCs vs. FO in our previously published study (29). Although the major function of adipocytes is to store excess energy, several recent findings have indicated that the adipocytes are also endocrine cells able to secrete adipokines and several pro-inflammatory molecules that modulate immune cell infiltration, immune cell activation and differentiation. We have preliminary evidence that leptin, the major adipokine secreted by the adipocytes, induces *in vitro* differentiation of splenic naïve B cells into ABCs secreting IgG2c autoantibodies (data not shown). Experiments currently under way in our laboratory are evaluating other adipocyte-derived molecules that may be involved in B cell differentiation in the VAT.

In conclusion, our results show for the first time that P2KO mice have decreased antibody responses, likely consequent to changes in B cell characteristics/function, chronic systemic inflammation supported by a continuous microbial translocation from the gut which cannot be controlled as these mice lack P2. These results are physiologically relevant for patients, although not frequent, with P2 deficiency who contract infections with intracellular bacteria (48) and therefore may need to be treated to improve their humoral immunity.

DATA AVAILABILITY STATEMENT

The data generated in this study are available upon request to the corresponding author.

ETHICS STATEMENT

The animal study was reviewed and approved by University of Miami IACUC approved protocols #16-252 and #16-006.

AUTHOR CONTRIBUTIONS

DF and BB conceived the experiments. DF coordinated the experiments. DF, AD, MR, and TV performed the experiments and analyzed data. DF and AD performed statistical analyses. RM, LR, and NS provided reagents. DF wrote the paper. All authors were involved in writing and had final approval of the submitted and published versions of the paper.

FUNDING

This study was supported by NIH R01 AG023717-11 (BB), NIH R01 NR015649 (NS), and by Department of Microbiology and Immunology P2 funds.

DEDICATION

This paper is dedicated to the memory of Eckhard R. Podack.

REFERENCES

1. Mccormack R, Podack ER. Perforin-2/Mpeg1 and other pore-forming proteins throughout evolution. *J Leukoc Biol.* (2015) 98:761–8. doi: 10.1189/jlb.4MR1114-523RR
2. Kleiman E, Salyakina D, De Heusch M, Hoek KL, Llanes JM, Castro I, et al. Distinct transcriptomic features are associated with transitional and mature B-cell populations in the mouse spleen. *Front Immunol.* (2015) 6:30. doi: 10.3389/fimmu.2015.00030
3. Mccormack RM, De Armas LR, Shiratsuchi M, Fiorentino DG, Olsson ML, Lichtenheld MG, et al. Perforin-2 is essential for intracellular defense of parenchymal cells and phagocytes against pathogenic bacteria. *Elife.* (2015) 4:37. doi: 10.7554/eLife.06508.037
4. Bai F, Mccormack RM, Hower S, Plano GV, Lichtenheld MG, Munson GP. Perforin-2 breaches the envelope of phagocytosed bacteria allowing antimicrobial effectors access to intracellular targets. *J Immunol.* (2018) 201:2710–20. doi: 10.4049/jimmunol.1800365
5. Sedman PC, Macfie J, Sagar P, Mitchell CJ, May J, Mancey-Jones B, et al. The prevalence of gut translocation in humans. *Gastroenterology.* (1994) 107:643–9. doi: 10.1016/0016-5085(94)90110-4
6. Frasca D, Romero M, Diaz A, Alter-Wolf S, Ratliff M, Landin AM, et al. A molecular mechanism for TNF-alpha-mediated downregulation of B cell responses. *J Immunol.* (2012) 188:279–86. doi: 10.4049/jimmunol.1003964
7. Frasca D, Diaz A, Romero M, Landin AM, Blomberg BB. High TNF-alpha levels in resting B cells negatively correlate with their response. *Exp Gerontol.* (2014) 54:116–22. doi: 10.1016/j.exger.2014.01.004
8. Frasca D, Diaz A, Romero M, Landin AM, Blomberg BB. Cytomegalovirus (CMV) seropositivity decreases B cell responses to the influenza vaccine. *Vaccine.* (2015) 33:1433–9. doi: 10.1016/j.vaccine.2015.01.071
9. Franceschi C, Bonafe M, Valensin S, Olivieri F, De Luca M, Ottaviani E, et al. Inflamm-aging. An evolutionary perspective on immunosenescence. *Ann N Y Acad Sci.* (2000) 908:244–54. doi: 10.1111/j.1749-6632.2000.tb06651.x
10. Miscia S, Marchisio M, Grilli A, Di Valerio V, Centurione L, Sabatino G, et al. Tumor necrosis factor alpha (TNF-alpha) activates Jak1/Stat3-Stat5B signaling through TNFR-1 in human B cells. *Cell Growth Differ.* (2002) 13:13–8.
11. Zhang X, Li L, Mayne J, Ning Z, Stintzi A, Figeys D. Assessing the impact of protein extraction methods for human gut metaproteomics. *J Proteomics.* (2018) 180:120–7. doi: 10.1016/j.jprot.2017.07.001

12. Takeda K, Kaisho T, Akira S. Toll-like receptors. *Annu Rev Immunol.* (2003) 21:335–76. doi: 10.1146/annurev.immunol.21.120601.141126
13. Moir S, Ho J, Malaspina A, Wang W, Dipoto AC, O'shea MA, et al. Evidence for HIV-associated B cell exhaustion in a dysfunctional memory B cell compartment in HIV-infected viremic individuals. *J Exp Med.* (2008) 205:1797–805. doi: 10.1084/jem.20072683
14. Parmigiani A, Alcaide ML, Freguja R, Pallikkuth S, Frasca D, Fischl MA, et al. Impaired antibody response to influenza vaccine in HIV-infected and uninfected aging women is associated with immune activation and inflammation. *PLoS ONE.* (2013) 8:e79816. doi: 10.1371/journal.pone.0079816
15. George VK, Pallikkuth S, Pahwa R, De Armas LR, Rinaldi S, Pan L, et al. Circulating inflammatory monocytes contribute to impaired influenza vaccine responses in HIV-infected participants. *AIDS.* (2018) 32:1219–28. doi: 10.1097/QAD.0000000000001821
16. Pallikkuth S, De Armas LR, Rinaldi S, George VK, Pan L, Arheart KL, et al. Dysfunctional peripheral T follicular helper cells dominate in people with impaired influenza vaccine responses: results from the FLORAH study. *PLoS Biol.* (2019) 17:e3000257. doi: 10.1371/journal.pbio.3000257
17. Frasca D, Van Der Put E, Riley RL, Blomberg BB. Reduced Ig class switch in aged mice correlates with decreased E47 and activation-induced cytidine deaminase. *J Immunol.* (2004) 172:2155–62. doi: 10.4049/jimmunol.172.4.2155
18. Frasca D, Van Der Put E, Landin AM, Gong D, Riley RL, Blomberg BB. RNA stability of the E2A-encoded transcription factor E47 is lower in splenic activated B cells from aged mice. *J Immunol.* (2005) 175:6633–44. doi: 10.4049/jimmunol.175.10.6633
19. Quong MW, Harris DP, Swain SL, Murre C. E2A activity is induced during B-cell activation to promote immunoglobulin class switch recombination. *EMBO J.* (1999) 18:6307–18. doi: 10.1093/emboj/18.22.6307
20. Sayegh CE, Quong MW, Agata Y, Murre C. E-proteins directly regulate expression of activation-induced deaminase in mature B cells. *Nat Immunol.* (2003) 4:586–93. doi: 10.1038/ni923
21. Gonda H, Sugai M, Nambu Y, Katakai T, Agata Y, Mori KJ, et al. The balance between Pax5 and Id2 activities is the key to AID gene expression. *J Exp Med.* (2003) 198:1427–37. doi: 10.1084/jem.20030802
22. Grundstrom C, Kumar A, Priya A, Negi N, Grundstrom T. ETS1 and PAX5 transcription factors recruit AID to Igh DNA. *Eur J Immunol.* (2018) 48:1687–97. doi: 10.1002/eji.201847625
23. Muramatsu M, Kinoshita K, Fagarasan S, Yamada S, Shinkai Y, Honjo T. Class switch recombination and hypermutation require activation-induced cytidine deaminase (AID), a potential RNA editing enzyme. *Cell.* (2000) 102:553–63. doi: 10.1016/S0092-8674(00)00078-7
24. Nagaoka H, Muramatsu M, Yamamura N, Kinoshita K, Honjo T. Activation-induced deaminase (AID)-directed hypermutation in the immunoglobulin Smu region: implication of AID involvement in a common step of class switch recombination and somatic hypermutation. *J Exp Med.* (2002) 195:529–34. doi: 10.1084/jem.20012144
25. Okazaki IM, Kinoshita K, Muramatsu M, Yoshikawa K, Honjo T. The AID enzyme induces class switch recombination in fibroblasts. *Nature.* (2002) 416:340–5. doi: 10.1038/nature727
26. Shaffer AL, Lin KI, Kuo TC, Yu X, Hurt EM, Rosenwald A, et al. Blimp-1 orchestrates plasma cell differentiation by extinguishing the mature B cell gene expression program. *Immunity.* (2002) 17:51–62. doi: 10.1016/S1074-7613(02)00335-7
27. Litinskiy MB, Nardelli B, Hilbert DM, He B, Schaffer A, Casali P, et al. DCs induce CD40-independent immunoglobulin class switching through BLyS and APRIL. *Nat Immunol.* (2002) 3:822–9. doi: 10.1038/ni829
28. Kaminski DA, Stavnezer J. Antibody class switching differs among SJL, C57BL/6 and 129 mice. *Int Immunol.* (2007) 19:545–56. doi: 10.1093/intimm/dxm020
29. Frasca D, Diaz A, Romero M, Vazquez T, Blomberg BB. Obesity induces pro-inflammatory B cells and impairs B cell function in old mice. *Mech Ageing Dev.* (2017) 162:91–9. doi: 10.1016/j.mad.2017.01.004
30. Tchkonia T, Morbeck DE, Von Zglinicki T, Van Deursen J, Lustgarten J, Scrable H, et al. Fat tissue, aging, and cellular senescence. *Aging Cell.* (2010) 9:667–84. doi: 10.1111/j.1474-9726.2010.00608.x
31. Zamboni M, Rossi AP, Fantin F, Zamboni G, Chirumbolo S, Zoico E, et al. Adipose tissue, diet and aging. *Mech Ageing Dev.* (2014) 136–7:129–37. doi: 10.1016/j.mad.2013.11.008
32. Frasca D, Diaz A, Romero M, Thaller S, Blomberg BB. Secretion of autoimmune antibodies in the human subcutaneous adipose tissue. *PLoS ONE.* (2018) 13:e0197472. doi: 10.1371/journal.pone.0197472
33. Frasca D, Diaz A, Romero M, Thaller S, Blomberg BB. Metabolic requirements of human pro-inflammatory B cells in aging and obesity. *PLoS ONE.* (2019) 14:e0219545. doi: 10.1371/journal.pone.0219545
34. Rubtsov AV, Rubtsova K, Fischer A, Meehan RT, Gillis JZ, Kappler JW, et al. Toll-like receptor 7 (TLR7)-driven accumulation of a novel CD11c(+) B-cell population is important for the development of autoimmunity. *Blood.* (2011) 118:1305–15. doi: 10.1182/blood-2011-01-331462
35. Tilg H, Kaser A. Gut microbiome, obesity, and metabolic dysfunction. *J Clin Invest.* (2011) 121:2126–32. doi: 10.1172/JCI58109
36. Brun P, Castagliuolo I, Di Leo V, Buda A, Pinzani M, Palu G, et al. Increased intestinal permeability in obese mice: new evidence in the pathogenesis of non-alcoholic steatohepatitis. *Am J Physiol Gastrointest Liver Physiol.* (2007) 292:G518–25. doi: 10.1152/ajpgi.00024.2006
37. Nagpal R, Newman TM, Wang S, Jain S, Lovato JF, Yadav H. Obesity-linked gut microbiome dysbiosis associated with derangements in gut permeability and intestinal cellular homeostasis independent of diet. *J Diabetes Res.* (2018) 2018:3462092. doi: 10.1155/2018/3462092
38. Wang Y, Ghoshal S, Ward M, De Villiers W, Woodward J, Eckhardt E. Chylomicrons promote intestinal absorption and systemic dissemination of dietary antigen (ovalbumin) in mice. *PLoS ONE.* (2009) 4:e8442. doi: 10.1371/journal.pone.0008442
39. Wang Y, Li J, Tang L, Wang Y, Charnigo R, De Villiers W, et al. T-lymphocyte responses to intestinally absorbed antigens can contribute to adipose tissue inflammation and glucose intolerance during high fat feeding. *PLoS ONE.* (2010) 5:e13951. doi: 10.1371/journal.pone.0013951
40. Hao Y, O'neill P, Naradikian MS, Scholz JL, Cancro MP. A B-cell subset uniquely responsive to innate stimuli accumulates in aged mice. *Blood.* (2011) 118:1294–304. doi: 10.1182/blood-2011-01-330530
41. Russell Knode LM, Naradikian MS, Myles A, Scholz JL, Hao Y, Liu D, et al. Age-associated B cells express a diverse repertoire of VH and Vkappa genes with somatic hypermutation. *J Immunol.* (2017) 198:1921–7. doi: 10.4049/jimmunol.1601106
42. Saadoun D, Terrier B, Bannock J, Vazquez T, Massad C, Kang I, et al. Expansion of autoreactive unresponsive CD21-/low B cells in Sjogren's syndrome-associated lymphoproliferation. *Arthritis Rheum.* (2013) 65:1085–96. doi: 10.1002/art.37828
43. Bulati M, Buffa S, Martorana A, Candore G, Lio D, Caruso C, et al. Trafficking phenotype and production of granzyme B by double negative B cells (IgG(+)IgD(–)CD27(–)) in the elderly. *Exp Gerontol.* (2014) 54:123–9. doi: 10.1016/j.exger.2013.12.011
44. Adlowitz DG, Barnard J, Biear JN, Cistrone C, Owen T, Wang W, et al. Expansion of activated peripheral blood memory B cells in rheumatoid arthritis, impact of B cell depletion therapy, and biomarkers of response. *PLoS ONE.* (2015) 10:e0128269. doi: 10.1371/journal.pone.0128269

45. Claes N, Fraussen J, Vanheusden M, Hellings N, Stinissen P, Van Wijmeersch B, et al. Age-associated B cells with proinflammatory characteristics are expanded in a proportion of multiple sclerosis patients. *J Immunol.* (2016) 197:4576–83. doi: 10.4049/jimmunol.1502448
46. Frasca D, Diaz A, Romero M, D'eramo F, Blomberg BB. Aging effects on T-bet expression in human B cell subsets. *Cell Immunol.* (2017) 321:68–73. doi: 10.1016/j.cellimm.2017.04.007
47. Campisi J. Cellular senescence: putting the paradoxes in perspective. *Curr Opin Genet Dev.* (2011) 21:107–12. doi: 10.1016/j.gde.2010.10.005
48. Mccormack RM, Szymanski EP, Hsu AP, Perez E, Olivier KN, Fisher E, et al. MPEG1/perforin-2 mutations in human pulmonary nontuberculous mycobacterial infections. *JCI Insight.* (2017) 2:89635. doi: 10.1172/jci.insight.89635

Conflict of Interest: RM and EP are inventors of patents and stand to gain royalties from future commercialization.

The remaining authors declare that the research was conducted in the absence of any commercial or financial relationships that could be construed as a potential conflict of interest.

frontiers in Immunology

ORIGINAL RESEARCH
published: 13 March 2020
doi: 10.3389/fimmu.2020.00428

Novel Role for Animal Innate Immune Molecules: Enterotoxic Activity of a Snail Egg MACPF-Toxin

*Matías L. Giglio[1], Santiago Ituarte[1], Andrés E. Ibañez[2], Marcos S. Dreon[1,3], Eduardo Prieto[4], Patricia E. Fernández[5] and Horacio Heras[1]**

[1] Instituto de Investigaciones Bioquímicas de La Plata "Prof. Dr. Rodolfo R. Brenner" (INIBIOLP), CONICET, CCT-La Plata, Universidad Nacional de la Plata (UNLP), La Plata, Argentina, [2] División de Vertebrados, Facultad de Ciencias Naturales y Museo (FCNyM), Universidad Nacional de La Plata, La Plata, Argentina, [3] Cátedra de Bioquímica y Biología Molecular, Facultad de Ciencias Médicas, Universidad Nacional de la Plata (UNLP), La Plata, Argentina, [4] Instituto de Investigaciones Físico-químicas Teóricas y Aplicadas (INIFTA), CONICET, CCT-La Plata, Universidad Nacional de La Plata, La Plata, Argentina, [5] Facultad de Ciencias Veterinarias (FEV), Instituto de Patología B. Epstein, Cátedra de Patología General Veterinaria, Universidad Nacional de La Plata (UNLP), La Plata, Argentina

OPEN ACCESS

Edited by:
George P. Munson,
University of Miami, United States

Reviewed by:
Nada Kraševec,
National Institute of Chemistry, Slovenia
Ruby Hong Ping Law,
Monash University, Australia

***Correspondence:**
Horacio Heras
h-heras@med.unlp.edu.ar

Specialty section:
This article was submitted to Molecular Innate Immunity, a section of the journal Frontiers in Immunology

Received: 24 December 2019
Accepted: 25 February 2020
Published: 13 March 2020

Citation:
Giglio ML, Ituarte S, Ibañez AE, Dreon MS, Prieto E, Fernández PE and Heras H (2020) Novel Role for Animal Innate Immune Molecules: Enterotoxic Activity of a Snail Egg MACPF-Toxin. Front. Immunol. 11:428. doi: 10.3389/fimmu.2020.00428

Gastropod Molluscs rely exclusively on the innate immune system to protect from pathogens, defending their embryos through maternally transferred effectors. In this regard, *Pomacea* snail eggs, in addition to immune defenses, have evolved the perivitellin-2 or PV2 combining two immune proteins into a neurotoxin: a lectin and a pore-forming protein from the Membrane Attack Complex/Perforin (MACPF) family. This binary structure resembles AB-toxins, a group of toxins otherwise restricted to bacteria and plants. Many of these are enterotoxins, leading us to explore this activity in PV2. Enterotoxins found in bacteria and plants act mainly as pore-forming toxins and toxic lectins, respectively. In animals, although both pore-forming proteins and lectins are ubiquitous, no enterotoxins have been reported. Considering that *Pomacea* snail eggs ingestion induce morpho-physiological changes in the intestinal mucosa of rodents and is cytotoxic to intestinal cells in culture, we seek for the factor causing these effects and identified PmPV2 from *Pomacea maculata* eggs. We characterized the enterotoxic activity of PmPV2 through *in vitro* and *in vivo* assays. We determined that it withstands the gastrointestinal environment and resisted a wide pH range and enzymatic proteolysis. After binding to Caco-2 cells it promoted changes in surface morphology and an increase in membrane roughness. It was also cytotoxic to both epithelial and immune cells from the digestive system of mammals. It induced enterocyte death by a lytic mechanism and disrupted enterocyte monolayers in a dose-dependent manner. Further, after oral administration to mice PmPV2 attached to enterocytes and induced large dose-dependent morphological changes on their small intestine mucosa, reducing the absorptive surface. Additionally, PmPV2 was detected in the Peyer's patches where it activated lymphoid follicles and triggered apoptosis. We also provide evidence that the toxin can traverse the intestinal barrier and induce oral adaptive immunity with evidence

of circulating antibody response. As a whole, these results indicate that PmPV2 is a true enterotoxin, a role that has never been reported to lectins or perforin in animals. This extends by convergent evolution the presence of plant- and bacteria-like enterotoxins to animals, thus expanding the diversity of functions of MACPF proteins in nature.

Keywords: *Pomacea maculata*, snail reproduction, PV2, intestinal morphology, antipredator defense, AB toxin, cytotoxicity

INTRODUCTION

The innate immune system is a protective line of defense toward foreign organisms present, to some extent, in all multicellular organisms. Mollusks, like all other invertebrates, rely exclusively on the innate immune system, using both cellular and humoral defense lines (1). Among the humoral effectors are reactive oxygen species, lectins, antimicrobial peptides, proteases, protease inhibitors, and pore-forming proteins, many of which are awaiting functional characterizations (2). In addition to protecting the adults, it has been shown that several of these compounds are also maternally transferred to eggs where they would provide immunity to the developing embryos. For instance, recent proteomic studies revealed the presence of many proteins with defensive roles in the egg fluid—referred to as perivitelline fluid (PVF)—of several snail species including *Biomphalaria glabrata*, *Marisa cornuarietis*, *Pomacea diffusa, P. canaliculata*, and *P. maculata* (3–7). Among these proteins, called perivitellins, an evolutionary novelty arose in the eggs of some *Pomacea* species, in which two immune effectors, a perforin from the Membrane Attack Complex and Perforin (MACPF) family and a tachylectin, combined and formed a neurotoxin, the perivitellin-2 or PV2 (8, 9). This binary structure is unique among animals and resembles those of bacterial and plant AB toxins, where a ¨B¨-moiety acts as a delivery unit of a toxic ¨A¨-moiety (10, 11). Unlike AB toxins from bacteria or plants, snail PV2 contains a unique arrangement of two AB toxins in a head-to-tail fashion (12). Interestingly, many of these AB toxins, such as the cholera toxin (CT), heat labile toxin (LT), and shiga toxins (Stxs) from bacteria and the type-2 ribosome inactivating proteins (RIPs) from plants, act as enterotoxins (11), an unexplored function in PV2.

Enterotoxins are a group of toxic proteins that target the digestive system. In many bacteria they intervene in pathogenic processes (13, 14) and most of them are cytotoxic to intestinal cells usually by forming pores in the plasma membrane hence known as pore-forming toxins (PFTs) (13, 15, 16). On the other hand, plant enterotoxins are mostly toxic lectins, particularly abundant in seeds, that play a role in the defense against herbivory (17–19). Both bacteria and plant enterotoxins adversely affect gut physiology and/or morphology usually by cytotoxicity on intestinal cells, disruption of the brush border, and changes in the digestive, absorptive, protective or secretory functions, that could eventually lead to death (14, 17, 19). Moreover, some bacterial enterotoxins elicit inflammatory processes and immune system activation in mammals (14, 15).

Remarkably, no enterotoxins have been reported in animals, although both pore-forming proteins and lectins are widely distributed (20, 21). Even more, when these animal proteins act as toxins they always target other systems (8, 9, 21, 22). This lack of enterotoxins is surprising given that plant and animal embryos are often exposed to similar selective pressures by predators and pathogens alike. However, recent studies in *Pomacea* snails have reported egg defensive compounds targeting the digestive system suggesting the presence of enterotoxins. For instance, ingestion of *P. canaliculata* PVF decreases rat growth rate, induces morphological changes in the small intestine mucosa, and decreases the absorptive surface in mice and rats (9, 23, 24). This PVF also showed cytotoxic effects on intestinal cells of the Caco-2 line (23). Moreover, the gastrointestinal tract of mice exposed to *P. canaliculata* PVF increases the permeability of the digestive barrier (24). Although the compounds responsible of these enterotoxic effects were unknown, some perivitellins with non-toxic defensive properties targeting the digestive system were isolated from *Pomacea* eggs such as protease inhibitors and non-digestible storage proteins (24–28). However, as PV2 is a toxin with the same structural domains as plant and bacteria enterotoxins, we wondered if it would be responsible for the enterotoxic effects observed for the *Pomacea* PVF.

Thus, the aim of this work was to evaluate the enterotoxic capacity of PmPV2. Using *in vitro* and *in vivo* approaches, we evaluated the ability of PmPV2 to resist enzymatic proteolysis and extreme pH, as well as its cytotoxicity, capacity to bind to intestinal cells, disrupt cell monolayers, cause morphological changes and traverse the intestinal barrier inducing adaptive immunity *via oral*. We found that PmPV2 was able to withstand a wide range of pHs and gastrointestinal proteases both *in vitro* and *in vivo*. Then, it binds to enterocytes which is followed by necrosis. Mice fed with the toxin showed strong morphological changes in their small intestine and a reduction of the absorptive surface. Additionally, PmPV2 was detected in the Peyer's patches where it induced cell apoptosis. PmPV2 triggered oral immunization indicating it can reach the circulatory system. All these results provide the first evidence that PmPV2, an animal PFT, besides neurotoxicity, exerts enterotoxicity when ingested further potentiating the multiple defenses of *Pomacea* eggs.

Abbreviations: MACPF, Membrane Attack Complex/Perforin; PFT, pore-forming toxin; PVF, perivitelline fluid; PV2, perivitellin-2; SAXS, small angle X-ray scattering; CD, circular dichroism; BSA, bovine serum albumin; ISAD, image surface area difference; TEER, transepithelial electric resistance; PPs, Peyer's patches; i.p, intraperitoneally; CT, cholera toxin; Stxs, Shiga toxins; LT, heat-labile enterotoxin; HlyA, alpha-hemolysin; PsSC, scalarin.

RESULTS

Stability at Physiologically Relevant PHs and Gastrointestinal Environments

A selective pressure faced by a defensive egg protein when ingested by a predator is the gastrointestinal tract pH and proteases. Therefore, stability of PmPV2 in a wide range of pH was analyzed by fluorescence, small angle X-ray scattering (SAXS) and circular dichroism (CD) spectroscopies. Fluorescence spectra did not change significantly between pH 4.0–10.0, while a change in emission spectra at extreme pH values, 2.0 and 12.0, was observed (**Figure 1A**). Likewise, SAXS analysis showed no significant changes in gyration radius (*Rg*) between pH 6.0 and 10.0 and protein denaturation was only evident at extreme pH values (**Figure 1B**). However, *Rg* increased from 53.7 nm (at pH 6.0) to 67.0 nm (at pH 4.0), together with its maximum intramolecular distance (*Dmax*), which went from 108 to 134 nm, at pH 6.0 and 4.0, respectively (**Figure S1**); molecular mass only increased slightly (**Figure S1**), indicating the protein expanded without oligomerization or aggregation. Far-UV CD spectra region showed structural stability in the pH range 4.0–8.0 (**Figure 1C**). These results indicate remarkable structural stability of the protein in a wide range of pH values and an expansion event at pH 4.0.

In addition, the susceptibility of PmPV2 to protease activity *in silico* and *in vitro* was also evaluated. *In silico* digestion showed that both PmPV2 subunits have putative cleavage sites for both pepsin and trypsin, indicating it is potentially susceptible to proteases. In particular, pepsin has 48 and 23 cleavage sites for the heavy (PmPV2-67) and light subunit (PmPV-31), respectively, while trypsin has 151 cleavage sites in PmPV2-67 and 76 in PmPV2-31. However, *in vitro* digestion assay showed that PmPV2 was able to withstand both gastric and duodenal phases with only minor protein degradation in the latter (**Figure 1D**). This result agreed with the immunodetection of PmPV2 attached to intestinal mucosae after oral administration to mice (*see below*).

Binding to Intestinal Cells and Effects on Cell Morphology and Small Intestinal Mucosa

Toxins that enter the predator's body by ingestion have first to bind to epithelial cells to be internalized to reach its target or exert its functions. In this regard, we analyzed PmPV2 binding to Caco-2 cells and enterocytes from the small intestine mucosa. Whereas, Caco-2 cells treated with Alexa-BSA showed no label (**Figure 2A**), after the incubation with Alexa-labeled

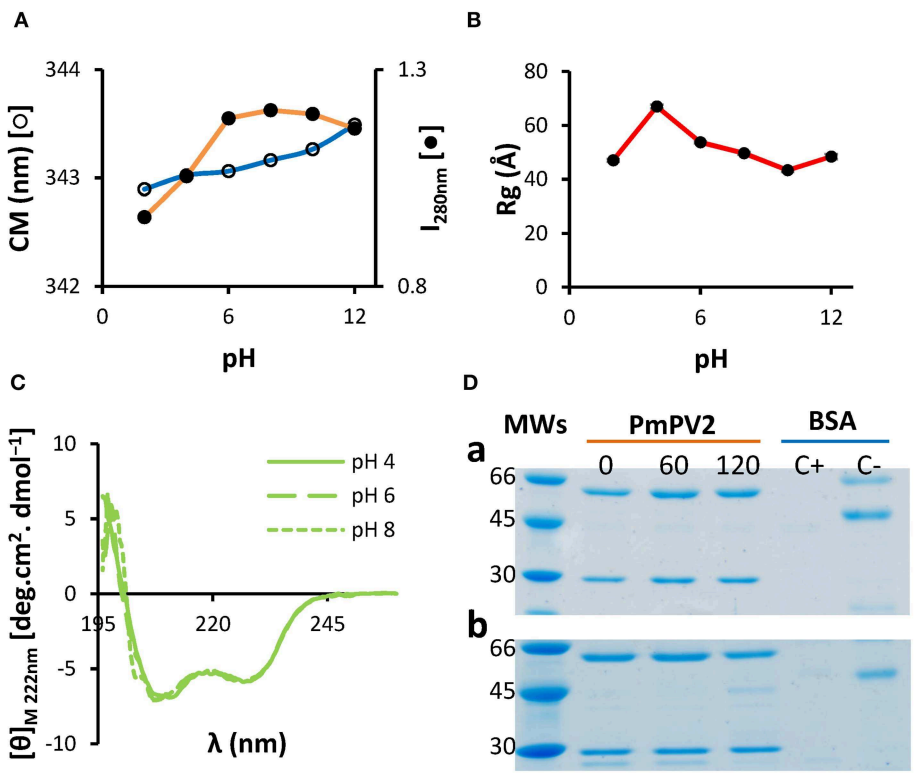

FIGURE 1 | PmPV2 is structurally stable in a wide range of pH and resists *in vitro* gastrointestinal digestion. **(A–C)** PmPV2 stability at different pH values. Stability was measured following the changes in: **(A)** Trp environment from pH 2.0 to pH 12.0, depicted as center of mass (CM) and fluorescence intensity at 280 nm (I_{280}); **(B)** gyration radii (*Rg*) obtained by SAXS; **(C)** secondary structure by CD spectra in the far-UV region at pH 4.0 (solid line), pH 6.0 (dashed line) and pH 8.0 (dotted line). **(D)** Gastric phase (a). PmPV2 exposed for 0, 60 and 120 min to pepsin at pH 2.5. MWs: molecular weight standard (kDa); Duodenal phase (b). PmPV2 exposed for 0, 60, and 120 min to trypsin at pH 8.5 after 120 min of gastric phase. Positive control (C+): BSA with enzyme, negative control (C–): BSA without enzyme.

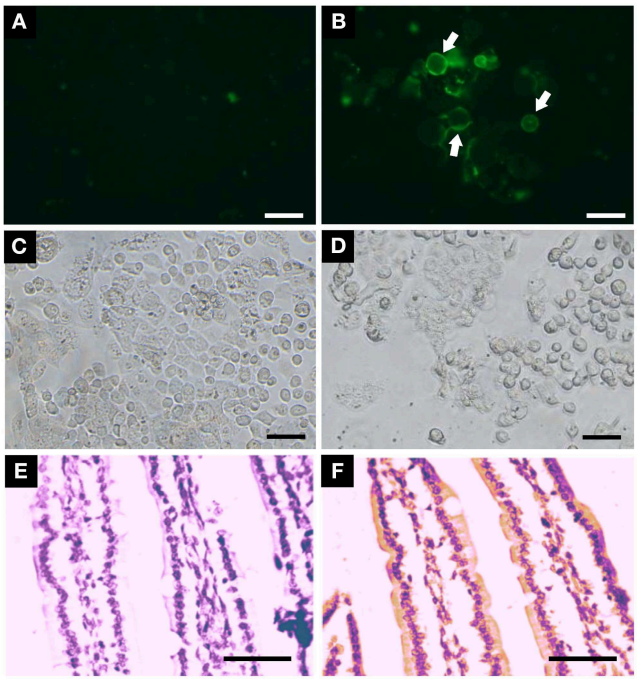

FIGURE 2 | PmPV2 binds to intestinal cells. **(A,B)** PmPV2 binding to intestinal cells in culture. Caco-2 cells were incubated for 1 h with Alexa-488 labeled BSA as control **(A)** or with PmPV2 **(B)**. PmPV2 attached to cell surface is highlighted with arrowheads. Bar 25 μm. **(C,D)** Same sections of BSA **(C)** and PmPV2 **(D)** treatments shown in A and B under bright field. Bar 25 μm. **(E,F)** Immunolocalization of PmPV2 at brush border intestinal mucosae of mice fed on a diet without **(E)** and with **(F)** 400 μg PmPV2 (PmPV2 location appears as yellowish regions). Bar 50 μm.

PmPV2 the surface of some of these cells was marked, indicating that the toxin attaches to the cell membrane, particularly to round-shaped and partially detached cells (**Figure 2B**). These morphological changes were presumably caused by the toxin since the cells that remained attached to the surface showed mild or no labeling. Accordingly, most Caco-2 cells treated with BSA remained attached and conserved a flat shape (**Figure 2C**) whereas PmPV2-treated cells showed an increased level of detached, rounded-shape cells (**Figure 2D**). In the same way, PmPV2 was immunodetected bound to the enterocyte surface of small intestine (**Figures 2E,F**), indicating that the toxin withstands gastrointestinal digestion *in vivo* and reaches the small intestine in an active form.

After having determined that PmPV2 binds to intestinal cell surfaces, we evaluated its effects on cell morphology and small intestinal mucosa. The alterations of Caco-2 cells were evaluated by quantifying changes on their surface with AFM. Whereas control cells were oval-shaped, with a maximum diameter of ∼35 μm and well-defined cell limits (**Figure 3A**), cells exposed to PmPV2 showed irregular form, granulated aspect and diffuse cell limits (**Figure 3B**). Additionally, small rounded structures of ∼1.8 μm of an unknown nature were observed on treated cells. Under greater magnification cell membranes showed a more homogeneous surface in control cells (**Figure 3C**) than in treated cells (**Figure 3D**). An important increase in membrane roughness was observed in PmPV2-treated cells: Roughness of 25 μm^2 sections was 40% higher in treated than in control cells as reflected in their *Rq* and *Ra* parameters (**Figures 3E,F**), while the ISAD increased ∼200% in treated cells (**Figure 2F**).

In addition to cell-level alterations, oral administration of PmPV2 caused notable morphological changes in the small intestinal mucosae of mice (**Figures 3G–L**). In comparison with control animals (**Figure 3G**), treated mice showed shortening and widening of villi, which were already evident after one dose of PmPV2 (**Figure 3H**) and even more evident in animals receiving four doses (**Figure 3I**). In the latter group, fused "tongue-like" villi were also observed. Besides, duodenal mucosae of treated animals showed a higher number of goblet cells (**Figures 3K–L**) than that of the control group (**Figure 3J**).

We calculated the effect of PmPV2 on the absorptive surface using the parameter of Kisielinski et al. (29). Control groups have a mucosal-to-serosal amplification ratio (M) of 14.5 ± 1.5 (mean ± SD). Mice treated with PmPV2 showed a decrease of this ratio with a reduction of 10 and 12% in animals fed with one dose ($M = 13.11 \pm 1.66$) and four doses ($M = 12.82 \pm 1.62$), respectively (1 dose of PmPV2: $P < 0.001$; 4 doses of PmPV2: $P < 0.0001$, vs. control mice).

Cytotoxicity and Cell Monolayer Disruption

We tested the effect of PmPV2 on cultured intestinal absorptive cells and intestinal cell monolayers, which the toxin would encounter when ingested by a predator. For this, we tested Caco-2 cells, widely used as a model of the intestinal epithelia that we knew showed reduced viability when exposed to *P. canaliculata* PVF (23). These cells were much affected by the PmPV2 toxin in a dose-dependent manner, with 0.11 mg/mL PmPV2 inducing 80% of cell death after 24 h (**Figure 4A**). The effect of PmPV2 on Caco-2 cells was also analyzed measuring its capacity to alter differentiated cells in a highly attached monolayer by measuring the transepitelial electric resistance (TEER) at three toxin concentrations (**Figure 4B**). Cell monolayers exposed to PmPV2 showed a decrease in TEER in <1 h at the highest toxin concentration (2 g/L). At the intermediate concentration (0.2 g/L), the TEER showed a progressive decrease between 3 and 10 h; after 10 h the lower TEER value was sustained until the end of the experiment. The lowest toxin concentration (0.02 g/L) showed no effect on TEER within the duration of the experiment. Together these results pointed out that PmPV2 is responsible for the effect of snail eggs on digestive cells.

We, therefore, analyzed whether cell death was caused by lytic or non-lytic mechanisms (i.e., necrosis or apoptosis). To evaluate the toxic mechanism, cells with or without treatment with PmPV2 were analyzed by flow cytometry and changes in cell populations were quantified. The control group showed a basal level of apoptotic cells (<2%) and necrotic cells (around 35%), while most cells remained viable (**Figures 4C,D**). PmPV2 exposed group showed an increase in necrotic cells with the concomitant decrease in viable cells, while the apoptotic cell population showed no significant changes (**Figures 4C,D**). In PmPV2-treated cells, necrotic cell population showed two subpopulations of high and low propidium iodide labeling

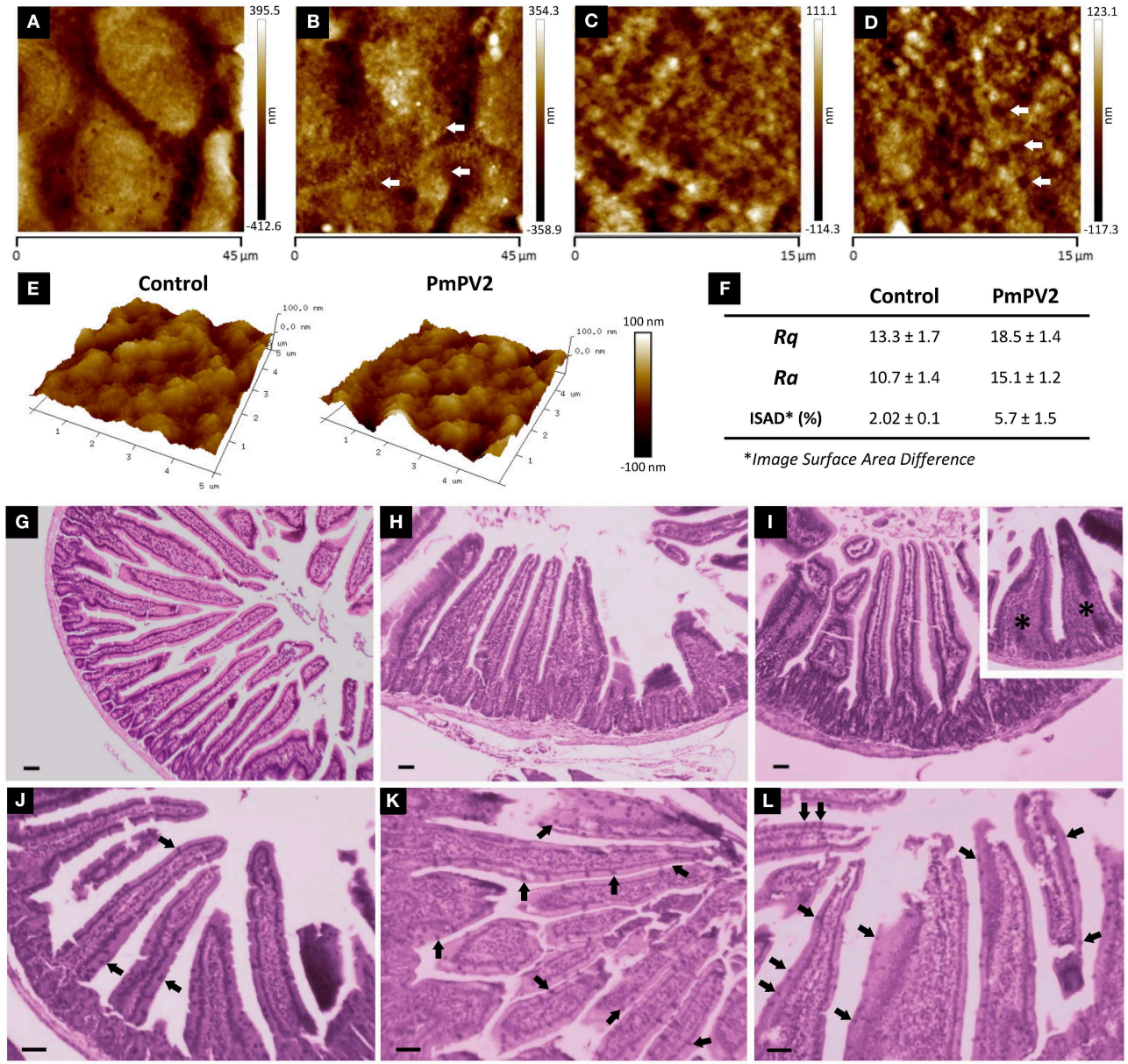

FIGURE 3 | PmPV2 affects Caco-2 and small intestine morphology. **(A–D)** AFM images obtained in tapping topography. Gross morphology of control cells **(A,C)** and PmPV2-treated Caco-2 cells **(B,D)** (**A,B**: 45 × 45 μm^2, **C,D**: 15 × 15 μm^2). Ring-like structures are highlighted with arrows. **(E)** 3D AFM topography images of control and PmPV2-treated Caco-2 cells at 10 x 10 μm^2 showing cell surface details. **(F)** *Ra*, *Rg* and *Image Surface Area Difference* values for control and PmPV2-treated Caco-2 cells. **(G–I)** Intestinal sections stained with HE of control mice **(G)** and mice treated with one **(H)** or four **(I)** doses of 400 µg of PmPV2. *Inset*: tongue-like fused villi (asterisks). **(J–L)** Intestinal sections stained with PAS. Globet cells are positively stained (some highlighted with arrowheads) in both control mice **(J)** and mice treated with one **(K)** and four **(L)** doses of 400 µg of PmPV2 each. Bars 100 µm.

intensities (**Figure 4C**). Necrotic cells were evident after 30 min of exposure and 50% of lethality was reached in ∼70 min (**Figure 4D**). In any case, apoptotic cells were always below 2%.

Fate and Internalization in the Intestinal Mucosa

As the content and proportion of gut proteases differ among organs and species, the ability of PmPV2 to withstand proteolytic activity *in vivo* was standardized using BSA as a control. In agreement with the *in vitro* resistance of PmPV2 to proteases, after oral administration at 2 and 6 h, higher amounts of PmPV2 were detected in the small intestine (2 h: $P < 0.0001$ 6 h: $P = 0.0291$ vs. BSA-administered mice). Moreover, at 2 and 6 h the ratio of PmPV2:BSA was 2.84 and 4.95, respectively, while at 8 h, only a slight difference in the amount of PmPV2 vs. BSA was observed (**Figure 5A**).

To understand the cytotoxic effect and the mechanism of entry of PmPV2, we studied whether internalization was occurring on

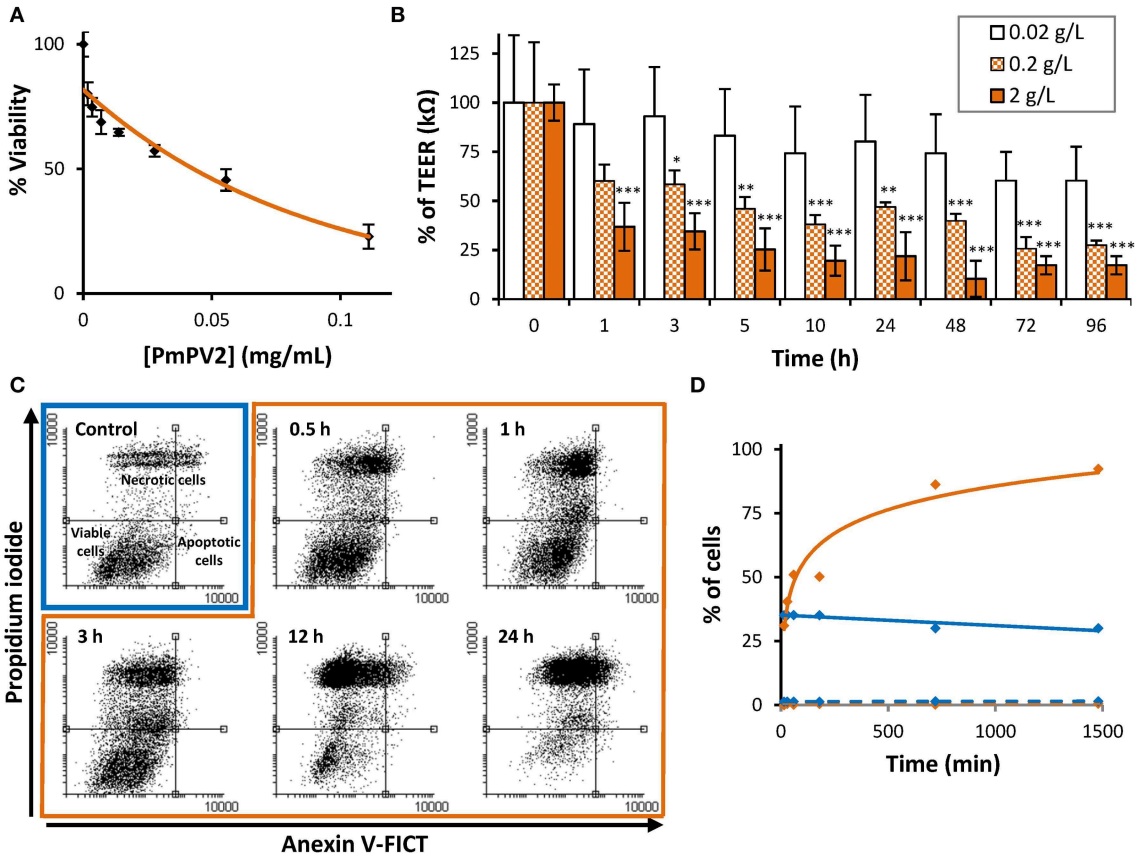

FIGURE 4 | PmPV2 is toxic to Caco-2 cells and disrupts enterocyte monolayers. **(A)** Cytotoxic effect of PmPV2 on Caco-2 cells evaluated using MTT assay. **(B)** Capacity of PmPV2 to disrupt a enterocyte monolayers (TEER assay) at three concentrations. Results are expressed as Mean ± SEM of three replicates. $^{*}P<0.05$, $^{**}P < 0.01$, $^{***}P <0.001$. **(C)** Flow cytometry analysis showing type of cell death caused by PmPV2. Cells were doubly-labeled with anexin V-FICT/propidium iodide (PI), without (control, blue box) and with 0.05 mg/mL PmPV2 (orange box) at 0.5, 1, 3, 12 and 24 h. Viable cells: $FICT^{-}/PI^{-}$; Apoptotic cells: $FICT^{+}/PI^{-}$; Necrotic cells: $FICT^{-}/PI^{+}$ and $FICT^{+}/PI^{+}$. **(D)** percentage of apoptotic (dashed line) and necrotic (full line) cells obtained in **(C)**. Blue lines: control; orange lines: treated with PmPV2.

inductive sites of the intestinal mucosa, the Peyer's patches (PPs). Interestingly, 2 h after inoculation a high amount of PmPV2 was detected in PPs ($P = 0.027$ vs. BSA administered mice), while at 6 h a non-significant increase was observed. As in the small intestine experiment, the PmPV2:BSA ratio was 3.6 and 7.8 at 2 and 6 h after administration, respectively, indicating that at these time periods a significant amount of PmPV2 was internalized in PPs (**Figure 5B**). In concordance with this latter result, PmPV2 effects on PPs *in vivo* were observed. Whereas, control animals showed regular, non-reactive lymphoid follicles (**Figure 5C**), treated animals had lymphoid follicles with pallid germinal center indicating induction of immune reaction (**Figure 5D**). In these secondary lymphoid follicles, cumuli of apoptotic bodies reactive to caspase-3 antibodies were observed (**Figure 5D**,*inset*), indicating that PmPV2 could also be toxic through apoptosis in some cell populations.

Oral Immunization

In agreement with PmPV2 internalization and detection in lymphoid follicles of the PPs, anti-PmPV2 IgG was detected in the sera of mice gavaged with 0.8 mg of PmPV2 (**Figure 5E**). Further, all the immunized mice survived to an i.p. injection of 1 mg of PmPV2 which is about 200% of its reported LD50 without any signs of intoxication (**Figure 5F**). Control groups showed no reaction to IgG detection and, when injected with PmPV2, all of the neurological signs previously reported were observed and all mice died after 48 h.

DISCUSSION

Eggs are usually an unattended life-cycle stage in gastropods and depend entirely on the defensive compounds maternally transferred that ensure embryos normal development and protection against pathogens. Notably, two distinctive immune-related polypeptides were found in the eggs of two *Pomacea* species, *P. canaliculata* and *P. maculata*: a tachylectin (PV2-31) and a MACPF-containing protein (PV2-67) (4, 5), which are combined into the perivitellin PV2 complex (8, 9). Comparative genomic analysis together with expression patterns and proteomic validation showed that although these lectin and MACPF are present in the genomes of four species of

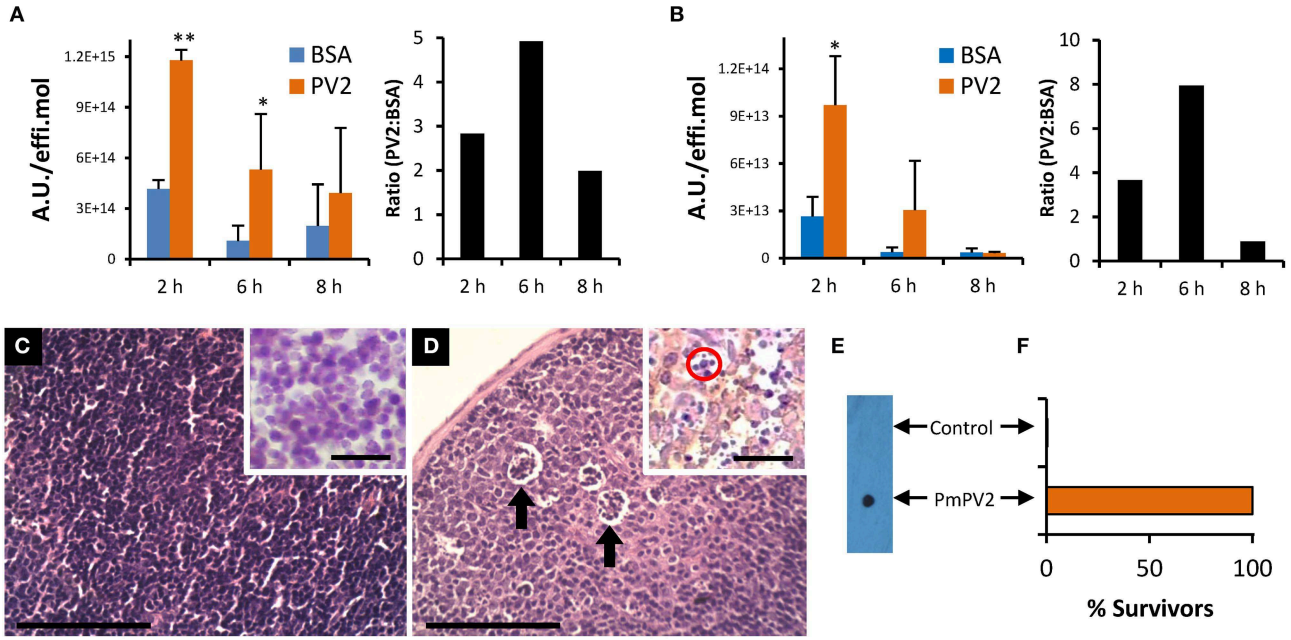

FIGURE 5 | PmPV2 fate, internalization and immune response after oral ingestion in mice. **(A,B)** Fate and internalization of fluorescently-labeled PmPV2 in mice intestine **(A)** and Peyer's patches **(B)** at different times after ingestion. Results are expressed as the Mean ± SEM of A.U./effi.mol ($n = 3$) and are representative of two independent experiments. *Right panels*: PmPV2:BSA ratio of values from left panel. $^{*}P<0.05$; $^{**}P<0.01$. **(C,D)** Peyer's patches of control mouse **(C)** and PmPV2-treated mouse **(D)**. Cumuli of apoptotic cells are highlighted with arrows. Bar 100 μm. *Insets*: IHC using mouse IgG anti-Caspase 3 antibodies (1:200). Mice treated with PmPV2 showed positive reaction; Caspase-3 location appears as yellowish regions. Apoptotic bodies were also evident in treated mice (red circle). Bar 50 μm. **(E,F)** Mice oral immunization against PmPV2. **(E)** Dot blot analysis of sera from mice gavaged with PBS (Control) or with 800 μg PmPV2 (PmPV2). **(F)** Effect of lethal (1 mg) i.p. dosis of PmPV2 on control and immunized mice survival ($n = 3$). Please note graph does not include error bars because all of the three immunized animals survived and all of the three control animals died after the intraperitoneal injection.

the family, as well as in the genomes of other Mollusks, only in *Pomacea* these two proteins experienced extensive gene expansion by tandem duplication and neofunctionalization into the PV2 complex, which is expressed as such only in an accessory gland of females and transferred to eggs (30). Although the immune role of these two proteins are largely unexplored in snails, a PV2-67-like protein found in the kidney of the snail *Littorina littorea* showed overexpression when infected with a trematode parasite (31), indicating a putative immune function in the common ancestor of mollusks MACPF (12). In addition to their immune role, another prominent role of animal MACPFs is in the embryonic development of several organisms, ranging from sea urchins to mammals (32). Similar to those proteins PmPV2 is maternally transferred to the eggs, where it is massively accumulated during the early developing stages, before the embryo consumes it (33). However, PV2 structure lacks some key structural features described in developmental MACPFs, such as absence of ancillary domains and shorter TMH1 (12, 32). Finally, a less-extended group of animal MACPFs also act as toxins such as those from some cnidarians and the stone fish, where they play a role in prey capture (22, 34). The co-option of PV2 into *Pomacea* eggs and its neurotoxicity to mice locates it within the group of MACPF toxins, although here it plays a defensive role against terrestrial predators (30). The novelty found in this work is that PV2 also exerts enterotoxic effects, a role never ascribed to MACPFs.

These *Pomacea* eggs have also other biochemical defenses targeting the digestive system, notably perivitellins that lower the nutritional value (i.e., antinutritive or indigestible) and others with antidigestive properties (i.e., digestive enzyme inhibitors) (9, 23, 27, 28, 35, 36). These noxious proteins, advertised by a warning (aposematic) pink-reddish coloration, seems to be an effective passive defense system since eggs have virtually no predators, except for the fire ant, *Solenopsis geminata* (37). Here we report a novel enterotoxic role for PV2, previously described as a neurotoxin (8).

Akin to other perivitellins, we found that PmPV2 is highly stable at pH values ranging from 4.0 to 10.0, a range that includes most digestive system environments of animals (38, 39). The increases in *Rg* and *Dmax* without changes in mass or secondary structure observed at pH 4.0 may be explained as a partial quaternary unfolding of some protein domains; a behavior already documented on model proteins like BSA using SAXS (40). In this regard, several reports in other pore-forming proteins (PFPs) suggest that the acidic microenvironment found at the membrane vicinity partially denatures the pore-forming domain to a more flexible state, leading to the conformational changes needed for membrane insertion (41–45). Moreover, it is worth to mention that the small intestine of mice has an acidic

pH (<5.2) relatively close to this experimental condition (46). However, whether these structural changes associated with pH are related with the PmPV2 function needs to be confirmed. We also demonstrate that it is resistant to the proteolytic activity of common digestive enzymes *in vitro,* and to gastrointestinal tract enzymes *in vivo* (see below), indicating that it is refractive to digestion and assimilation by predators. The non-digestible property of PV2, not only contributes to lower the nutritional value of eggs for a predator, but also allows PV2 to reach its intestinal tract in an active form to exert its toxic effect. The effects of the purified toxin on the gut are similar to those reported for diets supplemented with *P. canaliculata* PVF (23, 24), indicating that the PV2s are responsible, at least of some of the reported gut alterations. After reaching the intestinal lumen, oral toxins must either traverse the intestinal barrier to reach their target cells or exert its toxicity on the gut. In this regard, we provide evidence that PmPV2 does both. First it binds to intestinal cells and then induces strong morphological changes and cell detachment in a similar way as bacteria Cholera toxins (CT), Shiga toxins (Stxs) and heat-labile (LT) enterotoxins do (47). Then PmPV2 has a cytotoxic effect triggered by its structural components, because, like the above-mentioned bacterial toxins (10, 11, 13), PV2s have an AB-toxin structure, with a ¨B¨ lectin unit that delivers a toxic MACPF ¨A¨ module to the target cell (9, 12). Among the morphological changes that PmPV2 causes on Caco-2 cells, a notorious increase in plasma membrane roughness was observed by AFM. According to the bibliography, this increase could be due to three main reasons: (1) the formation of holes produced by the insertion of protein molecules into the membrane, as was observed for this and other PFPs (12, 48); (2) membrane vesiculation during protein internalization, a process commonly observed in AB toxins (10, 11, 49); (3) membrane and cytoskeleton reorganization as usually displayed by host cells in response to membrane damage (50–52). Further analyses are needed to confirm which of these processes -alone or combined- are triggered by PV2 toxins.

The ability of PmPV2 to bind to and kill enterocytes suggested a putative enterotoxic role for this toxin. Cytotoxic enterotoxins kill target cells through either lytic or non-lytic mechanisms by inducing necrosis or apoptosis, respectively (13, 47). Here, we demonstrate that PmPV2 triggers necrosis in Caco-2 cells, the same cell death pathway reported for bacterial pore-forming toxins such as alpha hemolysin (HlyA), staphylococcal alpha-toxin, pneumolysin, streptolysin-O and leukotoxin PFTs (15, 53). Interestingly, cells treated with PmPV2 showed two subpopulations of necrotic cells, which can be interpreted as different stages of cell damage. It has been reported that permeated living cells -which become transiently defective before total loss of the ability to exclude the dye- showed moderate labeling in comparison to the intensive labeling of dead cells (54). Besides necrosis, when using a rodent as a predator model, apoptotic bodies were also observed in lymphoid follicles after incorporation of the toxin indicating that another toxic mechanism is also present, an observation that requires future research to clarify.

In the present work, we were also able to detect orally ingested PmPV2 attached to the enterocyte glycocalyx of small intestine, indicating that the toxin reaches the intestinal mucosa in an active form. Binding to the mucosal surface may further protect this egg toxin from luminal digestive proteases as reported for plant enterotoxins (19). After binding, PmPV2 induced strong morphophysiological changes in the small intestine mucosa in <24 h. Several of these effects resemble those caused by plant seed dietary lectins, where toxicity is mainly attributed to interference with the digestive process and to anatomic abnormalities after binding to cell surface glycans on enterocytes (55, 56). We also demonstrate that PmPV2 not only causes morphological changes but also increases the permeability of enterocyte monolayers, indicating that it is able to disrupt the intestinal barrier. This provides an explanation of previous reports showing that oral administration of *P. canaliculata* PVF induced an increase of total absorption rate affecting both paracellular (i.e., between enterocytes) and transcellular (i.e., through enterocytes) pathways (24). This increased intestinal permeability may generate an uncontrolled income of dietary macromolecules (57, 58) further contributing to PV2 toxicity. Besides, the presence of high amounts of PmPV2 in the Peyer's patches suggests that it may also be entering the predator's body through a different pathway. Results suggest it may traverse the barrier through M cells, cells involved in the modulation of mucosal and systemic immune responses (59). In fact, lymphoid follicle activation was observed in treated mice. Independently of the mechanism through which PmPV2 traverses the intestinal barrier, ingestion of minute amounts (∼0.8 mg) stimulated the immune system of mice. This small amount of PV2 is biologically relevant if we consider that a single egg-clutch contains ∼67 mg PV2 (26). The immune response generated by PmPV2 was characterized by the presence of specific IgG antibodies that protected mice from an otherwise lethal injection of PV2, and also by the presence of apoptotic immune cells in the Peyer's patches. Remarkably, a similar response has been described for both invasive bacterial enterotoxins and plant dietary lectins ingested by mice and rats (14, 15, 19, 60, 61), pointing to a convergent mechanism among plant, bacteria, and animals' proteinaceous toxins. The resemblance between *Pomacea* eggs and plant seed defenses could be understood from an ecological point of view: both seeds and eggs are usually unattended life stages that are often exposed to similar selective pressures by predators and pathogens.

As a whole, these results indicate that PmPV2 not only affects the nervous system but also targets the digestive system. To our knowledge, there is no report of animal toxins with such dual effect. Furthermore, toxins having enterotoxic and neurotoxic activities at the same time were only reported in one bacterium, Stxs from *Shigella dysenteriae* (62). However, it is notable that the oral administration of PmPV2 did not cause the neurological signs observed when it is intraperitoneally injected. This absence of neurotoxicity through oral administration could be due to many causes still unclear.

Nowadays, there is an increasing biomedical interest on molecules capable of withstanding the harsh gastrointestinal environment and inducing immune responses to be used as adjuvants for oral vaccination (61, 63). Currently, bacterial enterotoxins (like CT from *Vibrio cholerae* and LT from

Escherichia coli) or their attenuated derivatives are mostly used for this purpose (64–66). The results gathered here indicate that PmPV2 is a good candidate to be tested as an adjuvant for oral vaccine design.

It is interesting to recall that other species of the *Pomacea* genus that lack PV2 enterotoxin have evolved different protective perivitellins such as the lectin PsSC from *P. scalaris* whose ingestion affects gut morphology but in a non-cytotoxic way (36). This suggests that it is likely that there are still other enterotoxic compounds yet to be discovered within the well-protected eggs of this rapidly diversifying group.

CONCLUSION

Avoiding attack is essential for survival and, under this selective pressure organisms have evolved a plethora of mechanisms to deter predators. In this study we unveiled part of the multiple defenses of *Pomacea* snails that suggest that the cooption of new functions in immune related egg proteins confer an advantage for survival and, even, diversification and spread of this highly invasive species.

By combining a lectin and a pore-forming protein, *Pomacea* PV2s have acquired enterotoxic properties, a role that has never been ascribed to lectins or perforin protein families in animals. This is also the first example of a eukaryotic toxin having both neuro- and enterotoxic activities. Finally, this work provides the first description of a true animal enterotoxin, extending by convergent evolution the presence of plant- and bacteria-like enterotoxins to unattended reproductive stages in animals and expanding the varied roles of MACPF in nature.

METHODS

Purification and Fluorescent Labeling of PmPV2

PmPV2 was purified from newly laid *P. maculata* egg clutches as previously described (8). Total protein was quantified following the method of Lowry et al. (67) using a standard curve prepared with bovine serum albumin (BSA) (Sigma-Aldrich, St. Louis, MO, USA). The protein was labeled using the Alexa Fluor 488 Protein Labeling Kit (Life Technologies-Molecular Probes, Eugine, OR, USA) following manufacturer instructions. Labeled BSA (Life Technologies-Molecular Probes, Eugine, OR, USA) was employed as negative control.

Cell Culture

For experimental analysis, we used the Caco-2 line of human colorectal adenocarcinoma cells, commonly used as a model of intestinal physiology and toxicology (68). Caco-2 cells were cultured in Dulbecco's modified Eagle's medium (DMEM) with 0.45% (w/v) D-glucose and supplemented with 10% (v/v) newborn calf serum, penicillin/streptomycin, amino acids and vitamins (Life Technologies-Invitrogen, Gaithersburg, MD, USA). Cells were cultured at 37°C in a humidified atmosphere of 5% CO_2. The culture medium was replaced every 2 days. After reaching 95% confluence, cells were subcultured by trypsinization. Cell viability was checked by trypan blue exclusion assay (69). Passages from 80 to 105 were used, with a window no higher than 10 passages within each experiment. All experiments were conducted with a confluence of cells above 90%.

Mice

BALB/c AnN mice, *Mus musculus* Linnaeus, 1758 (body mas $= 20.2 \pm 1.7$ g), were obtained from the Experimental Animals Laboratory of the School of Veterinary Science, UNLP. All experiments were performed in accordance with the Guide for the Care and Use of Laboratory Animals (70) and were approved by the Comité Institucional de Cuidado y Uso de Animales de Experimentación (CICUAL) of the School of Medicine, UNLP (Assurance No. P08-01-2013).

PmPV2 Resistance to *in silico* and *in vitro* Gastrointestinal Digestion

Before the *in vitro* assay, we analyzed the protein digestibility *in silico* using the amino acid sequences of both PmPV2 subunits already published (5). The number of putative cleavage sites of pepsin and trypsin was determined using the PeptideCutter server (https://web.expasy.org/peptide_cutter/) (71).

Gastric Phase

A simulated gastrointestinal digestion of PmPV2 was performed using the method described by Moreno et al. (72) with some modifications (9, 27). Briefly, PmPV2 in Mili-Q water was dissolved in simulated gastric fluid (0.15 M NaCl, pH 2.5) to a final concentration of 0.5 μg/μL. The gastric phase was conducted at 37°C in the presence of porcine pepsin (Sigma-Aldrich) at an enzyme:substrate ratio of 1:20 (w/w). Aliquots of 5 μg protein were taken at 0, 60 and 120 min after the addition of the pepsin. The reaction was stopped by increasing the pH with 150 mM Tris-HCl buffer pH 8.5.

Intestinal Phase

For *in vitro* duodenal digestion, 100 μL of the 120 min gastric digest was used as starting material. The pH of the digests was adjusted to 8.5 with 0.1 M NaOH and the following were added: 22.8 μL of 0.15 M Tris/HCl buffer (pH 8.5) and 4.17 μL of 0.25 M sodium taurocholate (Sigma-Aldrich) solution. The simulated duodenal digestion was conducted at 37°C using bovine pancreas trypsin (Sigma-Aldrich) at an enzyme:substrate ratio of 1:2.8 (w/w). Aliquots were taken at 0, 60, and 120 min.

Electrophoretic Analysis

Samples taken from both gastric and duodenal phases were immediately boiled for 10 min in SDS electrophoresis buffer with β-mercaptoethanol (4%) and analyzed by SDS-PAGE using 4–20% gradient gels prepared following the Laemmli (73) method. Gels were stained with Coomassie Brilliant Blue G-250 (Sigma-Aldrich). BSA (Sigma-Aldrich) in the presence and in absence of enzymes was used as positive and negative controls, respectively.

Structural Stability Against pH

Structural stability against pH was determined in PmPV2 (65 μg/mL) at pH values ranging from 2.0 to 12.0. Buffers of the desired pH were prepared using sodium phosphate salts and

citric acid buffers (74). After *overnight* incubation, samples were analyzed by fluorescence spectroscopy, CD, and SAXS as follows.

Fluorescence

Fluorescence emission spectra of PmPV2 (65 μg/mL) in PBS buffer (1.5 mM NaH_2PO_4, 8.1 mM Na_2HPO_4, 140 mM NaCl, 2.7 mM KCl, pH 7,4) were recorded in scanning mode in a Perkin-Elmer LS55 spectrofluorometer (Norwalk). Protein was exited at 280 nm (4 nm slit) and emission recorded between 275 and 437 nm. Fluorescence measurements were performed in 10 mm optical-path-length quartz-cells. The temperature was controlled at 25 ± 1°C using a circulating-water bath.

Circular Dichroism

Spectra of PmPV2 (70–140 μM) were recorded on a Jasco J-810 spectropolarimeter using quartz cylindrical cuvettes of 1-mm or 10-mm path lengths for the far-UV (200–250 nm) and near-UV (250–310 nm) regions, respectively. Data were converted into molar ellipticity $[\theta]_M$ ($deg.cm^2.\ dmol^{-1}$) using a mean residue weight value of 115.5 g/mol for PmPV2.

Small-Angle X-Ray Scattering (SAXS)

Synchrotron SAXS data from solutions of PmPV2 at different pH values (74) were collected on the SAXS2 beamline at the Laboratório Nacional de Luz Sincrotron (Campina, Brazil) using MAR 165 CDD detector at a sample-detector distance of 1.511 m and at a wavelength of $\lambda = 0.155$ nm ($I_{(s)}$ vs. s, where $s = 4\pi\sin\theta/\lambda$, and 2θ is the scattering angle). Protein concentrations ranging between 0.8 and 2 mg/mL were measured at 20°C; BSA (Sigma-Aldritch) was measured as a molecular mass standard. Five successive 300-s frames were collected. The data were normalized to the intensity of the transmitted beam and radially averaged; the scattering of the solvent-blank was subtracted. Radius of gyration (*Rg*), molecular mass and maximum intraparticle distance (D_{max}) were estimated from the final curves using ATSAS 3.0.1 (r12314) (75). Molecular mass was estimated from intensity at $s = 0$ (I_0) of the sample and reference (BSA) calculated by the software.

PmPV2 Interaction With Caco-2 Cells

Binding Assay

Caco-2 cells were seeded on a 24-well plate (Greiner Bio-One, Monroe, NC, USA) and were incubated at 37°C for 48 h. Then, cells were washed twice with PBS (1.5 mM NaH_2PO_4, 8.1 mM Na_2HPO_4, 140 mM NaCl, 2.7 mM KCl pH 7.4) and incubated with Alexa488-labeled PmPV2 or BSA in PBS (0.4 mg/mL) for 1 h at 37°C. Cells were observed in an inverted fluorescence microscope (Olympus IX-71).

Effect of PmPV2 on Cell Morphology

Changes in Caco-2 cell morphology and membrane roughness was determined by atomic force microscopy (AFM) following the protocol of Cattaneo et al. (76). Cells were cultured on slide covers and incubated at 37°C for 24 h. Then, the medium was replaced by a PmPV2 solution in DMEM (0.05 μg/μL) and incubated at 37°C for 24 h. After treatment cells were washed twice with PBS and fixed using an ethanol dehydration train (35°, 45°, 55°, 75°, 85°, 96°, and 100°) at room temperature and air-dried (77). Cells were photographed before and after fixation to check any morphological effect due to this step. Six different cell samples (three controls and three treated) were analyzed by AFM in air, using a MultiMode Scanning Probe Microscope (Veeco Instruments Inc., Santa Barbara, CA, USA) coupled with a Nanoscope V controller (Veeco Instruments Inc.). Measurements were obtained with Tapping® mode, using probes doped with silicon nitride (RTESP, Veeco Instruments Inc., with tip nominal radius of 8–12 nm, 271–311 kHz, force constant 20–80 N/m). The typical scan rate was 0.5 Hz. The analysis was performed on either a large area (50 × 50 μm) or a smaller area of the cell surface of 15 × 15 μm^2 and 5 × 5 μm^2. Membrane roughness was evaluated in 5 × 5 μm^2 sections taking into consideration the *Ra*, *Rq* and *Image Surface Area Difference (ISAD)* parameters determined using the Nanoscope Analysis 1.5 software package. The parameter *Ra* is the arithmetic mean of the deviations in height from the roughness mean value, *Rq* is the root mean square of the height distribution, and *ISAD* is the difference between the tridimensional area and the bidimensional area.

Cytotoxicity

The cytotoxic effect of the PmPV2 on enterocytes was evaluated on Caco-2 human colorectal adenocarcinoma cells following the method described in Dreon et al. (23). In brief, once cell cultures reached the desired confluence, 50 μl/well of a 2-fold serial dilution of PmPV2 (0.111 mg/mL) in PBS were added and incubated at 37°C for 24 h. Control wells were prepared with 50 μL/well of PBS. Cell viability was measured using the 3-(4,5-dimethythiazol-2-yl)-2,5-diphenyl tetrazolium bromide (MTT) assay (78), in a microplate Multimode Detector DTX-880 (Beckman Coulter, Inc., CA, USA). Cell viability was expressed as control percentage: % Viability = (OD treated cells/OD control cells) × 100.

Apoptosis vs. Necrosis Assay

Knowing that the PmPV2 was cytotoxic to Caco-2 cells we performed an assay to determine whether the toxin induces apoptosis or necrosis. Caco-2 cells were cultured in 6-well plates (Greiner Bio-One) and incubated at 37°C for 24 h. Then 100 μL of a PBS solution containing 100 μg of PmPV2 was added 24, 12, 3, 1, 0.5, and 0.25 h before trypsinization; 100 μL of PBS buffer was used as control. After harvest, cell suspensions were washed two times and resuspended in binding buffer (10 mM HEPES, 140 mM NaCl, 2.5 mM $CaCl_2$ pH 7.4) at 2 × 10^6 cells/mL. Next, 5 μL of annexin V-FICT (BD Biosciences, San Jose, CA, USA) and 10 μL of propidium iodide (PI, BD Biosciences) solutions were added to 100 μL of each cell suspension and incubated at room temperature for 15 min in the dark. After adding 300 μL of binding buffer and stirring, cell fluorescence was determined immediately using a BD FACSCalibur flow cytometer (BD Biosciences) and data were analyzed with Flowing Software v. 2.5.1. The percentage of apoptosis was taken as the percentage of only annexin V-positive ($FICT^+/PI^-$), the percentage of necrosis was either double-positive ($FICT^+/PI^+$) or only PI-positive cells ($FICT^-/PI^+$), while percentage of viable cells was double-negative cells ($FICT^-/PI^-$).

Transepithelial Electric Resistance (TEER) Assay

A volume of 500 μL of a Caco-2 cell suspension was cultured in 8.4 mm ThinCert transwell system of 0.4-μm pore size (Greiner Bio-One) for 24-well plates. Two milliliters of medium were added to each well. The medium was changed every 2 days in both compartments. Changes in TEER were followed by measuring the culture every 24 h using an EVOM-Epithelial voltohmmeter (World Precision Instruments Inc., Sarasota, FL, USA) until resistance reached a constant value (i.e., the monolayer was completely formed). Then, 100 μL of a 10-fold serial dilution of PmPV2 (2 mg/mL) in PBS was added. TEER was measured at different times within 96 h post-treatment. Data were expressed as percentage of TEER relative to the starting value at 0 h.

PmPV2 Interaction With Mice Intestine

Histological Analysis

Small intestine morphology was analyzed in three groups of treated mice, six animals each (three males and three females). One group was gavaged with a single dose of 300 μL of PBS containing 400 μg (<1% of the amount found in one clutch) of PmPV2 (1-dose group). Another group of mice was gavaged with doses of 300 μL of the same solution every 24 h during 4 days before intestine extraction (4-dose group). The control group (6 mice) received the equivalent volume of PBS. Oral gavage was performed using a winged needle infusion set and was completed within 30 s. Twelve hours after the single or last dose the intestines of the mice were removed and cylindrical tissue samples were fixed and analyzed as previously reported (24). Samples were stained using hematoxylin-eosin or PAS. PmPV2 binding to intestinal mucosae was analyzed by immunohistochemistry (IHC) using rabbit IgG anti-PcPV2 antibodies following previous reports (9). Apoptosis was also detected by IHC using mouse IgG anti-Caspase 3 monoclonal antibodies diluted 1:100 in PBS buffer (Santa Cruz Biotechnologies Inc., Santa Cruz, CA, USA).

Fate and Internalization of PmPV2 *in vivo*

To evaluate PmPV2 fate and internalization Alexa488-labeled PmPV2 and BSA in PBS were used. Three sets of nine mice (females and males) each were gavaged with (*i*) PBS, (*ii*) Alexa488-labeled BSA (75 μg) as control, or (*iii*) Alexa488-labeled PmPV2 (75 μg). At 2, 6 and 8 h post-administration three mice of each treatment were sacrificed and Peyer's patches (PPs) (9 PPs/mice) and the remaining small intestine (SI) were aseptically removed. SI was homogenized with 5 mL of PBS in a Potter type homogenizer OS-40 Pro (DLAB Scientific Inc., Riverside, CA, USA). Single-cell suspensions were prepared (79) from PPs and washed twice in PBS solution in order to remove extracellular labeled protein. Cell suspensions were resuspended in 5 mL of PBS. Then 100 μL of homogenate or cell suspensions were seeded in 96-well, flat-bottom, black microplate (Corning Inc., Corning, NY, USA) and fluorescence was measured in a microplate reader Multimode Detector DTX-880 (Beckman Coulter Inc., Brea, CA, USA). Arbitrary fluorescence units (A.U.) were corrected by labeling efficiency (effi) and molarity (A.U./effi.mol).

Oral Immunization

Groups of three female mice each were gavaged with two boosters of 100 μL of PBS containing 800 μg of PmPV2 with 19 days between each other; mice gavaged with 100 μL of PBS were used as control ($n = 3$). Immunization was determined by measuring IgG anti-PmPV2 in serum and by analyzing mice resistance to PmPV2 lethal toxic effect. Three days after the second boost blood was sampled by cheek puncture and serum obtained as previously described (9) and kept at −70°C until used. Spots of 0.05 μg of PmPV2 were pipetted onto nitrocellulose membranes (GE Healthcare-Amersham Biosciences Inc., Piscataway, NJ, USA) and membranes blocked with 5% (w/v) non-fat milk in PBS with 0.05% (v/v) Tween 20 (Anedra S.A., San Fernando, BA, Argentina) (PBST) at 4°C overnight. Then membranes were incubated with anti-sera solutions (1:100) in 3% (w/v) non-fat milk in PBST. After washing 5 times with PBST for 5 min each time, the presence of anti-PmPV2 antibodies was detected using anti-mouse IgG horseradish peroxidase conjugate (1:3,000, Bio-Rad Laboratories Inc., Hercules, CA, USA). Membranes were washed as above and revealed by chemiluminescence. Twelve days after the second boost, mice were intraperitoneally (i.p.) injected with 200 μL of a PBS solution containing 22.4 μg of PmPV2 (i.e., 1 mg/kg), a dose 4 times higher than the reported LD50, 96 h (8). Animals were observed every day for 4 days to check for neurological signs and survival.

Statistical Analysis

Statistical analyses were conducted with GraphPad PRISM v. 5.03 software and results expressed as mean ± 1 SEM. Mucosal-to-serosal amplification ratio (*M*), TEER and absorption parameters were determined by one-way analysis of variance (one-way ANOVA) with *post-hoc* Bonferroni's test. The significance level selected to accept difference for all statistical analysis performed was $\alpha < 0.05$.

DATA AVAILABILITY STATEMENT

All datasets generated for this study are included in the article/**Supplementary Material**.

ETHICS STATEMENT

The animal study was reviewed and approved by Comité Institucional de Cuidado y Uso de Animales de Experimentación (CICUAL) of the School of Medicine, National University of La Plata (Assurance No. P08-01-2013).

AUTHOR CONTRIBUTIONS

AI, HH, SI, and MG designed the research. AI, PF, SI, MG, EP, and MD performed research. AI, PF, SI, EP, MD, MG, and HH analyzed data and revised the draft. AI, MG, and HH drafted the article.

FUNDING

This work was supported by a grant from Agencia Nacional de Promoción Científica y Tecnológica (PICT 2014-0850 to HH).

ACKNOWLEDGMENTS

MG, SI, AI, EP, and HH are members of CONICET, Argentina. MD is member of CIC, Buenos Aires, Argentina. PF is member of National University of La Plata, Argentina. We thank N. Scelsio for her help with the histological techniques and L. Bauzá for help in PmPV2 purification. We thank Dr. W. Karasov for valuable comments on a draft of the ms and Dr. G. Docena for his help on the flow cytometry experiments.

SUPPLEMENTARY MATERIAL

The Supplementary Material for this article can be found online at: https://www.frontiersin.org/articles/10.3389/fimmu.2020.00428/full#supplementary-material

REFERENCES

1. McCormack R, Podack ER. Perforin-2/Mpeg1 and other pore-forming proteins throughout evolution. *J Leukoc Biol.* (2015) 98:761–8. doi: 10.1189/jlb.4MR1114-523RR
2. Loker ES. Gastropod immunobiology. In: Söderhäll K, editor. *Invertebrate Immunity*. New York, NY: Landes Biocience and Springer Science+Business Media (2010). p. 27.
3. Hathaway JJ, Adema CM, Stout BA, Mobarak CD, Loker ES. Identification of protein components of egg masses indicates parental investment in immunoprotection of offspring by Biomphalaria glabrata (Gastropoda, Mollusca). *Dev Comp Immunol.* (2010) 34:425–35. doi: 10.1016/j.dci.2009.12.001
4. Sun J, Zhang H, Wang H, Heras H, Dreon MS, Ituarte S, et al. First proteome of the egg perivitelline fluid of a freshwater gastropod with aerial oviposition. *J Proteome Res.* (2012) 11:4240–8. doi: 10.1021/pr3003613
5. Mu H, Sun J, Cheung SG, Fang L, Zhou H, Luan T, et al. Comparative proteomics and codon substitution analysis reveal mechanisms of differential resistance to hypoxia in congeneric snails. *J. Proteomics*. (2018) 172:36–48. doi: 10.1016/j.jprot.2017.11.002
6. Ip JCH, Mu H, Zhang Y, Heras H, Qiu J-W. Egg perivitelline fluid proteome of a freshwater snail (Caenogastropoda): insight into the transition from aquatic to terrestrial egg deposition. *Rapid Commun Mass Spectrom.* (2019) 34:e8605. doi: 10.1002/rcm.8605
7. Ip JCH, Mu H, Zhang Y, Sun J, Heras H, Chu KH, et al. Understanding the transition from water to land: insights from multi-omic analyses of the perivitelline fluid of apple snail eggs. *J Proteomics.* (2019) 194:79–88. doi: 10.1016/j.jprot.2018.12.014
8. Heras H, Frassa MV, Fernández PE, Galosi CM, Gimeno EJ, Dreon MS. First egg protein with a neurotoxic effect on mice. *Toxicon.* (2008) 52:481–8. doi: 10.1016/j.toxicon.2008.06.022
9. Dreon MS, Frassa MV, Ceolin M, Ituarte S, Qiu JW, Sun J, et al. Novel animal defenses against predation: a snail egg neurotoxin combining lectin and pore-forming chains that resembles plant defense and bacteria attack toxins. *PLoS ONE.* (2013) 8:e63782. doi: 10.1371/journal.pone.0063782
10. Falnes P, Sandvig K. Penetration of protein toxins into cells. *Curr Opin Cell Biol.* (2000) 12:407. doi: 10.1016/S0955-0674(00)00109-5
11. Odumosu O, Nicholas D, Yano H, Langridge W. AB toxins: a paradigm switch from deadly to desirable. *Toxins.* (2010) 2:1612–45. doi: 10.3390/toxins2071612
12. Giglio ML, Ituarte S, Milesi V, Dreon MS, Brola TR, Caramelo JJ, et al. Exaptation of two ancient immune proteins into a new dimeric pore-forming toxin in snails. *bioRxiv [Preprint]*. (2019). doi: 10.1101/2019.12.23.880021
13. Lin C-F, Chen C-L, Huang W-C, Cheng Y-L, Hsieh C-Y, Wang C-Y, et al. Different types of cell death induced by enterotoxins. *Toxins.* (2010) 2:2158–76. doi: 10.3390/toxins2082158
14. Taylor SL. Disease processes in foodborne illness. In: Dodd C, Aldsworth T, Stain R, Cliver D, Riemann H, editors. *Foodborne Diseases*. London: Stein Academic Press (2017). p. 576.
15. Bhakdi S, Bayley H, Valeva A, Walev I, Walker B, Weller U, et al. Staphylococcal alpha-toxin, streptolysin-0, and *Escrerichia coli* hemolysin: prototypes of pore-forming bacterial cytolysins. *Arch Microbiol.* (1996) 165:73–9. doi: 10.1007/s002030050300
16. Rosado CJ, Kondos S, Bull TE, Kuiper MJ, Law RH, Buckle AM, et al. The MACPF/CDC family of pore-forming toxins. *Cell Microbiol.* (2008) 10:1765–74. doi: 10.1111/j.1462-5822.2008.01191.x
17. Chrispeels MJ, Raikhel NV. Lectins, lectin genes, and their role in plant defense. *Plant Cell.* (1991) 3:1–9. doi: 10.1105/tpc.3.1.1
18. Peumans WJ, Van Damme EJ. Lectins as plant defense proteins. *Plant Physiol.* (1995) 109:347–52. doi: 10.1104/pp.109.2.347
19. Vasconcelos IM, Oliveira JT. Antinutritional properties of plant lectins. *Toxicon*. (2004) 44:385–403. doi: 10.1016/j.toxicon.2004.05.005
20. Vasta GR, Ahmed H. *Animal Lectins: A Functional View*. Boca Raton: CRC Press (2008). doi: 10.1201/9781420006971
21. Anderluh G, Kisovec M, Krasevec N, Gilbert RJ. Distribution of MACPF/CDC proteins. *Subcell Biochem.* (2014) 80:7–30. doi: 10.1007/978-94-017-8881-6_2
22. Ellisdon AM, Reboul CF, Panjikar S, Huynh K, Oellig CA, Winter KL, et al. Stonefish toxin defines an ancient branch of the perforin-like superfamily. *Proc Natl Acad Sci USA.* (2015) 112:15360–5. doi: 10.1073/pnas.1507622112
23. Dreon MS, Fernández PE, Gimeno EJ, Heras H. Insights into embryo defenses of the invasive apple snail *Pomacea canaliculata*: egg mass ingestion affects rat intestine morphology and growth. *PLoS Negl Trop Dis.* (2014) 8:e2961. doi: 10.1371/journal.pntd.0002961
24. Giglio ML, Garro C, Caviedes-Vidal E, Heras H. Egg perivitelline fluid of the invasive snail *Pomacea canaliculata* affects mice gastrointestinal function and morphology. *PeerJ.* (2018) 6:e5314. doi: 10.7717/peerj.5314
25. Dreon MS, Ituarte S, Heras H. The role of the proteinase inhibitor ovorubin in apple snail eggs resembles plant embryo defense against predation. *PLoS ONE.* (2010) 5:e15059. doi: 10.1371/journal.pone.0015059
26. Giglio ML, Ituarte S, Pasquevich MY, Heras H. The eggs of the apple snail *Pomacea maculata* are defended by indigestible polysaccharides and toxic proteins. *Can J Zool.* (2016) 94:777–85. doi: 10.1139/cjz-2016-0049
27. Pasquevich MY, Dreon MS, Qiu JW, Mu H, Heras H. Convergent evolution of plant and animal embryo defences by hyperstable non-digestible storage proteins. *Sci Rep.* (2017) 7:15848. doi: 10.1038/s41598-017-16185-9
28. Ituarte S, Brola TR, Dreon MS, Sun J, Qiu J-W, Heras H. Non-digestible proteins and protease inhibitors: implication for defense of the colored eggs of the freshwater apple snail *Pomacea canaliculata*. *Can J Zool.* (2019) 97:9. doi: 10.1139/cjz-2018-0210
29. Kisielinski K, Willis S, Prescher A, Klosterhalfen B, Schumpelick V. A simple new method to calculate small intestine absorptive surface in the rat. *Clin Exp Med.* (2002) 2:131–5. doi: 10.1007/s102380200018
30. Sun J, Mu H, Ip JCH, Li R, Xu T, Accorsi A, et al. Signatures of divergence, invasiveness, and terrestrialization revealed by four apple snail genomes. *Mol Biol Evol.* (2019) 36:1507–20. doi: 10.1093/molbev/msz084
31. Gorbushin AM. Membrane attack complex/perforin domain-containing proteins in a dual-species transcriptome of caenogastropod Littorina littorea and its trematode parasite Himasthla elongata. *Fish Shellfish Immunol.* (2016) 54:254–6. doi: 10.1016/j.fsi.2016.04.015
32. Johnson TK, Henstridge MA, Warr CG. MACPF/CDC proteins in development: insights from drosophila torso-like. *Semin Cell Dev Biol.* (2017) 72:163–70. doi: 10.1016/j.semcdb.2017.05.003

33. Heras H, Garín CF, and Pollero RJ. Biochemical composition and energy sources during embryo development and in early juveniles of the snail *Pomacea canaliculata* (Mollusca: Gastropoda). *J. Exp. Zool.* (1998) 280:375–83. doi: 10.1002/(SICI)1097-010X(19980415)280:6<375::AID-JEZ1>3.0.CO;2-K
34. Podobnik M, Anderluh G. Pore-forming toxins in Cnidaria. *Semin Cell Dev Biol.* (2017) 72:133–41. doi: 10.1016/j.semcdb.2017.07.026
35. Hayes KA, Burks RL, Castro-Vazquez A, Darby PC, Heras H, Martín PR, et al. Insights from an integrated view of the biology of apple snails (Caenogastropoda: Ampullariidae). *Malacologia.* (2015) 58:245–302. doi: 10.4002/040.058.0209
36. Ituarte S, Brola TR, Fernandez PE, Mu H, Qiu JW, Heras H, et al. A lectin of a non-invasive apple snail as an egg defense against predation alters the rat gut morphophysiology. *PLoS ONE.* (2018) 13:e0198361. doi: 10.1371/journal.pone.0198361
37. Yusa Y. Predation on eggs of the apple snail *Pomacea canaliculata* (Gastropoda: Ampullariidae) by the fire ant *Solenopsis geminata*. *J Mollus Stud.* (2001) 67:275–9. doi: 10.1093/mollus/67.3.275
38. Randall D, Burggren W, French K. Energy acquisition: feeding, digestion and metabolism. In: Randall D, Burggren W, French K, editors. *Eckert Animal Physiology. Mechanisms and Adaptations*. 4th ed. New York, NY: Freeman (1997). p. 683–724.
39. Nation JL. Digestion. In: Nation JL, editor. *Insect Physiology and Biochemistry*. Boca Raton: CRC press (2002). p. 27–64.
40. Yeh YQ, Liao KF, Shih O, Shiu YJ, Wu WR, Su CJ, et al. Probing the acid-induced packing structure changes of the molten globule domains of a protein near equilibrium unfolding. *J Phys Chem Lett.* (2017) 8:470–7. doi: 10.1021/acs.jpclett.6b02722
41. van der Goot FG, Lakey JH, Pattus F. The molten globule intermediate for protein insertion or translocation through membranes. *Trends Cell Biol.* (1992) 2:343–8. doi: 10.1016/0962-8924(92)90184-O
42. Ptitsyn OB. Molten globule and protein folding. *Adv Protein Chem.* (1995) 47:83–229. doi: 10.1016/S0065-3233(08)60546-X
43. Vecsey-Semjen B, Mollby R, van der Goot FG. Partial C-terminal unfolding is required for channel formation by staphylococcal alpha-toxin. *J Biol Chem.* (1996) 271:8655–60. doi: 10.1074/jbc.271.15.8655
44. Vecsey-Semjen B, Lesieur C, Mollby R, van der Goot FG. Conformational changes due to membrane binding and channel formation by staphylococcal alpha-toxin. *J Biol Chem.* (1997) 272:5709–17. doi: 10.1074/jbc.272.9.5709
45. Bortoleto RK, Ward RJ. A stability transition at mildly acidic pH in the alpha-hemolysin (alpha-toxin) from Staphylococcus aureus. *FEBS Lett.* (1999) 459:438–42. doi: 10.1016/S0014-5793(99)01246-6
46. McConnell EL, Basit AW, Murdan S. Measurements of rat and mouse gastrointestinal pH, fluid and lymphoid tissue, and implications for *in-vivo* experiments. *J Pharm Pharmacol.* (2008) 60:63–70. doi: 10.1211/jpp.60.1.0008
47. Keusch GT, Donta ST. Classification of enterotoxins on the basis of activity in cell culture. *J Infect Dis.* (1975) 131:58–63. doi: 10.1093/infdis/131.1.58
48. Liu Y, Zhang T, Zhou Y, Li J, Liang X, Zhou N, et al. Visualization of perforin/gasdermin/complement-formed pores in real cell membranes using atomic force microscopy. *Cell Mol Immunol.* (2019) 16:611–20. doi: 10.1038/s41423-018-0165-1
49. Yoshida A, Sakai N, Uekusa Y, Imaoka Y, Itagaki Y, Suzuki Y, et al. Morphological changes of plasma membrane and protein assembly during clathrin-mediated endocytosis. *PLoS Biol.* (2018) 16:e2004786. doi: 10.1371/journal.pbio.2004786
50. Pi J, Li B, Tu L, Zhu H, Jin H, Yang F, et al. Investigation of quercetin-induced HepG2 cell apoptosis-associated cellular biophysical alterations by atomic force microscopy. *Scanning.* (2016) 38:100–12. doi: 10.1002/sca.21245
51. Mesquita FS, Brito C, Cabanes D, Sousa S. Control of cytoskeletal dynamics during cellular responses to pore forming toxins. *Commun Integr Biol.* (2017) 10:e1349582. doi: 10.1080/19420889.2017.1349582
52. Brito C, Cabanes D, Sarmento Mesquita F, Sousa S. Mechanisms protecting host cells against bacterial pore-forming toxins. *Cell Mol Life Sci.* (2019) 76:1319–39. doi: 10.1007/s00018-018-2992-8
53. Karakelian D, Lear JD, Lally ET, Tanaka JC. Characterization of *Actinobacillus actinomycetemcomitans* leukotoxin pore formation in HL60 cells. *Biochim Biophys Acta.* (1997) 1406:175–87. doi: 10.1016/S0925-4439(98)00002-7
54. Darzynkiewicz Z, Juan G, Li X, Gorczyca W, Murakami T, Traganos F. Cytometry in cell necrobiology: analysis of apoptosis and accidental cell death (necrosis). *Cytometry.* (1997) 27:1–20. doi: 10.1002/(SICI)1097-0320(19970101)27:1<1::AID-CYTO2>3.0.CO;2-L
55. Cooper HS, Farano P, Coapman RA. Peanut lectin binding sites in colons of patients with ulcerative colitis. *Arch Pathol Lab Med.* (1987) 111:270–5.
56. Marzo F, Alonso R, Urdaneta E, Arricibita FJ, Ibanez F. Nutritional quality of extruded kidney bean (*Phaseolus vulgaris* L. var Pinto*)* and its effects on growth and skeletal muscle nitrogen fractions in rats. *J Anim Sci.* (2002) 80:875–9. doi: 10.2527/2002.804875x
57. Menard S, Cerf-Bensussan N, Heyman M. Multiple facets of intestinal permeability and epithelial handling of dietary antigens. *Mucosal Immunol.* (2010) 3:247–59. doi: 10.1038/mi.2010.5
58. Perrier C, Corthesy B. Gut permeability and food allergies. *Clin Exp Allergy.* (2011) 41:20–8. doi: 10.1111/j.1365-2222.2010.03639.x
59. Cirkovi C, Veličković T, Gavrović-Jankulović M. Intestinal permeability and trnsport of food antigens. In: Cirković T, Veličković Gavrović-Jankulović M, editors. *Food Allergens. Biochemistry and Molecular Nutrition.* Servia: Springer, (2014). p. 29–56.
60. Tchernychev B, Wilchek M. Natural human antibodies to dietary lectins. *FEBS Lett.* (1996) 397:139–42. doi: 10.1016/S0014-5793(96)01154-4
61. Lavelle EC, Grant G, Pusztai A, Pfuller U, O'Hagan DT. Mucosal immunogenicity of plant lectins in mice. *Immunology.* (2000) 99:30–7. doi: 10.1046/j.1365-2567.2000.00932.x
62. Eiklid K, Olsnes S. Animal toxicity of *Shigella dysenteriae* cytotoxin: evidence that the neurotoxin, enterotoxin, and cytotoxic activities are due to one toxin. *J Immunol.* (1983) 130:380–4.
63. Davitt CJ, Lavelle EC. Delivery strategies to enhance oral vaccination against enteric infections. *Adv Drug Deliv Rev.* (2015) 91:52–69. doi: 10.1016/j.addr.2015.03.007
64. Freytag LC, Clements JD. Mucosal adjuvants. *Vaccine.* (2005) 23:10. doi: 10.1016/j.vaccine.2004.11.010
65. Hill DR, Ford L, Lalloo DG. Oral cholera vaccines: use in clinical practice. *Lancet Infect Dis.* (2006) 6:361–73. doi: 10.1016/S1473-3099(06)70494-7
66. Norton EB, Lawson LB, Freytag LC, Clements JD. Characterization of a mutant *Escherichia coli* heat-labile toxin, LT(R192G/L211A), as a safe and effective oral adjuvant. *Clinical and Vaccine Immunology.* (2011) 18:546–51. doi: 10.1128/CVI.00538-10
67. Lowry OH, Rosenbrough NJ, Farr AL, Randall R. Protein measurement with the folin phenol reagent. *J Biol Chem.* (1951) 193:265–75.
68. Pinto M, Robine-Leon S, Appay MD, Kedinger M, Triadou N, Dussaulx E, et al. (1983). Enterocyte-like differentiation and polarization of the human colon carcinoma cell line Caco-2 in culture. *Biol. Cell.* 47:8.
69. Mishell BB, Shiigi SM, Henry C, Chan EL, North J, Gallily R, et al. Determination of viability by trypan blue exclusion. In: Mishell BB, Shiigi SM, editors. *Selected Methods in Cellular Immunology.* San Francisco, CA: W H Freeman and Company (1980) p. 124–37.
70. Council NR. *Guide for the Care and Use of Laboratory Animals*. (2011). Washington, DC: National Academies Press
71. Gasteiger E, Hoogland C, Gattiker A, Duvaud S, Wilkins MR, Appel RD, et al. Protein identification and analysis tools on the ExPASy server. In: Walker JM, editor. *The Proteomics Protocols Handbook*. Totowa, NJ: Humana Press (2005). p. 571–607.
72. Moreno FJ, Maldonado BM, Wellner N, Mills EN. Thermostability and *in vitro* digestibility of a purified major allergen 2S albumin (Ses i 1) from white sesame seeds (*Sesamum indicum* L.). *Biochim Biophys Acta.* (2005) 1752:142–53. doi: 10.1016/j.bbapap.2005.07.022
73. Laemmli UK. Cleavage of structural proteins during the assembly of the head of bacteriophage T4. *Nature.* (1970) 227:680–5. doi: 10.1038/227680a0
74. Deutscher MP. Section II. General methods for handling proteins and enzymes. In Deutscher MP, editors. *Guide to Protein Purification Methods in Enzymology*. New York, NY: Academic Press (1990). p. 19–92.
75. Franke D, Petoukhov MV, Konarev PV, Tuukkanen A, Mertens HDT, Kikhney AG, et al. ATSAS 2.8: a comprehensive data analysis suite for small-angle scattering from macromolecular solutions.

J Appl Crystallogr. (2017) 50:1212–5. doi: 10.1107/S1600576717007786

76. Cattaneo ER, Prieto ED, Garcia-Fabiani MB, Montanaro MA, Guillou H, Gonzalez-Baro MR. Glycerol-3-phosphate acyltransferase 2 expression modulates cell roughness and membrane permeability: an atomic force microscopy study. *PLoS ONE.* (2017) 12:e0189031. doi: 10.1371/journal.pone.0189031
77. Lara-Cruz C, Jimenez-Salazar JE, Ramon-Gallegos E, Damian-Matsumura P, Batina N. Increasing roughness of the human breast cancer cell membrane through incorporation of gold nanoparticles. *Int J Nanomed.* (2016) 11:5149–61. doi: 10.2147/IJN.S108768
78. Denizot F, Lang R. Rapid colorimetric assay for cell growth and survival Modifications to the tetrazolium dye procedure giving improved sensitivity and reliability *J Immunol Meth.* (1986) 89:271–7. doi: 10.1016/0022-1759(86)90368-6
79. Sheridan BS, Lefrancois L. Isolation of mouse lymphocytes from small intestine tissues. *Curr Protoc Immunol.* (2012) 99:3.19.1–11. doi: 10.1002/0471142735.im0319s99

Conflict of Interest: The authors declare that the research was conducted in the absence of any commercial or financial relationships that could be construed as a potential conflict of interest.

frontiers in Cellular and Infection Microbiology

ORIGINAL RESEARCH
published: 24 March 2020
doi: 10.3389/fcimb.2020.00121

Plasmodium Perforin-Like Protein Pores on the Host Cell Membrane Contribute in Its Multistage Growth and Erythrocyte Senescence

Swati Garg[1†], Abhishek Shivappagowdar[1†], Rahul S. Hada[1], Rajagopal Ayana[2], Chandramohan Bathula[3], Subhabrata Sen[3], Inderjeet Kalia[4], Soumya Pati[1], Agam P. Singh[4] and Shailja Singh[5]*

[1] Department of Life Science, School of Natural Sciences, Shiv Nadar University, Greater Noida, India, [2] Laboratory of Neuroplasticity and Neuroproteomics, Department of Biology, KU Leuven, Leuven, Belgium, [3] Department of Chemistry, School of Natural Sciences, Shiv Nadar University, Greater Noida, India, [4] Infectious Diseases Laboratory, National Institute of Immunology, New Delhi, India, [5] Special Centre for Molecular Medicine, Jawaharlal Nehru University, New Delhi, India

The pore forming *Plasmodium* Perforin Like Proteins (PPLP), expressed in all stages of the parasite life cycle are critical for completion of the parasite life cycle. The high sequence similarity in the central Membrane Attack Complex/ Perforin (MACPF) domain among PLPs and their distinct functional overlaps define them as lucrative target for developing multi-stage antimalarial therapeutics. Herein, we evaluated the mechanism of Pan-active MACPF Domain (PMD), a centrally located and highly conserved region of PPLPs, and deciphered the inhibitory potential of specifically designed PMD inhibitors. The *E. coli* expressed rPMD interacts with erythrocyte membrane and form pores of ~10.5 nm height and ~24.3 nm diameter leading to hemoglobin release and dextran uptake. The treatment with PMD induced erythrocytes senescence which can be hypothesized to account for the physiological effect of disseminated PLPs in loss of circulating erythrocytes inducing malaria anemia. The anti-PMD inhibitors effectively blocked intraerythrocytic growth by suppressing invasion and egress processes and protected erythrocytes against rPMD induced senescence. Moreover, these inhibitors also blocked the hepatic stage and transmission stage parasite development suggesting multi-stage, transmission-blocking potential of these inhibitors. Concievably, our study has introduced a novel set of anti-PMD inhibitors with pan-inhibitory activity against all the PPLPs members which can be developed into potent cross-stage antimalarial therapeutics along with erythrocyte senescence protective potential to occlude PPLPs mediated anemia in severe malaria.

Keywords: perforin like proteins, malaria, erythrocyte, anemia, invasion, egress, atomic force microscopy, Raman spectroscopy

OPEN ACCESS

Edited by:
Gabriele Pradel, RWTH Aachen University, Germany

Reviewed by:
Takafumi Tsuboi, Ehime University, Japan
Manuel Elkin Patarroyo, Colombian Institute of Immunology Foundation, Colombia

***Correspondence:**
Shailja Singh
shailja.jnu@gmail.com

[†]These authors share first authorship

Specialty section:
This article was submitted to Parasite and Host, a section of the journal Frontiers in Cellular and Infection Microbiology

Received: *21 November 2019*
Accepted: *04 March 2020*
Published: *24 March 2020*

Citation:
Garg S, Shivappagowdar A, Hada RS, Ayana R, Bathula C, Sen S, Kalia I, Pati S, Singh AP and Singh S (2020) Plasmodium Perforin-Like Protein Pores on the Host Cell Membrane Contribute in Its Multistage Growth and Erythrocyte Senescence. Front. Cell. Infect. Microbiol. 10:121. doi: 10.3389/fcimb.2020.00121

INTRODUCTION

Malaria remains a serious global health challenge and major roadblock for the economic growth of the poor and developing economies. The rapid emergence of drug-resistant malaria parasites has exceeded the rate at which anti-malarial therapies are presently being introduced. Though currently available antimalarial therapies target blood-stage to reduce the disease burden, the

next-generation therapeutics demands development of drugs with potent cross-stage protection, for complete prevention (WHO, 2018). Therefore, an efficient treatment regimen needs to be both curative and transmission-blocking. In lieu of the same, molecular players performing multiple roles across the life cycle of the malaria parasite would thus serve as ideal targets for developing pan-active therapeutic interventions. In this regard, *Plasmodium* Perforin like proteins (PPLPs) are excellent candidates in this regard and need to be further characterized.

Perforin like proteins (PLPs) are the eukaryotic pore forming proteins conserved across the apicomplexan parasites, and are the crucial players in the biology of malaria parasite across all the stages of *Plasmodium* life cycle (Tavares et al., 2014; Alaganan et al., 2017). The genome of *Plasmodium* spp. encodes for five PPLPs (PPLP1-5) that work in different combinations at different stages of the parasite life cycle, and are indispensable for the parasite growth and survival (Kadota et al., 2004; Ishino et al., 2005; Ecker et al., 2007; Deligianni et al., 2013; Wirth et al., 2014, 2015; Yang et al., 2017). In the liver stage, PPLP1 has a distinct role in the successful establishment of hepatocyte infection (Ishino et al., 2005; Yang et al., 2017). By HA tagging of the PPLP1 locus followed by immunoblotting with HA antibody, Yang et al. could not detect its expression in the blood stage. However, other reports confirm the expression of PPLP1 and PPLP2 in blood-stage schizonts and merozoites using LC-MS/MS (Lasonder et al., 2002; Garg et al., 2013). PPLP1 and PPLP2 are involved in the permeabilization of the host erythrocyte membrane during the egress of malarial parasites (Garg et al., 2013). In the gametocytes, PPLP2 is responsible for the egress of activated gametocytes from the host erythrocytes (Deligianni et al., 2013; Wirth et al., 2014). PPLP3, PPLP4, and PPLP5 are expressed in ookinete and are involved in mosquito midgut traversal to form oocysts (Kadota et al., 2004; Ecker et al., 2007; Wirth et al., 2015). Despite the importance that PPLPs have in the parasite life cycle, no chemotherapeutic interventions have been developed against them. Although single knockout suggests that individually they are not essential for the blood stage, functional knockout of both PfPLP1 and PfPLP2 can better reveal their role. Since the double knockout is a challenging task for malaria parasites, inhibitors can be mimic of functional knockout of PfPLPs. A few reported inhibitors for eukaryotic pore-forming proteins identified till date, mostly exert their effects indirectly through inhibition of protein processing, storage, or secretion from organelles rather than directly inhibiting perforin's function in the target cell (Kataoka et al., 1996a,b). Recently, a few small molecule inhibitors were identified from a high throughput screening which inhibited mouse perforin at sub-micromolar doses (Lena et al., 2008; Spicer et al., 2013). These studies proved motivational for the development of anti-PPLP molecules, which required identification and functional characterization of a common motif of PPLPs that can serve as the universal target for chemotherapeutics.

PPLPs have an N-terminal signal sequence, a central MACPF (membrane attack complex/ perforin) domain, and a C-terminal β-sheet rich domain (Garg et al., 2015). The central MACPF domain is the functional unit of PPLPs containing the characteristic signature motif of eukaryotic pore-forming proteins and two transmembrane helical domains (CH1 and CH2) that exhibit the typical arrangement of alternate hydrophilic and hydrophobic residues and is involved in membrane insertion (Hadders et al., 2007; Pipkin and Lieberman, 2007; Rosado et al., 2007). The C-terminal domain (CTD) is rich in the β-sheet and is involved in membrane binding similar to eukaryotic pore-forming proteins (Voskoboinik et al., 2005). PPLP molecules are initially secreted as monomers that bind to the target cell membrane and oligomerize on its surface to form functional, transmembrane pores (Pipkin and Lieberman, 2007; Baran et al., 2009). The structure of PPLPs remains unsolved, however, recently the crystal structure of a closely related PLP of another apicomplexan parasite *Toxoplasma gondii*, TgPLP1 was deciphered (Gilbert et al., 2018). The structure of TgPLP1 is similar to the reported eukaryotic pore-forming proteins, but, bulkier than others due to the presence of extra helices that may play roles in pore formation (Gilbert et al., 2018). The structure of PPLPs can now be predicted using TgPLP1 as a template for designing anti-malarial chemotherapeutics.

In this study, using various biochemical, biophysical, and pharmacological evidences, we characterized the pore forming activity of PLPs on erythrocytes. Further, the specifically designed inhibitors could restrict this pore formation, impede the exit/entry of the parasites and also could exert multiple-stage inhibition and rescue the uninfected erythrocytes from death. Together, we highlight the mechanism of pore formation by PPLPs and evaluate their potential for the development of pan-active inhibitors to provide both symptomatic and transmission-blocking cure for malaria.

MATERIALS AND METHODS

Expression and Activity of Recombinant Pan-MACPF Domain 1 (rPMD1) and Recombinant Pan-MACPF Domain 2 (rPMD1)

Codon optimized gene encoding for rPMD1 (**Figure S1A**) and rPMD2 domain (**Figure S1B**) were subcloned into bacterial expression vector PET28a (+) and protein expression in *E.coli* cells was induced with 1 mM isopropyl-β-D-thiogalactoside (IPTG). His-tagged rPMD1 was purified from inclusion bodies while his-tagged rPMD2 was purified from the soluble fraction using Ni-NTA chromatography. The gene encoding for rPLP2 C-terminal domain was subcloned into bacterial expression vector pQE 30. The protein expression in *E. coli* cells was induced with 1 mM isopropyl-β-D-thiogalactoside (IPTG) and the his-tagged protein was purified from the soluble fraction using Ni-NTA chromatography. The concentration of purified proteins was measured using the BCA estimation kit (Pierce, USA).

Erythrocyte Lysis and Permeabilization Assays

5×10^6 human erythrocytes were incubated with rPMD1 or rPMD2 in lysis buffer for 1 h at 37°C as described previously (Garg et al., 2013). The release of hemoglobin into the supernatant was estimated by measuring absorbance at 405 nm.

RBCs incubated in lysis buffer alone or rPPLP2-C-ter protein were taken as the negative control. Maximum hemoglobin release is lysis of 5×10^6 human RBCs in water which is considered as 100% lysis. For the permeabilization assays, lysis was performed in the presence of Rhodamine-phalloidin and 10 kDa FITC-dextran.

Binding and Oligomerization Assays

Binding of rPMD1and rPMD2 to human erythrocytes was performed as described previously (Gaur et al., 2007). Briefly, erythrocytes were incubated with rPMD1 or rPMD2 for 1 h at 4°C and bound proteins were eluted using 1.5 M NaCl and detected by Western blotting. For the oligomerization assay, rPMD1 or rPMD2 was incubated with human erythrocytes for 1 h at 37°C and centrifuged. The oligomerized protein was detected in erythrocyte pellets using Western Blot analysis (Garg et al., 2013).

Modified Cellular Thermal Shift Assay (CETSA)

Interaction between the PMIs with rPMDs was tested using CETSA as described previously (Jafari et al., 2014). Briefly, the rPMDs alone or in combination with the compounds were treated at 4, 60, and 80°C and cooled down followed by centrifugation. The supernatant was analyzed by SDS-PAGE. The band intensities for each of the protein lane was determined using Image J software (NIH, USA) and plotted considering the band intensity of untreated 4°C erythrocytes as maximum (100%).

In vitro Culture of *P. falciparum*

Laboratory strain of *P. falciparum*, 3D7 was cultured in RPMI 1640 (Invitrogen, USA) supplemented with 27.2 mg/L hypoxanthine (Sigma Aldrich, USA) and 0.5% Albumax I (Invitrogen, USA) using O+ erythrocytes in mixed gas environment (5% O_2, 5% CO_2, and 90% N_2) as described previously (Trager and Jensen, 1976). Parasites were synchronized by sorbitol selection of rings and percoll selection of schizonts.

HepG2 Cytotoxicity Assay

Human liver hepatocellular carcinoma cell line (HepG2 cells) were cultured in Dulbecco's Modified Eagle's Medium as described previously (Ramu et al., 2017). HepG2 cells were seeded at a density of 30,000 cells per well and allowed to grow overnight. Adhered cells were treated PMIs and kept for 48 h. Cytotoxic effect was assessed using MTT (3-[4,5-dimethylthiazol-2-yl]-2,5-diphenyl tetrazolium bromide) assay (Sigma-Aldrich, USA).

Parasite Growth Inhibition Assay (GIA)

To access the effect of PMIs on parasite growth, synchronized trophozoites were treated with different concentrations of C01 or C02 compounds along with DMSO control at 37°C for one cycle of parasite growth. The smears were prepared after 48 h and stained with Giemsa solution and scored for infection under a light microscope. IC_{50} was calculated using graph pad prism 8.0 (CA, USA). To access the non-specific effect of PMIs on erythrocytes, erythrocytes were treated with different concentrations of C01 or C02 at 37°C for 3 h and washed with incomplete RPMI. Purified schizonts were added to treated erythrocytes at a hematocrit of 2% and parasitemia of 1.0%. Parasites added to untreated erythrocytes were used as a control. The parasite invasion was scored after 8 h by counting the number of infected erythrocytes in Giemsa (Sigma, USA) stained smears under the light microscope.

Parasite Egress and Invasion Assay

To assess the effect of PMIs on parasite egress, late-stage schizonts [∼46 h post-invasion, (hpi)] were diluted to a final hematocrit of 2% and parasitemia of ∼10% and treated with different concentrations of C01 and C02 along with DMSO control for 6 h. Subsequently, the erythrocytes were smeared and counted for schizonts as well as rings by staining with Giemsa under the light microscope. Percent Egress was calculated as the fraction of schizonts ruptured in treatment and control during the incubation time as compared with the initial number of schizonts at 0 h, using the formula as described below. Percent Egress was then plotted considering the fraction of schizonts ruptured in control as 100% egress.

$$\%\text{Egress} = 100[(\text{I} - \text{T})/(\text{I} - \text{C})]$$

I, initial no. of schizonts; T, no. of schizonts in treatment; C, no. of schizonts in DMSO control.

For scoring invasion, the number of rings formed per egress of schizont was counted and plotted.

Ring and Trophozoites Toxicity Assay

To assess the effect of C01 and C02 on the ring stage, early rings (∼6 hpi) at a parasitemia of 1% were treated with different concentrations of PMIs along with DMSO control. All the wells were washed following 6 h and replenished with media and harvested after 48 h. The parasite growth was assessed by fluorimeter using SYBR green (Thermo Fisher Scientific, USA) staining. For trophozoites toxicity assay, early trophozoites instead of rings were taken and a similar protocol was performed.

In vitro Growth Inhibition Assay for Liver-Stage Parasites

The diluted PMI solutions were added to 24-well culture plates (final DMSO concentration was 1%) containing human HepG2 cells seeded a day prior to the experiment and 0.5 ml complete Dulbecco modified Eagle medium (DMEM) containing 10% fetal bovine serum (FBS), together with a cocktail of penicillin, streptomycin and amphotericin. Infection was initiated by adding 10,000 *Plasmodium berghei* ANKA sporozoites. Infected cultures were then allowed to grow at 37°C in a 5% CO_2 atmosphere for 51 h. The culture medium was changed 24 h after infection, and fresh compounds were added at the same concentration as on the previous day, to maintain inhibitor pressure throughout the growth period. At the end of the 51 h incubation period, total RNA was extracted using TrizolTM (Invitrogen, USA) reagent. Reverse transcription from 1 μg RNA

was performed using a cDNA synthesis kit (GCC Biotech, India) to obtain cDNA. In a real-time PCR mix (H-eff qPCR mix, GCC Biotech, India) of 20 μl, a cDNA equivalent of 0.1 μg RNA was used. The real-time PCR mix also contained *P. berghei* 18S rRNA specific primers. Real-time PCR was performed using an Eppendorf Mastercycler realplex4, and the copy numbers were calculated, using the known amount of plasmid standard having the amplification target sequence. Parasite growth inhibition was calculated by dividing the 18S rRNA copy number of the experimental group by that of the untreated control group. The fraction obtained was then converted into % inhibition (with respect to untreated as 100%).

Annexin and Calcium Staining Assays

Erythrocytes were treated with a sublethal concentration of rPMD1 or rPMD2 along with the different concentrations of C01 and C02. The samples were incubated for 48 h at 37°C and 5% CO_2. After 48 h, the samples were stained with Annexin-FITC (Life Technologies, USA) and Fluo-4 AM (Life Technologies, USA). The erythrocytes were imaged using a Nikon A1R microscope and also quantified using FACS BD Fortessa (Becton & Dickinson, USA) using Cell Quest software by scoring 100,000 cells per sample. Samples were analyzed using FlowJo software (Tree Star Inc, Ashland) by determining the proportion of FL-2 positive cells in comparison to the stained untreated erythrocytes.

Live-Cell Microscopy and Flow Cytometry for Calcium Influx

The erythrocytes were loaded with Fluo-4 AM (Life Technologies, USA), placed in coverslip bottom petri dishes and observed under a confocal microscope equipped with a temperature-controlled stage (Nikon A1R). These erythrocytes were treated with a sub-lethal concentration of rPMD1 (1 μg) or rPMD2 (50 ng) in the presence or absence of PMIs. DIC and fluorescent images were captured using a 100X, 1.4 numerical aperture lens at 1 frame per second. The recording was started for 30 s and then rPMD2 (rPMD2 along with PMI in case of inhibitor treatment) was added and captured for a total of 10 min at 37°C. The staining was also quantified using BD Fortessa (Becton & Dickinson, USA) by scoring 100,000 cells per sample and analyzed using FlowJo software (Tree Star Inc, Ashland).

Gametocyte Exflagellation Assay

To initiate *P. falciparum* gametocyte cultures, synchronized asexual blood-stage cultures were grown to a parasitemia of 10–15%, treated with 50 mM *N*-acetyl-D-glucosamine containing medium for 4 days to remove asexual stages and maintained in complete RPMI/HEPES to allow gametocyte development. Stage V gametocytes were incubated with activation medium (100 nM xanthuneric acid (XA), 20% AB+ human serum in RPMI1640/HEPES) in the presence of C01 and C02 at 25°C. Activated gametocytes were spread on glass slides 5 min after activation, fixed with methanol and stained with Giemsa (RAL Diagnostics, France). Around 200–250 gametocytes were scored to determine the percentage of rounded up gametocytes. The number of exflagellation centers was scored in gametocyte cultures by light microscopy at 40X magnification in 30 optical fields 15 min after activation.

Surface Plasmon Resonance

To determine the C01 and C02 interaction with rPMD11, SPR was performed using Auto-Lab Esprit SPR. rPMD1 (10 μM) was immobilized on the surface of the nickel-charged NTA SPR chip. Interaction analysis was studied by injecting C01, C02 along with rPMD1 over the chip surface, with association and dissociation time of 300 and 150 s, respectively. HEPES buffer was used both as immobilization and binding solutions. The surface of the sensor chip was then regenerated with a 50 mM NaOH solution. Data were fit by using Auto-Lab SPR Kinetic Evaluation software provided with the instrument.

In silico Docking

Using I-Tasser and PHYRE2, domain-based modeling and threading were performed to obtain the 3D structures of *P. falciparum* PLP1-5. Following this, structure refinement was done using ModRefiner. To characterize the catalytic pocket, SiteHound software was used while utilizing the structural motif of the MACPF domain in each of the proteins (PLP1-5). Further, molecular docking of two PMIs (C01 and C02) was done using AutodockTools and Autodock vina with an exhaustiveness cut-off of eight for each run. All the ligands were kept flexible by examining torsions.

Atomic Force Microscopy

Erythrocytes treated with rPMD or in combination with PMIs were smeared and air-dried on a clean grease-free glass slide and imaged using WITec alpha using NSG30 probes with force constant of 22–100 N/m, the resonant frequency of 240–440 Hz, tip curvature radius of 10 nm (Tips nano) in non-contact mode. Topographic images were obtained at points per line and lines per image of 512 × 512 with the scan rate of 0.5 times/line (Trace) (s). All the AFM images were recorded using the Control Four 4.1 software. The images were 3D processed and analyzed using software Project Four 4.1 software (WITec, Germany).

Raman Imaging and Analysis

The Raman measurements of all the samples were performed using WITec alpha 300RA combined confocal Raman microscope. The spectrometer was equipped with solid-state diode lasers operating 532 nm and a suitable CCD detector that was cooled to −60°C. A Zeiss Fluor (100X) EC Epiplan-NEOFLUAR objective was used. The spectral resolution was equal to $1 cm^{-1}$. The integration time for a single spectrum varied from 2 to 5 s. Raman measurements and data analysis were performed using software Project Four 4.1 software (WITec, Germany). All Raman spectra presented were after pre-processing (baseline correction, smoothening and background removal) using asymmetric least squares smoothing method.

Statistical Analysis

For all the experiments, the data are presented as the mean ± standard deviation of the results and the number of biological replicates per experimental variable (n) is given in the figure legends. The data for the half-maximal inhibitory concentration

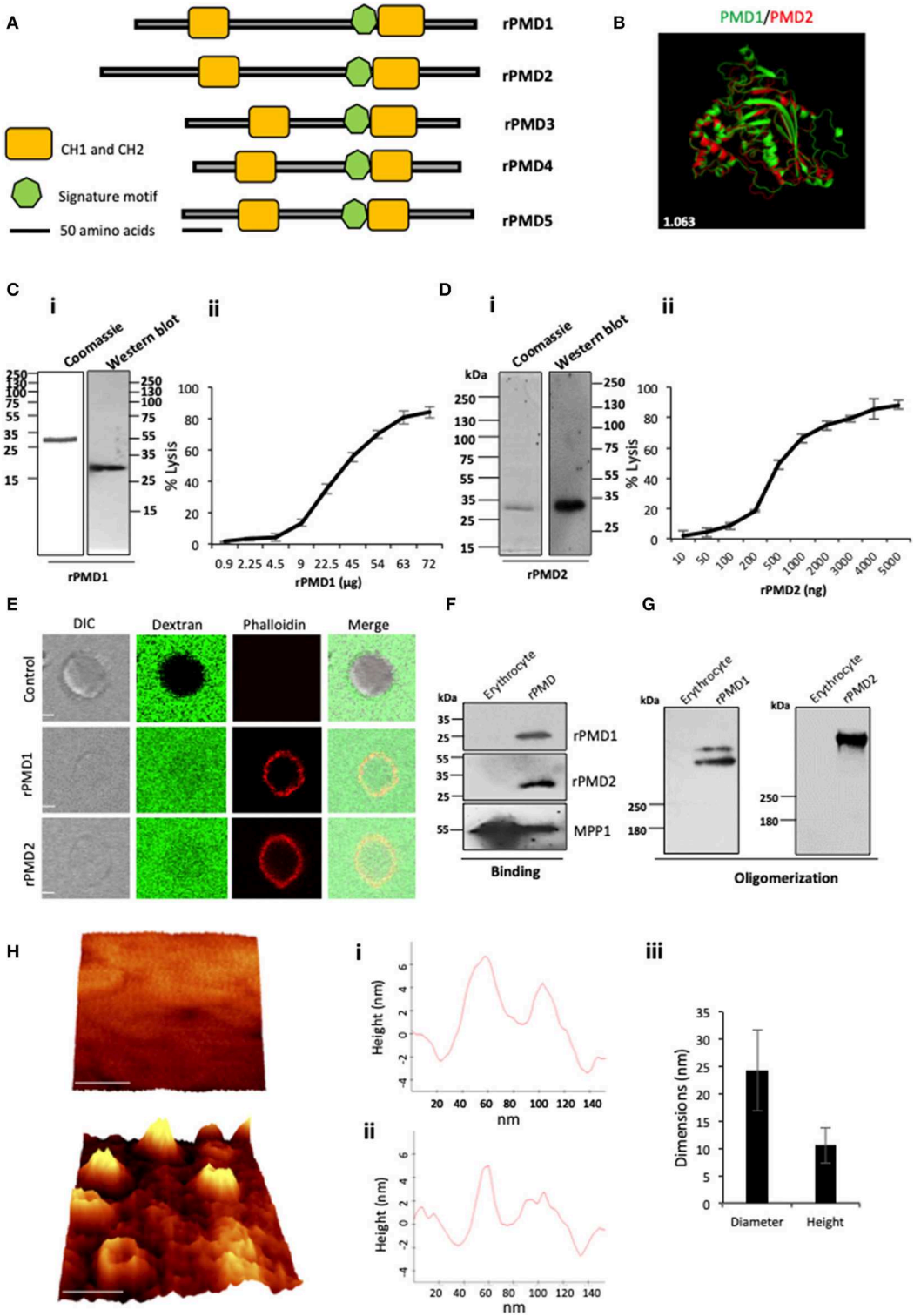

FIGURE 1 | Purification and activity of rPMDs. **(A)** Domain architecture of the MACPF domain of PfPLPs. The signature motif (green box) and two transmembrane helical domains, CH1 and CH2 (yellow boxes) are depicted. Scale bar represents 50 aa. **(B)** Structural superimposition of PMD domain of PfPLP1 and PfPLP2. RMSD value is indicated in white. **(C)** (i) Coomassie and Western blot of affinity-purified rPMD1 probed with the anti-his antibody. (ii) The dose-dependent membranolytic activity of rPMD1. The lysis of human erythrocytes was analyzed in the presence of different concentrations of rPMD1. The graph indicates the percent lysis of human erythrocytes by rPMD1 as compared with 100% hypotonic lysis of human erythrocytes in water ($n = 3$). **(D)** (i) Coomassie and Western blot of affinity-purified rPMD2

(Continued)

FIGURE 1 | probed with the anti-his antibody. (ii) The dose-dependent membranolytic activity of rPMD2. The lysis of human erythrocytes was analyzed in the presence of a different amount of rPMD2. The graph indicates the percent lysis of human erythrocytes by rPMD2 as compared with 100% hypotonic lysis of human erythrocytes in water ($n = 3$). **(E)** Permeabilization activity of rPMD1 and rPMD2. The human erythrocytes were incubated with Phalloidin Alexa 594 and 10 kDa FITC-Dextran in the presence and absence of rPMD1 and rPMD2 and visualized under a confocal microscope. Phalloidin staining was detected in the human erythrocytes treated with rPMD1 and rPMD2 but not in untreated human erythrocytes. **(F)** Western blot analysis of bound rPMD1 and rPMD2 eluted by 1.5 M NaCl. **(G)** Oligomerization of rPMD1 and rPMD2. rPMDs are incubated with human erythrocytes at 37°C for 30 min and analyzed for oligomeric rPMD1 and rPMD2 by Western blotting. **(H)** Visualization of oligomeric pores by AFM. (i) Erythrocytes were treated without (top) or with rPMD2 (bottom) for 30 min at 37°C and visualized under the AFM for pore formation. The image was 3D constructed using project Witec 4.1 software ($n = 2$). Scale bar represents 50 nm. (ii) Line profile of rPMD2 oligomers. Representative images of the height of the oligomer measured along the pore in AFM topographs are depicted. (iii) The average ring diameter and height of rPMD2 treated oligomers protruding from the erythrocytes membrane. Diameter and height were measured for oligomers formed on the erythrocyte membrane. Bars represent an average of 30 oligomers and error bars SD.

(IC_{50}) value and the % growth inhibition activity of compounds were analyzed and calculated using non-linear regression in Graph Pad Prism 8 (CA, USA). A student's *t*-test was performed to calculate the *p*-values, where $p < 0.05$ represents *, $p < 0.01$ represents **, and $p < 0.005$ represents *** significance.

RESULTS

The Pan-MACPF Domain of PfPLPs Forms Pores at Physiological Relevance

The presence of the MACPF domain in PfPLPs is necessary for pore formation. We mapped the minimal, active domain of PfPLPs and named it as pan-MACPF domain (PMD) (**Figure S2A**). The PMD harbors a signature motif ((Y/W)-X6-(F/Y)GTH(F/Y)-X6-GG) along with two clusters of helices (CH1 and CH2) to form pores in the cell membrane (**Figure 1A**). Interestingly, the sequence analysis of different PMDs revealed that they are highly conserved and closely related to each other. This stretch of a sequence is also evolutionarily conserved across *Plasmodium* spp. (**Figure S3**).

To investigate whether the conservation of sequence is also reflected in structural conservation, we *in silico* modeled the structure of PMDs based on the MACPF domain of a closely related apicomplexan parasite *T. gondii*, TgPLP1. Like other MACPF domains, PMDs contain a central β-pleated sheet, surrounded by CH1 and CH2 on either side. In addition, two helical inserts are additionally present in PMDs, similar to TgPLP1, that is absent in all other reported structures of the MACPF domain. Overall, the structural prediction revealed significant conservation of the MACPF domain fold across different PMDs (**Figure 1B** and **Figure S2B**).

The expression and purification of the recombinant MACPF domain from the earlier reported mammalian or insect cell system yield insufficient quantities of recombinant protein. To characterize, the pore-forming activity of PMDs *in vitro*, we cloned the codon optimized MACPF domain of PfPLP1 (rPMD1) and PfPLP2 (rPMD2) in pET28a (+) and recombinantly expressed rPMD1 and rPMD2 in *E. coli*. We could successfully purify the active protein from bacteria (**Figures 1C**i,**D**i) and demonstrate the erythrocyte lysis activity of both, rPMD1 and rPMD2, *in vitro* (**Figures 1C**ii,**D**ii). Both PMDs lysed erythrocytes in a dose-dependent manner which is due to their pore-forming activity on the erythrocyte membrane. Whereas, the histidine-tagged, C-terminal domain of PPLP2 did not demonstrate any lytic activity toward erythrocytes further confirming that the lytic activity of PPLPs is due to the central MACPF domain only (**Figures S4A–C**).

To confirm the permeabilization activity of rPMDs, the activity of rPMD1 and rPMD2 were monitored in the presence of rhodamine Phalloidin and 10 kDa FITC-dextran. The rPMD1 and 2 treated erythrocytes displayed phalloidin positivity accompanied by the uptake of 10 kDa FITC-dextran indicating permeabilization of the cell membrane (**Figure 1E**).

The PFPs binds to lipid bilayer and oligomerizes on it to create pores. To test the binding of rPMDs to the erythrocytes, sublytic concentration of rPMDs was incubated with erythrocytes and their binding was detected by Western blotting. We found that the monomers of rPMD1 and rPMD2 can bind to erythrocytes (**Figure 1F** and **Figure S4D**). We further investigated whether the binding of rPMDs leads to their oligomerization. To test this, lytic concentrations of rPMD1 and rPMD2 were incubated with erythrocytes and the ghosts thus formed were evaluated rPMD oligomers by Western Blot analysis. rPMD1 and rPMD2 formed SDS resistant, higher molecular weight oligomers (>250 kDa) suggesting the involvement of more than 8 monomers in the formation of pores (**Figure 1G**).

Although many studies indicate the pore-forming capacity of PPLPs, this process has not been characterized in detail. Hence, to gain in-depth insights into the characteristics of PPLP pores, we performed high-resolution atomic force microscopy (AFM) of oligomers on the erythrocyte membrane. Erythrocytes serve as the physiological host of PfPLP1 and PfPLP2 *in vivo* and hence we performed studies on red cells rather than model lipid bilayer membranes. AFM topographs of erythrocytes incubated with rPMD2 showed pore-forming oligomers in circular forms (**Figure 1H**). Height analysis demonstrated that rPMD2 oligomers have a vertical measurement of 10.55 ± 3.22 nm (mean ± SD, $n = 30$) on the erythrocyte surface (**Figure 1H**i,ii). The diameter of oligomers was distributed widely between 10 and 40 nm, showing a mean at 24.33 ± 7.42 nm (mean ± SD, $n = 30$). The line profile reveals the height and diameter of a single pore formed by rPMD2 (**Figure 1H**iii). Overall, this result confirms that PMD can drill pores in the membrane of erythrocytes.

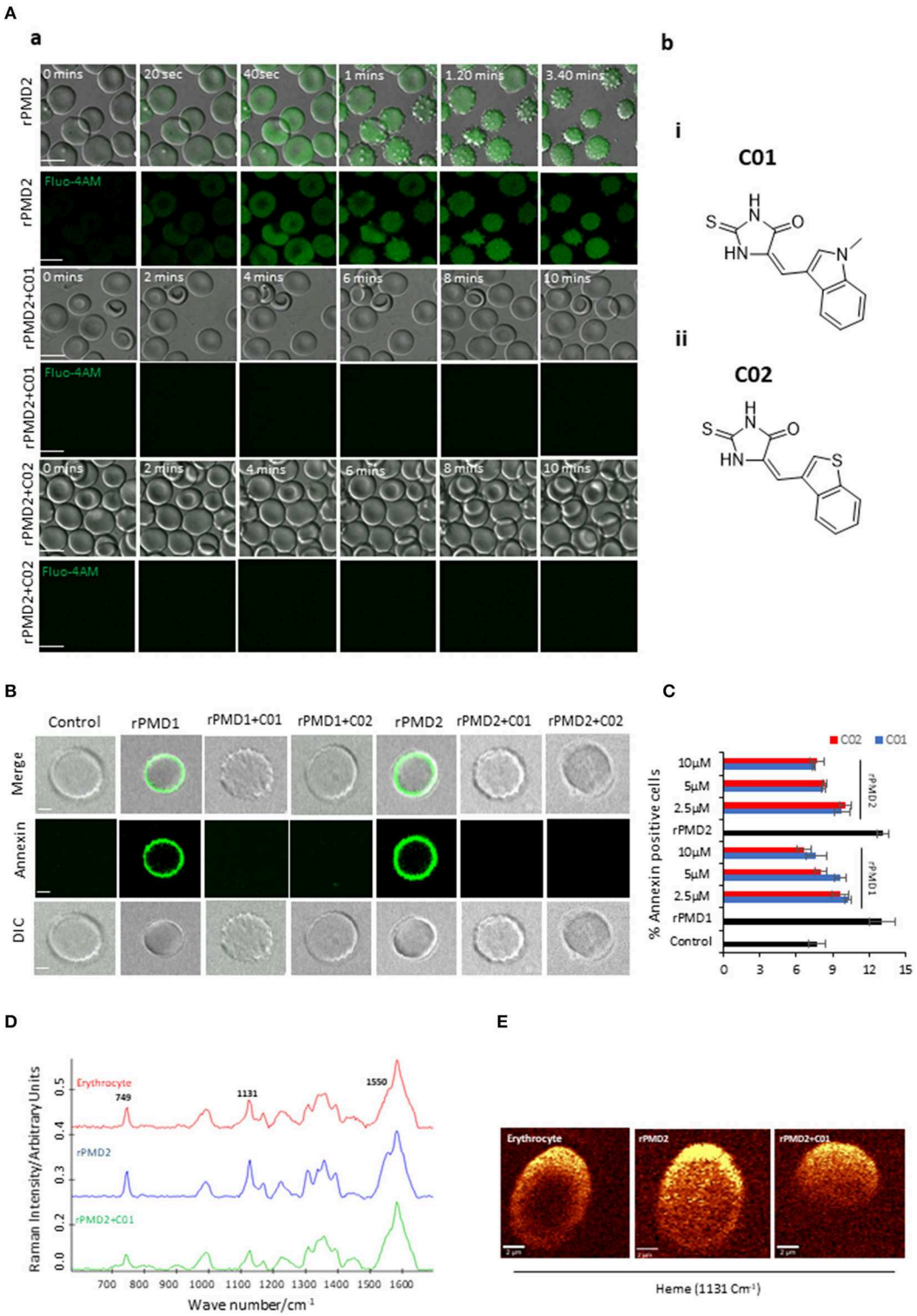

FIGURE 2 | Inhibition of bystander effect mediated by C01 and C02. **(A**-a**)** Time course of rPMD2-induced calcium channel formation. Erythrocytes were loaded with Fluo-4 AM. Sub lytic concentration of rPMD2 (50 ng) was added and the increase in calcium was monitored by confocal microscopy. Selected pairs of DIC and fluorescence images with time elapsed between frames in seconds (Sec) are shown. In the case of PMI treatment, C01 or C02 were added along with rPMD2. **(A-b)** (i) The structures depict scaffold of (Z)-5-((1-methyl-1H-indol-3-yl)methylene)-2-thioxoimidazolidin-4-one (C01) and (ii) (Z)-5-(benzo[b]thiophen-3-ylmethylene)-2-thioxoimidazolidin-4-one (C02). **(B)** Phosphatidylserine exposure on the erythrocyte surface. The erythrocytes were treated with rPMD1 or rPMD2 in the presence

(Continued)

FIGURE 2 | or absence of PMIs and stained with Annexin V-FITC after 48 h. The stained erythrocytes were visualized under a confocal microscope. **(C)** The annexin positive erythrocytes were quantitated using a flow cytometer. **(D)** Average Raman spectra of the untreated erythrocytes or erythrocytes treated with rPMD2 in the presence or absence of C01 was captured using 532 nm excitation. All the Raman spectra were presented after pre-processing (baseline correction, smoothening and background removal) using asymmetric least squares smoothing method ($n = 2$). **(E)** Raman images of erythrocytes were observed at 1,131 cm^{-1} which demonstrates the distribution of methemoglobin ($n = 2$).

Sub Lytic Concentration of PMDs Trigger Premature Senescence of Bystander Erythrocytes

The evolutionary conservation of PPLPs and their importance in disease pathogenesis prompted us to develop novel inhibitors against pan-MACPF domain. Recent reports demonstrate the identification of anti-perforin inhibitors through a high-throughput screen (Miller et al., 2016). Inspired by this, anti-PMD inhibitors (PMI), C01 and C02, were designed with a hypothesis that they can be pan-active against all PPLPs (**Figure 2A**b,i,ii).

An earlier report has revealed that secretion of TgPLP1 from one parasite can induce pore formation and egress of bystander parasites (Kafsack et al., 2009). Since PfPLP1 and PfPLP2 are secreted during the egress of merozoites and binds to the erythrocyte membrane (Garg et al., 2013), we thought to analyze the role of secreted PfPLPs on RBC senescence. We incubated the purified late-stage schizonts (∼44 h) with uninfected erythrocytes for 10 h at 37°C. To determine the effect of purified rPMDs on the bystander erythrocyte, time-lapse microscopy was performed, mimicking *in vivo* condition. Addition of sublytic concentration of rPMD1 (1 μg) and rPMD2 (50 ng) induced calcium influx in erythrocytes leading to changes in erythrocyte deformability followed by echinocytosis (**Figure 2A**-a, **Movie 1**). Initially, to check the non-specific calcium increase, we incubated the erythrocytes with PMIs that did not show any calcium increase (**Figure S5A**). Moreover, the PMIs alone also could not cause any erythrocyte lysis (**Figure S5B**). Inhibition of PMD binding to erythrocyte by PMIs restricted the influx of calcium and echinocytosis (**Figure 2A**-a, **Figure S5C**i,ii and **Movies 2, 3**). The calcium intake was further quantitated by flow cytometry also depicted an increase in intracellular calcium in response to rPMDs (**Figure S5C**). These results suggest that PfPLPs form smaller pores on erythrocytes at sub lytic concentrations that induce calcium influx but do not lead to lysis of erythrocytes.

Calcium influx also leads to phosphatidylserine (PS) exposure on the surface of erythrocytes that can lead to phagocytosis of cells by macrophages (Callahan et al., 2003; Brown and Neher, 2012). To assess this effect, erythrocytes were treated with sub lytic concentrations of rPMD1 and rPMD2 in the presence and absence of PMIs and stained with Annexin V-FITC after 48 h. The Annexin V-FITC positivity was analyzed by microscopy and flow cytometry (**Figures 2B,C** and **Figure S5D**). rPMDs treated erythrocytes in the absence of PMIs were Annexin-positive suggesting induction of PS exposure while the presence of PMIs abrogated their Annexin positivity (**Figure 2C**). This result indicates that at sub lytic concentrations, PfPLPs can induce delayed erythrocyte sequestration.

Oxidation of hemoglobin, leading to the formation of methemoglobin, is a marker for erythrocyte senescence (Umbreit, 2007). The methemoglobin carries the oxidized form of the heme (Fe^{3+}) that leads to changes in its porphyrin ring (Umbreit, 2007). To detect these changes in heme, we used Raman spectroscopy that is a non-invasive and label-free technique for the detection of metabolic changes at the single-cell level (Barkur et al., 2018). When 532 nm is applied to rPMD2 treated erythrocytes, ν_{15} gains intensity (pyrrole gains intensity) which is co-related well with the increase in intensity at band 749 cm^{-1}. A similar increase of band intensity was observed for the band located at 1,131 cm^{-1} that suggests the asymmetrical pyrrole half-ring stretching vibration (**Figure 2D**). The 1,550 cm^{-1} demonstrates the stretching mode ν (CbCb) (Dybas et al., 2018). The untreated and PMI treated erythrocytes demonstrated similar peak profiles (**Figure 2D**). Further, Raman imaging of 1,131 cm^{-1} also confirmed an increase in methemoglobin concentration within erythrocytes (**Figure 2E**). These results suggest the formation of methemoglobin following rPMD2 treatment that could lead to erythrocyte senescence.

Anti-PMD Inhibitors Bind to PfPLPs

To validate the binding of PMIs to PMDs *in silico* docking analysis was performed. The structure-refined models of PMD1-5 having an RMSD score of <2.0 were used for docking with PMIs. The molecular docking results revealed that C01 and C02 could efficiently bind to PMD1-5 as evident from strongly stable docking energy scores (**Figure 3A**i,ii, **Figures S6A**i–iii,**B**). The similar binding energy suggests that PMIs can inhibit PMDs with identical activity *in vitro*. *In silico* data further revealed that PMIs are binding in the same pocket of all PMDs. This pocket is not only structurally conserved but also has sequence identity as revealed by sequence alignment of PfPLP1-5 (**Figure S6C**).

To evaluate the binding of PMI to the rPMD, we modified and performed cellular thermal shift assay (CETSA). This technique involves the detection of a target protein by monitoring the thermostability of native protein in the presence of its selective inhibitor (Hashimoto et al., 2018). In principle, specific binding of the drug to its target protein increases the stability of protein at high temperatures (Jafari et al., 2014). In a similar line, we treated the purified rPMD1 and rPMD2 with C01 and C02 and heated them at 60 and 80°C while the sample at 4°C, served as a loading control. Analysis of band intensities demonstrated significant thermal protection of both rPMD1 and rPMD2 in the presence of compounds suggesting that C01 and C02 are interacting with rPMDs (**Figure 3B**i,ii). Further, the interaction of PMIs to PMDs is strong enough to impart thermal protection to the recombinant protein.

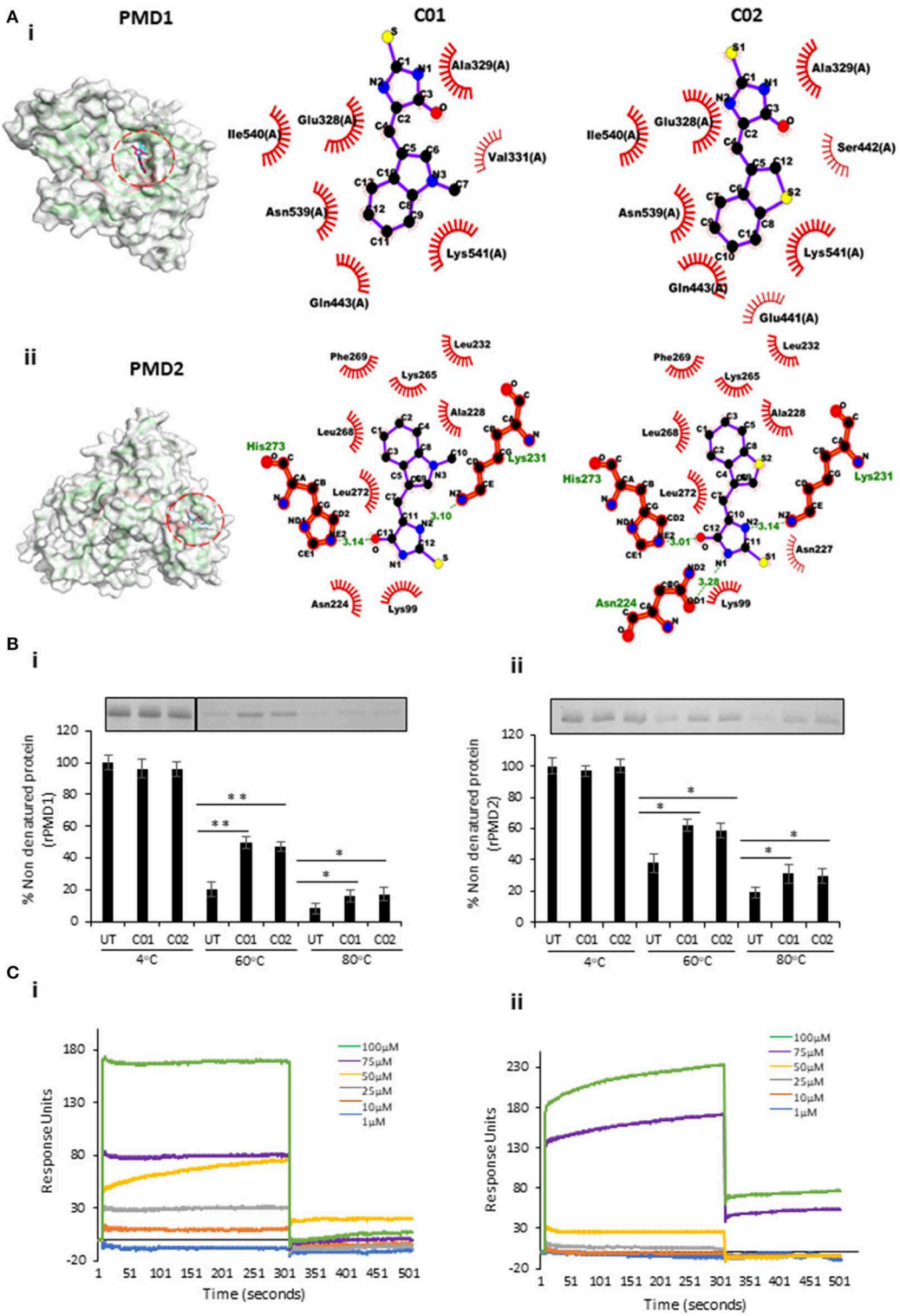

FIGURE 3 | *In silico* and *in vitro* interaction of C01 and C02 with rPMDs. **(A)** The PyMOL rendered surface structures of docked complexes have shown strong binding of C01 and C02 to the signature motif of PMD1 (i) and PMD2 (ii). The ligplot+ rendered scheme demonstrates strong interactions as shown by the close proximity between the C01 and C02 and hydrophobic amino acids (depicted by bold, eyelash-like structures), and hydrogen bonds formed with polar residues. **(B)** Interaction of PMIs and PMDs by CETSA. The drug-target engagement between the compounds and recombinant proteins was analyzed by subjecting the samples

(Continued)

FIGURE 3 | to thermal denaturation at 60 and 80°C (i) (ii). The protein intensity at 4°C was taken as control. The band intensities graph was plotted considering the 4°C samples as 100% non-denatured protein. UT indicates PMI untreated sample. Error bar represents SD (*$p < 0.05$; **$p < 0.01$). **(C)** rPMD1 was immobilized onto a nickel charged NTA SPR chip. C01 (i) and C02 (ii) were injected over immobilized rPMD1. The PMIs show concentration-dependent binding to rPMD1 with a K_d value of 0.1183 ± 0.0370 and 0.0866 ± 0.0709 for C01 and C02, respectively.

Surface Plasmon Resonance (SPR) is a sensitive technique to validate the protein-protein as well as protein-drug interactions (Vuignier et al., 2010; Frostell et al., 2013). To further confirm the interaction of PMIs with rMAC1, we performed SPR with different compound concentrations (1–100 μM). In both cases, the compounds showed concentration-dependent binding to the coated rMAC1 (**Figure 3C**i,ii). Together, SPR and CETSA confirm the binds of PMIs to rPMD.

PMIs Inhibit PMD Mediated Pore Formation

We analyzed the inhibitory activity of PMIs by performing rPMD mediated erythrocyte lysis assay in the presence of C01 and C02. The results demonstrated that C01 and C02 could inhibit the activity of both rPMD1 and rPMD2 in the sub-micromolar range (**Figures 4A,B**). Together, these data demonstrate the designing of anti-PMD inhibitors that inhibit the pore-forming ability of PMDs.

To investigate the complete disruption of pore formation in PMI treated erythrocytes, the influx of small molecules such as rhodamine-Phalloidin (∼1 kDa) and FITC-dextran (10 kDa) was investigated. PMD treated erythrocytes could not uptake dextran or Phalloidin in presence of PMI as compared to PMI treated erythrocytes (**Figure 4C**). This confirms that there is a complete abrogation of pore formation in the presence of PMIs.

Since the pore formation is chiefly dependent on the binding of monomers, we tested the binding of monomer to erythrocyte membrane in the presence of PMIs. rPMDs could not bind to the erythrocyte membrane in the presence of PMIs suggesting that inhibition in pore formation is due to the restriction of monomer binding to erythrocyte membrane (**Figure 4D**). Next, to closely monitor that PMIs are completely abrogating formation of pores and there is little to no change in membrane roughness due to rPMD binding, AFM was performed to evaluate surface topology of treated erythrocytes. We could clearly detect the formation of pores on the erythrocyte membrane treated with rPMD2 (**Figure 4E**ii). Also, the surface of rPMD treated erythrocytes was very rough and uneven. In comparison, treatment with rPMD2 in presence of PMIs, displayed no evident structures on the surface of erythrocytes, indicating the impairment in oligomerization and subsequent pore formation (**Figure 4E**iii,iv). Further, the smooth surface of PMI treated erythrocytes, similar to untreated erythrocytes, suggests that PMIs could revert all the phenotypes induced by rPMDs (**Figure 4E**i–iv). Taken together, this data indicates that C01 and C02 inhibit pore formation by a decrease in binding of the rPMD to the erythrocyte membrane.

PMIs Demonstrate Anti-parasitic Activity at Multiple Stages of Parasite Life Cycles

To monitor the effect of PMIs on parasite growth, Giemsa stained smears were prepared for the treated as well as untreated parasites at different time points. PMI treatment (10 μM) did not affect the parasite growth from ring to schizont stages. However, the treated parasites could not egress, and the merozoites that came out could be seen attached to erythrocytes but not forming rings (**Figure 5A**). Having confirmed the inhibitory activity of PMIs we further evaluated their anti-malarial activity. The ring infected parasites (∼5–6 hpi) were treated with different concentrations of drugs for 72 h. The parasites treated with DMSO served as a control and the parasite growth was measured by fluorimetry using SYBR green I-based assay. Both C01 and C02 demonstrated the ability to inhibit parasite growth with an IC_{50} of 3.54 μM for C01 and 3.31 μM for C02 (**Figure 5B**). This is similar to the reported role of PfPLPs in egress and invasion of merozoites suggesting the specific action of PMIs toward PMDs.

To confirm the egress defect, late schizonts (∼44–46 hpi) were treated with different concentrations of C01 and C02 for 6 h and a decrease in the number of schizonts was scored (**Figure 5C**). The intracellular Ca^{2+} chelator BAPTA-AM was used as a positive control. We observed a dose-dependent defect in egress. PfPLPs have a role in host erythrocyte permeabilization that facilitates the egress of merozoites. We observed that PMI treated schizonts demonstrated restriction in permeabilization of host erythrocyte as compared to untreated schizonts (**Figures 5C,D**), implying specific action of PMIs toward PfPLPs in egress.

Since the Giemsa scoring also suggested a defect in the invasion, we scored for ring formation after 10 h post-treatment. To specifically assess the effects of C01 and C02 on invasion and avoid the effects of their influence on egress, we calculated the number of rings formed per schizont egress. A drastic decrease in the number of rings formed in treated parasites as compared to the untreated control was noted (**Figure 5E**). To check the possibility of any non-specific effect of PMIs on erythrocytes, PMIs treated erythrocytes were incubated with purified schizonts and the parasite growth was accessed after 8 h. The data indicates no significant difference in parasite invasion to the untreated and the PMI erythrocytes, indicating that PMIs do not have any non-specific effect on erythrocytes (**Figure S7A**).

Further, to rule out the possibility that PMI treatment has any effect on ring and trophozoite stages, we devised a ring toxicity assay and trophozoite toxicity assay. In these assays, rings or trophozoites were treated for 6 h, washed and accessed for their growth during the next cycle. If the compounds have any toxicity on these stages, it will be reflected in this assay. Our data suggest that these compounds do not exhibit any toxicity toward either ring and trophozoite stages (**Figures S7B,C**). Taken together these findings imply that both compounds act only on the stages which involve the PPLP activity and can be used as a generic inhibitor of PPLPs.

Since PPLPs play a role during multiple stages of the parasite cycle, we studied their cross-stage inhibitory potential. PPLP2

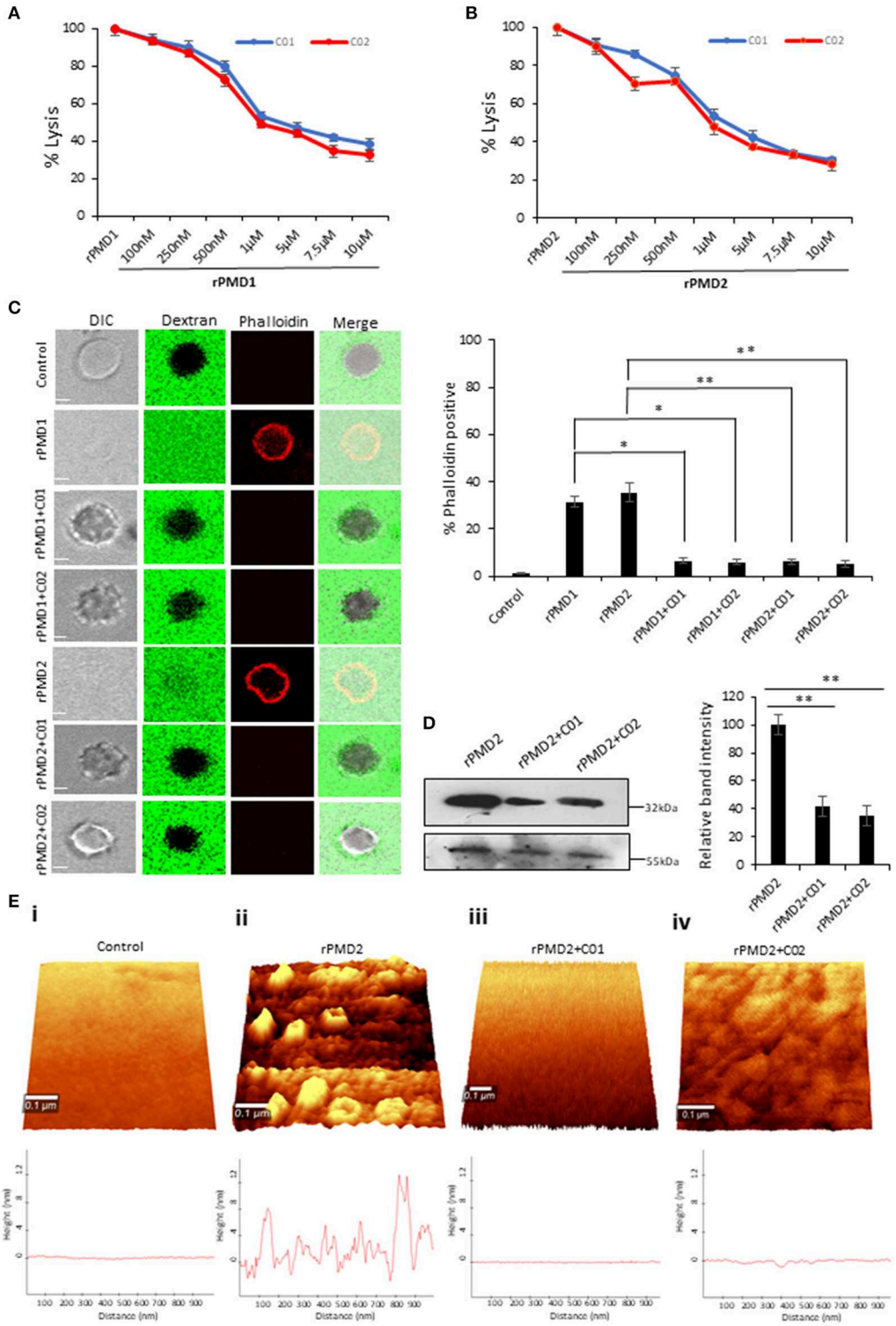

FIGURE 4 | C01 and C02 rescue RBCs from rPMD mediated lysis. **(A,B)** Anti-PLP effect of C01 and C02. The inhibition in erythrocytes lysis was evaluated by treating different concentrations of compounds with EC_{50} (effective concentration of rPMD that causes 50% erythrocyte lysis) of rPMD1 (45 μg) **(A)** and rPMD2 (500 ng) **(B)**. The lysis caused by recombinant protein alone was considered as 100% and was plotted respectively for the compound treated erythrocytes ($n = 3$). The error bar represents SD. **(C)** Inhibition of permeabilization activity by PMIs. The erythrocytes were incubated with Rhodamine-phalloidin and 10 kDa FITC-dextran in the

(Continued)

FIGURE 4 | presence of recombinant proteins in the presence or absence of PMIs and visualized under the confocal microscope. PMI treatment inhibited phalloidin staining and dextran entry into the erythrocytes. The phalloidin positive erythrocytes were counted under the microscope for different treatments and their relative percentage was plotted. Error bar represents SD (*$p < 0.05$; **$p < 0.01$). **(D)** Inhibition of PMD binding to erythrocyte membrane in the presence of PMI. Western blot was performed to detect the effect of PMIs on the binding of rPMD2 to the erythrocyte membrane. Membrane Palmitoylated Protein 1 (MPP1) was taken as the initial erythrocytes loading control. The relative band intensity of bound rPMD2 was analyzed using Image J. Error bar represents SD (**$p < 0.01$). **(E)** Erythrocytes were treated with rPMD2 in the presence and absence of PMIs and pore formation was observed under the AFM ($n = 2$). (ii) The PMD treated erythrocytes demonstrate the formation of pores on the erythrocyte surface. The line profile further depicts the roughness of erythrocytes. The PMD treated erythrocytes (iii, iv) in the presence of PMIs does not demonstrate the formation of pores and the surface roughness was also reduced to normal erythrocytes (i).

plays a role in gametocyte egress (Deligianni et al., 2013; Wirth et al., 2015) and hence the effect of PMI was monitored during this stage. The egress efficiency of male gametocytes, as revealed by counting exflagellation centers, was markedly reduced following PMI treatment (**Figure 5F**). To test the inhibitory effect of PMI on sporozoite infection, we infected HepG2 cells with *P. berghei* sporozoites treated with different concentrations of PMI for 72 h. The sporozoite infection was scored using real-time PCR analysis. As shown (**Figure 5G**), both compounds displayed an inhibitory effect toward *P. berghei* sporozoites. Both the compounds showed no defect in the viability of HepG2 cells suggesting the specific effect toward sporozoite but not host (**Figure S7D**).

Together, this suggests the cross-stage anti-malarial activity of PMIs which can be further exploited to deliver both symptomatic and transmission-blocking cure for the disease.

DISCUSSION

Despite abundant evidence that PPLPs are crucial for the life cycle progression of malaria parasites, the development of chemotherapeutic interventions against them has not been explored. In the blood stage of *P. falciparum*, PfPLP1 and PfPLP2 create pores on the erythrocyte membrane that help in the exit of merozoites (Garg et al., 2013). For the development of pan-active anti-PLP therapeutics, we first identified central, pan-active motif of PfPLPs, PMD domain, that is highly conserved across all *Plasmodium* spp (**Figure S3**) and oligomerize on host membranes to create pores (Pipkin and Lieberman, 2007; Baran et al., 2009). To visualize pore formation at physiological relevance, AFM was performed with a modified protocol to overcome the limitations associated with the non-adherent, rough cell surface of erythrocyte. The modified protocol could successfully demonstrate that rPMD2 drilled pores of 10.55 nm $\pm$ 3.22 nm height and 24.33 $\pm$ 7.42 nm width on the erythrocytes (**Figure 1H**). The characteristics of the pore formed by PfPLP are similar to earlier reported eukaryotic PFPs which form smaller pores as compared to prokaryotic PFPs which form larger pores (Metkar et al., 2015). The three-dimensional topology not only confirmed the presence of well-defined pores but also revealed that the rPMD2 treated erythrocyte surface is much rougher and more uneven as compared to the untreated erythrocytes (**Figure 1H**i,ii). The roughness of erythrocytes reflects its innate response toward any non-physiological, toxic agent which in this case is rPMD2. This information about the cellular response is usually missed in other studies where they studied pore formation on model membranes.

Given the multi-step process of pore formation by PLP, there exist multiple stages at which a PLP can be targeted for inhibition. The designed PMIs strongly bind to the PMD domain and inhibits its pore forming activity by restricting the initial attachment of the monomer to the erythrocyte surface (**Figure 4D**). The decreased binding of monomer inhibits the oligomerization of PMD to form pores confirming that PMIs completely abrogated the activity of PfPLPs. Ring stage parasites treated with PMIs progresse to schizonts without any growth defect, but the mature parasites could not egress and re-invade to new erythrocyte (**Figures 5A,C,D**). This finding is in line with the role of PfPLPs in schizont egress and merozoite invasion and suggests that PMIs are not showing any off-target effect *in vivo*. Furthermore, PMIs inhibited gametogenesis and sporozoite infection to HepG2 cells validating their potential in blocking the transmission of malaria parasites (**Figures 5F,G**). The invasion inhibitory activity of PMIs against sporozoite of *P. berghei* is suggestive of their cross-species activity due to evolutionary conservation and high similarity of PMDs. These scaffolds could be improved for their efficacy and development of better antimalarials.

In this study, we further propose that the secretion of PfPLPs in the blood leads to the formation of pores on bystander erythrocytes leading to their premature senescence and identifies it as one of the probable cause for anemia in severe malaria. This phenomenon was similar to earlier reports where it has been shown that binding of some parasite proteins to erythrocytes leads to anemia (Haldar and Mohandas, 2009; Gómez et al., 2011). But the mechanistic role underlying the induction of anemia remains to be fully elucidated. However, our data defines that the smaller pores created by PfPLPs induce calcium influx (**Figure 2A**-a) in erythrocytes leading to phosphatidylserine exposure (**Figure 2B**), as a signal for recognition by macrophages. This is in line with earlier studies that have demonstrated that an increase in intracellular calcium induces premature senescence of erythrocytes (Rettig et al., 1999; Arashiki et al., 2013).

The enhanced oxidative stress in erythrocyte senescence is represented by the formation of the oxidized form of hemoglobin, i.e., methemoglobin (**Figures 2D,E**) (Umbreit, 2007; Pamplona et al., 2009). The increased levels of methemoglobin *in vivo* are toxic to the plasma lipoproteins, endothelial cells, and other vascular organs. Therefore, the erythrocytes with increased methemoglobin concentrations are cleared from the body through spleen which is a cause of anemia in methemoglobinemia (Wagener et al., 2001; Umbreit, 2007). The presence of Fe^{3+} heme form in methemoglobin causes

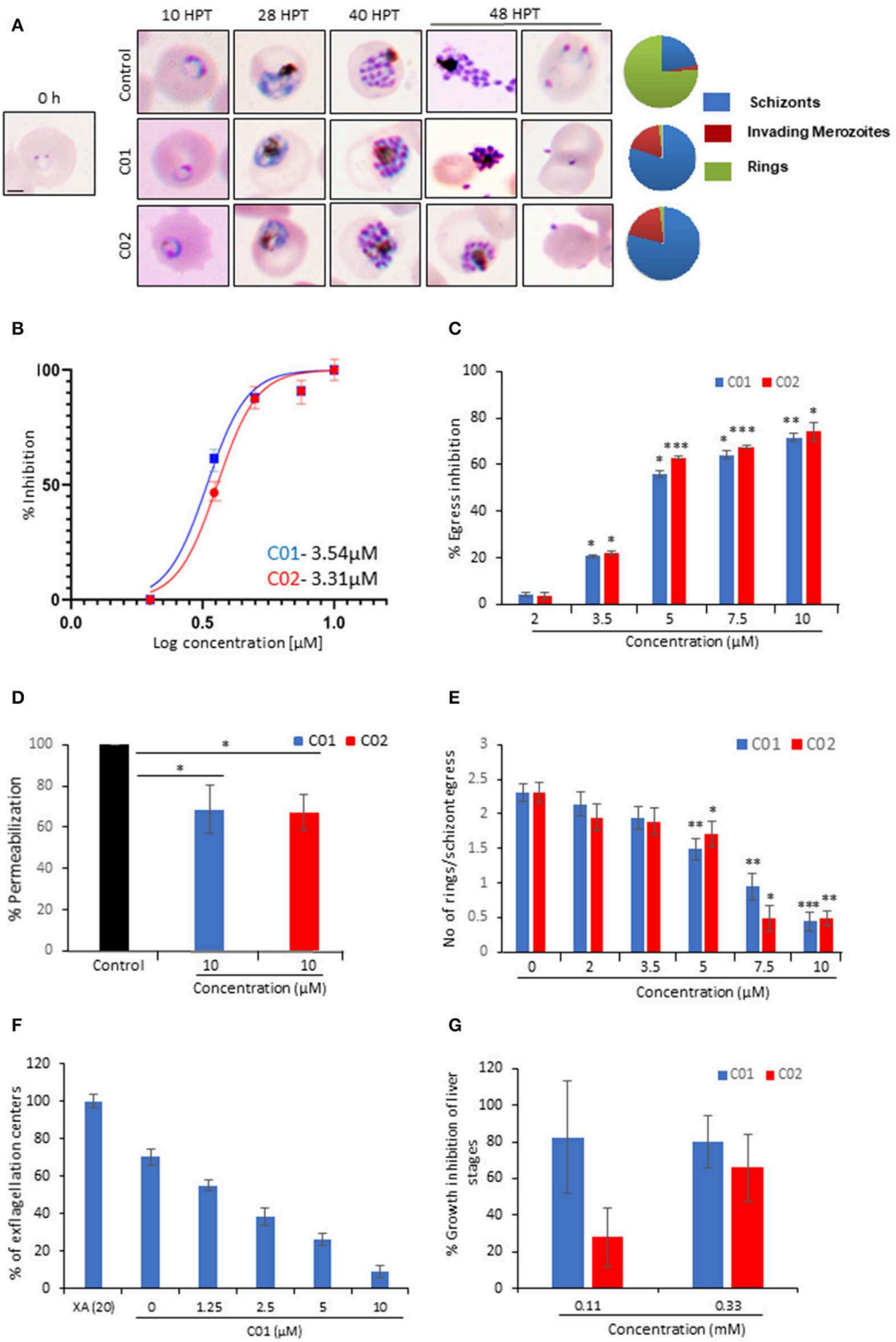

FIGURE 5 | C01 and C02 show multistage inhibition. **(A)** Images of Giemsa stained smears of PMI treated (10 μM) and untreated parasites. Early rings were treated with PMIs and smears were prepared 10, 28, 40, and 48 h post-treatment (HPT). Pie charts show relative proportions of schizonts, invading merozoites and rings. **(B)** C01 and C02 inhibit the *in vitro* growth of *P. falciparum*. The effect of PMIs on growth inhibition of *P. falciparum* was evaluated after one cycle of parasite growth ($n = 3$). Scale bar represents 2 μm. **(C)** Late-stage schizonts were treated with different concentrations of compounds. The relative inhibition in egress was calculated by

(Continued)

FIGURE 5 | counting the number of remaining schizonts after 7 h of treatment as compared to control ($n = 3$). Error bar represents SD (*$p < 0.05$; **$p < 0.01$; ***$p < 0.005$). **(D)** Permeabilization of PMI-treated schizonts was measured by flow cytometry using Phalloidin. Error bar represents SD (*$p < 0.05$). **(E)** Late-stage schizonts were treated with different concentrations of PMIs. The ability to form rings per schizont egress was calculated by counting the number of schizonts and rings after 7 h using Giemsa stained smears ($n = 3$). Error bar represents SD (*$p < 0.05$; **$p < 0.01$; ***$p < 0.005$). **(F)** Treatment of male gametocytes with PMIs inhibits exflagellation. The number of exflagellation centers was scored 15 min post-activation in 30 optical fields at 40X magnification by light microscopy. Exflagellation efficiency of PMI treated vs. untreated gametocytes is shown ($n = 2$). **(G)** HepG2 cells were infected with *P. berghei* sporozoites and treated with PMIs. Parasite growth was assessed after 51 h via real-time PCR using *P. berghei* 18S rRNA specific primers. Parasite growth inhibition was calculated by dividing the 18S rRNA copy number of the experimental group by that of the untreated control group. The fraction obtained was then converted into % inhibition (with respect to untreated as 100%) ($n = 2$).

changes in pyrrole ring breathing and asymmetrical pyrrole half-ring stretching vibrations (Dybas et al., 2018). Using Raman spectroscopy, we could detect the presence of these metabolic signatures in erythrocytes after 48 h of PfPLP treatment representing the formation of methemoglobin (**Figure 2E**). The earlier clinical reports advocate the identification of elevated levels of methemoglobin in severe malaria and directly correlates it with the death of patients (Behera et al., 2016). Our study supports the role of PfPLP in inducing premature senescence of erythrocytes leading to anemia in severe malaria.

Taken together, we identified novel pharmacological inhibitors against PPLPs that can preserve the cell membrane integrity and viability of all host cells and thus aid in facilitating parasite elimination by preventing further infection. Also, the proposed therapy can also be used as anti-virulence therapy along with routine medication for improving treatment outcomes. Since the anti-virulence strategies do not focus on directly killing the pathogen, the parasite is not under the selective pressure of resistance development. Therefore, our study lends weight for the development of novel pharmacological approaches against malaria to not only cure the disease but also ameliorate disease pathogenesis in clinical conditions.

DATA AVAILABILITY STATEMENT

The raw data supporting the conclusions of this article will be made available by the authors, without undue reservation, to any qualified researcher.

AUTHOR CONTRIBUTIONS

AS and SG performed the recombinant protein and inhibitors based *in vitro* and *in vivo* assays. SSe and CB synthesized and characterized the inhibitors. RH helped to design and perform *in vitro P. falciparum* assays. SP and RA performed the *in silico* experiments and data analysis. SG, AS, APS, and IK performed the liver stage inhibition assay. SSi performed the gametocyte inhibition assay. SSi and SG conceived and designed the experiments. AS, SG, APS, and SSi analyzed the data and wrote the manuscript. All the authors commented on the manuscript.

FUNDING

Funding from Science and Engineering Research Board (SERB), Drug and Pharmaceuticals Research Program (DPRP) (Project No. P/569/2016-1/TDT) and the National Bioscience Award from DBT for SS is acknowledged. The funders had no role in study design, data collection and analysis, decision to publish or preparation of the manuscript.

ACKNOWLEDGMENTS

AS, RH, RA, and CB, are supported by the Shiv Nadar University fellowship. SG is a recipient of the DST Inspire faculty award. SP is grateful for the support from the Shiv Nadar Foundation. The authors would like to thank AIRF for access to live-cell microscopy, AFM and Raman facilities at JNU. This manuscript has been released as a Pre-Print at bioRxiv (doi: 10.1101/756197) (Garg et al., 2019).

SUPPLEMENTARY MATERIAL

The Supplementary Material for this article can be found online at: https://www.frontiersin.org/articles/10.3389/fcimb.2020.00121/full#supplementary-material

REFERENCES

Alaganan, A., Singh, P., and Chitnis, C. E. (2017). Molecular mechanisms that mediate invasion and egress of malaria parasites from red blood cells. *Curr. Opin. Hematol.* 3, 208–214. doi: 10.1097/MOH.0000000000000334

Arashiki, N., Kimata, N., Manno, S., Mohandas, N., and Takakuwa, Y. (2013). Membrane peroxidation and methemoglobin formation are both necessary for band 3 clustering: mechanistic insights into human erythrocyte senescence. *Biochemistry* 52, 5760–5769. doi: 10.1021/bi400405p

Baran, K., Dunstone, M., Chia, J., Ciccone, A., Browne, K. A., Clarke, C. J. P., et al. (2009). The molecular basis for perforin oligomerization and transmembrane pore assembly. *Immunity* 30, 684–695. doi: 10.1016/j.immuni.2009.03.016

Barkur, S., Mathur, D., and Chidangil, S. (2018). A laser raman tweezers study of eryptosis. *J. Raman Spectrosc.* 49, 1155–1164. doi: 10.1002/jrs.5361

Behera, G. C., Behera, S. K., Jena, R. K., and Bharati, V. S. (2016). Study of methaemoglobin in malaria patients. *Indian J. Hematol. Blood Transfus.* 32, 100–103. doi: 10.1007/s12288-015-0522-5

Brown, G. C., and Neher, J. J. (2012). Eaten alive! cell death by primary phagocytosis: "Phagoptosis." *Trends Biochem. Sci.* 37, 325–32. doi: 10.1016/j.tibs.2012.05.002

Callahan, M. K., Halleck, M. S., Krahling, S., Henderson, A. J., Williamson, P., and Schlegel, R. A. (2003). Phosphatidylserine expression and phagocytosis of apoptotic thymocytes during differentiation of monocytic cells. *J. Leukoc. Biol.* 74, 846–856. doi: 10.1189/jlb.0902433

Deligianni, E., Morgan, R. N., Bertuccini, L., Wirth, C. C., Silmon de Monerri, N. C., Spanos, L., et al. (2013). A perforin-like protein mediates disruption of the erythrocyte membrane during egress of *Plasmodium berghei* male gametocytes. *Cell. Microbiol.* 15, 1438–1455. doi: 10.1111/cmi.12131

Dybas, J., Grosicki, M., Baranska, M., and Marzec, K. M. (2018). Raman imaging of heme metabolism: *in situ* in macrophages and Kupffer cells. *Analyst*. 143, 3489–3498. doi: 10.1039/C8AN00282G

Ecker, A., Pinto, S. B., Baker, K. W., Kafatos, F. C., and Sinden, R. E. (2007). Plasmodium berghei: plasmodium perforin-like protein 5 is required for mosquito midgut invasion in *Anopheles stephensi*. *Exp. Parasitol.* 116, 504–508. doi: 10.1016/j.exppara.2007.01.015

Frostell, Å., Vinterbäck, L., and Sjöbom, H. (2013). Protein-ligand interactions using SPR systems. *Methods Mol. Biol.* 1008, 139–165. doi: 10.1007/978-1-62703-398-5_6

Garg, S., Agarwal, S., Kumar, S., Shams Yazdani, S., Chitnis, C. E., and Singh, S. (2013). Calcium-dependent permeabilization of erythrocytes by a perforin-like protein during egress of malaria parasites. *Nat. Commun.* 4:1736. doi: 10.1038/ncomms2725

Garg, S., Sharma, V., Ramu, D., and Singh, S. (2015). *In silico* analysis of calcium binding pocket of perforin like protein 1: insights into the regulation of pore formation. *Syst. Synth. Biol.* 9(Suppl.1):17–21. doi: 10.1007/s11693-015-9166-x

Garg, S., Shivappagowdar, A., Hada, R. S., Ayana, R., Bathula, C., Sen, S., et al. (2019). Supression of perforin-like protein pores inhibit *plasmodium* multistage-growth, transmission and erythrocyte senescence. *bioRxiv* 756197. doi: 10.1101/756197

Gaur, D., Singh, S., Singh, S., Jiang, L., Diouf, A., and Miller, L. H. (2007). Recombinant *Plasmodium falciparum* reticulocyte homology protein 4 binds to erythrocytes and blocks invasion. *Proc. Natl. Acad. Sci. U. S. A.* 104, 17789–17794. doi: 10.1073/pnas.0708772104

Gilbert, R. J. C., Stansfeld, P. J., Harlos, K., Ni, T., Rezelj, S., Williams, S. I., et al. (2018). Structures of monomeric and oligomeric forms of the *Toxoplasma gondii* perforin-like protein 1. *Sci Adv.* 4:eaaq0762. doi: 10.1126/sciadv.aaq0762

Gómez, N. D., Safeukui, I., Adelani, A. A., Tewari, R., Reddy, J. K., Rao, S., et al. (2011). Deletion of a malaria invasion gene reduces death and anemia, in model hosts. *PLoS ONE* 6:e25477. doi: 10.1371/journal.pone.0025477

Hadders, M. A., Beringer, D. X., and Gros, P. (2007). Structure of C8alpha-MACPF reveals mechanism of membrane attack in complement immune defense. *Science* 317, 1552–1554. doi: 10.1126/science.1147103

Haldar, K., and Mohandas, N. (2009). Malaria, erythrocytic infection, and anemia. *Hematol. Am. Soc. Hematol. Educ. Program* 2009, 87–93. doi: 10.1182/asheducation-2009.1.87

Hashimoto, M., Girardi, E., Eichner, R., and Superti-Furga, G. (2018). Detection of chemical engagement of solute carrier proteins by a cellular thermal shift assay. *ACS Chem. Biol.* 13, 1480–1486. doi: 10.1021/acschembio.8b00270

Ishino, T., Chinzei, Y., and Yuda, M. (2005). A *Plasmodium sporozoite* protein with a membrane attack complex domain is required for breaching the liver sinusoidal cell layer prior to hepatocyte infection. *Cell. Microbiol.* 7, 199–208. doi: 10.1111/j.1462-5822.2004.00447.x

Jafari, R., Almqvist, H., Axelsson, H., Ignatushchenko, M., Lundbäck, T., Nordlund, P., et al. (2014). The cellular thermal shift assay for evaluating drug target interactions in cells. *Nat. Protoc.* 9, 2100–2122. doi: 10.1038/nprot.2014.138

Kadota, K., Matsuyama, T., Ishino, T., Yuda, M., and Chinzei, Y. (2004). From the cover: essential role of membrane-attack protein in malarial transmission to mosquito host. *Proc. Natl. Acad. Sci. U. S. A.* 101, 16310–16315. doi: 10.1073/pnas.0406187101

Kafsack, B. F. C., Pena, J. D. O., Coppens, I., Ravindran, S., Boothroyd, J. C., and Carruthers, V. B. (2009). Rapid membrane disruption by a perforin-like protein facilitates parasite exit from host cells. *Science* 323, 530–533. doi: 10.1126/science.1165740

Kataoka, T., Taniguchi, M., Yamada, A., Suzuki, H., Hamada, S., Magae, J., et al. (1996a). Identification of low molecular weight probes on perforin- and fas-based killing mediated by cytotoxic T lymphocytes. *Biosci. Biotechnol. Biochem.* 60, 1726–1728. doi: 10.1271/bbb.60.1726

Kataoka T., Shinohara N., Takayama H., Takaku K., Kondo S., Yonehara S., et al. (1996b). Concanamycin A, a powerful tool for characterization and estimation of contribution of perforin-and Fas-based lytic pathways in cellmediated cytotoxicity. *J Immunol.* 156, 3678–3686.

Lasonder, E., Ishihama, Y., Andersen, J. S., Vermunt, A. M. W., Pain, A., Sauerwein, R. W., et al. (2002). Analysis of the *Plasmodium falciparum* proteome by high-accuracy mass spedrometry. *Nature* 419, 537–542. doi: 10.1038/nature01111

Lena, G., Trapani, J. A., Sutton, V. R., Ciccone, A., Browne, K. A., Smyth, M. J., et al. (2008). Dihydrofuro[3,4-c]pyridinones as inhibitors of the cytolytic effects of the pore-forming glycoprotein perforin. *J. Med. Chem.* 51, 7614–7624. doi: 10.1021/jm801063n

Metkar, S. S., Marchioretto, M., Antonini, V., Lunelli, L., Wang, B., Gilbert, R. J., et al. (2015). Perforin oligomers form arcs in cellular membranes: a locus for intracellular delivery of granzymes. *Cell Death Differ.* 22, 74–85. doi: 10.1038/cdd.2014.110

Miller, C. K., Huttunen, K. M., Denny, W. A., Jaiswal, J. K., Ciccone, A., Browne, K. A., et al. (2016). Diarylthiophenes as inhibitors of the pore-forming protein perforin. *Bioorg. Med. Chem. Lett.* 26, 355–360. doi: 10.1016/j.bmcl.2015.12.003

Pamplona, A., Hanscheid, T., Epiphanio, S., Mota, M. M., and Vigário, A. M. (2009). Cerebral malaria and the hemolysis/methemoglobin/heme hypothesis: shedding new light on an old disease. *Int. J. Biochem. Cell Biol.* 41, 711–716. doi: 10.1016/j.biocel.2008.09.020

Pipkin, M. E., and Lieberman, J. (2007). Delivering the kiss of death: progress on understanding how perforin works. *Curr. Opin. Immunol.* 19, 301–308. doi: 10.1016/j.coi.2007.04.011

Ramu, D., Garg, S., Ayana, R., Keerthana, A. K., Sharma, V., Saini, C. P., et al. (2017). Novel β-carboline-quinazolinone hybrids disrupt *Leishmania donovani* redox homeostasis and show promising antileishmanial activity. *Biochem. Pharmacol.* 129, 26–42. doi: 10.1016/j.bcp.2016.12.012

Rettig, M. P., Low, P. S., Gimm, J. A., Mohandas, N., Wang, J., and Christian, J. A. (1999). Evaluation of biochemical changes during *in vivo* erythrocyte senescence in the dog. *Blood* 93, 376–384. doi: 10.1182/blood.V93.1.376.401k41_376_384

Rosado, C. J., Buckle, A. M., Law, R. H. P., Butcher, R. E., Kan, W. T., Bird, C. H., et al. (2007). A common fold mediates vertebrate defense and bacterial attack. *Science* 317, 1548–1551. doi: 10.1126/science.1144706

Spicer, J. A., Lena, G., Lyons, D. M., Huttunen, K. M., Miller, C. K., O'Connor, P. D., et al. (2013). Exploration of a series of 5-arylidene-2-thioxoimidazolidin-4-ones as inhibitors of the cytolytic protein perforin. *J. Med. Chem.* 56, 9542–9555. doi: 10.1021/jm401604x

Tavares, J., Amino, R., and Ménard, R. (2014). The role of MACPF proteins in the biology of malaria and other apicomplexan parasites. *Subcell. Biochem.* 80, 241–253. doi: 10.1007/978-94-017-8881-6_12

Trager, W., and Jensen, J. B. (1976). Human malaria parasites in continuous culture. *Science* 193:673–675. doi: 10.1126/science.781840

Umbreit, J. (2007). Methemoglobin—it's not just blue: a concise review. *Am. J. Hematol.* 82, 134–144. doi: 10.1002/ajh.20738

Voskoboinik, I., Thia, M. C., Fletcher, J., Ciccone, A., Browne, K., Smyth, M. J., et al. (2005). Calcium-dependent plasma membrane binding and cell lygis by perforin are mediated through its C2 domain: a critical role for aspartate residues 429, 435, 483, and 485 but not 491. *J. Biol. Chem.* 280, 8426–8434. doi: 10.1074/jbc.M413303200

Vuignier, K., Schappler, J., Veuthey, J. L., Carrupt, P. A., and Martel, S. (2010). Drug-protein binding: a critical review of analytical tools. *Anal. Bioanal. Chem.* 398, 53–66. doi: 10.1007/s00216-010-3737-1

Wagener, F. A., Eggert, A., Boerman, O. C., Oyen, W. J., Verhofstad, A., Abraham, N. G., et al. (2001). Heme is a potent inducer of inflammation

in mice and is counteracted by heme oxygenase. *Blood* 98, 1802–1811. doi: 10.1182/blood.V98.6.1802

WHO (2018). *World Malaria Report 2018*. Geneva: World Health Organization.

Wirth, C. C., Bennink, S., Scheuermayer, M., Fischer, R., and Pradel, G. (2015). Perforin-like protein PPLP4 is crucial for mosquito midgut infection by *Plasmodium falciparum*. *Mol. Biochem. Parasitol.* 201, 90–99. doi: 10.1016/j.molbiopara.2015.06.005

Wirth, C. C., Glushakova, S., Scheuermayer, M., Repnik, U., Garg, S., Schaack, D., et al. (2014). Perforin-like protein PPLP2 permeabilizes the red blood cell membrane during egress of *Plasmodium falciparum* gametocytes. *Cell. Microbiol.* 16, 709–733. doi: 10.1111/cmi.12288

Yang, A. S. P., O'Neill, M. T., Jennison, C., Lopaticki, S., Allison, C. C., Armistead, J. S., et al. (2017). Cell traversal activity is important for *Plasmodium falciparum* liver infection in humanized mice. *Cell Rep.* 18, 3105–3116. doi: 10.1016/j.celrep.2017.03.017

Conflict of Interest: The authors declare that the research was conducted in the absence of any commercial or financial relationships that could be construed as a potential conflict of interest.

frontiers in Microbiology

MINI REVIEW
published: 02 July 2020
doi: 10.3389/fmicb.2020.01543

Pneumolysin: Pathogenesis and Therapeutic Target

*Andrew T. Nishimoto, Jason W. Rosch and Elaine I. Tuomanen**

Department of Infectious Disease, St. Jude Children's Research Hospital, Memphis, TN, United States

Streptococcus pneumoniae is an opportunistic pathogen responsible for widespread illness and is a major global health issue for children, the elderly, and the immunocompromised population. Pneumolysin (PLY) is a cholesterol-dependent cytolysin (CDC) and key pneumococcal virulence factor involved in all phases of pneumococcal disease, including transmission, colonization, and infection. In this review we cover the biology and cytolytic function of PLY, its contribution to *S. pneumoniae* pathogenesis, and its known interactions and effects on the host with regard to tissue damage and immune response. Additionally, we review statins as a therapeutic option for CDC toxicity and PLY toxoid as a vaccine candidate in protein-based vaccines.

Keywords: *Streptococcus pneumoniae*, pneumococcus, pneumolysin, cholesterol-dependent cytolysin, invasive pneumococcal disease, vaccine

OPEN ACCESS

Edited by:
George P. Munson, University of Miami Leonard M. Miller School of Medicine, United States

Reviewed by:
Carlos J. Orihuela, University of Alabama at Birmingham, United States
James C. Paton, The University of Adelaide, Australia
Jianfeng Wang, Jilin University, China
Lucy Hathaway, University of Bern, Switzerland

****Correspondence:***
Elaine I. Tuomanen
elaine.tuomanen@stjude.org

Specialty section:
This article was submitted to Infectious Diseases, a section of the journal Frontiers in Microbiology

Received: *14 May 2020*
Accepted: *15 June 2020*
Published: *02 July 2020*

Citation:
Nishimoto AT, Rosch JW and Tuomanen EI (2020) Pneumolysin: Pathogenesis and Therapeutic Target. Front. Microbiol. 11:1543. doi: 10.3389/fmicb.2020.01543

INTRODUCTION

Streptococcus pneumoniae is a commensal organism responsible for a wide array of disease and is the source of considerable morbidity and mortality. Able to colonize the nasopharynx of adults and more frequently of children, *S. pneumoniae* manifests as infections of the ear, respiratory tract, and even severe, life-threatening sepsis and meningitis. The cholesterol-dependent cytolysin (CDC) pneumolysin (PLY), is critical at many steps of pneumococcal disease, working in concert with adhesins, invasins, and proteases to achieve pathogenesis (Cundell et al., 1995; Zhang et al., 2000; Radin et al., 2005; Orihuela et al., 2009). Consequently, PLY's effects in the body are numerous and diverse – contributing to inflammation and bacterial penetration, causing direct damage to cells through pore-forming cytolytic activity, aiding bacterial escape through blocking complement activation, and being a key factor in host-to-host pneumococcal transmission (Berry et al., 1989b; Rayner et al., 1995; Berry and Paton, 2000; Alcantara et al., 2001; Rogers et al., 2003; Mitchell and Dalziel, 2014; Zafar et al., 2017). Recognizing the multifaceted role of PLY in host-pathogen interactions is therefore paramount to better understand pneumococcal infection and address it as a therapeutic target.

BIOLOGY OF PNEUMOLYSIN

Pneumolysin is a 471 amino acid CDC whose properties and characteristics have been closely studied since the early 20th century (Neill, 1926; Cohen et al., 1942; Walker et al., 1987). Structurally, PLY has four functional domains, which were initially attributed based on sequence similarity to the bacterial pore-forming toxin perfringolysin from *Clostridium perfringens* (Kelly and Jedrzejas, 2000a,b). Domains 1 and 3 are linked via domain 2 to the membrane-sensing C-terminal domain 4 (Lawrence et al., 2015; Marshall et al., 2015). Like other CDCs, PLY

contains the highly conserved undecapeptide sequence known as the tryptophan-rich loop and a threonine-leucine amino acid pair involved in membrane-bound cholesterol recognition and binding (Nollmann et al., 2004; Farrand et al., 2010).

During the course of pore-formation, PLY monomers bind to the targeted cell membrane and interact with other PLY molecules, packing side-by-side to form the pre-pore complex (Marshall et al., 2015) (**Figure 1**). After undergoing further conformational changes, the final ring-like pore of roughly 30–50 PLY subunits inserts into the membrane (Tilley et al., 2005). These pore and pre-pore formations at the cell membrane are initially shed in toxin-induced microvesicules as a mechanism of repair, with cytotoxic effects occurring via dysregulation of cell homeostasis through influx of calcium (Wolfmeier et al., 2016). Repeated insertion of numerous pore-forming PLY complexes can result in membrane destabilization, loss of ion homeostasis, and ultimately cell death. Intracellular calcium influx via formed pores at the cell membrane can trigger changes in host cell mitochondrial membrane ultrastructure, loss of mitochondrial membrane potential and release of mitochondrial apoptosis-inducing factor (Braun et al., 2007; Nerlich et al., 2018). In addition, PLY can induce double-strand breaks in cellular DNA resulting in loss of genomic integrity and further cytotoxicity (Rai et al., 2016). As will be discussed, PLY's effects extend beyond cell damage and death, altering cells, cell components, and their respective functions to modulate and facilitate transmission, invasion, and colonization.

While it is popularly accepted that cholesterol is a PLY cellular receptor, this has not been definitively demonstrated with intact pneumococcal cells. Early studies observed PLY inhibition in the presence of cholesterol (Walker et al., 1987), possibly due to saturation of binding sites on PLY, indicating that membrane cholesterol may be the target receptor as suggested for other CDCs (Watson et al., 1972). Furthermore, cholesterol was shown to have specific 1:1 stoichiometric interactions with PLY and to be required for PLY hemolytic activity (Nollmann et al., 2004). Recent investigations studied lipid–lipid and lipid–protein interactions at different pore-forming stages of PLY upon exposure to cholesterol-containing liposomes. Gradual decreases in membrane order and increases in rotational diffusion of the lipids during pre-pore oligomerization stages but not during PLY oligomer binding and insertion into the membrane have been described (Faraj et al., 2020). Some evidence suggests that PLY-membrane cholesterol interactions may have more to do with toxin activation than cell binding (Soltani et al., 2007). Notably, PLY has been shown to interact with cellular glycolipid receptors at the surface of human red blood cells, supporting growing evidence that pore-forming toxins possess non-cholesterol receptors (Shewell et al., 2014).

Pneumolysin is not actively secreted by *S. pneumoniae* owing to a lack of an N-terminal secretion signal (Walker et al., 1987). It is the only member of the CDC class to behave in this manner, though interestingly this trait is universally conserved across pneumococci (Martner et al., 2008). While it was thought that PLY relied on the pneumococcal autolysin LytA and cellular autolysis for release (Berry et al., 1989a; Canvin et al., 1995), it was later revealed that the amount of extracellular PLY released by a *lytA*-mutant was comparable to the wildtype strain (Balachandran et al., 2001) and that PLY release can occur in early growth phases when the autolytic cascade is inactive (Benton et al., 1997) In the absence of autolysis, PLY localizes to the cell wall (Price and Camilli, 2009). Furthermore, domain 2 is required for PLY export to the cell wall compartment, and interestingly fusion of a secretion signal sequence to PLY did not result in detectable release of PLY protein (Price et al., 2012). While factors such as pyruvate oxidase enhance PLY release, possibly via intracellular H_2O_2-dependent mechanisms, *S. pneumoniae* may also modulate the release of PLY exported to the cell wall based on the composition of branched stem peptides and choline-binding proteins in the peptidoglycan cell wall network, and peptidoglycan remodeling by hydrolases may contribute to PLY release (Greene et al., 2015; Bryant et al., 2016).

PNEUMOLYSIN IN HOST TISSUE INJURY

The pneumococcus is a highly successful pathogen that infects the middle ear, lungs, blood, heart, and brain. In the host, PLY works on multiple levels to facilitate invasion by contributing to direct cell damage and escape from the host's immune system. It has long been known that PLY exhibits cytotoxic activity for virtually every cell type in the body. Lung endothelial cells as well as nasal and tracheobronchial epithelial cells are damaged as a result of pore-forming activity (Steinfort et al., 1989; Rubins et al., 1992; Rayner et al., 1995). Mutants lacking PLY fail to induce lung mucosal damage (Rubins et al., 1995). Acute lung injury has also been attributed to PLY's effects on specific host factors, such as the increased release of platelet activating factor, which contributes to proinflammatory actions, increased vascular permeability, and vasoconstriction (Witzenrath et al., 2007). Pneumolysin can activate platelets *in vitro* via calcium influx due to sub-lytic pore formation, which may similarly potentiate lung inflammation (Nel et al., 2016).

In addition to the lung, invasive pneumococcal disease can also lead to cardiac pathologies. For example, intraperitoneal injections into mice with *S. pneumoniae* led to microlesions in the ventricular myocardium, indicating bacterial translocation into the heart (Brown et al., 2014). Fluorescence microscopy showed that PLY localized to these microlesions and induced cardiomyocyte injury (Alhamdi et al., 2015). Furthermore, even sub-lytic PLY concentrations induced cardiomyocyte dysfunction via calcium influx and a resulting reduction in contractility.

Pneumolysin plays a key role in pathogenesis of pneumococcal meningitis by facilitating bacterial crossing of the blood-brain barrier. *In vitro* models using human and bovine brain microvascular endothelial cells indicated that PLY induces loss of tight junctions, and this endothelial cell damage may contribute to bacterial translocation (Ring et al., 1998; Zysk et al., 2001). Additionally, PLY-induced remodeling of brain tissue through astrocyte reorganization, in combination with interstitial fluid retention, may promote bacterial invasion (Hupp et al., 2012). Pneumolysin released in the CSF directly damages the ependymal cells lining the ventricles of the brain, resulting in loss of cilia and reduction in ciliary beat frequency indicative of decreased

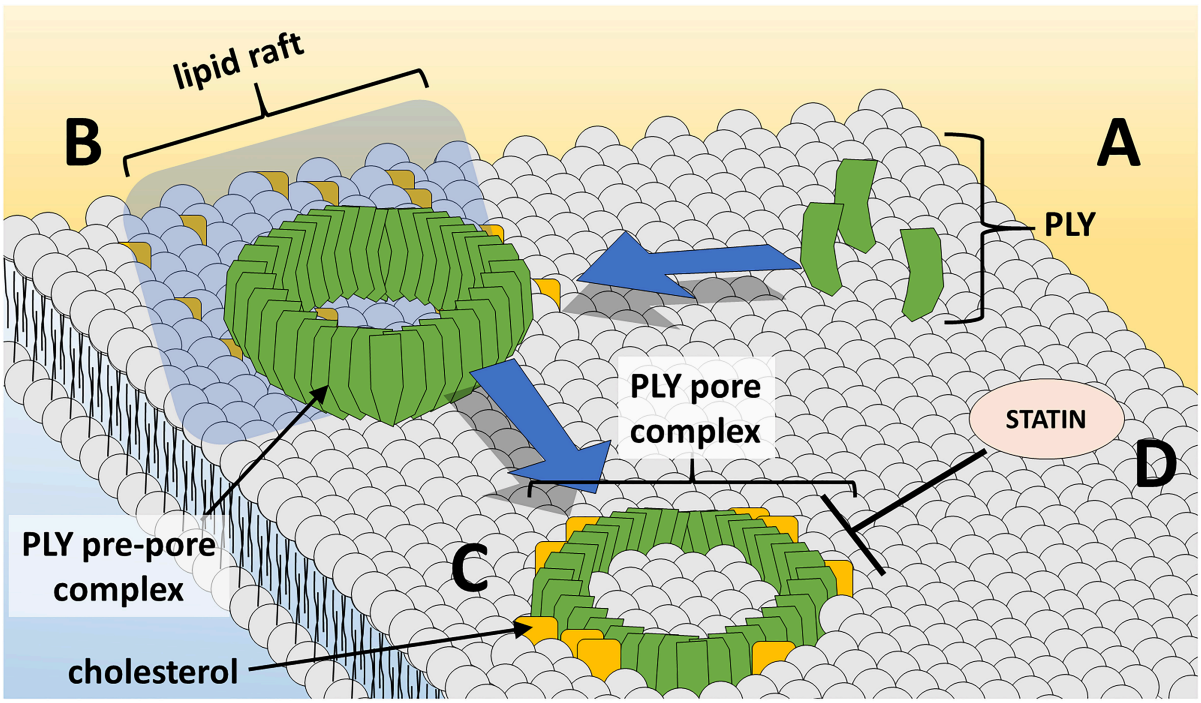

FIGURE 1 | PLY pore formation at the host cell membrane. **(A)** PLY monomers gather at cholesterol-rich lipid rafts at the cell membrane and **(B)** assemble in the ring-shaped pre-pore complex. **(C)** Insertion of the PLY pore-forming complex into lipid bilayer results in loss of membrane integrity and cell damage/death. **(D)** Statin medications oppose PLY-induced pore-formation at the cell membrane.

cell viability and flow of cerebrospinal fluid (Mohammed et al., 1999; Hirst et al., 2000a). Subsequently, additional studies have demonstrated that PLY-deficient strains possessed decreased virulence in murine meningitis and, in rabbit models, decreased hippocampal damage via neuronal apoptosis (Braun et al., 2002; Wellmer et al., 2002).

Pneumolysin additionally affects pathogenesis in acute otitis media. Using chinchilla otitis models, the PLY deletion mutant yielded a reduced recovery of bacteria from middle ear fluid and reduced biofilm formation (Keller et al., 2016). Pneumolysin deletion resulted in reduced pathological changes to the round window membrane and less recovered bacteria from middle ear effusions, supporting PLY's role in virulence during middle ear infections (Schachern et al., 2013).

Pneumolysin demonstrates not only cytolytic activity, but direct interference with host responses. Pneumolysin shows complement-activating and complement consumption properties that divert opsonization and subsequent phagocytosis of intact pneumococcal cells (Paton et al., 1984; Mitchell et al., 1991; Rubins et al., 1995). An early *in vitro* study showed that PLY inhibited polymorphonuclear leukocytes by interfering with opsonization, reducing respiratory burst response and decreasing leukocyte migratory ability (Paton and Ferrante, 1983). Within the lungs, PLY acts to help *S. pneumoniae* escape detection via creating a refuge inside dendritic cells. At low doses, PLY binds to the mannose receptor C type 1 (MRC-1) on dendritic cells and, in addition to inhibiting proinflammatory cytokine release, causes dendritic cells to internalize *S. pneumoniae* (Subramanian et al., 2019). Pneumolysin's interaction with MRC-1 also inhibits pneumococcal-infected vacuoles from fusing with lysosomes, promoting intracellular pneumococcal survival (Subramanian et al., 2019).

It is especially important to note that many murine studies may underestimate the actual contributions of PLY to pathogenesis. Compared to human serum, pooled mouse serum had a greater ability (62-fold vs. >3000-fold change in EC_{50}) to inhibit PLY hemolytic activity (Wade et al., 2014). Closer inspection revealed that cholesterol carried by mouse ApoB-100 lipoprotein, but not human ApoB-100, possessed potent PLY inhibitory activity, causing premature pore formation and subsequent inactivation of PLY's lytic activities. Consequently, PLY studies involving mice must be closely examined, as these findings imply that PLY activity in mice may underestimate PLY's role in human disease and that mouse models expressing human ApoB-100 may represent a better translation to human infections.

PNEUMOLYSIN IN TRANSMISSION AND COLONIZATION

Host-to-host transmission is an important component in the development of pneumococcal infection in which PLY also plays a role. In a study evaluating *S pneumoniae* transmission between mouse pups, recombinant PLY administered intranasally in doses of 100 ng/pup or greater caused increased levels of

bacterial shedding in nasal secretions (Zafar et al., 2017). This increased shedding appeared to be related to acute inflammation since wildtype recombinant PLY resulted in increased proinflammatory cytokine IL-1β, while a mutant PLY_{W433F}, defective in pore-formation, did not show increased inflammation or bacterial shedding. Furthermore, only strains expressing native PLY, and not the PLY-deficient or mutant PLY_{W433F} strains, successfully transmitted (Zafar et al., 2017).

S. pneumoniae is known to form biofilms when colonizing the nasopharyngeal passages and middle ear (Hoa et al., 2009). Biofilm formation plays a significant role in fomite-mediated pneumococcal transmission, allowing *S. pneumoniae* to survive longer in the environment (Marks et al., 2014). Also, pneumococcal biofilms appear more suited for enhancing colonization and transmission, at the cost of attenuated virulence (Gilley and Orihuela, 2014). Pneumolysin-deficient mutants show significantly reduced biofilm formation compared to the wildtype, even though PLY's contribution to biofilm development is not dependent on hemolytic ability (Shak et al., 2013; Keller et al., 2016).

PNEUMOLYSIN AS A MEDIATOR OF CELL DEATH AND INFLAMMATION

Due to its pore-forming cytolytic activity, PLY is capable of damaging and killing multiple cell types not just by necrosis but also by triggering programmed cell death pathways (**Table 1**). This occurs in lung and myocardial tissue during pneumococcal invasive disease and applies to other pneumococcal infections as well (Steinfort et al., 1989; Rubins et al., 1992; Alhamdi et al., 2015; Rashwan et al., 2018). For example, PLY has been shown to induce severe damage to cochlear cells resulting in hearing loss and deafness (Winter et al., 1997). In rat cochlear hair cells, PLY showed preferential killing of inner vs. outer cochlear hair cells via mitochondria-mediated apoptosis due to intracellular increases in calcium (Beurg et al., 2005). Induction of apoptosis is a major mechanism of brain injury in meningitis (Braun et al., 1999, 2001, 2002; Mitchell et al., 2004). Waves of apoptosis are seen in cortical and hippocampal neurons and in microglia in mouse models (Braun et al., 2007). Pneumolysin colocalizes with apoptotic neurons, and damage is significantly decreased during infection by PLY-/- strains. Thus, PLY is a major determinant of the poor outcome and permanent sequelae of meningitis.

TABLE 1 | Classifications of PLY-induced cell death pathways.

Cell death	Affected tissue	References
Apoptosis	Cochlear hair cells	Beurg et al., 2005
	Cortical neurons	Braun et al., 2002, 2007
	Dendritic cells	Littmann et al., 2009
Necroptosis	Respiratory epithelium	Gonzalez-Juarbe et al., 2017
	Alveolar macrophages	Riegler et al., 2019
Direct cytotoxicity	Lung endothelium	Rubins et al., 1992
	Nasal/tracheobronchial epithelium	Steinfort et al., 1989;Rayner et al., 1995
	Polymorphonuclear leukocytes	Johnson et al., 1981
	Platelets	Johnson et al., 1981
	Cardiomyocytes	Alhamdi et al., 2015
	Brain microvascular endothelium	Zysk et al., 2001
	Ependymal cells	Mohammed et al., 1999; Hirst et al., 2000b

In addition to the necrotic cell death accomplished directly by PLY, the pneumococcal CDC can also induce programmed necroptosis in respiratory epithelial cells and alveolar macrophages (Gonzalez-Juarbe et al., 2017). By inhibiting regulatory kinases (RIP1, RIP3, and MLKL) in the necroptosis pathway, mouse macrophages or human macrophage-like THP-1 cells were partially protected from PLY-induced cell death (Gonzalez-Juarbe et al., 2015). Necroptosis was detected in infiltrating macrophages during *S. pneumoniae* invasion of the myocardium and was believed to contribute to adverse remodeling in the heart (Gilley et al., 2016). A PLY-dependent increase in nasopharyngeal epithelial cell necroptosis was observed in asymptomatically colonized mice and indicated that this may benefit bacterial clearance at early stages of mucosal colonization (Riegler et al., 2019).

Pneumolysin itself is also a critical mediator of inflammation. An *in vivo* study in rats showed that PLY injection alone replicated the inflammation and histological findings consistent with pneumococcal pneumonia and found that PLY, independent of hemolytic activity, induced considerable pneumonitis *in vivo* (Feldman et al., 1991). *In vitro*, *S. pneumoniae* increases expression of proinflammatory cytokines like IL-1β and TNF-α in human epithelial cells (Yoo et al., 2010). A calcium-dependent increase in the proinflammatory mediators leukotriene B_4 and prostaglandin E_2 has also been seen *in vitro* when examining human neutrophils treated with recombinant PLY, further supporting PLY's proinflammatory role during invasive disease (Cockeran et al., 2001).

Multiple mechanisms are responsible for the inflammation in response to PLY. Pneumolysin's ability to activate the classical complement pathway likely contributes to generalized inflammation through the host's release of C3a and C5a anaphylatoxins (Paton et al., 1984). Several studies have also identified toll-like receptor (TLR) 4 for its role in recognizing PLY and subsequent inflammatory response regulation in murine and human cells (Malley et al., 2003; Bernatoniene et al., 2008; Dessing et al., 2009). Additionally, mice defective for TLR4 signaling were found to be hypersusceptible to pneumococcal disease and more susceptible to nasopharyngeal colonization with *S. pneumoniae*, suggesting that TLR4 is key to orchestrating proper response to pneumococcal disease.

PLY is necessary for IFN-γ and IL-17A induction in *in vivo* murine pneumonia models, suggesting that PLY is required for release of some inflammatory cytokines while synergistic with TLR agonists to enhance secretion of others. Of particular significance was the finding that PLY activates the NLRP3 inflammasome in order to induce the processing and secretion of IL-1β from dendritic cells, and interestingly, the PLY-induced cytokine release from mouse dendritic cells was found to be independent of TLR4 (Mcneela et al., 2010).

More recently, PLY has been suggested to incite inflammatory cytokine release in neutrophils and THP-1 monocyte-derived macrophages, but actually inhibit release of TNF-α, IL-1β, and IL-12 in human-derived dendritic cells (Subramanian et al., 2019). Infection of dendritic cells showed a STAT1- and NF-κB-dependent inhibition of proinflammatory cytokine release compared to infection with a PLY-deficient mutant. The observed interaction of PLY with the phagocytic receptor, MRC-1, which is highly expressed in dendritic cells compared to neutrophils or GM-CSF derived macrophages, suggests that this dose-dependent inhibition of inflammatory cytokines aids in allowing *S. pneumoniae* to establish intracellular residency within the dendritic cells (Subramanian et al., 2019). Moreover, these mechanisms may help identify PLY's contribution to inflammation in the nasopharynx, as MRC-1-expressing macrophages have been observed to be present in low-density pneumococcal carriage (Neill et al., 2014).

PNEUMOLYSIN AS A THERAPEUTIC TARGET

To date, there has been limited study of non-antibiotic strategies for the prevention or improvement of outcome of pneumococcal infection. Statins, the popularly prescribed cholesterol-lowering medication class, inhibit 3-hydroxy-3-methylglutaryl CoA reductase – the rate-limiting step in cholesterol biosynthesis. Furthermore, statins possess beneficial immunomodulatory and anti-inflammatory properties in infection and cardiovascular disease, and some evidence supports a beneficial effect of statins in community-acquired pneumonia outcomes (Ray and Cannon, 2005; Terblanche et al., 2007; Chalmers et al., 2008). One study demonstrated efficacy in using statins to inhibit cell-damaging PLY activity (**Figure 1**) to improve outcomes in sickle-cell mice (Rosch et al., 2010). Patients with sickle-cell disease experience a 600-fold increase in lethality due to pneumococcus and thus, sickle-cell mice are an excellent animal model to test interventions. Pretreatment of sickle-cell mice with simvastatin resulted in decreased mortality, pneumococcal burden in the lungs and bloodstream, and severity of lung pathology.

Based on this study, statins seemed to have a two-pronged effect on pneumococcal infection. First, statin's anti-inflammatory activity reduced the expression of platelet activating factor receptor (PAFr) in mouse lungs and vascular endothelium, thus reducing PAFr-mediated bacterial endocytosis and invasion. Second, statins directly reduced PLN cytotoxicity *in vivo* and *in vitro* at physiologic concentrations. Protection extended to tetanolysin and streptolysin, suggesting that therapeutic statin levels may be sufficient to impact CDC toxicity in general (Rosch et al., 2010). This was further shown not only for simvastatin and PLN but also for pravstatin protection of airway epithelial cells treated with alpha-hemolysin Statt et al., 2015). Evidence for a commercially available drug class to alter PLY function has far-reaching implications for immediately improving outcomes of pneumococcal infection. Moreover, if drug-mediated inhibition of PLY extends its roles in transmission and colonization, these agents may prevent spread of pneumococcal disease. Future studies are needed to investigate the mechanisms by which statins may affect PLY and prevent fulminant pneumococcal disease and whether their beneficial effects persist in combination with current antibiotic therapies.

It is also important to note the existence of other natural compounds that have been studied as inhibitors of PLY. β-sitosterol, for instance, was shown to bind with high affinity to PLY, inhibit PLY-induced hemolysis, protect human alveolar epithelial cells from injury, and prevent lethal pneumococcal infection (Li et al., 2015). Investigation of other natural compounds have identified chemical moieties important to blocking of PLY hemolytic activity and perhaps to the design of future inhibitors of PLY (Li et al., 2017). Similar studies have also reported prevention and attenuation of pneumococcal infection using compounds that prohibit PLY oligomerization (Li et al., 2020; Lv et al., 2020; Xu et al., 2020). These compounds potentially show promise as tools for developing small molecule adjuvant therapies in the prevention or treatment pneumococcal infection and studying PLY interactions.

The presence of anti-PLY antibodies has shown protective effects in delaying time to first pneumococcal carriage in newborns (Holmlund et al., 2006; Francis et al., 2009). Conversely, there is supportive evidence that patients with low serum antibody to PLY may be at higher risk for developing pneumococcal pneumonia (Huo et al., 2004). Mice administered anti-PLY antibodies showed significantly lower nasopharyngeal colonization compared to mice given nonspecific control antibodies (Kaur et al., 2014). It is therefore not surprising that PLY is one among several pneumococcal antigens studied as a potential vaccine candidate (Rapola et al., 2000; Holmlund et al., 2006; Francis et al., 2009). Pneumococcal protein based vaccines are particularly attractive in that the antigens are independent of capsular serotype and therefore may provide additional coverage compared to current serotype-based pneumococcal vaccines or may enhance protection when conjugated to capsular polysaccharide (Paton et al., 1991; Feldman and Anderson, 2014). Even so, PLY may present some challenges to its effective development as a vaccine target. For example, PLY is released from cells into the supernatant and thus is not present on the pneumococcal cell surface where an antibody could promote opsonization.

Fortunately, PLY shows relatively limited variation between strains and serotypes (Han and Zhang, 2019). Furthermore, PLY cytolytic effects can easily be attenuated with single amino acid substitutions (Boulnois et al., 1991). Specifically, a PLY L460D amino acid substitution disrupting the conserved CDC cholesterol-recognition motif abolishes any detectable cytotoxic effects (Farrand et al., 2010; Chen et al., 2015). This, in combination with the importance of PLY in immune cell recognition, makes PLY toxoid a key component in many protein-based vaccine trials (Malley et al., 2003; Witzenrath et al., 2011). Pneumolysin and attenuated PLY toxoid have since been extensively studied in animals for protective effects as an immunogenic agent (Paton et al., 1983; Alexander et al., 1994; Musher et al., 2001; Ogunniyi et al., 2001; Garcia-Suarez Mdel et al., 2004; Sanders et al., 2010; Denoel et al., 2011; Lu et al., 2014; Hermand et al., 2017). Many pre-clinical

studies have additionally investigated protein-based vaccines using PLY toxoid combined with additional surface antigens. For example, a vaccine utilizing fusions of PLY toxoid and the major pneumococcal virulence factor choline-binding protein A was found to have broadly protective activities against pneumococcal infection in mouse nasopharyngeal carriage and infection models of sepsis, meningitis, otitis media, and pneumonia (Mann et al., 2014). Immunization with PLY-peptide fusions results in expanded PLY epitope recognition, indicating such fusions may engender enhanced protective capacity by facilitating recognition of protective epitopes that typically do not elicit a robust antibody response (Mann et al., 2014). While antibody responses against PLY are clearly one important component in protective immunity against *S. pneumoniae*, protective immunity requires responses against multiple protein antigens underscoring the important of multicomponent vaccines (Wilson et al., 2017).

Human trials using PLY-based vaccines have also been successful in demonstrating protection and immunogenicity (Bologa et al., 2012; Seiberling et al., 2012; Berglund et al., 2014). A detoxified PLY-derivative given to healthy adult humans demonstrated increased IgG titers against the PLY toxoid and increased toxin-neutralizing antibody activity (Kamtchoua et al., 2013). However, a pneumococcal vaccine containing PLY toxoid has yet to show protection in humans. Phase II trials showed no additional protection against infant pneumococcal nasopharyngeal carriage, acute otitis media or pneumonia by adding PLY toxoid in combinations with other antigens (Odutola et al., 2017; Hammitt et al., 2019). This suggests that PLY toxicity may not be a major driver of mucosal disease but the question remains open, as it is generally accepted to be an important component of future protein-based vaccines. As vaccine development continues, the efficacy, safety, and immunogenicity of PLY-based vaccines should be reassessed not only for effectiveness against disease prevention and carriage but also for changes in immune response mediated by PLY.

CONCLUSION

The CDC PLY has multiple interactions with the host leading to extensive spread of disease, intense inflammation and abundant cell damage. Pneumolysin appears to incite tissue damage to increase bacterial penetration and transmissibility while simultaneously disarming elements of host defense. These effects of PLY promoting virulence are balanced against increased bacterial clearance and enhanced immune responses induced via cell damage and inflammation; thus, the timing, magnitude, and localization of PLY release can have a major impact on invasion and host response. Attenuation of tissue damage by statins that interfere with cholesterol in membranes may be a feasible therapeutic strategy for CDCs. Current research into PLY as a vaccine target shows promise especially when addressing infection from strains not currently covered in commercially available pneumococcal vaccines or non-typeable *S. pneumoniae*.

AUTHOR CONTRIBUTIONS

JR and ET conceived the manuscript and provided the groundwork of relevant content. AN drafted the manuscript. All authors reviewed and edited the manuscript.

FUNDING

ET is supported by NIAID R01-12111585 and ALSAC. JR is supported by NIAID U01-AI124302, R01-AI110618 and ALSAC. The content is solely the responsibility of the authors and does not necessarily represent the official views of the National Institutes of Health.

REFERENCES

Alcantara, R. B., Preheim, L. C., and Gentry-Nielsen, M. J. (2001). Pneumolysin-induced complement depletion during experimental pneumococcal bacteremia. *Infect. Immun.* 69, 3569–3575. doi: 10.1128/iai.69.6.3569-3575.2001

Alexander, J. E., Lock, R. A., Peeters, C. C., Poolman, J. T., Andrew, P. W., Mitchell, T. J., et al. (1994). Immunization of mice with pneumolysin toxoid confers a significant degree of protection against at least nine serotypes of *Streptococcus pneumoniae*. *Infect. Immun.* 62, 5683–5688. doi: 10.1128/iai.62.12.5683-5688.1994

Alhamdi, Y., Neill, D. R., Abrams, S. T., Malak, H. A., Yahya, R., Barrett-Jolley, R., et al. (2015). Circulating pneumolysin is a potent inducer of cardiac injury during pneumococcal infection. *PLoS Pathog.* 11:e1004836. doi: 10.1371/journal.ppat.1004836

Balachandran, P., Hollingshead, S. K., Paton, J. C., and Briles, D. E. (2001). The autolytic enzyme LytA of *Streptococcus pneumoniae* is not responsible for releasing pneumolysin. *J. Bacteriol.* 183, 3108–3116. doi: 10.1128/jb.183.10.3108-3116.2001

Benton, K. A., Paton, J. C., and Briles, D. E. (1997). Differences in virulence for mice among *Streptococcus pneumoniae* strains of capsular types 2, 3, 4, 5, and 6 are not attributable to differences in pneumolysin production. *Infect. Immun.* 65, 1237–1244. doi: 10.1128/iai.65.4.1237-1244.1997

Berglund, J., Vink, P., Tavares Da Silva, F., Lestrate, P., and Boutriau, D. (2014). Safety, immunogenicity, and antibody persistence following an investigational *Streptococcus pneumoniae* and *Haemophilus influenzae* triple-protein vaccine in a phase 1 randomized controlled study in healthy adults. *Clin. Vaccine Immunol.* 21, 56–65. doi: 10.1128/cvi.00430-13

Bernatoniene, J., Zhang, Q., Dogan, S., Mitchell, T. J., Paton, J. C., and Finn, A. (2008). Induction of CC and CXC chemokines in human antigen-presenting dendritic cells by the pneumococcal proteins pneumolysin and CbpA, and the role played by toll-like receptor 4, NF-kappaB, and mitogen-activated protein kinases. *J. Infect. Dis.* 198, 1823–1833. doi: 10.1086/593177

Berry, A. M., Lock, R. A., Hansman, D., and Paton, J. C. (1989a). Contribution of autolysin to virulence of *Streptococcus pneumoniae*. *Infect. Immun.* 57, 2324–2330. doi: 10.1128/iai.57.8.2324-2330.1989

Berry, A. M., and Paton, J. C. (2000). Additive attenuation of virulence of *Streptococcus pneumoniae* by mutation of the genes encoding pneumolysin and other putative pneumococcal virulence proteins. *Infect. Immun.* 68, 133–140. doi: 10.1128/iai.68.1.133-140.2000

Berry, A. M., Yother, J., Briles, D. E., Hansman, D., and Paton, J. C. (1989b). Reduced virulence of a defined pneumolysin-negative mutant of *Streptococcus pneumoniae*. *Infect. Immun.* 57, 2037–2042. doi: 10.1128/iai.57.7.2037-2042.1989

Beurg, M., Hafidi, A., Skinner, L., Cowan, G., Hondarrague, Y., Mitchell, T. J., et al. (2005). The mechanism of pneumolysin-induced cochlear hair cell death in the rat. *J. Physiol.* 568, 211–227. doi: 10.1113/jphysiol.2005.092478

Bologa, M., Kamtchoua, T., Hopfer, R., Sheng, X., Hicks, B., Bixler, G., et al. (2012). Safety and immunogenicity of pneumococcal protein vaccine candidates: monovalent choline-binding protein A (PcpA) vaccine and bivalent PcpA-pneumococcal histidine triad protein D vaccine. *Vaccine* 30, 7461–7468. doi: 10.1016/j.vaccine.2012.10.076

Boulnois, G. J., Paton, J. C., Mitchell, T. J., and Andrew, P. W. (1991). Structure and function of pneumolysin, the multifunctional, thiol-activated toxin of *Streptococcus pneumoniae*. *Mol. Microbiol.* 5, 2611–2616. doi: 10.1111/j.1365-2958.1991.tb01969.x

Braun, J. S., Hoffmann, O., Schickhaus, M., Freyer, D., Dagand, E., Bermpohl, D., et al. (2007). Pneumolysin causes neuronal cell death through mitochondrial damage. *Infect. Immun.* 75, 4245–4254. doi: 10.1128/iai.00031-07

Braun, J. S., Novak, R., Herzog, K. H., Bodner, S. M., Cleveland, J. L., and Tuomanen, E. I. (1999). Neuroprotection by a caspase inhibitor in acute bacterial meningitis. *Nat. Med.* 5, 298–302. doi: 10.1038/6514

Braun, J. S., Novak, R., Murray, P. J., Eischen, C. M., Susin, S. A., Kroemer, G., et al. (2001). Apoptosis-inducing factor mediates microglial and neuronal apoptosis caused by pneumococcus. *J. Infect. Dis.* 184, 1300–1309. doi: 10.1086/324013

Braun, J. S., Sublett, J. E., Freyer, D., Mitchell, T. J., Cleveland, J. L., Tuomanen, E. I., et al. (2002). Pneumococcal pneumolysin and H(2)O(2) mediate brain cell apoptosis during meningitis. *J. Clin. Invest.* 109, 19–27. doi: 10.1172/jci12035

Brown, A. O., Mann, B., Gao, G., Hankins, J. S., Humann, J., Giardina, J., et al. (2014). *Streptococcus pneumoniae* translocates into the myocardium and forms unique microlesions that disrupt cardiac function. *PLoS Pathog.* 10:e1004383. doi: 10.1371/journal.ppat.1004383

Bryant, J. C., Dabbs, R. C., Oswalt, K. L., Brown, L. R., Rosch, J. W., Seo, K. S., et al. (2016). Pyruvate oxidase of *Streptococcus pneumoniae* contributes to pneumolysin release. *BMC Microbiol.* 16:271. doi: 10.1186/s12866-016-0881-6

Canvin, J. R., Marvin, A. P., Sivakumaran, M., Paton, J. C., Boulnois, G. J., Andrew, P. W., et al. (1995). The role of pneumolysin and autolysin in the pathology of pneumonia and septicemia in mice infected with a type 2 pneumococcus. *J. Infect. Dis.* 172, 119–123. doi: 10.1093/infdis/172.1.119

Chalmers, J. D., Singanayagam, A., Murray, M. P., and Hill, A. T. (2008). Prior statin use is associated with improved outcomes in community-acquired pneumonia. *Am. J. Med.* 121, 1002.e–1007.e.

Chen, A., Mann, B., Gao, G., Heath, R., King, J., Maissoneuve, J., et al. (2015). Multivalent pneumococcal protein vaccines comprising pneumolysoid with epitopes/fragments of CbpA and/or PspA elicit strong and broad protection. *Clin. Vaccine Immunol.* 22, 1079–1089. doi: 10.1128/cvi.00293-15

Cockeran, R., Steel, H. C., Mitchell, T. J., Feldman, C., and Anderson, R. (2001). Pneumolysin potentiates production of prostaglandin E(2) and leukotriene B(4) by human neutrophils. *Infect. Immun.* 69, 3494–3496. doi: 10.1128/iai.69.5.3494-3496.2001

Cohen, B., Halbert, S. P., and Perkins, M. E. (1942). Pneumococcal hemolysin: the preparation of concentrates, and their action on red cells. *J. Bacteriol.* 43, 607–627.

Cundell, D. R., Gerard, N. P., Gerard, C., Idanpaan-Heikkila, I., and Tuomanen, E. I. (1995). *Streptococcus pneumoniae* anchor to activated human cells by the receptor for platelet-activating factor. *Nature* 377, 435–438. doi: 10.1038/377435a0

Denoel, P., Philipp, M. T., Doyle, L., Martin, D., Carletti, G., and Poolman, J. T. (2011). A protein-based pneumococcal vaccine protects rhesus macaques from pneumonia after experimental infection with *Streptococcus pneumoniae*. *Vaccine* 29, 5495–5501. doi: 10.1016/j.vaccine.2011.05.051

Dessing, M. C., Hirst, R. A., De Vos, A. F., and Van Der Poll, T. (2009). Role of Toll-like receptors 2 and 4 in pulmonary inflammation and injury induced by pneumolysin in mice. *PLoS One* 4:e7993. doi: 10.1371/journal.pone.0007993

Faraj, B. H. A., Collard, L., Cliffe, R., Blount, L. A., Lonnen, R., Wallis, R., et al. (2020). Formation of pre-pore complexes of pneumolysin is accompanied by a decrease in short-range order of lipid molecules throughout vesicle bilayers. *Sci. Rep.* 10:4585.

Farrand, A. J., Lachapelle, S., Hotze, E. M., Johnson, A. E., and Tweten, R. K. (2010). Only two amino acids are essential for cytolytic toxin recognition of cholesterol at the membrane surface. *Proc. Natl. Acad. Sci. U.S.A.* 107, 4341–4346. doi: 10.1073/pnas.0911581107

Feldman, C., and Anderson, R. (2014). Review: current and new generation pneumococcal vaccines. *J. Infect.* 69, 309–325. doi: 10.1016/j.jinf.2014.06.006

Feldman, C., Munro, N. C., Jeffery, P. K., Mitchell, T. J., Andrew, P. W., Boulnois, G. J., et al. (1991). Pneumolysin induces the salient histologic features of pneumococcal infection in the rat lung in vivo. *Am. J. Respir. Cell Mol. Biol.* 5, 416–423. doi: 10.1165/ajrcmb/5.5.416

Francis, J. P., Richmond, P. C., Pomat, W. S., Michael, A., Keno, H., Phuanukoonnon, S., et al. (2009). Maternal antibodies to pneumolysin but not to pneumococcal surface protein A delay early pneumococcal carriage in high-risk Papua New Guinean infants. *Clin. Vaccine Immunol.* 16, 1633–1638. doi: 10.1128/cvi.00247-09

Garcia-Suarez Mdel, M., Cima-Cabal, M. D., Florez, N., Garcia, P., Cernuda-Cernuda, R., Astudillo, A., et al. (2004). Protection against pneumococcal pneumonia in mice by monoclonal antibodies to pneumolysin. *Infect. Immun.* 72, 4534–4540. doi: 10.1128/iai.72.8.4534-4540.2004

Gilley, R. P., Gonzalez-Juarbe, N., Shenoy, A. T., Reyes, L. F., Dube, P. H., Restrepo, M. I., et al. (2016). Infiltrated macrophages die of pneumolysin-mediated necroptosis following pneumococcal myocardial invasion. *Infect. Immun.* 84, 1457–1469. doi: 10.1128/iai.00007-16

Gilley, R. P., and Orihuela, C. J. (2014). Pneumococci in biofilms are non-invasive: implications on nasopharyngeal colonization. *Front. Cell Infect. Microbiol.* 4:163. doi: 10.3389/fcimb.2014.00163

Gonzalez-Juarbe, N., Bradley, K. M., Shenoy, A. T., Gilley, R. P., Reyes, L. F., Hinojosa, C. A., et al. (2017). Pore-forming toxin-mediated ion dysregulation leads to death receptor-independent necroptosis of lung epithelial cells during bacterial pneumonia. *Cell Death Differ.* 24, 917–928. doi: 10.1038/cdd.2017.49

Gonzalez-Juarbe, N., Gilley, R. P., Hinojosa, C. A., Bradley, K. M., Kamei, A., Gao, G., et al. (2015). Pore-forming toxins induce macrophage necroptosis during acute bacterial pneumonia. *PLoS Pathog* 11:e1005337. doi: 10.1371/journal.ppat.1005337

Greene, N. G., Narciso, A. R., Filipe, S. R., and Camilli, A. (2015). Peptidoglycan branched stem peptides contribute to *Streptococcus pneumoniae* virulence by inhibiting pneumolysin release. *PLoS Pathog* 11:e1004996. doi: 10.1371/journal.ppat.1004996

Hammitt, L. L., Campbell, J. C., Borys, D., Weatherholtz, R. C., Reid, R., Goklish, N., et al. (2019). Efficacy, safety and immunogenicity of a pneumococcal protein-based vaccine co-administered with 13-valent pneumococcal conjugate vaccine against acute otitis media in young children: a phase IIb randomized study. *Vaccine* 37, 7482–7492. doi: 10.1016/j.vaccine.2019.09.076

Han, C., and Zhang, M. (2019). Genetic diversity and antigenicity analysis of *Streptococcus pneumoniae* pneumolysin isolated from children with pneumococcal infection. *Int. J. Infect. Dis.* 86, 57–64. doi: 10.1016/j.ijid.2019.06.025

Hermand, P., Vandercammen, A., Mertens, E., Di Paolo, E., Verlant, V., Denoel, P., et al. (2017). Preclinical evaluation of a chemically detoxified pneumolysin as pneumococcal vaccine antigen. *Hum. Vaccin. Immunother.* 13, 220–228. doi: 10.1080/21645515.2016.1234553

Hirst, R. A., Rutman, A., Sikand, K., Andrew, P. W., Mitchell, T. J., and O'callaghan, C. (2000a). Effect of pneumolysin on rat brain ciliary function: comparison of brain slices with cultured ependymal cells. *Pediatr. Res.* 47, 381–384. doi: 10.1203/00006450-200003000-00016

Hirst, R. A., Sikand, K. S., Rutman, A., Mitchell, T. J., Andrew, P. W., and O'callaghan, C. (2000b). Relative roles of pneumolysin and hydrogen peroxide from *Streptococcus pneumoniae* in inhibition of ependymal ciliary beat frequency. *Infect. Immun.* 68, 1557–1562. doi: 10.1128/iai.68.3.1557-1562.2000

Hoa, M., Syamal, M., Sachdeva, L., Berk, R., and Coticchia, J. (2009). Demonstration of nasopharyngeal and middle ear mucosal biofilms in an animal model of acute otitis media. *Ann. Otol. Rhinol. Laryngol.* 118, 292–298. doi: 10.1177/000348940911800410

Holmlund, E., Quiambao, B., Ollgren, J., Nohynek, H., and Kayhty, H. (2006). Development of natural antibodies to pneumococcal surface protein A, pneumococcal surface adhesin A and pneumolysin in Filipino pregnant women and their infants in relation to pneumococcal carriage. *Vaccine* 24, 57–65. doi: 10.1016/j.vaccine.2005.07.055

Huo, Z., Spencer, O., Miles, J., Johnson, J., Holliman, R., Sheldon, J., et al. (2004). Antibody response to pneumolysin and to pneumococcal capsular polysaccharide in healthy individuals and *Streptococcus pneumoniae* infected patients. *Vaccine* 22, 1157–1161. doi: 10.1016/j.vaccine.2003.09.025

Hupp, S., Heimeroth, V., Wippel, C., Fortsch, C., Ma, J., Mitchell, T. J., et al. (2012). Astrocytic tissue remodeling by the meningitis neurotoxin pneumolysin facilitates pathogen tissue penetration and produces interstitial brain edema. *Glia* 60, 137–146. doi: 10.1002/glia.21256

Johnson, M. K., Boese-Marrazzo, D., and Pierce, W. A. Jr. (1981). Effects of pneumolysin on human polymorphonuclear leukocytes and platelets. *Infect. Immun.* 34, 171–176. doi: 10.1128/iai.34.1.171-176.1981

Kamtchoua, T., Bologa, M., Hopfer, R., Neveu, D., Hu, B., Sheng, X., et al. (2013). Safety and immunogenicity of the pneumococcal pneumolysin derivative PlyD1 in a single-antigen protein vaccine candidate in adults. *Vaccine* 31, 327–333. doi: 10.1016/j.vaccine.2012.11.005

Kaur, R., Surendran, N., Ochs, M., and Pichichero, M. E. (2014). Human antibodies to PhtD, PcpA, and Ply reduce adherence to human lung epithelial cells and murine nasopharyngeal colonization by *Streptococcus pneumoniae*. *Infect. Immun.* 82, 5069–5075. doi: 10.1128/iai.02124-14

Keller, L. E., Bradshaw, J. L., Pipkins, H., and Mcdaniel, L. S. (2016). Surface proteins and pneumolysin of encapsulated and nonencapsulated *streptococcus pneumoniae* mediate virulence in a chinchilla model of otitis media. *Front. Cell Infect. Microbiol.* 6:55. doi: 10.3389/fcimb.2016.00055

Kelly, S. J., and Jedrzejas, M. J. (2000a). Crystallization and preliminary X-ray diffraction analysis of a functional form of pneumolysin, a virulence factor from *Streptococcus pneumoniae*. *Acta Crystallogr. D Biol. Crystallogr.* 56, 1452–1455. doi: 10.1107/s0907444900010143

Kelly, S. J., and Jedrzejas, M. J. (2000b). Structure and molecular mechanism of a functional form of pneumolysin: a cholesterol-dependent cytolysin from *Streptococcus pneumoniae*. *J. Struct. Biol.* 132, 72–81. doi: 10.1006/jsbi.2000.4308

Lawrence, S. L., Feil, S. C., Morton, C. J., Farrand, A. J., Mulhern, T. D., Gorman, M. A., et al. (2015). Crystal structure of *Streptococcus pneumoniae* pneumolysin provides key insights into early steps of pore formation. *Sci. Rep.* 5:14352.

Li, H., Zhao, X., Deng, X., Wang, J., Song, M., Niu, X., et al. (2017). Insights into structure and activity of natural compound inhibitors of pneumolysin. *Sci. Rep.* 7:42015.

Li, H., Zhao, X., Wang, J., Dong, Y., Meng, S., Li, R., et al. (2015). beta-sitosterol interacts with pneumolysin to prevent *Streptococcus pneumoniae* infection. *Sci. Rep.* 5:17668.

Li, S., Lv, Q., Sun, X., Tang, T., Deng, X., Yin, Y., et al. (2020). Acacetin inhibits *Streptococcus pneumoniae* virulence by targeting pneumolysin. *J. Pharm. Pharmacol.* [Epub ahead of print],

Littmann, M., Albiger, B., Frentzen, A., Normark, S., Henriques-Normark, B., and Plant, L. (2009). *Streptococcus pneumoniae* evades human dendritic cell surveillance by pneumolysin expression. *EMBO Mol. Med.* 1, 211–222. doi: 10.1002/emmm.200900025

Lu, J., Sun, T., Hou, H., Xu, M., Gu, T., Dong, Y., et al. (2014). Detoxified pneumolysin derivative Plym2 directly protects against pneumococcal infection via induction of inflammatory cytokines. *Immunol. Invest.* 43, 717–726. doi: 10.3109/08820139.2014.930478

Lv, Q., Zhang, P., Quan, P., Cui, M., Liu, T., Yin, Y., et al. (2020). Quercetin, a pneumolysin inhibitor, protects mice against *Streptococcus pneumoniae* infection. *Microb. Pathog.* 140:103934. doi: 10.1016/j.micpath.2019.103934

Malley, R., Henneke, P., Morse, S. C., Cieslewicz, M. J., Lipsitch, M., Thompson, C. M., et al. (2003). Recognition of pneumolysin by Toll-like receptor 4 confers resistance to pneumococcal infection. *Proc. Natl. Acad. Sci. U.S.A.* 100, 1966–1971. doi: 10.1073/pnas.0435928100

Mann, B., Thornton, J., Heath, R., Wade, K. R., Tweten, R. K., Gao, G., et al. (2014). Broadly protective protein-based pneumococcal vaccine composed of pneumolysin toxoid-CbpA peptide recombinant fusion protein. *J. Infect. Dis.* 209, 1116–1125. doi: 10.1093/infdis/jit502

Marks, L. R., Reddinger, R. M., and Hakansson, A. P. (2014). Biofilm formation enhances fomite survival of *Streptococcus pneumoniae* and *Streptococcus pyogenes*. *Infect. Immun.* 82, 1141–1146. doi: 10.1128/iai.01310-13

Marshall, J. E., Faraj, B. H., Gingras, A. R., Lonnen, R., Sheikh, M. A., El-Mezgueldi, M., et al. (2015). The crystal structure of pneumolysin at 2.0 A resolution reveals the molecular packing of the pre-pore complex. *Sci. Rep.* 5:13293.

Martner, A., Dahlgren, C., Paton, J. C., and Wold, A. E. (2008). Pneumolysin released during *Streptococcus pneumoniae* autolysis is a potent activator of intracellular oxygen radical production in neutrophils. *Infect. Immun.* 76, 4079–4087. doi: 10.1128/iai.01747-07

Mcneela, E. A., Burke, A., Neill, D. R., Baxter, C., Fernandes, V. E., Ferreira, D., et al. (2010). Pneumolysin activates the NLRP3 inflammasome and promotes proinflammatory cytokines independently of TLR4. *PLoS Pathog.* 6:e1001191. doi: 10.1371/journal.ppat.1001191

Mitchell, L., Smith, S. H., Braun, J. S., Herzog, K. H., Weber, J. R., and Tuomanen, E. I. (2004). Dual phases of apoptosis in pneumococcal meningitis. *J. Infect. Dis.* 190, 2039–2046. doi: 10.1086/425520

Mitchell, T. J., Andrew, P. W., Saunders, F. K., Smith, A. N., and Boulnois, G. J. (1991). Complement activation and antibody binding by pneumolysin via a region of the toxin homologous to a human acute-phase protein. *Mol. Microbiol.* 5, 1883–1888. doi: 10.1111/j.1365-2958.1991.tb00812.x

Mitchell, T. J., and Dalziel, C. E. (2014). The biology of pneumolysin. *Subcell Biochem.* 80, 145–160.

Mohammed, B. J., Mitchell, T. J., Andrew, P. W., Hirst, R. A., and O'callaghan, C. (1999). The effect of the pneumococcal toxin, pneumolysin on brain ependymal cilia. *Microb. Pathog.* 27, 303–309. doi: 10.1006/mpat.1999.0306

Musher, D. M., Phan, H. M., and Baughn, R. E. (2001). Protection against bacteremic pneumococcal infection by antibody to pneumolysin. *J. Infect. Dis.* 183, 827–830. doi: 10.1086/318833

Neill, D. R., Coward, W. R., Gritzfeld, J. F., Richards, L., Garcia-Garcia, F. J., Dotor, J., et al. (2014). Density and duration of pneumococcal carriage is maintained by transforming growth factor beta1 and T regulatory cells. *Am. J. Respir. Crit. Care Med.* 189, 1250–1259. doi: 10.1164/rccm.201401-0128oc

Neill, J. (1926). Studies on the oxidation-reduction of immunological substances. I. *Pneumococcus hemotoxin*. *J. Exptl. Med.* 44, 199–213. doi: 10.1084/jem.44.2.199

Nel, J. G., Durandt, C., Mitchell, T. J., Feldman, C., Anderson, R., and Tintinger, G. R. (2016). Pneumolysin mediates platelet activation in vitro. *Lung* 194, 589–593. doi: 10.1007/s00408-016-9900-5

Nerlich, A., Mieth, M., Letsiou, E., Fatykhova, D., Zscheppang, K., Imai-Matsushima, A., et al. (2018). Pneumolysin induced mitochondrial dysfunction leads to release of mitochondrial DNA. *Sci. Rep.* 8:182.

Nollmann, M., Gilbert, R., Mitchell, T., Sferrazza, M., and Byron, O. (2004). The role of cholesterol in the activity of pneumolysin, a bacterial protein toxin. *Biophys. J.* 86, 3141–3151. doi: 10.1016/s0006-3495(04)74362-3

Odutola, A., Ota, M. O. C., Antonio, M., Ogundare, E. O., Saidu, Y., Foster-Nyarko, E., et al. (2017). Efficacy of a novel, protein-based pneumococcal vaccine against nasopharyngeal carriage of *Streptococcus pneumoniae* in infants: A phase 2, randomized, controlled, observer-blind study. *Vaccine* 35, 2531–2542. doi: 10.1016/j.vaccine.2017.03.071

Ogunniyi, A. D., Woodrow, M. C., Poolman, J. T., and Paton, J. C. (2001). Protection against *Streptococcus pneumoniae* elicited by immunization with pneumolysin and CbpA. *Infect. Immun.* 69, 5997–6003. doi: 10.1128/iai.69.10.5997-6003.2001

Orihuela, C. J., Mahdavi, J., Thornton, J., Mann, B., Wooldridge, K. G., Abouseada, N., et al. (2009). Laminin receptor initiates bacterial contact with the blood brain barrier in experimental meningitis models. *J. Clin. Invest.* 119, 1638–1646. doi: 10.1172/jci36759

Paton, J. C., and Ferrante, A. (1983). Inhibition of human polymorphonuclear leukocyte respiratory burst, bactericidal activity, and migration by pneumolysin. *Infect. Immun.* 41, 1212–1216. doi: 10.1128/iai.41.3.1212-1216.1983

Paton, J. C., Lock, R. A., and Hansman, D. J. (1983). Effect of immunization with pneumolysin on survival time of mice challenged with *Streptococcus pneumoniae*. *Infect. Immun.* 40, 548–552. doi: 10.1128/iai.40.2.548-552.1983

Paton, J. C., Lock, R. A., Lee, C. J., Li, J. P., Berry, A. M., Mitchell, T. J., et al. (1991). Purification and immunogenicity of genetically obtained pneumolysin toxoids and their conjugation to *Streptococcus pneumoniae* type 19F polysaccharide. *Infect. Immun.* 59, 2297–2304. doi: 10.1128/iai.59.7.2297-2304.1991

Paton, J. C., Rowan-Kelly, B., and Ferrante, A. (1984). Activation of human complement by the pneumococcal toxin pneumolysin. *Infect. Immun.* 43, 1085–1087. doi: 10.1128/iai.43.3.1085-1087.1984

Price, K. E., and Camilli, A. (2009). Pneumolysin localizes to the cell wall of *Streptococcus pneumoniae*. *J. Bacteriol.* 191, 2163–2168. doi: 10.1128/jb.01489-08

Price, K. E., Greene, N. G., and Camilli, A. (2012). Export requirements of pneumolysin in *Streptococcus pneumoniae*. *J. Bacteriol.* 194, 3651–3660. doi: 10.1128/jb.00114-12

Radin, J. N., Orihuela, C. J., Murti, G., Guglielmo, C., Murray, P. J., and Tuomanen, E. I. (2005). beta-Arrestin 1 participates in platelet-activating factor receptor-mediated endocytosis of *Streptococcus pneumoniae*. *Infect. Immun.* 73, 7827–7835. doi: 10.1128/iai.73.12.7827-7835.2005

Rai, P., He, F., Kwang, J., Engelward, B. P., and Chow, V. T. (2016). Pneumococcal pneumolysin induces DNA damage and cell cycle arrest. *Sci. Rep.* 6:22972.

Rapola, S., Jantti, V., Haikala, R., Syrjanen, R., Carlone, G. M., Sampson, J. S., et al. (2000). Natural development of antibodies to pneumococcal surface protein A, pneumococcal surface adhesin A, and pneumolysin in relation to pneumococcal carriage and acute otitis media. *J. Infect. Dis.* 182, 1146–1152. doi: 10.1086/315822

Rashwan, R., Varano Della Vergiliana, J. F., Lansley, S. M., Cheah, H. M., Popowicz, N., Paton, J. C., et al. (2018). *Streptococcus pneumoniae* potently induces cell death in mesothelial cells. *PLoS One* 13:e0201530. doi: 10.1371/journal.pone.0201530

Ray, K. K., and Cannon, C. P. (2005). The potential relevance of the multiple lipid-independent (pleiotropic) effects of statins in the management of acute coronary syndromes. *J. Am. Coll. Cardiol.* 46, 1425–1433. doi: 10.1016/j.jacc.2005.05.086

Rayner, C. F., Jackson, A. D., Rutman, A., Dewar, A., Mitchell, T. J., Andrew, P. W., et al. (1995). Interaction of pneumolysin-sufficient and -deficient isogenic variants of *Streptococcus pneumoniae* with human respiratory mucosa. *Infect. Immun.* 63, 442–447. doi: 10.1128/iai.63.2.442-447.1995

Riegler, A. N., Brissac, T., Gonzalez-Juarbe, N., and Orihuela, C. J. (2019). Necroptotic cell death promotes adaptive immunity against colonizing pneumococci. *Front. Immunol.* 10:615. doi: 10.3389/fimmu.2019.00615

Ring, A., Weiser, J. N., and Tuomanen, E. I. (1998). Pneumococcal trafficking across the blood-brain barrier. Molecular analysis of a novel bidirectional pathway. *J. Clin. Invest.* 102, 347–360. doi: 10.1172/jci2406

Rogers, P. D., Thornton, J., Barker, K. S., Mcdaniel, D. O., Sacks, G. S., Swiatlo, E., et al. (2003). Pneumolysin-dependent and -independent gene expression identified by cDNA microarray analysis of THP-1 human mononuclear cells stimulated by *Streptococcus pneumoniae*. *Infect. Immun.* 71, 2087–2094. doi: 10.1128/iai.71.4.2087-2094.2003

Rosch, J. W., Boyd, A. R., Hinojosa, E., Pestina, T., Hu, Y., Persons, D. A., et al. (2010). Statins protect against fulminant pneumococcal infection and cytolysin toxicity in a mouse model of sickle cell disease. *J. Clin. Invest.* 120, 627–635. doi: 10.1172/jci39843

Rubins, J. B., Charboneau, D., Paton, J. C., Mitchell, T. J., Andrew, P. W., and Janoff, E. N. (1995). Dual function of pneumolysin in the early pathogenesis of murine pneumococcal pneumonia. *J. Clin. Invest.* 95, 142–150. doi: 10.1172/jci117631

Rubins, J. B., Duane, P. G., Charboneau, D., and Janoff, E. N. (1992). Toxicity of pneumolysin to pulmonary endothelial cells in vitro. *Infect. Immun.* 60, 1740–1746. doi: 10.1128/iai.60.5.1740-1746.1992

Sanders, M. E., Norcross, E. W., Moore, Q. C. III, Fratkin, J., Thompson, H., and Marquart, M. E. (2010). Immunization with pneumolysin protects against both retinal and global damage caused by *Streptococcus pneumoniae* endophthalmitis. *J. Ocul. Pharmacol. Ther.* 26, 571–577. doi: 10.1089/jop.2010.0077

Schachern, P. A., Tsuprun, V., Goetz, S., Cureoglu, S., Juhn, S. K., Briles, D. E., et al. (2013). Viability and virulence of pneumolysin, pneumococcal surface protein A, and pneumolysin/pneumococcal surface protein A mutants in the ear. *JAMA Otolaryngol. Head Neck Surg.* 139, 937–943.

Seiberling, M., Bologa, M., Brookes, R., Ochs, M., Go, K., Neveu, D., et al. (2012). Safety and immunogenicity of a pneumococcal histidine triad protein D vaccine candidate in adults. *Vaccine* 30, 7455–7460. doi: 10.1016/j.vaccine.2012.10.080

Shak, J. R., Ludewick, H. P., Howery, K. E., Sakai, F., Yi, H., Harvey, R. M., et al. (2013). Novel role for the *Streptococcus pneumoniae* toxin pneumolysin in the assembly of biofilms. *mBio* 4:e00655-13.

Shewell, L. K., Harvey, R. M., Higgins, M. A., Day, C. J., Hartley-Tassell, L. E., Chen, A. Y., et al. (2014). The cholesterol-dependent cytolysins pneumolysin and streptolysin O require binding to red blood cell glycans for hemolytic activity. *Proc. Natl. Acad. Sci. U.S.A.* 111, E5312–E5320.

Soltani, C. E., Hotze, E. M., Johnson, A. E., and Tweten, R. K. (2007). Structural elements of the cholesterol-dependent cytolysins that are responsible for their cholesterol-sensitive membrane interactions. *Proc. Natl. Acad. Sci. U.S.A.* 104, 20226–20231. doi: 10.1073/pnas.0708104105

Statt, S., Ruan, J. W., Hung, L. Y., Chang, C. Y., Huang, C. T., Lim, J. H., et al. (2015). Statin-conferred enhanced cellular resistance against bacterial pore-forming toxins in airway epithelial cells. *Am. J. Respir. Cell Mol. Biol.* 53, 689–702. doi: 10.1165/rcmb.2014-0391oc

Steinfort, C., Wilson, R., Mitchell, T., Feldman, C., Rutman, A., Todd, H., et al. (1989). Effect of *Streptococcus pneumoniae* on human respiratory epithelium in vitro. *Infect. Immun.* 57, 2006–2013. doi: 10.1128/iai.57.7.2006-2013.1989

Subramanian, K., Neill, D. R., Malak, H. A., Spelmink, L., Khandaker, S., Dalla Libera Marchiori, G., et al. (2019). Pneumolysin binds to the mannose receptor C type 1 (MRC-1) leading to anti-inflammatory responses and enhanced pneumococcal survival. *Nat. Microbiol.* 4, 62–70. doi: 10.1038/s41564-018-0280-x

Terblanche, M., Almog, Y., Rosenson, R. S., Smith, T. S., and Hackam, D. G. (2007). Statins and sepsis: multiple modifications at multiple levels. *Lancet Infect. Dis.* 7, 358–368. doi: 10.1016/s1473-3099(07)70111-1

Tilley, S. J., Orlova, E. V., Gilbert, R. J., Andrew, P. W., and Saibil, H. R. (2005). Structural basis of pore formation by the bacterial toxin pneumolysin. *Cell* 121, 247–256. doi: 10.1016/j.cell.2005.02.033

Wade, K. R., Hotze, E. M., Briles, D. E., and Tweten, R. K. (2014). Mouse, but not human, ApoB-100 lipoprotein cholesterol is a potent innate inhibitor of *Streptococcus pneumoniae* pneumolysin. *PLoS Pathog.* 10:e1004353. doi: 10.1371/journal.ppat.1004353

Walker, J. A., Allen, R. L., Falmagne, P., Johnson, M. K., and Boulnois, G. J. (1987). Molecular cloning, characterization, and complete nucleotide sequence of the gene for pneumolysin, the sulfhydryl-activated toxin of *Streptococcus pneumoniae*. *Infect. Immun.* 55, 1184–1189. doi: 10.1128/iai.55.5.1184-1189.1987

Watson, K. C., Rose, T. P., and Kerr, E. J. (1972). Some factors influencing the effect of cholesterol on streptolysin O activity. *J. Clin. Pathol.* 25, 885–891. doi: 10.1136/jcp.25.10.885

Wellmer, A., Zysk, G., Gerber, J., Kunst, T., Von Mering, M., Bunkowski, S., et al. (2002). Decreased virulence of a pneumolysin-deficient strain of *Streptococcus pneumoniae* in murine meningitis. *Infect. Immun.* 70, 6504–6508. doi: 10.1128/iai.70.11.6504-6508.2002

Wilson, R., Cohen, J. M., Reglinski, M., Jose, R. J., Chan, W. Y., Marshall, H., et al. (2017). Naturally acquired human immunity to pneumococcus is dependent on antibody to protein antigens. *PLoS Pathog.* 13:e1006137. doi: 10.1371/journal.ppat.1006137

Winter, A. J., Comis, S. D., Osborne, M. P., Tarlow, M. J., Stephen, J., Andrew, P. W., et al. (1997). A role for pneumolysin but not neuraminidase in the hearing loss and cochlear damage induced by experimental pneumococcal meningitis in guinea pigs. *Infect. Immun.* 65, 4411–4418. doi: 10.1128/iai.65.11.4411-4418.1997

Witzenrath, M., Gutbier, B., Owen, J. S., Schmeck, B., Mitchell, T. J., Mayer, K., et al. (2007). Role of platelet-activating factor in pneumolysin-induced acute lung injury. *Crit. Care Med.* 35, 1756–1762. doi: 10.1097/01.ccm.0000269212.84709.23

Witzenrath, M., Pache, F., Lorenz, D., Koppe, U., Gutbier, B., Tabeling, C., et al. (2011). The NLRP3 inflammasome is differentially activated by pneumolysin variants and contributes to host defense in pneumococcal pneumonia. *J. Immunol.* 187, 434–440. doi: 10.4049/jimmunol.1003143

Wolfmeier, H., Radecke, J., Schoenauer, R., Koeffel, R., Babiychuk, V. S., Drucker, P., et al. (2016). Active release of pneumolysin prepores and pores by mammalian cells undergoing a *Streptococcus pneumoniae* attack. *Biochim. Biophys. Acta* 1860, 2498–2509. doi: 10.1016/j.bbagen.2016.07.022

Xu, Y., Wei, L., Wang, Y., Ding, L., Guo, Y., Sun, X., et al. (2020). Inhibitory effect of the traditional chinese medicine ephedra sinica granules on *Streptococcus pneumoniae* pneumolysin. *Biol. Pharm. Bull.* 43, 994–999. doi: 10.1248/bpb.b20-00034

Yoo, I. H., Shin, H. S., Kim, Y. J., Kim, H. B., Jin, S., and Ha, U. H. (2010). Role of pneumococcal pneumolysin in the induction of an inflammatory response in human epithelial cells. *FEMS Immunol. Med. Microbiol.* 60, 28–35. doi: 10.1111/j.1574-695x.2010.00699.x

Zafar, M. A., Wang, Y., Hamaguchi, S., and Weiser, J. N. (2017). Host-to-host transmission of *Streptococcus pneumoniae* is driven by its inflammatory

toxin, pneumolysin. *Cell Host Microbe* 21, 73–83. doi: 10.1016/j.chom.2016.12.005

Zhang, J. R., Mostov, K. E., Lamm, M. E., Nanno, M., Shimida, S., Ohwaki, M., et al. (2000). The polymeric immunoglobulin receptor translocates pneumococci across human nasopharyngeal epithelial cells. *Cell* 102, 827–837. doi: 10.1016/s0092-8674(00)00071-4

Zysk, G., Schneider-Wald, B. K., Hwang, J. H., Bejo, L., Kim, K. S., Mitchell, T. J., et al. (2001). Pneumolysin is the main inducer of cytotoxicity to brain microvascular endothelial cells caused by *Streptococcus pneumoniae*. *Infect. Immun.* 69, 845–852. doi: 10.1128/iai.69.2.845-852.2001

Conflict of Interest: The authors declare that the research was conducted in the absence of any commercial or financial relationships that could be construed as a potential conflict of interest.

frontiers in Immunology

REVIEW
published: 14 July 2020
doi: 10.3389/fimmu.2020.01490

An Ancient Molecular Arms Race: *Chlamydia* vs. Membrane Attack Complex/Perforin (MACPF) Domain Proteins

*Gabrielle Keb and Kenneth A. Fields**

Department of Microbiology, Immunology & Molecular Genetics, University of Kentucky College of Medicine, Lexington, KY, United States

Dynamic interactions that govern the balance between host and pathogen determine the outcome of infection and are shaped by evolutionary pressures. Eukaryotic hosts have evolved elaborate and formidable defense mechanisms that provide the basis for innate and adaptive immunity. Proteins containing a membrane attack complex/Perforin (MACPF) domain represent an important class of immune effectors. These pore-forming proteins induce cell killing by targeting microbial or host membranes. Intracellular bacteria can be shielded from MACPF-mediated killing, and *Chlamydia* spp. represent a successful paradigm of obligate intracellular parasitism. Ancestors of present-day *Chlamydia* likely originated at evolutionary times that correlated with or preceded many host defense pathways. We discuss the current knowledge regarding how chlamydiae interact with the MACPF proteins Complement C9, Perforin-1, and Perforin-2. Current evidence indicates a degree of resistance by *Chlamydia* to MACPF effector mechanisms. In fact, chlamydiae have acquired and adapted their own MACPF-domain protein to facilitate infection.

Keywords: immunity, evolution, pathogenesis, pore-forming, obligate intracellular

OPEN ACCESS

Edited by:
George P. Munson, The University of Miami Leonard M. Miller School of Medicine, United States

Reviewed by:
Mary M. Weber, University of Iowa, United States
Erika Ildiko Lutter, Oklahoma State University, United States
David E. Nelson, Indiana University School of Medicine, United States
Kevin Hybiske, University of Washington, United States

****Correspondence:***
Kenneth A. Fields
Ken.fields@uky.edu

Specialty section:
This article was submitted to Microbial Immunology, a section of the journal Frontiers in Immunology

Received: *20 April 2020*
Accepted: *08 June 2020*
Published: *14 July 2020*

Citation:
Keb G and Fields KA (2020) An Ancient Molecular Arms Race: Chlamydia vs. Membrane Attack Complex/Perforin (MACPF) Domain Proteins. Front. Immunol. 11:1490. doi: 10.3389/fimmu.2020.01490

INTRODUCTION

Obligate intracellular bacteria depend on survival within eukaryotic host cells. The family *Chlamydiaceae* contains at least nine designated species of obligate intracellular pathogens exhibiting a diverse host range in higher eukaryotes. *C. trachomatis* and *C. pneumoniae* represent species commonly impacting human health. *C. pneumoniae* infects the upper respiratory tract and is associated with 10–20% of adult community-acquired pneumonia (1). *C. trachomatis* urogenital infection (serovars D-K) continues to be the most common sexually transmitted bacterial infection in the US (2) and ocular infection (serovars A-C) is the leading cause of infectious blindness in developing countries (3). Interestingly, anecdotal evidence suggests that chlamydial ocular infections have affected humans for millennia (4). Regardless of species, all *Chlamydia* share a biphasic developmental cycle that alternates between infectious elementary bodies (EBs) and non-infectious reticulate bodies (RBs). EBs have minimal metabolic activity and are often referred to as "spore-like" due to a durable cell wall that is resistant to mechanical and osmotic pressures [reviewed in (5)]. EB envelopes are comprised of an "atypical" Gram-negative lipid bilayer that is stabilized through disulfide bonds among cysteine-rich outer membrane proteins [reviewed in (6)]. During invasion, EBs traverse the host-cell plasma membrane and establish an intracellular

niche within a membrane bound vesicle termed the inclusion. Once the inclusion is established, EBs differentiate into non-infectious RBs which are capable of robust protein synthesis and replication. This stage of the developmental cycle occurs entirely within the protection of the infected host cell. The cycle is completed by asynchronous differentiation of RBs back into EBs capable of infecting neighboring cells after release. Escape of EBs from the host cell is accomplished by either lysis of the host cell or extrusion of intact inclusions (7).

The *Chlamydiales* order also contains *Chlamydia*-related bacteria often referred to as environmental *Chlamydia* due to their obligate intracellular parasitism of amoeba (8). The *Chlamydiaceae* family diverged from *Chlamydia*-related bacteria an estimated 700 million years ago at a time when all eukaryotes were single cell [reviewed in (9)]. Due to a dependence on intracellular survival and long evolution with eukaryotic hosts, it is not surprising that *Chlamydia* may have adapted multiple immune evasion strategies. During *C. trachomatis* genital infection, both innate and adaptive immune responses are clearly elicited with innate immunity functioning to limit ascension of infection and a Th1-, IFNγ-dependent adaptive response being required for control and resolution [reviewed in (10)]. Reinfection is common, and the majority of infections are asymptomatic, particularly in women (11). Progress in developing an efficacious vaccine has been challenged by poor protective immunity and increased pathology (12). Detrimental patient outcomes, such as tubal factor infertility and pelvic inflammatory disease, are associated with severe immunopathology which is initiated by the infected epithelium (13). Taken together, it is evident that *Chlamydia* maintain a finely tuned relationship with their host to interfere with productive immune recognition and clearance.

Formation of targeted membrane spanning pores using membrane attack complex/Perforin (MACPF)-domain proteins represents one mechanism used by both innate and adaptive arms of immunity. The MACPF-containing host proteins Perforin-2 and Complement C9 represent innate immune effectors whereas Perforin-1 functions during adaptive immunity (14). Both C9 and Perforin-2 are evolutionarily ancient whereas Perforin-1 likely arose by gene duplication of Perforin-2 during evolution of adaptive immunity in multi-cellular organisms (15, 16). All three function by killing microbes (C9 and Perforin-2) or host cells (Perforin-1) via polymerization and pore formation in target membranes (17). Interestingly, chlamydial genomes also contain a gene encoding a MACPF domain protein. It is hypothesized that this domain was acquired through horizontal gene transfer with a mammalian host (18, 19). A recent metagenomic study found only a small number of protein families that were taxonomically restricted within *Chlamydiaceae* (20). MACPF-containing proteins were among factors related to specific host interactions, providing further evidence that *Chlamydia* likely acquired this domain through co-evolution with a mammalian host.

Given the apparent long co-evolution of the host-pathogen interaction exemplified by *Chlamydia*, this review will summarize current evidence of chlamydial resistance and susceptibility to MACPF domain-mediated attack strategies while highlighting immune evasion mechanisms adapted through co-evolution. The discussion will focus on the more thoroughly characterized human pathogen *C. trachomatis* and corresponding immune modeling in mice using *C. muridarum*. We will also discuss the implications of the endogenous chlamydial MACPF domain protein in infection biology.

THE C9 MACPF DOMAIN

Complement is a central defense mechanism of the innate immune system that evolved to inactivate extracellularly localized pathogens (16). The complement system consists of more than 30 soluble serum proteins culminating in formation of the membrane attack complex (MAC) for complement-mediated cell lysis. The pore forming complex targets outer membranes of Gram-negative bacteria, enveloped viruses, and parasites. Activation of the complement cascade can occur via lectin, classical, or alternative pathways. Each pathway differs in the early mechanism used to recognize pathogens, but all converge through the covalent attachment of C3b to the target cell which then recruit downstream factors leading to MAC formation. Complement activation clearly occurs during chlamydial infection with the antibody-independent alternative pathway playing a major role (21). Multiple studies using a tissue-culture infection model have demonstrated that *Chlamydia* inclusion formation is significantly inhibited when EBs are pre-incubated with normal human sera (21–25) indicating complement factors may be important for controlling infection.

After typical C3b deposition on a bacterial surface, subsequently recruitmented components C5b-C8 then recruit soluble C9 monomers and facilitate C9 polymerization and the assembly of an 88-strand β-barrel membrane spanning pore (26). CryoEM studies have revealed that active pores contain 6 poly peptide chains, C5b, C6, C7, C8a, C8β, and C8γ, with 18 C9 monomers (27, 28). In experiments using C3 deficient mice, *C. muridarum* infectivity was not impacted during genital infections (29), however, *C. psittaci* pneumonia was significantly exacerbated when chlamydiae were introduced via a respiratory route (30). These data raise the possibility that C5b-C8 recruitment of C9 and pore formation may lead to fatal disruption of the chlamydial envelope; yet, formation of the MAC appears to be dispensable as a primary control mechanism for *Chlamydia* infections. Depletion of factors C5 and C8 from serum had no effect on *in vitro* anti-chlamydial activity (24). Additionally, *C. muridarum* shedding and ascension into the upper genital tract was not impacted in C5-deficient mice (29). Together these data indicate that late complement factors do not play a significant role in directly inactivating *Chlamydia*. The anaphylatoxin activities of C5a and C3a have been proposed as mediators of complement-dependent effects on infectivity and pathogenesis in mice (29–31). The antibody-independent inhibitory activity of complement in human serum could be mediated by opsonization and inactivation of chlamydial surface proteins required for cellular attachment and invasion (21), or deposition of other components such as properdin leading to targeting of *Chlamydia* to the lysosomal pathway for

degradation (32). It remains undefined, however, how findings in cell culture are related to those observed *in vivo*. Clearly, further investigation of this interesting area is warranted.

Given that the complement system primarily targets extracellular invaders, the obligate intracellular lifestyle of all *Chlamydia* spp. represents the most obvious defense mechanism. Beyond that, the biphasic developmental cycle represents an additional layer of protection. The extracellular, infectious EB possess a rigid and highly disulfide crosslinked outer envelope. Assembly of the MAC requires a fluid membrane capable of allowing lateral diffusion of MAC components and dramatic structural changes associated with pore formation (33). We therefore speculate that the EB envelope would be impervious to the MAC. A highly conserved chlamydial protease, CPAF, cleaves C3, and factor B *in vitro* and may inhibit activation of the alternate complement pathway (25). Host cell escape through extrusion, one of two chlamydial exit strategies, may be another defense mechanism. During extrusion, the inclusion pinches off from the host cell in an exocytosis-like mechanism. Both the host cell and inclusion remain intact, and the now double-membrane-bound inclusion is released into the extracellular space where it is stable up to 4 h *in vitro* (7, 34–36). We predict that it is unlikely that complement factors could gain access through the multiple layers of membrane comprising this barrier. *Chlamydia*-mediated recruitment of CD59 to the inclusion membrane (37) would represent an additional layer of defense. CD59 regulates formation of the MAC to prevent uncontrolled complement-mediated cell lysis (38) and would prevent any lytic pore formation should barrier integrity be compromised.

PERFORIN

The cytotoxic functions of natural killer cells (NKs) and cytotoxic T lymphocytes (CTLs) represent an adaptive defense mechanism against viral and intracellular pathogens. NKs and CTLs release cytoplasmic granules containing Perforin and proteolytic granzymes onto the surface of infected cells. In the presence of Ca^{2+}, Perforin binds to the target membrane and forms a transmembrane β-barrel pore. The N-terminal domain of Perforin contains a MACPF domain that allows insertion into lipid bilayers (39). Once assembled, the Perforin pore functions to deliver the proteolytic granzymes to the cytosol of the targeted cell. Two models of Perforin mediated granzyme delivery exist. The original model proposes that the Perforin pore provides direct delivery of granzymes to the cytosol, and a second model proposes that both Perforin and granzymes are endocytosed into the cell with subsequent delivery of granzymes by Perforin (40, 41). This model is supported by data demonstrating Perforin alters membrane curvature and stimulates the formation of endocytic vesicles (42).

During respiratory infection with *C. muridarum*, NKs infiltrate the lungs and become activated (43). Multiple studies have shown that NKs contribute modestly to clearance of chlamydial infection, however, this effect may be driven by IFN-γ expression and independent of Perforin targeting (43–45). *Chlamydia* infected cells are highly resistant to induction of apoptosis which is predicted to be due to chlamydial proteins that interrupt events such as cytochrome C release from mitochondria (46). NK cells extracted from *C. trachomatis* infected patients have also be shown to have decreased lytic capability (47). In two studies, Perforin knockout mice were not compromised in their ability to clear *C. muridarum* genital infection (48, 49), indicating Perforin-mediated cytotoxicity is not required for clearance of primary chlamydial infection. A third study, using lower infectious doses, did note a delayed clearance of infection in Perforin -/- mice (50); however, the authors concluded from their additional data that the phenotype occurred independently of direct interaction of cytotoxic cells with infected epithelia. Finally, the IFN-γ dependent/Perforin independent clearance of *Chlamydia* is supported by the finding that NK cells have a differential effect during infection where IFN-γ production is increased, yet cytolytic function is decreased (43).

Although some studies indicated *Chlamydia*-mediated interference with inducible expression of class I MHC on infected cells (51), primary chlamydial defense against Perforin may be more passive. *Ex vivo* studies indicated that *Chlamydia*-infected epithelial cells can be lysed by cytotoxic cells (52–54). Whether host cell lysis would directly contribute to control of chlamydial infection, however, is unclear since the disrupted cells would merely release any infectious EBs that had formed. Indeed, *in vivo* work noted above is consistent with Perforin-independent control mechanisms. In addition, the female genital tract represents one location where tolerance to foreign antigens must be greater for sustainment of the natural microbial flora. In both the gastrointestinal and female genital tracts, CD8+ T-cells have decreased expression of Perforin, thus comparatively limited cytotoxic activity (8, 55). In endocervical samples from both non-infected and *C. trachomatis* infected patients, effector memory T cell subsets showed decreased Perforin expression as compared to paired blood controls (55). Therefore, infection of the genital tract likely provides an advantageous niche for chlamydial infection.

PERFORIN-2

In contrast to the relative lack of susceptibility of *Chlamydia* to Perforin-1 and Complement C9, there does appear to be a role for the most recently described MACPF protein, Perforin-2. Perforin-2, encoded by the intronless *MPEG1*, represents perhaps the most evolutionary ancient and conserved member of the MACPF family of proteins (16, 56, 57). Originally shown to have anti-bacterial properties in sponges (58) and zebrafish (59), it is now established that Perforin-2 is capable of killing a range of cell-associated bacteria including Gram positive, Gram negative, and acid fast bacteria (60). A model has emerged where Perforin-2 is trafficked to bacteria-containing vacuoles and disrupts the integrity of bacterial envelopes by polymerizing into multi-subunit pores (14, 57). To date, the susceptibility of *Chlamydia* spp. to Perforin-2 represents the sole indication for how an obligate intracellular bacterium might respond to this novel innate immune mechanism (61).

Professional phagocytes, including macrophages and neutrophils, represent a functionally important arm of innate immunity, and Perforin-2 expression is constitutive in these cells (60). Cumulative data using murine-specific *C. muridarum* in a well-established mouse model of genital tract infection indicate robust recruitment of professional phagocytes to infected tissues. Although innate immunity is not required for resolution of infection, it has been proposed to function in opposing ascension of chlamydial infection into the upper genital tract (10). Although some degree of chlamydial growth can be detected in macrophage cell lines, *Chlamydia* spp. do not productively infect primary cells (62). RNAi knock-down of *MPEG1* message was used to provide direct evidence for Perforin-2-mediated eradication of *Chlamydia* in infected macrophages (61). Transmission electron microscopy revealed that mock-treated murine BV2 macrophages contained vacuoles harboring debris and few intact chlamydiae, whereas Perforin-2-deficient cells contained intact inclusions that yielded 10^3 more progeny 24 h post infection. Knock-down of Perforin-2 resulted in levels of progeny *C. trachomatis* L2 EB production equivalent to similarly infected HeLa cells. Comparable results were seen for *C. trachomatis* serovars B and D indicating that Perforin-2 is capable of inhibiting a range of *C. trachomatis* serovars. In addition, *C. muridarum* was also susceptible to Perforin-2 activity. The BV2 line was initially tested due to the comparatively high level of constitutive Perforin-2 expression, yet similar results were obtained using the murine RAW 264.7 cell line (61). To date, the potential role of Perforin-2-dependent inhibition of *Chlamydia* has not been tested in human cell lines such as THP-1 or HL-60; however, Perforin-2 has been shown in these cells to limit growth of other bacteria such as *Salmonella, S. aureus,* and *Mycobacterium* (60) raising the probability that the observed anti-*Chlamydia* potential of Perforin-2 also occurs in humans cells.

These data are consistent with macrophage-produced Perforin-2 having a significant role in controlling chlamydial infection. How Perforin-2 inactivates intra-inclusion chlamydiae remains an open question. *Chlamydia* are rapidly targeted to lysosomal compartments in macrophages (61), yet develop normally in Perforin-2 deficient macrophages. Hence, Perforin-2 plays an active role in clearance at the cellular level. Based on a proposed working model for susceptibility of intracellular bacteria (14), deployment of Perforin-2 to the luminal face of subsequent *Chlamydia*-containing vacuolar membranes would culminate in insertion and polymerization of the Perforin-2 pore in chlamydial membranes. This would be predicted to disrupt the integrity of the RB envelope and lead to lysis. This model is supported by electron micrographs of Perforin-2 sufficient and deficient cells were clearly lysed chlamydial material is detected within an apparently intact vacuole (61). The *Chlamydia* highly cross-linked envelope of the EB developmental form (6) is likely resistant to Perforin-2 insertion. However, Perforin-2-mediated killing of *Mycobacteria* spp., which possess a highly impermeable, mycolic acid-containing envelope, suggest that the atypical RB envelope may be susceptible to Perforin-2 attack. Perforation of bacterial envelopes has also been shown to promote access of antimicrobial substances like reactive oxygen species (63). This mechanism may contribute to observed *Chlamydia* clearance since RAW 264.7 macrophages generate ROS and iNOS in response to infection, and pharmacologic inhibitors or scavengers of reactive species benefit chlamydial survival (64). Finally, macrophage-mediated killing of *C. trachomatis* has also been linked to autophagy (65–67). It is possible that Perforin-2 and autophagy mechanisms are linked, yet Perforin-2 has been proposed to function upstream of autophagy based on the greater impact on chlamydial survival (61).

Interestingly, chlamydial exit from infected epithelial cells via extrusion may subvert Perforin-2-mediated killing. *Chlamydia*-containing extrusionsare phagocytosed by bone marrow-derived macrophages and retain infectivity compared to non-encapsulated *Chlamydia* (36). In this scenario, the extra lipid bilayer could shield *Chlamydia* from detection and Perforin-2-mediated killing since machinery necessary for targeting Perforin-2 to membranes would be absent from the extrusion membrane (68) Finally, *C. pneumoniae* appears to be capable of replication in a subset of primary phagocytes (62), raising the possibility of additional, species-specific protective mechanisms. This would be consistent with observations that other pathogens such as *Salmonella* and enteropathogenic *E. coli* have evolved Perforin-2-specific mitigation mechanisms (68).

Columnar epithelial cells lining target mucosa represent the productive replication niche for all *Chlamydia* spp. Therefore, *Chlamydia* would be predicted to possess effective Perforin-2 protective mechanisms in this cell type. *MPEG1* is inducible in non-myeloid cells, and Perforin-2-specific signal is below detection in multiple epithelial lines (60). Indeed, Perforin-2 was absent in both mock-treated and *Chlamydia*-infected cells in a HeLa-cell infection model (61). In contrast, treatment of cells with heat-killed *Chlamydia* resulted in significant up-regulation of Perforin-2, indicating that stealthy subversion of signals leading to *MPEG1* expression as one protective mechanism. *MPEG1* is inducible with IFNγ and type I interferons (60), both of which play important roles in limiting chlamydial infection *in vivo* (10). Indeed, *MPEG1* upregulation was evident in early microarray analyses of IFNγ-treated oviduct epithelial cells (69). Interestingly, cells containing established inclusions prevent IFNγ-mediated induction of Perforin-2 in epithelial cells. This effect required viable *Chlamydia*. The role of IFNβ-mediated induction of *MPEG1* during chlamydial infection has not been tested, yet a recent report indicated a requirement of Perforin-2 in transducing activation signals through the cognate receptor, IFNAR (70). Hence, Perforin-2 mediated killing is counter-indicated in infected epithelial cells. Importantly, *ex vivo* treatment of murine genital tract-derived epithelial cells with *Chlamydia*-conditioned media resulted in upregulation of *MPEG1* (50). Proinflammatory signals are certainly capable of acting on uninfected, bystander cells which could then be more resistant to chlamydial infection in a Perforin-2-dependent manner. In support of this notion, ectopic overexpression of RFP-tagged Perforin-2 in HeLa cells resulted in efficient killing of *Chlamydia* (61). It is important to note that polymerization of Perforin-2 for crystallographic studies required an acidic environment and is postulated to reflect delivery of Perforin-2 to acidified phagolysosomes (71, 72). The chlamydial inclusion,

however, does not acidify and remains segregated from the lysosomal pathway (73), raising the possibility of alternative polymerization mechanisms. It is also possible that non-physiologic levels due to ectopic expression favor polymerization *in vivo*. Regardless, it seems apparent that *Chlamydia* avoid Perforin-2 killing in epithelial cells by avoiding and suppressing *MPEG1* expression. Although Perforin-2 proteins levels were not shown, inhibition of *C. muridarum* in IFNγ-primed murine embryonic fibroblasts was unchanged after Perforin-2 knockdown using siRNAs (74). These data may, once again, elude to alternative, species-specific susceptiblity of *Chlamydia* to Perforin-2.

Mice deficient in *MPEG1* have subsequently been employed to test the anti-bacterial role of Perforin-2 in an animal model. Cells derived from *MPEG1* -/- mice are deficient in *ex vivo* killing of a range of bacteria including *L. monocytogenes* (75), *Mycobacteria* spp., *S. aureus*, *S. enterica* Typhimurium, and enteropathogenic *E. coli* (60, 68). *MPEG1* -/- mice are more susceptible to systemic listeriosis (75) and succumb to sublethal doses of *S. aureus* and *Salmonella* in cutaneous and orogastric infection models, respectively (60). Collectively, these data indicate the fundamental importance of Perforin-2 in controlling a diverse array of bacterial infections. It remained unclear how the impact of Perforin-2 would manifest during a mammalian model of chlamydial infection. To that end, the well-established intravaginal infection model was employed were *Chlamydia* are deposited at the cervical vault and bacterial shedding is enumerated by swabbing over time. We infected groups of 5 wild type or *MPEG1* -/- mice with 5×10^4 infectious particles of *C. muridarum* and monitored chlamydial shedding and mouse body weight over time (**Figure 1**). Time to resolution was not extended in the absence of Perforin-2. However, MPEG -/- mice shed statistically fewer IFUs overall with a ca. $\log_{10}$ decrease observed on days 11 and 15. Interestingly, the *MPEG1* -/- mice did appear ill with ruffled fur (Fields, unpublished) and decreased body weight (**Figure 1B**). These symptoms persisted until times corresponding to resolution. We speculate that these data could indicate systemic dissemination of chlamydiae beyond the genital tract. Infiltration of macrophages and neutrophils to the sites of active infection functions to contain chlamydiae (10). Less efficient killing by professional phagocytes could allow rapid ascension and seeding of peripheral sites. The role of these myeloid cells could be easily tested using bone-marrow chimeric mice expressing or lacking *MPEG1*. A functional adaptive response is likely intact given that infections in *MPEG1* -/- mice were resolved comparable to wild type. As is the case with the molecular mechanisms of Perforin-2 function in cell culture, many provocative questions remain to be resolved.

THE CHLAMYDIAL MACPF

Whole-genome sequencing of *Chlamydia* spp. originally identified a gene encoding a MACPF domain protein (18). In the reference strain *C. trachomatis* serovar D, this protein is designated CT153 (76). Gene orthologs were conserved in all *C. trachomatis* genomes sampled and located within the highly variable plasticity zone, immediately upstream pzPLD genes encoding putative lipid-modifying proteins (77, 78). Although similarity varies, orthologs are also present in other *Chlamydia* spp (**Figure 2**). Consistent with acquisition through horizontal gene transfer during co-evolution, the MACPF gene sequence of *C. pneumoniae* can differentiate bacteria isolated from indigenous and non-indigenous human sources from varying geographical regions (79). C-terminal amino acid residues 427–621 share homology with the MACPF domain found in C9 and Perforin. CT153 appears to undergo some proteolytic processing (78). The full length p91 was observed as the dominant polypeptide in EBs and is rapidly cleaved (15 min) into p57 and p41 fragments independent of *de novo* chlamydial protein synthesis. Processing may occur through host-mediated proteolytic cleavage or auto-proteolysis. This suggests distinct functions for full-length and processed peptides, yet it should be noted that the possibility of post-lysis degradation has not been ruled out (80). Currently, there is limited understanding

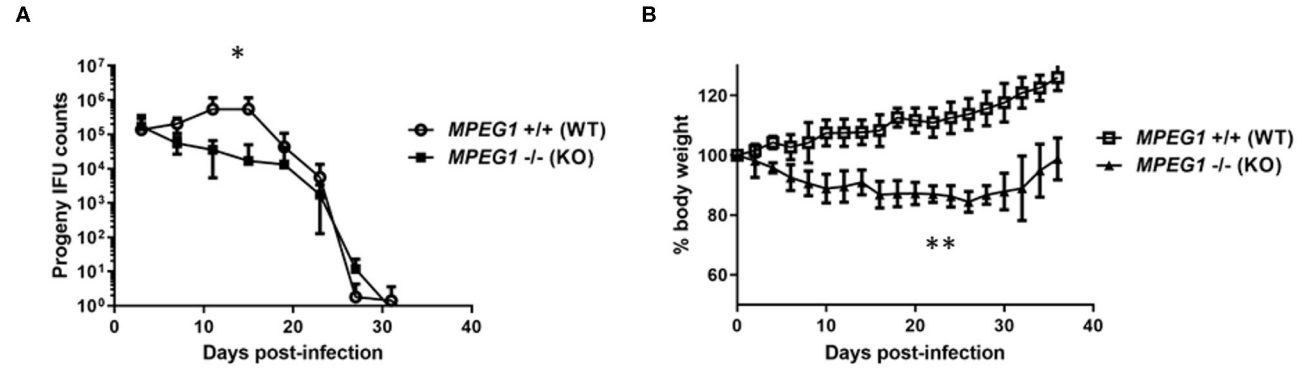

FIGURE 1 | *C. muridarum* infection of Perforin-2 KO mice. Groups of 5, 6–7 week-old female wild type (*MPEG1*+/+) or KO (*MPEG1* -/-) C57BL/6 × 129 × 1/SJV mice (60) were infected intravaginally with 5×10^4 *C. muridarum* 5 days after synchronization with medroxyprogesterone. Shed IFUs **(A)** and body weights **(B)** were measured over time (days). **(A)** Shed IFUs were enumerated every 4 days according to standard protocols and averages within groups are shown with standard deviations. Curves were different (*$p < 0.01$) by two-way ANOVA. **(B)** Average body weights (+/– standard deviation) within groups are shown. KO weights were significantly different (**$p < 0.0001$) from WT via two-way ANOVA. Data represent one of two replicate experiments ($n = 2$).

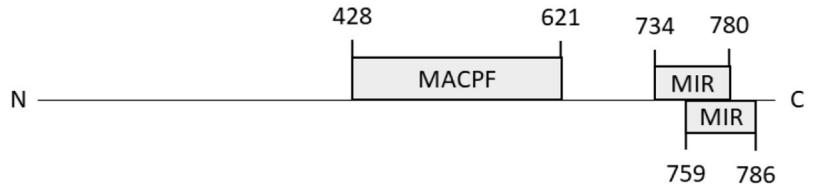

Species	N-Terminal Domain (1-427)	MACPF (428-621)	Intervening (622-733)	MIR (734-780)	MIR (759-786)
C. pneumoniae	47%	54%	45%	65%	68%
C. muridarum	67%	79%	77%	76%	71%
C. psittaci	48%	59%	41%	61%	57%
C. pecorum	48%	53%	45%	55%	64%
C. felis	62%	70%	61%	78%	86%
C. suis	77%	84%	83%	85%	86%

FIGURE 2 | Similarity of *C. trachomatis* CT153 domains to orthologs in other *Chlamydia* spp. The 810 residue CT153 of *C. trachomatis* D/UW-3 is shown schematically with predicted functional domains highlighted. These include the MACPF and Mannosyltransferase, Inositol 1,4,5-trisphosphate receptor and Ryanodine receptor (MIR) domains. Residues corresponding to the N-Terminal domain (aa 1-427), MACPF (aa 428-621), Intervening domain (aa 622-733), or MIR (aa 734-780 and aa 759-786) were used as query sequences in NCBI BLAST searches. Searches were performed using *C. pneumoniae* TW-183, *C. psittaci* 6 BC, *C. muridarum* Nigg, *C. suis* S45, *C. felis* DSM:26967, and C. *pecorum* Bo/E58 data bases. Calculated percent identity in respective species is shown for each domain.

regarding the function and cytolytic activity of this protein. It was originally postulated that the MACPF domain protein may be essential for *Chlamydia* since a saturating screen for chemically-induced mutations in *C. muridarum* failed to reveal nonsense mutations in *tc0431* (81). However, inactivating transposon insertions were subsequently observed in both *C. muridarum* and *C. trachomatis* (82, 83). None of the mutations abolished intracellular survival, indicating that this protein is not essential for cultivation in tissue culture. These data are in line with the apparent lack of a MACPF-encoding gene in *C. abortus* which can infect the same cells (84). CT153 is expressed during mid-cycle (85) and has been shown to localize with both RBs near the inclusion membrane and within the inclusion membrane (78). These data suggest that CT153 may permeabilize the inclusion membrane. Complete lysis of the inclusion membrane is likely retarded by structural integrity conferred by chlamydial inclusion membrane proteins (86). For example, loss of specific Incs results in premature lysis of the parasitophorous vacuole (87, 88). The embedded pore could instead facilitate diffusion of small molecules into or out of the inclusion or be involved in fusion events during exocytic exit from cells. Clearly, this is a rich area needing further investigation.

CONCLUDING REMARKS

Chlamydia are ancient bacteria that have evolved with mammalian hosts for of millions of years. To sustain a privileged niche and intracellular survival, *Chlamydia* have adapted resistance mechanisms to major host defenses that include formation of the MAC and Perforin mediated cytotoxicity. *Chlamydia* are not completely resistant to MACPF attack strategies since these pathogens are susceptible to Perforin-2 activities of professional phagocytes. Finally, acquisition of the MACPF domain from hosts may have given the bacteria an edge for survival, however it is unclear whether this domain is responsible for resistance to host immunity or has other functions.

AUTHOR CONTRIBUTIONS

Article preparation and writing was performed by GK and KF. KF performed work associated with **Figure 1**. All authors contributed to the article and approved the submitted version.

FUNDING

KF and GK were supported by Public Health Service grants from the National Institutes of Health/NIAD including AI117876 to KF and AI147417 to GK.

ACKNOWLEDGMENTS

We thank Dr. K. Wolf, R. Hayman, and M. Clouse for critical reading of the manuscript.

REFERENCES

1. Grayston JT, Campbell LA, Kuo C-C, Mordhorst CH, Saikku P, Thorn DH, et al. A new respiratory tract pathogen: *Chlamydia pneumoniae* strain TWAR. *J Infect Dis.* (1990) 161:618–25. doi: 10.1093/infdis/161.4.618
2. National Center for HIV/AIDS Viral Hepatitis STD and TB Prevention (U.S.). Division of STD Prevention. *Sexually Transmitted Disease Surveillance 2018*. Atlanta, GA: CDC (2019).
3. Mariotti SP, Pascolini D, Rose-Nussbaumer J. Trachoma: global magnitude of a preventable cause of blindness. *Br J Ophthalmol.* (2009) 93:563–8. doi: 10.1136/bjo.2008.148494
4. Halberstädter L, Prowazek SV. Über zelleinschlüsse parasitärer natur beim trachom. *Arb Aus Dem Kais Gesundheitsamte*. (1907) 26:44–7.
5. Cossé MM, Hayward RD, Subtil A. One face of *Chlamydia trachomatis*: the infectious elementary body. *Curr Top Microbiol Immunol.* (2018) 412:35–58. doi: 10.1007/82_2016_12
6. Christensen S, McMahon RM, Martin JL, Huston WM. Life inside and out: making and breaking protein disulfide bonds in *Chlamydia*. *Crit Rev Microbiol.* (2019) 45:33–50. doi: 10.1080/1040841X.2018.1538933
7. Hybiske K, Stephens RS. Mechanisms of host cell exit by the intracellular bacterium *Chlamydia*. *Proc Natl Acad Sci. USA*. (2007) 104:11430–5. doi: 10.1073/pnas.0703218104
8. Bayramova F, Jacquier N, Greub G. Insight in the biology of *Chlamydia*-related bacteria. *Microbes Infect.* (2018) 20:432–40. doi: 10.1016/j.micinf.2017.11.008
9. Nunes A, Gomes JP. Evolution, phylogeny, and molecular epidemiology of *Chlamydia*. *Infect Genet Evol.* (2014) 23:49–64. doi: 10.1016/j.meegid.2014.01.029
10. Darville T, Hiltke TJ. Pathogenesis of genital tract disease due to *Chlamydia trachomatis*. *J Infect Dis.* (2010) 201(Suppl. 2):S114–25. doi: 10.1086/652397
11. Hosenfeld CB, Workowski KA, Berman S, Zaidi A, Dyson J, Mosure D, et al. Repeat infection with *Chlamydia* and gonorrhea among females: a systematic review of the literature. *Sex Transm Dis.* (2009) 36:478–89. doi: 10.1097/OLQ.0b013e3181a2a933
12. Schachter J. Overview of *Chlamydia trachomatis* infection and the requirements for a vaccine. *Rev Infect Dis.* (1985) 7:713–6. doi: 10.1093/clinids/7.6.713
13. Stephens RS. The cellular paradigm of chlamydial pathogenesis. *Trends Microbiol.* (2003) 11:44–51. doi: 10.1016/S0966-842X(02)00011-2
14. McCormack R, de Armas L, Shiratsuchi M, Podack ER. Killing machines: three pore-forming proteins of the immune system. *Immunol Res.* (2013) 57:268–78. doi: 10.1007/s12026-013-8469-9
15. Sunyer JO, Boshra H, Lorenzo G, Parra D, Freedman B, Bosch N. Evolution of complement as an effector system in innate and adaptive immunity. *Immunol Res.* (2003) 27:549–64. doi: 10.1385/IR:27:2-3:549
16. McCormack R, Podack ER. Perforin-2/Mpeg1 and other pore-forming proteins throughout evolution. *J Leukoc Biol.* (2015) 98:761–8. doi: 10.1189/jlb.4MR1114-523RR
17. Podack ER, Munson GP. Killing of microbes and cancer by the immune system with three mammalian pore-forming killer proteins. *Front Immunol.* (2016) 7:464. doi: 10.3389/fimmu.2016.00464
18. Ponting CP. Chlamydial homologues of the MACPF (MAC/perforin) domain. *Curr Biol.* (1999) 9:R911–3. doi: 10.1016/S0960-9822(00)80102-5
19. Wolf YI, Aravind L, Koonin EV. Rickettsiae and *Chlamydiae*: evidence of horizontal gene transfer and gene exchange. *Trends Genet.* (1999) 15:173–5. doi: 10.1016/S0168-9525(99)01704-7
20. Dharamshi JE, Tamarit D, Eme L, Stairs CW, Martijn J, Homa F, et al. Marine sediments illuminate *Chlamydiae* diversity and evolution. *Curr Biol.* (2020) 30:1032–48.e7. doi: 10.1016/j.cub.2020.02.016
21. Hall RT, Strugnell T, Wu X, Devine DV, Stiver HG. Characterization of kinetics and target proteins for binding of human complement component C3 to the surface-exposed outer membrane of *Chlamydia trachomatis* serovar L2. *Infect Immun.* (1993) 61:1829–34. doi: 10.1128/IAI.61.5.1829-1834.1993
22. Johnson AP, Osborn MF, Rowntree S, Thomas BJ, Taylor-Robinson D. A study of inactivation of *Chlamydia trachomatis* by normal human serum. *Br J Vener Dis.* (1983) 59:369–72. doi: 10.1136/sti.59.6.369
23. Osborn MF, Johnson AP, Taylor-Robinson D. Susceptibility of different serovars of *Chlamydia trachomatis* to inactivation by normal human serum. *Genitourin Med.* (1985) 61:244–6. doi: 10.1136/sti.61.4.244
24. Lin JS, Yan LL, Ho Y, Rice PA. Early complement components enhance neutralization of *Chlamydia trachomatis* infectivity by human sera. *Infect Immun.* (1992) 60:2547–50. doi: 10.1128/IAI.60.6.2547-2550.1992
25. Yang Z, Tang L, Zhou Z, Zhong G. Neutralizing antichlamydial activity of complement by chlamydia-secreted protease CPAF. *Microbes Infect.* (2016) 18:669–74. doi: 10.1016/j.micinf.2016.07.002
26. Dudkina NV, Spicer BA, Reboul CF, Conroy PJ, Lukoyanova N, Elmlund H, et al. Structure of the poly-C9 component of the complement membrane attack complex. *Nat Commun.* (2016) 7:10588. doi: 10.1038/ncomms10588
27. Sharp TH, Koster AJ, Gros P. Heterogeneous MAC initiator and pore structures in a lipid bilayer by phase-plate cryo-electron tomography. *Cell Rep.* (2016) 15:1–8. doi: 10.1016/j.celrep.2016.03.002
28. Menny A, Serna M, Boyd CM, Gardner S, Joseph AP, Morgan BP, et al. CryoEM reveals how the complement membrane attack complex ruptures lipid bilayers. *Nat Commun.* (2018) 9:5316. doi: 10.1038/s41467-018-07653-5
29. Yang Z, Conrad T, Zhou Z, Chen J, Dutow P, Klos A, et al. Complement factor C5 but not C3 contributes significantly to hydrosalpinx development in mice infected with *Chlamydia muridarum*. *Infect Immun.* (2014) 82:3154–63. doi: 10.1128/IAI.01833-14
30. Bode J, Dutow P, Sommer K, Janik K, Glage S, Tümmler B, et al. A new role of the complement system: C3 provides protection in a mouse model of lung infection with intracellular *Chlamydia psittaci*. *PLoS ONE.* (2012) 7:e50327. doi: 10.1371/journal.pone.0050327
31. Dutow P, Fehlhaber B, Bode J, Laudeley R, Rheinheimer C, Glage S, et al. The complement C3a receptor is critical in defense against *Chlamydia psittaci* in mouse lung infection and required for antibody and optimal T cell response. *J Infect Dis.* (2014) 209:1269–78. doi: 10.1093/infdis/jit640
32. Cortes C, Ferreira VP, Pangburn MK. Native properdin binds to *Chlamydia pneumoniae* and promotes complement activation. *Infect Immun.* (2011) 79:724–31. doi: 10.1128/IAI.00980-10
33. Bayly-Jones C, Bubeck D, Dunstone M. The mystery behind membrane insertion: a review of the complement membrane attack complex. *Philos Trans R Soc Lond Biol Sci.* (2017) 372:20160221. doi: 10.1098/rstb.2016.0221
34. Doughri AM, Storz J, Altera KP. Mode of entry and release of *Chlamydiae* in infections of intestinal epithelial cells. *J Infect Dis.* (1972) 126:652–7. doi: 10.1093/infdis/126.6.652
35. Chin E, Kirker K, Zuck M, James G, Hybiske K. Actin recruitment to the *Chlamydia* inclusion is spatiotemporally regulated by a mechanism that requires host and bacterial factors. *PLoS ONE.* (2012) 7:e46949. doi: 10.1371/journal.pone.0046949
36. Zuck M, Ellis T, Venida A, Hybiske K. Extrusions are phagocytosed and promote *Chlamydia* survival within macrophages: extrusions are phagocytosed and promote *Chlamydia* survival within macrophages. *Cell Microbiol.* (2017) 19:e12683. doi: 10.1111/cmi.12683
37. Hasegawa A, Sogo LF, Tan M, Sutterlin C. Host complement regulatory protein CD59 is transported to the chlamydial inclusion by a golgi apparatus-independent pathway. *Infect Immun.* (2009) 77:1285–92. doi: 10.1128/IAI.01062-08
38. Kim DD, Song W-C. Membrane complement regulatory proteins. *Clin Immunol.* (2006) 118:127–36. doi: 10.1016/j.clim.2005.10.014
39. Law RHP, Lukoyanova N, Voskoboinik I, Caradoc-Davies TT, Baran K, Dunstone MA, et al. The structural basis for membrane binding and pore formation by lymphocyte perforin. *Nature.* (2010) 468:447–51. doi: 10.1038/nature09518
40. Froelich CJ, Orth K, Turbov J, Seth P, Gottlieb R, Babior B, et al. New paradigm for lymphocyte granule-mediated cytotoxicity: target cells bind and internalize granzyme b, but an endosomolytic agent is necessary for cytosolic delivery and subsequent apoptosis. *J Biol Chem.* (1996) 271:29073–9. doi: 10.1074/jbc.271.46.29073
41. Pipkin ME, Lieberman J. Delivering the kiss of death: progress on understanding how perforin works. *Curr Opin Immunol.* (2007) 19:301–8. doi: 10.1016/j.coi.2007.04.011
42. Praper T, Sonnen AF-P, Kladnik A, Andrighetti AO, Viero G, Morris KJ, et al. Perforin activity at membranes leads to invaginations and vesicle formation. *Proc Natl Acad Sci. USA.* (2011) 108:21016–21. doi: 10.1073/pnas.1107473108

43. Zhao L, Gao X, Peng Y, Joyee AG, Bai H, Wang S, et al. Differential modulating effect of natural killer (NK) T cells on interferon-γ production and cytotoxic function of NK cells and its relationship with NK subsets in *Chlamydia muridarum* infection: differential modulation of NKT on NK function. *Immunology*. (2011) 134:172–84. doi: 10.1111/j.1365-2567.2011.03477.x
44. Williams DM, Grubbs BG, Schachter J, Magee DM. Gamma interferon levels during *Chlamydia trachomatis* pneumonia in mice. *Infect Immun.* (1993) 61:3556–8. doi: 10.1128/IAI.61.8.3556-3558.1993
45. Tseng C-TK, Rank RG. Role of NK cells in early host response to chlamydial genital infection. *Infect Immun.* (1998) 66:5867–75. doi: 10.1128/IAI.66.12.5867-5875.1998
46. Fan T, Lu H, Hu H, Shi L, McClarty GA, Nance DM, et al. Inhibition of apoptosis in *Chlamydia*-infected cells: blockade of mitochondrial cytochrome c release and caspase activation. *J Exp Med.* (1998) 187:487–96. doi: 10.1084/jem.187.4.487
47. Mavoungou E, Poaty-Mavoungou V, Touré FS, Sall A, Delicat A, Yaba P, et al. Impairment of natural killer cell activity in *Chlamydia trachomatis* infected individuals. *Trop Med Int Health*. (1999) 4:719–27. doi: 10.1046/j.1365-3156.1999.00479.x
48. Perry LL, Feilzer K, Hughes S, Caldwell HD. Clearance of *Chlamydia trachomatis* from the murine genital mucosa does not require perforin-mediated cytolysis or fas-mediated apoptosis. *Infect Immun.* (1999) 67:1379–85. doi: 10.1128/IAI.67.3.1379-1385.1999
49. Murthy AK, Li W, Chaganty BKR, Kamalakaran S, Guentzel MN, Seshu J, et al. Tumor necrosis factor alpha production from CD8+ T cells mediates oviduct pathological sequelae following primary genital chlamydia muridarum infection. *Infect Immun.* (2011) 79:2928–35. doi: 10.1128/IAI.05022-11
50. Johnson RM, Kerr MS, Slaven JE. Perforin is detrimental to controllinγ *C.* muridarum replication *in vitro*, but not *in vivo*. *PLoS ONE*. (2013) 8:e63340. doi: 10.1371/journal.pone.0063340
51. Zhong G, Liu L, Fan T, Fan P, Ji H. Degradation of transcription factor RFX5 during the inhibition of both constitutive and interferon gamma-inducible major histocompatibility complex class I expression in chlamydia-infected cells. *J Exp Med.* (2000) 191:1525–34. doi: 10.1084/jem.191.9.1525
52. Beatty PR, Stephens RS. CD8+ T lymphocyte-mediated lysis of *Chlamydia*-infected L cells using an endogenous antigen pathway. *J Immunol Baltim Md.* (1994) 153:4588–95.
53. Starnbach MN, Bevan MJ, Lampe MF. Protective cytotoxic T lymphocytes are induced during murine infection with *Chlamydia trachomatis*. *J Immunol Baltim Md.* (1994) 153:5183–9.
54. Starnbach MN, Bevan MJ, Lampe MF. Murine cytotoxic T lymphocytes induced following *Chlamydia trachomatis* intraperitoneal or genital tract infection respond to cells infected with multiple serovars. *Infect Immun.* (1995) 63:3527–30. doi: 10.1128/IAI.63.9.3527-3530.1995
55. Ibana JA, Myers L, Porretta C, Lewis M, Taylor SN, Martin DH, et al. The major CD8 T cell effector memory subset in the normal and *Chlamydia trachomatis*-infected human endocervix is low in perforin. *BMC Immunol.* (2012) 13:66. doi: 10.1186/1471-2172-13-66
56. McCormack R, de Armas LR, Shiratsuchi M, Ramos JE, Podack ER. Inhibition of intracellular bacterial replication in fibroblasts is dependent on the perforin-like protein (Perforin-2) encoded by macrophage-expressed gene 1. *J Innate Immun.* (2013) 5:185–94. doi: 10.1159/000345249
57. Ni T, Gilbert RJC. Repurposing a pore: highly conserved perforin-like proteins with alternative mechanisms. *Philos Trans R Soc B Biol Sci.* (2017) 372:20160212. doi: 10.1098/rstb.2016.0212
58. Wiens M, Korzhev M, Krasko A, Thakur NL, Perović-Ottstadt S, Breter HJ, et al. Innate immune defense of the sponge *Suberites domuncula* against bacteria involves a MyD88-dependent signaling pathway: induction of a perforin-like molecule. *J Biol Chem.* (2005) 280:27949–59. doi: 10.1074/jbc.M504049200
59. Benard EL, Racz PI, Rougeot J, Nezhinsky AE, Verbeek FJ, Spaink HP, et al. Macrophage-expressed perforins Mpeg1 and Mpeg1.2 have an anti-bacterial function in zebrafish. *J Innate Immun.* (2015) 7:136–52. doi: 10.1159/000366103
60. McCormack RM, de Armas LR, Shiratsuchi M, Fiorentino DG, Olsson ML, Lichtenheld MG, et al. Perforin-2 is essential for intracellular defense of parenchymal cells and phagocytes against pathogenic bacteria. *eLife*. (2015) 4:e06508. doi: 10.7554/eLife.06508
61. Fields KA, McCormack R, de Armas LR, Podack ER. Perforin-2 restricts growth of *Chlamydia trachomatis* in macrophages. *Infect Immun.* (2013) 81:3045–54. doi: 10.1128/IAI.00497-13
62. Herweg J-A, Rudel T. Interaction of *Chlamydiae* with human macrophages. *FEBS J.* (2016) 283:608–18. doi: 10.1111/febs.13609
63. Bai F, McCormack RM, Hower S, Plano GV, Lichtenheld MG, Munson GP. Perforin-2 breaches the envelope of phagocytosed bacteria allowing antimicrobial effectors access to intracellular targets. *J Immunol Baltim Md.* (2018) 201:2710–20. doi: 10.4049/jimmunol.1800365
64. Rajaram K, Nelson DE. Chlamydia muridarum infection of macrophages elicits bactericidal nitric oxide production via reactive oxygen species and cathepsin B. *Infect Immun.* (2015) 83:3164–75. doi: 10.1128/IAI.00382-15
65. Yasir M, Pachikara ND, Bao X, Pan Z, Fan H. Regulation of chlamydial infection by host autophagy and vacuolar ATPase-bearing organelles. *Infect Immun.* (2011) 79:4019–28. doi: 10.1128/IAI.05308-11
66. Sun HS, Eng EWY, Jeganathan S, Sin AT-W, Patel PC, Gracey E, et al. *Chlamydia trachomatis* vacuole maturation in infected macrophages. *J Leukoc Biol.* (2012) 92:815–27. doi: 10.1189/jlb.0711336
67. Al-Zeer MA, Al-Younes HM, Lauster D, Abu Lubad M, Meyer TF. *Autophagy* restricts *Chlamydia trachomatis* growth in human macrophages via IFNG-inducible guanylate binding proteins. *Autophagy*. (2013) 9:50–62. doi: 10.4161/auto.22482
68. McCormack RM, Lyapichev K, Olsson ML, Podack ER, Munson GP. Enteric pathogens deploy cell cycle inhibiting factors to block the bactericidal activity of Perforin-2. *eLife*. (2015) 4:e06505. doi: 10.7554/eLife.06505
69. Nelson DE, Virok D, Wood H, Roshick C, Johnson RM, Whitmire WM, et al. Chlamydial IFN-gamma immune evasion is linked to host infection tropism. *Proc Natl Acad Sci USA*. (2005) 26:10658–63. doi: 10.1073/pnas.0504198102
70. McCormack R, Hunte R, Podack ER, Plano GV, Shembade N. An essential role for Perforin-2 in type I IFN signaling. *J Immunol Baltim Md.* (2020) 204:2242–56. doi: 10.4049/jimmunol.1901013
71. Pang SS, Bayly-Jones C, Radjainia M, Spicer BA, Law RHP, Hodel AW, et al. The cryo-EM structure of the acid activatable pore-forming immune effector macrophage-expressed gene 1. *Nat Commun.* (2019) 10:4288. doi: 10.1038/s41467-019-12279-2
72. Ni T, Jiao F, Yu X, Aden S, Ginger L, Williams SI, et al. Structure and mechanism of bactericidal mammalian Perforin-2, an ancient agent of innate immunity. *Sci Adv.* (2020) 6:eaax8286. doi: 10.1126/sciadv.aax8286
73. Heinzen RA, Scidmore MA, Rockey DD, Hackstadt T. Differential interaction with endocytic and exocytic pathways distinguish parasitophorous vacuoles of *Coxiella burnetii* and *Chlamydia trachomatis*. *Infect Immun.* (1996) 64:796–809. doi: 10.1128/IAI.64.3.796-809.1996
74. Giebel AM, Hu S, Rajaram K, Finethy R, Toh E, Brothwell JA, et al. Genetic screen in *Chlamydia muridarum* reveals role for an interferon-induced host cell death program in antimicrobial inclusion rupture. *MBio.* (2019) 10:e00385–19. doi: 10.1128/mBio.00385-19
75. McCormack R, Bahnan W, Shrestha N, Boucher J, Barreto M, Barrera CM, et al. Perforin-2 protects host cells and mice by restricting the vacuole to cytosol transitioning of a bacterial pathogen. *Infect Immun.* (2016) 84:1083–91. doi: 10.1128/IAI.01434-15
76. Stephens RS, Kalman S, Lammel C, Fan J, Marathe R, Aravind L, et al. Genome sequence of an obligate intracellular pathogen of humans: *Chlamydia trachomatis*. *Science*. (1998) 282:754–9. doi: 10.1126/science.282.5389.754
77. Read TD. Genome sequences of *Chlamydia trachomatis* MoPn and *Chlamydia pneumoniae* AR39. *Nucleic Acids Res.* (2000) 28:1397–406. doi: 10.1093/nar/28.6.1397
78. Taylor LD, Nelson DE, Dorward DW, Whitmire WM, Caldwell HD. Biological characterization of *Chlamydia trachomatis* plasticity zone MACPF domain family protein CT153. *Infect Immun.* (2010) 78:2691–9. doi: 10.1128/IAI.01455-09
79. Mitchell CM, Hutton S, Myers GSA, Brunham R, Timms P. *Chlamydia pneumoniae* is genetically diverse in animals and appears to have crossed the host barrier to humans on (at least) two occasions. *PLoS Pathog.* (2010) 6:e1000903. doi: 10.1371/journal.ppat.1000903
80. Chen AL, Johnson KA, Lee JK, Sutterlin C, Tan M. CPAF: a chlamydial protease in search of an authentic substrate. *PLoS Path.* (2012) 8:e1002842. doi: 10.1371/Journal.ppat.1002842

81. Rajaram K, Giebel AM, Toh E, Hu S, Newman JH, Morrison SG, et al. Mutational analysis of the *Chlamydia muridarum* plasticity zone. *Infect Immun.* (2015) 83:2870–81. doi: 10.1128/IAI.00106-15
82. LaBrie SD, Dimond ZE, Harrison KS, Baid S, Wickstrum J, Suchland RJ, et al. Transposon mutagenesis in *Chlamydia trachomatis* identifies CT339 as a ComEC homolog important for DNA uptake and lateral gene transfer. *MBio.* (2019) 10:e01343–19. doi: 10.1128/mBio.01343-19
83. Wang Y, LaBrie SD, Carrell SJ, Suchland RJ, Dimond ZE, Kwong F, et al. Development of transposon mutagenesis for *Chlamydia muridarum*. *J Bacteriol.* (2019) 201:e00366–19. doi: 10.1128/JB.00366-19
84. Thomson NR, Yeats C, Bell K, Holden MTG, Bentley SD, Livingstone M, et al. The *Chlamydophila abortus* genome sequence reveals an array of variable proteins that contribute to interspecies variation. *Genome Res.* (2005) 15:629–40. doi: 10.1101/gr.3684805
85. Belland RJ, Zhong G, Crane DD, Hogan D, Sturdevant D, Sharma J, et al. Genomic transcriptional profiling of the developmental cycle of *Chlamydia trachomatis*. *Proc Natl Acad Sci USA.* (2003) 100:8478–83. doi: 10.1073/pnas.1331135100
86. Moore ER, Ouellette SP. Reconceptualizing the chlamydial inclusion as a pathogen-specified parasitic organelle: an expanded role for Inc proteins. *Front Cell Infect Microbiol.* (2014) 4:157. doi: 10.3389/fcimb.2014.00157
87. Sixt BS, Bastidas RJ, Finethy R, Baxter RM, Carpenter VK, Kroemer G, et al. The *Chlamydia trachomatis* inclusion membrane protein CpoS counteracts STING-mediated cellular surveillance and suicide programs. *Cell Host Microbe.* (2017) 21:113–21. doi: 10.1016/j.chom.2016.12.002
88. Weber MM, Lam JL, Dooley CA, Noriae NF, Hansen BT, Hoyt FH, et al. Absence of specific *Chlamydia Trachomatis* inclusion membrane proteins triggers premature inclusion membrane lysis and host cell death. *Cell Rep.* (2017) 19:1406–17. doi: 10.1016/j.celrep.2017.04.058

Conflict of Interest: The authors declare that the research was conducted in the absence of any commercial or financial relationships that could be construed as a potential conflict of interest.

frontiers in Immunology

PERSPECTIVE
published: 06 August 2020
doi: 10.3389/fimmu.2020.01690

The Complicated Evolutionary Diversification of the Mpeg-1/Perforin-2 Family in Cnidarians

Brian M. Walters[1], *Michael T. Connelly*[2], *Benjamin Young*[2] *and Nikki Traylor-Knowles*[2]*

[1] Department of Biology, University of Miami, Coral Gables, FL, United States, [2] Rosenstiel School of Marine and Atmospheric Science, University of Miami, Coral Gables, FL, United States

The invertebrate innate immune system is surprisingly complex, yet our knowledge is limited to a few select model systems. One understudied group is the phylum Cnidaria (corals, sea anemones, etc.). Cnidarians are the sister group to Bilateria and by studying their innate immunity repertoire, a better understanding of the ancestral state can be gained. Corals in particular have evolved a highly diverse innate immune system that can uncover evolutionarily basal functions of conserved genes and proteins. One rudimentary function of the innate immune system is defense against harmful bacteria using pore forming proteins. Macrophage expressed gene 1/Perforin-2 protein (Mpeg-1/P2) is a particularly important pore forming molecule as demonstrated by previous studies in humans and mice, and limited studies in non-bilaterians. However, in cnidarians, little is known about Mpeg-1/P2. In this perspective article, we will summarize the current state of knowledge of Mpeg-1/P2 in invertebrates, analyze identified Mpeg-1/P2 homologs in cnidarians, and demonstrate the evolutionary diversity of this gene family using phylogenetic analysis. We will also show that Mpeg-1 is upregulated in one species of stony coral in response to lipopolysaccharides and downregulated in another species of stony coral in response to white band disease. This data presents evidence that Mpeg-1/P2 is conserved in cnidarians and we hypothesize that it plays an important role in cnidarian innate immunity. We propose that future research focus on the function of Mpeg-1/P2 family in cnidarians to identify its primary role in innate immunity and beyond.

Keywords: perforin, perforin-2, Mpeg-1, cnidarian, immunity, evolution, phylogenetics, macrophage expressed gene 1

OPEN ACCESS

Edited by:
Gabriele Pradel,
RWTH Aachen University, Germany

Reviewed by:
Stefan Oehlers,
University of Sydney, Australia
Yehu Moran,
Hebrew University of Jerusalem, Israel

***Correspondence:**
Nikki Traylor-Knowles
ntraylorknowles@rsmas.miami.edu

Specialty section:
This article was submitted to Microbial Immunology, a section of the journal Frontiers in Immunology

Received: *02 April 2020*
Accepted: *24 June 2020*
Published: *06 August 2020*

Citation:
Walters BM, Connelly MT, Young B and Traylor-Knowles N (2020) The Complicated Evolutionary Diversification of the Mpeg-1/Perforin-2 Family in Cnidarians. Front. Immunol. 11:1690. doi: 10.3389/fimmu.2020.01690

OVERVIEW OF CNIDARIA, INNATE IMMUNITY, AND MACROPHAGE EXPRESSED GENE 1/PERFORIN-2 PROTEIN

The phylum of Cnidaria possesses over 10,000 extant species which are united by the innovation of stinging cnidocyte cells and a polyp life stage (1). Cnidarians include stony corals, soft corals, sea anemones, and jellyfish and are known to be some of the most important organisms for promoting ocean biodiversity, as well as sources of novel compound discovery (2, 3). From an evolutionary perspective, Cnidaria is critical for our understanding of ancestral traits because they are the sister group with Bilateria, from which they split ∼604–748 million years ago [**Figure 1A**; (6, 7)].

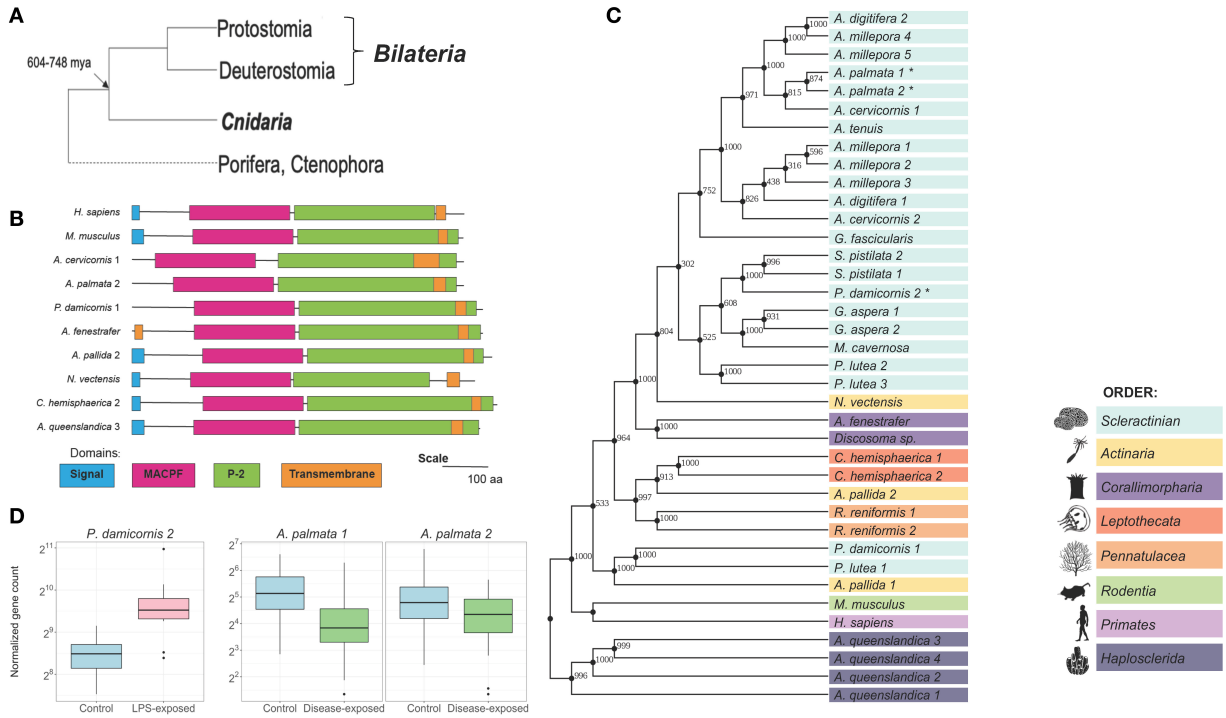

FIGURE 1 | Mpeg-1/P2 is highly diversified in Cnidarians. **(A)** Between 604–748 million years ago, bilaterians split from cnidarians. Cnidaria as sister group to Bilateria can inform our understanding of ancestral traits. **(B)** Domain architecture of P2. Amino acid sequence and domain lengths are drawn to scale. Signal peptide (blue), membrane attack complex/perforin (MACPF; pink), and transmembrane (orange) domains were identified using Hmmer. The P2 (green) domain was identified by aligning the P2 sequence of the human P2 protein. **(C)** A Maximum likelihood tree created in PhyML using the WAG +G +I model, as predicted by Smart Model Selection and ProtTest [Version 3.4.2; (4, 5)]. This tree shows the predicted evolutionary relationship of the whole P2 protein using 38 protein sequences. The percentage of replicate trees associated with the given taxa clustered together using 1000 bootstrap tests are shown at the nodes. All amino acid positions with <95% coverage were eliminated from the model. Tree is rooted taxonomically by *A. queenslandica*. **(D)** The response of Mpeg-1 to an immune stimulus and active white band disease infection in two coral species. In *P. damicornis* LPS exposure causes significant upregulation of a Mpeg-1 transcript (pdam_00017055, Swiss-prot E-value = 7.43E-143) compared with control. In *A. palmata,* exposure to white band disease identified two significantly differentially expressed downregulated Mpeg-1 transcripts (Apalm_v2_evm.model.Sc0a5M3_382_HRSCAF_692.335, Swiss-prot E = 3.55E-158; Apalm_v2_evm.model.Sc0a5M3_382_HRSCAF_692.340 Swiss-prot E-value = 1.69E-159).

The advent of next-generation sequencing technologies has revealed that stony corals possess a highly redundant and diverse innate immune system at the gene and protein levels (8–10). Stony corals maintain symbiotic associations with a diverse microbial community including bacteria, fungi, archaea, and dinoflagellates of the family Symbiodiniaceae (11). To maintain these relationships, they must possess a complex innate immune repertoire that can decipher between symbiont and pathogen (12). These intricate symbioses, paired with old evolutionary age are hypothesized to be the primary factors that have led to the complex diversity of stony coral innate immune proteins (13–15). We currently do not understand the function of many of these innate immune factors, but by examining their phylogenetics, protein domain architecture, and gene expression we can begin to better understand their possible significance.

Macrophage expressed gene 1/Perforin-2 protein (Mpeg-1/P2) is a pore forming effector molecule that is crucial for the innate immune response of both vertebrates and invertebrates (16). It has been identified in multiple organisms, including sponges, mollusks, zebrafish, ctenophores, sea anemones, and humans (16–27). Within invertebrates, limited studies have shown that both sponges and oysters upregulate Mpeg-1 in response to viral or bacterial infections (18, 28). In other invertebrates, including stony corals, little is known about the function or diversity of the Mpeg-1/P2 family. Previous studies have identified MACPF containing proteins in stony corals including within toxins from cnidocyte cells (29–34), however proteins containing both MACPF and P2 domains such as Mpeg-1/P2 have not been well-described.

In this perspective article, we will discuss the diversity of the Mpeg-1/P2 family within Cnidaria, with a focus on stony corals. Additionally, we describe the conserved protein domains of P2 in Cnidaria and show that Mpeg-1 homologs react to both a natural disease challenge, as well as a synthetic pathogen mimic. Lastly, we discuss the possible role of Mpeg-1/P2 in cnidarian innate immunity and future areas of investigation.

CNIDARIA MPEG-1/P2 IS HIGHLY CONSERVED, DUPLICATED, AND COMPLICATED

To identify cnidarian homologs, BLASTp (Version 2.2.29+) searches using the *Mus musculus* P2 protein sequence were employed (35). To locate the P2 domain, each sequence was aligned against the isolated *Homo sapiens* P2 domain (amino acids 351–653) using Clustal Omega (36). From this, we identified cnidarian P2 protein homologs as highly conserved (**Figure 1B**, **Supplementary Table 1**). This is supported by both protein domain analysis and phylogenetic analysis (**Figures 1B,C**). There is a diversity of P2 homologs present indicating multiple duplication events within each cnidarian species and thus paralogs. One hypothesis for the retention of multiple P2 paralogs is that it may have evolved additional functions in cnidarians through the process of neofunctionalization. Alternatively, subfunctionalization could have occurred requiring multiple paralogs to perform the original ancestral function.

P2 proteins consist of an N-terminus regulatory signal peptide, the membrane attack complex/perforin (MACPF) domain, the perforin-2 (P2) domain, and the C-terminus transmembrane anchor (16). The MACPF domain generates pores in the lipid bilayer of bacteria cell membranes that leads to bacterial lysis (37). The defining P2 domain is important for Mpeg-1/P2 identification, but little is known about the functional mechanisms of this domain. A single missense or stop mutation in the P2 domain causes an inability to fight off bacterial infections indicating that it is important for the overall primary function of the P2 protein (38).

Using PhyML (Version 3.0) phylogenetic trees were constructed to identify the relationships between cnidarian, mammalian, and sponge P2 proteins (**Figure 1C**) (39). A maximum-likelihood tree was created using the WAG +G +I model as recommended by both Smart Model Selection and ProtTest [Version 3.4.2; (4, 5)]. The resulting tree shows P2 homologs partitioning into groups based on the major clades of stony corals with Corallimorpharia forming a paraphyletic group sister to the stony corals in accordance with their known evolutionary relationship (40, 41). The 60% of the bootstrap support are over 90% indicating high confidence in our model (**Figure 1C**).

Taken together these results show that P2 proteins are highly conserved and diverse within Cnidaria, a pattern which has also been observed in other innate immunity genes (13, 14). The phylogenetic relationship of P2 clearly shows that diversification of this protein occurred within species which resulted in many unique paralogs for P2. Given this protein domain analysis and phylogenetic information, understanding if the genes associated with Mpeg-1 are expressed in response to an active infection or a synthetic immune stimulus would further bolster our hypothesis that Cnidaria possesses functional Mpeg-1/P2.

STONY CORAL MPEG-1 GENES EXHIBIT ALTERNATE REACTIONS TO IMMUNE STIMULUS AND ACTIVE INFECTION

Two scleractinian coral transcriptomic datasets were mined for homologs of P2; one from *Pocillopora damicornis* exposed to the synthetic immune stimulus lipopolysaccharide (LPS), NCBI SRA BioProject PRJNA587509, (34) and the second from *Acropora palmata* exposed to the naturally occurring white band disease (WBD); NCBI SRA BioProject PRJNA529682, (42); **Figure 1D**. In *P. damicornis*, one Mpeg-1 homolog was found to be significantly upregulated (pdam_00017055, LFC = 1.21), while in *A. palmata* two paralogs of Mpeg-1 were found to be significantly downregulated in response to WBD (Apalm_v2_evm.model.Sc0a5M3_382_HRSCAF_692.340, LFC = −1.38; Apalm_v2_evm.model.Sc0a5M3_382_HRSCAF_692.335, LFC = −0.94). The presence of Mpeg-1 significant differential gene expression in these different coral species is evidence that it is responding to bacteria much like what has been previously seen in other organisms, however, unlike these other organisms, the response is more complicated and variable (16–24, 26, 43). With the presence of multiple paralogs, it is possible that some of these genes are not involved in innate immunity. Additionally, the variation in gene expression in *A. palmata* could be due to environmental challenges, as these were nursery reared corals (42). Further investigation into the function of these genes in multiple species of coral will be valuable for our understanding of the functional repertoire of this gene family in cnidarians, as well as, the effects of environmental stress.

FUTURE DIRECTIONS FOR CNIDARIAN MPEG-1/P2

The conservation of Mpeg-1/P2, across both the cnidarian lineage and throughout evolutionary history provides evidence that it is an ancient immune factor important for survival. Specifically, within cnidarians, there is much we do not understand: (1) What is the function of Mpeg-1/P2? (2) What is the protein structure? (3) Why are there abundant gene duplications? (4) What other proteins do cnidarian Mpeg-1/P2 associate with? (5) Why do different Mpeg-1/P2 respond differently in distinct cnidarians? (6) In what cell lineage is Mpeg-1/P2 expressed? Investigating Mpeg-1/P2 within non-traditional model systems such as cnidarians will shed light on its full functional capabilities and lead to novel discoveries on the function of this family that could have medically relevant applications.

DATA AVAILABILITY STATEMENT

Publicly available datasets were analyzed in this study. This data can be found here: https://github.com/brianwalters7/Cnidarian-Mpeg1/tree/v1.3.3.20. *Pocillopora damicornis* sequence data is available through NCBI: SRA BioProject PRJNA587509. *Acropora palmata* sequence data is available through NCBI: SRA BioProject PRJNA529682.

AUTHOR CONTRIBUTIONS

BW and NT-K conceived the project and performed the phylogenetic analysis and protein analysis. MC and BY performed the transcriptomic analysis and figure production. All authors were involved in editing and writing of this paper.

FUNDING

BW was supported by the 2018 Lou and Chosun Mastriani Award for Coral Research. NT-K was supported by start up funds provided by University of Miami, Rosenstiel School of Marine and Atmospheric Sciences, and the National Science Foundation Award # 2013692.

ACKNOWLEDGMENTS

We would like to thank reviewers for their valuable comments. BW would like to thank members of the Cnidarian Immunity Lab for comments and conversations. Lastly, BW and NT-K would like to thank Dr. George Munson for his advice and conversations on Mpeg-1/P2.

SUPPLEMENTARY MATERIAL

The Supplementary Material for this article can be found online at: https://www.frontiersin.org/articles/10.3389/fimmu.2020.01690/full#supplementary-material

Supplementary Table 1 | Summary of P2 homologs found in Cnidarians. P2 homologs were identified through BLASTp (Version 2.2.29+) using the Mus musculus protein sequence (NP_001361597.1). Twenty cnidarians genomes, one cnidarian transcript shotgun assembly, and one sponge genome were searched. This included 12 scleractinian corals, one soft coral, two coral-like anemones, three anemones, one hydra, one jellyfish, and one parasitic myxozoa. Candidate homologs from the BLAST searches were limited to E-value cut off (E-6). Sequences were further culled by removing candidates which lacked MACPF or P2 domain. Only three cnidarians (Anemonia viridis, Hydra vulgaris, and Thelohanellus kitauei) did not have homologs present. Lastly, an Orbicella faveolata homolog, was identified, but removed from analysis due to truncation.

REFERENCES

1. Appeltans W, Ahyong ST, Anderson G, Angel MV, Artois T, Bailly N, et al. The magnitude of global marine species diversity. *Curr Biol.* (2012) 22:2189–202. doi: 10.1016/j.cub.2012.09.036
2. Hughes TP, Baird AH, Bellwood DR, Card M, Connolly SR, Folke C, et al. Climate change, human impacts, and the resilience of coral reefs. *Science.* (2003) 301:929–33. doi: 10.1126/science.1085046
3. Rocha J, Peixe L, Gomes N, Calado R. Cnidarians as a source of new marine bioactive compounds—an overview of the last decade and future steps for bioprospecting. *Mar Drugs.* (2011) 9:1860–86. doi: 10.3390/md9101860
4. Lefort V, Longueville JE, Gascuel O. SMS: Smart Model Selection in PhyML. *Mol Biol Evol.* (2017) 34:2422–24. doi: 10.1093/molbev/msx149
5. Darriba D, Taboada GL, Doallo R, Posada D. ProtTest 3: fast selection of best-fit models of protein evolution. *Bioinformatics.* (2011) 27:1164–5. doi: 10.1093/bioinformatics/btr088
6. Ryan JF, Burton PM, Mazza ME, Kwong GK, Mullikin JC, Finnerty JR. The cnidarian-bilaterian ancestor possessed at least 56 homeoboxes: evidence from the starlet sea anemone, *Nematostella vectensis*. *Genome Biol.* (2006) 7:R64. doi: 10.1186/gb-2006-7-7-r64
7. Bosch TCG. Cnidarian-microbe interactions and the origin of innate immunity in metazoans. *Annu Rev Microbiol.* (2013) 67:499–518. doi: 10.1146/annurev-micro-092412-155626
8. Palmer CV, Traylor-Knowles N. Towards an integrated network of coral immune mechanisms. *Proc R Soc B Biol Sci.* (2012) 279. doi: 10.1098/rspb.2012.1477
9. Quistad SD, Traylor-Knowles N. Precambrian origins of the TNFR superfamily. *Cell Death Discov.* (2016) 2:16058. doi: 10.1038/cddiscovery.2016.58
10. Traylor-Knowles N, Connelly MT. What is currently known about the effects of climate change on the coral immune response. *Curr Clim Chang Rep.* (2017) 3:252–60. doi: 10.1007/s40641-017-0077-7
11. Rohwer F, Seguritan V, Azam F. Diversity and distribution of coral-associated bacteria. *Mar Ecol Prog Ser.* (2002) 243:1–10. doi: 10.3354/meps243001
12. Palmer CV, Traylor-Knowles NG. Cnidaria: Anthozoans in the hot seat. In: Cooper EL, editor. *Advances in Comparative Immunology*. Cham: Springer (2018). p. 51–93. doi: 10.1007/978-3-319-76768-0_3
13. Hamada M, Shoguchi E, Shinzato C, Kawashima T, Miller DJ, Satoh N. The complex NOD-like receptor repertoire of the coral acropora digitifera includes novel domain combinations. *Mol Biol Evol.* (2013) 30:167–76. doi: 10.1093/molbev/mss213
14. Poole AZ, Weis VM. TIR-domain-containing protein repertoire of nine anthozoan species reveals coral–specific expansions and uncharacterized proteins. *Dev Comp Immunol.* (2014) 46:480–8. doi: 10.1016/j.dci.2014.06.002
15. Cunning R, Bay RA, Gillette P, Baker AC, Traylor-Knowles N. Comparative analysis of the Pocillopora damicornis genome highlights role of immune system in coral evolution. *Sci Rep.* (2018) 8:16134. doi: 10.1038/s41598-018-34459-8
16. McCormack R, Podack ER. Perforin-2/Mpeg1 and other pore-forming proteins throughout evolution. *J Leukoc Biol.* (2015) 98:761–8. doi: 10.1189/jlb.4MR1114-523RR
17. Mah SA, Moy GW, Swanson WJ, Vacquier VD. A perforin-like protein from a marine mollusk. *Biochem Biophys Res Commun.* (2004) 316:468–75. doi: 10.1016/j.bbrc.2004.02.073
18. Wiens M, Korzhev M, Krasko A, Thakur NL, Perović-Ottstadt S, Breter HJ, et al. Innate immune defense of the sponge suberites domuncula against bacteria involves a MyD88-dependent signaling pathway: induction of a perforin-like molecule. *J Biol Chem.* (2005) 280:27949–59. doi: 10.1074/jbc.M504049200
19. Miller DJ, Hemmrich G, Ball EE, Hayward DC, Khalturin K, Funayama N, et al. The innate immune repertoire in Cnidaria - ancestral complexity and stochastic gene loss. *Genome Biol.* (2007) 8:R59. doi: 10.1186/gb-2007-8-4-r59
20. Wang K-J, Ren H-L, Xu D-D, Cai L, Yang M. Identification of the up-regulated expression genes in hemocytes of variously colored abalone (Haliotis diversicolor Reeve, 1846) challenged with bacteria. *Dev Comp Immunol.* (2008) 32:1326–47. doi: 10.1016/j.dci.2008.04.007
21. Wang G-D, Zhang K-F, Zhang Z-P, Zou Z-H, Jia X-W, Wang S-H, et al. Molecular cloning and responsive expression of macrophage expressed gene from small abalone Haliotis diversicolor supertexta. *Fish Shellfish Immunol.* (2008) 24:346–59. doi: 10.1016/j.fsi.2007.12.008
22. He X, Zhang Y, Yu Z. An Mpeg (macrophage expressed gene) from the Pacific oyster Crassostrea gigas: Molecular characterization and gene expression. *Fish Shellfish Immunol.* (2011) 30:870–6. doi: 10.1016/j.fsi.2011.01.009
23. Kemp IK, Coyne VE. Identification and characterisation of the Mpeg1 homologue in the South African abalone, Haliotis midae. *Fish Shellfish Immunol.* (2011) 31:754–64. doi: 10.1016/j.fsi.2011.07.010
24. Bathige SDNK, Umasuthan N, Whang I, Lim B-S, Won SH, Lee J. Antibacterial activity and immune responses of a molluscan macrophage expressed gene-1 from disk abalone, Haliotis discus. *Fish Shellfish Immunol.* (2014) 39:263–72. doi: 10.1016/j.fsi.2014.05.012
25. Zakrzewska A, van Eikenhorst G, Burggraaff JE. Genome-wide analysis of yeast stress survival and tolerance acquisition to analyze the central trade-off

between growth rate and cellular robustness. *Mol Biol Cell*. (2011) 22:4435–46. doi: 10.1091/mbc.e10-08-0721
26. Gorbushin AM. Membrane Attack Complex/Perforin domain-containing proteins in a dual-species transcriptome of caenogastropoda Littorina littorea and its trematode parasite Himasthla elongata. *Fish Shellfish Immunol.* (2016) 54:254–6. doi: 10.1016/j.fsi.2016.04.015
27. Traylor-Knowles N, Vandepas LE, Browne WE. Still enigmatic: innate immunity in the ctenophore Mnemiopsis leidyi. *Integr Comp Biol*. (2019) 59:811–8. doi: 10.1093/icb/icz116
28. Renault T, Faury N, Barbosa-Solomieu V, Moreau K. Suppression substractive hybridisation (SSH) and real time PCR reveal differential gene expression in the Pacific cupped oyster, Crassostrea gigas, challenged with Ostreid herpesvirus 1. *Dev Comp Immunol.* (2011) 35:725–35. doi: 10.1016/j.dci.2011.02.004
29. Oshiro C, Bradley EK, Eksterowicz J, Evensen E, Lamb ML, Lanctot JK, et al. Performance of 3D-database molecular docking studies into homology models. *J Med Chem*. (2004) 47:764–7. doi: 10.1021/jm0300781
30. Satoh H, Nakamura Y, Okabe S. Influences of infaunal burrows on the community structure and activity of ammonia-oxidizing bacteria in intertidal sediments. *Appl Environ Microbiol.* (2007) 73:1341–8. doi: 10.1128/AEM.02073-06
31. Nagai T, Ibata K, Park ES, Kubota M, Mikoshiba K, Miyawaki A. A variant of yellow fluorescent protein with fast and efficient maturation for cell-biological applications. *Nat Biotechnol*. (2002) 20:87–90. doi: 10.1038/nbt0102-87
32. Mizuno D, Tardin C, Schmidt CF, Mackintosh FC. Nonequilibrium mechanics of active cytoskeletal networks. *Science*. (2007) 315:370–73. doi: 10.1126/science.1134404
33. Oliveira JS, Fuentes-Silva D, King GF. Development of a rational nomenclature for naming peptide and protein toxins from sea anemones. *Toxicon*. (2012) 60:539–50. doi: 10.1016/j.toxicon.2012.05.020
34. Connelly MT, McRae CJ, Liu PJ, Traylor-Knowles N. Lipopolysaccharide treatment stimulates Pocillopora coral genotype-specific immune responses but does not alter coral-associated bacteria communities. *Dev Comp Immunol.* (2020) 109:103717. doi: 10.1016/j.dci.2020.103717
35. Altschul SF, Gish W, Miller W, Myers EW, Lipman DJ. Basic local alignment search tool. *J Mol Biol.* (1990) 215:403–10. doi: 10.1016/S0022-2836(05)80360-2
36. Madeira F, Park Y, Mi, Lee J, Buso N, Gur T, Madhusoodanan N, et al. The EMBL-EBI search and sequence analysis tools APIs in 2019. *Nucleic Acids Res.* (2019) 47:W636–41. doi: 10.1093/nar/gkz268
37. Smyth MJ, Browne KA, Thia KYT, Apostolidis VA, Kershaw MH, Trapani JA. Hypothesis: cytotoxic lymphocyte granule serine proteases activate target cell endonucleases to trigger apoptosis. *Clin Exp Pharmacol Physiol.* (1994) 21:67–70. doi: 10.1111/j.1440-1681.1994.tb02438.x
38. McCormack RM, Szymanski EP, Hsu AP, Perez E, Olivier KN, Fisher E, et al. MPEG1/perforin-2 mutations in human pulmonary nontuberculous mycobacterial infections. *JCI Insight.* (2017) 2:e89635. doi: 10.1172/jci.insight.89635
39. Guindon S, Dufayard JF, Lefort V, Anisimova M, Hordijk W, Gascuel O. New algorithms and methods to estimate maximum-likelihood phylogenies: assessing the performance of PhyML 3.0. *Syst Biol*. (2010) 59:307–21. doi: 10.1093/sysbio/syq010
40. Kitahara MV, Cairns SD, Stolarski J, Blair D, Miller DJ. A comprehensive phylogenetic analysis of the scleractinia (cnidaria, anthozoa) based on mitochondrial CO1 sequence data. *PLoS ONE.* (2010) 5:e11490. doi: 10.1371/journal.pone.0011490
41. Lin MF, Chou WH, Kitahara MV, Chen CLA, Miller DJ, Forêt S. Corallimorpharians are not "naked corals": insights into relationships between Scleractinia and Corallimorpharia from phylogenomic analyses. *PeerJ*. (2016) 4:e2463. doi: 10.7717/peerj.2463
42. Young B, Serrano XM, Rosales S, Miller MW, Williams D, Traylor-Knowles N. Innate immune gene expression in Acropora palmata is consistent despite variance in yearly disease events. *bioRxiv*. (2020). doi: 10.1101/2020.01.20.912410
43. Benard EL, Racz PI, Rougeot J, Nezhinsky AE, Verbeek FJ, Spaink HP, et al. Macrophage-expressed perforins Mpeg1 and Mpeg1.2 have an anti-bacterial function in Zebrafish. *J Innate Immun*. (2015) 7:136–52. doi: 10.1159/000366103

Conflict of Interest: The authors declare that the research was conducted in the absence of any commercial or financial relationships that could be construed as a potential conflict of interest.

frontiers in Microbiology

ORIGINAL RESEARCH
published: 14 August 2020
doi: 10.3389/fmicb.2020.01788

Contribution of Nlrp3 Inflammasome Activation Mediated by Suilysin to Streptococcal Toxic Shock-like Syndrome

Liqiong Song[1,2†], Xianping Li[1,2†], Yuchun Xiao[1,2], Yuanming Huang[1,2], Yongqiang Jiang[3], Guangxun Meng[4]* and Zhihong Ren[1,2]**

[1]State Key Laboratory for Infectious Disease Prevention and Control, National Institute for Communicable Disease Control and Prevention, Collaborative Innovation Center for Diagnosis and Treatment of Infectious Diseases, Chinese Center for Disease Control and Prevention, Beijing, China, [2]Research Units of Discovery of Unknown Bacteria and Function (2018 RU010), Chinese Academy of Medical Sciences, Beijing, China, [3]State Key Laboratory of Pathogen and Biosecurity, Institute of Microbiology and Epidemiology, Academy of Military Medical Sciences, Beijing, China, [4]The Center for Microbes, Development and Health, CAS Key Laboratory of Molecular Virology and Immunology, Institut Pasteur of Shanghai, Chinese Academy of Sciences, University of Chinese Academy of Sciences, Shanghai, China

OPEN ACCESS

Edited by:
George P. Munson,
University of Miami, United States

Reviewed by:
Rebecca Leigh Schmidt,
Upper Iowa University, United States
Hridayesh Prakash,
Amity University, India

***Correspondence:**
Yongqiang Jiang
jiang_yongqiang@sina.cn
Guangxun Meng
gxmeng@ips.ac.cn;
gxmeng@sibs.ac.cn
Zhihong Ren
renzhihong@icdc.cn

†These authors have contributed equally to this work

Specialty section:
This article was submitted to Microbial Immunology, a section of the journal Frontiers in Microbiology

Received: 07 April 2020
Accepted: 08 July 2020
Published: 14 August 2020

Citation:
Song L, Li X, Xiao Y, Huang Y, Jiang Y, Meng G and Ren Z (2020) Contribution of Nlrp3 Inflammasome Activation Mediated by Suilysin to Streptococcal Toxic Shock-like Syndrome. Front. Microbiol. 11:1788. doi: 10.3389/fmicb.2020.01788

Objective: The aim of this study was to investigate the molecular mechanism of inflammasome activation in response to *Streptococcus suis* serotype 2 (SS2) infection and its contribution to the development of streptococcal toxic shock-like syndrome (STSS).

Methods: To verify the role of suilysin (SLY) in STSS, we infected bone-marrow-derived macrophages (BMDMs) *in vitro* and C57BL/6J mice intraperitoneally (IP) with the SS2 wild-type (WT) strain or isogenic *sly* mutant (ΔSLY) to measure the interleukin (IL)-1β release and survival rate. To determine the role of inflammasome activation and pyroptosis in STSS, we infected BMDMs from WT and various deficient mice, including *Nlrp3*-deficient (Nlrp3$^{-/-}$), *Nlrc4*-deficient (Nlrc4$^{-/-}$), *Asc*-deficient (Asc$^{-/-}$), *Aim2*-deficient (Aim2$^{-/-}$), *Caspase*-1/11-deficient (Caspase-1/11$^{-/-}$), and *Gsdmd*-deficient (Gsdmd$^{-/-}$) *ex vivo*, and IP injected WT, Nlrp3$^{-/-}$, Caspase-1/11$^{-/-}$, and Gsdmd$^{-/-}$ mice with SS2, to compare the IL-1β releases and survival rate *in vivo*.

Results: The SS2-induced IL-1β production in mouse macrophages is mediated by SLY *ex vivo*. The survival rate of WT mice infected with SS2 was significantly lower than that of mice infected with the ΔSLY strain *in vivo*. Furthermore, SS2-triggered IL-1β releases, and the cytotoxicity in the BMDMs required the activation of the NOD-Like Receptors Family Pyrin Domain Containing 3 (Nlrp3), Caspase-1/11, and gasdermin D (Gsdmd) inflammasomes, but not the Nlrc4 and Aim2 inflammasomes *ex vivo*. The IL-1β production and survival rate of WT mice infected with SS2 were significantly lower than those of the Nlrp3$^{-/-}$, Caspase-1/11$^{-/-}$, and Gsdmd$^{-/-}$ mice *in vivo*. Finally, the inhibitor of the Nlrp3 inflammasome could reduce the IL-1β release and cytotoxicity of SS2-infected macrophages *ex vivo* and protect SS2-infected mice from death *in vivo*.

Conclusion: Nlrp3 inflammasome activation triggered by SLY in macrophages played an important role in the pathogenesis of STSS.

Keywords: *Streptococcus suis*, suilysin, interlukin-1β, inflammasome, caspase-1

INTRODUCTION

Streptococcus suis is a common swine pathogen, which not only results in a great loss to swine industry every year but also causes meningitis and streptococcal toxic shock-like syndrome (STSS) in humans (Ye et al., 2006; Yu et al., 2006; Gottschalk et al., 2007; Huong et al., 2014). More than 30 serotypes of *S. suis* have been identified (King et al., 2001), among which serotype 2 is considered as the most common and virulent. *Streptococcus suis* serotype 2 (SS2) is further divided into four predominant sequence types using multilocus sequence typing, including sequence types 1, 7, 25, and 28 (Fittipaldi et al., 2011). Among patients infected with strain ST7 of *S. suis*, the incidence of STSS is significantly higher than that among patients infected with the other sequence type of SS2. ST7 is thought to have been responsible for two large outbreaks of human SS2 infections in China in 1998 and 2005 (Hu et al., 2000; Ye et al., 2006; Yu et al., 2006). The serum proinflammatory cytokines in STSS patients, especially interleukin 6 (IL-6), IL-1β, and tumor necrosis factor (TNF), gamma interferon (IFN-ɣ), IL-12, and monocyte chemoattractant protein 1 (MCP-1), are significantly higher than those in meningitis patients (Ye et al., 2009). It was generally accepted that the severe outcome of the SS2 infection was closely related to the excess innate immune response of the host. However, how the overproduction of proinflammatory cytokines occurs in STSS is not fully understood.

A variety of virulence factors participate in the *S. suis* pathogenesis, for example, the capsular polysaccharide and lipoprotein (LP). Among these virulence factors, suilysin (SLY) was found to be closely related to bacterial dissemination and host inflammation (Lun et al., 2003). SLY, an extracellular protein secreted by SS2, belongs to a family of cholesterol-dependent cytolysins, including listeriolysin O of *Listeria monocytogenes* and pneumolysin of *Streptococcus pneumonia*, which are the multifunctional proteins responsible for hemolytic activity, apoptosis, and cytokine-inducing activity (Kim et al., 2010; Witzenrath et al., 2011). Notably, a highly virulent strain (ST7) that causes a more severe invasive infection can produce a greater amount of SLYs than non-epidemic strains (He et al., 2014). SLY-positive strains have also been reported to result in more severe symptoms than SLY-negative strains (Jacobs et al., 1996; He et al., 2014). Moreover, it was reported that SLY could stimulate the host immune system to produce massive amounts of proinflammatory cytokines, for example, IL-1β, IL-6, and TNF-α (Lun et al., 2003; Tenenbaum et al., 2016). The vaccine containing purified SLY derived from SS2 had immunoprotective effects against SS2-induced STSS for swine and mice due to its reduction of the proinflammatory response during SS2 infection (Jacobs et al., 1996). Furthermore, passive immunization using anti-SLY antisera protected mice from acute death after infection with SS2 and significantly reduced levels of proinflammatory cytokines. Therefore, it is necessary to further explore the role of SLY in the pathogenesis of SS2 infection.

Lavagna et al. (2019) reported that the IL-1β release plays a protective role during SS2 systemic infection by activating various inflammasomes, thus promoting host survival. The inflammasome is commonly composed of NOD-like receptors (NLRs) and the adapter molecule Asc. Multiple inflammasomes are involved in the host defense responses against various pathogens. The activated inflammasome can recruit and activate proinflammatory protease, Caspase-1. The activated form of Caspase-1 then cleaves the precursors of some subsequent cytokines (pro-IL-1β and pro-IL-18) into their corresponding mature forms, and it cleaves gasdermin D (Gsdmd) to remove its auto-inhibition. The N-terminal of Gsdmd generated by the cleavage induces cell pyroptosis, a programmed cell necrosis accompanied by the activation of the inflammatory cytokines IL-1β and IL-18, and forms pores on the cell membrane for IL-1β secretion (Shi et al., 2017). However, existing studies have not revealed the comprehensive molecular mechanism for the inflammasome activation triggered by SLY of SS2 and have not clarified the role of Nlrp3 inflammasome activation and pyroptosis in the pathogenesis of SS2-induced STSS.

To investigate the issues mentioned above, we constructed a SLY-mutant strain and used mouse macrophages deficient in Nlrp3, Nlrc4, Aim2, Caspase-1/11, Asc, and Gsdmd to determine whether SLY mediates inflammasome activation and pyroptosis and explored the role of inflammasome activation and pyroptosis in SS2-induced STSS. Our findings demonstrate a critical role of SLY in activating inflammasomes during STSS; the deficiencies in the Nlrp3 or Nlrp3 inhibitors could protect SS2-infected mice from death.

MATERIALS AND METHODS

Ethics Statement

This study was approved by the Laboratory Animal Welfare & Ethics Committee of the National Institute for Communicable Disease Control and Prevention, Chinese Center for Disease Prevention and Control. This study was carried out in accordance with the recommendations of the Animal Management Regulations (2017/03) and measures for the Ethical Review of Biomedical Research Involving Humans (2016/12) [SYXK (Beijing 2012-0022)].

All operations in our study are performed in the Biosafety Level II laboratory and Animal Biosafety Level II laboratory.

Bacterial Culture and Preparation of the Concentrated Supernatant Protein (SS2-S/N and ΔSLY-S/N)

The wild-type (WT) SS2 strain 05ZYH33 (ST-7) and its isogenic *sly* mutant (ΔSLY; He et al., 2014; Pian et al., 2015) were obtained from Yongqiang Jiang's laboratory at the Institute of Microbiology and Epidemiology, Academy of Chinese Military Medical Sciences. These bacteria were cultured on goat blood

Abbreviations: SLY, suilysin; SS2, *Streptococcus suis* serotype 2; STSS, streptococcal toxic-shock-like syndrome; NLRs, NOD-like receptors; Asc, adapter molecule; Nlrp3, NLR family pyrin domain containing 3; ROS, reactive oxygen species; WT, wild-type; ΔSLY, isogenic *sly* mutant; PLF, peritoneal lavage fluid; $Asc^{-/-}$, Asc-deficient; $Nlrp3^{-/-}$, Nlrp3-deficient; $Casp\text{-}1/11^{-/-}$, Caspase-1/11-deficient; BMDMs, mouse bone marrow derived macrophages; PMs, mouse peritoneal macrophages; IP, intraperitoneally; MOI, multiplicity of infection; LDH, lactate dehydrogenase; Gsdmd, gasdermin D.

agar at 37°C overnight. The isolated colonies were inoculated into Todd–Hewitt broth (BD, USA).

Bacterial culture supernatants of the SS2 WT or ΔSLY strain were centrifuged at 10,000 rpm for 10 min and then filtrated with a 0.22 μM filter. Then, both the cell-free supernatants were centrifuged using Amicon Ultra-4 10 K Centrifugal Filter Devices (Millipore, USA) and concentrated. The concentration of the supernatant protein containing SLY (SS2-S/N) or without SLY (ΔSLY-S/N) was measured using a Pierce™ BCA protein kit (Pierce, USA).

Mice and Cell Culture

All mice used in our experiments are on a C57BL/6 genetic background and all experiments were carried out with age and gender matched mice (8–10 weeks old, female). C57BL/6 WT mice were obtained from Beijing Vital River Laboratory Animal Technology Co. Ltd., *Asc*-deficient (Asc$^{-/-}$) mice were provided by Vishva M. Dixit of Genentech, and *Nlrp3*-deficient (Nlrp3$^{-/-}$) mice were provided by Warren Strober from NIH, *Aim2*-deficient (Aim2$^{-/-}$) were obtained from Dr. Meng Guangxun's lab (Mariathasan et al., 2004; Hornung et al., 2009; Meng et al., 2009; Mao et al., 2013), and Caspase-1$^{-/-}$mice were obtained from the Jackson Laboratory and crossed onto the C57BL/6 genetic background for 10 generations. These mice are also deficient for functional Caspase-11 (Kayagaki et al., 2011). *Nlrc4*-deficient (Nlrc4$^{-/-}$) and *Gsdmd*-deficient (Gsdmd$^{-/-}$) mice on a C57BL/6 background were obtained from Feng Shao's lab at the Beijing Institute of Life Sciences (Shi et al., 2015).

Mouse bone-marrow-derived macrophages (BMDMs) were isolated from the abovementioned mice and cultured as previously described (Song et al., 2015). Peritoneal macrophages (PMs) were collected from peritoneal lavage using the procedure utilized by Kumagai et al. (1979). The purity of the macrophages obtained was around 90%, which was assessed by a flow cytometer using the F4/80 antibody. Differentiation of the THP-1 human monocytic cell line was achieved after incubation for 48 h in the presence of 10 nM phorbolmyristate acetate (PMA, P8139). All of the cultured cells were grown in RPMI 1640 at a maximum density of 1×10^6 cells/ml.

BMDMs Infected With Bacteria (SS2 or ΔSLY) and Treated With Concentrated Supernatant Proteins (SS2-S/N or ΔSLY-S/N) *ex vivo*

BMDMs from WT mice or deficient mice (Asc$^{-/-}$, Nlrc4$^{-/-}$, Aim2$^{-/-}$, Nlrp3$^{-/-}$, Casp-1/11$^{-/-}$, and Gsdmd$^{-/-}$) were infected with the SS2 WT or ΔSLY strain *ex vivo* at a multiplicity of infection (MOI) of 1 for 16 h without lipopolysaccharide (LPS,100 ng/ml, L3012, Sigma) priming. BMDMs treated with phosphate buffer saline (PBS) or LPS plus adenosine triphosphate (ATP; 500 μM, A2383, Sigma) were used as the negative and positive control, respectively.

In parallel, BMDMs from the WT mice or deficient mice (Asc$^{-/-}$, Nlrc4$^{-/-}$, Aim2$^{-/-}$, Nlrp3$^{-/-}$, Casp-1/11$^{-/-}$, and Gsdmd$^{-/-}$) were pretreated with LPS priming (100 ng/ml) for 3 h and washed off with PBS. Then, the cell-free concentrated supernatant proteins SS2-S/N (containing SLY) or ΔSLY-S/N (without SLY) were incubated with the primed BMDMs in a 24-well plates at a concentration of 200 ng/ml for 16 h, respectively.

Both the unprimed BMDMs and LPS-primed BMDMs were pre-incubated with various inhibitors, including KCl (50 mM, PB0440), oxidized ATP (oATP, 500 μM, A6779), N-acetyl-L-cysteine (NAC; 20 mM, A7250), Nlrp3 inhibitor MCC950 (10 μM, S7809), and Caspase-1 inhibitor Z-YVAD-FMK (10 μM, A3707) at the indicated concentrations for 1 h. Then, these unprimed BMDMs were infected with the SS2 WT or ΔSLY strain, and LPS-primed BMDMs were treated with the concentrated supernatant proteins SS2-S/N or ΔSLY-S/N for 16 h *ex vivo*, as described above.

Mice Infection *in vivo*

To observe the survival of mice from a high-dose infection, C57BL/6J WT mice (female, 18–20 g) and various deficient mice (Nlrp3$^{-/-}$, Casp-1/11$^{-/-}$, and Gsdmd$^{-/-}$) were injected intraperitoneally (IP) with 2×10^9 CFU SS2 or its mutant (ΔSLY) strain in 200 μl PBS. The mice of the negative control group received the same volume of PBS. There were 10 mice in each group, and their survival was monitored every 2 h up to 24 h.

To detect the inflammatory response to a low dose of SS2 infection without death, BMDMs of C57BL/6J WT and various deficient mice (Nlrp3$^{-/-}$, Casp-1/11$^{-/-}$, and Gsdmd$^{-/-}$) were injected IP with 2×10^8 CFU SS2 in 200 μl PBS, and the negative control mice were treated with the same volume of PBS (six mice per group). Mice were sacrificed 24 h after injection. The peritoneal lavage fluid (PLF) was harvested by rinsing the peritoneal cavity with 500 μl PBS. The harvested PLF was used for the IL-1β detection by ELISA.

To determine the effect of the Nlrp3 inhibitor MCC950 on the survival and inflammatory response of SS2-infected mice *in vivo*, mice were injected IP with MCC950 (50 mg/kg, qd) for 2 days and then infected with 2×10^8 CFU SS2 2 h after injection. Mice were sacrificed 24 h after infection, then the PLF was harvested for IL-1β detection by ELISA. Those mice infected with 2×10^9 CFU SS2 were monitored for their survival for 24 h.

The WT mice group infected with SS2 was used as common positive control group in all *in vivo* experiments. The WT mice treated with PBS were used as shared negative control group in all *in vivo* experiments.

Detection of Cytokines and Lactate Dehydrogenase

All the cultured supernatants mentioned above were collected at the indicated time in this study. Lactate dehydrogenase (LDH) was measured for the cytotoxicity assessment using the Cytotox96 assay kit (Promega, USA). Interlukin 1β (IL-1β) and IL-6 were tested using ELISA kits (BD Biosciences, USA).

Western Blotting Analysis

The cultured supernatants and bacterial lysates were collected at the indicated time after treatment (Liu et al., 2015). Proteins in the supernatants were extracted using the methanol – chloroform approach, and the cell pellets were lysed with the RIPA Lysis buffer (89901, Thermo) supplemented with a protease

inhibitor cocktail (Roche). Finally, all the protein pellets were mixed with the SDS loading buffer. Both of the obtained proteins were applied to detection for pro-IL-1β/IL-1β, and pro-Caspase-1/Caspase-1 by immunoblotting. β-actin was chosen as the positive control. The antibodies against IL-1β (sc-52012), Caspase-1 (sc-56036), β-actin (4967S), and the secondary antibodies (IRDye 800-labeled anti-rabbit IgG; 611-132-002) were obtained from Santa Cruz Biotechnology. The proteins were quantified using an Odyssey infrared imaging system (LI-COR, Lincoln, NE).

Statistical Analysis

All continuous variables were represented as the means ± standard deviations. The unpaired 2-tailed Student's *t* test was used to compare the differences between two groups. Differences among three or more groups were compared using ANOVA. The survivals of different groups of mice were plotted with Kaplan Meir and their comparison was performed using the log-rank method. A value of $p < 0.05$ was considered statistically significant. Statistical analysis was done using SPSS 17.0 (SPSS Inc., Chicago, IL).

RESULTS

IL-1β Releases and Cytotoxicity Are Induced by SS2 *in vitro*

To measure the kinetics of the IL-1β secretion and cytotoxicity induction by SS2 in macrophages, we infected mice PMs with SS2, as explained in the "Materials and Methods" section, and the data showed that SS2 gradually increased IL-1β and the cytotoxicity during the time course after the SS2 challenge. The optimal stimulation conditions for SS2 to induce IL-1β production was 16 h post infection and a MOI of 1 (**Figures 1A,C**) with peaked IL-1β production (2,200 ± 605 pg/ml) without too much cytotoxicity (20.2 ± 4.6%). Thus, this optimal condition was used for subsequent *ex vivo* experiments. **Figures 1B,D** show that SS2 induced cytotoxicity in a time- and dose-dependent manner.

SLY Contributes to the IL-1β Release and Cytotoxicity of BMDMs *in vitro* and a Deficiency of SLY Protects Mice From Death *in vivo* in Response to the SS2 Infection

To determine which component of SS2 mediates the IL-1β secretion and cytotoxicity in multiple cells, PMs, BMDMs, and human THP-1 cells were infected with SS2 and its SLY-deficient isogenic mutant (ΔSLY; MOI, 1). SS2 induced significantly more IL-1β and cytotoxicity compared with the Δ SLY strain 16 h post infection (**Figures 2A,B**). To confirm whether the secreted SLY triggered the IL-1β and LDH release, we treated BMDMs with concentrated supernatant proteins (SS2-S/N containing SLY or ΔSLY-S/N without SLY). The SS2-S/N induced a significantly greater IL-1β and LDH release in BMDMs than ΔSLY-S/N did (**Figures 2C,D**). In contrast, the IL-6 secretions induced by different strains were comparable, suggesting that the production of IL-6 was not affected by SLY and was independent of the IL-1β release (**Figure 2E**). These results further confirmed that the SS2-induced-IL-1β secretion and cytotoxicity in the BMDMs were mediated by SLY.

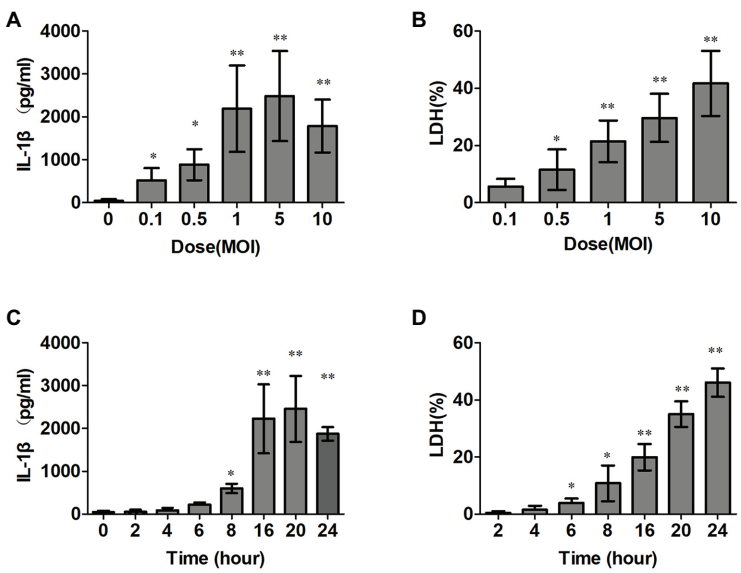

FIGURE 1 | *Streptococcus suis* serotype 2 (SS2) trigged interleukin (IL)-1β production and induced cytotoxicity *in vitro*. **(A,B)** Bone marrow derived macrophages (BMDMs; 1 × 10^6 cells/ml) were infected with SS2. The supernatants were harvested at different time points after infection. The IL-1β release was measured with ELISA **(A)**, and lactate dehydrogenase (LDH) leakage was detected using the CytoTox96® non-radioactive cytotoxicity kit **(B)**. **(C,D)** BMDMs were infected with SS2 at different doses, and the supernatants were harvested for IL-1β **(C)** and LDH detections **(D)** The data shown have the means ± standard deviations from three independent experiments. *$p < 0.05$; **$p < 0.01$.

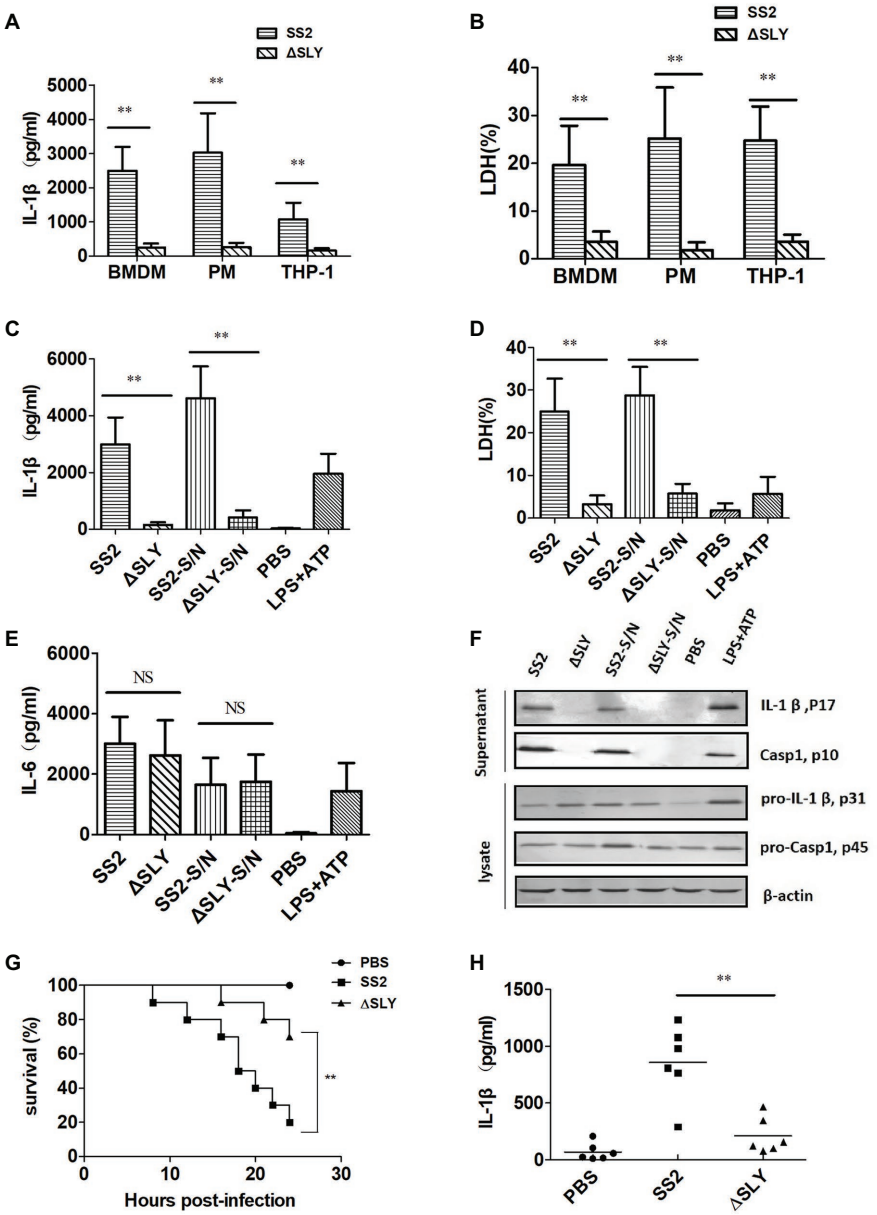

FIGURE 2 | SS2-induced secretion of IL-1β is dependent on suilysin (SLY) *in vitro* and *in vivo*. **(A,B)** Three types of cells, including human monocytic THP-1 cells, mouse peritoneal macrophages (PMs), and BMDMs, were infected with SS2 or its SLY-deficient mutant (ΔSLY); multiplicity of infection (MOI, 1) for 16 h. The supernatants were harvested for the measurement of IL-1β **(A)** and LDH **(B)**. **(C–E)** BMDMs (1×10^6 cells/ml) were infected with SS2 or ΔSLY (MOI, 1) for 16 h and also treated in parallel with the concentrated supernatant proteins SS2-S/N (200 ng/ml) or ΔSLY-S/N (200 ng/ml) for 16 h after LPS priming for 3 h. Phosphate buffer saline (PBS) and LPS plus adenosine triphosphate (ATP) were used as the negative control and positive control, respectively. The supernatants were collected for IL-1β **(C)** and IL-6 **(E)** by ELISA and LDH assay **(D)**. **(F)** Immunoblotting was performed, and the culture supernatants were measured for IL-1β p17 and Caspase1 p10, and the cell lysates were analyzed for proIL-1β p31 and pro-Caspase1 p45. **(G)** 8-week-old C57BL/6J WT mice were injected intraperitoneally (IP) with a higher dose of SS2 or ΔSLY (2×10^9 CFU/mouse in 200 μl PBS) and their survivals were observed every 2 h up to 24 h, with 10 mice in each group. The WT mice treated with SS2 and PBS were considered as the positive and negative control group, respectively. **(H)** 8-week-old WT C57BL/6J mice were injected IP with a lower dose of SS2 or ΔSLY (2×10^8 CFU in 200 μl PBS). The WT mice treated with SS2 and PBS were considered as the positive and negative control group, respectively. These mice were sacrificed 24 h after injection. Their peritoneal lavage fluids (PLFs) were harvested by rinsing the peritoneal cavity with 500 μl PBS and measured for IL-1β by ELISA (six mice in each group). The data shown in panels **(A–E)** are the means ± standard deviations from three independent experiments. The data shown in panels **(F–H)** are from one of two independent experiments. *$p < 0.05$; **$p < 0.01$.

To explore the molecular mechanisms of the SS2-induced IL-1β in BMDMs, we measured the amount of IL-1β (p17) and its immature precursor pro-IL-1β (p31) and the amount of Caspase-1 (p10) and its immature precursor pro-Caspase-1 (p45) in both supernatants and cell lysates using western blotting. The BMDMs were treated as indicated in the "Materials and Methods"

section and LPS plus ATP was used as a positive control to stimulate the secretion of IL-1β. The data showed that all strains and concentrated supernatant proteins induced similar levels of immature pro-IL-1β in the cell lysates, but SS2 or SS2-S/N induced significantly more mature IL-1β in the supernatants than the ΔSLY strains or ΔSLY-S/N did. We also observed the presence of active Caspase-1 in the supernatants of the BMDMs treated with SS2 or SS2-S/N, but not in the supernatants of the cells treated with ΔSLY or ΔSLY-S/N (**Figure 2F**).

To verify the role of SLY in the pathogenicity of SS2 *in vivo*, we infected WT mice as noted in the "Materials and Methods" section and observed their activity and survival every 2 h until 24 h post infection. Eight out of ten WT mice infected with a higher dose of 2×10^9 CFU SS2 strain died within 24 h, but only 2 out of 10 WT mice infected with 2×10^9 CFU ΔSLY strains died within 24 h post infection (**Figure 2G**). To further evaluate whether SLY was involved in the IL-1β release in response to the SS2 infection *in vivo*, we injected IP WT mice with a lower dose of 2×10^8 CFU SS2 or ΔSLY. Our results proved that the IL-1β production in the PLF from the SS2-infected WT mice was significantly higher than that in the ΔSLY-infected WT mice (**Figure 2H**). These findings suggested that SLY is a very important virulent factor.

SS2-Triggered IL-1β Releases and Cytotoxicity Require the Activation of Caspase-1/11 and Gsdmd

To verify the role of Caspase-1 and Gsdmd during SS2-induced-IL-1β release and the cytotoxicity in macrophages, we treated BMDMs isolated from WT, Caspase-1/11$^{-/-}$ and Gsdmd$^{-/-}$ mice with SS2, ΔSLY, SS2-S/N, and ΔSLY-S/N. The data showed the SS2 and SS2-S/N that induced IL-1β and the cytotoxicity were abolished in BMDMs isolated from Caspase-1/11$^{-/-}$ mice, but partly inhibited in BMDMs from Gsdmd$^{-/-}$ mice, compared with the cells of WT mice (**Figures 3A,B**).

To confirm the roles of Caspase-1/11 and Gsdmd in the pathogenicity of SS2-induced STSS *in vivo*, we infected IP WT, Caspase-1/11$^{-/-}$, and Gsdmd$^{-/-}$ mice with a higher dose of 2×10^9 CFU SS2 and observed their activity and survival every 2 h until 24 h post infection. Three (3/10) Gsdmd$^{-/-}$ mice and one (1/10) Caspase-1-deficient mouse died within 24 h post infection, and the deaths all decreased significantly compared to those of WT mice (8/10 died; **Figure 3C**).

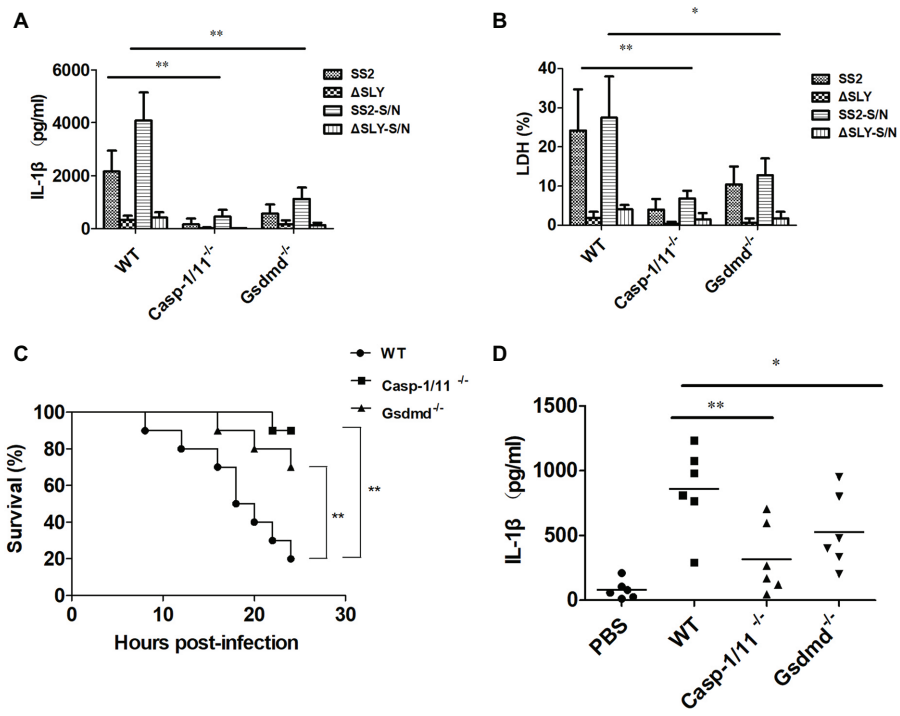

FIGURE 3 | The SS2-induced IL-1β secretion was dependent on Caspase-1/11 and gasdermin D (Gsdmd) *in vitro* and *in vivo*. **(A,B)** BMDMs were isolated from 8-week-old WT C57BL/6J, *Caspase1/11*-deficient (Caspase-1/11$^{-/-}$) and *Gsdmd*-deficient (Gsdmd$^{-/-}$) mice, which were treated with SS2 (MOI, 1), ΔSLY (MOI, 1), SS2-S/N (200 ng/ml), and ΔSLY-S/N (200 ng/ml) for 16 h (LPS priming for 3 h was needed prior to the treatments of SS2-S/N and ΔSLY-S/N). The supernatants were collected for the IL-1β ELISA **(A)** and LDH assays **(B)**. **(C)** 8-week-old WT C57BL/6J, Caspase-1/11$^{-/-}$, and Gsdmd$^{-/-}$ mice were injected IP with a higher dose of SS2 (2×10^9 CFU in 200 μl PBS) and monitored for 24 h for their survival, with 10 mice per group. The WT mice infected with SS2 were considered as the positive control group. **(D)** 8-week-old WT C57BL/6J, Caspase-1/11$^{-/-}$, and Gsdmd$^{-/-}$ mice were injected IP with a lower dose of SS2 (2×10^8 CFU in 200 μl PBS). The wild-type (WT) mice infected with SS2 and PBS were considered as the positive and negative control group respectively. These mice were sacrificed 24 h after injection and their PLFs were harvested for the measurement of IL-1β (six mice per group). The data in panels **(A,B)** are the means ± standard deviations from three independent experiments. The data in panels **(C,D)** are from one of two independent experiments. *$p < 0.05$; **$p < 0.01$.

To further evaluate whether Caspase-1/11 and Gsdmd were involved in the IL-1β release in response to the SS2 infection *in vivo*, we also injected IP WT, Caspase-1/11$^{-/-}$, and Gsdmd$^{-/-}$ mice with lower dose of 2×10^8 CFU SS2. Our results showed that the IL-1β production in the PLF from SS2-infected WT mice was significantly higher than that in Caspase-1/11$^{-/-}$ mice and Gsdmd$^{-/-}$ mice (**Figure 3D**).

Thus, we confirmed that the activation of Caspase-1/11 and Gsdmd was required for the SS2-induced IL-1β release and cytotoxicity in BMDMs *ex vivo*, and this activation contributes to mouse death and IL-1β release in response to the SS2 infection *in vivo*.

SS2-Triggered Caspase-1 Activation *via* the Nlrp3 Inflammasome, but Not the Nlrc4 and Aim2 Inflammasome

To characterize the specific inflammasome involved in SS2-induced Caspase-1 activation, we infected BMDMs of WT, Nlrp3$^{-/-}$, Nlrc4$^{-/-}$, Asc$^{-/-}$, and Aim2$^{-/-}$ mice with SS2, ΔSLY, SS2-S/N, and ΔSLY-S/N and measured the IL-1β release and cytotoxicity. The SS2-induced IL-1β and the cytotoxicity were completely abrogated in the Nlrp3$^{-/-}$ and Asc$^{-/-}$ BMDMs but unaltered in the Nlrc4$^{-/-}$ and Aim2$^{-/-}$ BMDMs (**Figures 4A,B**). Similarly, SS2-S/N induced significantly a greater amount of IL-1β and cytotoxicity in the BMDMs of WT, Nlrc4$^{-/-}$, and Aim2$^{-/-}$ BMDMs compared with those in the BMDMs of the Nlrp3$^{-/-}$ and Asc$^{-/-}$ mice (**Figures 4C,D**). In contrast, the IL-6 secretions from different genotypes of BMDMs were comparable, suggesting that Nlrp3 and Asc were dispensable for the production of IL-6 in response to the SS2 and ΔSLY strains (**Figure 4E**). Thus, the SS2-induced IL-1β secretions depend primarily on the Nlrp3 inflammasome activation.

We then measured the amount of inactive pro-IL-1β (p31), pro-Caspase-1 (p45), mature active IL-1β (p17), and Caspase-1 (p10) in the supernatants and cell lysates in SS2-infected-BMDMs from the WT and various deficient mice with immunoblotting. Consistent with the ELISA results, SS2 induced significantly more active IL-1β and Caspase-1 in the supernatants of the BMDMs of the WT, Nlrc4$^{-/-}$, and Aim2$^{-/-}$ mice but not in the BMDMs isolated from the Nlrp3$^{-/-}$ and Asc$^{-/-}$ mice. However, SS2 induced similar levels of biologically inactive pro-IL-1β and pro-Caspase-1 in cell lysates from various cells (**Figure 4F**). Thus, we demonstrated that the Nlrp3 inflammasome mediated the SS2-induced IL-1β release.

To further clarify the role of the Nlrp3 inflammasome activation in developing STSS caused by SS2, we infected three genotypes of mice [WT mice, Nlrp3$^{-/-}$ mice, and WT mice injected with the Nlrp3 inhibitor (MCC950) prior to infection] with a high dose of 2×10^9 CFU SS2. The results showed that the survival of the Nlrp3$^{-/-}$ group (2 of 10 died) and WT mice treated with the inhibitor group (3 of 10 died) was both significantly higher than that of the WT group (8 of 10 died; **Figure 4G**). Therefore, we confirmed that the Nlrp3 inflammasome played a crucial role in the host's combat against SS2 infection *in vivo*.

To further evaluate the role of the Nlrp3 inflammasome in the IL-1β release in response to the SS2 infection *in vivo*, we also injected IP three groups of the abovementioned mice with a lower dose of 2×10^8 CFU SS2. The results showed that the IL-1β production in the PLF from the SS2-infected WT mice was significantly higher than that in the Nlrp3$^{-/-}$ mice and WT mice injected with the Nlrp3 inhibitor (**Figure 4H**).

SS2 and SS2-S/N-Induced IL-1β Release in BMDMs Requires K^+ Efflux and ROS Production

To find whether potassium (K^+) efflux participates in the inflammasome activation induced by SS2 in BMDMs, a high concentration of KCl was added to the supernatants of a cell culture to block the K^+ efflux before the cells were treated with SS2. The IL-1β production and cytotoxicity were almost completely abrogated by KCl (**Figures 5A,B**). To investigate whether SS2 activated the inflammasome *via* the ATP receptor P2X7R, BMDMs were pretreated with the P2X7R inhibitor (oATP) prior to the SS2 infection. The results showed that the IL-1β release and cytotoxicity were significantly reduced by blocking the ATP receptor P2X7R (**Figures 5A,B**). To study the involvement of the ROS production in activating the inflammasome in response to the SS2 infection, BMDMs were pretreated with the ROS inhibitor (NAC). The IL-1β release and cytotoxicity triggered by SS2 was impaired by inhibiting ROS (**Figures 5A,B**). Together, these results indicated that the K^+ efflux, ATP receptor P2X7, and production of reactive oxygen species (ROS) were all involved in IL-1β secretion during the SS2 infection. Furthermore, we pretreated BMDMs with the Nlrp3 inhibitor (MCC950) and Caspase-1 inhibitor (Z-YVAD-FMK) prior to the infection with SS2, and we observed the expected significant inhibitions to the IL-1β release and cytotoxicity (**Figures 5A,B**).

Similarly, the abovementioned five kinds of inhibitors, including KCl, P2X7R receptor inhibitor (oATP), ROS inhibitor (NAC), Nlrp3 inhibitor (MCC950), and Caspase-1 inhibitor (Z-YVAD-FMK), impaired the IL-1β release and cytotoxicity induced by SS2-S/N (**Figures 5C,D**).

All of the data suggested that the IL-1β secretion in BMDMs induced by SS2 or SS2-S/N was mediated by K^+ efflux and ROS production *via* the Nlrp3 inflammasome activation.

DISCUSSION

Innate immunity is critical to the pathogenesis of the SS2 infection. The infected individuals rely exclusively on their innate immune response to clear bacteria but the massive release of proinflammatory mediators by innate immune cells can cause severe pathophysiological injury to the host (Li et al., 2019). In this study, we focused on the role of SLY and inflammasome activation in the pathogenesis of STSS-induced by SS2. Our results demonstrated that SLY mediated IL-1β release and cytotoxicity in the BMDMs, which contributed to the higher mortality of mice infected with SS2. We also found that the activation of the Nlrp3

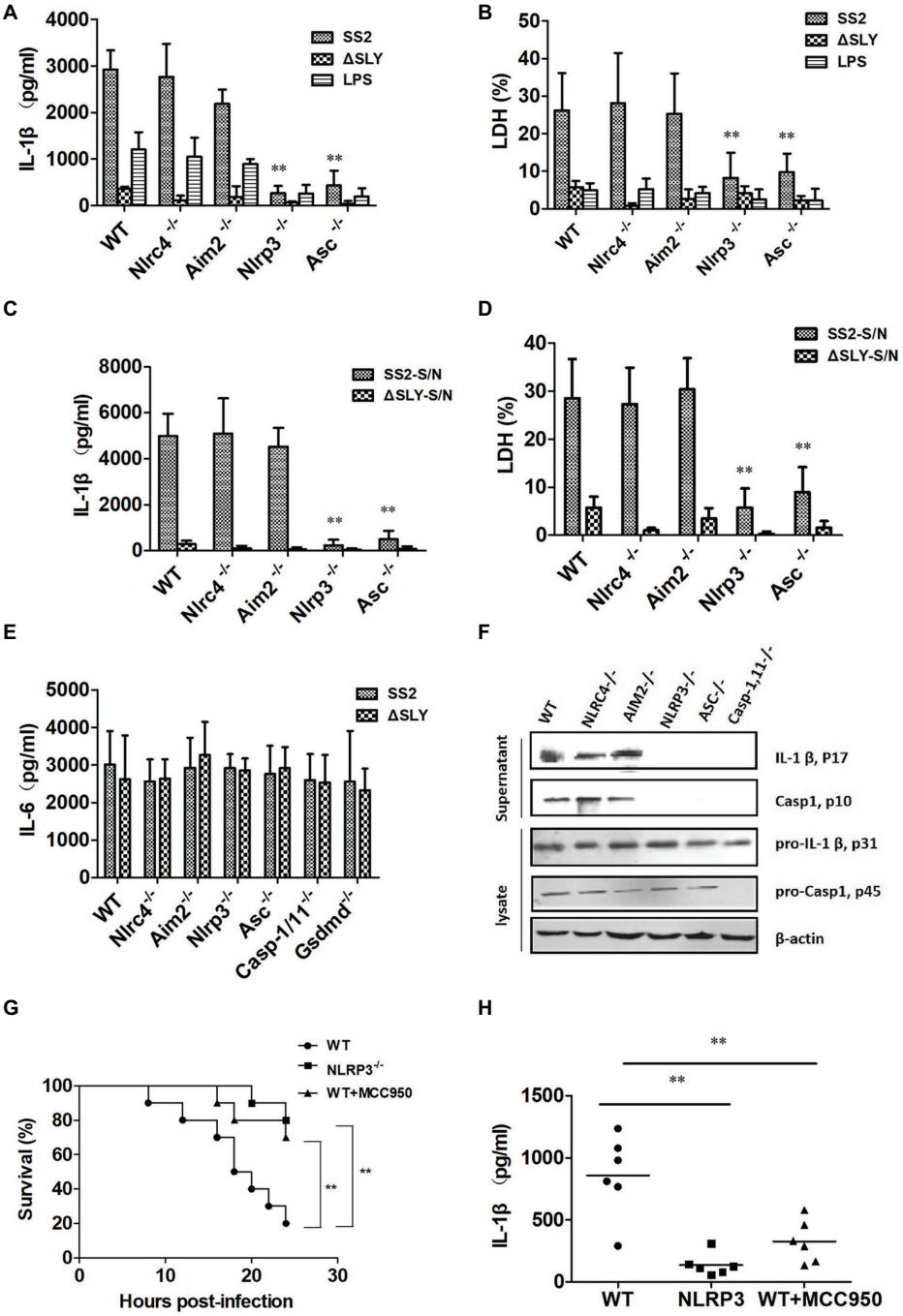

FIGURE 4 | The SS2-induced IL-1β secretion is dependent on the Nlrp3 inflammasome activation *in vitro* and *in vivo*. BMDMs were isolated from WT C57BL/6J mice and multiple deficient mice [*Nlrc4*-deficient (Nlrc4$^{-/-}$), *Aim2*-deficient (Aim2$^{-/-}$), *Nlrp3*-deficient (Nlrp3$^{-/-}$), and *Asc*-deficient (Asc$^{-/-}$)] and infected with SS2 (MOI, 1) and ΔSLY (MOI, 1) for 16 h. The supernatants were harvested and assayed for IL-1β **(A)**, LDH **(B)**, and IL-6 **(E)**. These cells were also treated parallel with SS2-S/N (200 ng/ml) and ΔSLY-S/N (200 ng/ml) for 16 h after LPS priming for 3 h. Their supernatants were collected for IL-1β ELISA **(C)** and LDH assays **(D)**. **(F)** Along with immunoblotting, the supernatants were also measured for IL-1β p17 and Caspase1 p10, and the cell lysates were analyzed for pro-IL-1β p31 and pro-Caspase1 p45. **(G)** Three groups of 8-week-old mice, including WT mice (C57BL/6J), Nlrp3$^{-/-}$ mice, and WT mice treated with the Nlrp3 inhibitor MCC950 (the WT mice were injected IP with Nlrp3 inhibitor MCC950 prior to SS2 infection), were injected IP with a higher dose of SS2 (2×10^9 CFU in 200 μl PBS), and their survival was monitored for 24 h, with 10 mice per group. The WT mice infected with SS2 were considered as the positive control group. **(H)** Three groups of the abovementioned mice were injected IP with a lower dose of SS2 (2×10^8 CFU in 200 μl PBS). The WT mice infected with SS2 were considered as the positive control group. These mice were sacrificed 24 h after injection and their PLF was harvested and measured for IL-1β (six mice in each group). The data in panels **(A–E)** are the means ± standard deviations from three independent experiments. The data in panels **(F–H)** are obtained from one of two independent experiments. *$p < 0.05$; **$p < 0.01$.

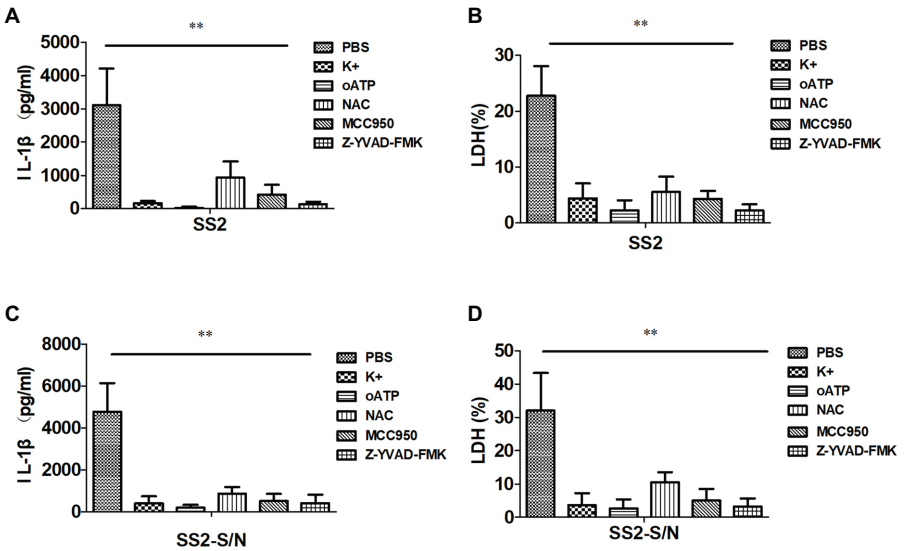

FIGURE 5 | SS2-induced IL-1β secretion in BMDMs requires potassium (K^+) efflux, ATP, and reactive oxygen species (ROS) production. BMDMs were infected with SS2 (MOI, 1) 16 h in the absence or presence of the K^+ efflux blocker (KCl, 50 mM), ATP blocker (oxidized ATP, oATP, 500 μM), ROS inhibitor (N-acetyl-L-cysteine, NAC, 20 mM), Nlrp3 inhibitor (MCC950, 10 μM), and Caspase-1 inhibitor (Z-YVAD-FMK, 10 μM). IL-1β in the supernatants was measured with ELISA **(A)** and LDH was assayed using a Cytotox96 kit **(B)**. BMDMs were also incubated with SS2-S/N 16 h after lipopolysaccharide (LPS) priming for 3 h in the absence or presence of the above-mentioned inhibitors. The IL-1β in the supernatants was measured with ELISA **(C)**, and LDH was assayed using a Cytotox96 Kit **(D)**. The results are represented as the means ± standard deviations of three independent experiments. *$p < 0.05$; **$p < 0.01$.

inflammasome mediated by SLY played a key role in the IL-1β release, cytotoxicity, and protecting mice from early death due to the high dose of the SS2 infection in a mouse STSS model.

In this study, we proved that SLY, a member of cholesterol-dependent cytolysins, contributed to the IL-1β release, cytotoxicity, and activation of the Nlrp3 inflammasome that was involved in STSS caused by SS2. Our results add SLY to the growing list of bacterial toxins, including various pore-forming toxins, hemolysins, and cholesterol-dependent cytolysins, which can trigger the Nlrp3 inflammasome activation (Muñoz-Planillo et al., 2009; Meixenberger et al., 2010). SLY was also studied as a potential vaccine candidate (Du et al., 2013) because the increased SLY release promotes *S. suis* entering into and surviving in the blood stream, thereby contributing to the infection (Jacobs et al., 1996). Therefore, SLY plays a key role in the pathogenesis of SS2-induced STSS.

It has been reported that both Caspase-1- and Caspase-11-deficient mice are more resistant to LPS-induced shock than WT mice controls (Wang et al., 1998). SS2 is a gram-positive bacterium without LPS to activate Caspase-11. Therefore, we speculated that the STSS and pyroptosis induced by SS2 were mainly attributed to the canonical inflammatory Caspase pathway. Two studies reported that Gsdmd as a key mediator of pyroptosis was essential for IL-1β secretion in both the canonical- and non-canonical inflammatory Caspase pathways (He et al., 2015; Shi et al., 2015). The 31 kDa N-terminal fragment of Gsdmd is cytotoxic and capable of triggering pyroptosis when expressed aberrantly. Gsdmd-deficient macrophages failed to induce pyroptosis after exposure to cytosolic LPS and other known inflammasome stimuli, and therefore, Gsdmd was regarded as a shared component of Caspase-1- and -11-mediated pyroptosis. Whether Gsdmd is involved in the development of STSS in SS2 infection is uncertain. In this study, SS2-infected BMDMs from Caspase-1/11$^{-/-}$and Gsdmd$^{-/-}$ mice had a lower IL-1β release and cytotoxicity than the BMDMs from WT mice *ex vivo*. *In vivo* results further confirmed that Caspase-1/11$^{-/-}$ mice and Gsdmd$^{-/-}$ mice had a lower IL-1β production in the PLF and were more resistant to SS2-induced STSS and death compared with WT mice. These findings suggest that IL-1β release and pyroptosis mediated by activations of Caspase-1/11 and Gsdmd contribute to STSS during SS2 infection. Recent studies (Antonopoulos et al., 2015; Gurung and Kanneganti, 2015) revealed novel non-apoptotic function of caspase-8 to modulate IL-1β production *via* NLRP3 inflammasomes activation. It is proposed that caspase-8 regulates expression of pro-IL-1β and NLRP3 mRNA activation *via* nuclear factor-kB (NF-kB) pathway. In the NLRP3 inflammasome, caspase-8 is required for both canonical- and non-canonical assembly and activation of the inflammasome complex. In the absence of caspase-1, NLRP3 inflammasomes directly utilize caspase-8 as both a proapoptotic initiator and major IL-1β-converting protease. In the presence of caspase-1, caspase-8 acts as a positive modulator of the NLRP3-dependent caspase-1 signaling cascades that drive both IL-1β production and pyroptotic death. It remains to be determined whether caspase-8 is involved in SLY-induced NLRP3 activation and IL-1β production during SS2 infection.

Several types of streptococci have been reported to activate inflammasomes. For example, production of IL-1β in macrophages infected with *Streptococcus pyogenes* depends on the TLR and Nlrp3 signaling and the activation of Caspase-1 is mediated by the pore-forming toxin streptolysin O (Harder et al., 2009). Furthermore, Nlrp3 activation depends on pneumolysin, which is required for the protection against respiratory infections with *S. pneumonia* (McNeela et al., 2010). Moreover, the IL-1β secretion in Group B *Streptococcus*-stimulated mouse dendritic cells depended on the Nlrp3 inflammasome and on production of β-hemolysin by Group B *Streptococcus* (Costa et al., 2012). Recent studies indicated that *Streptococcus sanguinis* could trigger the IL-1β release *via* Nlrp3 inflammasome in macrophage and dendritic cells and that interaction of purinergic receptors with ATP released is involved in the activity (Saeki et al., 2017). How SS2 activates inflammasomes has not been well studied.

Coll et al. (2015) found that a small-molecule inhibitor, MCC950, showed its potential as a therapeutic drug in many NLRP3-associated syndromes, including autoinflammatory and autoimmune diseases. MCC950 specifically inhibits NLRP3 activation but not AIM2, NLRC4, or NLRP1 activation, and it blocks both canonical- and non-canonical inflammasome activation at nanomolar concentrations. Here, we reported that SS2-infected BMDMs from Nlrp3$^{-/-}$ mice had a lower IL-1β release and cytotoxicity *ex vivo*. Both Nlrp3$^{-/-}$ mice and WT mice treated with the Nlrp3 inhibitor MCC950 had a lower IL-1β production in the PLF and were more resistant to STSS and death caused by SS2 in comparison to the WT mice. Consistent with our results, Li et al. (2019) reported that myricetin, a natural compound, could reduce the production of the proinflammatory cytokines TNF-α and IL-1β effectively, and confirmed that myricetin exerted an obvious protective effect against SS2 infection *in vitro* and *in vivo*. Similarly, Shen et al. (2018) chose a mentoflavone, a biflavonoid compound that has been widely used in traditional Chinese medicine, to block SLY oligomerization and inhibit its pore-forming activity and suppress the excessive inflammation without interfering with SS2 growth, which were observed to clearly increase the survival of mice infected with highly virulent SS2. In contrast, Lavagna et al. (2019) reported that the survival of IL-1β receptor-deficient mice decreased compared to that of the WT mice when infected with 1×10^7 CFU highly virulent SS2. The infection doses in Lavagna's study were significantly lower than those in our study (2×10^9 CFU) and Shen's studies (2×10^9 CFU; Shen et al., 2018). Besides the virulence of the pathogen and the genetic characters of the host, the infection dose of the pathogen may be another important risk factor that can induce an excessive inflammatory response and cause a severe outcome from the infection. We compared different infection doses and found that a higher infection dose can quickly induce an acute excessive inflammatory response as a cytokine storm and cause septic shock and death within 24 h. However, mice infected with a lower infection dose almost all survived. The inflammatory response to infection is beneficial to the host to combat bacterial growth. However, the massive release of proinflammatory mediators may cause severe pathophysiological phenomena that are the hallmark of SS2-induced septic shock and lethality. Therefore, reducing an excessive inflammatory response by using the SLY antibody or NLPR3 pathway inhibitor at an early stage may protect the host from severe acute STSS but might not play protective role at any stage of infection for any host with a different immune function.

The Nlrp3 inflammasome activation can be induced by diverse stimuli, including bacterial toxins and endogenous danger signals. We still do not know how the activation of the Nlrp3 inflammasome was initiated in the BMDMs infected with SS2. The K^+ efflux occurs upon the extracellular ATP engagement with the ATP receptor P2X7R. Bacterial pore-forming toxins can cause plasma membranes to become more permeable, allowing the K^+ efflux to be independent of the ATP receptor (Muñoz-Planillo et al., 2013). In this study, the IL-1β release in BMDMs was significantly reduced *via* blocking the K^+ efflux and A2X7R receptor and inhibiting ROS generation. The roles of blocking the K^+ efflux and A2X7R receptor were more effective than the inhibition of the ROS generation, suggesting that the K^+ efflux may play the most important role in the SS2-induced IL-1β release. Lavagna et al. (2019) also reported consistent findings on the role of the K^+ efflux in the Nlrp3 activation induced by SS2, although they also observed the activation of the NLRP1, Nlrc4, and Aim2 inflammasomes; Nlrp3 was the major one being activated (Mariathasan et al., 2006; Rathinam et al., 2010). The precise mechanism of the Nlrp3 inflammasome activation induced by SS2 should be further investigated.

In summary, we reported that SLY was essential for mediating the IL-1β secretion and triggering pyroptosis during the SS2 infection *in vitro* and *in vivo*. Our data suggested that Nlrp3 inflammasome activation and pyroptosis participated in the proinflammatory response upon SS2 infection. Furthermore, the K^+ efflux and ROS generation are involved in the SLY-induced Nlrp3 inflammasome activation. Our study sheds light on the role of SLY and the activation of Nlrp3 inflammasomes and pyroptosis in the pathogenesis of STSS caused by the SS2 infection, and this may hold promise for the potential prevention and therapy for STSS.

DATA AVAILABILITY STATEMENT

The raw data supporting the conclusions of this article will be made available by the authors, without undue reservation.

ETHICS STATEMENT

The animal study was reviewed and approved by the Laboratory Animal Welfare & Ethics Committee of the National Institute for Communicable Disease Control and Prevention, Chinese Center for Disease Prevention and Control.

AUTHOR CONTRIBUTIONS

LS and ZR conceptualized the experiments. LS, XL, YH, and YX conducted the experiments. LS analyzed the data. LS and

ZR wrote the paper. YJ provided the strains and GM provided the deficient mice and both contributed to the discussion. All authors contributed to the article and approved the submitted version.

FUNDING

This work was supported by grants from the National Natural Science Foundation of China (No. 81371761 to ZR; No 31170868 for GM), the Ministry of Science and Technology of China (Grant No. 2018ZX10301403-003, 2018ZX10712-001-006, 2018ZX10305409-003-001).

ACKNOWLEDGMENTS

We appreciated the help of Dr. Warren Strober for sharing the Nlrp3-deficient mice, Dr. Vishva M. Dixit for providing the Asc-deficient mice, and Dr. Feng Shao for providing the Gsdmd-deficient mice.

REFERENCES

Antonopoulos, C., Russo, H. M., El Sanadi, C., Martin, B. N., Li, X., Kaiser, W. J., et al. (2015). Caspase-8 as an effector and regulator of NLRP3 inflammasome signaling. *J. Biochem.* 290, 20167–20184. doi: 10.1074/jbc.M115.652321

Coll, R. C., Robertson, A. A., Chae, J. J., Higgins, S. C., Muñoz-Planillo, R., Inserra, M. C., et al. (2015). A small-molecule inhibitor of the NLRP3 inflammasome for the treatment of inflammatory diseases. *Nat. Med.* 21, 248–255. doi: 10.1038/nm.3806

Costa, A., Gupta, R., Signorino, G., Malara, A., Cardile, F., Biondo, C., et al. (2012). Activation of the NLRP3 inflammasome by group B streptococci. *J. Immunol.* 188, 1953–1960. doi: 10.4049/jimmunol.1102543

Du, H., Huang, W., Xie, H., Ye, C., Jing, H., Ren, Z., et al. (2013). The genetically modified suilysin, rSLY (P353L), provides a candidate vaccine that suppresses proinflammatory response and reduces fatality following infection with *Streptococcus suis*. *Vaccine* 31, 4209–4215. doi: 10.1016/j.vaccine.2013.07.004

Fittipaldi, N., Xu, J., Lacouture, S., Tharavichitkul, P., Osaki, M., Sekizaki, T., et al. (2011). Lineage and virulence of *Streptococcus suis* serotype 2 isolates from North America. *Emerg. Infect. Dis.* 17, 2239–2244. doi: 10.3201/eid1712.110609

Gottschalk, M., Segura, M., and Xu, J. (2007). *Streptococcus suis* infections in humans: the Chinese experience and the situation in North America. *Anim. Health Res. Rev.* 8, 29–45. doi: 10.1017/S1466252307001247

Gurung, P., and Kanneganti, T. D. (2015). Novel roles for caspase-8 in IL-1β and inflammasome regulation. *Am. J. Pathol.* 185, 17–25. doi: 10.1016/j.ajpath.2014.08.025

Harder, J., Franchi, L., Muñoz-Planillo, R., Park, J. H., Reimer, T., and Núñez, G. (2009). Activation of the Nlrp3 inflammasome by *Streptococcus pyogenes* requires streptolysin O and NF-kappa B activation but proceeds independently of TLR signaling and P2X7 receptor. *J. Immunol.* 183, 5823–5829. doi: 10.4049/jimmunol.0900444

He, Z., Pian, Y., Ren, Z., Bi, L., Yuan, Y., Zheng, Y., et al. (2014). Increased production of suilysin contributes to invasive infection of the *Streptococcus suis* strain 05ZYH33. *Mol. Med. Rep.* 10, 2819–2826. doi: 10.3892/mmr.2014.2586

He, W. T., Wan, H., Hu, L., Chen, P., Xin Wang, X., Huang, Z., et al. (2015). Gasdermin D is an executor of pyroptosis and required for interleukin-1β secretion. *Cell Res.* 25, 1285–1298. doi: 10.1038/cr.2015.139

Hornung, V., Ablasser, A., Charrel-Dennis, M., Bauernfeind, F., Horvath, G., Caffrey, D. R., et al. (2009). AIM2 recognizes cytosolic dsDNA and forms a caspase-1-activating inflammasome with ASC. *Nature* 458, 514–518. doi: 10.1038/nature07725

Hu, X., Zhu, F., Wang, H., Chen, S., Wang, G., Sun, J., et al. (2000). Studies on human streptococcal infectious syndrome caused by infected pigs. *Zhonghua Yu Fang Yi Xue Za Zhi* 34, 150–152.

Huong, V. T., Ha, N., Huy, N. T., Horby, P., Nghia, H. D., Thiem, V. D., et al. (2014). Epidemiology, clinical manifestations, and outcomes of *Streptococcus suis* infection in humans. *Emerg. Infect. Dis.* 20, 1105–1114. doi: 10.3201/eid2007.131594

Jacobs, A. A., van den Berg, A. J., and Loeffen, P. L. (1996). Protection of experimentally infected pigs by suilysin, the thiol-activated haemolysin of *Streptococcus suis*. *Vet. Rec.* 139, 225–228. doi: 10.1136/vr.139.10.225

Kayagaki, N., Warming, S., Lamkanfi, M., Vande Walle, L., Louie, S., Dong, J., et al. (2011). Non-canonical inflammasome activation targets caspase-11. *Nature* 479, 117–121. doi: 10.1038/nature10558

Kim, S., Bauernfeind, F., Ablasser, A., Hartmann, G., Fitzgerald, K. A., Latz, E., et al. (2010). *Listeria monocytogenes* is sensed by the NLRP3 and AIM2 inflammasome. *Eur. J. Immunol.* 40, 1545–1551. doi: 10.1002/eji.201040425

King, S. J., Heath, P. J., Luque, I., Tarradas, C., Dowson, C. G., and Whatmore, A. M. (2001). Distribution and genetic diversity of suilysin in *Streptococcus suis* isolated from different diseases of pigs and characterization of the genetic basis of suilysin absence. *Infect. Immun.* 69, 7572–7582. doi: 10.1128/IAI.69.12.7572-7582.2001

Kumagai, K., Itoh, K., Hinuma, S., and Tada, M. (1979). Pretreatment of plastic petri dishes with fetal calf serum. A simple method for macrophage isolation. *J. Immunol. Methods* 29, 17–25. doi: 10.1016/0022-1759(79)90121-2

Lavagna, A., Auger, J. P., Dumesnil, A., Roy, D., Girardin, S. E., Gisch, N., et al. (2019). Interleukin-1 signaling induced by *Streptococcus suis* serotype 2 is strain-dependent and contributes to bacterial clearance and inflammation during systemic disease in a mouse model of infection. *Vet. Res.* 50:52. doi: 10.1186/s13567-019-0670-y

Li, G., Wang, G., Si, X., Zhang, X., Liu, W., Li, L., et al. (2019). Inhibition of suilysin activity and inflammation by myricetin attenuates *Streptococcus suis* virulence. *Life Sci.* 223, 62–68. doi: 10.1016/j.lfs.2019.03.024

Liu, L., Hao, S., Lan, R., Wang, G., Xiao, D., Sun, H., et al. (2015). The type VI secretion system modulates flagellar gene expression and secretion in *Citrobacter freundii* and contributes to adhesion and cytotoxicity to host cells. *Infect. Immun.* 83, 2596–2604. doi: 10.1128/IAI.03071-14

Lun, S., Perez-Casal, J., Connor, W., and Willson, P. J. (2003). Role of suilysin in pathogenesis of *Streptococcus suis* capsular serotype 2. *Microb. Pathog.* 34, 27–37. doi: 10.1016/S0882-4010(02)00192-4

Mao, K., Chen, S., Chen, M., Ma, Y., Wang, Y., Huang, B., et al. (2013). Nitric oxide suppresses NLRP3 inflammasome activation and protects against LPS-induced septic shock. *Cell Res.* 23, 201–212. doi: 10.1038/cr.2013.6

Mariathasan, S., Newton, K., Monack, D. M., Vucic, D., French, D. M., Lee, W. P., et al. (2004). Differential activation of the inflammasome by caspase-1 adaptors ASC and Ipaf. *Nature* 430, 213–218. doi: 10.1038/nature02664

Mariathasan, S., Weiss, D. S., Newton, K., McBride, J., O'Rourke, K., Roose-Girma, M., et al. (2006). Cryopyrin activates the inflammasome in response to toxins and ATP. *Nature* 440, 228–232. doi: 10.1038/nature04515

McNeela, E. A., Burke, A., Neill, D. R., Baxter, C., Fernandes, V. E., Ferreira, D., et al. (2010). Pneumolysin activates the NLRP3 inflammasome and promotes proinflammatory cytokines independently of TLR4. *PLoS Pathog.* 6:e1001191. doi: 10.1371/journal.ppat.1001191

Meixenberger, K., Pache, F., Eitel, J., Schmeck, B., Hippenstiel, S., Slevogt, H., et al. (2010). *Listeria monocytogenes*-infected human peripheral blood mononuclear cells produce IL-1beta, depending on listeriolysin O and NLRP3. *J. Immunol.* 184, 922–930. doi: 10.4049/jimmunol.0901346

Meng, G., Zhang, F., Fuss, I., Kitani, A., and Strober, W. (2009). A mutation in the Nlrp3 gene causing inflammasome hyperactivation potentiates Th17 cell-dominant immune responses. *Immunity* 30, 860–874. doi: 10.1016/j.immuni.2009.04.012

Muñoz-Planillo, R., Franchi, L., Miller, L. S., and Núñez, G. (2009). A critical role for hemolysins and bacterial lipoproteins in *Staphylococcus aureus*-induced

activation of the Nlrp3 inflammasome. *J. Immunol.* 183, 3942–3948. doi: 10.4049/jimmunol.0900729

Muñoz-Planillo, R., Kuffa, P., Martínez-Colón, G., Smith, B. L., Rajendiran, T. M., and Núñez, G. (2013). K^+ efflux is the common trigger of NLRP3 inflammasome activation by bacterial toxins and particulate matter. *Immunity* 38, 1142–1153. doi: 10.1016/j.immuni.2013.05.016

Pian, Y., Wang, P., Liu, P., Zheng, Y., Zhu, L., Wang, H., et al. (2015). Proteomics identification of novel fibrinogen-binding proteins of *Streptococcus suis* contributing to antiphagocytosis. *Front. Cell. Infect. Microbiol.* 5:19. doi: 10.3389/fcimb.2015.00019

Rathinam, V. A., Jiang, Z., Waggoner, S. N., Sharma, S., Cole, L. E., Waggoner, L., et al. (2010). The AIM2 inflammasome is essential for host defense against cytosolic bacteria and DNA viruses. *Nat. Immunol.* 11, 395–402. doi: 10.1038/ni.1864

Saeki, A., Suzuki, T., Hasebe, A., Kamezaki, R., Fujita, M., Nakazawa, F., et al. (2017). Activation of nucleotide-binding domain-like receptor containing protein 3 inflammasome in dendritic cells and macrophages by *Streptococcus sanguinis*. *Cell. Microbiol.* 19:e12663. doi: 10.1111/cmi.12663

Shen, X., Niu, X., Li, G., Deng, X., and Wang, J. (2018). Amentoflavone ameliorates *Streptococcus suis*-induced infection *in vitro* and *in vivo*. *Appl. Environ. Microbiol.* 84, e01804–e01818. doi: 10.1128/AEM.01804-18

Shi, J., Gao, W., and Shao, F. (2017). Pyroptosis: gasdermin-mediated programmed necrotic cell death. *Trends Biochem. Sci.* 42, 245–254. doi: 10.1016/j.tibs.2016.10.004

Shi, J., Zhao, Y., Wang, K., Shi, X., Wang, Y., Huang, H., et al. (2015). Cleavage of GSDMD by inflammatory caspases determines pyroptotic cell death. *Nature* 526, 660–665. doi: 10.1038/nature15514

Song, L., Huang, Y., Zhao, M., Wang, Z., Wang, S., Sun, H., et al. (2015). A critical role for hemolysin in vibrio fluvialis-induced IL-1β secretion mediated by the NLRP3 inflammasome in macrophages. *Front. Microbiol.* 6:510. doi: 10.3389/fmicb.2015.00510

Tenenbaum, T., Asmat, T. M., Seitz, M., Schroten, H., and Schwerk, C. (2016). Biological activities of suilysin: role in *Streptococcus suis* pathogenesis. *Future Microbiol.* 11, 941–954. doi: 10.2217/fmb-2016-0028

Wang, S., Miura, M., Jung, Y. K., Zhu, H., Li, E., and Yuan, J. (1998). Murine caspase-11, an ICE-interacting protease, is essential for the activation of ICE. *Cell* 92, 501–209. doi: 10.1016/S0092-8674(00)80943-5

Witzenrath, M., Pache, F., Lorenz, D., Koppe, U., Gutbier, B., Tabeling, C., et al. (2011). The NLRP3 inflammasome is differentially activated by pneumolysin variants and contributes to host defense in pneumococcal pneumonia. *J. Immunol.* 187, 434–440. doi: 10.4049/jimmunol.1003143

Ye, C., Zheng, H., Zhang, J., Jing, H., Wang, L., Xiong, Y., et al. (2009). Clinical, experimental, and genomic differences between intermediately pathogenic, highly pathogenic, and epidemic *Streptococcus suis*. *J. Infect. Dis.* 199, 97–107. doi: 10.1086/594370

Ye, C., Zhu, X., Jing, H., Du, H., Segura, M., Zheng, H., et al. (2006). *Streptococcus suis* sequence type 7 outbreak, Sichuan, China. *Emerg. Infect. Dis.* 12, 1203–1208. doi: 10.3201/eid1708.060232

Yu, H., Jing, H., Chen, Z., Zheng, H., Zhu, X., Wang, H., et al. (2006). Human *Streptococcus suis* outbreak, Sichuan, China. *Emerg. Infect. Dis.* 12, 914–920. doi: 10.3201/eid1206.051194

Conflict of Interest: The authors declare that the research was conducted in the absence of any commercial or financial relationships that could be construed as a potential conflict of interest.

frontiers in Immunology

MINI REVIEW
published: 14 August 2020
doi: 10.3389/fimmu.2020.01839

Perforins Expression by Cutaneous Gamma Delta T Cells

Katelyn O'Neill[1], *Irena Pastar*[2], *Marjana Tomic-Canic*[2] *and Natasa Strbo*[1]*

[1] Department of Microbiology and Immunology, Miller School of Medicine, University of Miami, Miami, FL, United States, [2] Wound Healing and Regenerative Medicine Research Program, Dr. Phillip Frost Department of Dermatology and Cutaneous Surgery, Miller School of Medicine, University of Miami, Miami, FL, United States

Gamma delta (GD) T cells are an unconventional T cell type present in both the epidermis and the dermis of human skin. They are critical to regulating skin inflammation, wound healing, and anti-microbial defense. Similar to CD8+ cytotoxic T cells expressing an alpha beta (AB) TCR, GD T cells have cytolytic capabilities. They play an important role in elimination of cutaneous tumors and virally infected cells and have also been implicated in pathogenicity of several autoimmune diseases. T cell cytotoxicity is associated with the expression of the pore forming protein Perforin. Perforin is an innate immune protein containing a membrane attack complex perforin-like (MACPF) domain and functions by forming pores in the membranes of target cells, which allow granzymes and reactive oxygen species to enter the cells and destroy them. Perforin-2, encoded by the gene *MPEG1*, is a newly discovered member of this protein family that is critical for clearance of intracellular bacteria. Cutaneous GD T cells express both Perforin and Perforin-2, but many questions remain regarding the role that these proteins play in GD T cell mediated cytotoxicity against tumors and bacterial pathogens. Here, we review what is known about Perforin expression by skin GD T cells and the mechanisms that contribute to Perforin activation.

Keywords: pore forming proteins, perforin, perforin-2, mpeg-1, gamma delta T cells, skin, cytotoxicity

OPEN ACCESS

Edited by:
Gabriele Pradel,
RWTH Aachen University, Germany

Reviewed by:
Ilia Voskoboinik,
Peter MacCallum Cancer Centre, Australia
Ruby Hong Ping Law,
Monash University, Australia
Michael Walch,
Université de Fribourg, Switzerland

***Correspondence:**
Natasa Strbo
nstrbo@med.miami.edu

Specialty section:
This article was submitted to Microbial Immunology, a section of the journal Frontiers in Immunology

Received: *21 April 2020*
Accepted: *08 July 2020*
Published: *14 August 2020*

Citation:
O'Neill K, Pastar I, Tomic-Canic M and Strbo N (2020) Perforins Expression by Cutaneous Gamma Delta T Cells. Front. Immunol. 11:1839. doi: 10.3389/fimmu.2020.01839

INTRODUCTION

Gamma delta (GD) T cells are an unconventional T cell type that constitutes about 1–5% of circulating lymphocytes (1, 2). Despite low numbers in circulation, GD T cells are enriched in barrier tissues including the skin, gut, and reproductive tract (3–8). The skin is an epithelial tissue that serves as a barrier to protect against physical and chemical insults as well as potentially pathogenic microorganisms. It is composed of two main layers, the epidermis and dermis, and GD T cells are present in both layers in both mice and humans (2, 9). Epidermal GD T cells in mice are referred to as dendritic epidermal T cells (DETCs) because of the dendritic processes they use to survey surrounding keratinocytes for signs of stress or damage (10, 11). These cells all express an identical invariant TCR and are potent producers of IFN-g (12–14). Dermal GD T cells on the other hand are not dendritic and they produce IL-17 (5, 6). Human GD T cells, however, exist primarily in the dermis (15, 16). Small numbers are observed in the epidermis in steady state, but unlike mouse DETCs, they do not exhibit dendritic processes (17). Human GD T cells also express an invariant TCR. Skin resident cells express a delta 1 TCR, while circulating GD T cells express a delta 2 TCR (18–20).

In recent years, researchers have begun to elucidate the vast roles that GD T cells play in skin inflammation and anti-microbial defense. GD T cells serve as bridges between the innate and adaptive immune system. Although they express a recombinant TCR as alpha beta (AB) T cells do, they can bind to and recognize antigens directly without processing and presentation by MHC molecules (21). They can also respond to antigens without the need for pre-stimulation (6, 22). These innate-like characteristics position GD T cells to respond quickly to signs of stress caused by damage or infection. GD T cells play an important role in the response to pathogens in the skin. They produce IL-17 and IL-22 upon stimulation with IL-23, which triggers antimicrobial peptide production by keratinocytes as well as neutrophil recruitment to the site of infection (5, 9, 23). GD T cells also contribute to wound healing, particularly through their production of fibroblast growth factor-7 (FGF-7) and insulin-like growth factor-1 (IGF-1), which promote keratinocyte proliferation and reepithelialization (24, 25), as well as through their production of IL-17 (26). They also secrete fibroblast growth factor-9 (FGF-9), which triggers Wnt activation in wound fibroblasts and modulates hair follicle regeneration after wounding (27). In addition, GD T cells play a role in tumor surveillance. They have the ability to kill a variety of cutaneous tumors including melanoma and carcinomas, and they express cytotoxic molecules including Perforins and granzymes (18, 28, 29). Although researchers have documented Perforin production by GD T cells, the mechanisms regulating Perforin production and the pathways through which it stimulates GD T cell cytotoxicity are not fully understood. This review will cover what is known about the role of Perforin as well as the novel pore forming protein Perforin-2 in GD T cells in the skin.

OVERVIEW OF THE PERFORINS

Some of the most well-characterized pore forming proteins include the pore forming toxins expressed by pathogenic bacteria (30). One example is the cholesterol dependent cytolysins (CDC) which are produced by several gram-positive bacterial species. These virulence factors promote bacterial pathogenesis by lysing or permeabilizing host cell membranes or intracellular organelles (30–32). CDC proteins share a complex core fold with proteins from the membrane attack complex/perforin (MACPF) superfamily (33–35). This structural homology underlies the similar mechanism of pore formation and membrane disruption shared by both protein families. Pore forming proteins in the MACPF family are named as such because they all contain a domain that is shared by the proteins that form the membrane attack complex and the Perforins (36). Hundreds of MACPF domain- containing proteins have been identified, but some of the most well-characterized are the mammalian MACPF immune proteins, which include complement proteins C6-C9, Perforin, and Perforin-2 (34, 37, 38). Perforin, encoded by the gene *PRF1*, is located within cytolytic granules inside cytotoxic T cells and natural killer (NK) cells (39). When the cytotoxic cell recognizes a transformed or infected target cell, the granules containing Perforin, granzymes, and granulysin migrate to the cell membrane and release their contents into the immune synapse (40). Perforin binds to the plasma membrane of the target cell and forms pores in the cell membrane, allowing delivery of cytolytic effector proteins and subsequent destruction of the cell (39–41). Perforin-2, encoded by the gene *MPEG1*, is a recently discovered innate immune protein that is highly conserved throughout the animal kingdom (42–44). Perforin-2 is the more ancient of the two Perforins and it is thought that Perforin originated as a gene duplication of *MPEG1* (45). Perforin-2 differs from other MACPF pore formers in that it has a transmembrane domain and localizes to endosomal membranes. The Perforin-2 cytosolic tail directs the endosomes to bacteria- encapsulating phagosomes (46). Acidification of the phagosome stimulates reconfiguration of the MACPF domain, resulting in pore formation on the bacterial cell membrane (46, 47). Our group was the first to demonstrate the essential role of Perforin-2 in eliminating intracellular bacterial infections (48, 49), confirming the importance of this protein as an antimicrobial effector protein expressed by both phagocytic and tissue forming cells.

PERFORIN EXPRESSION BY SKIN GD T CELLS

The tumor-lysing capabilities of GD T cells have been well-documented in human skin (**Figure 1A**). Human skin derived GD T cells were purified using single cell sorting and tested in cytotoxicity assays against a variety of melanoma cell lines. They demonstrated cytotoxicity against SK-Mel2 and HS-294 melanoma cells, resulting in up to 90% cell death. This was comparable to the cytotoxic activity of the CD8+ AB T cells and NK cells that were also tested (18). GD T cells, CD8+ AB T cells, and NK cells only expressed Perforin after being cultured in the presence of IL-2, which is a previously established mechanism of Perforin induction in cytotoxic CD8+ T cells (18, 50, 51). Murine cutaneous Vdelta1+ GD T cells also express Perforin both at the mRNA and protein levels (51). They exhibited cytotoxicity against several tumor cell lines and also expressed granzyme B in amounts comparable to cytotoxic CD8+ AB T cells. Cytotoxic GD and AB T cells both produced IFN-g and TNF-a (18, 52, 53). Additionally, increased numbers of circulating CD3+TCR GD+ cells were observed in melanoma patients in comparison to healthy controls. These cells highly expressed Perforin in both normal individuals and melanoma patients, which may be important to anticancer surveillance (54). However, a study using a mouse model of skin carcinoma reported that circulating IL-17 producing GD T cells supported cutaneous tumor progression by promoting angiogenesis (55). In contrast to cytotoxic skin resident GD T cells, these non-skin resident IL-17 producing GD T cells that infiltrated the skin after tumor formation expressed low levels of Perforin and increased levels of the tumor-promoting factor COX-2. Although this paper did not establish a causative link between reduced Perforin expression and IL-17 production by circulating GD T cells, it implies that low levels of Perforin in these cells may contribute to their lack of cytotoxic activity and allow them to acquire a

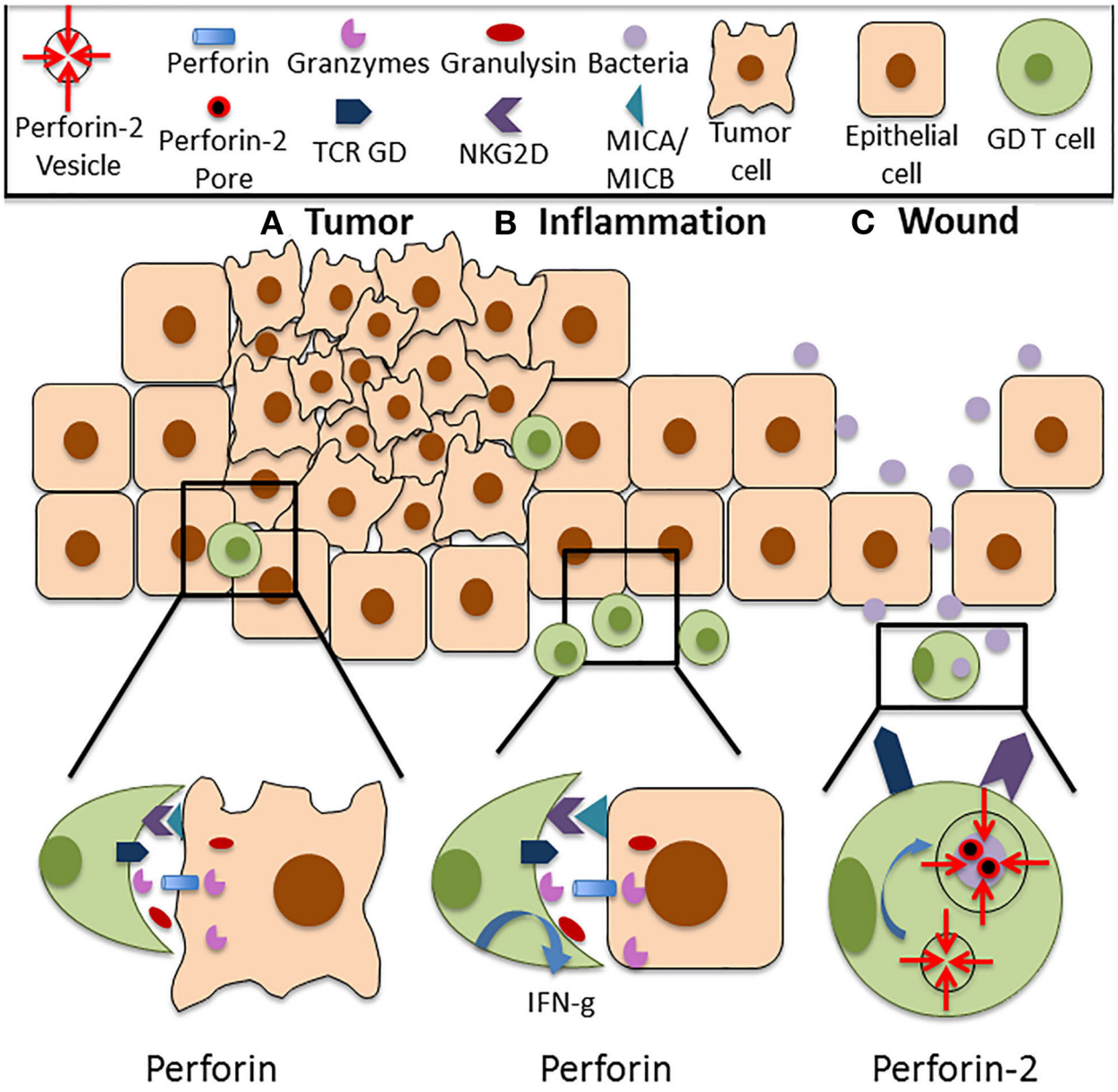

FIGURE 1 | Functions of Perforin in cutaneous GD T cells. **(A)** Cutaneous GD T cells exhibit cytotoxicity against an array of tumor cell types, and this is associated with Perforin expression both at the mRNA and protein level. Perforin is located within cytolytic granules inside cytotoxic GD T cells and they are released upon degranulation into the immune synapse. Perforin binds to the plasma membrane of the target cell and forms pores in the cell membrane, allowing granzymes, granulysin, and reactive oxygen species to enter the cell and destroy it. Cytotoxic GD T cells can become activated through TCR stimulation or through ligation of several costimulatory surface molecules, particularly NKG2D. NKG2D recognizes the stress induced ligands MICA and MICB, and NKG2D signaling is sufficient for activation of skin GD T cell cytotoxicity. **(B)** Perforin expressing GD T cells are also implicated in autoimmune and inflammatory skin diseases. Increased percentages of GD T cells have been observed in the skin of patients with systemic sclerosis, pemphigus vulgaris, Behcet's disease, and psoriasis. These cells express Perforin and granzymes and demonstrate enhanced cytotoxicity in comparison to cells from healthy controls. They also exhibit increased IFN-g expression. **(C)** Cutaneous GD T cells also express the newly discovered innate immune protein Perforin-2. Unlike other MACPF pore formers, Perforin-2 localizes to endosomes that fuse with the phagosome upon intracellular bacterial infection, facilitating pore formation on the bacterial cell membrane. Perforin-2 is essential for the elimination of intracellular bacteria. Given the established role of GD T cells in the antimicrobial response, it is likely that damage to the skin barrier and bacterial entry into the skin contribute to Perforin-2 induction in these immune surveillance cells.

pro-tumor GD T cell phenotype. These results underscore the importance of Perforin as an effector molecule in GD T cell mediated cytotoxicity in the skin.

Despite the clear importance of Perforin expressing cytotoxic GD T cells in the cutaneous anti-tumor response, these cells have the potential to develop into aggressive T cell lymphomas

(56, 57). Primary cutaneous GD T cell lymphomas constitute a subgroup of aggressive T cell lymphomas that express a mature cytotoxic phenotype. These tumors are characterized by their expression of T-cell-restricted intracellular antigen-1 (TIA-1), granzyme B, and Perforin (56–58) and there is also a strong correlation between CD30 expression and cytotoxic protein production (59). Cutaneous GD T cell lymphomas, while rare, have a poor prognosis; therefore, appropriate tumor phenotyping could be a useful tool for diagnosing this disease.

Perforin expressing GD T cells are also implicated in autoimmune and inflammatory skin diseases (**Table 1**). Patients with the autoimmune disease systemic sclerosis exhibit an increased percentage of Vdelta 1+ GD T cells that demonstrate cytotoxic activity in the skin (69, 70). Increased percentages of CD27+ GD T cells expressing Perforin and granzyme B are also present (71). Patients with Pemphigus vulgaris, an autoimmune disease that causes skin blistering, also have an increased percentage of circulating GD T cells. These cells demonstrate increased activation and cytotoxic activity in comparison to healthy controls (72). Behcet's disease, a disorder that causes blood vessel inflammation, is also associated with the expansion of GD T cells exhibiting increased Perforin and granzyme A expression (73, 74). Increased Perforin and granzyme B expression by CD3+ T cells is also evident in the epidermis of psoriasis patients (75–77). Only the CD8+ and CD4+ T cell subsets were analyzed, so Perforin expression by GD T cells in psoriasis has not yet been confirmed. It has been confirmed, however, that dermal GD T cells are recruited to the epidermis in psoriasis by activated keratinocytes that produce the chemokines CCL2 and CCL20 (78). Recruited dermal GD T cells induce an innate-like immune response by producing IL-17 and IL-22 upon IL-1 and IL-23 stimulation. IL-1 is expressed by keratinocytes while IL-23 is expressed by dermal dendritic cells and macrophages. IL-17 and IL-22 production further drives keratinocyte hyperplasia, neutrophil recruitment and disease progression (5). Since pro-inflammatory GD T cells are recruited to psoriatic skin, they are likely to be among the Perforin expressing CD3+ T cells observed in psoriasis patients (**Figure 1B**). Overall, studies have shown that GD T cells in the skin express Perforin, and this is associated with an activated cytotoxic phenotype. This can contribute positively to skin immune function via induction of the anti-tumor immune response, or it may have deleterious effects in the case of autoimmune and inflammatory skin disorders or cutaneous GD T cell lymphomas.

MECHANISMS REGULATING PERFORIN EXPRESSION IN SKIN GD T CELLS

Although it is clear that cutaneous cytotoxic GD T cells express Perforin, the mechanisms that regulate its expression are still unclear. Perforin is copiously expressed once these cells become activated (18). In contrast to CD8+ AB T cells which require TCR binding to MHC for activation (79), cytotoxic GD T cells can become activated through a non-MHC-restricted mechanism (61). In fact, recognition and killing of target cells can proceed through ligation of several costimulatory surface molecules in the absence of TCR stimulation (53). One of these surface molecules is the activating NK receptor NKG2D. It recognizes the MHC class I polypeptide-related sequence A and B (MICA and MICB), which are induced on stressed cells (53). NKG2D is expressed by most NK and CD8+ AB T cells, but it was found that both mouse and human GD T cells constitutively express NKG2D as well (53, 80, 81). Its expression is maintained during cell culture of freshly isolated GD T cells (13, 18, 53). NKG2D ligation stimulates epidermal GD T cell degranulation using a phosphatidylinositol 3-kinase (PI3K)–dependent pathway, and killing of NKG2DL expressing target cells occurs in the absence of CD3 and TCR signaling (60). Treatment of skin GD T cells with anti-NKG2D antibodies impaired lysis of A20 B cell lymphoma cells, but treatment with anti-TCR antibodies had no effect, indicating that NKG2D signaling is sufficient to activate cytotoxicity in skin GD T cells (53). Skin GD T cells also express the surface glycoprotein 2B4. Removal of IL-2 from GD T cell culture media reduced surface expression of 2B4 and also reduced their capacity to lyse target cells (61). Their cytotoxicity was enhanced by treatment with a stimulatory anti-2B4 antibody, indicating the importance of this receptor in cutaneous GD T cell mediated cytotoxicity. B7-1 (CD80) also provides costimulatory signals to both AB and GD T cells by binding to CD28 on the T cell surface, increasing adhesion to the target cell. B7-1 surface expression on Pam212, murine squamous cell carcinoma cells, stimulated cutaneous GD T cell proliferation and increased carcinoma cell sensitivity to GD T cell mediated lysis (62). Cutaneous GD T cell cytotoxicity is regulated through expression of several inhibitory receptors that block cytotoxicity upon binding with their appropriate ligands. Murine skin GD T cells express the inhibitory receptors Ly49 and CD94/NKG2. Presentation with Qdm, the ligand for CD94/NKG2, prevented the epidermal GD T cells from killing target cells (67).

GD T cell cytotoxicity is also activated by their recognition of stress-induced molecules on target cell surfaces. Macrophages and neutrophils externalize the heat shock proteins Hsp60 and Hsp70 under inflammatory conditions to target them for destruction, thus resolving the inflammation and preventing excess tissue damage. Cytotoxic GD T cells recognize these molecules and kill the target cells via direct cell-cell interactions (64). Activation of Perforin expressing cytotoxic GD T cells is also mediated through cytokine expression. IL-2, IL-15, and IL-12 enhance cytolytic activity of cutaneous GD T cells, and the transcription factor IFN regulatory factor-1 (IRF-1) is essential for induction of cytotoxicity (61, 63). The Perforin dependent anti-tumor properties of GD T cells can be enhanced pharmacologically. For example, rapamycin enhances the perforin-dependent cytotoxicity of human GD T cells against squamous cell carcinomas *in vitro* and in a mouse xenograft model of human squamous cell carcinoma (65). Additionally, Resveratrol enhances Perforin expression in NK cells through an NKG2D dependent pathway, implicating its potential to increase Perforin expression by NKG2D expressing GD T cells as well (82). Given the deleterious effects of Perforin expressing cells in the context of autoimmune and inflammatory disorders, blocking therapeutics targeting Perforin may benefit patients

TABLE 1 | Perforins expressed by cutaneous GD T cells.

	Perforin	Perforin-2
Location in the cell	Intracellular cytolytic granules (39)	Membranes of intracellular endosomes (46, 47)
Function in GD T cells	Lysis of transformed or infected cells (39–41)	Destruction of intracellular bacteria (46, 47)
Stimulatory factors	Surface receptors: - GD TCR (53) - NKG2D (13, 18, 53, 60) - 2B4 (61) - B7-1 (62) Cytokines: - IL-2 (61) - IL-12 (63) - IL-15 (63) Stress induced molecules: - Hsp60 (64) - Hsp70 (64) Transcription Factors: - IRF-1 (63) Therapeutics: - Rapamycin (65)	Commensal bacteria: - *S. epidermidis* (66)
Inhibitory factors	Surface receptors: - Ly49 (67) - CD94 (67)	Pathogenic bacteria: - *S. aureus* (68)
Role in disease	Expressed by cutaneous GD T cell lymphomas (56–59) Upregulated in autoimmune and inflammatory diseases: - Systemic sclerosis (69–71) - Pemphigus vulgaris (72) - Behcet's disease (73, 74) - Psoriasis (75–77)	Upregulated in response to wounding (68) Downregulation may contribute to persistent wound infection (68)

Summary of the information currently known about Perforin and Perforin-2 expression by cutaneous GD T cells. Listed are the location of the Perforins within the cell, functions of the Perforins in GD T cells, Perforin stimulatory and inhibitory factors, and the role of Perforins in cutaneous diseases.

suffering from these illnesses. Compounds identified as Perforin inhibitors in NK and AB T cells include diarylthiophenes and benzenesulfonamide based therapeutics (83–85). In short, cutaneous GD T cells express Perforin upon activation and this activation can be achieved through a variety of mechanisms including stimulation of the TCR, ligation of costimulatory molecules, and cytokine stimulation (**Table 1**). The critical role of Perforin in executing GD T cell mediated cytotoxicity in the skin warrants further studies on the mechanisms that induce Perforin expression by these cells.

PERFORIN-2 EXPRESSION BY GD T CELLS

Perforin-2 is a recently identified member of the MACPF domain containing pore forming family of innate immune proteins that plays a critical role in clearance of intracellular bacterial infections. However, the mechanisms behind Perforin-2 activation and the extent of its contributions to host immunity have not been fully characterized. Our group was the first to report Perforin-2 expression in a variety of cell types in human skin including keratinocytes, fibroblasts and GD T cells (68). Although it is known that both murine and human GD T cells express Perforin-2, the role that it plays in GD T cell mediated cytotoxicity toward bacterial pathogens is still unknown. We demonstrated that Perforin-2 expression is upregulated in CD45+ cells upon wounding in an *ex vivo* human skin model. However, infection of the wounds with *Staphylococcus aureus* inhibited Perforin-2 expression in these cells (68). This indicates a potential role for Perforin-2 in promoting skin homeostasis and barrier integrity by aiding in the clearance of bacteria from the wound site (**Figure 1C**). This was confirmed by our finding that human keratinocyte cells constitutively expressing a Perforin-2-GFP fusion protein demonstrate improved clearance of intracellular *S. aureus* infection in comparison to control cells (68). Our group has also demonstrated that Perforin-2 deficient mice infected epicutaneously are unable to clear *S. aureus* and eventually succumb to the infection (48). Interestingly, in this issue we provide evidence that *S. epidermidis*, a skin commensal microorganism, induces Perforin-2 in GD T cells in human skin *ex vivo* (66). Given the established role of GD T cells in the antimicrobial response and in keratinocyte proliferation and migration upon wounding, it is likely that disruption of the epidermal barrier and signals from microorganisms can result in Perforin-2 induction. This warrants further studies on Perforin-2 regulation and its function as an effector protein in GD T cell mediated skin immune responses.

CONCLUSIONS

Maintaining skin homeostasis and barrier function is essential for protection against physical and chemical stress, infections, and malignancies. Recent research has highlighted the significant contributions of GD T cells to skin health through their role in bacterial clearance, wound healing, and tumor killing. Expression of both Perforin and Perforin-2 by GD T cells has been implicated in the activation of these effector functions (**Figure 1**, **Table 1**). GD T cells lyse a variety of tumor cell lines and exhibit many characteristics of conventional cytotoxic T cells. Although GD T cells have been shown to produce Perforin, little is known about the signals that stimulate its expression. Additionally, Perforin-2 was recently identified as another member of the MACPF domain containing pore forming protein family. It is critical for clearance of intracellular bacterial infections, and it is expressed constitutively by GD T cells. Given the established role of GD T cells as first responders to bacterial infections in the skin, it is important to further investigate the regulation of Perforin-2 in this GD T cell function. Understanding the signals that activate Perforin expression by GD T cells can help to elucidate the mechanisms governing their diverse roles in skin immunity.

AUTHOR CONTRIBUTIONS

KO'N wrote the manuscript and prepared the figures. IP, MT-C, and NS revised the manuscript and provided critical comments. All authors contributed to the article and approved the submitted version.

FUNDING

This work was supported by NIH NR015649 (MT-C and NS), DK119085 (MT-C), Dwoskin family gift to the Dr. Phillip Frost Department of Dermatology and Cutaneous Surgery (MT-C) and by Department of Microbiology and Immunology P2 funds (NS).

ACKNOWLEDGMENTS

We dedicate this work to the late Dr. Eckhard Podack without whom studies of Perforin-2 would not be possible. We are grateful to all members of Tomic-Canic and Strbo laboratories for their overall support.

REFERENCES

1. Chien Y, Meyer C, Bonneville M. γδ T cells: first line of defense and beyond. *Annu Rev Immunol.* (2014) 32:121–55. doi: 10.1146/annurev-immunol-032713-120216
2. Havran WL, Jameson JM, Witherden DA. Epithelial cells and their neighbors. III. Interactions between intraepithelial lymphocytes and neighboring epithelial cells. *Am J Physiol Liver Physiol.* (2005) 289:G627–30. doi: 10.1152/ajpgi.00224.2005
3. Groh V, Porcelli S, Fabbi M, Lanier LL, Picker LJ, Anderson T, et al. Human lymphocytes bearing T cell receptor gamma/delta are phenotypically diverse and evenly distributed throughout the lymphoid system. *J Exp Med.* (1989) 169:1277–94. doi: 10.1084/jem.169.4.1277
4. Parker CM, Groh V, Band H, Porcelli SA, Morita C, Fabbi M, et al. Evidence for extrathymic changes in the T cell receptor gamma/delta repertoire. *J Exp Med.* (1990) 171:1597–612. doi: 10.1084/jem.171.5.1597
5. Cai Y, Shen X, Ding C, Qi C, Li K, Li X, et al. Pivotal role of dermal IL-17-producing γδ T cells in skin inflammation. *Immunity.* (2011) 35:596–610. doi: 10.1016/j.immuni.2011.08.001
6. Gray EE, Suzuki K, Cyster JG. Cutting edge: identification of a motile IL-17-producing gammadelta T cell population in the dermis. *J Immunol.* (2011) 186:6091–5. doi: 10.4049/jimmunol.1100427
7. Itohara S, Farr AG, Lafaille JJ, Bonneville M, Takagaki Y, Haas W, et al. Homing of a γδ thymocyte subset with homogeneous T-cell receptors to mucosal epithelia. *Nature.* (1990) 343:754–7. doi: 10.1038/343754a0
8. Goodman T, Lefrancois L. Intraepithelial lymphocytes. Anatomical site, not T cell receptor form, dictates phenotype and function. *J Exp Med.* (1989) 170:1569–81. doi: 10.1084/jem.170.5.1569
9. Laggner U, Di Meglio P, Perera GK, Hundhausen C, Lacy KE, Ali N, et al. Identification of a novel proinflammatory human skin-homing Vγ9Vδ2 T cell subset with a potential role in psoriasis. *J Immunol.* (2011) 187:2783–93. doi: 10.4049/jimmunol.1100804
10. Witherden DA, Havran WL. Cross-talk between intraepithelial γδ T cells and epithelial cells. *J Leukoc Biol.* (2013) 94:69–76. doi: 10.1189/jlb.0213101
11. Whang MI, Guerra N, Raulet DH. Costimulation of dendritic epidermal γδ T cells by a new NKG2D ligand expressed specifically in the skin. *J Immunol.* (2009) 182:4557–64. doi: 10.4049/jimmunol.0802439
12. Bonneville M, O'Brien RL, Born WK. γδ T cell effector functions: a blend of innate programming and acquired plasticity. *Nat Rev Immunol.* (2010) 10:467–78. doi: 10.1038/nri2781
13. Strid J, Sobolev O, Zafirova B, Polic B, Hayday A. The intraepithelial T cell response to NKG2D-ligands links lymphoid stress surveillance to atopy. *Science.* (2011) 334:1293–7. doi: 10.1126/science.1211250
14. Havran WL, Allison JP. Origin of Thy-1+ dendritic epidermal cells of adult mice from fetal thymic precursors. *Nature.* (1990) 344:68–70. doi: 10.1038/344068a0
15. Bos JD, Teunissen MBM, Cairo I, Krieg SR, Kapsenberg ML, Das PK, et al. T-Cell receptor γδ bearing cells in normal human skin. *J Invest Dermatol.* (1990) 94:37–42. doi: 10.1111/1523-1747.ep12873333
16. Clark RA, Chong B, Mirchandani N, Brinster NK, Yamanaka K-I, Dowgiert RK, et al. The vast majority of CLA+ T cells are resident in normal skin. *J Immunol.* (2006) 176:4431–9. doi: 10.4049/jimmunol.176.7.4431
17. Alaibac M, Morris J, Yu R, Chu AC. T lymphocytes bearing the γδ T-cell receptor: a study in normal human skin and pathological skin conditions. *Br J Dermatol.* (1992) 127:458–62. doi: 10.1111/j.1365-2133.1992.tb14840.x
18. Ebert LM, Meuter S, Moser B. Homing and function of human skin gammadelta T cells and NK cells: relevance for tumor surveillance. *J Immunol.* (2006) 176:4331–6. doi: 10.4049/jimmunol.176.7.4331
19. Cruz MS, Diamond A, Russell A, Jameson JM. Human αβ and γδ T cells in skin immunity and disease. *Front Immunol.* (2018) 9:1304. doi: 10.3389/fimmu.2018.01304
20. Vantourout P, Hayday A. Six-of-the-best: unique contributions of γδ T cells to immunology. *Nat Rev Immunol.* (2013) 13:88–100. doi: 10.1038/nri3384
21. Morita CT, Lee HK, Leslie DS, Tanaka Y, Bukowski JF, Märker-Hermann E. Recognition of nonpeptide prenyl pyrophosphate antigens by human γδ T cells. *Microbes Infect.* (1999) 1:175–86. doi: 10.1016/S1286-4579(99)80032-X
22. Sumaria N, Roediger B, Ng LG, Qin J, Pinto R, Cavanagh LL, et al. Groth B, Triccas JA, Weninger W. Cutaneous immunosurveillance by self-renewing dermal γδ T cells. *J Exp Med.* (2011) 208:505–18. doi: 10.1084/jem.20101824
23. Pantelyushin S, Haak S, Ingold B, Kulig P, Heppner FL, Navarini AA, et al. Rorγt+ innate lymphocytes and γδ T cells initiate psoriasiform plaque formation in mice. *J Clin Invest.* (2012) 122:2252–6. doi: 10.1172/JCI61862
24. Toulon A, Breton L, Taylor KR, Tenenhaus M, Bhavsar D, Lanigan C, et al. A role for human skin–resident T cells in wound healing. *J Exp Med.* (2009) 206:743–50. doi: 10.1084/jem.20081787
25. Jameson J, Ugarte K, Chen N, Yachi P, Fuchs E, Boismenu R, et al. A role for skin gamma delta T cells in wound repair. *Science.* (2002) 296:747–9. doi: 10.1126/science.1069639
26. MacLeod AS, Hemmers S, Garijo O, Chabod M, Mowen K, Witherden DA, et al. Dendritic epidermal T cells regulate skin antimicrobial barrier function. *J Clin Invest.* (2013) 123:4364–74. doi: 10.1172/JCI70064
27. Gay D, Kwon O, Zhang Z, Spata M, Plikus M V, Holler PD, et al. Fgf9 from dermal γδ T cells induces hair follicle neogenesis after wounding. *Nat Med.* (2013) 19:916–23. doi: 10.1038/nm.3181
28. Kaminski MJ, Cruz PD, Bergstresser PR, Takashima A. Killing of skin-derived tumor cells by mouse dendritic epidermal T-cells. *Cancer Res.* (1993) 53:4014–9.
29. Girardi M, Oppenheim DE, Steele CR, Lewis JM, Glusac E, Filler R, et al. Regulation of cutaneous malignancy by gamma delta T Cells. *Science.* (2001) 294:605–9. doi: 10.1126/science.1063916
30. Rosado CJ, Kondos S, Bull TE, Kuiper MJ, Law RHP, Buckle AM, et al. The MACPF/CDC family of pore-forming toxins. *Cell Microbiol.* (2008) 10:1765–74. doi: 10.1111/j.1462-5822.2008.01191.x
31. Gilbert RJC. Cholesterol-dependent cytolysins. *Adv Exp Med Biol.* (2010) 677:56–66. doi: 10.1007/978-1-4419-6327-7_5
32. Tweten RK. Cholesterol-dependent cytolysins, a family of versatile pore-forming toxins. *Infect Immun.* (2005) 73:6199–209. doi: 10.1128/IAI.73.10.6199-6209.2005
33. Hadders MA, Beringer DX, Gros P. Structure of C8α-MACPF reveals mechanism of membrane attack in complement immune defense. *Science.* (2007) 317:1552–4. doi: 10.2210/pdb2qqh/pdb
34. Rosado CJ, Buckle AM, Law RHP, Butcher RE, Kan WT, Bird CH, et al. A common fold mediates vertebrate defense and bacterial attack. *Science.* (2007) 317:1548–51. doi: 10.1126/science.1144706
35. Slade DJ, Lovelace LL, Chruszcz M, Minor W, Lebioda L, Sodetz JM. Crystal structure of the MACPF domain of human complement protein C8α in complex with the C8γ subunit. *J Mol Biol.* (2008) 379:331–42. doi: 10.1016/j.jmb.2008.03.061
36. Tschopp J, Masson D, Stanley KK. Structural/functional similarity between proteins involved in complement- and cytotoxic T-lymphocyte-mediated cytolysis. *Nature.* (1986) 322:831–4. doi: 10.1038/322831a0
37. Lovelace LL, Cooper CL, Sodetz JM, Lebioda L. Structure of human C8 protein provides mechanistic insight into membrane pore formation by complement. *J Biol Chem.* (2011) 286:17585–92. doi: 10.1074/jbc.M111.219766

38. Kondos SC, Hatfaludi T, Voskoboinik I, Trapani JA, Law RHP, Whisstock JC, et al. The structure and function of mammalian membrane-attack complex/perforin-like proteins. *Tissue Antigens.* (2010) 76:341–51. doi: 10.1111/j.1399-0039.2010.01566.x
39. Podack ER, Young JDE, Cohn ZA. Isolation and biochemical and functional characterization of perforin 1 from cytolytic T-cell granules. *Proc Natl Acad Sci USA*. (1985) 82:8629–33. doi: 10.1073/pnas.82.24.8629
40. Lopez JA, Susanto O, Jenkins MR, Lukoyanova N, Sutton VR, Law RHP, et al. Perforin forms transient pores on the target cell plasma membrane to facilitate rapid access of granzymes during killer cell attack. *Blood*. (2013) 121:2659–68. doi: 10.1182/blood-2012-07-446146
41. Leung C, Hodel AW, Brennan AJ, Lukoyanova N, Tran S, House CM, et al. Real-time visualization of perforin nanopore assembly. *Nat Nanotechnol.* (2017) 12:467–73. doi: 10.1038/nnano.2016.303
42. Benard EL, Racz PI, Rougeot J, Nezhinsky AE, Verbeek FJ, Spaink HP, et al. Macrophage-expressed perforins mpeg1 and mpeg1.2 have an anti-bacterial function in zebrafish. *J Innate Immun.* (2015) 7:136–52. doi: 10.1159/000366103
43. Wiens M, Korzhev M, Krasko A, Thakur NL, Perović-Ottstadt S, Breter HJ, et al. Innate immune defense of the sponge *suberites domuncula* against bacteria involves a myD88-dependent signaling pathway. *J Biol Chem.* (2005) 280:27949–59. doi: 10.1074/jbc.M504049200
44. McCormack R, Podack ER. Perforin-2/Mpeg1 and other pore-forming proteins throughout evolution. *J Leukoc Biol.* (2015) 98:761–8. doi: 10.1189/jlb.4MR1114-523RR
45. D'Angelo ME, Dunstone MA, Whisstock JC, Trapani JA, Bird PI. Perforin evolved from a gene duplication of MPEG1, followed by a complex pattern of gene gain and loss within luteleostomi. *BMC Evol Biol.* (2012) 12:59. doi: 10.1186/1471-2148-12-59
46. Ni T, Jiao F, Yu X, Aden S, Ginger L, Williams SI, et al. Structure and mechanism of bactericidal mammalian perforin-2, an ancient agent of innate immunity. *Sci Adv.* (2020) 6:eaax8286. doi: 10.1126/sciadv.aax8286
47. Pang SS, Bayly-Jones C, Radjainia M, Spicer BA, Law RHP, Hodel AW, et al. The cryo-EM structure of the acid activatable pore-forming immune effector macrophage-expressed gene 1. *Nat Commun.* (2019) 10:4288. doi: 10.1038/s41467-019-12279-2
48. McCormack RM, de Armas LR, Shiratsuchi M, Fiorentino DG, Olsson ML, Lichtenheld MG, et al. Perforin-2 is essential for intracellular defense of parenchymal cells and phagocytes against pathogenic bacteria. *Elife.* (2015) 4:e508. doi: 10.7554/eLife.06508
49. McCormack R, de Armas LR, Shiratsuchi M, Ramos JE, Podack ER. Inhibition of intracellular bacterial replication in fibroblasts is dependent on the perforin-like protein (perforin-2) encoded by macrophage-expressed gene 1. *J Innate Immun.* (2013) 5:185–94. doi: 10.1159/000345249
50. Smyth MJ, Ortaldo JR, Shinkaij YI, Yagita H, Nakata M, Okumura K, et al. Interleukin 2 induction of pore-forming protein gene expression in human peripheral blood CD8+ T cells. *J Exp Med*. (1990) 171:1269–81. doi: 10.1084/jem.171.4.1269
51. Krähenbühl O, Gattesco S, Tschopp J. Murine Thy-1+ dendritic epidermal t cell lines express granule-associated perforin and a family of granzyme molecules. *Immunobiology.* (1992) 184:392–401. doi: 10.1016/S0171-2985(11)80596-6
52. Kägi D, Ledermann B, Bürki K, Zinkernagel RM, Hengartner H. Molecular mechanisms of lymphocyte-mediated cytotoxicity and their role in immunological protection and pathogenesis *in vivo*. *Annu Rev Immunol.* (1996) 14:207–32. doi: 10.1146/annurev.immunol.14.1.207
53. Nitahara A, Shimura H, Ito A, Tomiyama K, Ito M, Kawai K. NKG2D ligation without T cell receptor engagement triggers both cytotoxicity and cytokine production in dendritic epidermal T Cells. *J Invest Dermatol.* (2006) 126:1052–8. doi: 10.1038/sj.jid.5700112
54. Campillo JA, Martínez-Escribano JA, Minguela A, López-Álvarez R, Marín LA, García-Alonso AM, et al. Increased number of cytotoxic CD3+CD28- γδ T cells in peripheral blood of patients with cutaneous malignant melanoma. *Dermatology.* (2007) 214:283–8. doi: 10.1159/000100878
55. Wakita D, Sumida K, Iwakura Y, Nishikawa H, Ohkuri T, Chamoto K, et al. Tumor-infiltrating IL-17-producing γδ T cells support the progression of tumor by promoting angiogenesis. *Eur J Immunol.* (2010) 40:1927–37. doi: 10.1002/eji.200940157
56. Toro JR, Beaty M, Sorbara L, Turner ML, White J, Kingma DW, et al. γδ T-cell lymphoma of the skin. *Arch Dermatol.* (2000) 136:1024–32. doi: 10.1001/archderm.136.8.1024
57. Rodríguez-Pinilla SM, Ortiz-Romero PL, Monsalvez V, Tomás IE, Almagro M, Sevilla A, et al. TCR-γ expression in primary cutaneous T-cell lymphomas. *Am J Surg Pathol.* (2013) 37:375–84. doi: 10.1097/PAS.0b013e318275d1a2
58. Salhany KE, Macon WR, Choi JK, Elenitsas R, Lessin SR, Felgar RE, et al. Subcutaneous panniculitis-like T-cell lymphoma. *Am J Surg Pathol.* (1998) 22:881–93. doi: 10.1097/00000478-199807000-00010
59. Boulland ML, Wechsler J, Bagot M, Pulford K, Kanavaros P, Gaulard P. Primary CD30-positive cutaneous T-cell lymphomas and lymphomatoid papulosis frequently express cytotoxic proteins. *Histopathology.* (2000) 36:136–44. doi: 10.1046/j.1365-2559.2000.00799.x
60. Ibusuki A, Kawai K, Yoshida S, Uchida Y, Nitahara-Takeuchi A, Kuroki K, et al. NKG2D triggers cytotoxicity in murine epidermal γδ T cells via PI3K-dependent, Syk/ZAP70-independent signaling pathway. *J Invest Dermatol.* (2014) 134:396–404. doi: 10.1038/jid.2013.353
61. Schuhmachers G, Ariizumi K, Mathew PA, Bennett M, Kumar V, Takashima A. 2B4, a new member of the immunoglobulin gene superfamily, is expressed on murine dendritic epidermal T cells and plays a functional role in their killing of skin tumors. *J Invest Dermetol.* (1995). 105:592–6. doi: 10.1111/1523-1747.ep12323533
62. Yeh K-Y, Zhong C, Nasir A, Ohsuga Y, Takashima A, Lord EM, et al. Expression of B7–1 by pam 212 squamous cell carcinoma enhances tumor cell interactions with dendritic epidermal t cells but does not affect *in vivo* tumor growth. *J Invest Dermatol.* (1997). 109:728–33. doi: 10.1111/1523-1747.ep12340723
63. De Creus A, Van Beneden K, Stevenaert F, Debacker V, Plum J, Leclercq G. Developmental and functional defects of thymic and epidermal V gamma 3 cells in IL-15-deficient and IFN regulatory factor-1-deficient mice. *J Immunol.* (2002) 168:6486–93. doi: 10.4049/jimmunol.168.12.6486
64. Hirsh MI, Junger WG. Roles of heat shock proteins and gamma delta T cells in inflammation. *Am J Respir Cell Mol Biol.* (2008) 39:509–13. doi: 10.1165/rcmb.2008-0090TR
65. Dao V, Liu Y, Pandeswara S, Svatek RS, Gelfond JA, Liu A, et al. Immune-stimulatory effects of rapamycin are mediated by stimulation of antitumor γδ T cells. *Cancer Res.* (2016) 76:5970–82. doi: 10.1158/0008-5472.CAN-16-0091
66. Strbo N, O'Neill KE, Head CR, Padula L, Stojadinovic O, Pastar I, et al. *Staphylococcus epidermidis* facilitates intracellular pathogen clearance through upregulation of antimicrobial protein perforin-2 (P-2) in the human skin gamma delta T cells. *J Immunol*. (2020) 204(1 Supplement):157.10.
67. Van Beneden K, De Creus A, Stevenaert F, Debacker V, Plum J, Leclercq G. Expression of inhibitory receptors ly49e and cd94/nkg2 on fetal thymic and adult epidermal tcr vγ3 lymphocytes. *J Immunol.* (2002) 168:3295–302. doi: 10.4049/jimmunol.168.7.3295
68. Strbo N, Pastar I, Romero L, Chen V, Vujanac M, Sawaya AP, et al. Single cell analyses reveal specific distribution of anti-bacterial molecule perforin-2 in human skin and its modulation by wounding and *Staphylococcus aureus* infection. *Exp Dermatol.* (2019) 28:225–32. doi: 10.1111/exd.13870
69. Giacomelli R, Cipriani P, Fulminis A, Barattelli G, Matucci-Cerinic M, D'Alo S, et al. Circulating gamma/delta T lymphocytes from systemic sclerosis (SSc) patients display a T helper (Th) 1 polarization. *Clin Exp Immunol.* (2001) 125:310–5. doi: 10.1046/j.1365-2249.2001.01603.x
70. Giacomelli R, Matucci-Cerinic M, Cipriani P, Ghersetich I, Lattanzio R, Pavan A, et al. Circulating Vδ1 + T cells are activated and accumulate in the skin of systemic sclerosis patients. *Arthritis Rheum.* (1998) 41:327–34. doi: 10.1002/1529-013141:2<327::AID–ART17>3.0.CO;2-S
71. Henriques A, Silva C, Santiago M, Henriques MJ, Martinho A, Trindade H, et al. Subset-specific alterations in frequencies and functional signatures of γδ T cells in systemic sclerosis patients. *Inflamm Res.* (2016) 65:985–94. doi: 10.1007/s00011-016-0982-6
72. Das D, Anand V, Khandpur S, Sharma VK, Sharma A. T helper type 1 polarizing *γδ* T cells and scavenger receptors contribute to the pathogenesis of pemphigus vulgaris. *Immunology.* (2018) 153:97–104. doi: 10.1111/imm.12814
73. Accardo-Palumbo A, Giardina AR, Ciccia F, Ferrante A, Principato A, Impastato R, et al. Phenotype and functional changes of Vγ9/Vδ2 T lymphocytes in behçet's disease and the effect of infliximab on Vγ9/Vδ2 T

cell expansion, activation and cytotoxicity. *Arthritis Res Ther.* (2010) 12:R109. doi: 10.1186/ar3043
74. Cañete JD, Celis R, Noordenbos T, Moll C, Gómez-Puerta JA, Pizcueta P, et al. Distinct synovial immunopathology in Behçet disease and psoriatic arthritis. *Arthritis Res Ther.* (2009) 11:R17. doi: 10.1186/ar2608
75. Kastelan M, Prpic Massari L, Gruber F, Zamolo G, Zauhar G, Coklo M, et al. Perforin expression is upregulated in the epidermis of psoriatic lesions. *Br J Dermatol.* (2004) 151:831–6. doi: 10.1111/j.1365-2133.2004.06168.x
76. Prpić Massari L, Kaštelan M, Laškarin G, Zamolo G, Massari D, Rukavina D. Analysis of perforin expression in peripheral blood and lesions in severe and mild psoriasis. *J Dermatol Sci.* (2007) 47:29–36. doi: 10.1016/j.jdermsci.2007.02.007
77. Yawalkar N, Schmid S, Braathen LR, Pichler WJ. Perforin and granzyme B may contribute to skin inflammation in atopic dermatitis and psoriasis. *Br J Dermatol.* (2001) 144:1133–9. doi: 10.1046/j.1365-2133.2001.04222.x
78. Polese B, Zhang H, Thurairajah B, King IL. Innate lymphocytes in psoriasis. *Front Immunol.* (2020) 11:242. doi: 10.3389/fimmu.2020.00242
79. Bousso P, Robey E. Dynamics of CD8+ T cell priming by dendritic cells in intact lymph nodes. *Nat Immunol.* (2003) 4:579–85. doi: 10.1038/ni928
80. Maasho K, Opoku-Anane J, Marusina AI, Coligan JE, Borrego F. Cutting edge: NKG2D Is a costimulatory receptor for human naive CD8 + T Cells. *J Immunol.* (2005) 174:4480–4. doi: 10.4049/jimmunol.174.8.4480
81. Bauer S, Groh V, Wu J, Steinle A, Phillips JH, Lanier LL, et al. Activation of NK cells and T cells by NKG2D, a receptor for stress- inducible MICA. *Science.* (1999) 174:4480–4. doi: 10.1126/science.285.5428.727
82. Lu C-C, Chen J-K. Resveratrol enhances perforin expression and NK cell cytotoxicity through NKG2D-dependent pathways. *J Cell Physiol.* (2010) 223:343–51. doi: 10.1002/jcp.22043
83. Miller CK, Huttunen KM, Denny WA, Jaiswal JK, Ciccone A, Browne KA, et al. Diarylthiophenes as inhibitors of the pore-forming protein perforin. *Bioorg Med Chem Lett.* (2016) 26:355. doi: 10.1016/j.bmcl.2015.12.003
84. Spicer JA, Miller CK, O'Connor PD, Jose J, Huttunen KM, Jaiswal JK, et al. Benzenesulphonamide inhibitors of the cytolytic protein perforin. *Bioorg Med Chem Lett.* (2017) 27:1050–4. doi: 10.1016/j.bmcl.2016.12.057
85. Welz M, Eickhoff S, Abdullah Z, Trebicka J, Gartlan KH, Spicer JA, et al. Perforin inhibition protects from lethal endothelial damage during fulminant viral hepatitis. *Nat Commun.* (2018) 9:4805. doi: 10.1038/s41467-018-07213-x

Conflict of Interest: The authors declare that the research was conducted in the absence of any commercial or financial relationships that could be construed as a potential conflict of interest.

frontiers in Cellular and Infection Microbiology

MINI REVIEW
published: 15 September 2020
doi: 10.3389/fcimb.2020.578883

Perforin-Like Proteins of Apicomplexan Parasites

*Juliane Sassmannshausen, Gabriele Pradel and Sandra Bennink**

Division of Cellular and Applied Infection Biology, Institute of Zoology, Rheinisch-Westfälische Technische Hochschule Aachen University, Aachen, Germany

Perforins are secreted proteins of eukaryotes, which possess a membrane attack complex/perforin (MACPF) domain enabling them to form pores in the membranes of target cells. In higher eukaryotes, they are assigned to immune defense mechanisms required to kill invading microbes or infected cells. Perforin-like proteins (PLPs) are also found in apicomplexan parasites. Here they play diverse roles during lifecycle progression of the intracellularly replicating protozoans. The apicomplexan PLPs are best studied in *Plasmodium* and *Toxoplasma*, the causative agents of malaria and toxoplasmosis, respectively. The PLPs are expressed in the different lifecycle stages of the pathogens and can target and lyse a variety of cell membranes of the invertebrate and mammalian hosts. The PLPs thereby either function in host cell destruction during exit or in overcoming epithelial barriers during tissue passage. In this review, we summarize the various PLPs known for apicomplexan parasites and highlight their roles in *Plasmodium* and *Toxoplasma* lifecycle progression.

Keywords: apicomplexa, *Plasmodium falciparum*, malaria, *Toxoplasma gondii*, perforin, MACPF domain, host cell egress, cell traversal

OPEN ACCESS

Edited by:
Kai Matuschewski, Humboldt University of Berlin, Germany

Reviewed by:
Elena Deligianni, Foundation of Research and Technology (FORTH), Greece
Chris J. Janse, Leiden University Medical Center, Netherlands

****Correspondence:***
Sandra Bennink
bennink@bio2.rwth-aachen.de

Specialty section:
This article was submitted to Parasite and Host, a section of the journal Frontiers in Cellular and Infection Microbiology

Received: *01 July 2020*
Accepted: *13 August 2020*
Published: *15 September 2020*

Citation:
Sassmannshausen J, Pradel G and Bennink S (2020) Perforin-Like Proteins of Apicomplexan Parasites. Front. Cell. Infect. Microbiol. 10:578883. doi: 10.3389/fcimb.2020.578883

INTRODUCTION

Members of the pore-forming Membrane Attack Complex/Perforin (MACPF) superfamily are highly conserved in both prokaryotes and eukaryotes, and are mainly used for immune defense or virulence. During the co-evolution of pathogens and hosts, both have developed pore-forming proteins facilitating target membrane lysis and translocation of molecules.

Eukaryotic parasites of the phylum Apicomplexa express MACPF domain-containing proteins termed perforin-like proteins (PLPs). The Apicomplexa comprises a diverse group of intracellularly replicating protozoans that share the apical complex, composed of secretory organelles, such as the micronemes and rhoptries—and structural elements. Calcium-regulated protein discharge from the micronemes is fundamental to motility, cell invasion and egress of apicomplexan parasites (e.g., reviewed in Blackman and Bannister, 2001; Dubois and Soldati-Favre, 2019). Members of the phylum Apicomplexa include parasites that can cause infectious diseases relevant to human or veterinary medicine, such as the malaria parasite *Plasmodium* or representatives of the genera *Toxoplasma*, *Babesia*, and *Eimeria*.

Many apicomplexan parasites exhibit complex lifecycles, during which they reproduce both asexually and sexually, and which include one or more hosts. For example, the malaria parasite *Plasmodium* is transmitted from human to human via the bite of an *Anopheles* mosquito, which serves as the definitive host. The parasite *Toxoplasma gondii* on the other hand infects members of the family Felidae (domestic cats and their relatives) as its definitive host, but can use other vertebrates as intermediate hosts. Lifecycle progression of apicomplexan parasites is highly dependent on host cell traversal as well as invasion of and egress from host cells.

We here review the role of apicomplexan PLPs (ApiPLPs) during lifecycle progression, with special focus on the processes of cell traversal and host cell egress. As most work about ApiPLPs has been done on *Plasmodium* and *T. gondii*, we will concentrate on these species as representatives.

CONSERVATION OF APICOMPLEXAN MACPF PROTEINS

The MACPF superfamily is named after the central protein domain shared by the membrane attack complex (MAC) proteins of the human complement system (C6, C7, C8α, C8β, and C9) and the cytolytic perforin (PF) of cytotoxic T lymphocytes and natural killer cells. However, members of the superfamily can be found in all three domains of life, i.e., eubacteria, archaebacteria, and eukaryotes (Moreno-Hagelsieb et al., 2017). In eukaryotes, they are not only involved in immune defense mechanisms, but additionally play important roles in various biological processes, such as embryonic development or neural migration (reviewed in Lukoyanova et al., 2016).

Among the phylum of Apicomplexa, which almost exclusively comprises obligatory intracellular parasites, MACPF domain-containing proteins are encoded in all genomes sequenced so far, except for *Cryptosporidium*, which might have lost the genes during evolution. The number of MACPF proteins however varies between the different species, which might be linked to the degree of lifecycle complexity (see **Table 1**). In general, parasites that are transmitted to vertebrates via insects, such as *Plasmodium*, *Theileria*, or *Babesia*, seem to express more PLPs than parasites, which are restricted to vertebrates, e.g., *Toxoplasma*, *Neospora*, or *Eimeria*. While *Plasmodium* parasites express five and *Theileria* and *Babesia* six to nine PLPs, *Toxoplasma*, *Neospora*, and *Eimeria* only express two to three PLPs.

DOMAIN ARCHITECTURE AND MECHANISM OF PORE FORMATION

The apicomplexan PLPs characterized so far share the basic architecture of canonical MACPF proteins but additionally exhibit some unique features. They are composed of a central MACPF domain, surrounded by a variable N-terminal region and an apicomplexan-specific β-pleated sheet-rich C-terminal region (reviewed in Kafsack and Carruthers, 2010). The N-terminal region does not only vary in length and sequence between different apicomplexan PLPs (see **Figure 1**), but also between proteins of the same species. For example the two MACPF-domain containing proteins that are expressed in *T. gondii*, TgPLP1, and TgPLP2, only share 13% sequence identity in the N-terminal regions, while the C-terminal regions are 36% identical.

The canonical MACPF domain, which is structurally similar to prokaryotic cholesterol-dependent cytolysins (CDCs), consists of a central four-stranded β-sheet that is flanked by two α-helical clusters (Hadders et al., 2007; Rosado et al., 2007). The α-helical clusters display the typical pattern of alternating hydrophilic and hydrophobic amino acids and convert into amphipathic transmembrane β-hairpins during pore-formation (Shepard et al., 1998; Shatursky et al., 1999; reviewed in Tweten, 2005; Law et al., 2010; Aleshin et al., 2012). Interestingly, *Theileria* and *Babesia* are predicted to encode PLPs that comprise more than one MACPF domain (see **Figure 1** and **Table 1**), which might enable pore-formation using a reduced number of monomers. Further, the MACPF domains of ApiPLPs exhibit several unique characteristics that are absent in canonical MACPF domains. They consist of a pair of anti-parallel α-helices and two pairs of cysteine residues, which are presumably responsible for stabilization. While the first pair is thought to stabilize the unique anti-parallel α-helices in the MACPF domain, the second one might support two strands of the central β-sheet (reviewed in Kafsack and Carruthers, 2010). The C-terminal regions of ApiPLPs contain a β-sheet-rich domain, called APC-β (ApiPLP C-terminal β-pleated sheet) domain, unique to the Apicomplexa, which is probably necessary for initial binding to the target membrane. Analyses of the *T. gondii* PLP TgPLP1 revealed that both, the N-terminal domain as well as the C-terminal domain, have membrane-binding activity, as shown in membrane flotation experiments with recombinant N- and C-terminal domains of the protein. However, Roiko and Carruthers (2013) demonstrated that only the C-terminal domain is critical for protein function. The authors generated several domain deletion strains expressing separate domains or domain combinations of the protein and subjected them to lysis assays, PVM permeabilization experiments and mouse virulence assays. In these experiments, parasites expressing the MACPF domain and C-terminal region of TgPLP1 mostly behaved like the wildtype, whereas parasites lacking one of these domains had no TgPLP1 activity (Roiko and Carruthers, 2013).

Recently published crystal structures of purified APC-β domains of TgPLP1 gave insight into the architecture and membrane-binding properties of ApiPLPs (Guerra et al., 2018; Ni et al., 2018). The studies revealed that the TgPLP1 APC-β domain has an unusual β-prism fold comprising three subdomains. One of these subdomains exhibits a protruding hydrophobic loop tipped by an exposed tryptophan that is presumably responsible for membrane insertion upon binding (Guerra et al., 2018; Ni et al., 2018). Accordingly, mutant parasites expressing TgPLP1 with a loop that is either shortened or changed in amino acid identity or hydrophobicity display an impaired egress phenotype recapitulating the TgPLP1-knock out phenotype, including the formation of smaller plaques compared to wildtype parasites, impaired PVM rupture and delayed egress as determined via LDH activity measurement in culture supernatants (see below; Kafsack et al., 2009; Guerra et al., 2018).

Successful pore formation by perforin-like proteins relies on several consecutive steps and begins with the release of soluble monomers that bind to their target membrane typically via their C-terminal domain. Oligomerization of PLP monomers by lateral interactions results in the formation of a ring-like structure, the so-called pre-pore that is not yet fully inserted into the membrane. Only after conformational rearrangement of the MACPF domain, during which the two α-helical clusters transform into transmembrane β-hairpins, a

TABLE 1 | Putative apicomplexan PLPs with their gene identification numbers according to EuPathDB.org (Aurrecoechea et al., 2017), molecular weight (MW), peak expression of the plasmodial genes (López-Barragán et al., 2011; Otto et al., 2014), and function.

Organism	GeneID EuPathDB and protein name	MW (kDa)	Peak expression	Function	References
Plasmodium falciparum	PF3D7_0408700 (PPLP1)	94	GC	Traversal of human cells (sporozoite); Host cell egress (merozoite)	Garg et al., 2013; Yang et al., 2017
	PF3D7_1216700 (PPLP2)	124	OK	Host cell egress (gametocyte)	Wirth et al., 2014; Hentzschel et al., 2020
	PF3D7_0923300 (PPLP3)	93	OK		
	PF3D7_0819400 (PPLP4)	76	OK	Traversal of mosquito midgut epithelium (ookinete)	Wirth et al., 2015
	PF3D7_0819200 (PPLP5)	79	OK		
Plasmodium berghei	PBANKA_1006300 (PPLP1)	90	OK	Traversal of sinusoidal endothelium (sporozoite)	Ishino et al., 2005
	PBANKA_1432400 (PPLP2)	114	GC	Host cell egress (gametocyte)	Deligianni et al., 2013
	PBANKA_0824200 (PPLP3)	92	GC, OK	Traversal of mosquito midgut epithelium (ookinete)	Kadota et al., 2004
	PBANKA_0711400 (PPLP4)	79	OK	Traversal of mosquito midgut epithelium (ookinete)	Deligianni et al., 2018
	PBANKA_0711600 (PPLP5)	80	OK	Traversal of mosquito midgut epithelium (ookinete)	Ecker et al., 2007
Toxoplasma gondii	TGME49_204130 (TgPLP1)	125		Vacuolar and host cell egress (tachyzoite)	Kafsack et al., 2009; Roiko and Carruthers, 2013; Guerra et al., 2018
	TGME49_272430 (TgPLP2)	92			
Theileria annulata	TA19210	126			
	TA11680	92			
	TA07905	57			
	TA07910	67			
	TA18285[a]	140			
	TA18325	39			
	TA14315	13			
Babesia bovis	BBOV_IV001370	108			
	BBOV_II007150	84			
	BBOV_III000410[a]	143			
	BBOV_II002020	46			
	BBOV_II001970	61			
	BBOV_III000320	56			
	BBOV_II006750	45			
Neospora caninum	NCLIV_020990	114			
	NCLIV_034870	95			
	NCLIV_035170	151			
Eimeria tenella	ETH_00005740	83			
	ETH_00025550	148			

GC, gametocyte; OK, ookinete.
[a]*Three MACPF domains predicted.*

β-barrel pore is formed that finally inserts into the target membrane (Shepard et al., 1998, 2000; Shatursky et al., 1999; Law et al., 2010; Lukoyanova et al., 2015). MACPF pores are typically between 80 and 200 Å in diameter and contain 13-20 monomers (reviewed in Pipkin and Lieberman, 2007; Rosado et al., 2007; Lukoyanova et al., 2015). Although gel analyses of TgPLP1 complexes indicated the presence of more than 20 monomers comprising the pore complex (Roiko and Carruthers, 2013), recent crystallographic studies suggested that the TgPLP1 MACPF domain forms rather small, hexameric assemblies (Ni et al., 2018).

In order to ensure membrane specificity, the pore-forming process has to be tightly controlled. Mechanisms to avoid lysis of non-target membranes have been best studied for the

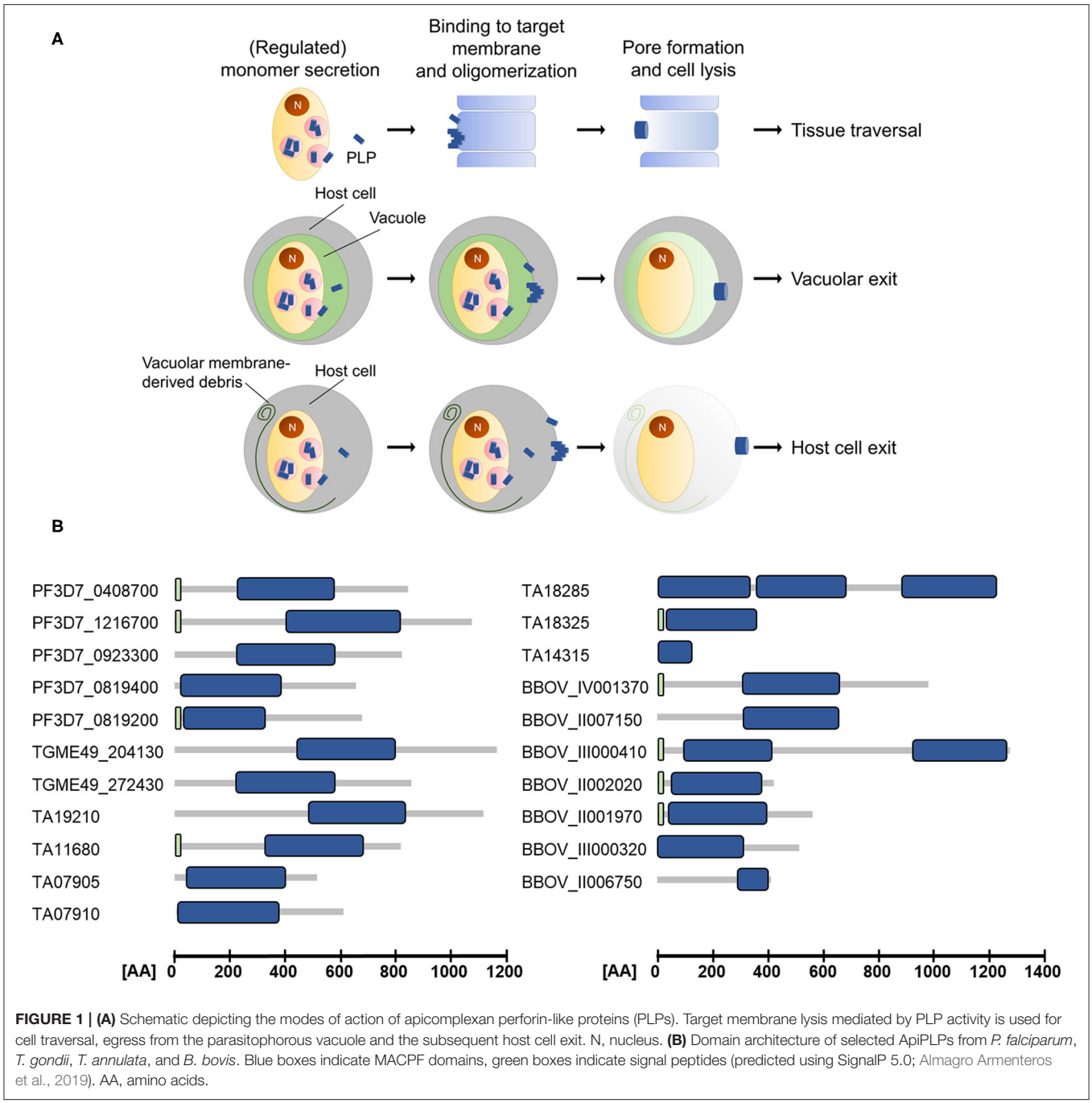

FIGURE 1 | (A) Schematic depicting the modes of action of apicomplexan perforin-like proteins (PLPs). Target membrane lysis mediated by PLP activity is used for cell traversal, egress from the parasitophorous vacuole and the subsequent host cell exit. N, nucleus. **(B)** Domain architecture of selected ApiPLPs from *P. falciparum*, *T. gondii*, *T. annulata*, and *B. bovis*. Blue boxes indicate MACPF domains, green boxes indicate signal peptides (predicted using SignalP 5.0; Almagro Armenteros et al., 2019). AA, amino acids.

pore-formation by human immune molecules, such as perforins and members of the complement system, but potentially also apply for the pore-formation by apicomplexan PLPs. These mechanisms might include the binding to an inhibitor protein prior to the lytic function of the PLP, regulated secretion, pH-dependent activity, protease-mediated activation or the interaction with specific phospholipids in the target membranes, as it has been shown for TgPLP1 (see below). Non-target membranes might further be protected from lysis through the presence of inhibitor proteins as it has been shown in humans as a mechanism to avoid self-cell destruction by the complement system (e.g., reviewed in Pipkin and Lieberman, 2007; Kafsack and Carruthers, 2010; Meri, 2016).

APICOMPLEXAN PERFORINS IN HOST CELL EGRESS

PLPs are involved in the exit of apicomplexan parasites from their respective host cells and hence have important roles for parasite propagation. Apicomplexan parasites mainly egress from their host cells by active lysis of the surrounding membranes,

the parasitophorous vacuole membrane (PVM), and the host cell membrane (HCM). Host cell exit follows a strictly regulated programme, during which rupture of the PVM precedes HCM breakdown (the so-called inside-out egress). Both steps may involve lytic PLPs (**Figure 1**). The involvement of PLPs in host cell lysis, however, has so far only been shown experimentally for *Toxoplasma* and *Plasmodium* parasites (reviewed in Kafsack and Carruthers, 2010; Wirth and Pradel, 2012; Flieger et al., 2018).

Of the two PLPs detected in *T. gondii*, only TgPLP1 hitherto showed a clear involvement in host cell exit (Kafsack et al., 2009; Roiko and Carruthers, 2013; Guerra et al., 2018). TgPLP1 localizes to the micronemes of tachyzoites and is secreted in a calcium-dependent manner during egress similar to other micronemal proteins. Parasites lacking TgPLP1 remain enclosed by the PVM and the HCM, demonstrating its role in lysis of these membranes (Kafsack et al., 2009; Roiko and Carruthers, 2013). Before egress, cytosolic calcium concentrations are suppressed by the activity of a protein kinase A (PKA) and *T. gondii* tachyzoites impaired in PKA signaling spontaneously egress from their host cells in a TgPLP1-dependent fashion (Uboldi et al., 2018). However, it is not yet known if PKA directly regulates TgPLP1 secretion and activity or if they are part of two different pathways that are required for parasite egress.

It is postulated that the egress of *T. gondii* tachyzoites from the host cell is dependent on PV acidification, which promotes membrane binding of TgPLP1 (Roiko et al., 2014). TgPLP1 activity appears to be further regulated by interaction with specific phospholipids located in the respective membrane, particularly phosphatidylethanolamine (PE) or phosphatidylserine (PS), which are characteristic components of the inner leaflet of the red blood cell membrane. The availability of PE and PS, e.g., during egress, increases TgPLP1 activity, whereas the absence of these preferred phospholipid receptors in the outer leaflet of the target cell, e.g., during cell invasion, strongly limits the activity of TgPLP1 (Guerra et al., 2018). In a first model of tachyzoite egress, it has been postulated that TgPLP1 is transported to the PV after secretion, where it interacts with the PVM. This interaction triggers the lytic activity of the protein. After dissolution of the PVM, TgPLP1 binds to phospholipids of the HCM and, hence, further lyses this membrane, in consequence facilitating the final exit of the parasite from its host cell (Guerra et al., 2018).

Active host cell lysis by membrane breaching is also a typical mechanism used by the *Plasmodium* blood stages during exit from the red blood cell (RBC) (reviewed in Wirth and Pradel, 2012; Flieger et al., 2018). Two types of blood stages actively destroy the enveloping RBC during egress, the merozoites and the gametocytes, and for both stages, the involvement of plasmodial PLPs (PPLPs) has been reported. Like for *T. gondii*, egress of *Plasmodium* from the host cell is mediated by a signaling cascade that involves the sequential activation of a PKG by cGMP and of CDPKs by increased cytosolic calcium and this process results in the discharge of vesicles important for RBC lysis (reviewed in Flieger et al., 2018). While five PPLPs (termed PPLP1 to PPLP5) are encoded in the *Plasmodium* genome, only for PPLP1 and PPLP2, an involvement in RBC egress was hitherto shown (Kaiser et al., 2004; Deligianni et al., 2013; Garg et al., 2013; Wirth et al., 2014).

In *P. falciparum*, PPLP1 expression starts in the trophozoite stage and peaks in the mature schizont, where it initially localizes to the micronemes of the merozoites. Similar to TgPLP1, PPLP1 is secreted by the micronemes in a calcium-dependent fashion at the onset of RBC egress (Garg et al., 2013). Later, PPLP1 localizes to the PVM and RBC membrane (RBCM). Since recombinant PPLP1 demonstrates membrane-lytic activities, a role in membrane rupture during merozoite egress from the RBC was postulated. In this context, inhibition of the type-2 phosphatic acid phosphatase PAP2 of *P. falciparum* by propranolol results in the early microneme secretion of PPLP1 by merozoites and in consequence RBCM lysis (Kumar Sah et al., 2019). In general, PAP2s are able to phosphorylate diacylglycerol to generate phosphatidic acid, the latter of which was previously shown to be crucial for triggering microneme secretion in *T. gondii* tachyzoites (Bullen et al., 2016).

PPLP2 is involved in RBC lysis during egress of the *Plasmodium* gametocytes at the onset of gametogenesis (Deligianni et al., 2013; Wirth et al., 2014). In gametocytes, PPLP2 localizes to distinct vesicles which probably represent specialized egress vesicles presumably containing further egress-related molecules. Interestingly, these PPLP2-harboring vesicles are negative for the protein G377 which is a known component of osmiophilic bodies (OBs) (Wirth et al., 2014). OBs constitute vesicles of mature gametocytes that release their content into the PV lumen during the first minutes after gametocyte activation. They contain a variety of proteins, e.g., G377, MDV-1/Peg3, GEST, and several proteases, which are probably involved in PVM rupture (reviewed in Flieger et al., 2018). In a subsequent step, PPLP2 is discharged from the second type of vesicles in a calcium-dependent process. In accord with these data, PPLP2 was found to be a component of the *P. berghei* gametocyte egressome (Kehrer et al., 2016). In both *P. berghei* and *P. falciparum*, activated gametocytes deficient of PPLP2 remain trapped in the host RBCs (Deligianni et al., 2013; Wirth et al., 2014; Hentzschel et al., 2020). While the PVM ruptures normally, lack of PPLP2 leads to impaired perforation of the RBC membrane, which is essential to release the erythrocyte cytoplasm prior to the final rupture of the RBCM. In agreement with these data, recombinant PPLP2 was shown to form pores in RBCMs leading to hemoglobin release (Garg et al., 2020; this issue). The recombinant protein was further able to induce senescence in bystander RBCs. The lytic activity of recombinant PPLP2 could be blocked by specific MACPF domain inhibitors, suggesting that the plasmodial perforins may represent targets for future antimalarials.

APICOMPLEXAN PERFORINS IN TISSUE TRAVERSAL

The PPLPs of *Plasmodium* are further crucial for tissue traversal during lifecycle progression of the parasite (**Figure 1**). With the exception of PPLP2, all of the PPLPs were shown to be involved in crossing of epithelial barriers.

The passage through host cell epithelia is particularly important for the infective sporozoites during their journey to the human liver. An initial study on *P. berghei* demonstrated

that PPLP1 (originally termed SPECT2) is present in sporozoite micronemes and secreted, when these traverse the sinusoidal endothelium (Ishino et al., 2005). Crossing of cells lining capillaries and the subsequent traversal of hepatocytes is a mandatory step of sporozoites, before these are able to settle down in a host hepatocyte to initiate replication (Mota et al., 2001, 2002; Pradel and Frevert, 2001; Amino et al., 2008; Tavares et al., 2013). *P. berghei* sporozoites deficient of PPLP1 remain in the blood circulation and are unable to establish an infection in mice (Ishino et al., 2005). Similarly, PPLP1-deficient *P. falciparum* sporozoites could not initiate an infection in the humanized mouse model (Yang et al., 2017). A subsequent study on the rodent malaria parasite *P. yoelii* showed that sporozoites traverse cell barriers via a transient vacuole, which is independent of moving junction formation, and that the sporozoites escape this vacuole with the help of PPLP1 (Risco-Castillo et al., 2015). The final invasion of hepatocytes requires a moving junction-dependent PV formation, in which the parasite in then able to grow.

Another epithelial crossing occurs during exit of the mosquito midgut by the motile *Plasmodium* ookinetes. In *P. berghei*, PPLP3 (originally termed MAOP), PPLP4 and PPLP5 were shown to be essential for the traversal of the mosquito midgut epithelium by ookinetes, while in *P. falciparum*, only PPLP4 has been attributed a role in this process so far (Kadota et al., 2004; Ecker et al., 2007; Wirth et al., 2015; Deligianni et al., 2018). Ookinetes lacking any of the three PPLPs are unable to infect female *Anopheles* mosquitoes. Interestingly, while in *P. falciparum*, PPLP4 is initially expressed in female gametocytes and later localizes to the ookinete micronemes, in *P. berghei*, PPLP4 was reported to be present on the entire surface of the ookinete (Wirth et al., 2015; Deligianni et al., 2018). While these data demonstrate a crucial role for PPLP3, PPLP4, and PPLP5 in the mosquito-specific lifecycle phase of the malaria parasite, the detailed mode of action and any potential synergistic interplay of the three perforins during mosquito midgut traversal still needs to be elucidated.

CONCLUSION

Despite an increasing number of publications that shed light on the structure of apicomplexan PLPs and their functions during parasitic lifecycle progression, many questions about their mode of action and regulation remain. For instance, further studies are needed to determine how membrane specificity is achieved. What are the receptors for initial membrane binding and how are non-target membranes protected from lysis? How many monomers are involved in complex formation, and, given the fact that some apicomplexan PLPs are predicted to encode multiple MACPF domains, are less of these monomers necessary to form a pore? Furthermore, the role of the unconserved N-terminal regions of apicomplexan PLPs, which vary in length and sequence, remains to be elucidated. Interestingly, some processes, such as the traversal of epithelial cells of the mosquito midgut by *Plasmodium* ookinetes involve several different PLPs. The interplay of these proteins and potential co-dependencies will be the focus of further studies.

AUTHOR CONTRIBUTIONS

JS, GP, and SB wrote the manuscript. All authors contributed to the manuscript and approved the submitted version.

ACKNOWLEDGMENTS

The authors acknowledge funding by the priority programme SPP1580 of the Deutsche Forschungsgemeinschaft (DFG).

REFERENCES

Aleshin, A. E., Schraufstatter, I. U., Stec, B., Bankston, L. A., Liddington, R. C., and DiScipio, R. G. (2012). Structure of complement C6 suggests a mechanism for initiation and unidirectional, sequential assembly of membrane attack complex (MAC). *J. Biol. Chem.* 287, 10210–10222. doi: 10.1074/jbc.M111.327809

Almagro Armenteros, J. J., Tsirigos, K. D., Sønderby, C. K., Petersen, T. N., Winther, O., Brunak, S., et al. (2019). SignalP 5.0 improves signal peptide predictions using deep neural networks. *Nat. Biotechnol.* 37, 420–423. doi: 10.1038/s41587-019-0036-z

Amino, R., Giovannini, D., Thiberge, S., Gueirard, P., Boisson, B., Dubremetz, J. F., et al. (2008). Host cell traversal is important for progression of the malaria parasite through the dermis to the liver. *Cell Host Microbe* 3, 88–96. doi: 10.1016/j.chom.2007.12.007

Aurrecoechea, C., Barreto, A., Basenko, E. Y., Brestelli, J., Brunk, B. P., Cade, S., et al. (2017). EuPathDB: the eukaryotic pathogen genomics database resource. *Nucleic Acids Res.* 45, D581–D591. doi: 10.1093/nar/gkw1105

Blackman, M. J., and Bannister, L. H. (2001). Apical organelles of apicomplexa: biology and isolation by subcellular fractionation. *Mol. Biochem. Parasitol.* 117, 11–25. doi: 10.1016/S0166-6851(01)00328-0

Bullen, H. E., Jia, Y., Yamaryo-Bott,é, Y., Bisio, H., Zhang, O., Jemelin, N. K., et al. (2016). Phosphatidic acid-mediated signaling regulates microneme secretion in toxoplasma. *Cell Host Microbe* 19, 349–360. doi: 10.1016/j.chom.2016.02.006

Deligianni, E., Morgan, R. N., Bertuccini, L., Wirth, C. C., Silmon de Monerri, N. C., Spanos, L., et al. (2013). A perforin-like protein mediates disruption of the erythrocyte membrane during egress of *Plasmodium berghei* male gametocytes. *Cell. Microbiol.* 15, 1438–1455. doi: 10.1111/cmi.12131

Deligianni, E., Silmon de Monerri, N. C., McMillan, P. J., Bertuccini, L., Superti, F., Manola, M., et al. (2018). Essential role of plasmodium perforin-like protein 4 in ookinete midgut passage. *PLoS ONE* 13:e0201651. doi: 10.1371/journal.pone.0201651

Dubois, D. J., and Soldati-Favre, D. (2019). Biogenesis and secretion of micronemes in *Toxoplasma gondii*. *Cell. Microbiol.* 21:e13018. doi: 10.1111/cmi.13018

Ecker, A., Pinto, S. B., Baker, K. W., Kafatos, F. C., and Sinden, R. E. (2007). *Plasmodium berghei*: plasmodium perforin-like protein 5 is required for mosquito midgut invasion in *Anopheles stephensi*. *Exp. Parasitol.* 116, 504–508. doi: 10.1016/j.exppara.2007.01.015

Flieger, A., Frischknecht, F., Häcker, G., Hornef, M. W., and Pradel, G. (2018). Pathways of host cell exit by intracellular pathogens. *Microb. Cell* 5, 525–544. doi: 10.15698/mic2018.12.659

Garg, S., Agarwal, S., Kumar, S., Shams Yazdani, S., Chitnis, C. E., and Singh, S. (2013). Calcium-dependent permeabilization of erythrocytes by a perforin-like protein during egress of malaria parasites. *Nat. Commun.* 4:1736. doi: 10.1038/ncomms2725

Garg, S., Shivappagowdar, A., Hada, R. S., Ayana, R., Bathula, C., Sen, S., et al. (2020). Plasmodium perforin-like protein pores on the host cell membrane contribute in its multistage growth and erythrocyte senescence. *Front. Cell. Infect. Microbiol.* 10:121. doi: 10.3389/fcimb.2020.00121

Guerra, A. J., Zhang, O., Bahr, C. M. E., Huynh, M. H., DelProposto, J., Brown, W. C., et al. (2018). Structural basis of *Toxoplasma gondii* perforin-like protein

1 membrane interaction and activity during egress. *PLoS Pathog.* 14:e1007476. doi: 10.1371/journal.ppat.1007476

Hadders, M. A., Beringer, D. X., and Gros, P. (2007). Structure of C8α-MACPF reveals mechanism of membrane attack in complement immune defense. *Science.* 317, 1552–1554. doi: 10.1126/science.1147103

Hentzschel, F., Mitesser, V., Fraschka, S. A. K., Krzikalla, D., Carrillo, E. H., Berkhout, B., et al. (2020). Gene knockdown in malaria parasites via non-canonical RNAi. *Nucleic Acids Res.* 48:e2. doi: 10.1093/nar/gkz927

Ishino, T., Chinzei, Y., and Yuda, M. (2005). A Plasmodium sporozoite protein with a membrane attack complex domain is required for breaching the liver sinusoidal cell layer prior to hepatocyte infection. *Cell. Microbiol.* 7, 199–208. doi: 10.1111/j.1462-5822.2004.00447.x

Kadota, K., Ishino, T., Matsuyama, T., Chinzei, Y., and Yuda, M. (2004). Essential role of membrane-attack protein in malarial transmission to mosquito host. *Proc. Natl. Acad. Sci. U.S.A.* 101, 16310–16315. doi: 10.1073/pnas.0406187101

Kafsack, B. F. C., and Carruthers, V. B. (2010). Apicomplexan perforin-like proteins. *Commun. Integr. Biol.* 3, 18–23. doi: 10.4161/cib.3.1.9794

Kafsack, B. F. C., Pena, J. D. O., Coppens, I., Ravindran, S., Boothroyd, J. C., and Carruthers, V. B. (2009). Rapid membrane disruption by a perforin-like protein facilitates parasite exit from host cells. *Science* 323, 530–533. doi: 10.1126/science.1165740

Kaiser, K., Camargo, N., Coppens, I., Morrisey, J. M., Vaidya, A. B., and Kappe, S. H. I. (2004). A member of a conserved plasmodium protein family with membrane-attack complex/perforin (MACPF)-like domains localizes to the micronemes of sporozoites. *Mol. Biochem. Parasitol.* 133, 15–26. doi: 10.1016/j.molbiopara.2003.08.009

Kehrer, J., Frischknecht, F., and Mair, G. R. (2016). Proteomic analysis of the plasmodium berghei gametocyte egressome and vesicular bioID of osmiophilic body proteins identifies merozoite TRAP-like protein (MTRAP) as an essential factor for parasite transmission. *Mol. Cell. Proteomics* 15, 2852–2862. doi: 10.1074/mcp.M116.058263

Kumar Sah, R., Garg, S., Dangi, P., Ponnusamy, K., and Singh, S. (2019). Phosphatidic acid homeostasis regulated by a type-2 phosphatidic acid phosphatase represents a novel druggable target in malaria intervention. *Cell Death Discov.* 5:107. doi: 10.1038/s41420-019-0187-1

Law, R. H. P., Lukoyanova, N., Voskoboinik, I., Caradoc-Davies, T. T., Baran, K., Dunstone, M. A., et al. (2010). The structural basis for membrane binding and pore formation by lymphocyte perforin. *Nature* 468, 447–451. doi: 10.1038/nature09518

López-Barragán, M. J., Lemieux, J., Quiñones, M., Williamson, K. C., Molina-Cruz, A., Cui, K., et al. (2011). Directional gene expression and antisense transcripts in sexual and asexual stages of *Plasmodium falciparum*. *BMC Genomics* 12:587. doi: 10.1186/1471-2164-12-587

Lukoyanova, N., Hoogenboom, B. W., and Saibil, H. R. (2016). The membrane attack complex, perforin and cholesteroldependent cytolysin superfamily of pore-forming proteins. *J. Cell Sci.* 129, 2125–2133. doi: 10.1242/jcs.182741

Lukoyanova, N., Kondos, S. C., Farabella, I., Law, R. H. P., Reboul, C. F., Caradoc-Davies, T. T., et al. (2015). Conformational changes during pore formation by the perforin-related protein pleurotolysin. *PLoS Biol.* 13:e1002049. doi: 10.1371/journal.pbio.1002049

Meri, S. (2016). Self-nonself discrimination by the complement system. *FEBS Lett.* 590, 2418–2434. doi: 10.1002/1873-3468.12284

Moreno-Hagelsieb, G., Vitug, B., Medrano-Soto, A., and Saier, M. H. J. (2017). The membrane attack complex/perforin (MACPF) superfamily. *J. Mol. Microbiol. Biotechnol.* 27, 252–267. doi: 10.1159/000481286

Mota, M. M., Hafalla, J. C. R., and Rodriguez, A. (2002). Migration through host cells activates plasmodium sporozoites for infection. *Nat. Med.* 8, 1318–1322. doi: 10.1038/nm785

Mota, M. M., Pradel, G., Vanderberg, J. P., Hafalla, J. C. R., Frevert, U., Nussenzweig, R. S., et al. (2001). Migration of plasmodium sporozoites through cells before infection. *Science* 291, 141–144. doi: 10.1126/science.291.5501.141

Ni, T., Williams, S. I., Rezelj, S., Anderluh, G., Harlos, K., Stansfeld, P. J., et al. (2018). Structures of monomeric and oligomeric forms of the *Toxoplasma gondii* perforin-like protein 1. *Sci. Adv.* 4:eaaq0762. doi: 10.1126/sciadv.aaq0762

Otto, T. D., Böhme, U., Jackson, A. P., Hunt, M., Franke-Fayard, B., Hoeijmakers, W. A. M., et al. (2014). A comprehensive evaluation of rodent malaria parasite genomes and gene expression. *BMC Biol.* 12:86. doi: 10.1186/s12915-014-0086-0

Pipkin, M. E., and Lieberman, J. (2007). Delivering the kiss of death: progress on understanding how perforin works. *Curr. Opin. Immunol.* 19, 301–308. doi: 10.1016/j.coi.2007.04.011

Pradel, G., and Frevert, U. (2001). Malaria sporozoites actively enter and pass through rat Kupffer cells prior to hepatocyte invasion. *Hepatology* 33, 1154–1165. doi: 10.1053/jhep.2001.24237

Risco-Castillo, V., Topcu, S., Marinach, C., Manzoni, G., Bigorgne, A., Briquet, S., et al. (2015). Malaria sporozoites traverse host cells within transient vacuoles. *Cell Host Microbe* 18, 593–603. doi: 10.1016/j.chom.2015.10.006

Roiko, M. S., and Carruthers, V. B. (2013). Functional dissection of Toxoplasma gondii perforin-like protein 1 reveals a dual domain mode of membrane binding for cytolysis and parasite egress. *J. Biol. Chem.* 288, 8712–8725. doi: 10.1074/jbc.M113.450932

Roiko, M. S., Svezhova, N., and Carruthers, V. B. (2014). Acidification activates *Toxoplasma gondii* motility and egress by enhancing protein secretion and cytolytic activity. *PLoS Pathog.* 10:e1004488. doi: 10.1371/journal.ppat.1004488

Rosado, C. J., Buckle, A. M., Law, R. H. P., Butcher, R. E., Kan, W. T., Bird, C. H., et al. (2007). A common fold mediates vertebrate defense and bacterial attack. *Science* 317, 1548–1551. doi: 10.1126/science.1144706

Shatursky, O., Heuck, A. P., Shepard, L. A., Rossjohn, J., Parker, M. W., Johnson, A. E., et al. (1999). The mechanism of membrane insertion for a cholesterol-dependent cytolysin: a novel paradigm for pore-forming toxins. *Cell* 99, 293–299. doi: 10.1016/S0092-8674(00)81660-8

Shepard, L. A., Heuck, A. P., Hamman, B. D., Rossjohn, J., Parker, M. W., Ryan, K. R., et al. (1998). Identification of a membrane-spanning domain of the thiol-activated pore-forming toxin *Clostridium perfringens* perfringolysin O: an α-helical to β-sheet transition identified by fluorescence spectroscopy. *Biochemistry* 37, 14563–14574. doi: 10.1021/bi981452f

Shepard, L. A., Shatursky, O., Johnson, A. E., and Tweten, R. K. (2000). The mechanism of pore assembly for a cholesterol-dependent cytolysin: formation of a large prepore complex precedes the insertion of the transmembrane β-hairpins. *Biochemistry* 39, 10284–10293. doi: 10.1021/bi000436r

Tavares, J., Formaglio, P., Thiberge, S., Mordelet, E., Van Rooijen, N., Medvinsky, A., et al. (2013). Role of host cell traversal by the malaria sporozoite during liver infection. *J. Exp. Med.* 210, 905–915. doi: 10.1084/jem.20121130

Tweten, R. K. (2005). Cholesterol-dependent cytolysins, a family of versatile pore-forming toxins. *Infect. Immun.* 73, 6199–6209. doi: 10.1128/IAI.73.10.6199-6209.2005

Uboldi, A. D., Wilde, M. L., McRae, E. A., Stewart, R. J., Dagley, L. F., Yang, L., et al. (2018). Protein kinase A negatively regulates Ca^{2+} signalling in *Toxoplasma gondii*. *PLoS Biol.* 16:e2005642. doi: 10.1371/journal.pbio.2005642

Wirth, C. C., Bennink, S., Scheuermayer, M., Fischer, R., and Pradel, G. (2015). Perforin-like protein PPLP4 is crucial for mosquito midgut infection by *Plasmodium falciparum*. *Mol. Biochem. Parasitol.* 201, 90–99. doi: 10.1016/j.molbiopara.2015.06.005

Wirth, C. C., Glushakova, S., Scheuermayer, M., Repnik, U., Garg, S., Schaack, D., et al. (2014). Perforin-like protein PPLP2 permeabilizes the red blood cell membrane during egress of *Plasmodium falciparum* gametocytes. *Cell. Microbiol.* 16, 709–733. doi: 10.1111/cmi.12288

Wirth, C. C., and Pradel, G. (2012). Molecular mechanisms of host cell egress by malaria parasites. *Int. J. Med. Microbiol.* 302, 172–178. doi: 10.1016/j.ijmm.2012.07.003

Yang, A. S. P., O'Neill, M. T., Jennison, C., Lopaticki, S., Allison, C. C., Armistead, J. S., et al. (2017). Cell traversal activity is important for *Plasmodium falciparum* liver infection in humanized mice. *Cell Rep.* 18, 3105–3116. doi: 10.1016/j.celrep.2017.03.017

Conflict of Interest: The authors declare that the research was conducted in the absence of any commercial or financial relationships that could be construed as a potential conflict of interest.

frontiers in Immunology

ORIGINAL RESEARCH
published: 16 September 2020
doi: 10.3389/fimmu.2020.550946

Staphylococcus epidermidis Boosts Innate Immune Response by Activation of Gamma Delta T Cells and Induction of Perforin-2 in Human Skin

Irena Pastar[1†], Katelyn O'Neill[2†], Laura Padula[2], Cheyanne R. Head[1], Jamie L. Burgess[1], Vivien Chen[1], Denisse Garcia[2], Olivera Stojadinovic[1], Suzanne Hower[2], Gregory V. Plano[2], Seth R. Thaller[3], Marjana Tomic-Canic[1] and Natasa Strbo[2]**

[1] Wound Healing and Regenerative Medicine Research Program, Dr. Phillip Frost Department of Dermatology and Cutaneous Surgery, University of Miami Miller School of Medicine, Miami, FL, United States, [2] Department of Microbiology and Immunology, University of Miami Miller School of Medicine, Miami, FL, United States, [3] Division of Plastic Surgery Dewitt Daughtry, Department of Surgery, University of Miami Miller School of Medicine, Miami, FL, United States

Perforin-2 (P-2) is an antimicrobial protein with unique properties to kill intracellular bacteria. Gamma delta (GD) T cells, as the major T cell population in epithelial tissues, play a central role in protective and pathogenic immune responses in the skin. However, the tissue-specific mechanisms that control the innate immune response and the effector functions of GD T cells, especially the cross-talk with commensal organisms, are not very well understood. We hypothesized that the most prevalent skin commensal microorganism, *Staphylococcus epidermidis*, may play a role in regulating GD T cell-mediated cutaneous responses. We analyzed antimicrobial protein P-2 expression in human skin at a single cell resolution using an amplified fluorescence *in situ* hybridization approach to detect P-2 mRNA in combination with immunophenotyping. We show that *S. epidermidis* activates GD T cells and upregulates P-2 in human skin *ex vivo* in a cell-specific manner. Furthermore, P-2 upregulation following *S. epidermidis* stimulation correlates with increased ability of skin cells to kill intracellular *Staphylococcus aureus*. Our findings are the first to reveal that skin commensal bacteria induce P-2 expression, which may be utilized beneficially to modulate host innate immune responses and protect from skin infections.

Keywords: perforin-2/mpeg-1, human skin, innate immunity, *Staphylococcus epidermidis*, gamma delta T cells, cytotoxicity

OPEN ACCESS

Edited by:
Gabriele Pradel, RWTH Aachen University, Germany

Reviewed by:
Michael Otto, National Institutes of Health (NIH), United States
Juan Carlos Cancino-Diaz, National Polytechnic Institute of Mexico (IPN), Mexico

***Correspondence:**
Marjana Tomic-Canic
MTcanic@med.miami.edu
Natasa Strbo
nstrbo@med.miami.edu

† These authors have contributed equally to this work and share first authorship

Specialty section:
This article was submitted to Microbial Immunology, a section of the journal Frontiers in Immunology

Received: *11 April 2020*
Accepted: *18 August 2020*
Published: *16 September 2020*

Citation:
Pastar I, O'Neill K, Padula L, Head CR, Burgess JL, Chen V, Garcia D, Stojadinovic O, Hower S, Plano GV, Thaller SR, Tomic-Canic M and Strbo N (2020) Staphylococcus epidermidis Boosts Innate Immune Response by Activation of Gamma Delta T Cells and Induction of Perforin-2 in Human Skin. Front. Immunol. 11:550946. doi: 10.3389/fimmu.2020.550946

INTRODUCTION

Skin, in the same fashion as all other epithelial barrier sites (gastrointestinal, reproductive, and respiratory tracts) harbors a distinct community of commensal microbes that modulate the host immune system (1–3). One of the most common members of the healthy cutaneous microbiome is *Staphylococcus epidermidis*. *S. epidermidis* stimulates antimicrobial peptide production by skin cells (4–11), which may provide protection against pathogenic bacteria (4, 5, 10–12). Recent studies reported that colonization of mouse skin with *S. epidermidis* induced commensal-specific tissue

(skin)-resident memory T cells that demonstrated immunoregulatory and tissue repair properties. This was proposed as a novel *S. epidermidis* mediated mechanism for rapid immune response and tissue protection from invasive pathogens (13–15).

Multiple lines of evidence have shown that gamma delta (GD) T cells display strong activities against bacteria (16–20), parasites (21), and viruses (22, 23). In marked contrast to αβ T lymphocytes (24–29), GD T cells recognize antigens independently of peptide processing and major histocompatibility complex (MHC)-restricted antigen presentation. They are activated by signs of tissue stress, including infected or transformed cells, and respond by deploying an immediate and efficient killing response or by regulating the immune response against them. Phosphoantigens and several other molecules of microbial origin have been proposed as GD T cell antigens accounting for the specific recognition of infected cells. These candidates include the *Staphylococcus aureus* superantigens Staphylococcal enterotoxin A (SEA) (and to a lesser extent staphylococcal enterotoxin E (SEE) (30, 31), which are recognized by the GD T cell receptor (TCR) independently from antigen processing and MHC presentation. Although GD T cells are one of the predominant lymphocyte subsets in mouse and human skin (32) that are essential for skin homeostatic and protective pathways against *S. aureus* (33), the contribution of commensal-derived antigens to the activation of GD T cells and their effector function, particularly their cytotoxic potential, has not been established. Furthermore, the extent to which GD T cells promote cutaneous tissue physiology remains to be determined.

Perforin-2 (P-2)/MPEG1 is a highly conserved member of the membrane attack complex (MAC)/perforin-like (PF)/cholesterol-dependent cytolysin (MACPF/CDC) superfamily (34–36). In contrast to all other MACPF/CDC members, P-2 is a type-1 transmembrane protein that traffics throughout the endosomal pathway to the late-endosome and phagosome (37–39). Therefore, P-2 can form pores in bacterial membranes and damage engulfed microbes within the phagolysosome (37, 40). In the absence of P-2, the other innate defense effectors including reactive oxygen species and nitric oxide, were unable to prevent the replication and systemic dissemination of intracellular pathogens (37, 41, 42). Dr. Eckhard Podack's group was the first to report about major P-2 functions as an antibacterial effector protein of the innate immune system in phagocytic and in tissue forming cells (37, 41). Although we recently reported specific distribution of P-2 in normal human skin (43), the mechanisms involved in the regulation of P-2 expression have not been well established. Moreover, the effect of P-2 function within the complex system of host-microbe interactions has important implication for our understanding of skin immunity and diseases.

Here we established a human skin *ex vivo* model to study the effect of *S. epidermidis* on the skin innate immune response and on the novel antimicrobial protein P-2. We report that *S. epidermidis* activates skin GD T cells, specifically through P-2 induction, which has demonstrated antibacterial effects in other cell subsets (macrophages and fibroblasts) (37, 42). Importantly, *S. epidermidis* mediated induction of P-2 correlated with an enhanced ability of the skin cells to eliminate intracellular *S. aureus*.

MATERIALS AND METHODS

Bacterial Strains and Culture Conditions

Staphylococcus epidermidis CCN021 and CCN0024, human commensal *S. epidermidis* strains, were obtained from GP (University of Miami). *S. epidermidis* ATCC 12228 was a gift from Prof. Davis (University of Miami). *S. epidermidis* CCN021 and CCN0024 were isolated from a healthy volunteer and characterized by phenotypic and qPCR identification techniques (44, 45). Staphylococci were routinely grown aerobically with agitation, at 37°C, in Luria-Bertani (LB) broth. For pre-treatment, bacteria were diluted in fresh LB and grown to mid-log growth phase. Before application on *ex vivo* human skin or single cell suspension, bacteria were harvested by centrifugation and washed with phosphate buffered saline (PBS). The bacterial density and the absence of contamination were controlled by numeration of colony forming units (CFU).

The GFP containing USA300 Methicillin resistant *Staphylococcus aureus* (MRSA) strain AH1726 [MRSA LAC (AH1263) + pCM29 (CmR)] (46) was obtained from GP (University of Miami). MRSA was grown aerobically with agitation overnight at 37°C in LB supplemented with 10 μg/mL chloramphenicol to retain the GFP plasmid.

Ex vivo Human Skin Explant System

Discarded human skin tissue was obtained from voluntary reduction surgeries (n = 6) at the University of Miami (UM) Hospital and as such were found to be exempt from human subject research under CFR46.101.2 by the Institutional Review Board at the UM Miller School of Medicine.

Skin samples were processed to remove subcutaneous fat and washed with PBS. Multiple 8 mm punch biopsies were obtained from each specimen and placed individually into 0.4 μm PET-membrane *trans*-wells (Millipore) in a 12 well plate containing 1 ml media per well (RPMI, 10% FBS, 1% HEPES). Skin specimens were maintained at the air-liquid interface as previously described (43, 47–50).

Human Skin Single Cell Suspension

Cells were isolated from healthy human skin using the MACS Whole Skin Dissociation Kit (Miltenyi 130-101-540). Briefly, subcutaneous fat was removed, and sterilization of human skin was optimized to remove any commensal or pathogenic microorganisms. Skin was washed with Gibco® Antibiotic-Antimycotic (ABAM) (Life Technologies) to prevent bacterial and fungal contamination. This solution contains 10,000 units/mL of penicillin, 10,000 μg/mL of streptomycin, and 25 μg/mL of Gibco Amphotericin B. After washings with ABAM, skin was washed in PBS (46). Three 4 mm diameter punches were digested overnight at 37°C using enzymes from a whole-skin dissociation kit (Miltenyi, Bergisch Gladbach, Germany). The resulting cell suspension was filtered through a 70 μm cell strainer and centrifuged at 1,500 r.p.m. for 10 min

at 4°C. The supernatant was removed, and the pellet was washed once with PBS. Obtained cell suspensions were washed with IMDM (Gibco-Thermo Fisher Scientific) supplemented with 10% heat-inactivated FBS, 2 mM L-glutamine, 0.15% sodium hydrogencarbonate, 1 mM sodium pyruvate, and non-essential amino acids.

Ex vivo and *in vitro* Skin Stimulation With *S. epidermidis*

Staphylococcus epidermidis CCN021 was prepared for stimulation experiments as described above and 20 μL of the bacteria solution (approx. 6 Log CFU) was added centrally onto the epidermis while control samples were treated with PBS. After 24, 48, 72, and 96 h of incubation at 37°C in a 5% CO2 atmosphere, tissue samples were either digested with collagenase for further cell viability and FISH/Flow analysis (**Supplementary Figure S2**), preserved in RNA-later for RNA isolation, or used for CFU enumeration. CFU count was determined after overnight colony growth and expressed as CFU/ml.

Skin cell suspension obtained after whole-skin dissociation was used for *in vitro* stimulation with *S. epidermidis* CCN021, CCN0024, and ATCC 12228. Cells were plated on 24 well plates with 1 million cells per well and treated with *S. epidermidis* at a multiplicity of infection (MOI) of 20 for 24 h. The control cells were exposed to media only.

Intracellular MRSA Killing Assay

After 24 h stimulation with *S. epidermidis,* skin cells were washed twice with warmed plain IMDM and infected with MRSA at an MOI of 20 for 1 h. Cells were washed twice with IMDM after infection and fresh media containing gentamicin (50 μg/mL) was added for 30 min to eliminate extracellular bacteria. Samples were collected 30 and 90 min after intracellular infection for enumeration of intracellular colony forming units (CFU) and for FISH flow analysis as described before (43). To release intracellular bacterial load, cells were subjected to hypotonic lysis with 0.1% Triton X in PBS. Lysates were plated on agar plates containing 10 μg/mL chloramphenicol for CFU quantification (43).

FISH-Flow P-2 RNA Assay and Flow Cytometric Analysis

Single cell suspensions obtained from full thickness samples or after stimulation with *S. epidermidis* and MRSA were first labeled with live/dead detection kit (Yellow Amine, Thermo Fisher Scientific) and then with the following fluorescently labeled antibodies: CD45-Alexa Fluor 700, TCR GD-PE-Cy7, CD31-PacBlue, CD104-FITC, CD325-PerCPCy5.5, and CCRL1-PE (Biolegend, San Diego, CA, United States). We also stained cells with fluorescently labeled antibodies for TLR1-BV570, TLR2-PE, TLR6-BV605, and TCR GD 1 FITC (Biolegend, San Diego, CA, United States). P-2 mRNA was detected using an amplified signal FISH technique (PrimeFlow; Affymetrix/eBioscience-Thermo Fisher Scientific). For mRNA detection, target probe hybridization was performed using type 1 (AlexaFluor647) probes for P-2 as described (43). Approximately 20,000 cell events were acquired from each sample on flow cytometer equipped with 405 nm, 488 nm, 642 nm, and 785 nm (SSC) lasers (Fortessa X-50, BD Immunocytometry Systems, San Jose, CA, United States). Spectral compensation was completed using single color control samples and antibody capture beads (BD Biosciences). Data were analyzed using FlowJo version 10.2 (TreeStar).

GD T Cell Sorting and Real-Time PCR

Two-way sorting was performed to obtain purified GD T cells by sterile sorting on a SONY SH800S cell sorter (SONY Biotechnology, San Jose, CA, United States). Briefly, single cell suspensions were labeled with Live/Dead Violet, CD45, CD3, and TCR GD. GD T cells were sorted as Live/Dead-CD45+ CD3+ TCR GD+ cell population. 5,000–10,000 sorted cells were collected from three donors. Purity of sorted GD T population was >97%.

After sorting, cells were stimulated with *S. epidermidis* at an MOI of 20 for 1 h, washed with PBS, spun down, and kept on ice briefly prior to performing one-step reverse transcription and cDNA amplification of specific targets using a pool of TaqmanTM gene expression assays (Thermo Fisher Scientific). Resulting cDNA was loaded onto BioMark IFC 96 × 96 chip (Fluidigm) according to the manufacturer's protocol. Raw data underwent "cellular detection rate" (CDR) filtering to remove outlier samples and genes based on dataset distribution (51, 52). CD74 (also known as HLADG) was used as a surrogate for the presence of a cell (i.e., loading control) due to its stable expression in lymphocytes. Cells that had low or absent CD74 expression exhibited reduced gene expression globally and were removed from analysis. Differential gene expression analysis was subsequently performed to contrast transcriptional profiles of GD T cells between unstimulated and *S. epidermidis* stimulated samples.

RT-PCR for Antimicrobial Peptides and Pro-inflammatory Cytokines

Total RNA from human skin was extracted using the miRNeasy kit (QIAGEN, Valencia, CA, United States) per manufacturer's instructions as previously described (49). cDNA was made with qScript™ Synthesis kit (Quanta BioSciences Inc.,Gaithersburg, MD, United States). ARPC2 was used as a reference gene for normalization, forward 5′-TCCGGGACTACCTGCACTAC-3′, reverse 5′-GGTTCAGCACCTTGAGGAAG-3′. All real-time PCR (qPCR) reactions were performed in triplicate using PerfeCTa® SYBR® Green SuperMix (Quanta BioSciences) and quantified using the ddCT method. The primer sequences were IL-1α forward 5′-AGATGCCTGAGATACCCAAAACC-3′ reverse 5′-CCAAGCACACCCAGTAGTCT-3′, defensin β4 (DefB4) forward 5′-GGTGGTATAGGCGATCCTGTT-3′ reverse 5′-AGGGCAAAAGACTGGATGACA-3′, and cathelicidin (LL37) forward 5′-GGGCAAAAGACTGGATGACA-3′ reverse 5′-TCTTGAAGTCACAATCCTCTGGT-3′.

Statistical Analysis

All experiments were conducted independently at least three times on different days. Comparisons of flow cytometry cell

frequencies was measured by the two-way ANOVA test with Holm-Sidak multiple-comparison test, $^{*}p < 0.05$, $^{**}p < 0.01$, and $^{***}p < 0.001$ or Student *t*-test using the Prism software (GraphPad software). Comparisons of PCR array data were performed using *t*-test (two tail distribution and equal variances between the two groups) based on the triplicate 2^(−ΔCT) values for each gene in the *S. epidermidis* treated group and control group. Error bars in all figures are reported as a SEM.

RESULTS

S. epidermidis Contributes to Increased Number of Human GD T Cells

Staphylococcus epidermidis is an important skin commensal organism and modulator of cutaneous innate immune responses (9, 10). Here we established an *ex vivo* skin model of *S. epidermidis* colonization to study the effect of this commensal microorganism on skin innate immune responses including GD T cell activity. *S. epidermidis* was topically applied onto the epidermis. Tissue was collected at different time points during colonization and then dissociated into single cell suspensions (**Figure 1**). There were no statistical differences in viability of *S. epidermidis* treated and control tissue (**Supplementary Figure S1**). We analyzed the GD T cell subset in the control and *S. epidermidis* colonized human skin by flow cytometry and observed a statistically significant ($p < 0.01$) increase in the frequency as well as in the total number of GD T cells within live, CD45+ CD3+ skin cells after 72 h of *S. epidermidis* stimulation compared to control tissue (**Figures 1A,B**). We confirmed *S. epidermidis* colonization in human skin by CFU quantification (**Figure 1C**).

S. epidermidis Induces P-2 in Human GD T Cells, Keratinocytes, and Papillary Fibroblasts *ex vivo*

We have previously described an amplified fluorescence *in situ* hybridization (FISH) technique for detection of mRNA in combination with immune-phenotyping in human skin (43). We and others found that P-2 is an antimicrobial protein crucial for intracellular bacteria killing (37, 38, 40, 41). Here, we analyzed P-2 expression in different skin cell subsets after stimulation with *S. epidermidis*. First, we found that P-2 expression was significantly upregulated ($p < 0.05$ and $p < 0.01$) in GD T cells from human skin explants colonized with *S. epidermidis* at 24, 48, and 72 h compared to the uncolonized control (**Figures 2A,B**). Moreover, our analysis revealed that *S. epidermidis* stimulation for 96 h upregulated P-2 in the basal layer keratinocytes after an initial suppression observed at 24 h (CD45-CD31-CD104+ cells) (**Figure 3**). Two major human skin fibroblast subsets, papillary and reticular fibroblasts, based on their expression of CCRL1 and CD325, respectively (53, 54) were also tested. We found that only papillary fibroblasts, CCRL1+ cells, upregulate P-2 96 h post *S. epidermidis* colonization. P-2 expression in reticular fibroblasts was not affected at any time point and was lower overall compared to other cell subtypes (**Figure 3**).

Antimicrobial Peptides Are Upregulated in Human Skin by *S. epidermidis*

Staphylococcus epidermidis isolates from healthy adults have been reported to show widespread production of bacteriocins (55) and in addition they can stimulate keratinocytes to produce antimicrobial peptides (4). We investigated if *S. epidermidis* triggers expression of antimicrobial peptides in our *ex vivo* skin model. We found that 24 h of *S. epidermidis* colonization significantly induced expression of defensin β4 (Defβ4) and cathelicidin (LL37) ($p < 0.01$) (**Figure 4**). Upregulation of LL37 was maintained 48 h post *S. epidermidis* colonization ($p < 0.01$) in contrast to defensin Defβ4 that was downregulated ($p < 0.05$). In addition, *S. epidermidis* colonization of human skin resulted in downregulation of pro-inflammatory IL-1α after 24 and 96 h ($p < 0.05$) (**Figure 4**).

Early Regulation of GD T Cell Gene Expression by *S. epidermidis*

Human GD T cells in the skin exhibit both pro-inflammatory and regulatory functions (32). Deciphering the underlying mechanisms that contribute to induction of effector vs. regulatory GD T cell functions, including expression of cytotoxic molecules, is key to understanding skin homeostasis. To understand the effect of *S. epidermidis* on skin GD T cells during initial phases of colonization, we sorted GD T cells from normal skin (**Figure 5A**) and stimulated them with *S. epidermidis for* 1 h. We evaluated the expression of well-known genes previously described to play a role in GD T cell cytotoxic functions. We found a 6-7-fold induction in Fas ligand (FASLG) and Granulysin (GNLY) in *S. epidermidis* treated cells compared to control, untreated GD T cells (**Figure 5B**). Additionally, we observed increased expression of the transcription factor PLZF, which is responsible for selection of GD innate natural killer T cells (56), as well as CCL4, a monokine with inflammatory and chemokinetic properties (**Figure 5B**). Previous studies have observed increased CCL4 expression by GD T cells following engagement of the natural cytotoxicity receptor NKp30 on the GD T cell surface (57).

Intracellular MRSA Killing Is Enhanced After Exposure to *S. epidermidis*

We have previously reported that MRSA, the most common cutaneous pathogen, suppresses P-2 induction in skin cells (43), revealing a novel mechanism by which *S. aureus* may escape cutaneous immunity to cause persistent infections. Here, we report that in contrast to MRSA (43), *S. epidermidis* up-regulates P-2 expression in an *ex vivo* skin model (see **Figure 1**) and in the single cell suspension culture model (**Figure 6**). In order to further analyze *S. epidermidis*-mediated induction of P-2 in *ex vivo* human skin, we isolated skin cells and established a single cell type culture system. We found an increase in the frequency of GD T cells after 24 h stimulation with *S. epidermidis* (**Figure 6A**), which agrees with findings from the *ex vivo* human skin model (**Figure 1**). Furthermore, expression of P-2 was also increased in the GD T cells after 24 h of *S. epidermidis* stimulation (**Figure 6B**). Most importantly, we show that cells stimulated with *S. epidermidis* demonstrate an

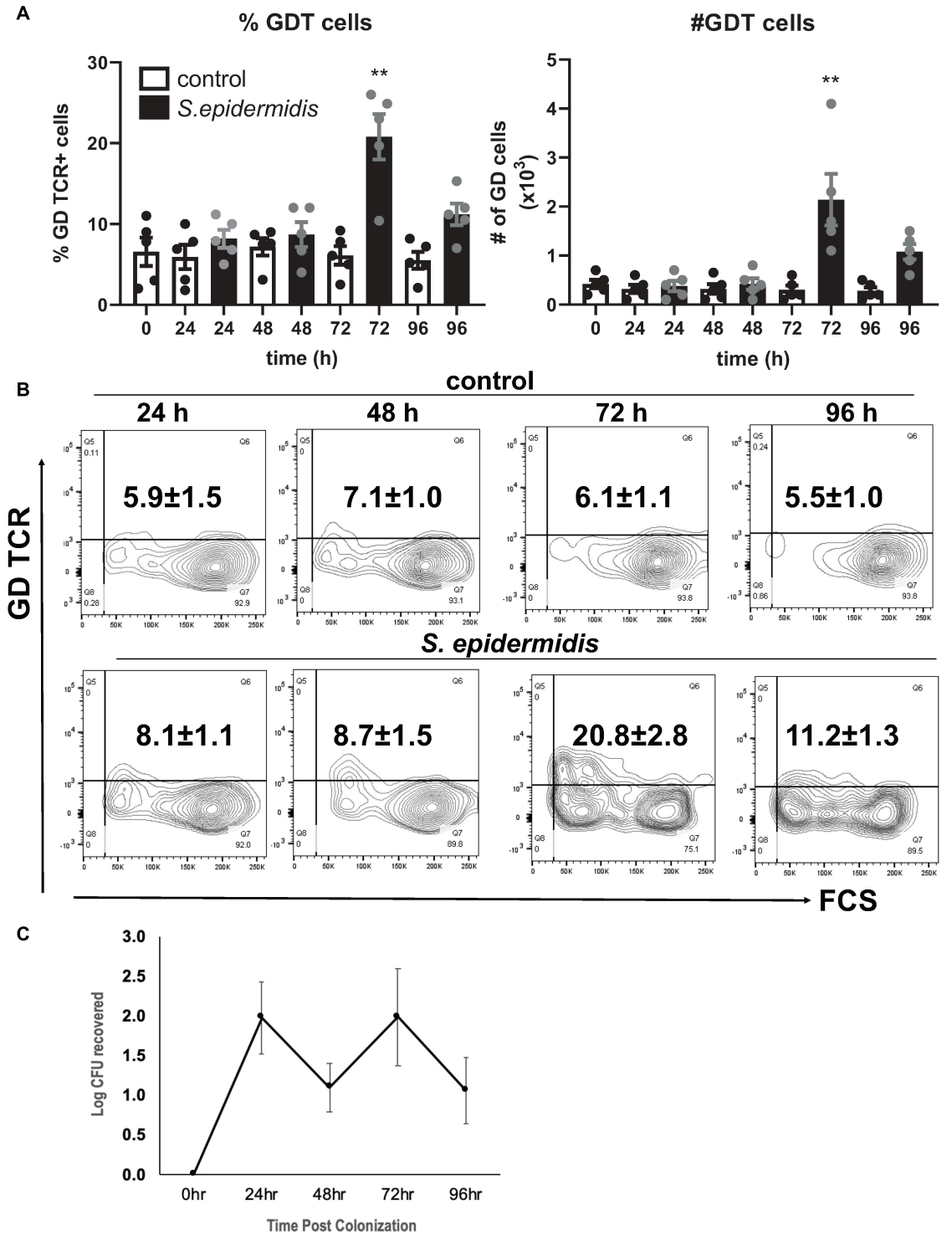

FIGURE 1 | *Staphylococcus epidermidis* increases the number of GD T cells in human skin *ex vivo*. Control, uncolonized, and *S. epidermidis* colonized skin was maintained on air liquid interface and collected at indicated time points (0, 24, 48, 72, and 96 h). Single cell suspensions were obtained and labeled with live/dead stain, CD45, CD3, and GD TCR. **(A)** Cells were analyzed using flow cytometry and gated on the CD45+ CD3+ GDT+ population. Bar graphs show SEM frequency (%) and SEM number (#) of skin GD T cells ($n = 5$). **(B)** Representative contour plots showing frequency of GD TCR in control and *S. epidermidis* colonized skin. **(C)** Number of *S. epidermidis* colony forming units (CFU) recovered from *ex vivo* skin explants colonized with *S. epidermidis* CCN021 on day 0 through day 4. Data represent at least two technical replicates and five independent biological replicates per group. $^{**}p < 0.01$ (two-way ANOVA with Holm-Sidak multiple-comparison test).

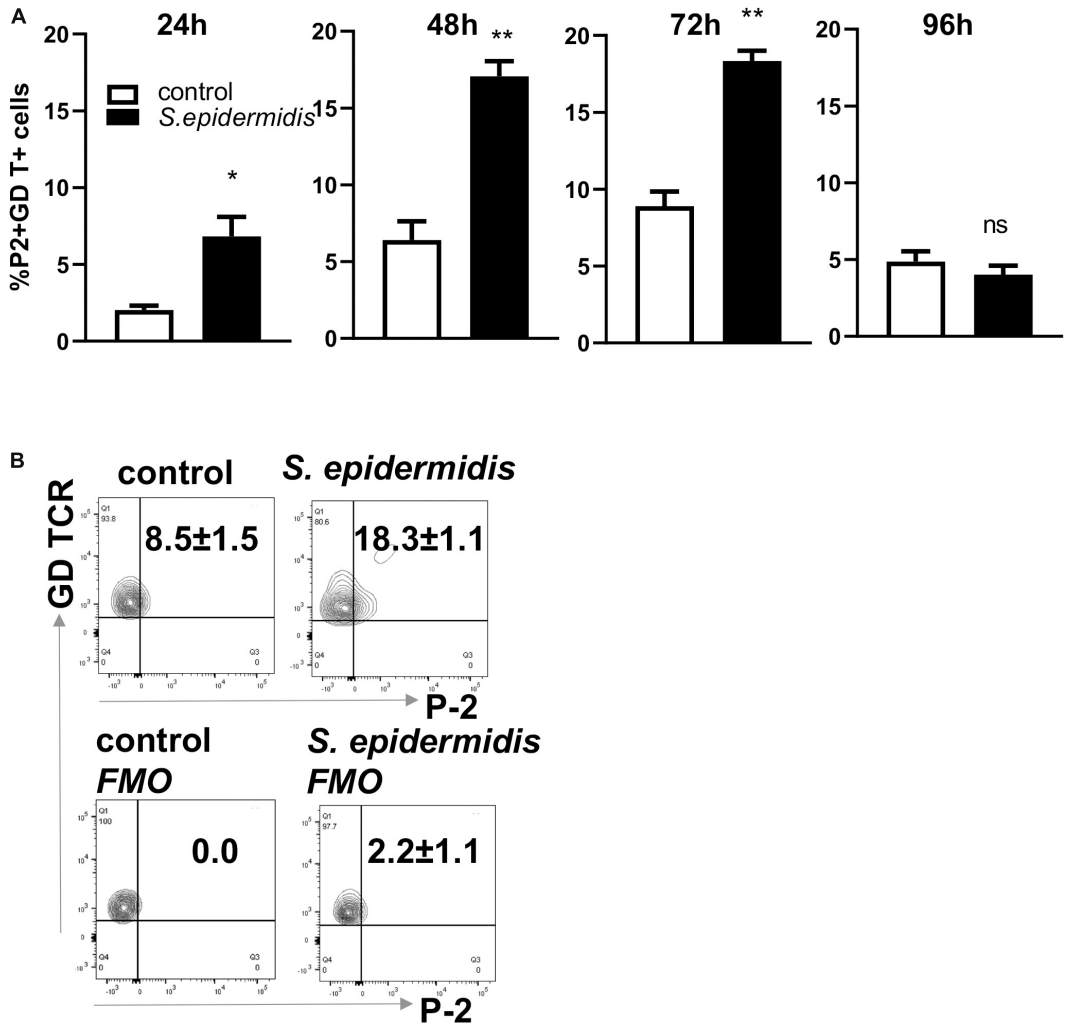

FIGURE 2 | Colonization of human skin with *Staphylococcus epidermis* induces P-2 in GD T cells. **(A)** Control and *S. epidermidis* colonized human skin was collected at indicated time points (24, 48, 72, and 96 h) for FISH-Flow. Single cell suspensions were obtained using Collagenase D and labeled with live/dead stain. Using FISH-Flow RNA assay, P-2 RNA levels were analyzed in the CD45+, CD3+ GD TCR+ cell population. **(B)** Representative dot plot graph showing expression of mRNA P-2 in gated CD45+ CD3+ GD TCR+ T cells at 72 h in *S. epidermidis* colonized skin or non-colonized (control). FMO-fluorescence minus one. Bar graphs show SEM of P-2 mRNA positive cells within skin GD T cells ($n = 3$). Data represent at least two technical replicates with three independent biological replicates per group. $^{*}p < 0.05$, $^{**}p < 0.01$ as calculated using Student *t*-test.

increased capability to kill intracellular MRSA (**Figure 6C**). We observed this same result after repeating stimulations with 2 additional *S. epidermidis* strains, *S. epidermidis* ATCC 12228 and commensal isolate *S. epidermidis* CCN0024 (**Supplementary Figure S2**). In addition, we found that *S. epidermidis* CCN021 stimulated GD T cells upregulate expression of TLR2 and TLR1, but not TLR6 (**Figure 6D**).

DISCUSSION

Pore-forming proteins permeabilize membranes of infected cells targeted for immune elimination and together with antimicrobial peptides represent the key effector molecules of the epithelial barriers. GD T cells, as surveillance cells in the skin, constitutively express mRNA for granzyme A and B and perforin and contain significant esterase activity (58). We provided the first evidence to show that human skin GD T cells constitutively express antimicrobial protein P-2 (43). In contrast to other secreted pore forming proteins, P-2 is a transmembrane protein that efficiently kills intracellular bacteria. IFNγ, type I interferons, and LPS have been implicated in the regulation of its expression (37, 38). We have previously reported that MRSA, the most common skin pathogen, suppresses P2-induction in skin cells (43), revealing a novel mechanism by which *S. aureus* may escape cutaneous immunity to cause persistent infections. Here we show that, in contrast to MRSA, *S. epidermidis* up-regulates P-2 expression in human skin and in single cell suspensions. We also demonstrate that *S. epidermidis* upregulates P-2 mRNA expression in multiple skin cell types including GD T cells,

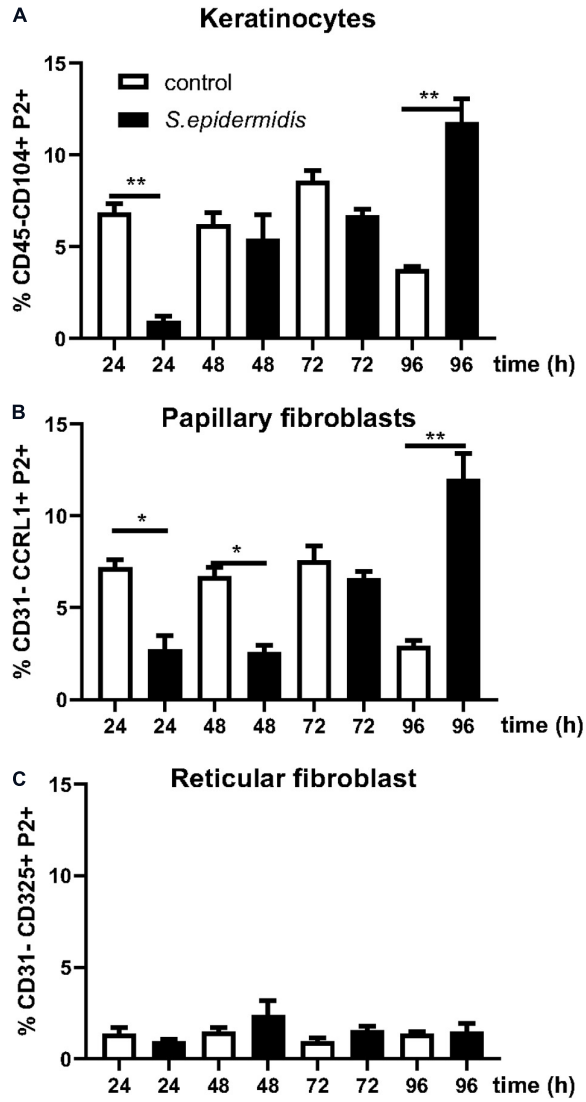

FIGURE 3 | *Staphylococcus epidermidis* colonization induces P-2 in human keratinocytes and papillary fibroblasts. Control, non-colonized, and *S. epidermidis* colonized human skin was maintained at air liquid interface and collected at indicated time points (24, 48, 72, and 96 h) for FISH-Flow. Single cell suspensions were labeled with live/dead stain. Using FISH-Flow RNA assay, P-2 RNA levels were analyzed in **(A)** CD45-, CD31-, CD104+ cells (keratinocytes), or **(B)** CD45-, CD31-, CCRL1+ (papillary fibroblasts), and **(C)** CD45-, CD31-, CD325+ cells (reticular fibroblasts). Bar graphs show percentage of P-2 mRNA positive cells within each CD45-CD31-skin cell population. Data represent at least two experiments with three independent biological replicates per group. $^{*}p < 0.05$, $^{**}p < 0.01$ (two-way ANOVA with Holm-Sidak multiple-comparison test).

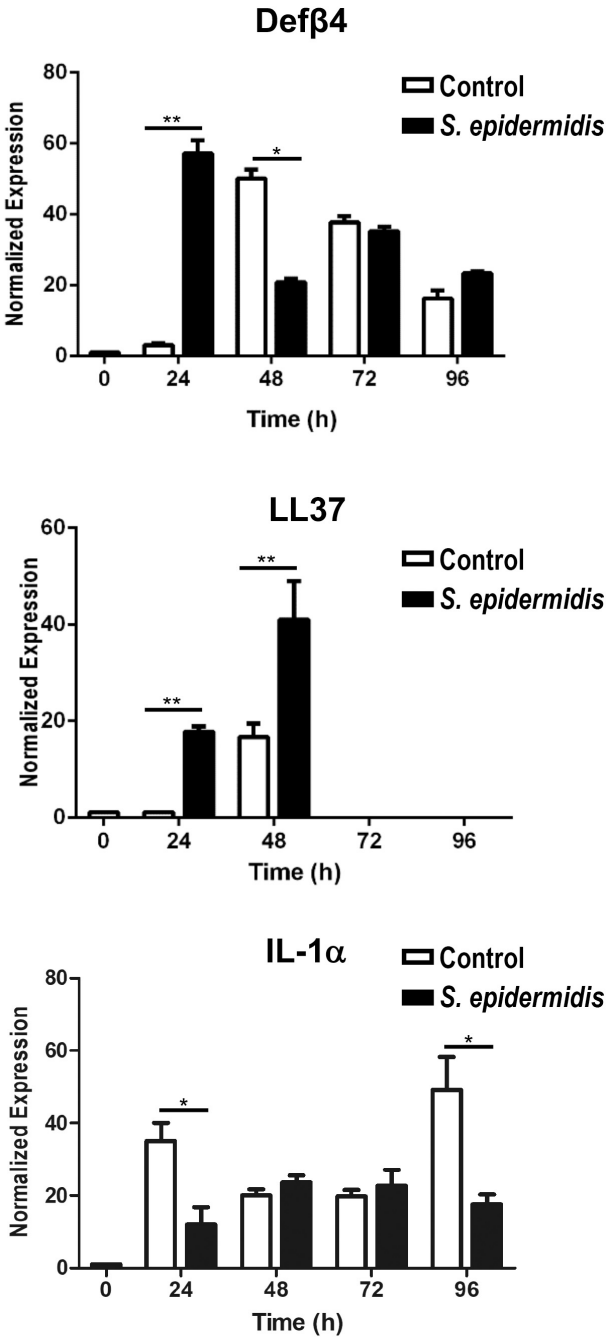

FIGURE 4 | Antimicrobial and inflammatory responses mediated by *Staphylococcus epidermidis* in human *ex vivo* model. Expression levels of antimicrobial peptides Defβ4, LL-37, and pro-inflammatory cytokine IL-1α were evaluated by qPCR from non-colonized and *S. epidermidis* colonized skin at 24, 48, 72, and 96 h ($n = 3$ for each treatment group and time point). $^{*}p < 0.05$, $^{**}p < 0.01$ as calculated using Student *t*-test.

basal keratinocytes, and papillary fibroblasts. Most importantly, we observed a decrease in number of intracellular MRSA in skin stimulated by *S. epidermidis*, which correlates with *S. epidermidis*-mediated P-2 induction. These data provide new insights regarding mechanisms of P-2 expression and function and elucidate novel approaches to protect skin from infections caused by intracellular pathogens.

Gamma delta T cells represent a major T cell subset involved in the surveillance of epithelial surfaces (skin, gastrointestinal, reproductive, and respiratory tracts). It is well establish that GD T cells, upon recognition of pathogens, effectively proliferate,

A

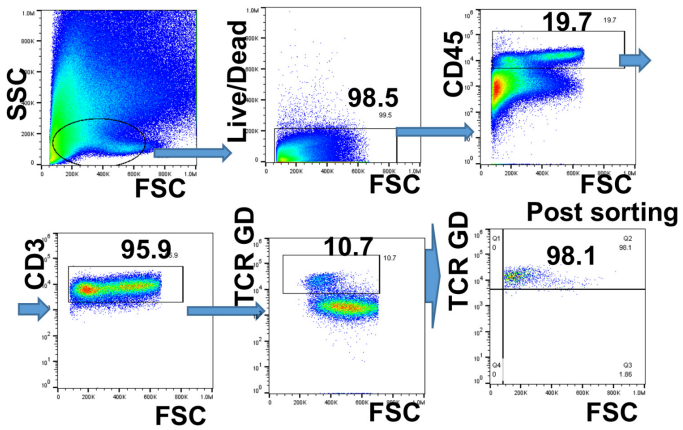

B

Gene	Gene name	Fold change*	P value
GNLY	Granulysin	7.61	0.015
FASLG	Fas Ligand	6.76	0.021
PLZF	Promyelocytic Leukemia Zinc Finger	6.52	0.028
CCL4	C-C Motif Chemokine Ligand 4	5.40	0.046

*Fold change of log2-transformed, normalized data.

FIGURE 5 | Differential gene expression in human GD T cells as an early response to *Staphylococcus epidermidis*. Human skin cells were isolated using the Miltenyi Whole Skin Dissociation kit (Miltenyi, Bergisch-Gladbach, Germany) and GD T cells were sorted from the skin cell suspension using fluorescence-activated cell sorting. **(A)** Gating strategy for GD T cell sorting. **(B)** Cells were stimulated with *S. epidermidis* for 1 h and changes in gene expression between uninfected and infected cells were measured using the BioMark IFC 96 × 96 chip (Fluidigm). Changes in gene expression are expressed as log2 of fold change (n = 3). *P*-values were calculated using Student *t*-test.

secrete pro-inflammatory cytokines, and activate their cytolytic machinery (perforin and granzymes) to kill the pathogen (59). Clonally expanded GD T cells can establish long-lasting immunity against recurrent *S. aureus* skin infections (33). In contrast, GD T cell deficient mice develop large skin lesions after infection with *S. aureus* (60). However, encounters with commensal microbes by skin GD T cells and how such interactions affect their response to pathogens remains poorly understood. Here we provide the first evidence that the common skin commensal, *S. epidermidis,* upregulates the frequency of GD T cells and induces the expression of P-2, which is associated with an increased capability to eliminate intracellular MRSA. Our data on increased frequency of skin GD T cells after colonization with *S. epidermidis* supports the hypothesis that under normal conditions the presence of *S. epidermidis* on the skin surface strengthens cutaneous innate defenses (9, 10).

We observed that during the early steps of colonization, prior to P-2 induction, *S. epidermidis* upregulates the GD T cell cytotoxic molecules Fas Ligand (FASLG) and granulysin (GNLY). This may contribute to the GD T cell mediated antimicrobial immune response, in addition to P-2 induction at later time points. We are currently expanding these studies to *in vivo* animal models. *S. epidermidis*, when topically applied to murine skin, induces specific IL-17 producing T cells that persist as tissue-resident memory T cells (13). However, to the best of our knowledge, our study is the first report that shows specific effect of *S. epidermidis* on induction of human skin GD T cell responses.

Previous reports indicate that a commensal strain of *S. epidermidis* and non-commensal strain *S. carnosus* have different modifications of the lipoprotein (Lpp) lipid moieties (61). The essential receptor for recognition of bacterial Lpp is TLR2. However, the degree of acylation at the lipid moiety can be discriminated by additional TLRs, such as TLR1 and TLR6, which form heterodimers with TLR2 (62–64). Importantly, these lipoprotein modifications were implicated in the differential immune responses where commensal staphylococcal species dampened IFNγ, TNFα, and IL-12 production compared to pathogenic staphylococcal species (61). We have found that

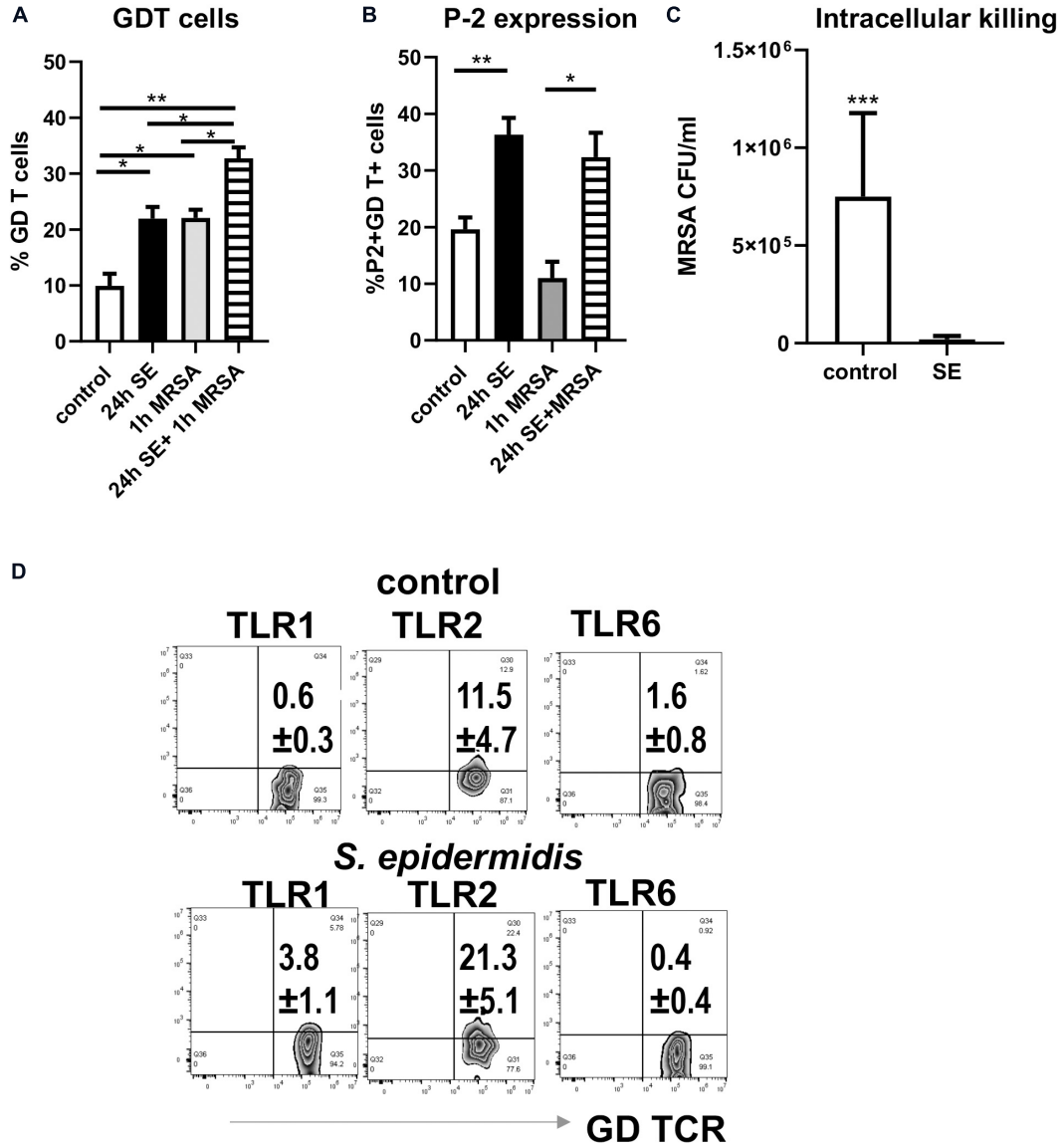

FIGURE 6 | Pre-treatment of skin cells with *Staphylococcus epidermidis* increases frequency of GD T cells, stimulates P-2 expression, and limits survival of intracellular MRSA. Single skin cells were exposed to *S. epidermidis* at MOI 1:20 or media control for 24 h. After washing to remove *S. epidermidis*, cells were infected with MRSA (MOI 1:20) for 1 h to allow intracellular infection, and extracellular bacteria were subsequently removed by gentamicin treatment. **(A)** Frequency of GDT cells and **(B)** P2 mRNA expression in CD45+ CD3+ GD TCR+ cells as determined by FISH-Flow ($n = 3$ biological replicates). **(C)** Bar graph showing the number of intracellular MRSA (CFU/ml) upon hypotonic lysis of control and *S. epidermidis* pre-treated cells ($n = 3$ biological replicates). **(D)** Expression of TLR1, TLR2, and TLR6 on gated CD45+ CD3+ TCR GD+ T cells. Data represent at least two experiments with three independent biological replicates per group. $^{*}p < 0.05$, $^{**}p < 0.01$ as calculated using two-way ANOVA with Holm-Sidak multiple-comparison **(A)** and $^{***}p < 0.001$ as calculated using Student *t*-test **(B)**.

a 24 h stimulation with *S. epidermidis* upregulates TLR2 and TLR1, but not TLR6 on GD T cells. We postulate that *S. epidermidis*, through recognition of TLR2/TLR1 heterodimers on cutaneous GD T cells, regulates not only Th1 responses but also cytotoxic mediators such as P-2. The recognition of TLR2/TLR1 heterodimers may even be strain specific (12) warranting further studies on the mechanisms of P-2 induction by *S. epidermidis* CCN021.

It has been shown that *S. epidermidis* colonization of skin induces AMP production by keratinocytes (5, 7, 8, 65). Our findings regarding induction of LL37 and Defβ4 during early phases of human skin colonization with *S. epidermidis* are in line with these results. Kinetics of P-2 induction upon *S. epidermidis* colonization shows dynamic control and cell specificity that integrates with the kinetics of AMP production. In GD T cells, the induction of P-2 is rapid and maintained, persisting from 24 to 72 h post colonization whereas in keratinocytes and papillary fibroblasts it shows complementary activation at 96 h. These data suggest that the initial protective response derives from GD T cells whereas in keratinocytes activation of P-2 follows initial

activation of AMPs, cathelicidin, and β-defensin. The human skin *ex vivo* model is comprised of the epidermis and dermis with no circulation, thus limiting the studies on modulation of the immune response by *S. epidermidis* to resident innate immune cells, while the potential role of adaptive immunity would require *in vivo* models.

The initial findings presented here also provide a functional readout of *S. epidermidis* colonization and P-2 upregulation: decrease of the intracellular pathogen *S. aureus*. We observed suppression of the pro-inflammatory cytokine IL-1α after colonization with *S. epidermidis*. Previously, we showed that *S. aureus* induces IL-1α in non-healing diabetic foot ulcers (50), suggesting that *S. epidermidis* may have additional mechanisms to neutralize the damaging effects of pathogenic organisms. The limitation of our study was sequential stimulation of human skin and primary cells by *S. epidermidis* and *S. aureus*. Future *in vivo* studies are required to confirm antimicrobial effects of *S. epidermidis* in the presence of pathogenic *S. aureus*. Additionally, future studies that block P-2 expression will be necessary to confirm that enhanced *S. aureus* killing upon *S. epidermidis* treatment is solely due to P-2 upregulation. Despite these limitations, this work provides an intriguing possibility that colonization of *S. epidermidis* may prevent and/or protect from bacterial skin infections through modulation of P-2.

In summary, we confirmed that colonization with commensal *S. epidermidis* in human *ex vivo* skin modulates the innate immune system by activating GD T cells, promoting antimicrobial peptide production, and upregulating the antimicrobial protein P-2. Understanding how commensal bacteria regulate P-2 expression represents the first step toward identifying mechanisms by which P-2 contributes to cutaneous homeostasis and host defense mechanisms and may reveal new approaches for preventing and treating skin infections.

DATA AVAILABILITY STATEMENT

The raw data supporting the conclusions of this article will be made available by the authors, without undue reservation.

ETHICS STATEMENT

The studies involving human participants were reviewed and approved by Institutional Review Board at the UM Miller School of Medicine (exempt from human subject research under CFR46.101.2). The patients provided their written informed consent to participate in this study.

AUTHOR CONTRIBUTIONS

MT-C and NS obtained funding, and conceived and coordinated the experiments. IP, KO'N, LP, CH, JB, VC, DG, OS, and SH performed the experiments and analyzed the data. KO'N, IP, and NS performed the statistical analyses. GP and ST provided reagents. NS, IP, and MT-C wrote the manuscript. All authors were involved in writing and had final approval of the submitted and published versions of the manuscript.

FUNDING

This work was supported by NIH NR015649 (MT-C and NS), DK119085 (MT-C), Dwoskin family gift to the Dr. Phillip Frost Department of Dermatology and Cutaneous Surgery (MT-C), and by Department of Microbiology and Immunology P2 funds (NS). VC was supported by Wound Healing Society Summer Research Fellowship.

ACKNOWLEDGMENTS

We dedicate this work to late Dr. Eckhard Podack without whom studies of Perforin-2 would not be possible. We are grateful to all members of MT-C and NS laboratories for their overall support and Prof. Stephen C. Davis for the gift of *S. epidermidis* ATCC 12228.

SUPPLEMENTARY MATERIAL

The Supplementary Material for this article can be found online at: https://www.frontiersin.org/articles/10.3389/fimmu.2020.550946/full#supplementary-material

FIGURE S1 | Cell viability of *ex vivo* skin tissue with or without *S. epidermidis* colonization via flow cytometry (data represented as mean ± SEM, n = 3–4 skin samples).

FIGURE S2 | Pre-treatment of skin cells with *S. epidermidis* CCN0024 and ATCC 12228 strains limits intracellular MRSA survival. Single skin cells were exposed to single *S. epidermidis* strain at MOI 1:20 or media control for 24 h. After washing to remove *S. epidermidis*, cells were infected with MRSA (MOI 1:20) for 1 h to allow intracellular infection, and extracellular bacteria were subsequently removed by gentamicin treatment. Bar graph shows the number of intracellular MRSA (CFU/ml) upon hypotonic lysis of control and *S. epidermidis* pre-treated cells. $^{****}p < 0.0001$ as calculated using one-way ANOVA with Dunnett's multiple comparisons test, which compared each *S. epidermidis* pre-treatment with non-pretreated control cells.

REFERENCES

1. Belkaid Y, Harrison OJ. Homeostatic immunity and the microbiota. *Immunity.* (2017) 46:562–76. doi: 10.1016/j.immuni.2017.04.008
2. Stacy A, Belkaid Y. Microbial guardians of skin health. *Science.* (2019) 363:227–8. doi: 10.1126/science.aat4326
3. Lukic J, Chen V, Strahinic I, Begovic J, Lev-Tov H, Davis SC, et al. Probiotics or pro-healers: the role of beneficial bacteria in tissue repair. *Wound Repair Regen.* (2017) 25:912–22. doi: 10.1111/wrr.12607
4. Lai Y, Cogen AL, Radek KA, Park HJ, Macleod DT, Leichtle A, et al. Activation of TLR2 by a small molecule produced by *Staphylococcus epidermidis* increases antimicrobial defense against bacterial skin infections. *J Invest Dermatol.* (2010) 130:2211–21. doi: 10.1038/jid.2010.123
5. Ommori R, Ouji N, Mizuno F, Kita E, Ikada Y, Asada H. Selective induction of antimicrobial peptides from keratinocytes by staphylococcal bacteria. *Microb Pathog.* (2013) 56:35–9. doi: 10.1016/j.micpath.2012.11.005
6. Nakatsuji T, Chen TH, Narala S, Chun KA, Two AM, Yun T, et al. Antimicrobials from human skin commensal bacteria protect against

Staphylococcus aureus and are deficient in atopic dermatitis. *Sci Transl Med.* (2017) 9:eaah4680. doi: 10.1126/scitranslmed.aah4680
7. Li D, Lei H, Li Z, Li H, Wang Y, Lai Y. A novel lipopeptide from skin commensal activates TLR2/CD36-p38 MAPK signaling to increase antibacterial defense against bacterial infection. *PLoS One.* (2013) 8:e58288. doi: 10.1371/journal.pone.0058288
8. Liu Q, Liu Q, Meng H, Lv H, Liu Y, Liu J, et al. *Staphylococcus epidermidis* contributes to healthy maturation of the nasal microbiome by stimulating antimicrobial peptide production. *Cell Host Microbe.* (2020) 27:68–78.e5. doi: 10.1016/j.chom.2019.11.003
9. Christensen GJ, Bruggemann H. Bacterial skin commensals and their role as host guardians. *Benef Microbes.* (2014) 5:201–15. doi: 10.3920/BM2012.0062
10. Gallo RL, Nakatsuji T. Microbial symbiosis with the innate immune defense system of the skin. *J Invest Dermatol.* (2011) 131:1974–80. doi: 10.1038/jid.2011.182
11. Cogen AL, Yamasaki K, Muto J, Sanchez KM, Crotty Alexander L, Tanios J, et al. *Staphylococcus epidermidis* antimicrobial delta-toxin (phenol-soluble modulin-gamma) cooperates with host antimicrobial peptides to kill group A Streptococcus. *PLoS One.* (2010) 5:e8557. doi: 10.1371/journal.pone.0008557
12. Zhou W, Spoto M, Hardy R, Guan C, Fleming E, Larson PJ, et al. Host-specific evolutionary and transmission dynamics shape the functional diversification of *Staphylococcus epidermidis* in human skin. *Cell.* (2020) 180:454–470.e18. doi: 10.1016/j.cell.2020.01.006
13. Naik S, Bouladoux N, Linehan JL, Han SJ, Harrison OJ, Wilhelm C, et al. Commensal-dendritic-cell interaction specifies a unique protective skin immune signature. *Nature.* (2015) 520:104–8. doi: 10.1038/nature14052
14. Linehan JL, Harrison OJ, Han SJ, Byrd AL, Vujkovic-Cvijin I, Villarino AV, et al. Non-classical immunity controls microbiota impact on skin immunity and tissue repair. *Cell.* (2018) 172:784–796.e18. doi: 10.1016/j.cell.2017.12.033
15. Scharschmidt TC, Vasquez KS, Truong HA, Gearty SV, Pauli ML, Nosbaum A, et al. A wave of regulatory T cells into neonatal skin mediates tolerance to commensal microbes. *Immunity.* (2015) 43:1011–21. doi: 10.1016/j.immuni.2015.10.016
16. Young JL, Goodall JC, Beacock-Sharp H, Gaston JS. Human gamma delta T-cell recognition of *Yersinia enterocolitica*. *Immunology.* (1997) 91:503–10. doi: 10.1046/j.1365-2567.1997.00289.x
17. Barisa M, Kramer AM, Majani Y, Moulding D, Saraiva L, Bajaj-Elliott M, et al. *E. coli* promotes human Vgamma9Vdelta2 T cell transition from cytokine-producing bactericidal effectors to professional phagocytic killers in a TCR-dependent manner. *Sci Rep.* (2017) 7:2805. doi: 10.1038/s41598-017-02886-8
18. Chen ZW. Protective immune responses of major Vgamma2Vdelta2 T-cell subset in *M. tuberculosis* infection. *Curr Opin Immunol.* (2016) 42:105–12. doi: 10.1016/j.coi.2016.06.005
19. Marx S, Wesch D, Kabelitz D. Activation of human gamma delta T cells by *Mycobacterium tuberculosis* and Daudi lymphoma cells: differential regulatory effect of IL-10 and IL-12. *J Immunol.* (1997) 158:2842–8.
20. Hara T, Mizuno Y, Takaki K, Takada H, Akeda H, Aoki T, et al. Predominant activation and expansion of V gamma 9-bearing gamma delta T cells in vivo as well as in vitro in *Salmonella* infection. *J Clin Invest.* (1992) 90:204–10. doi: 10.1172/JCI115837
21. Kurup SP, Harty JT. gammadelta T cells and immunity to human malaria in endemic regions. *Ann Transl Med.* (2015) 3(Suppl. 1):S22. doi: 10.3978/j.issn.2305-5839.2015.02.22
22. Poccia F, Agrati C, Martini F, Capobianchi MR, Wallace M, Malkovsky M. Antiviral reactivities of gammadelta T cells. *Microbes Infect.* (2005) 7:518–28. doi: 10.1016/j.micinf.2004.12.009
23. Knight A, Madrigal AJ, Grace S, Sivakumaran J, Kottaridis P, Mackinnon S, et al. The role of Vdelta2-negative gammadelta T cells during cytomegalovirus reactivation in recipients of allogeneic stem cell transplantation. *Blood.* (2010) 116:2164–72. doi: 10.1182/blood-2010-01-255166
24. Fisch P, Malkovsky M, Kovats S, Sturm E, Braakman E, Klein BS, et al. Recognition by human V gamma 9/V delta 2 T cells of a GroEL homolog on Daudi Burkitt's lymphoma cells. *Science.* (1990) 250:1269–73. doi: 10.1126/science.1978758
25. Fisch P, Oettel K, Fudim N, Surfus JE, Malkovsky M, Sondel PM. MHC-unrestricted cytotoxic and proliferative responses of two distinct human gamma/delta T cell subsets to Daudi cells. *J Immunol.* (1992) 148:2315–23.
26. Havran WL, Allison JP. Developmentally ordered appearance of thymocytes expressing different T-cell antigen receptors. *Nature.* (1988) 335:443–5. doi: 10.1038/335443a0
27. Havran WL, Fitch FW. Characterization of murine cytolytic-helper hybrid T cell clones. *Nature.* (1987) 325:65–7. doi: 10.1038/325065a0
28. Havran WL, Grell S, Duwe G, Kimura J, Wilson A, Kruisbeek AM, et al. Limited diversity of T-cell receptor gamma-chain expression of murine Thy-1+ dendritic epidermal cells revealed by V gamma 3-specific monoclonal antibody. *Proc Natl Acad Sci USA.* (1989) 86:4185–9. doi: 10.1073/pnas.86.11.4185
29. Weintraub BC, Jackson MR, Hedrick SM. Gamma delta T cells can recognize nonclassical MHC in the absence of conventional antigenic peptides. *J Immunol.* (1994) 153:3051–8.
30. Rust C, Orsini D, Kooy Y, Koning F. Reactivity of human gamma delta T cells to staphylococcal enterotoxins: a restricted reaction pattern mediated by two distinct recognition pathways. *Scand J Immunol.* (1993) 38:89–94. doi: 10.1111/j.1365-3083.1993.tb01698.x
31. Rust CJ, Koning F. Gamma delta T cell reactivity towards bacterial superantigens. *Semin Immunol.* (1993) 5:41–6. doi: 10.1006/smim.1993.1006
32. Nielsen MM, Witherden DA, Havran WL. gammadelta T cells in homeostasis and host defence of epithelial barrier tissues. *Nat Rev Immunol.* (2017) 17:733–45. doi: 10.1038/nri.2017.101
33. Dillen CA, Pinsker BL, Marusina AI, Merleev AA, Farber ON, Liu H, et al. Clonally expanded gammadelta T cells protect against *Staphylococcus aureus* skin reinfection. *J Clin Invest.* (2018) 128:1026–42. doi: 10.1172/JCI96481
34. He X, Zhang Y, Yu Z. An Mpeg (macrophage expressed gene) from the Pacific oyster *Crassostrea gigas*: molecular characterization and gene expression. *Fish Shellfish Immunol.* (2011) 30:870–6. doi: 10.1016/j.fsi.2011.01.009
35. Kemp IK, Coyne VE. Identification and characterisation of the Mpeg1 homologue in the South African abalone, *Haliotis midae*. *Fish Shellfish Immunol.* (2011) 31:754–64. doi: 10.1016/j.fsi.2011.07.010
36. McCormack R, Podack ER. Perforin-2/Mpeg1 and other pore-forming proteins throughout evolution. *J Leukoc Biol.* (2015) 98:761–8. doi: 10.1189/jlb.4MR1114-523RR
37. McCormack RM, de Armas LR, Shiratsuchi M, Fiorentino DG, Olsson ML, Lichtenheld MG, et al. Perforin-2 is essential for intracellular defense of parenchymal cells and phagocytes against pathogenic bacteria. *eLife.* (2015) 4:e06508. doi: 10.7554/eLife.06508
38. McCormack RM, Lyapichev K, Olsson ML, Podack ER, Munson GP. Enteric pathogens deploy cell cycle inhibiting factors to block the bactericidal activity of Perforin-2. *eLife.* (2015) 4:e06505. doi: 10.7554/eLife.06505
39. McCormack R, Bahnan W, Shrestha N, Boucher J, Barreto M, Barrera CM, et al. Perforin-2 protects host cells and mice by restricting the vacuole to cytosol transitioning of a bacterial pathogen. *Infect Immun.* (2016) 84:1083–91. doi: 10.1128/IAI.01434-15
40. Pang SS, Bayly-Jones C, Radjainia M, Spicer BA, Law RHP, Hodel AW, et al. The cryo-EM structure of the acid activatable pore-forming immune effector Macrophage-expressed gene 1. *Nat Commun.* (2019) 10:4288. doi: 10.1038/s41467-019-12279-2
41. McCormack R, de Armas L, Shiratsuchi M, Podack ER. Killing machines: three pore-forming proteins of the immune system. *Immunol Res.* (2013) 57:268–78. doi: 10.1007/s12026-013-8469-9
42. McCormack R, de Armas LR, Shiratsuchi M, Ramos JE, Podack ER. Inhibition of intracellular bacterial replication in fibroblasts is dependent on the perforin-like protein (perforin-2) encoded by macrophage-expressed gene 1. *J Innate Immun.* (2013) 5:185–94. doi: 10.1159/000345249
43. Strbo N, Pastar I, Romero L, Chen V, Vujanac M, Sawaya AP, et al. Single cell analyses reveal specific distribution of anti-bacterial molecule Perforin-2 in human skin and its modulation by wounding and *Staphylococcus aureus* infection. *Exp Dermatol.* (2019) 28:225–32. doi: 10.1111/exd.13870
44. Martineau F, Picard FJ, Ke D, Paradis S, Roy PH, Ouellette M, et al. Development of a PCR assay for identification of staphylococci at genus and species levels. *J Clin Microbiol.* (2001) 39:2541–7. doi: 10.1128/JCM.39.7.2541-2547.2001
45. Vandecasteele SJ, Peetermans WE, Merckx R, Van Eldere J. Quantification of expression of *Staphylococcus epidermidis* housekeeping genes with Taqman quantitative PCR during in vitro growth and under different conditions. *J Bacteriol.* (2001) 183:7094–101. doi: 10.1128/JB.183.24.7094-7101.2001

46. Pang YY, Schwartz J, Thoendel M, Ackermann LW, Horswill AR, Nauseef WM. *agr*-Dependent interactions of *Staphylococcus aureus* USA300 with human polymorphonuclear neutrophils. *J Innate Immun.* (2010) 2:546–59. doi: 10.1159/000319855
47. Yoon DJ, Fregoso DR, Nguyen D, Chen V, Strbo N, Fuentes JJ, et al. A tractable, simplified ex vivo human skin model of wound infection. *Wound Repair Regen.* (2019) 27:421–5. doi: 10.1111/wrr.12712
48. Pastar I, Stojadinovic O, Krzyzanowska A, Barrientos S, Stuelten C, Zimmerman K, et al. Attenuation of the transforming growth factor beta-signaling pathway in chronic venous ulcers. *Mol Med.* (2010) 16:92–101. doi: 10.2119/molmed.2009.00149
49. Ramirez HA, Pastar I, Jozic I, Stojadinovic O, Stone RC, Ojeh N, et al. *Staphylococcus aureus* triggers induction of miR-15B-5P to diminish DNA repair and deregulate inflammatory response in diabetic foot ulcers. *J Invest Dermatol.* (2018) 138:1187–96. doi: 10.1016/j.jid.2017.11.038
50. Stojadinovic O, Tomic-Canic M. Human ex vivo wound healing model. *Methods Mol Biol.* (2013) 1037:255–64. doi: 10.1007/978-1-62703-505-7_14
51. Finak G, McDavid A, Yajima M, Deng J, Gersuk V, Shalek AK, et al. MAST: a flexible statistical framework for assessing transcriptional changes and characterizing heterogeneity in single-cell RNA sequencing data. *Genome Biol.* (2015) 16:278. doi: 10.1186/s13059-015-0844-5
52. Bolton DL, McGinnis K, Finak G, Chattopadhyay P, Gottardo R, Roederer M. Combined single-cell quantitation of host and SIV genes and proteins ex vivo reveals host-pathogen interactions in individual cells. *PLoS Pathog.* (2017) 13:e1006445. doi: 10.1371/journal.ppat.1006445
53. Janson DG, Saintigny G, van Adrichem A, Mahe C, El Ghalbzouri A. Different gene expression patterns in human papillary and reticular fibroblasts. *J Invest Dermatol.* (2012) 132:2565–72. doi: 10.1038/jid.2012.192
54. Woodley DT. Distinct fibroblasts in the papillary and reticular dermis: implications for wound healing. *Dermatol Clin.* (2017) 35:95–100. doi: 10.1016/j.det.2016.07.004
55. Janek D, Zipperer A, Kulik A, Krismer B, Peschel A. High frequency and diversity of antimicrobial activities produced by nasal *Staphylococcus* strains against bacterial competitors. *PLoS Pathog.* (2016) 12:e1005812. doi: 10.1371/journal.ppat.1005812
56. Dimova T, Brouwer M, Gosselin F, Tassignon J, Leo O, Donner C, et al. Effector Vgamma9Vdelta2 T cells dominate the human fetal gammadelta T-cell repertoire. *Proc Natl Acad Sci USA.* (2015) 112:E556–65. doi: 10.1073/pnas.1412058112
57. Hudspeth K, Fogli M, Correia DV, Mikulak J, Roberto A, Della Bella S, et al. Engagement of NKp30 on Vdelta1 T cells induces the production of CCL3, CCL4, and CCL5 and suppresses HIV-1 replication. *Blood.* (2012) 119:4013–6. doi: 10.1182/blood-2011-11-390153
58. Mohamadzadeh M, McGuire MJ, Smith DJ, Gaspari AA, Bergstresser PR, Takashima A. Functional roles for granzymes in murine epidermal gamma(delta) T-cell-mediated killing of tumor targets. *J Invest Dermatol.* (1996) 107:738–42. doi: 10.1111/1523-1747.ep12365634
59. Bonneville M, O'Brien RL, Born WK. Gammadelta T cell effector functions: a blend of innate programming and acquired plasticity. *Nat Rev Immunol.* (2010) 10:467–78. doi: 10.1038/nri2781
60. Cho JS, Pietras EM, Garcia NC, Ramos RI, Farzam DM, Monroe HR, et al. IL-17 is essential for host defense against cutaneous *Staphylococcus aureus* infection in mice. *J Clin Invest.* (2010) 120:1762–73. doi: 10.1172/JCI40891
61. Nguyen MT, Uebele J, Kumari N, Nakayama H, Peter L, Ticha O, et al. Lipid moieties on lipoproteins of commensal and non-commensal staphylococci induce differential immune responses. *Nat Commun.* (2017) 8:2246. doi: 10.1038/s41467-017-02234-4
62. Kang JY, Nan X, Jin MS, Youn SJ, Ryu YH, Mah S, et al. Recognition of lipopeptide patterns by Toll-like receptor 2-Toll-like receptor 6 heterodimer. *Immunity.* (2009) 31:873–84. doi: 10.1016/j.immuni.2009.09.018
63. Takeda K, Takeuchi O, Akira S. Recognition of lipopeptides by Toll-like receptors. *J Endotoxin Res.* (2002) 8:459–63. doi: 10.1179/096805102125001073
64. Takeuchi O, Kawai T, Muhlradt PF, Morr M, Radolf JD, Zychlinsky A, et al. Discrimination of bacterial lipoproteins by Toll-like receptor 6. *Int Immunol.* (2001) 13:933–40. doi: 10.1093/intimm/13.7.933
65. Wanke I, Steffen H, Christ C, Krismer B, Gotz F, Peschel A, et al. Skin commensals amplify the innate immune response to pathogens by activation of distinct signaling pathways. *J Invest Dermatol.* (2011) 131:382–90. doi: 10.1038/jid.2010.328

Conflict of Interest: The authors declare that the research was conducted in the absence of any commercial or financial relationships that could be construed as a potential conflict of interest.

frontiers in Immunology

CORRECTION
published: 10 August 2021
doi: 10.3389/fimmu.2021.741437

Corrigendum: *Staphylococcus epidermidis* Boosts Innate Immune Response by Activation of Gamma Delta T Cells and Induction of Perforin-2 in Human Skin

Irena Pastar[1†], Katelyn O'Neill[2†], Laura Padula[2], Cheyanne R. Head[1], Jamie L. Burgess[1], Vivien Chen[1], Denisse Garcia[2], Olivera Stojadinovic[1], Suzanne Hower[2], Gregory V. Plano[2], Seth R. Thaller[3], Marjana Tomic-Canic[1] and Natasa Strbo[2*]*

[1] Wound Healing and Regenerative Medicine Research Program, Dr. Phillip Frost Department of Dermatology and Cutaneous Surgery, University of Miami Miller School of Medicine, Miami, FL, United States, [2] Department of Microbiology and Immunology, University of Miami Miller School of Medicine, Miami, FL, United States, [3] Division of Plastic Surgery Dewitt Daughtry Department of Surgery, University of Miami Miller School of Medicine, Miami, FL, United States

OPEN ACCESS

Edited and reviewed by:
Gabriele Pradel,
RWTH Aachen University, Germany

***Correspondence:**
Marjana Tomic-Canic
MTcanic@med.miami.edu
Natasa Strbo
nstrbo@med.miami.edu

[†]These authors have contributed equally to this work and share first authorship

Specialty section:
This article was submitted to Microbial Immunology, a section of the journal Frontiers in Immunology

Received: 14 July 2021
Accepted: 23 July 2021
Published: 10 August 2021

Citation:
Pastar I, O'Neill K, Padula L, Head CR, Burgess JL, Chen V, Garcia D, Stojadinovic O, Hower S, Plano GV, Thaller SR, Tomic-Canic M and Strbo N (2021) Corrigendum: Staphylococcus epidermidis Boosts Innate Immune Response by Activation of Gamma Delta T Cells and Induction of Perforin-2 in Human Skin. Front. Immunol. 12:741437. doi: 10.3389/fimmu.2021.741437

Keywords: perforin-2/mpeg-1, human skin, innate immunity, *Staphylococcus epidermidis*, gamma delta T cells, cytotoxicity

A Corrigendum on

Staphylococcus epidermidis Boosts Innate Immune Response by Activation of Gamma Delta T Cells and Induction of Perforin-2 in Human Skin

By Pastar I, O'Neill K, Padula L, Head CR, Burgess JL, Chen V, Garcia D, Stojadinovic O, Hower S, Plano GV, Thaller SR, Tomic-Canic M and Strbo N (2020). Front. Immunol. 11:550946. doi: 10.3389/fimmu.2020.550946

In the original article, there was a mistake in **Figure 1B** as published. The incorrect contour plots for the conditions Control 24 h and *S. epidermidis* 48 h were mistakenly included into **Figure 1B**. The correct representative contour plots in **Figure 1B** appear below.

The authors apologize for this error and state that this does not change the scientific conclusions of the article in any way. The original article has been updated.

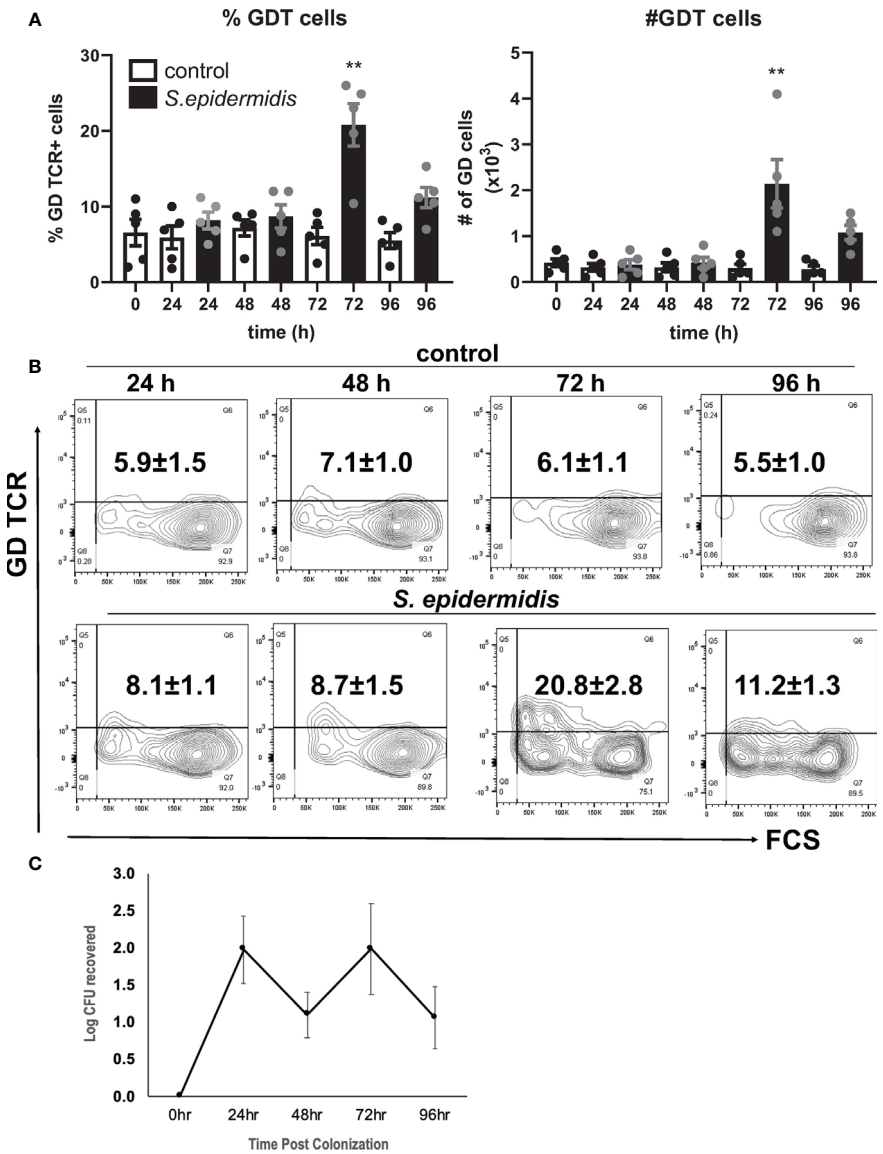

FIGURE 1 | *Staphylococcus epidermidis* increases the number of GD T cells in human skin ex vivo. Control, uncolonized, and S. epidermidis colonized skin was maintained on air liquid interface and collected at indicated time points (0, 24, 48, 72, and 96 h). Single cell suspensions were obtained and labeled with live/dead stain, CD45, CD3, and GD TCR. **(A)** Cells were analyzed using flow cytometry and gated on the CD45+ CD3+ GDT+ population. Bar graphs show SEM frequency (%) and SEM number (#) of skin GD T cells (n = 5). **(B)** Representative contour plots showing frequency of GD TCR in control and S. epidermidis colonized skin. **(C)** Number of S. epidermidis colony forming units (CFU) recovered from ex vivo skin explants colonized with S. epidermidis CCN021 on day 0 through day 4. Data represent at least two technical replicates and five independent biological replicates per group. **$p < 0.01$ (two-way ANOVA with Holm-Sidak multiple-comparison test).

frontiers in Immunology

REVIEW
published: 15 October 2020
doi: 10.3389/fimmu.2020.581906

OPEN ACCESS

Edited by:
George P. Munson,
University of Miami,
United States

Reviewed by:
Doryen Bubeck,
Imperial College London,
United Kingdom
Marjetka Podobnik,
National Institute of Chemistry
Slovenia, Slovenia
Horacio Heras,
CONICET Mar del Plata, Argentina

***Correspondence:**
Charles Bayly-Jones
Charles.Bayly-Jones@monash.edu
James C. Whisstock
James.Whisstock@monash.edu
Michelle A. Dunstone
Michelle.Dunstone@monash.edu

†ORCID:
Charles Bayly-Jones
orcid.org/0000-0002-7573-7715
Bradley Alan Spicer
orcid.org/0000-0002-9595-918X
James Whisstock
orcid.org/0000-0003-4200-5611
Michelle Dunstone
orcid.org/0000-0002-6026-648X

Specialty section:
This article was submitted to
Microbial Immunology,
a section of the journal
Frontiers in Immunology

Received: 10 July 2020
Accepted: 25 September 2020
Published: 15 October 2020

Citation:
Bayly-Jones C, Pang SS, Spicer BA,
Whisstock JC and Dunstone MA
(2020) Ancient but Not Forgotten: New
Insights Into MPEG1, a Macrophage
Perforin-Like Immune Effector.
Front. Immunol. 11:581906.
doi: 10.3389/fimmu.2020.581906

Ancient but Not Forgotten: New Insights Into MPEG1, a Macrophage Perforin-Like Immune Effector

Charles Bayly-Jones[1,2*†], *Siew Siew Pang*[1,2], *Bradley A. Spicer*[1,2†], *James C. Whisstock*[1,2,3*†] *and Michelle A. Dunstone*[1,2*†]

[1] ARC Centre of Excellence in Advanced Molecular Imaging, Monash University, Melbourne, VIC, Australia, [2] Department of Biochemistry and Molecular Biology, Biomedicine Discovery Institute, Monash University, Melbourne, VIC, Australia, [3] John Curtin School of Medical Research, Australian National University, Canberra, ACT, Australia

Macrophage-expressed gene 1 [MPEG1/Perforin-2 (PRF2)] is an ancient metazoan protein belonging to the Membrane Attack Complex/Perforin (MACPF) branch of the MACPF/Cholesterol Dependent Cytolysin (CDC) superfamily of pore-forming proteins (PFPs). MACPF/CDC proteins are a large and extremely diverse superfamily that forms large transmembrane aqueous channels in target membranes. In humans, MACPFs have known roles in immunity and development. Like perforin (PRF) and the membrane attack complex (MAC), MPEG1 is also postulated to perform a role in immunity. Indeed, bioinformatic studies suggest that gene duplications of MPEG1 likely gave rise to PRF and MAC components. Studies reveal partial or complete loss of MPEG1 causes an increased susceptibility to microbial infection in both cells and animals. To this end, MPEG1 expression is upregulated in response to proinflammatory signals such as tumor necrosis factor α (TNFα) and lipopolysaccharides (LPS). Furthermore, germline mutations in MPEG1 have been identified in connection with recurrent pulmonary mycobacterial infections in humans. Structural studies on MPEG1 revealed that it can form oligomeric pre-pores and pores. Strikingly, the unusual domain arrangement within the MPEG1 architecture suggests a novel mechanism of pore formation that may have evolved to guard against unwanted lysis of the host cell. Collectively, the available data suggest that MPEG1 likely functions as an intracellular pore-forming immune effector. Herein, we review the current understanding of MPEG1 evolution, regulation, and function. Furthermore, recent structural studies of MPEG1 are discussed, including the proposed mechanisms of action for MPEG1 bactericidal activity. Lastly limitations, outstanding questions, and implications of MPEG1 models are explored in the context of the broader literature and in light of newly available structural data.

Keywords: MACPF/CDC, MACPF domain, pore-forming protein, immune effector, immunology, PRF2, MPEG1

INTRODUCTION

The superfamily of MACPF/CDCs consists of proteins ubiquitously found in many kingdoms of life, including bacteria, plants, fungi and animals. Collectively, these molecules perform diverse functions, including roles in plant defence (*e.g. Arabidopsis thaliana*; CAD1, NSL1) (1–3), microbial virulence (Gram-positive bacteria; CDCs) (4–6), ingress and egress (*e.g. Plasmodium* spp.; SPECT, MAOP) (7, 8), as venom components (*e.g.* sea anemone toxin PsTX-60B, stonustoxin, perivitellin-2) (9–12), and nutrition (*e.g.* fungi; pleurotolysin) (13, 14). In humans MACPF proteins play key roles in immunity and development [*e.g.* mammalian perforin (PRF) and complement component 9 (C9)] (15–18).

The first indirect observations of a MACPF pore-forming complex were made by Jules Bordet in 1898 (19). Here, it was observed that certain blood factors complemented antibodies in their function and could lyse red blood cells. These early studies led to the identification of the Membrane Attack Complex (MAC), which is the terminal effector of the complement pathway (16). The MAC is formed *via* the recruitment of C5, C6, C7, C8, and, finally, multiple copies of C9 (20–23). The latter protein forms a transmembrane pore that can function in immunity to clear a wide variety of invading microorganisms including gram-negative bacteria (24–27), protozoa, enveloped viruses, and helminths (28, 29). These microbes can be eliminated by either direct lysis of cells or *via* facilitating the entry of other immune effectors (30, 31). Formation of sub-lytic levels of the MAC on local host cells also triggers cellular signal transduction pathways to control local inflammatory and immune responses (32–34). Loss of MAC activity can lead to recurrent infections (35, 36), while aberrant and excessive MAC activity can lead to life-threatening disease, such as paroxysmal nocturnal hemoglobinuria, where red blood cells become lysed due to unregulated MAC activity (37, 38).

A second immune pore-forming MACPF protein, perforin (PRF), was identified in the mid 1980s through the work of Podack, Tschopp and colleagues (39, 40). PRF is held inside of granules within cytotoxic T lymphocytes and natural killer cells (40). Upon formation of the immune synapse with a virally infected or transformed cell, PRF is secreted into the synapse, whereupon it oligomerizes to form pores in the target cell membrane (41–43). These pores permit the translocation of granzymes (which are secreted with PRF) into the target cell, an event that results in apoptosis (44, 45). Complete loss of PRF results in familial hemophagocytic lymphohistiocytosis type II, where expansion of antigen presenting cells becomes uncontrolled as normal apoptotic clearance is disrupted (46). This disease manifests itself in individuals as high levels of circulating active leukocytes, which secrete proinflammatory cytokines resulting in fever and a cytokine storm which, if untreated, ultimately leads to patient death (46, 47).

Outside the realm of immunology, several MACPFs appear to govern developmental processes within humans, namely the astrotactins (ASTN1 and ASTN2) and the bone morphogenetic protein/retinoic acid inducible neural-specific proteins (BRINP1, BRINP2 and BRINP3) (48). While the biological functions of the ASTNs and BRINPs are unknown, they have been implicated in brain development. Specifically, ASTNs are involved in neuronal migration and glial cell adhesion (49–51). Conversely the roles of BRINPs are poorly understood, with some suggestions that they function in neuroplasticity or regulating cell cycles (52, 53). Mutations in both ASTNs and BRINPs have been associated with intellectual disabilities, ADHD, and other neuropathies (54–56). It is currently unclear whether ASTNs or BRINPs form pores as part of their function.

An intriguing family of pore-forming proteins (PFPs), the gasdermins (GSDMs), represents a class of intracellular immune effectors which like MACPFs form giant β-barrel pores (57, 58). Specifically cleaved and activated by caspases during microbial infection or after detection of danger signals, GSDMs are converted from an autoinhibited state into two fragments (59). Cleaved-GSDMs rapidly form pores in the cell membrane (from the cytosolic side) and are considered effectors of cellular pyroptosis, a form of programmed cell death (60, 61). The GSDM fold is suggested to define a unique family, although striking similarities with MACPF proteins have been noted (62, 63).

The primary topic of this review, MPEG1, was identified through the *in situ* analysis of differential gene expression comparing mature with immature cell lines of mouse macrophages (64). Numerous names for this pore-forming protein have since arisen, including macrophage-expressed gene 1 (MPEG1 or sometimes MPG1), perforin-2 (PRF2 or P2) and macrophage specific gene 1 (MSP1). We elect to use the original name, MPEG1, owing to its widespread use and to distinguish MPEG1 from PRF. MPEG1 is postulated to represent the closest paralog of the common MACPF ancestor gene in metazoa (65, 66). Bioinformatic analyses reveal that complete MPEG1 homologs can be found throughout the kingdom *Animalia* with exemplars identifiable in phyla including sea sponges (Porifera), sea anemones (Cnidaria) (67), comb jellies (Ctenophora) (68), flatworms (Platyhelminthes) (69), molluscs (Mollusca) (70–76) and all chordate organisms (66, 77). These studies also suggest that gene duplications of MPEG1 likely gave rise to the mammalian immune effectors PRF and the terminal components of the complement system (MAC), which are observed after notochord evolution. Resultantly, MPEG1 represents the earliest known and most ancient MACPF protein identified to date in metazoan immune and defense systems (66, 78).

Abbreviations: MACPF, Membrane Attack Complex/Perforin; CDC, Cholesterol Dependent Cytolysin; MPEG1, Macrophage-expressed gene 1; MAC, Membrane Attack Complex; PRF, Perforin; ASTN, Astrotactin; BRINP, bone morphogenetic protein/retinoic acid inducible neural-specific proteins; MVB12, multi-vesicular body-12; MABP, MVB12-associated β-prism; PNH, paroxysmal nocturnal hemoglobinuria; SPECT, sporozoite microneme proteins essential for cell traversal; LPS, lipopolysaccharide; IFN, interferon; TNF, tumor necrosis factor; MRSA, Methicillin-resistant *Staphylococcus aureus;* LAMP, lysosomal-associated membrane protein 1; EEA1, early endosome antigen 1; ESCRT, endosomal sorting complexes required for transport machinery; MyD88, Myeloid differentiation primary response 88; NFκB, nuclear factor kappa-light-chain-enhancer of activated B cells; EGF, epidermal growth factor; (Cryo-)EM, (cryogenic) electron microscopy; (Cryo-)ET, (cryogenic) electron tomography; BMDM, bone marrow derived macrophages; MEF, Mouse embryonic fibroblast.

From the structural perspective, MPEG1 is an intracellular type-1 transmembrane MACPF protein with both a vacuole-based ectodomain and cytosolic region (endodomain). MPEG1 traffics *via* the ER, Golgi, and secretory vesicles to localize to early endosomes and phagosomes/lysosomes (79–81). It is thought that MPEG1 functions in the phagosome in an anti-microbial capacity. Furthermore, recent structural studies strongly support the idea that MPEG1 is a *bona fide* pore-forming immune effector. In this regard, early electron-microscopy (EM) studies revealed that MPEG1 is able to form oligomers of a size and shape typical for members of the MACPF/CDC superfamily (79). The first three-dimensional structure of human MPEG1 revealed the molecule was able to assemble into an oligomeric prepore intermediate, and that this material was able to form pores upon acidification (82). This is consistent with MPEG1 performing a role in the phagosomal system. Indeed, analysis of the primary structure of MPEG1, together with imaging data, suggests that the pore-forming machinery of the MPEG1 MACPF domain is positioned within the luminal environment of the membrane vesicles (78–81). Consistent with these data, a low-resolution detergent solubilized structure of murine MPEG1 suggests the molecule can form membrane spanning pores (83). Finally, germline mutations in MPEG1 have been found in patients suffering from recurrent pulmonary non-tuberculous mycobacterial infections (84). Thus, the available data to date suggests that MPEG1 is an immune effector involved in defense against invading intracellular pathogens and processing of engulfed pathogens. Overall, several mechanisms are proposed to explain MPEG1 mode of action *in vivo*.

In this review, we discuss the current understanding of MPEG1 evolution, regulation, and structure–function. We furthermore evaluate the contrasting proposed mechanisms of bactericidal activity. Taken together, we explore the implications of cellular and whole-organism research in the context of new MPEG1 structure–function studies and discuss the outstanding questions surrounding this ancient immune effector.

OVERALL DOMAIN ARCHITECTURE OF MPEG1

The majority of the MPEG1 sequence forms an ectodomain component, which comprises an N-terminal MACPF domain, followed by a multi-vesicular body-12 (**M**VB12)-**a**ssociated β-prism (MABP) domain (**Figure 1**). A signal peptide (SP) precedes the ectodomain and directs MPEG1 to the endoplasmic reticulum (ER) (**Figure 1**). While the SP is proteolytically removed shortly after translation, it positions the MPEG1 ectodomain within the lumen of the ER. Between the MACPF and MABP domains, MPEG1 also possesses a small folded linker region which is postulated to be an EGF-like domain (**Figure 1**). Furthermore, a second small folded region exists between the MABP domain and the Type I transmembrane helix of unknown fold named either the L-domain (82) or CTT (83) (**Figure 1**). Directly after the L-domain there follows a single pass type I transmembrane helix and a cytosolic region (**Figure 1A**).

A shorter isoform of MPEG1 has also been described (81), whereby alternative splicing gives rise to a product that is truncated at residue K511 within the MABP domain (**Figure 1B**). This shorter isoform, named MPEG1b (or PRF2b), therefore lacks a part of the MABP domain and the entire transmembrane and cytosolic regions. For the purposes of this review, when referring to the shorter isoform we will use MPEG1b, otherwise MPEG1 is used to denote the full-length isoform.

Prior to its structural characterization (82), the MPEG1 MABP domain was referred to as the P2 domain (for PRF2 domain), since the homology with the MABP fold could not be identified through sequence analysis alone (79). The MPEG1 MABP domain appears to be somewhat divergent, possessing an inserted hyper-extended β-hairpin motif, which likely explains why sequence analysis failed to identify the domain. Previously, MABP domains have been implicated in lipid binding (85, 86).

MPEG1 EXPRESSION AND REGULATION IN THE CELLULAR CONTEXT

Historically, MPEG1 was discovered in macrophages; however, it is now clear that many cell types can express MPEG1 (79). Constitutive MPEG1 expression is common in macrophages and leukocytes (**Figure 2i**); however, others have observed that

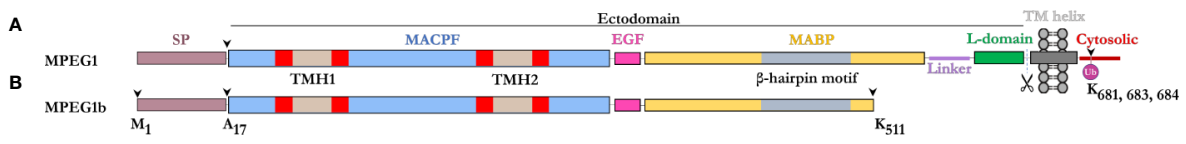

FIGURE 1 | Domain schematic of MPEG1 in two isoforms. **(A)** The majority of MPEG1 consists of a MACPF (blue) and MABP (yellow) domain. The MACPF domain contains functional motifs, namely the TMH regions (tan/red) that unfurl to form a β-barrel upon pore formation. The MABP domain contains a β-hairpin motif (gray) that recognizes and binds to negatively charged phospholipids. A small EGF-like motif (pink) is located between the MACPF and MABP domains. The MABP domain is followed by a small linker region (purple) and conformationally labile motif, denoted the L-domain (green). These directly precede the transmembrane helix (dark gray) and cytosolic (red) regions. The cytosolic region contains a lysine rich motif that is monoubiquitinated during immune response. Scissors depict the putative cleavage site of MPEG1. The majority of MPEG1 constitutes the ectodomain and is postulated to be proteolytically shed from the bilayer. **(B)** MPEG1b is a shorter secreted isoform that is truncated in the MABP domain at K511 (arrow). Both MPEG1 and MPEG1b are directed to the ER by a signal peptide (SP; copper rose) that is cleaved (arrow) shortly after translation.

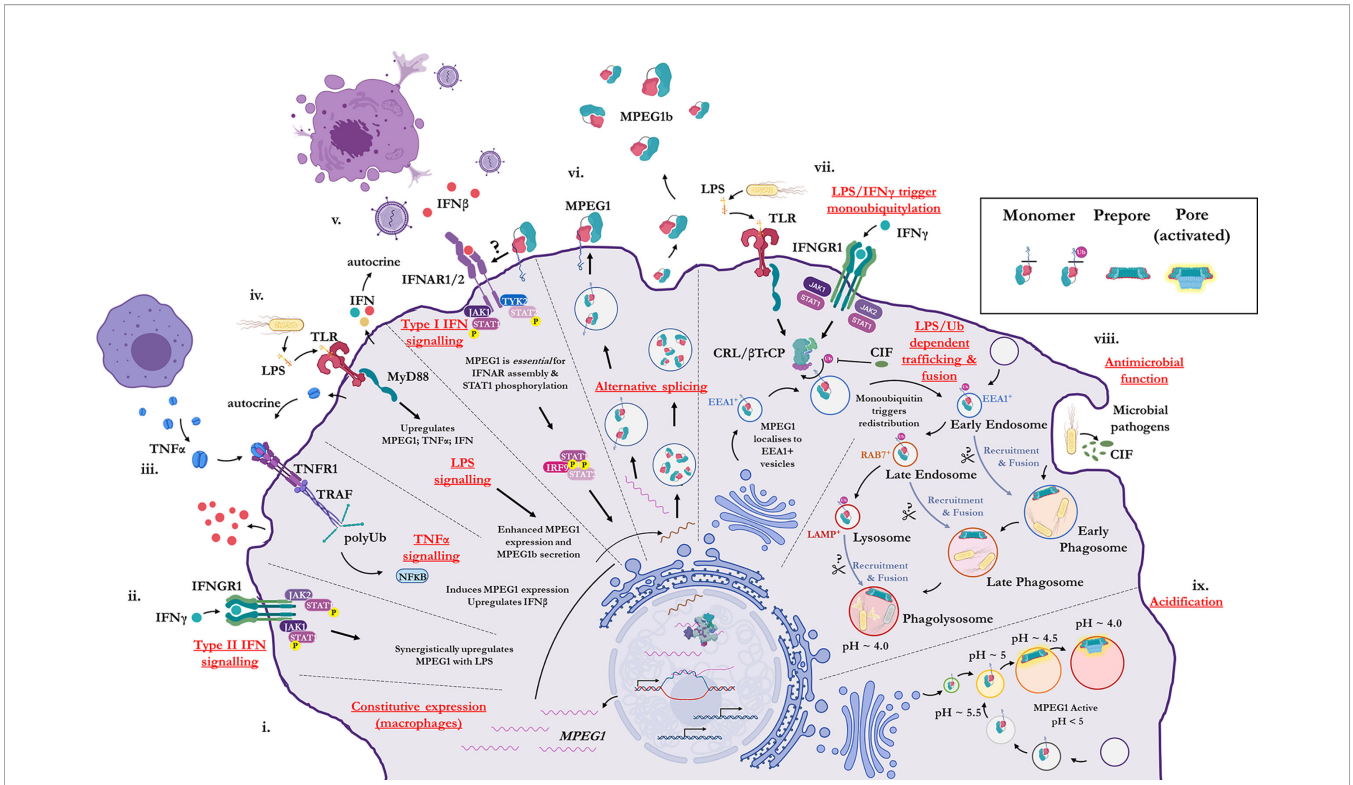

FIGURE 2 | Illustration of the cellular context and key processes in which MPEG1 is implicated. **(i)** MPEG1 is constitutively expressed in macrophages and phagocytes. **(ii, iii, iv)** Type II IFN, TNFα and LPS signaling are involved in the regulation of MPEG1 expression. **(v)** Surface bound MPEG1 is essential for the correct assembly and signaling of the type I IFN pathway. **(vi)** MPEG1 is expressed either as a membrane tethered isoform (MPEG1) or as a secreted, truncated form (MPEG1b). **(vii)** LPS and IFNγ signaling are important for triggering monoubiquitination of MPEG1 in EEA1$^+$ vesicles. Some pathogens produce CIF which inhibits the monoubiquitination of MPEG1 and confers resistance. **(viii)** Once monoubiquitinated, EEA1$^+$/MPEG1$^+$ vesicles traffic to and fuse with the early phagosome. The phagocytic and secretory pathways cooperate to enrich intracellular compartments with MPEG1 to aid in the disruption and killing of engulfed microbes. Proteases (scissors) may be important for MPEG1 function. **(ix)** As phagosomal and endosomal vesicles become acidified, MPEG1 is activated to form lytic pores. Figure produced with BioRender.

expression can be induced in a wide variety of other cell types such as epithelial and fibroblast lines (79, 87) (**Figures 2ii–iv**). Furthermore, proinflammatory signals were observed to trigger the upregulation of MPEG1 expression (**Figures 2ii–v**). For example, parenchymal, epithelial, and fibroblast cells, which usually do not express MPEG1, can be induced to express MPEG1 upon stimulus during an inflammatory response (**Figures 2ii–v**) (79). In this regard, tumor necrosis factor α (TNFα) and lipopolysaccharide (LPS) signaling have been shown to drive the expression of MPEG1 independently. Hence, MyD88 and NFκB pathways have been implicated for MPEG1 expression (65, 88). When used in combination, TNFα and LPS were observed to have an additive effect upon MPEG1 gene expression. Similarly, interferon (IFN)-γ upregulates MPEG1 expression synergistically with LPS, while IFNγ alone has no effect (81) (**Figures 2ii–iv**). In addition to these effects, in the context of MPEG1b, stimulation of cells by LPS alone also triggered enhanced secretion of MPEG1b (81) (**Figure 2iv**).

MPEG1 is expressed as a type-I transmembrane protein where, upon translation, the C-terminal transmembrane helix anchors MPEG1 into the bilayer (**Figure 1A; Figure 2vi**). As such, the folded ectodomain of MPEG1 is located on the luminal side of the ER with the cytoplasmic tail protruding into the cytoplasm. The cytoplasmic tail and transmembrane helix act to facilitate correct trafficking *via* the secretory pathway whereby MPEG1 migrates through the ER, Golgi, *via* secretory vesicles to fuse and accumulate within early endosome antigen 1 (EEA1+) vesicles (79) (**Figure 2vii**). MPEG1 is also found associated with the plasma membrane, with the ectodomain oriented into the extracellular space (81, 89) (**Figure 2vi**), where surface bound MPEG1 is implicated in type I IFN signaling (89) (**Figure 2v**). Conversely, since MPEG1b lacks the transmembrane domain, this short isoform is not membrane tethered and is therefore secreted into the extracellular space (**Figure 2vi**). While MPEG1 likely functions in a bactericidal capacity, the function of extracellular MPEG1b remains poorly characterized.

LPS/IFNγ DEPENDENT MONOUBIQUITINATION AND TRANSLOCATION

In addition to stimulating expression, proinflammatory stimuli prompt the redistribution and translocation of MPEG1 (**Figure 2vii**) (80). Specifically, LPS and type II interferon signaling lead

to post translational modification of the MPEG1 cytosolic region (**Figure 2vii**). Upon engulfing microbes, cells are stimulated by LPS and IFNγ which initiates monoubiquitination of MPEG1 by a Cullin-RING ligase (CRL) and β-Transducin Repeat Containing Protein (βTrCP) complex (**Figure 2vii**). A conserved, lysine rich region (K681, K684, K685) located in the cytosolic tail of MPEG1 (**Figure 1A**), is resultantly modified by a monoubiquitin. When monoubiquitinated, $EEA1^+/MPEG1^+$ vesicles traffic and fuse with $LAMP^+$ vesicles (late phagosomes, phagolysosomes and/or lysosomes) (80, 81) (**Figure 2viii**). These cellular re-distribution events ultimately result in MPEG1 co-localization with phagosomal vesicles containing engulfed microbes (79–81) (**Figures 2vii–ix**).

This re-organization is paramount for the function of MPEG1. Mutation of the lysine rich region produces a form of MPEG1 that prevents trafficking and accordingly a null phenotype (80). Indeed, certain intracellular pathogens produce molecules (CIF; cycle inhibiting factor) that inhibit the ubiquitination machinery of mammalian cells, thus disrupting the post translational modification of MPEG1 and therefore preventing further maturation and trafficking (80) (**Figure 2viii**). It is, therefore, unsurprising that inhibition of MPEG1 trafficking confers resistance to microbes, such as enteropathogenic *Escherichia coli* and *Yersinia pseudotuberculosis*, from the host cell (**Figures 2vii, viii**). Hence, the cytosolic tail functions as a signal-dependent trafficking motif. This implies monoubiquitination-dependent trafficking of MPEG1b cannot occur, since it lacks the signaling motif present in the cytosolic tail. Thus, external stimulation from microbes by proinflammatory molecules coordinates the re-organization of MPEG1 in preparation for phagocytosis.

MPEG1 FUNCTION IN IMMUNITY

The available evidence to date suggests that MPEG1 functions as an immune effector. Despite the significance of MPEG1 as a likely ancestor to the better-known immune effectors C9 and PRF, its precise function has remained poorly understood. However, given the role of the MAC and PRF, and the localization of MPEG1 to macrophages, it was suggested that MPEG1 may perform an anti-microbial role. Indeed, recombinantly produced sponge MPEG1 and the MACPF domain of oyster MPEG1, have anti-microbial activity *in vitro* (65, 72). MPEG1 expression is induced by proinflammatory signals in several dozen cell lines and, furthermore, multiple cell lines succumb to bacterial infection when MPEG1 is knocked-down or knocked-out (79–81, 90, 91). In vertebrates, MPEG1-deficient mice and zebrafish are more susceptible to infections (by Methicillin-resistant *Staphylococcus aureus*, *Salmonella typhimurium* and *Mycobacterium marinum*) compared to wild-type counterparts (88, 90). Likewise, several studies have illustrated MPEG1 antibacterial activity in invertebrates (67, 68, 70–74).

Recombinant forms of MPEG1 from sponge (65), oyster (MACPF domain only) (72) and fish (92) were all observed to be bactericidal *in vitro*. When challenged by *M. marinum*, one of the three MPEG1 paralogs in zebrafish (*mpeg1.2*) becomes upregulated. Of the remaining two, one is thought to be a pseudogene (*mpeg1.3)*, while the other (*mpeg1)* is surprisingly suppressed. Knock-down experiments of *mpeg1.2* resulted in an increased bacterial burden on zebrafish challenged with *M. marinum*, while knock-down of *mpeg1* gave a survival advantage compared to wild type fish, suggesting an altered immune response (88). Several studies of MPEG1 in vertebrates and invertebrates now support the model that suppression or complete loss of MPEG1 results in a loss of bactericidal activity. Collectively, these studies demonstrate the essential role MPEG1 plays as an immune effector against microbes and bacteria.

In one experiment McCormack and colleagues observed *Mycobacterium smegmatis* swelling (albeit not killing) after treatment with MPEG1. The addition of minute quantities of lysozyme, however, were sufficient to kill pre-treated *M. smegmatis*, putatively indicating MPEG1 perforates the outer membrane but does not affect the integrity of the peptidoglycan layer (90). Indeed, more recent studies have found MPEG1 facilitates the entry of myriad anti-microbial effectors into cells including; proteases, reactive oxygen and nitrogen species, bactericidal peptides and the harsh acidic environment of the phagosome (93). Notably, recombinant MPEG1 possesses lytic activity which is strictly dependent on low pH (82, 83). Lastly, MPEG1 has been observed to form membrane spanning pores similar to the lytic MAC and PRF (13, 94).

To date, no severe disease state has been described in humans with complete loss of MPEG1 function. Like many aspects of biology, there may be compensating redundancies in the immune system that maintain a sufficient immune response in the absence of MPEG1. One retrospective case study, however, has described recurrent pulmonary non-tuberculous mycobacterial infections in individuals with germline mutations in MPEG1 (84). The association of these mutations with recurrent infections suggests there may be subtle clinical outcomes in individuals with a defective form of MPEG1; however, further clinical data is required to definitively implicate MPEG1 in these pathologies. Furthermore, there are presently no examples of excessive MPEG1 function, which contrasts to MAC and PRF where hyperactivity can lead to severe disease states in humans (47, 95, 96).

INTERFERON SIGNALING/LPS INDUCED SHOCK

Apart from anti-microbial function by pore formation, MPEG1 has been implicated in regulating type I IFN signaling and is critical for the correct assembly and signaling of the Interferon-α/β receptor (IFNAR) proximal complexes (89) (**Figure 2v**). Transfection studies, using several MPEG1 truncation variants, illustrate the assembly of proximal complexes and phosphorylation of downstream signaling effectors are dependent on MPEG1. Type I IFN signaling was found to be defective in MPEG1-deficient cell lines (BMDM, MEFs) due to loss of IFNAR mediated phosphorylation of STAT1, STAT2, JAK1, and TYK2. It was

observed that both the MACPF and MABP domains appear to mediate interactions with IFNAR1 and IFNAR2, respectively, while the intracellular cytosolic region was required for phosphorylation of STAT2. Currently, however, the nature of MPEG1–IFNAR interactions is poorly understood.

Animal models have shed light on the MPEG1–IFNAR association and the significance of this poorly understood signaling pathway. Under normal circumstances excessive LPS can overwhelm the host immune response and lead to septic shock. Mice lacking MPEG1 were found to be resistant to LPS induced septic shock (89). Consistently, the suppression of an MPEG1 paralog in zebrafish was observed to reduce the likelihood that fish would succumb to infection (88). Taken together, these studies suggest MPEG1 plays a role in the excessive IFN signaling during an overwhelming immune response.

Overall, these findings suggest MPEG1 is not only important for cellular immunity, but also the regulation of immune response *via* IFNα/β signaling. This has implications for both autoimmune disorders and cancer. In a recent example studying MPEG1-deficient, aged mice, there was an increased proportion of microbial migration into serum from the gastrointestinal tracts, which resulted in a state of chronic inflammation (97). A significantly reduced antibody response was also observed in these MPEG1-deficient mice. Furthermore, an increased level of inflammation was observed in splenic B cells, as well as an increased frequency of pro-inflammatory B cells. These data suggest that an increased bacterial burden in those who lack MPEG1 may be responsible for chronic inflammation, which is proposed to affect the normal immune responses of B cells. Chronic inflammation is a known determinant of many autoimmune diseases, and hence, reduced levels of MPEG1 may also contribute to a number of chronic, progressive diseases in humans.

MPEG1 PROTEOLYSIS

Proteolytic shedding of MPEG1 has been proposed for proper MPEG1 regulation and function. It is hypothesized that proteolysis may be required for the release of the ectodomain from the host membrane to allow for pathogen targeting and pore-forming function. Proteolytic processing may function two-fold to regulate MPEG1 function. Firstly, proteolysis may be necessary for oligomerization to occur (79). Secondly, anchoring MPEG1 to the host bilayers (endosome, secretory vesicles, *etc.*) may prevent unintended lytic function. Lastly, sequestration of MPEG1 by the transmembrane region is important for trafficking (81, 89). Therefore, untimely proteolytic processing may result in MPEG1 mis-trafficking (**Figure 2viii**).

In the context of invading microbes, fragments of MPEG1 corresponding to the ectodomain (among others) have been identified in bacterial membranes treated with MPEG1 (79). Notably, the C-terminal cytosolic region was not detectable, consistent with suggestions that the transmembrane and cytosolic tail remains in the host membrane. Furthermore, limited proteolysis experiments of MPEG1-enriched bilayers derived from transfected cells resulted in membrane-bound ring-like oligomers (79), whereas, these oligomers were not observed in the absence of proteolytic treatment. This supports the current model whereby the ectodomain is shed during MPEG1 anti-microbial function.

These findings suggest that spatio-temporal regulation of MPEG1 proteolysis is associated with normal function. The mechanism of this proteolysis is still being determined and the endogenous protease responsible for MPEG1 cleavage has not been identified. Further studies will be required to confirm the sites of MPEG1 cleavage and their functional role within the cellular context. While the relevance and functional importance of MPEG1 proteolysis is unclear, it is notable that the GSDMs require the specific and coordinated proteolytic processing by caspases for subsequent activation and pore-forming function (59, 60). In this regard, it is possible that such a mechanism could also exist to coordinate proper MPEG1 function.

MPEG1 STRUCTURE AND MECHANISM

Pore-forming MACPF proteins generally adopt two different stable conformations—a soluble, metastable monomeric form and a membrane inserted hyper-stable oligomeric pore form (**Figure 3**). The pathways from the metastable monomer to the stable oligomer pore can vary. These topics have been extensively reviewed elsewhere in detail (15, 17, 18, 58, 98–102).

Structural Biology of the MACPF Domain

The MACPF domain has two well documented functions; firstly, oligomerization into rings and, secondly, insertion into membranes. The domain is a well characterized fold that is centered around a contorted four stranded antiparallel β-sheet that features an L-shaped bend (**Figure 4**). The β-sheet is flanked at one end by two clusters of α-helices, termed transmembrane β-hairpin-1 (TMH-1) and TMH-2 (**Figure 4A**). The term, seemingly a misnomer, refers to the end-state conformation of these microdomains. Structural comparisons reveal that the MACPF domain undergoes a dramatic concerted conformational transition (104). These two bundles of α-helices (in the monomeric form) undergo structural rearrangement, unfurling to form a set of amphipathic β-hairpins (in the final pore form) (13, 21, 22, 83, 105) (**Figures 4A, B**). As they unwind the TMH regions are postulated to concurrently zipper up into β-hairpins, these protrude below the MACPF domain and thereby form a giant, amphipathic β-barrel that inserts into the membrane. Together these two β-hairpins each contribute four β-strands to the final oligomeric β-barrel pore (**Figure 4C**). From the perspective of the MACPF domain, the initial membrane associated oligomerization event includes the formation of β-sheet hydrogen bonds between the central β-sheets of adjacent subunits to form a nascent β-barrel. During the prepore-to-pore transition, the unfurling of the TMH regions is also accompanied by a straightening of the central MACPF β-sheet that permits more substantive β-sheet hydrogen bonding between adjacent

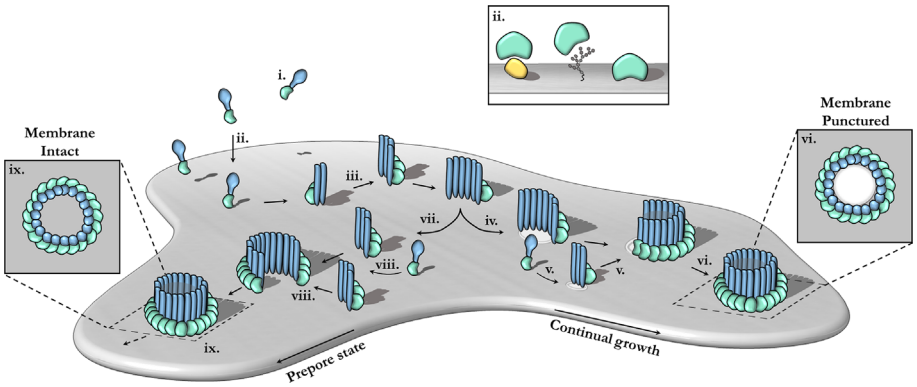

FIGURE 3 | The canonical pathway of pore formation. A generic pore forming protein is shown, with a green ancillary (or receptor binding) domain and blue pore forming domain. Freely diffusing monomers **(i)** bind to the target bilayer (gray) **(ii)** *via* target recognition domains (green) that are ancillary to the pore forming machinery (blue). The target receptor can be proteins (yellow), glycans or lipids (**ii**; inset). Membrane-bound monomers undergo two-dimensional diffusion, colliding and eventually oligomerizing **(iii)**. Maturation *via* the prepore-to-pore conformational change may occur at different stages. For example, incomplete oligomers may transition into arc-pores **(iv)**. Other smaller arcs or monomers may also be recruited to a growing arc pore **(v)**. Ultimately complete pores are formed upon the closure of the oligomeric ring **(vi)**. In this context pore growth can occur in a continuous mechanism. Completed pores define large aqueous channels, capable of facilitating the passive diffusion of additional effector molecules (not shown) *via* the membrane channel (**vi**; inset). Alternatively, arc prepores may continue to grow without inserting into the membrane **(vii)** by recruiting additional monomers or other smaller arcs **(viii)**. These can ultimately form complete prepores that have yet to punch into the lipid bilayer **(ix)**. Fully formed prepores are most commonly observed for CDCs **(ix)**. The prepore-to-pore transition is triggered resulting in a conformational change of the MACPF core machinery that unfurls into a giant β-barrel (**ix** goes to **vi**). These inserted pores possess an amphipathic region that is fully inserted into the lipid membrane (not shown). Insets **(ix, vi)** show top-down views.

subunits (**Figures 4A, B**) (13). A short helix-turn-helix (HTH) region sits on top of TMH1 and forms additional inter-subunit interactions (**Figures 4A, C**). This region is observed to shift during the prepore-to-pore transition in some studies (13, 22). A second larger "helix elbow", which contains the MACPF consensus motif (Y-X(6)-[FY]-G-T-H-[FY]), protrudes away from the core β-sheet and forms contacts around the periphery of the complex (**Figures 4A, C**). This helix elbow forms a complementary surface to accommodate TMH2 (**Figure 4A**). Outside the MACPF domain, studies on C9 and MPEG1 reveal that extensive inter-subunit interactions are also formed by the ancillary domains N- and C-terminal to the MACPF domain (23, 82). These interactions aid in the formation of oligomers (**Figure 4C**). The ancillary domain varies substantially between

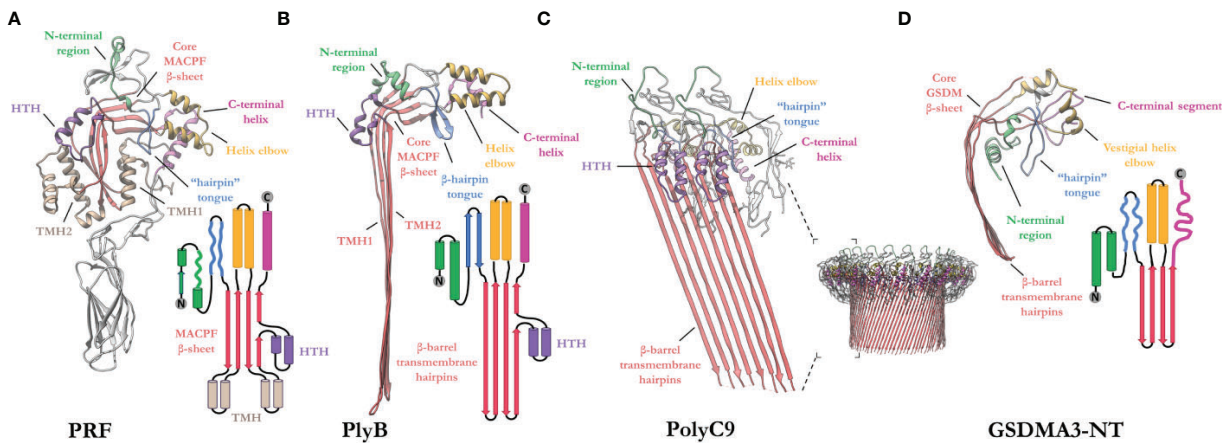

FIGURE 4 | Exemplar structures of MACPF pore forming proteins in the monomeric and pore states. **(A)** Crystal structure of lymphocyte PRF in the monomeric state [PDB: 3NSJ] (43). The ancillary domain is colored gray and omitted from the topology diagram for clarity. **(B)** The cryoEM pore structure of the fungal MACPF protein, pleurotolysin (PlyB)[PDB: 4V2T] (13). Pleurotolysin is a homolog of PRF found in oyster mushroom. The β-trefoil domain of PlyB is not shown for clarity. **(C)** A dimer of the polyC9 cryoEM reconstruction (bottom right) is shown to illustrate the intra-subunit contacts at the MACPF interface [PDB: 6DLW] (22, 23). **(D)** The cryoEM pore structure of the intracellular GSDMA3-NT shows structural and topological similarity to the MACPF domain [PDB: 6CB8] (103). HTH, helix-turn-helix (purple); TMH, transmembrane β-hairpin (pale brown). Topology diagrams are colored consistently with the PDB coordinates.

superfamily members, but its function is typically associated with membrane binding or targeting (15, 17, 100, 101).

A similar fold, from the GSDM family has strong topological parallels to the MACPF domain (**Figure 4D**). Indeed, DALI analysis revealed the pore-forming domain of GSDMs is a *bona fide* homolog of MAPCFs (62). Like MPEG1, GSDMs are regulated by proinflammatory signals and rely on proteolytic processing for activation (106). While the two families appear substantially different, GSDMs and MACPFs share mechanistic similarities—namely PRF, MAC, and GSDMs assemble and form transmembrane pores in a "growing-pore" like the model discussed below (20, 63, 94). Additionally, both families share topologically equivalent transmembrane β-hairpins which contribute to a giant β-barrel (86, 104, 107). The relation between the two families, however, still remains controversial.

Overview of the MACPF Mechanism of Pore Formation

In the archetypal pathway of pore assembly, soluble monomers (**Figure 3i**) are generally recruited to the membrane surface *via* the function of domains that are ancillary to the MACPF domain and that function to directly bind to lipids or membrane associated protein receptors (**Figure 3ii**). In the monomeric form, the pore forming MACPF domain is folded into a compact structure that represents a state of high potential energy—it is primed and ready to punch into a lipid bilayer, akin to a compressed spring (**Figure 4A**). Membrane-bound monomers then undergo two-dimensional lateral diffusion and oligomerize to form prepore oligomers perched above the target membrane (**Figure 3iii**). These prepores are short-lived intermediate complexes comprised of rings or arcs that are yet to insert into the bilayer (83, 94, 104). These arciform or complete prepores can undergo the MACPF prepore-to-pore transition and insert into the lipid membrane (**Figures 3iv–vi**). Both membrane-inserted and uninserted arcs can continue to grow by recruiting subunits (**Figures 3iv–vi**). Both the mechanisms of prepore-to-pore transition and how prepores are triggered to form pores remain to be fully understood. In the final structure, each monomer contributes two amphipathic β-hairpins, and the final pore comprises a giant membrane spanning β-barrel (23, 43, 86, 104, 108). The oligomeric pore form represents the final, highly stable, membrane inserted state of the MACPF domain (**Figure 3vi**).

The archetypal MACPF mechanism described above was originally derived from extensive studies of the bacterial CDC branch of the superfamily (100, 104, 109, 110) (**Figures 3vii–ix**). However, in the context of MACPF proteins it is clear that numerous variations of this mechanism have been identified. Most importantly the concept of a prepore is less applicable to the MACPF branch of the superfamily. For example, the complement MAC forms a hetero-oligomer that assembles by recruitment of multiple different MACPF domain-containing subunits (C6, C7, C8, and C9) (21, 105). The MAC is also distinct in that membrane insertion into the target bilayer most likely takes place in a sequential, non-concerted manner with individual monomers progressively undergoing conformational change and membrane insertion one-by-one (20, 22). In addition, the MAC lacks membrane recognition domains, instead it is recruited to the target membrane *via* opsonization and the formation of complement component 5b on the surface of pathogenic microbes. Studies on PRF also reveal variations from the archetypal CDC-like mechanism—most notably the "prepore" form of PRF oligomers is highly mobile and flexible (94). PRF is thought to assemble and insert into the membrane in a growing pore model—where subunits or smaller arcs are recruited to a growing membrane inserted form (94, 111). PRF appears to only form ordered ring-like structures upon transition to the final pore form (94). Deviations of the common mechanism also are evident in pleurotolysin and perivitellin-2, which are two-component toxins (12, 13).

Three-Dimensional Structure of MPEG1

Two studies have reported high resolution structures of truncated MPEG1 (82, 83). These studies employ MPEG1 constructs that lack the transmembrane and cytosolic regions, under the assumption that proteolysis of MPEG1 *in vivo* results in the same final primary sequence. These structures thereby represent presumed late matured MPEG1. These discoveries have propelled our understanding with respect to MPEG1 biology.

Membrane-Bound Prepore

Overall, the ultrastructure of MPEG1 strongly reflects other pore forming proteins (**Figures 5A–E**). The membrane-bound structure of the MPEG1 ectodomain exists as a hexadecameric homo-oligomer, whose central core consists of the MACPF domain in a yet-to-unfurl, prepore state (**Figure 5A**). The MACPF core β-sheet is oriented such that release of the TMH helices would result in a β-barrel pore in an adjacent membrane.

The MABP domain of each subunit is positioned around the periphery of the central MACPF core. An extended, twisted β-hairpin protrudes from the MABP domain, in the opposite direction to the MACPF β-sheet and TMH regions, to make contact with the lipid membrane. All sixteen subunits coordinate the lipid bilayer in this manner and act to adhere the MPEG1 prepore to the membrane surface (**Figure 5A**). The hydrophobic tip of the MABP β-hairpin is surrounded by positively charged residues that together interact with the lipid bilayer and charged head groups of phospholipids (82, 83). This binding mode was observed for the canonical MABP domain and suggests the β-hairpin is an elongated variant of the similarly charged membrane-binding loop of the ESCRT MABP (85).

The L-domain (CTT domain) is located in close proximity to the lipid bilayer and, in the primary sequence, directly precedes the transmembrane helix and cytosolic tail (**Figure 1A**). However, in the membrane-bound prepore structure the L-domain is unresolved and, therefore, is presumed to be disordered (not shown).

Prepore (Soluble)—Role of the L-Domain

In vitro studies of the MPEG1 ectodomain have demonstrated that MPEG1 can adopt various conformational states (82, 83). Human MPEG1 was seen to form dimeric ring/ring complexes that are loosely associated (denoted the α-conformation) (**Figure 5B**).

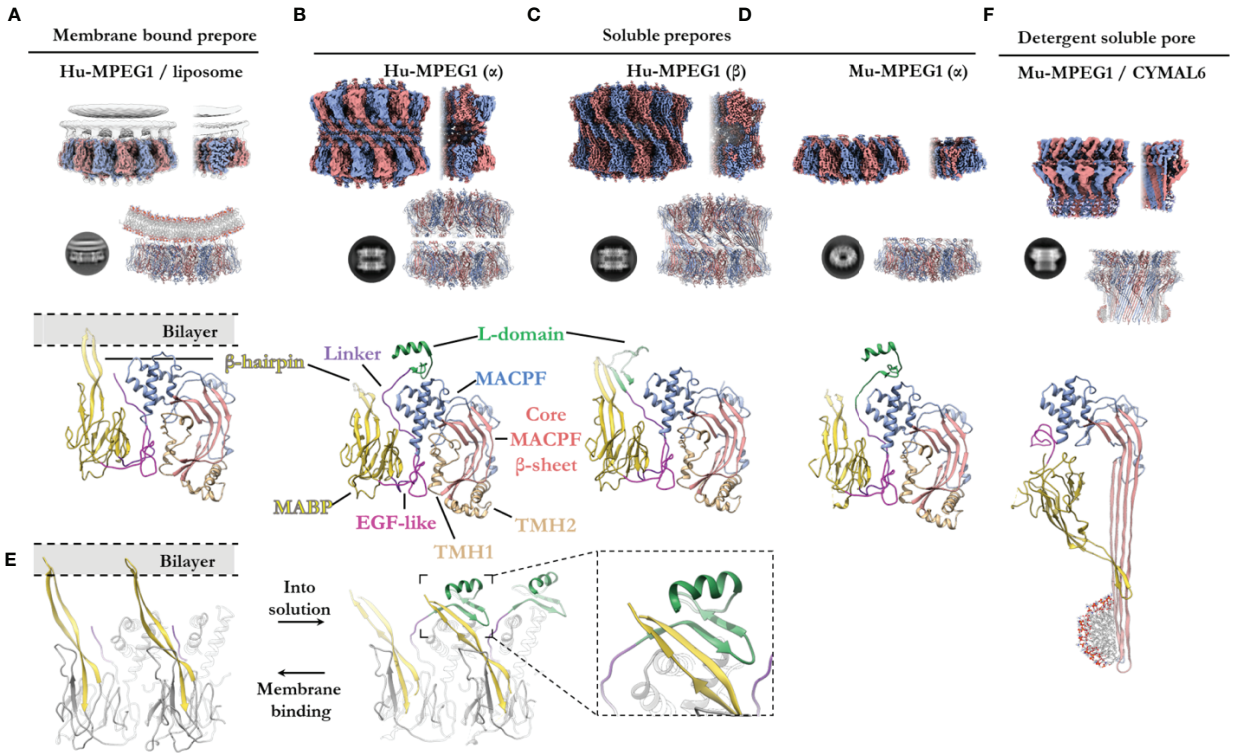

FIGURE 5 | The various structural states of MPEG1. **(A)** When incubated with liposomes (gray), MPEG1 binds the lipid bilayer as a single prepore ring, *via* the MABP β-hairpin (yellow), orienting the MACPF domain away from the lipid bilayer [PDB: 6U2W] (82). Lipids are illustrated with a cartoon model. Both the unsharpened (gray) and sharpened (alternating color) maps are superimposed to illustrate the lipid density (gray). **(B)** In solution, recombinant MPEG1 (truncated between the L-domain [green] and TM region [not shown]) forms a loosely associated ring–ring dimer whereby the helix of the L-domain mediates interactions between rings (termed the α-conformation) [PDB: 6U2J, 6U2K] (82). **(C)** A second, tightly associated ring–ring dimer is also possible; this conformation is defined by inter-ring strand swapping (termed the β-conformation) [PDB: 6U2L] (82). This is achieved by the L-domain which adopts an extended β-sheet conformation. **(D)** Murine MPEG1 truncated at a similar position to **(A, B)**, forms single ring structures after prolonged incubation in acidic conditions [PDB: 6SB3] (83). These rings were observed in the α-conformation (with respect to the L-domain). **(E)** A view of an MPEG1 dimer is shown from the periphery of the complex in both the membrane-bound (left) and soluble prepore (right) states. Upon interchanging between these states, the L-domain and β-hairpin undergo conformational change. Inset shows a magnified view of the interaction. **(F)** Incubation of murine MPEG1 at low pH and in the presence of the detergent CYMAL6 results in MPEG1 pores [PDB: 6SB5] (83) where the MABP domain is flipped relative to **(A–D)**. This conformational change re-orients the MACPF and MABP domains into the same direction. The extremity of the β-barrel forms an amphipathic region (illustrated by a cartoon micelle). Top row: CryoEM reconstructions of MPEG1 (alternating colors show individual subunits) of the overall quaternary structure. Both the full reconstruction (left) and a partial cross section (right) are shown for each panel **(A–D, F)**. The cross section enables visualization of the inner structure of the complex. Second row: Exemplar 2D class averages are shown below each reconstruction [reproduced from (82, 83)]. The atomic coordinates for the full reconstruction are shown next to the corresponding 2D class average (alternating colours show individual subunits). Third row: A single magnified subunit from each complex is shown. MACPF β-sheet (red), TMH regions (tan), MACPF core (blue), MABP/β-hairpin (yellow), EGF-like (pink), linker region (purple), L-domain (green).

Some of these dimeric complexes were observed to undergo inter-ring, β-strand swapping to form tightly associated double-ring complexes (denoted the β-conformation) (**Figure 5C**). These different interactions are mediated by the L-domain and, hence, it was named due to its labile (L) conformational states. It is unclear whether the double-ring assemblies of human MPEG1 exist *in vivo* and it is suggested they likely represent *in vitro* artefacts (82). Unlike human MPEG1, murine MPEG1 was observed to form monomeric material that readily oligomerized to form single rings on membrane bilayers or in solution after prolonged incubation at pH 5.5 and 37°C (**Figure 5D**). With the exception of the β-conformation, both murine and human soluble MPEG1 complexes are very similar overall.

Comparison between the soluble and membrane-bound prepore conformations reveals relatively few differences, with one notable exception. In the soluble prepore (α-conformation; **Figures 5B, D**), the β-hairpin of the MABP domain interacts with the L-domain of the neighboring subunit (**Figure 5E** [right]). Due to this interaction, the β-hairpin is shifted relative to the membrane-bound prepore (**Figures 5D, E** [left]). These interactions stabilize the L-domain, which forms a small β-hairpin motif capped by an α-helix (**Figures 5B, D**). The β-hairpin and L-domain interaction creates a four strand β-sheet (**Figure 5E; inset**), and hence these inter-subunit contacts anchor adjacent subunits in place. These interactions presumably provide stability to the complex and, therefore,

were suggested to mediate oligomerization in solution. Truncation of the L-domain was reported not to affect membrane binding, however oligomerization in solution was not reported (83).

Therefore, in order for the soluble prepore to bind membranes it must undergo a conformational change. To accommodate the interactions with the membrane bilayer the MABP β-hairpin in the soluble prepore must bend upward ~25° and shift laterally away from the L-domain (**Figure 5E**). This movement breaks the intermolecular interactions with the L-domain of the adjacent subunit and positions the β-hairpin to interact with lipid head groups. In the absence of the interactions with the β-hairpin, the L-domain of the adjacent subunit becomes flexible or disordered. Furthermore, movement of the L-domain helix is necessary to accommodate the bending of the β-hairpin, which would otherwise produce steric clashes.

Detergent Solubilized Pore

Recently Ni and colleagues reported a structure of the murine MPEG1 pore (**Figure 5F**) (83). Incubation of murine MPEG1 in mildly acidified buffer led to oligomerization in solution, with further incubation in strongly acidified buffer (pH 4.0–3.6) promoting pore formation. Performing these reactions in the presence of the detergent, Cymal-6, stabilized the exposed hydrophobic regions of the β-barrel for structural studies. As expected, these experiments revealed that, like polyC9 and CDCs, the MPEG1 TMH regions unfurl to form giant β-barrels (**Figure 5F**).

Strikingly, the MPEG1 pore revealed significant structural rearrangement of the MABP domain relative to the MACPF domain (**Figures 5D, F**). The large rotation of the MABP domain results in the membrane-binding β-hairpin region oriented in the same direction with the β-barrel of the MACPF domain. Unlike most MACPF mechanisms studied to date, the peripheral ancillary domains typically do not undergo such drastic conformational changes, and hence these data suggest MPEG1 adopts an entirely unique mechanism. It remains unclear how and when this conformational change occurs, *i.e.* from a structural perspective and at which point of the MPEG1 assembly pathway. Higher resolution structures, as well as studies in the presence of lipid bilayers, will be required to fully understand the mechanism and structural motifs that mediate this unique transition.

Control and Regulation of Oligomerization

In most PFPs studied to date, oligomerization on the target bilayer results in a rapid trajectory into a final lytic pore. In this regard, the correct spatiotemporal control of oligomerization represents a key regulatory mechanism of PFP activity and safeguards the host cell from premature lytic activity. For example, in the PRF system, storage of PRF monomers within acidified vesicles prevents key aspartic acid residues in the C2 domain from chelating Ca^{2+}, which prevents the C2 from adopting the membrane binding conformation (112). Therefore, PRF cannot bind membranes and does not oligomerize within granules. Subsequent release into the junction of the immune synapse causes a pH shift, and Ca^{2+} binding is restored, thus PRF binds the cell plasma membrane and rapidly oligomerizes to form pores (**Figure 6A**). During off-target assembly of the MAC on host cells, the inhibitor CD59 directly binds the nascent growing MAC and therefore blocks subsequent recruitment of C9 monomers, halting further oligomerization and safeguarding the cell (113). Notably, patients who lack CD59 develop PNH due to uncontrolled MAC activity (37). Given the intracellular context of the MPEG1 system, it is unclear what triggers oligomerization and when it occurs. Like the MAC and PRF systems, controlling MPEG1 oligomerization may act to prevent premature lytic activity that may have detrimental effects on the cell. In this regard, the coordinated cellular re-distribution of MPEG1 is critical in ensuring MPEG1 is appropriately located and poised to encounter microbes. However, cellular redistribution may additionally function to control the oligomerization event itself. As discussed earlier, proteolysis is suggested to regulate MPEG1 oligomerization (79). Moreover, sufficiently low pH was observed to be important for murine MPEG1 oligomerization (83). Thus, delivery of MPEG1 to acidified vesicles that possess the appropriate proteases may represent an additional level of functional regulation.

Role of MABP β-Hairpin for Membrane Association

In agreement with structural data, independent studies found the MABP β-hairpin directly mediates lipid binding *in vitro*, preferentially recognizing negatively charged phospholipids (phosphatidylserine, cardiolipin, phosphatidylinositol(s), *E. coli* lipid extract, LPS) but not neutrally charged lipids (phosphatidylcholine, phosphatidylethanolamine, sphingomyelin) (82, 83). Therefore, consistent with other MACPF superfamily members (13, 43, 102, 104), the ancillary domain of MPEG1 appears to function for membrane targeting.

In all other MACPF systems studied to date, both assembly of the pore and perforation of the bilayer occurs on the same membrane, *i.e.* the assembly and target membrane are the same (13, 20, 21, 43, 94, 105, 114) (**Figure 6A**). In contrast, the MPEG1 assembly pathway may not follow this simple concept (**Figure 6B**). As discussed, the MABP and MACPF domains are functionally positioned in opposite directions. As such the MPEG1 system was observed to form soluble oligomers that were capable of diffusing and binding membranes (orienting the MACPF domain away from the bilayer). Therefore, the assembly membrane may not correspond to the target membrane.

Pang, Bayly-Jones and colleagues suggest this may function as a control mechanism to prevent MPEG1 oligomers from mediating autolysis (*i.e.* of the assembly membrane) (82). While the MABP β-hairpin is associated with the endosomal host bilayer (assembly membrane) (**Figures 6B iv–v**), the orientation of the MACPF domain would prevent membrane perforation of the host bilayer. Hence, these data suggest the MABP β-hairpin may act to sequester MPEG1 to the host bilayer and orient it in a protective capacity.

Conversely, *in vitro* high speed AFM imaging suggests these prepores could undergo a conformational change upon acidification that can be interpreted as pore formation (83).

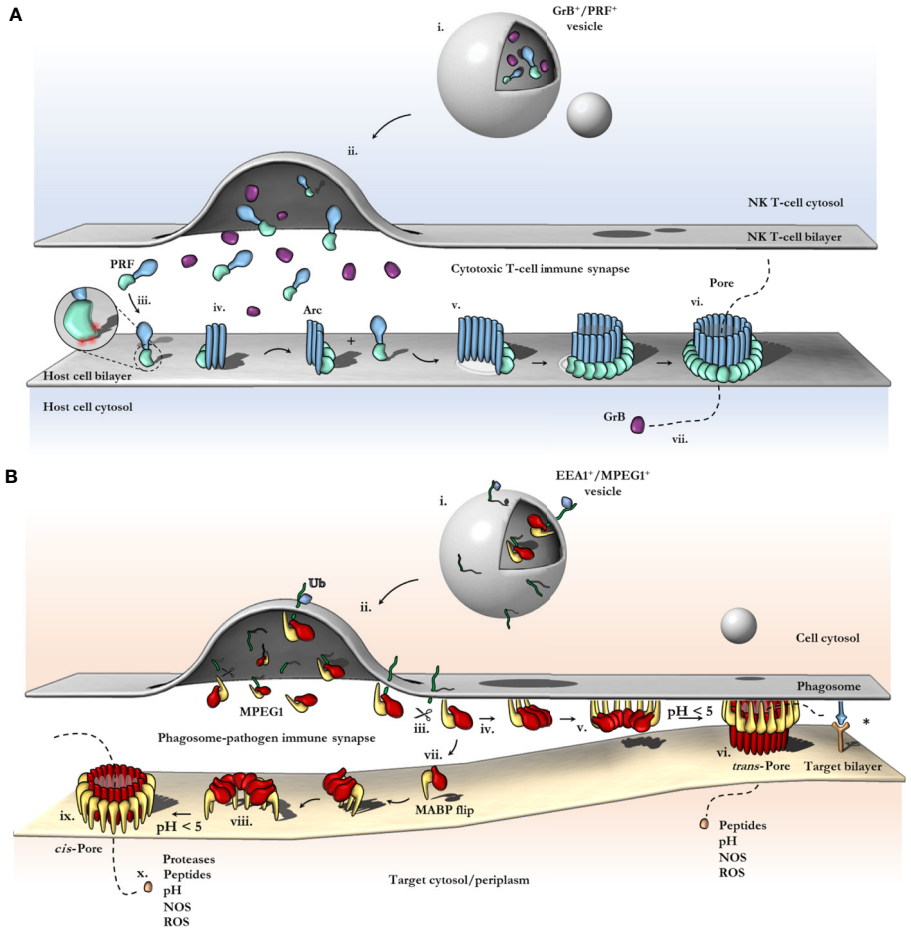

FIGURE 6 | Schematic comparison between current models of PRF and MPEG1 assembly. **(A)** At the T-cell immune synapse, vesicles (i) containing PRF [only the MAPCF (blue) and C2 domains (green) are shown] and granzymes (purple) fuse with the plasma membrane releasing their contents onto the target cell (ii). Within these cytotoxic granules (i), PRF is kept in a Ca^{2+}-deficient environment at low pH, therefore PRF is unable to bind membranes. Upon being released into the immune synapse (ii), PRF encounters Ca^{2+} (zoomed inset; red spheres) and therefore, binds the lipid bilayer *via* a target recognition C2 domain (iii). PRF begins to oligomerize into arcs (iv) and, later, fully formed pores (vi). In the PRF mechanism, early arc intermediates can puncture the lipid membrane (v); these can continue to grow in a continuous manner by recruiting monomers or other arcs. Functional arcs that have punctured into the lipid bilayer are depicted with a white membrane lesion (v). The final PRF pore enables granzyme B (GrB; purple) to diffuse into the target cell (vii). **(B)** $EEA1^+$ vesicles containing MPEG1 (i) are triggered to traffic toward and fuse with the phagosomal membrane by monoubiquitination (blue diamond) (ii). Tethered MPEG1 [only the MACPF (red) and MABP domains (yellow) are shown] is proteolyzed from the lipid bilayer [transmembrane region and cytosolic tail are shown as a line (green)] (iii). Cleaved MPEG1 oligomerizes into a prepore (v). Upon strong acidification (pH < 5), MPEG1 is activated and transitions into a pore (vi or ix). MPEG1 may follow two proposed pathways (iv or vii). In the trans-pore model, oligomerization occurs on the host bilayer (iv to v) and *trans*-pores breach the bilayer of target membranes in close proximity (vi) (82). Other receptor complexes may be required to drive the formation of a close membrane–membrane junction (blue/orange receptor complex; asterisk). Alternatively, MPEG1 monomers diffuse within the synapse (vii) and oligomerize on microbial bilayers (vii to viii). The MACPF or MABP domains rotate, to re-orient the MACPF machinery toward the microbial bilayer [vii or viii; unclear (83)]. A *cis*-pore breaches the microbial bilayer (ix). The stage of MACPF or MABP domain rotation is unclear. After either a *trans*- or *cis*-pore has formed, effector molecules enter the target cell *via* the MPEG1 pore (x).

These experiments suggest that, rather than a protective role, the MABP β-hairpin may perform a targeting role as an ancillary domain in a more typical MACPF/CDC sense (**Figures 6Bvii–viii**). However, in this context the assembly of the prepore occurs independently from the target membrane (either in solution or on another bilayer)—this ability itself is unique when compared to other family members.

These features suggest that MPEG1, unlike other MACPF/CDC systems studied to date, may follow a distinct assembly pathway with independent assembly and target membranes (regardless of the role of the MABP β-hairpin). Both the ability to form soluble active prepore oligomers and the unique domain arrangement distinguish MPEG1 from other characterized MACPF/CDCs. Indeed, the canonical mechanism of pore formation and the notion of a single assembly/target membrane may not be consistent with the MPEG1 system.

Acid Induced Pore Formation

Recent structure–functions studies reveal MPEG1 activity is strictly dependent on acidification, with recombinant MPEG1

becoming increasingly active at lower pH, with pH 5.5 representing an upper limit for detectable activity (82, 83) (**Figure 2ix**). How exactly pH triggers the prepore-to-pore transition of MPEG1 is not understood. The motifs and residues that mediate this acid trigger have not yet been established. Inspection of the core domain of MPEG1 does not reveal titratable residues that clearly govern key interactions for activation. As an alternative hypothesis, perhaps the low pH has an overall destabilizing effect and thus reduces the necessary activation energy. In any case, the acid trigger represents an important negative regulatory mechanism employed by the cell. This mechanism also explains why MPEG1 activity occurs within the matured endosomal vesicles and the phagolysosome. Furthermore, inhibition of endosomal acidification, for example by inhibitors of vacuolar-type H^+-ATPases, would likely confer resistance to intracellular microbes by preventing the activation of MPEG1. This is a known mechanism of microbial evasion and is described for several pathogens, reviewed elsewhere (115). In contrast, earlier studies of MPEG1 function examined endosomal pH levels and found vesicles occupied by the intracellular pathogen *L. monocytogenes* rapidly acidify in MPEG1 deficient cell lines (116). Conversely, acidification was significantly delayed when MPEG1 expression was rescued. These data suggest that MPEG1 somehow functions to slow the rapid acidification of these phagosomal vesicles. These observations appear paradoxical. Specifically, it is unclear how exactly MPEG1 functions to reduce the acidification of vesicles *in situ*, while being strictly dependent on low pH for activity *in vitro*.

MPEG1 Proposed Models and Mechanisms

The archetypal model of pore formation has largely arisen to describe PRF and CDCs (**Figure 3**); however, this canonical mechanism fails to explain how intracellular MACPFs operate within membranous compartments without detrimental effects to the host cell. Furthermore, membrane tethered MACPF systems, such as MPEG1 and ASTN1/2, challenge the notions of diffusion, membrane recognition, and oligomerization; in particular, the sequence of events may be different or additional steps may be required, such as proteolysis. There are currently two proposed models of pore formation, both of which may co-exist depending on context, together these represent an exciting frontier in understanding MPEG function (**Figure 6B**). In this regard, *in situ* data, such as cryo-electron tomography (cryoET) of MPEG1 in cells, will be important to determine the final pore state, mechanism of bactericidal activity and whether the prepore observed thus far represents a productive intermediate on the way to pore formation.

The Immunosynapse and *Trans*-Pore Formation

The advances in MPEG1 biology highlighted by recent studies address a critical question of how an intracellular MACPF can function within membrane compartments without killing the host cell. Specifically, the orientation of membrane-bound MPEG1 suggests pore formation can occur in an adjacent membrane (**Figure 6B vi**). As a result, MPEG1 may bridge two bilayers; one membrane is coordinated by the MABP β-hairpin, while the other becomes the target of the MACPF β-barrel of the MPEG1 pore (**Figure 6B vi**). Such a mechanism is akin to a primordial (intracellular) immune synapse, where the phagosomal membrane and target membrane are brought into close proximity by conjugate cellular mechanisms *e.g.* immune receptor:antigen interactions (**Figure 6B**; right). Such proximity would then allow for MPEG1 pores to preferentially damage pathogen bilayers, while providing a method of protecting the host bilayer. Of course, to ensure that pore formation results in damage to a target membrane, it is important that acidification occur after a synapse has been established such that membranes are in sufficient proximity. Importantly, these *trans*-pores were observed in cryo-EM data sets of MPEG1 proteoliposomes (82); however, these were a rare population, and 3D reconstructions were not possible. Further structural and biochemical studies will be required to confirm or exclude their existence.

A key implication of the *trans*-pore model is that MPEG1 has little target specificity, rather MPEG1 would damage any membrane that is sufficiently close upon activation. Similarly, broad anti-membrane activity is thought to occur for the MAC, which employs an atypical target-recognition mechanism (20–22, 105). Likewise, upon its delivery, PRF must recognize any host cell membrane in the immune synapse. In this regard, PRF has been shown to form pores on several lipid compositions, relying more specifically on the physical properties of lipid fluidity to distinguish its target (117) (**Figure 6A**). An evolutionary advantage would be conferred by immune effectors that can broadly target and damage a variety of membrane compositions and thus a range of pathogens. Therefore, metazoan immune complexes such as MPEG1, MAC, and PRF may have evolved greater flexibility in their target recognition, while relying more heavily on conjugate cellular mechanisms to govern their regulation *e.g.* PRF granules, or the MAC-inhibitor CD59 (118) or the domain arrangement in MPEG1 (82, 83). Broad anti-membrane activity would maximize the spectrum of potential vulnerable targets; however, it would also simultaneously make the organism more susceptible to collateral damage. Therefore, conjugate cellular mechanisms might be more important in governing the regulation, delivery, and activation of the mammalian perforin-like immune effectors (**Figure 6A**). The promiscuity of these immune effectors is highlighted when juxtaposed against other PFPs that have highly specific target recognition requirements (*e.g.* pleurotolysin, intermedilysin) (13, 119).

MABP Rotation and *Cis*-Pore Formation

In contrast, the recent structure of a murine MPEG1 pore at 5 Å illustrates an unexpected conformational rearrangement of the MABP domain (83) (**Figure 6B viii**). Comparison of MPEG1 structures as a soluble prepore and a detergent solubilized pore suggests a different model of pore formation occurs, whereby rotation of the MABP domain and β-hairpin motif is responsible for recognition of the target membrane (**Figure 6B vi**). The drastic conformational rearrangement corresponds to a lateral 180° rotation of the MABP domain (such that the peripheral region remains on the periphery), resulting in the MABP

β-hairpin and MACPF domains being re-oriented in the same direction (**Figure 5E**, **Figure 6B viii**). It is not clear whether this rearrangement would occur prior to acid-induced pore formation or accompany pore formation. One possibility is that the MABP β-hairpin swings down to recognize the target membrane, engaging the bilayer *via* the lipid binding motif (**Figure 6B vi**). Subsequently, upon acidification, the MPEG1 prepore (here in a late stage) unfurls to form a giant β-barrel in the target. In support of this model is a disulfide trapped mutant, which locks the MABP domain to the linker region, preventing domain movement. This mutant loses lytic activity until a reducing agent is added, restoring activity to that of wild type. These data suggest that MPEG1 activity is dependent on the movement of the MABP domain.

While there are some parallels between this model and the archetypal mechanism, the model is nevertheless unique. Specifically, MPEG1 may adopt two prepore states, both an early stage (either soluble or membrane-bound; **Figure 6B iv**) and a late stage (MABP and MACPF in the same orientation; **Figure 6B vii**) [also depicted in Ni et al. (83)]. Furthermore, this model provides a simpler explanation of target recognition, without postulating coupled processes or receptors, as the MABP β-hairpin alone would be sufficient. Problematically, the *cis*-pore model fails to explain how freely diffusing MPEG1 could function within a membrane compartment without damaging the cell's own membranes. A similar conundrum exists for PRF, which functions at the immunosynapse between a host and target cell (**Figure 6A**). One recent study suggests that differences in the fluidity of the lipid bilayer of cytotoxic T cells, compared to that in target cells, can protect T-cell membranes from PRF pore formation (117). Therefore, potential differences in membrane properties of the host and pathogen may likewise provide selectivity in the MPEG1 system.

DISCUSSION

In vitro studies of MPEG1 have provided key biophysical and structural insights into the MPEG1 assembly pathway. Two models have emerged that attempt to explain the MPEG1 mechanism, namely the *cis*- and *trans*-pore models; however, there remain several questions that neither assembly model fully addresses (**Figure 6**). At this point in time the field cannot resolve both models. In this regard it is obvious that the MPEG1 system deviates from other MACPFs. Indeed, the MPEG1 system appears to adopt a unique mechanism of pore formation altogether. Further work is required such as characterization of other potential structural states, as well as higher resolution data of current models. Particularly, *in situ* studies would be beneficial to ascertain the stepwise events in MPEG1 function, *e.g.* data acquired by imaging pores within the cellular environment by cryoET.

One issue with the *trans*-pore model is the apparent redundancy of the MABP domain and the transmembrane helix. It seems mysterious that MPEG1 would evolve two independent mechanisms for anchoring to the host membrane (**Figures 6B iii, iv**). In contrast, the *cis*-pore model is consistent with a need for both a transmembrane helix and a secondary membrane recognition domain for targeting, namely the MABP domain. Matters are complicated by the role of proteolysis where it is hypothesized that cleavage of the transmembrane helix is necessary for oligomerization (**Figure 6B iii**). The *trans*-pore model encompasses the possibility of proteolysis, whereby the MABP β-hairpin functions in sequestering MPEG1. In contrast, in the *cis*-pore model, proteolysis raises the issue of host cell protection where membrane compartments become susceptible to collateral damage by freely diffusing MPEG1.

Nevertheless, there is structural and biochemical evidence to support a *cis*-pore model, where it is proposed the MABP domain rotates to contact the target bilayer (**Figures 6 vii–xi**) (83). However, it is unclear how such a conformational shift would be physically possible in an oligomeric form, since significant clashes with neighbouring subunits would prohibit the MABP rotation. Secondly, substantial energy would be required to dissociate all sixteen MABP β-hairpins from the bilayer to allow for MABP rotation. Assuming the MPEG1 complex does not dissociate from the bilayer (**Figures 6 iv–vi**), structural comparison of the membrane-bound prepore (**Figure 5D**) and the inserted pore state (**Figures 5E**) suggests that the point of rotation is about the MACPF domain rather than the MABP domain. However, rotation of the MACPF domain seems highly unlikely. This would require extensive interactions formed at the MACPF interface to break or require subunits to dissociate entirely to accommodate the large motion. Taken together, within an oligomeric state, rotation of either the MACPF or MABP domains is difficult to reconcile. One possibility is that structural rearrangement occurs prior to oligomerization, *i.e.* as monomers (**Figures 6B iv, vi**); however this is inconsistent with the observed lytic activity of pre-assembled oligomers (82, 83). Alternatively, it is possible that the observed *cis*-pore may be artefactual, resulting from detergent solubilization or partial denaturation at pH 3.6–4.0. Further studies will be required in order to address these issues and confirm if, and how, the MABP domain rotates in the presence of lipid bilayers and under more physiological conditions.

It is worth considering similarities between MPEG1—the most ancient pore forming MACPF protein described to date—and the GSDMs—a somewhat recently described family of pore forming proteins that drive programmed cell death *via* pyroptosis. Both are intracellular pore forming proteins that share a similar function that is pore formation in immunity. Our analysis further reveals these molecules clearly share the same overall core topological fold (**Figures 4A–C**) in agreement with others (62), and both MPEG1 and GSDMs require activation *via* proteolysis. These comparisons reveal that both MACPF proteins and GSDMs utilize common mechanistic features to form large β-barrel lined pores—*i.e.* oligomerization of a substantial number of monomers and the unwinding of two topologically equivalent regions within each monomer to form membrane spanning amphipathic β-hairpins (**Figures 4A–C**).

Despite these observations, sequence comparisons reveal no obvious sequence conservation between the two families.

Furthermore, certain structural features of MACPF proteins (*e.g.* the HTH motif) are absent in GSDMs. Thus, some controversy exists with respect to whether the similarities between GSDMs and MACPF proteins have arisen through convergent or divergent evolution. Based on bioinformatic studies of other protein families (120), we, and others (62, 63), suggest that the structural, functional, and mechanistic data collectively present a reasonably compelling argument for a common ancestry between MACPF proteins and GSDMs. Such a relationship, if further supported (for example through identification and structural characterization of proteins that link the two families), may reveal intriguing new aspects of how members of the MACPF superfamily have been deployed and re-deployed throughout the breadth of the immune response.

Herein, we have discussed the role MPEG1 plays within the cellular environment and its involvement as an immune effector. While several features of MPEG1 have been elucidated, many new questions have correspondingly arisen. For example, few studies have been performed that investigate the short MPEG1 isoform (MPEG1b), and hence, its role is poorly understood. Overall, the structural advances to date will provide a strong foundation for future work by guiding experiments and *in situ* studies. Of particular interest will be the impact of more directed mutagenesis and targeted changes to MPEG1 domains and key structural elements, to ascertain what effects these have on phenotypes in cellular and animal models. In this regard, further studies will be highly informative in delineating the physiological roles of MPEG1 and its assembly.

AUTHOR CONTRIBUTIONS

Drafting of manuscript by CB-J, JW and MD. Figures made by CB-J. Critical review and editing of manuscript by BS and SP. All authors contributed to the article and approved the submitted version.

FUNDING

CB-J acknowledges the support of the Australian Government RTP scholarship. JW is an Australian Research Council (ARC) Laureate Fellow (FL180100019) and an Honorary National Health and Medical Research Council (NHMRC) Senior Principal Research Fellow (APP1127593). He acknowledges the previous support of an Australian Research Council (ARC) Federation Fellowship. MD acknowledges the support of an ARC Future Fellowship (FT150100049) and ARC Discovery Project (DP180100040). We thank the staff of the Monash Ramaciotti Centre for Electron Microscopy, the Monash protein production and proteomics platforms, and the support of the MASSIVE supercomputer team.

REFERENCES

1. Morita-Yamamuro C, Tsutsui T, Sato M, Yoshioka H, Tamaoki M, Ogawa D, et al. The Arabidopsis gene CAD1 controls programmed cell death in the plant immune system and encodes a protein containing a MACPF domain. *Plant Cell Physiol* (2005) 46(6):902–12. doi: 10.1093/pcp/pci095
2. Fukunaga S, Sogame M, Hata M, Singkaravanit-Ogawa S, Piślewska-Bednarek M, Onozawa-Komori M, et al. Dysfunction of Arabidopsis MACPF domain protein activates programmed cell death via tryptophan metabolism in MAMP-triggered immunity. *Plant J* (2017) 89(2):381–93. doi: 10.1111/tpj.13391
3. Noutoshi Y, Kuromori T, Wada T, Hirayama T, Kamiya A, Imura Y, et al. Loss of necrotic spotted lesions 1 associates with cell death and defense responses in Arabidopsis thaliana. *Plant Mol Biol* (2006) 62(1–2):29–42. doi: 10.1007/s11103-006-9001-6
4. Hirst RA, Kadioglu A, O'Callaghan C, Andrew PW. The role of pneumolysin in pneumococcal pneumonia and meningitis. *Clin Exp Immunol* (2004) 138(2):195–201. doi: 10.1111/j.1365-2249.2004.02611.x
5. Awad MM, Ellemor DM, Boyd RL, Emmins JJ, Rood JI. Synergistic effects of alpha-toxin and perfringolysin O in Clostridium perfringens-mediated gas gangrene. *Infect Immun* (2001) 69(12):7904–10. doi: 10.1128/IAI.69.12.7904-7910.2001
6. Hamon MA, Ribet D, Stavru F, Cossart P. Listeriolysin O: The Swiss army knife of Listeria. *Trends Microbiol* (2012) 20(8):360–8. doi: 10.1016/j.tim.2012.04.006
7. Kadota K, Ishino T, Matsuyama T, Chinzei Y, Yuda M. Essential role of membrane-attack protein in malarial transmission to mosquito host. *Proc Natl Acad Sci U S A* (2004) 101(46):16310–5. doi: 10.1073/pnas.0406187101
8. Ishino T, Chinzei Y, Yuda M. A Plasmodium sporozoite protein with a membrane attack complex domain is required for breaching the liver sinusoidal cell layer prior to hepatocyte infection. *Cell Microbiol* (2005) 7 (2):199–208. doi: 10.1111/j.1462-5822.2004.00447.x
9. Ellisdon AM, Reboul CF, Panjikar S, Huynh K, Oellig CA, Winter KL, et al. Stonefish toxin defines an ancient branch of the perforin-like superfamily. *Proc Natl Acad Sci U S A* (2015) 112(50):15360–5. doi: 10.1073/pnas.1507622112
10. Nagai H, Oshiro N, Takuwa-Kuroda K, Iwanaga S, Nozaki M, Nakajima T. Novel proteinaceous toxins from the nematocyst venom of the Okinawan sea anemone Phyllodiscus semoni Kwietniewski. *Biochem Biophys Res Commun* (2002) 294(4):760–3. doi: 10.1016/S0006-291X(02)00547-8
11. Oshiro N, Kobayashi C, Iwanaga S, Nozaki M, Namikoshi M, Spring J, et al. A new membrane-attack complex/perforin (MACPF) domain lethal toxin from the nematocyst venom of the Okinawan sea anemone Actineria villosa. *Toxicon* (2004) 43(2):225–8. doi: 10.1016/j.toxicon.2003.11.017
12. Giglio ML, Ituarte S, Milesi V, Dreon MS, Brola TR, Caramelo J, et al. Exaptation of two ancient immune proteins into a new dimeric pore-forming toxin in snails. *J Struct Biol* (2020) 211(2):107531. doi: 10.1016/j.jsb.2020.107531
13. Lukoyanova N, Kondos SC, Farabella I, Law RHP, Reboul CF, Caradoc-Davies TT, et al. Conformational Changes during Pore Formation by the Perforin-Related Protein Pleurotolysin. *PLoS Biol* (2015) 13(2):1–15. doi: 10.1371/journal.pbio.1002049
14. Panevska A, Hodnik V, Skočaj M, Novak M, Modic Š, Pavlic I, et al. Pore-forming protein complexes from Pleurotus mushrooms kill western corn rootworm and Colorado potato beetle through targeting membrane ceramide phosphoethanolamine. *Sci Rep* (2019) 9(1):5073. doi: 10.1038/s41598-019-41450-4
15. Anderluh G, Kisovec M, Kraševec N, Gilbert RJC. MACPF/CDC Proteins - Agents of Defence, Attack and Invasion. *Sub-cellular Biochem* (2014) 80:7–30 p. doi: 10.1007/978-94-017-8881-6_2
16. Bayly-Jones C, Bubeck D, Dunstone MA. The mystery behind membrane insertion: A review of the complement membrane attack complex. *Philos Trans R Soc B Biol Sci* (2017) 372(1726):20160221. doi: 10.1098/rstb.2016.0221

17. Rosado CJ, Kondos S, Bull TE, Kuiper MJ, Law RHP, Buckle AM, et al. The MACPF/CDC family of pore-forming toxins. *Cell Microbiol* (2008) 10 (9):1765–74. doi: 10.1111/j.1462-5822.2008.01191.x
18. Podack ER, Munson GP. Killing of microbes and cancer by the immune system with three mammalian pore-forming killer proteins. *Front Immunol* (2016) 7:464. doi: 10.3389/fimmu.2016.00464
19. Kaufmann SHE. Immunology's foundation: The 100-year anniversary of the Nobel Prize to Paul Ehrlich and Elie Metchnikoff. *Nat Immunol* (2008) 9:705–12. doi: 10.1038/ni0708-705
20. Parsons ES, Stanley GJ, Pyne ALB, Hodel AW, Nievergelt AP, Menny A, et al. Single-molecule kinetics of pore assembly by the membrane attack complex. *Nat Commun* (2019) 10(1):2066. doi: 10.1038/s41467-019-10058-7
21. Serna M, Giles JL, Morgan BP, Bubeck D. Structural basis of complement membrane attack complex formation. *Nat Commun* (2016) 7:1–7. doi: 10.1038/ncomms10587
22. Spicer BA, Law RHP, Caradoc-davies TT, Ekkel SM, Bayly-Jones C, Pang S, et al. The first transmembrane region of complement component-9 acts as a brake on its self-assembly. *Nat Commun* (2018) 9(3266):3266. doi: 10.1038/s41467-018-05717-0
23. Dudkina NV, Spicer BA, Reboul CF, Conroy PJ, Lukoyanova N, Elmlund H, et al. Structure of the poly-C9 component of the complement membrane attack complex. *Nat Commun* (2016) 7:10588. doi: 10.1038/ncomms10588
24. Doorduijn DJ, Rooijakkers SHM, Heesterbeek DAC. How the Membrane Attack Complex Damages the Bacterial Cell Envelope and Kills Gram-Negative Bacteria. *BioEssays* (2019) 41(10):1900074. doi: 10.1002/bies.201900074
25. Heesterbeek DA, Bardoel BW, Parsons ES, Bennett I, Ruyken M, Doorduijn DJ, et al. Bacterial killing by complement requires membrane attack complex formation via surface-bound C5 convertases. *EMBO J* (2019) 38(4):e99852. doi: 10.15252/embj.201899852
26. Doorduijn DJ, Bardoel BW, Heesterbeek DAC, Ruyken M, Benn G, Parsons ES, et al. Bacterial killing by complement requires direct anchoring of membrane attack complex precursor C5b-7. *PLoS Pathog* (2020) 16(6): e1008606. doi: 10.1371/journal.ppat.1008606
27. Heesterbeek DAC, Martin NI, Velthuizen A, Duijst M, Ruyken M, Wubbolts R, et al. Complement-dependent outer membrane perturbation sensitizes Gram-negative bacteria to Gram-positive specific antibiotics. *Sci Rep* (2019) 9(1):7841. doi: 10.1038/s41598-019-43208-4
28. Zhang Z, Yang J, Wei J, Yang Y, Chen X, Zhao X, et al. Trichinella spiralis paramyosin binds to c8 and c9 and protects the tissue-dwelling nematode from being attacked by host complement. *PLoS Negl Trop Dis* (2011) 5(7): e1225. doi: 10.1371/journal.pntd.0001225
29. Parizade M, Arnon R, Lachmann PJ, Fishelson Z. Functional and antigenic similarities between a 94-kD protein of Schistosoma mansoni (SCIP-1) and human CD59. *J Exp Med* (1994) 179(5):1625–36. doi: 10.1084/jem.179.5.1625
30. Schreiber RD, Morrison DC, Podack ER, Müller-Eberhard HJ. Bactericidal activity of the alternative complement pathway generated from 11 isolated plasma proteins. *J Exp Med* (1979) 149(4):870–82. doi: 10.1084/jem.149.4.870
31. Martinez RJ, Carroll SF. Sequential metabolic expressions of the lethal process in human serum-treated Escherichia coli: Role of lysozyme. *Infect Immun* (1980) 28(3):735–45.
32. Kim SH, Carney DF, Hammer CH, Shin ML. Nucleated cell killing by complement: effects of C5b-9 channel size and extracellular Ca2+ on the lytic process. *J Immunol* (1987) 138(5):1530–6.
33. Niculescu F, Rus H, van Biesen T, Shin ML. Activation of Ras and mitogen-activated protein kinase pathway by terminal complement complexes is G protein dependent. *J Immunol* (1997) 158(9):4405–12.
34. Morgan BP. The membrane attack complex as an inflammatory trigger. *Immunobiology* (2016) 221:747–51. doi: 10.1016/j.imbio.2015.04.006
35. Nagata M, Hara T, Aoki T, Mizuno Y, Akeda H, Inaba S, et al. Inherited deficiency of ninth component of complement: An increased risk of meningococcal meningitis. *J Pediatr* (1989) 114(2):260–3. doi: 10.1016/S0022-3476(89)80793-0
36. Inai S, Akagaki Y, Moriyama T, Fukumori Y, Yoshimura K, Ohnoki S, et al. Inherited deficiencies of the late-acting complement components other than C9 found among healthy blood donors. *Int Arch Allergy Immunol* (1989) 90 (3):274–9. doi: 10.1159/000235037
37. Takeda J, Miyata T, Kawagoe K, Iida Y, Endo Y, Fujita T, et al. Deficiency of the GPI anchor caused by a somatic mutation of the PIG-A gene in paroxysmal nocturnal hemoglobinuria. *Cell* (1993) 73(4):703–11. doi: 10.1016/0092-8674(93)90250-T
38. Bessler M, Mason PJ, Hillmen P, Miyata T, Yamada N, Takeda J, et al. Paroxysmal nocturnal haemoglobinuria (PNH) is caused by somatic mutations in the PIG-A gene. *EMBO J* (1994) 13(1):110–7. doi: 10.1002/j.1460-2075.1994.tb06240.x
39. Podack ER, Young JDE, Cohn ZA. Isolation and biochemical and functional characterization of perforin 1 from cytolytic T-cell granules. *Proc Natl Acad Sci U S A* (1985) 82(24):8629–33. doi: 10.1073/pnas.82.24.8629
40. Masson D, Tschopp J. Isolation of a lytic, pore-forming protein (perforin) from cytolytic T-lymphocytes. *J Biol Chem* (1985) 260(16):9069–72.
41. Stinchcombe JC, Bossi G, Booth S, Griffiths GM. The immunological synapse of CTL contains a secretory domain and membrane bridges. *Immunity* (2001) 15(5):751–61. doi: 10.1016/S1074-7613(01)00234-5
42. Baran K, Dunstone M, Chia J, Ciccone A, Browne KA, Clarke CJP, et al. The Molecular Basis for Perforin Oligomerization and Transmembrane Pore Assembly. *Immunity* (2009) 30(5):684–95. doi: 10.1016/j.immuni.2009.03.016
43. Law RHP, Lukoyanova N, Voskoboinik I, Caradoc-Davies TT, Baran K, Dunstone MA, et al. The structural basis for membrane binding and pore formation by lymphocyte perforin. *Nature* (2010) 468(7322):447–51. doi: 10.1038/nature09518
44. Talanian RV, Yang XH, Turbov J, Seth P, Ghayur T, Casiano CA, et al. Granule-mediated killing: Pathways for granzyme B-initiated apoptosis. *J Exp Med* (1997) 186(8):1323–31. doi: 10.1084/jem.186.8.1323
45. Lopez JA, Jenkins MR, Rudd-Schmidt JA, Brennan AJ, Danne JC, Mannering SI, et al. Rapid and Unidirectional Perforin Pore Delivery at the Cytotoxic Immune Synapse. *J Immunol* (2013) 191(5):2328–34. doi: 10.4049/jimmunol.1301205
46. Jenkins MR, Rudd-Schmidt JA, Lopez JA, Ramsbottom KM, Mannering SI, Andrews DM, et al. Failed CTL/NK cell killing and cytokine hypersecretion are directly linked through prolonged synapse time. *J Exp Med* (2015) 212 (3):307–17. doi: 10.1084/jem.20140964
47. Voskoboinik I, Whisstock JC, Trapani JA. Perforin and granzymes: Function, dysfunction and human pathology. *Nat Rev Immunol* (2015) 15:388–400. doi: 10.1038/nri3839
48. Berkowicz SR, Giousoh A, Bird PI. Neurodevelopmental MACPFs: The vertebrate astrotactins and BRINPs. *Semin Cell Dev Biol* (2017) 72:171–81. doi: 10.1016/j.semcdb.2017.05.005
49. Hatten ME. New directions in neuronal migration. *Science* (2002) 297:1660–3. doi: 10.1126/science.1074572
50. Fink JM, Hirsch BA, Zheng C, Dietz G, Hatten ME, Ross ME. Astrotactin (ASTN), a gene for glial-guided neuronal migration, maps to human chromosome 1q25.2. *Genomics* (1997) 40(1):202–5. doi: 10.1006/geno.1996.4538
51. Zheng C, Heintz N, Hatten ME. CNS gene encoding astrotactin, which supports neuronal migration along glial fibers. *Sci (80-)* (1996) 272 (5260):417–9. doi: 10.1126/science.272.5260.417
52. Kawano H, Nakatani T, Mori T, Ueno S, Fukaya M, Abe A, et al. Identification and characterization of novel developmentally regulated 5neural-specific proteins, BRINP family. *Mol Brain Res* (2004) 125(1–2):60–75. doi: 10.1016/j.molbrainres.2004.04.001
53. Terashima M, Kobayashi M, Motomiya M, Inoue N, Yoshida T, Okano H, et al. Analysis of the expression and function of BRINP family genes during neuronal differentiation in mouse embryonic stem cell-derived neural stem cells. *J Neurosci Res* (2010) 88(7):1387–93. doi: 10.1002/jnr.22315
54. Lionel AC, Tammimies K, Vaags AK, Rosenfeld JA, Ahn JW, Merico D, et al. Disruption of the ASTN2/TRIM32 locus at 9q33.1 is a risk factor in males for autism spectrum disorders, ADHD and other neurodevelopmental phenotypes. *Hum Mol Genet* (2014) 23(10):2752–68. doi: 10.1093/hmg/ddt669
55. Wang KS, Tonarelli S, Luo X, Wang L, Su B, Zuo L, et al. Polymorphisms within ASTN2 gene are associated with age at onset of Alzheimer's disease. *J Neural Transm* (2015) 122(5):701–8. doi: 10.1007/s00702-014-1306-z

56. Adams NC, Tomoda T, Cooper M, Dietz G, Hatten ME. Mice that lack astrotactin have slowed neuronal migration. *Development* (2002) 129 (4):965–72.
57. Broz P, Pelegrín P, Shao F. The gasdermins, a protein family executing cell death and inflammation. *Nat Rev Immunol* (2020) 20:143–57. doi: 10.1038/s41577-019-0228-2
58. Liu X, Lieberman J. Knocking rsquoem Dead: Pore-Forming Proteins in Immune Defense. *Annu Rev Immunol* (2020) 38:455–85. doi: 10.1146/annurev-immunol-111319-023800
59. Shi J, Zhao Y, Wang K, Shi X, Wang Y, Huang H, et al. Cleavage of GSDMD by inflammatory caspases determines pyroptotic cell death. *Nature* (2015) 526(7575):660–5. doi: 10.1038/nature15514
60. Ding J, Wang K, Liu W, She Y, Sun Q, Shi J, et al. Pore-forming activity and structural autoinhibition of the gasdermin family. *Nature* (2016) 535 (7610):111–6. doi: 10.1038/nature18590
61. Sborgi L, Rühl S, Mulvihill E, Pipercevic J, Heilig R, Stahlberg H, et al. GSDMD membrane pore formation constitutes the mechanism of pyroptotic cell death. *EMBO J* (2016) 35(16):1766–78. doi: 10.15252/embj.201694696
62. Rogers C, Fernandes-Alnemri T, Mayes L, Alnemri D, Cingolani G, Alnemri ES. Cleavage of DFNA5 by caspase-3 during apoptosis mediates progression to secondary necrotic/pyroptotic cell death. *Nat Commun* (2017) 8:1–14. doi: 10.1038/ncomms14128
63. Mulvihill E, Sborgi L, Mari SA, Pfreundschuh M, Hiller S, Müller DJ. Mechanism of membrane pore formation by human gasdermin-D. *EMBO J* (2018) 37(14):e98321. doi: 10.15252/embj.201798321
64. Spilsbury K, O'Mara MA, Wu WM, Rowe PB, Symonds G, Takayama Y. Isolation of a novel macrophage-specific gene by differential cDNA analysis. *Blood* (1995) 85(6):1620–9. doi: 10.1182/blood.V85.6.1620.bloodjournal8561620
65. Wiens M, Korzhev M, Krasko A, Thakur NL, Breter HJ, Ushijima H, et al. Innate Immune Defense of the Sponge Suberites domuncula against Bacteria Involves a MyD88-dependent Signaling Pathway. *J Biol Chem* (2005) 280 (30):27949–59. doi: 10.1074/jbc.M504049200
66. D'Angelo ME, Dunstone MA, Whisstock JC, Trapani JA, Bird PI. Perforin evolved from a gene duplication of MPEG1, followed by a complex pattern of gene gain and loss within Euteleostomi. *BMC Evol Biol* (2012) 12:59. doi: 10.1186/1471-2148-12-59
67. Miller DJ, Hemmrich G, Ball EE, Hayward DC, Khalturin K, Funayama N, et al. The innate immune repertoire in Cnidaria - Ancestral complexity and stochastic gene loss. *Genome Biol* (2007) 8(4):R59. doi: 10.1186/gb-2007-8-4-r59
68. Traylor-Knowles N, Vandepas LE, Browne WE. Still Enigmatic: Innate Immunity in the Ctenophore Mnemiopsis leidyi. *Integr Comp Biol* (2019) 59(4):811–8. doi: 10.1093/icb/icz116
69. Gorbushin AM. Membrane Attack Complex/Perforin domain-containing proteins in a dual-species transcriptome of caenogastropoda Littorina littorea and its trematode parasite Himasthla elongata. *Fish Shellfish Immunol* (2016) 54:254–6. doi: 10.1016/j.fsi.2016.04.015
70. Mah SA, Moy GW, Swanson WJ, Vacquier VD. A perforin-like protein from a marine mollusk. *Biochem Biophys Res Commun* (2004) 316(2):468–75. doi: 10.1016/j.bbrc.2004.02.073
71. Kemp IK, Coyne VE. Identification and characterisation of the Mpeg1 homologue in the South African abalone, Haliotis midae. *Fish Shellfish Immunol* (2011) 31(6):754–64. doi: 10.1016/j.fsi.2011.07.010
72. He X, Zhang Y, Yu Z. An Mpeg (macrophage expressed gene) from the Pacific oyster Crassostrea gigas: Molecular characterization and gene expression. *Fish Shellfish Immunol* (2011) 30(3):870–6. doi: 10.1016/j.fsi.2011.01.009
73. Wang G, Zhang K, Zhang Z, Zou Z, Jia X-W, Wang S-H, et al. Molecular cloning and responsive expression of macrophage expressed gene from small abalone Haliotis diversicolor supertexta. *Fish Shellfish Immunol* (2008) 24 (3):346–59. doi: 10.1016/j.fsi.2007.12.008
74. Bathige SDNK, Umasuthan N, Whang I, Lim BS, Won SH, Lee J. Antibacterial activity and immune responses of a molluscan macrophage expressed gene-1 from disk abalone, Haliotis discus discus. *Fish Shellfish Immunol* (2014) 39 (2):263–72. doi: 10.1016/j.fsi.2014.05.012
75. Renault T, Faury N, Barbosa-Solomieu V, Moreau K. Suppression substractive hybridisation (SSH) and real time PCR reveal differential gene expression in the Pacific cupped oyster, Crassostrea gigas, challenged with Ostreid herpesvirus 1. *Dev Comp Immunol* (2011) 35(7):725–35. doi: 10.1016/j.dci.2011.02.004
76. Wang KJ, Ren HL, Xu DD, Cai L, Yang M. Identification of the up-regulated expression genes in hemocytes of variously colored abalone (Haliotis diversicolor Reeve, 1846) challenged with bacteria. *Dev Comp Immunol* (2008) 32(11):1326–47. doi: 10.1016/j.dci.2008.04.007
77. Walters BM, Connelly MT, Young B, Traylor-Knowles N. The Complicated Evolutionary Diversification of the Mpeg-1/Perforin-2 Family in Cnidarians. *Front Immunol* (2020) 11:1690. doi: 10.3389/fimmu.2020.01690
78. McCormack RM, Podack ER. Perforin-2 / Mpeg1 and other pore-forming proteins throughout evolution. *J Microbiol Immunol* (2015) 98(5):761–8. doi: 10.1189/jlb.4MR1114-523RR
79. McCormack RM, de Armas LR, Shiratsuchi M, Fiorentino DG, Olsson ML, Lichtenheld MG, et al. Perforin-2 is essential for intracellular defense of parenchymal cells and phagocytes against pathogenic bacteria. *Elife* (2015) 4 (September):e06508. doi: 10.7554/eLife.06508
80. McCormack RM, Lyapichev K, Olsson ML, Podack ER, Munson GP. Enteric pathogens deploy cell cycle inhibiting factors to block the bactericidal activity of Perforin-2. *Elife* (2015) 4:e065051–22. doi: 10.7554/eLife.06505
81. Xiong P, Shiratsuchi M, Matsushima T, Liao J, Tanaka E, Nakashima Y, et al. Regulation of expression and trafficking of perforin-2 by LPS and TNF-α. *Cell Immunol* (2017) 320(May):1–10. doi: 10.1016/j.cellimm.2017.07.001
82. Pang SS, Bayly-Jones C, Radjainia M, Spicer BA, Law RHP, Hodel AW, et al. The cryo-EM structure of the acid activatable pore-forming immune effector Macrophage-expressed gene 1. *Nat Commun* (2019) 10(1):1–9. doi: 10.1038/s41467-019-12279-2
83. Ni T, Jiao F, Yu X, Aden S, Ginger L, Williams SI, et al. Structure and mechanism of bactericidal mammalian perforin-2, an ancient agent of innate immunity. *Sci Adv* (2020) 6(5):1–13. doi: 10.1126/sciadv.aax8286
84. McCormack RM, Szymanski EP, Hsu AP, Perez E, Olivier KN, Fisher E, et al. MPEG1/perforin-2 mutations in human pulmonary nontuberculous mycobacterial infections. *JCI insight* (2017) 2(8):1–8. doi: 10.1172/jci.insight.89635
85. Boura E, Hurley JH. Structural basis for membrane targeting by the MVB12-associated β-prism domain of the human ESCRT-I MVB12 subunit. *Proc Natl Acad Sci* (2012) 109(6):1901–6. doi: 10.1073/pnas.1117597109
86. Rosado CJ, Buckle AM, Law RHP, Butcher RE, Kan WT, Bird CH, et al. A common fold mediates vertebrate defense and bacterial attack. *Sci (80-)* (2007) 317(5844):1548–51. doi: 10.1126/science.1144706
87. Strbo N, Pastar I, Romero L, Chen V, Vujanac M, Sawaya AP, et al. Single cell analyses reveal specific distribution of anti-bacterial molecule Perforin-2 in human skin and its modulation by wounding and Staphylococcus aureus infection. *Exp Dermatol* (2019) 28(3):225–32. doi: 10.1111/exd.13870
88. Benard EL, Racz PI, Rougeot J, Nezhinsky AE, Verbeek FJ, Spaink HP, et al. Macrophage-Expressed Perforins Mpeg1 and Mpeg1.2 Have an Anti-Bacterial Function in Zebrafish. *J Innate Immun* (2014) 7):136–52. doi: 10.1159/000366103
89. McCormack RM, Hunte R, Podack ER, Plano GV, Shembade N. An Essential Role for Perforin-2 in Type I IFN Signaling. *J Immunol* (2020) 204(8):2242–56. doi: 10.4049/jimmunol.1901013
90. McCormack RM, De Armas LR, Shiratsuchi M, Ramos JE, Podack ER. Inhibition of intracellular bacterial replication in fibroblasts is dependent on the perforin-like protein (Perforin-2) encoded by macrophage-expressed gene 1. *J Innate Immun* (2012) 5(2):185–94. doi: 10.1159/000345249
91. Fields KA, McCormack RM, De Armas LR, Podack ER. Perforin-2 Restricts Growth of Chlamydia trachomatis in Macrophages. *Infect Immun* (2013) 81 (8):3045–54. doi: 10.1128/IAI.00497-13
92. Ni LY, Han Q, Chen HP, Luo XC, Li AX, Dan XM, et al. Grouper (Epinephelus coioides) Mpeg1s: Molecular identification, expression analysis, and antimicrobial activity. *Fish Shellfish Immunol* (2019) 92:690–7. doi: 10.1016/j.fsi.2019.06.060
93. Bai F, McCormack RM, Hower S, Plano GV, Lichtenheld MG, Munson GP. Perforin-2 Breaches the Envelope of Phagocytosed Bacteria Allowing Antimicrobial Effectors Access to Intracellular Targets. *J Immunol* (2018) 201(9):2710–20. doi: 10.4049/jimmunol.1800365

94. Leung C, Hodel AW, Brennan AJ, Lukoyanova N, Tran S, House CM, et al. Real-time visualization of perforin nanopore assembly. *Nat Nanotechnol* (2017) 12(5):467–73. doi: 10.1038/nnano.2016.303
95. Carroll MV, Sim RB. Complement in health and disease. *Adv Drug Deliv Rev* (2011) 63(12):965–75. doi: 10.1016/j.addr.2011.06.005
96. Spicer BA, Conroy PJ, Law RHP, Voskoboinik I, Whisstock JC. Perforin—A key (shaped) weapon in the immunological arsenal. *Semin Cell Dev Biol* (2017) 72:117–23. doi: 10.1016/j.semcdb.2017.07.033
97. Frasca D, Diaz A, Romero M, Vazquez T, Strbo N, Romero L, et al. Impaired B Cell Function in Mice Lacking Perforin-2. *Front Immunol* (2020) 11 (February):1–12. doi: 10.3389/fimmu.2020.00328
98. Kondos SC, Hatfaludi T, Voskoboinik I, Trapani JA, Law RHP, Whisstock JC, et al. The structure and function of mammalian membrane-attack complex/perforin-like proteins. *Tissue Antigens* (2010) 76(5):341–51. doi: 10.1111/j.1399-0039.2010.01566.x
99. Dunstone MA, Tweten RK. Packing a punch: The mechanism of pore formation by cholesterol dependent cytolysins and membrane attack complex/perforin-like proteins. *Curr Opin Struct Biol* (2012) 22(3):342–9. doi: 10.1016/j.sbi.2012.04.008
100. Reboul CF, Whisstock JC, Dunstone MA. Giant MACPF/CDC pore forming toxins: A class of their own. *Biochim Biophys Acta - Biomembr* (2015) 1858 (3):475–86. doi: 10.1016/j.bbamem.2015.11.017
101. Gilbert RJC, Mikelj M, Dalla Serra M, Froelich CJ, Anderluh G. Effects of MACPF/CDC proteins on lipid membranes. *Cell Mol Life Sci* (2012) 70 (12):2083–98. doi: 10.1007/s00018-012-1153-8
102. Ni T, Gilbert RJC. Repurposing a pore: Highly conserved perforin-like proteins with alternative mechanisms. *Philos Trans R Soc B: Biol Sci* (2017) 372(1726):20160212. doi: 10.1098/rstb.2016.0212
103. Ruan J, Xia S, Liu X, Lieberman J, Wu H. Cryo-EM structure of the gasdermin A3 membrane pore. *Nature* (2018) 557(7703):62–7. doi: 10.1038/s41586-018-0058-6
104. Tilley SJ, Orlova EV, Gilbert RJC, Andrew PW, Saibil HR. Structural basis of pore formation by the bacterial toxin pneumolysin. *Cell* (2005) 121(2):247–56. doi: 10.1016/j.cell.2005.02.033
105. Menny A, Serna M, Boyd CM, Gardner S, Joseph AP, Morgan BP, et al. CryoEM reveals how the complement membrane attack complex ruptures lipid bilayers. *Nat Commun* (2018) 9(1):5316. doi: 10.1038/s41467-018-07653-5
106. Lieberman J, Wu H, Kagan JC. Gasdermin D activity in inflammation and host defense. *Sci Immunol* (2019) 4(39):eaav1447. doi: 10.1126/sciimmunol.aav1447
107. Ramachandran R, Tweten RK, Johnson AE. The domains of a cholesterol-dependent cytolysin undergo a major FRET-detected rearrangement during pore formation. *Proc Natl Acad Sci U S A* (2005) 102(20):7139–44. doi: 10.1073/pnas.0500556102
108. Rossjohn J, Feil SC, McKinstry WJ, Tweten RK, Parker MW. Structure of a cholesterol-binding, thiol-activated cytolysin and a model of its membrane form. *Cell* (1997) 89(5):685–92. doi: 10.1016/S0092-8674(00)80251-2
109. Shatursky O, Heuck AP, Shepard LA, Rossjohn J, Parker MW, Johnson AE, et al. The mechanism of membrane insertion for a cholesterol-dependent cytolysin: A novel paradigm for pore-forming toxins. *Cell* (1999) 99(3):293–9. doi: 10.1016/S0092-8674(00)81660-8
110. Shepard LA, Heuck AP, Hamman BD, Rossjohn J, Parker MW, Ryan KR, et al. Identification of a membrane-spanning domain of the thiol-activated pore-forming toxin Clostridium perfringens perfringolysin O: An α-helical to β-sheet transition identified by fluorescence spectroscopy. *Biochemistry* (1998) 37 (41):14563–74. doi: 10.1021/bi981452f
111. Metkar SS, Marchioretto M, Antonini V, Lunelli L, Wang B, Gilbert RJ, et al. Perforin oligomers form arcs in cellular membranes: a locus for intracellular delivery of granzymes. *Cell Death Differ* (2015) 22(1):1–12. doi: 10.1038/cdd.2014.110
112. Yagi H, Conroy PJ, Leung EWW, Law RHP, Trapani JA, Voskoboinik I, et al. Structural basis for Ca2+-mediated interaction of the Perforin C2 domain with lipid membranes. *J Biol Chem* (2015) 290(42):25213–26. doi: 10.1074/jbc.M115.668384
113. Farkas I, Baranyi L, Ishikawa Y, Okada N, Bohata C, Budai D, et al. CD59 blocks not only the insertion of C9 into MAC but inhibits ion channel formation by homologous C5b-8 as well as C5b-9. *J Physiol* (2002) 539 (2):537–45. doi: 10.1113/jphysiol.2001.013381
114. Leung C, Dudkina NV, Lukoyanova N, Hodel AW, Farabella I, Pandurangan AP, et al. Stepwise visualization of membrane pore formation by suilysin, a bacterial cholesterol-dependent cytolysin. *Elife* (2014) 3:e04247. doi: 10.7554/eLife.04247
115. Uribe-Quero E, Rosales C. Control of phagocytosis by microbial pathogens. *Front Immunol* (2017) 8:1368. doi: 10.3389/fimmu.2017.01368
116. McCormack RM, Bahnan W, Shrestha N, Boucher J, Barreto M, Barrera CM, et al. Perforin-2 Protects Host Cells and Mice by Restricting the Vacuole to Cytosol Transitioning of a Bacterial Pathogen. *Infect Immun* (2016) 84 (4):1083–91. doi: 10.1128/IAI.01434-15
117. Rudd-Schmidt JA, Hodel AW, Noori T, Lopez JA, Cho HJ, Verschoor S, et al. Lipid order and charge protect killer T cells from accidental death. *Nat Commun* (2019) 10(1):5396. doi: 10.1038/s41467-019-13385-x
118. Fletcher CM, Harrison RA, Lachmann PJ, Neuhaus D. Structure of a soluble, glycosylated form of the human complement regulatory protein CD59. *Structure* (1994) 2(3):185–99. doi: 10.1016/S0969-2126(00)00020-4
119. Giddings KSK, Zhao J, Sims PPJ, Tweten RKR. Human CD59 is a receptor for the cholesterol-dependent cytolysin intermedilysin. *Nat Struct Mol Biol* (2004) 11(12):1173–8. doi: 10.1038/nsmb862
120. Murzin AG. How far divergent evolution goes in proteins. *Curr Opin Struct Biol* (1998) 8(3):380–7. doi: 10.1016/S0959-440X(98)80073-0

Conflict of Interest: The authors declare that the research was conducted in the absence of any commercial or financial relationships that could be construed as a potential conflict of interest.

frontiers in Immunology

MINI REVIEW
published: 23 October 2020
doi: 10.3389/fimmu.2020.599439

Vibrio vulnificus Hemolysin: Biological Activity, Regulation of *vvhA* Expression, and Role in Pathogenesis

Yuan Yuan, Zihan Feng and Jinglin Wang**

State Key Laboratory of Pathogen and Biosecurity, Beijing Institute of Microbiology and Epidemiology, Academy of Military Medical Sciences (AMMS), Beijing, China

The *Vibrio vulnificus* (*V. vulnificus*) hemolysin (VVH) is a pore-forming cholesterol-dependent cytolysin (CDC). Although there has been some debate surrounding the *in vivo* virulence effects of the VVH, it is becoming increasingly clear that it drives different cellular outcomes and is involved in the pathogenesis of *V. vulnificus*. This minireview outlines recent advances in our understanding of the regulation of *vvhA* gene expression, the biological activity of the VVH and its role in pathogenesis. An in-depth examination of the role of the VVH in *V. vulnificus* pathogenesis will help reveal the potential targets for therapeutic and preventive interventions to treat fatal *V. vulnificus* septicemia in humans. Future directions in VVH research will also be discussed.

Keywords: *Vibrio vulnificus* hemolysin (VVH), cholesterol-dependent cytolysin (CDC), biological activity, gene regulation, sepsis, pathogenesis

OPEN ACCESS

Edited by:
George P. Munson, University of Miami, United States

Reviewed by:
Jessica Jones, United States Food and Drug Administration, United States
Shin-ichi Miyoshi, Okayama University, Japan
Takashige Kashimoto, Kitasato University Japan
Carmen Amaro, University of Valencia, Spain

****Correspondence:***
Jinglin Wang
wangjlin@bmi.ac.cn
Yuan Yuan
miniminiyuan@163.com

Specialty section:
This article was submitted to Microbial Immunology, a section of the journal Frontiers in Immunology

Received: *27 August 2020*
Accepted: *30 September 2020*
Published: *23 October 2020*

Citation:
Yuan Y, Feng Z and Wang J (2020) Vibrio vulnificus Hemolysin: Biological Activity, Regulation of vvhA Expression, and Role in Pathogenesis. Front. Immunol. 11:599439. doi: 10.3389/fimmu.2020.599439

INTRODUCTION

V. vulnificus is an opportunistic human pathogen commonly found in estuarine environments. Human infections usually occur following the consumption of contaminated seafood or *via* an open wound exposed to a contaminated water source (1). Consumption of contaminated raw oysters can result in rapidly fatal septicemia in susceptible individuals, with *V. vulnificus* having the highest fatality rate among all food-borne pathogens (2). However, many aspects related to the biology, genomics, and virulence capabilities of *V. vulnificus* remain elusive or poorly understood (1, 3). During the last decade, research has mainly been focused on the pathogenic mechanisms and virulence factors adopted by *V. vulnificus* (2, 4). The capsule has proven to be a critical virulence factor, with non-encapsulated *V. vulnificus* isogenic mutants readily phagocytosed by host immune cells (5). The *V. vulnificus* multifunctional-auto processing repeats-in-toxin (MARTX) toxin is also likely to be critical to the success of infection. Supporting this, Gavin et al. showed that the MARTX toxin is essential for bacterial dissemination from the intestine (6), while Jones and Oliver demonstrated that the overwhelming tissue destruction that characterizes *V. vulnificus* infections contracted either *via* ingestion or wound infection likely results from the powerful collagenase, metalloproteases, and lipases/phospholipases produced by the bacterium (4). Moreover, MARTX is also known to take part in resistance to phagocytosis, cell destruction, and sepsis (7, 8).

Although the VVH belongs to the cytolytic pore-forming family of toxins (PFTs), all of which cause cytolysis in a variety of mammalian cells, VVH as a virulence factor is under debate. An earlier

study has shown that disruption of hemolysin gene *vvhA* had no effect on the virulence of *V. vulnificus* in a mouse lethality model (9). However, other studies have confirmed that *vvhA* gene is substantially regulated and expressed *in vivo* and is likely to play important roles in the pathogenesis of *V. vulnificus* (10, 11). For example, V. *vulnificus* is known for a siderophilic bacterium and iron as one of the factors that regulate *vvhA* expression (12–14). Fan JJ et al. indicate that there was a small difference in mortality when wild type and *vvhA*-deficient mutant strains were force-fed to mice, but VVH seemed to be important for causing damage in the alimentary tract of the mice (15). Moreover, another study suggested that in addition to the MARTX toxin, the VVH may contribute to bacterial invasion from the intestine into the bloodstream and other organs (16). These results would suggest that VVH may not be responsible for the lethality of *V. vulnificus*, but may be a contributor to the tissue damage in pathogenesis. Moreover, other proposed virulence factors characterized to date are not sufficient to explain the acute process of *V. vulnificus* septicemia. The *vvhA* gene is found in most *V. vulnificus* isolates, which was often used as a detecting marker for *V. vulnificus* (17, 18). However, unlike other Vibrio spp. such as *V. cholerae* and *V. parahaemolyticus*, where distinct molecular attributes, such as toxin genes, are normally associated with clinical strains (19, 20). More researchers contend that infections may be driven more by factors associated with host susceptibility than the virulence of *V. vulnificus* (1, 12). Besides *V. vulnificus*, the hemolysins produced by *Vibrio cholerae* and Gram-positive species such as *Streptococcus pneumoniae*, *Streptococcus suis*, *Bacillus Cereus*, have been extensively reviewed (21–23). Like most Gram-negative bacteria, the X-ray crystal structure of VVH remains unknown. However, the mechanisms of pore formation by VVH have been studied in crucial amino acid residues and domains related to the activity of VVH (24–27). Molecular architecture and functional analysis of *V. cholerae* cytolysin (VCC) revealed that VVH has a similar cytolysin domain and a lectin-like domain of VCC (28). However, although these pore-forming cholesterol-dependent cytolysins share structural similarity, they drive divergent cellular outcomes during pathogenesis. In comparison to PFTs in Gram-positive bacteria, more research is needed to clarify the role of VVH in pathogenesis, especially in infections with raw oyster consumption, which can produce rapidly fatal *V. vulnificus* septicemia.

In this review, we explore the features of VVH in its biological activity, regulation of v*vhA* expression, and possible roles in pathogenesis. Future directions in VVH research was also discussed in this review. This in-depth evaluation of the contribution of the VVH to *V. vulnificus* pathogenesis may aid in the development of novel therapies aimed at treating and preventing sepsis in humans.

EFFECTS OF THE VVH ON EUKARYOTIC CELLS

VVH is a 51-kDa water-soluble protein thought to be a member of CDC family of PFT; its hemolytic activity was inhibited by adding cholesterol or divalent cations (29). The VVH causes necrosis, apoptosis, pyroptosis, and lysis in a range of host cell types. First described as a hemolysin, the VVH causes hemolysis of red blood cells in many species, with human erythrocytes being the most susceptible. Although active against erythrocytes from sheep, horses, cows, rabbits, and chickens, the amount of VVH required to cause 50% hemolysis under identical conditions differed between species, suggesting that erythrocyte susceptibility may be closely associated with the binding ability of the VVH and erythrocyte membrane stability (30). *In vitro* studies have illuminated the effects of the VVH in various host cell types, including human epithelial cells, human umbilical vein endothelial cells (HUVECs), mice macrophages and lymphocytes (**Figure 1**), and commonly used cell lines, such as Chinese hamster ovary (CHO) cells (26, 27). However, similar cytotoxic effects have not been reported in human platelets or monocytes.

While *in vitro* studies have revealed the comprehensive effects of the VVH on eukaryotic cells, researchers have also examined the impact of host effectors on the activity of the VVH. Cholesterol is well known for its ability to inactivate the VVH through oligomerization of the toxin monomer (29). However, there are some reports that the VVH recognizes and binds to certain kinds of carbohydrates (38, 39), which suggested that cellular cholesterol is not a receptor for VVH. It may be a trigger factor of conformational changes from membrane bound form to pore-form (39). Moreover, although two studies indicate VVH induces cell death *via* lipid raft-mediated signaling pathway in human intestinal epithelial cells (31, 32), there is no evidence that the VVH localizes at lipid raft so far. One study shows that binding of VVH to target cells does not change by the methyl-beta-cyclodextrin (MβCD) treatment (40), and the author subsequently indicates that MβCD induces oligomerization of VVH by binding to VVH directly (41).

Besides that, several other factors have also been reported to affect the cytotoxicity of the VVH. Although albumin affects the activity of many different bacterial toxins, Choi et al. reported that neither human serum albumin (HAS) nor bovine serum albumin (BSA) affected *vvhA* transcription or the growth of *V. vulnificus*. However, both HSA and BSA stabilized VVH and delayed its inactivation by oligomerization, thus enhancing VVH activity (42). Blood lipoproteins have also been shown to be an important defense factor against bacterial infection. Park et al. found that low density lipoprotein inactivates the VVH through the oligomerization of the toxin monomer (43). It was widely reported that calcium prevented hemolysis caused by a variety of bacterial hemolysins (44). Jin-Woo Park showed that calcium exerts its major inhibitory effect on *V. vulnificus* cytolysin-induced hemolysis as an osmotic protectant (45). Consequently, trifluoperazine, a calcium-calmodulin antagonist, was found to block the hyperpermeability induced by *V. vulnificus* cytolysin in an *in vitro* modeled endothelium and prevented the deaths of mice (46). Additionally, a recent study showed that melatonin, an endogenous hormone molecule, inhibits apoptotic cell death induced by VVH *via* melatonin receptor 2 coupling with NCF-1 (47). While promising, these results emphasize the fact that we still

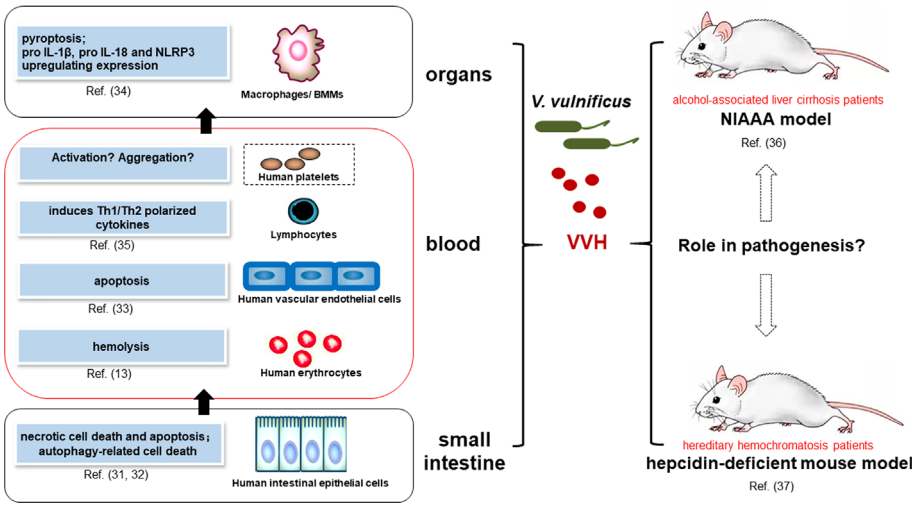

FIGURE 1 | Major activity of VVH's interactions with host cells and a future perspective of *in vivo* studies involved in pathogenesis. Major activity and mechanism of VVH's Interactions with host cells mainly focus on intestinal epithelial cells (31, 32), vascular endothelial cells (33), macrophages, (34) and lymphocytes (35), which are possibly involved in bacterial invasion from intestine to blood stream and other organs. However, the effects of VVH on platelets have not been reported. The animal models that mimick human infection will provide a perspective to elucidate the role of VVH in pathogenesis, mainly including the National Institute on Alcohol Abuse and Alcoholism (NIAAA) model (36) and a hepcidin-deficient mouse model (37).

have much to learn about how the VVH displays its cytotoxic effects *in vivo*, knowledge that will provide important insights into the potential for development of therapeutic strategies and agents to combat *V. vulnificus* infection.

Of special interest is the question of whether the VVH contributes to bacterial invasion from the intestine into the bloodstream and other organs by interacting with host cells. Intestinal epithelial cell death is a host defense response that eliminates damaged cells as well as pathogens to maintain gut homeostasis. However, many bacterial pathogens eventually elicit epithelial cell death and disrupt the gut barrier function to propagate persistent bacterial colonization. A study performed in human intestinal epithelial cells (INT-407) showed that infection with low doses of recombinant VVH protein induces necrotic cell death and apoptosis. The study further demonstrated that (r)VVH induces NF-κB-dependent mitochondrial cell death *via* lipid raft-mediated reactive oxygen species production by the distinct activation of PKCα and ERK/JNK in intestinal epithelial cells (31). Besides VVH has the ability to induce two general modes of cell death, apoptosis and necrosis mentioned above; another study indicated that the VVH induced autophagy-related cell death through the lipid raft-dependent c-Src/NOX signaling pathway in human intestinal epithelial Caco-2 cells. This study further showed that, in an *in vivo* model, VVH increased autophagy activation and paracellular permeabilization in the intestinal epithelium, indicating that VVH plays a pivotal role in the pathogenesis and dissemination of *V. vulnificus via* the upregulation of autophagy, which may provide potential therapeutic targets for strategic modulations of *V. vulnificus* infections (32).

V. vulnificus has been shown to produce sufficient VVH in the small intestine to accelerate invasion into the bloodstream (16). Once *V. vulnificus* is in the bloodstream, the VVH interacts with erythrocytes, white blood cells, and vascular endothelial cells. In fact, a recent study has shown that VVH together with MARTX mediates erythrocytes lyses *ex vivo* and, therefore, could contribute to the bacterial growth in human blood that provokes sepsis (13). Researchers observed *in vitro* proliferation of lymphocytes upon re-stimulation of recombinant VVH leukocidin domain (rL/VvhA)-primed splenocytes with formalin-inactivated VVH toxin, while co-expression of T-cell-polarizing cytokines (interferon-γ, interleukin (IL)-12, and IL-4) was detected in the cell culture supernatant (35). In an *in vitro* study, the recombinant VVH induces apoptosis in HUVEC cells *via* caspase-9/3-dependent pathway (33). The VVH can also spread to other tissues *via* the bloodstream. Macrophages are large phagocytes found in almost all tissues and play a critical role in increasing inflammation and stimulating the immune system. Claudia Toma et al. indicate that VVH-stimulated NLRP3 Inflammasome activation of bone marrow derived macrophages (BMM), which was induced by TLR and nucleotide-binding oligomerization domain 1/2 ligand-mediated NF-*k*B activation (34). Recently, analysis of VVH-induced inflammation in mice showed that the VVH induces inflammatory responses in RAW264.7 macrophages *via* calcium signaling and causes inflammation *in vivo* (48).

REGULATION OF VVH GENE (*VVHA*) EXPRESSION

In this review, we will outline the roles of environmental and host factors and global regulators in the regulation of the *vvhA* in terms of expression and transport (**Figure 2**). Cyclic-AMP

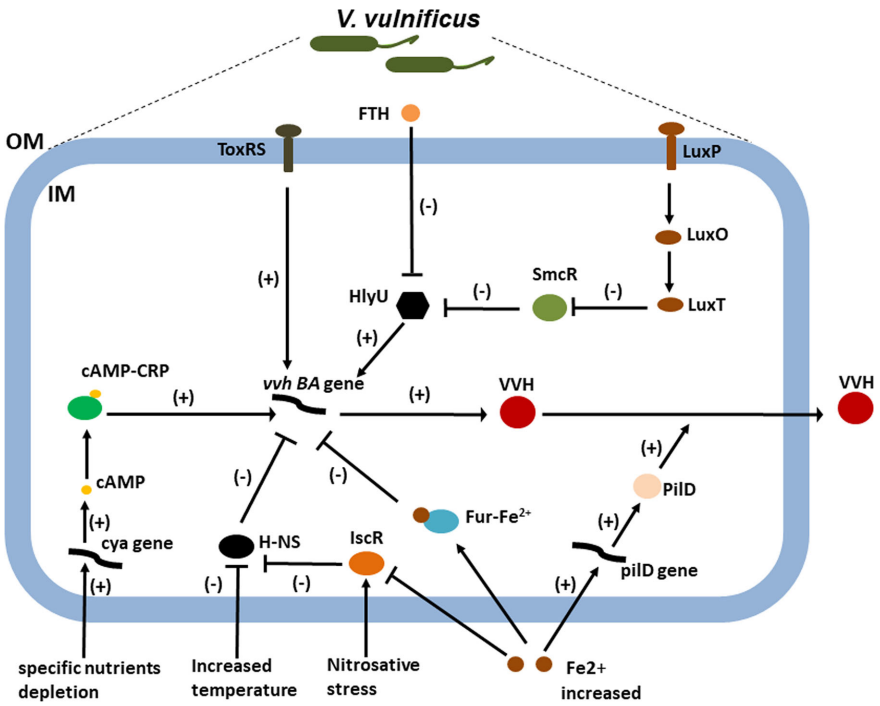

FIGURE 2 | The roles of environmental and host factors and global regulators in the regulation of the VVH expression. CRP activates *vvhBA* transcription in *V. vulnificus* by sensing the depletion of specific nutrients, possibly as a result of increased cAMP levels under glucose starvation (32). Increased iron can repress *vvhA* transcription *via* the ferric uptake regulator (Fur) and IscR (41, 46). However, it increases extracellular VVH secretion through increased transcription of pilD, which encodes PilD, a component responsible for extracellular VVH secretion (41). IscR activates *vvhBA* by relieving H-NS repression by sensing nitrosative stress (46). Meanwhile, a repressive interaction of H-NS would be relieved in response to the increase in temperature (39, 49). LuxO is a central response regulator of the QS circuit in *V. vulnificus*, which negatively regulates *vvhA* expression *via* SmcR and HlyU (42, 43). However, the transmembrane transcriptional activator ToxRS positively regulates the expression of the *vvhA* (47). Taken together, the transcriptional regulators integrate diverse environmental and host signals to collaboratively regulate *vvhA* transcription during the course of infection. Lastly, FTH, an inhibitor target HlyU, was identified to inhibit the transcription of *vvhA* along with that of other HlyU-regulated virulence genes.; OM, outer membrane; IM, inner membrane; FTH, fursultiamine hydrochloride; H-NS, histone-like nucleoid structuring protein; cya, gene encoding adenylate cyclase; cAMP, cyclic AMP; CRP, cAMP receptor protein.

(cAMP) and bacterial cyclic-AMP receptor proteins (CRPs) represent a classic regulatory system that has been adapted to respond to distinct external and internal signals in many bacteria (50). Hemolysin production in *V. vulnificus* increased after the addition of cAMP but was undetectable in a putative *crp* mutant, suggesting that *vvh* expression is positively regulated by cAMP-CRP in *V. vulnificus* (49). In *V. vulnificus*, cAMP can be produced from adenylate cyclase-encoding gene *cya*. Hemolysin and protease production, motility, and cytotoxicity were all negatively affected by mutation of *cya* (51). CRP activates *vvhBA* transcription in *V. vulnificus* by sensing the depletion of specific nutrients, possibly as a result of increased cAMP levels under glucose starvation (52). In *Escherichia coli*, glucose starvation results in an increase in intracellular cAMP concentrations in response to the altered phosphorylation state of the phosphotransferase system; however, this is difficult to reconcile with observations that the glucose phosphotransferase system remains saturated when intracellular cAMP concentrations increase (53). The regulation of *vvhBA* expression can be more easily examined in the intestine because the availability of free glucose is quite limited. *V. vulnificus* is a ferrophilic bacterium that requires high levels of available iron for growth (12, 13). Although iron can repress *vvhA* transcription *via* the ferric uptake regulator (Fur), it increases extracellular VVH secretion through increased transcription of *pilD*, which encodes PilD, a component of the type II general secretion system responsible for extracellular VVH secretion (14). But there are infection models that suggest that high iron levels (susceptible patients) could also increase *vvhA* transcription (13). So, the regulation of this gene expression should be more complex.

In many pathogenic bacteria, including *V. vulnificus*, quorum sensing (QS) is one of the most important cellular regulatory cascades. QS is responsible for cell–cell communication and is mediated by a small diffusible molecule called autoinducer 2 (AI-2). LuxO is a central response regulator of the QS circuit in *V. vulnificus*, with disruption of *luxO* shown to increase the expression of *smcR*, *crp*, and *luxS*, which encodes the autoinducer 2 synthetase (54). In comparison, SmcR regulates cytotoxicity in *V. vulnificus via* QS signaling by repressing HlyU, which positively regulates *vvhA* expression (55). Temperature is one of the important host parameters regulating the expression of virulence factors in bacteria. The histone-like nucleoid structuring protein (H-NS) global regulator is known to play a crucial role in the expression of temperature-dependent virulence factors. A study on the role of H-NS in temperature-dependent regulation indicated that *hns*

expression levels were higher at 26 °C than at 37 °C and that *vvhA* expression and the resulting VVH production were increased following disruption of *hns* (56). Moreover, H-NS, in its role as a *vvhA* repressor, competes with HlyU for binding to the *vvhA* promoter region (57); however, the exact mechanisms of HlyU and H-NS regulation have yet to be fully characterized (56). In addition to cAMP-CRP, Fur, and H-NS, the Fe-S cluster, containing transcriptional regulator IscR, was recently described as an important regulator of *V. vulnificus* virulence in host environments. IscR activates the *vvhBA* operon in response to nitrosative stress and iron starvation, thereby aiding successful host infection (58). Lastly, transmembrane transcriptional activator ToxRS, a homolog of the *V. cholerae* ToxRS transmembrane virulence regulator, may also positively regulate the expression of the *vvhA* (59). In summary, recognition of the subtle regulation of v*vhA* gene expression and hemolysin delivery by *V. vulnificus* has furthered our understanding of how the VVH contributes to disease pathogenesis.

The complicated *vvhA* regulatory system that emerges from this data suggests that inhibition of global regulators may be a promising approach for the development of alternatives to antibiotic treatment. Recently, an inhibitor-screening reporter platform was used to target HlyU, a master virulence factor transcriptional regulator in *V. vulnificus*. The study identified a small molecule called fursultiamine hydrochloride that inhibited the transcription of *vvhA* along with that of other HlyU-regulated virulence genes. Fursultiamine hydrochloride therefore has the potential to inhibit the pathogenesis of *V. vulnificus* without inducing antimicrobial resistance (60).

THE ROLE OF THE VVH IN DISEASE AND PATHOGENESIS

V. vulnificus most commonly causes severe gastroenteritis following the consumption of contaminated raw seafood, with sepsis infection mortality rates of 50% (12). Moreover, because *V. vulnificus* is responsible for >95% of seafood-associated infection deaths in the United States (4), a significant number of studies have focused on the effects of the VVH on human intestinal epithelial cells mentioned above. In addition, small intestine-associated host factors together with mouse models have been used to investigate the role of the VVH in pathogenesis. The human intestine usually secretes cationic antimicrobial peptides to prevent pathogen colonization, with Paneth cells in the small intestine secreting antimicrobial molecule alpha-defensin 5 (HD-5). However, while HD-5 inactivated the *Vibrio mimicus* hemolysin, it had no effect on VVH. The inability of *V. mimicus* to penetrate the small intestinal epithelium suggests that the cytolytic activity of the *V. mimicus* hemolysin is abolished by HD-5 (61). In contrast, *V. vulnificus* causes intestinal tissue damage and inflammation, which then promotes dissemination of the pathogen from the small intestine into the bloodstream and other organs in infected mice (6, 7). Notably, the small intestine is recognized as the site of the most severe tissue necrosis in humans based on autopsy results from *V. vulnificus*-infected patients (62). Indeed, VVH and MARTX are the two *V. vulnificus* virulence factors associated with both enhanced growth *in vivo* and necrosis of tissue in the small intestine, followed by dissemination into the bloodstream and other tissues. In the absence of these two secreted factors, *V. vulnificus* is unable to cause intestinal infection in mice (16).

V. vulnificus also causes primary septicemia in patients with underlying liver disease or who are immunocompromised (63). Patients with septicemia tend to die of hypovolemic shock complicated by multi-organ failure. A study in rats found that the VVH dilates the thoracic aorta by activating guanylate cyclase, causing hypotension *in vivo* and vasodilatation *in vitro* (64, 65). *V. vulnificus* can be spreading from the intestine to bloodstream. To survive and proliferate in blood, *V. vulnificus* requires to overcome the innate immune defenses, including complement-mediated phagocytosis. Recently, capsular polysaccharide and Flp (fimbrial low-molecular-weight protein) pili are reported to play critical roles in evasion of the host innate immune system by resistance to complement-mediated killing (66, 67). Although an earlier work showed that virulent isolates produced high titers of hemolysin, were resistant to inactivation by serum complement (68), further information is needed to uncover the mechanism of VVH-mediated evasion of complement killing, which may help us to better understand the basis of the *V. vulnificus* infection process in human blood. Being at the crossroads between the immune system, clotting cascade, and endothelial cells, platelets seem to be an appealing central mediator and possible therapeutic target for sepsis (69–71). The mechanism of bacterial-induced platelet activation by pore-forming toxins has been well characterized in other Gram-positive bacteria (72). However, despite the significant fatality rate associated with *V. vulnificus*-induced sepsis, the interaction between the VVH and platelets is not clear. Because the CDC of Vibrio spp. share structural similarity (28), it is possible that VVH represents a critical molecule of Vibrio spp. involved in pathogenesis by interacting with platelets. Linked to this, efforts should be focused on the mechanisms of VVH-induced platelet activation for future work.

CONCLUSIONS AND FUTURE PERSPECTIVE

Cholesterol-dependent cytolysins are a diverse group of proteins that differ between bacterial species. However, it is these differences that have informed much of our understanding of the biological activities of the proteins, as well as their role in pathogenesis. Despite this insight, further studies are needed to determine the structure–function relationships of the VVH. Functionally, the major roles of the VVH are to induce cytotoxicity by binding to the cellular membrane to form pores and activating the host inflammatory response. These functions, along with the subtle regulation of VVH gene expression and other potentially unrecognized activities, contribute to the pathogenesis of *V. vulnificus* disease. Although the host

response to the VVH involves lipid raft-dependent signaling pathway-mediated cell death, it is likely that other mechanisms may also be involved in the host response to the VVH.

V. vulnificus infection can result in severe disease. In fact, most cases occur in patients with underlying conditions resulting in hereditary hemochromatosis, primarily alcohol-associated liver cirrhosis or immuno-compromised males, but it does not cause severe illness in healthy individuals (73). Although there have been many studies on the effects of the VVH on eukaryotic cells *in vitro*, few animal models that mimick human infection were used to elucidate the role of VVH in pathogenesis. As a result, we still have much to learn about how this toxin contributes to disease pathogenesis *in vivo* (**Figure 1**). An interesting study found that hepcidin has a critical role in host defense against *V. vulnificus* by inducing reactive hypoferremia during early phases of infection (74). Hepcidin is a 25 amino acid peptide secreted by hepatocytes. Hereditary hemochromatosis is caused by deficiency of the iron-regulatory hormone hepcidin (75). Therefore, a hepcidin-deficient mouse model of severe hemochromatosis (37) could be considered for the future work about the role of VVH in the lethal infections by *V. vulnificus*, a siderophilic bacterium. Additionally, the National Institute on Alcohol Abuse and Alcoholism (NIAAA) model is a mouse model of chronic and binge ethanol feeding, which mimics acute-on-chronic alcoholic liver injury in patients (36). This simple model will be very useful for the study of the function of VVH *in vivo*, and the underlying mechanisms that contribute to acute infections by *V. vulnificus* in liver disease patient.

AUTHOR CONTRIBUTIONS

YY contributed to the research of the literature and the writing and revision of the manuscript. ZF and JW contributed to the revision of the manuscript. All authors contributed to the article and approved the submitted version.

REFERENCES

1. Baker-Austin C, Oliver JD. *Vibrio vulnificus*: new insights into a deadly opportunistic pathogen. *Environ Microbiol* (2018) 20(2):423–30. doi: 10.1111/1462-2920.13955
2. Heng SP, Letchumanan V, Deng CY, Ab Mutalib NS, Khan TM, Chuah LH, et al. *Vibrio vulnificus*: An Environmental and Clinical Burden. *Front Microbiol* (2017) 8:997. doi: 10.3389/fmicb.2017.00997
3. Rippey SR. Infectious diseases associated with molluscan shellfish consumption. *Clin Microbiol Rev* (1994) 7(4):419–25. doi: 10.1128/cmr.7.4.419
4. Jones MK, Oliver JD. *Vibrio vulnificus*: disease and pathogenesis. *Infect Immun* (2009) 77(5):1723–33. doi: 10.1128/IAI.01046-08
5. Yoshida S, Ogawa M, Mizuguchi Y. Relation of capsular materials and colony opacity to virulence of *Vibrio vulnificus*. *Infect Immun* (1985) 47(2):446–51. doi: 10.1128/IAI.47.2.446-451.1985
6. Gavin HE, Beubier NT, Satchell KJ. The Effector Domain Region of the *Vibrio vulnificus* MARTX Toxin Confers Biphasic Epithelial Barrier Disruption and Is Essential for Systemic Spread from the Intestine. *PLoS Pathog* (2017) 13(1):e1006119. doi: 10.1371/journal.ppat.1006119
7. Lo HR, Lin JH, Chen YH, Chen CL, Shao CP, Lai YC, et al. RTX toxin enhances the survival of *Vibrio vulnificus* during infection by protecting the organism from phagocytosis. *J Infect Dis* (2011) 203(12):1866–74. doi: 10.1093/infdis/jir070
8. Murciano C, Lee CT, Fernandez-Bravo A, Hsieh TH, Fouz B, Hor LI, et al. MARTX Toxin in the Zoonotic Serovar of *Vibrio vulnificus* Triggers an Early Cytokine Storm in Mice. *Front Cell Infect Microbiol* (2017) 7:332. doi: 10.3389/fcimb.2017.00332
9. Wright AC, Morris JGJr. The extracellular cytolysin of *Vibrio vulnificus*: inactivation and relationship to virulence in mice. *Infect Immun* (1991) 59(1):192–7. doi: 10.1128/IAI.59.1.192-197.1991
10. Elgaml A, Miyoshi SI. Regulation systems of protease and hemolysin production in *Vibrio vulnificus*. *Microbiol Immunol* (2017) 61(1):1–11. doi: 10.1111/1348-0421.12465
11. Lee SE, Ryu PY, Kim SY, Kim YR, Koh JT, Kim OJ, et al. Production of *Vibrio vulnificus* hemolysin in vivo and its pathogenic significance. *Biochem Biophys Res Commun* (2004) 324(1):86–91. doi: 10.1016/j.bbrc.2004.09.020
12. Horseman MA, Surani S. A comprehensive review of *Vibrio vulnificus*: an important cause of severe sepsis and skin and soft-tissue infection. *Int J Infect Dis* (2011) 15(3):e157–66. doi: 10.1016/j.ijid.2010.11.003
13. Hernandez-Cabanyero C, Lee CT, Tolosa-Enguis V, Sanjuan E, Pajuelo D, Reyes-Lopez F, et al. Adaptation to host in *Vibrio vulnificus*, a zoonotic pathogen that causes septicemia in fish and humans. *Environ Microbiol* (2019) 21(8):3118–39. doi: 10.1111/1462-2920.14714
14. Kim CM, Chung YY, Shin SH. Iron differentially regulates gene expression and extracellular secretion of *Vibrio vulnificus* cytolysin-hemolysin. *J Infect Dis* (2009) 200(4):582–9. doi: 10.1086/600869
15. Fan JJ, Shao CP, Ho YC, Yu CK, Hor LI. Isolation and characterization of a *Vibrio vulnificus* mutant deficient in both extracellular metalloprotease and cytolysin. *Infect Immun* (2001) 69(9):5943–8. doi: 10.1128/iai.69.9.5943-5948.2001
16. Jeong HG, Satchell KJ. Additive function of *Vibrio vulnificus* MARTX(Vv) and VvhA cytolysins promotes rapid growth and epithelial tissue necrosis during intestinal infection. *PLoS Pathog* (2012) 8(3):e1002581. doi: 10.1371/journal.ppat.1002581
17. Panicker G, Myers ML, Bej AK. Rapid detection of *Vibrio vulnificus* in shellfish and Gulf of Mexico water by real-time PCR. *Appl Environ Microbiol* (2004) 70(1):498–507. doi: 10.1128/aem.70.1.498-507.2004
18. Panicker G, Bej AK. Real-time PCR detection of *Vibrio vulnificus* in oysters: comparison of oligonucleotide primers and probes targeting vvhA. *Appl Environ Microbiol* (2005) 71(10):5702–9. doi: 10.1128/AEM.71.10.5702-5709.2005
19. Waldor MK, Mekalanos JJ. Lysogenic conversion by a filamentous phage encoding cholera toxin. *Science* (1996) 272(5270):1910–4. doi: 10.1126/science.272.5270.1910
20. Bej AK, Patterson DP, Brasher CW, Vickery MC, Jones DD, Kaysner CA. Detection of total and hemolysin-producing Vibrio parahaemolyticus in shellfish using multiplex PCR amplification of tl, tdh and trh. *J Microbiol Methods* (1999) 36(3):215–25. doi: 10.1016/s0167-7012(99)00037-8
21. Heuck AP, Moe PC, Johnson BB. The cholesterol-dependent cytolysin family of gram-positive bacterial toxins. *Subcell Biochem* (2010) 51:551–77. doi: 10.1007/978-90-481-8622-8_20
22. Kathuria R, Chattopadhyay K. *Vibrio cholerae* cytolysin: Multiple facets of the membrane interaction mechanism of a beta-barrel pore-forming toxin. *IUBMB Life* (2018) 70(4):260–6. doi: 10.1002/iub.1725
23. Ramarao N, Sanchis V. The pore-forming haemolysins of *Bacillus cereus*: a review. *Toxins (Basel)* (2013) 5(6):1119–39. doi: 10.3390/toxins5061119
24. Miyoshi S, Abe Y, Senoh M, Mizuno T, Maehara Y, Nakao H. Inactivation of *Vibrio vulnificus* hemolysin through mutation of the N- or C-terminus of the lectin-like domain. *Toxicon* (2011) 57(6):904–8. doi: 10.1016/j.toxicon.2011.03.013
25. Senoh M, Okita Y, Shinoda S, Miyoshi S. The crucial amino acid residue related to inactivation of *Vibrio vulnificus* hemolysin. *Microb Pathog* (2008) 44(1):78–83. doi: 10.1016/j.micpath.2007.07.002
26. Kashimoto T, Akita T, Kado T, Yamazaki K, Ueno S. Both polarity and aromatic ring in the side chain of tryptophan 246 are involved in binding activity of *Vibrio vulnificus* hemolysin to target cells. *Microb Pathog* (2017) 109:71–7. doi: 10.1016/j.micpath.2017.05.029

27. Kashimoto T, Ueno S, Koga T, Fukudome S, Ehara H, Komai M, et al. The aromatic ring of phenylalanine 334 is essential for oligomerization of *Vibrio vulnificus* hemolysin. *J Bacteriol* (2010) 192(2):568–74. doi: 10.1128/JB.01049-09
28. Olson R, Gouaux E. Crystal structure of the *Vibrio cholerae* cytolysin (VCC) pro-toxin and its assembly into a heptameric transmembrane pore. *J Mol Biol* (2005) 350(5):997–1016. doi: 10.1016/j.jmb.2005.05.045
29. Shinoda S, Miyoshi S, Yamanaka H, Miyoshi-Nakahara N. Some properties of *Vibrio vulnificus* hemolysin. *Microbiol Immunol* (1985) 29(7):583–90. doi: 10.1111/j.1348-0421.1985.tb00862.x
30. Yamanaka H, Shimatani S, Tanaka M, Katsu T, Ono B, Shinoda S. Susceptibility of erythrocytes from several animal species to *Vibrio vulnificus* hemolysin. *FEMS Microbiol Lett* (1989) 52(3):251–5. doi: 10.1016/0378-1097(89)90206-1
31. Lee SJ, Jung YH, Oh SY, Song EJ, Choi SH, Han HJ. *Vibrio vulnificus* VvhA induces NF-kappaB-dependent mitochondrial cell death via lipid raft-mediated ROS production in intestinal epithelial cells. *Cell Death Dis* (2015) 6:1655. doi: 10.1038/cddis.2015.19
32. Song EJ, Lee SJ, Lim HS, Kim JS, Jang KK, Choi SH, et al. *Vibrio vulnificus* VvhA induces autophagy-related cell death through the lipid raft-dependent c-Src/NOX signaling pathway. *Sci Rep* (2016) 6:27080. doi: 10.1038/srep27080
33. Zhao JF, Sun AH, Ruan P, Zhao XH, Lu MQ, Yan J. Vibrio vulnificus cytolysin induces apoptosis in HUVEC, SGC-7901 and SMMC-7721 cells via caspase-9/3-dependent pathway. *Microb Pathog* (2009) 46(4):194–200. doi: 10.1016/j.micpath.2008.12.005
34. Toma C, Higa N, Koizumi Y, Nakasone N, Ogura Y, McCoy AJ, et al. Pathogenic Vibrio activate NLRP3 inflammasome via cytotoxins and TLR/nucleotide-binding oligomerization domain-mediated NF-kappa B signaling. *J Immunol* (2010) 184(9):5287–97. doi: 10.4049/jimmunol.0903536
35. Lohith GK, Kingston JJ, Singh AK, Murali HS, Batra HV. Evaluation of recombinant leukocidin domain of VvhA exotoxin of *Vibrio vulnificus* as an effective toxoid in mouse model. *Immunol Lett* (2015) 167(1):47–53. doi: 10.1016/j.imlet.2015.06.015
36. Bertola A, Mathews S, Ki SH, Wang H, Gao B. Mouse model of chronic and binge ethanol feeding (the NIAAA model). *Nat Protoc* (2013) 8(3):627–37. doi: 10.1038/nprot.2013.032
37. Lesbordes-Brion JC, Viatte L, Bennoun M, Lou DQ, Ramey G, Houbron C, et al. Targeted disruption of the hepcidin 1 gene results in severe hemochromatosis. *Blood* (2006) 108(4):1402–5. doi: 10.1182/blood-2006-02-003376
38. Kaus K, Lary JW, Cole JL, Olson R. Glycan specificity of the *Vibrio vulnificus* hemolysin lectin outlines evolutionary history of membrane targeting by a toxin family. *J Mol Biol* (2014) 426(15):2800–12. doi: 10.1016/j.jmb.2014.05.021
39. Kashimoto T, Sugiyama H, Kawamidori K, Yamazaki K, Kado T, Matsuda K, et al. Vibiro vulnificus hemolysin associates with gangliosides. *BMC Microbiol* (2020) 20(1):69. doi: 10.1186/s12866-020-01755-1
40. Sugiyama H, Kashimoto T, Ueno S, Ehara H, Kodama T, Iida T, et al. Relationship between localization on cellular membranes and cytotoxicity of *Vibrio vulnificus* hemolysin. *PLoS One* (2011) 6(10):e26018. doi: 10.1371/journal.pone.0026018
41. Sugiyama H, Kashimoto T, Ueno S, Susa N. Inhibition of binding of *Vibrio vulnificus* hemolysin (VVH) by MbetaCD. *J Vet Med Sci* (2013) 75(5):649–52. doi: 10.1292/jvms.12-0387
42. Choi MH, Sun HY, Park RY, Bai YH, Chung YY, Kim CM, et al. Human serum albumin enhances the hemolytic activity of *Vibrio vulnificus*. *Biol Pharm Bull* (2006) 29(1):180–2. doi: 10.1248/bpb.29.180
43. Park KH, Yang HB, Kim HG, Lee YR, Hur H, Kim JS, et al. Low density lipoprotein inactivates *Vibrio vulnificus* cytolysin through the oligomerization of toxin monomer. *Med Microbiol Immunol* (2005) 194(3):137–41. doi: 10.1007/s00430-004-0227-0
44. Korchev YE, Bashford CL, Pasternak CA. Differential sensitivity of pneumolysin-induced channels to gating by divalent cations. *J Membr Biol* (1992) 127(3):195–203. doi: 10.1007/BF00231507
45. Park JW, Jahng TA, Rho HW, Park BH, Kim NH, Kim HR. Inhibitory mechanism of Ca^{2+} on the hemolysis caused by *Vibrio vulnificus* cytolysin. *Biochim Biophys Acta* (1994) 1194(1):166–70. doi: 10.1016/0005-2736(94)90216-x
46. Lee YR, Park KH, Lin ZZ, Kho YJ, Park JW, Rho HW, et al. A calcium-calmodulin antagonist blocks experimental *Vibrio vulnificus* cytolysin-induced lethality in an experimental mouse model. *Infect Immun* (2004) 72(10):6157–9. doi: 10.1128/IAI.72.10.6157-6159.2004
47. Lee SJ, Lee HJ, Jung YH, Kim JS, Choi SH, Han HJ. Melatonin inhibits apoptotic cell death induced by *Vibrio vulnificus* VvhA via melatonin receptor 2 coupling with NCF-1. *Cell Death Dis* (2018) 9(2):48. doi: 10.1038/s41419-017-0083-7
48. Qin K, Fu K, Liu J, Wu C, Wang Y, Zhou L. *Vibrio vulnificus* cytolysin induces inflammatory responses in RAW264.7 macrophages through calcium signaling and causes inflammation in vivo. *Microb Pathog* (2019) 137:103789. doi: 10.1016/j.micpath.2019.103789
49. Bang YB, Lee SE, Rhee JH, Choi SH. Evidence that expression of the *Vibrio vulnificus* hemolysin gene is dependent on cyclic AMP and cyclic AMP receptor protein. *J Bacteriol* (1999) 181(24):7639–42. doi: 10.1128/JB.181.24.7639-7642.1999
50. Green J, Stapleton MR, Smith LJ, Artymiuk PJ, Kahramanoglou C, Hunt DM, et al. Cyclic-AMP and bacterial cyclic-AMP receptor proteins revisited: adaptation for different ecological niches. *Curr Opin Microbiol* (2014) 18:1–7. doi: 10.1016/j.mib.2014.01.003
51. Kim YR, Kim SY, Kim CM, Lee SE, Rhee JH. Essential role of an adenylate cyclase in regulating *Vibrio vulnificus* virulence. *FEMS Microbiol Lett* (2005) 243(2):497–503. doi: 10.1016/j.femsle.2005.01.016
52. Choi HK, Park NY, Kim DI, Chung HJ, Ryu S, Choi SH. Promoter analysis and regulatory characteristics of vvhBA encoding cytolytic hemolysin of *Vibrio vulnificus*. *J Biol Chem* (2002) 277(49):47292–9. doi: 10.1074/jbc.M206893200
53. Notley-McRobb L, Death A, Ferenci T. The relationship between external glucose concentration and cAMP levels inside Escherichia coli: implications for models of phosphotransferase-mediated regulation of adenylate cyclase. *Microbiology* (1997) 143(Pt 6):1909–18. doi: 10.1099/00221287-143-6-1909
54. Elgaml A, Higaki K, Miyoshi S. Effects of temperature, growth phase and luxO-disruption on regulation systems of toxin production in *Vibrio vulnificus* strain L-180, a human clinical isolate. *World J Microbiol Biotechnol* (2014) 30(2):681–91. doi: 10.1007/s11274-013-1501-3
55. Shao CP, Lo HR, Lin JH, Hor LI. Regulation of cytotoxicity by quorum-sensing signaling in *Vibrio vulnificus* is mediated by SmcR, a repressor of hlyU. *J Bacteriol* (2011) 193(10):2557–65. doi: 10.1128/JB.01259-10
56. Elgaml A, Miyoshi S. Role of the Histone-Like Nucleoid Structuring Protein (H-NS) in the Regulation of Virulence Factor Expression and Stress Response in *Vibrio vulnificus*. *Biocontrol Sci* (2015) 20(4):263–74. doi: 10.4265/bio.20.263
57. Liu M, Naka H, Crosa JH. HlyU acts as an H-NS antirepressor in the regulation of the RTX toxin gene essential for the virulence of the human pathogen *Vibrio vulnificus* CMCP6. *Mol Microbiol* (2009) 72(2):491–505. doi: 10.1111/j.1365-2958.2009.06664.x
58. Choi G, Jang KK, Lim JG, Lee ZW, Im H, Choi SH. The transcriptional regulator IscR integrates host-derived nitrosative stress and iron starvation in activation of the vvhBA operon in *Vibrio vulnificus*. *J Biol Chem* (2020) 295(16):5350–61. doi: 10.1074/jbc.RA120.012724
59. Lee SE, Shin SH, Kim SY, Kim YR, Shin DH, Chung SS, et al. *Vibrio vulnificus* has the transmembrane transcription activator ToxRS stimulating the expression of the hemolysin gene vvhA. *J Bacteriol* (2000) 182(12):3405–15. doi: 10.1128/jb.182.12.3405-3415.2000
60. Imdad S, Chaurasia AK, Kim KK. Identification and Validation of an Antivirulence Agent Targeting HlyU-Regulated Virulence in *Vibrio vulnificus*. *Front Cell Infect Microbiol* (2018) 8:152 doi: 10.3389/fcimb.2018.00152
61. Miyoshi S, Ikehara H, Kumagai M, Mizuno T, Kawase T, Maehara Y. Defensive effects of human intestinal antimicrobial peptides against infectious diseases caused by *Vibrio mimicus* and *V. vulnificus*. *Biocontrol Sci* (2014) 19(4):199–203. doi: 10.4265/bio.19.199
62. Chen Y, Satoh T, Tokunaga O. *Vibrio vulnificus* infection in patients with liver disease: report of five autopsy cases. *Virchows Arch* (2002) 441(1):88–92. doi: 10.1007/s00428-002-0613-1
63. Menon MP, Yu PA, Iwamoto M, Painter J. Pre-existing medical conditions associated with *Vibrio vulnificus* septicaemia. *Epidemiol Infect* (2014) 142(4):878–81. doi: 10.1017/S0950268813001593
64. Kook H, Lee SE, Baik YH, Chung SS, Rhee JH. *Vibrio vulnificus* hemolysin dilates rat thoracic aorta by activating guanylate cyclase. *Life Sci* (1996) 59(3):PL41–7. doi: 10.1016/0024-3205(96)00292-5

65. Kook H, Rhee JH, Lee SE, Kang SY, Chung SS, Cho KW, et al. Activation of particulate guanylyl cyclase by *Vibrio vulnificus* hemolysin. *Eur J Pharmacol* (1999) 365(2-3):267–72. doi: 10.1016/s0014-2999(98)00870-x
66. Pettis GS, Mukerji AS. Structure, Function, and Regulation of the Essential Virulence Factor Capsular Polysaccharide of *Vibrio vulnificus*. *Int J Mol Sci* (2020) 21(9):3259. doi: 10.3390/ijms21093259
67. Duong-Nu TM, Jeong K, Hong SH, Puth S, Kim SY, Tan W, et al. A stealth adhesion factor contributes to *Vibrio vulnificus* pathogenicity: Flp pili play roles in host invasion, survival in the blood stream and resistance to complement activation. *PLoS Pathog* (2019) 15(8):e1007767. doi: 10.1371/journal.ppat.1007767
68. Stelma GNJr., Reyes AL, Peeler JT, Johnson CH, Spaulding PL. Virulence characteristics of clinical and environmental isolates of *Vibrio vulnificus*. *Appl Environ Microbiol* (1992) 58(9):2776–82. doi: 10.1128/AEM.58.9.2776-2782.1992
69. Greco E, Lupia E, Bosco O, Vizio B, Montrucchio G. Platelets and Multi-Organ Failure in Sepsis. *Int J Mol Sci* (2017) 18(10):2200. doi: 10.3390/ijms18102200
70. Wang Y, Ouyang Y, Liu B, Ma X, Ding R. Platelet activation and antiplatelet therapy in sepsis: A narrative review. *Thromb Res* (2018) 166:28–36. doi: 10.1016/j.thromres.2018.04.007
71. Kerris EWJ, Hoptay C, Calderon T, Freishtat RJ. Platelets and platelet extracellular vesicles in hemostasis and sepsis. *J Invest Med* (2020) 68 (4):813–20. doi: 10.1136/jim-2019-001195
72. Cox D, Kerrigan SW, Watson SP. Platelets and the innate immune system: mechanisms of bacterial-induced platelet activation. *J Thromb Haemost* (2011) 9(6):1097–107. doi: 10.1111/j.1538-7836.2011.04264.x
73. Bross MH, Soch K, Morales R, Mitchell RB. *Vibrio vulnificus* infection: diagnosis and treatment. *Am Fam Physician* (2007) 76(4):539–44.
74. Arezes J, Jung G, Gabayan V, Valore E, Ruchala P, Gulig PA, et al. Hepcidin-induced hypoferremia is a critical host defense mechanism against the siderophilic bacterium *Vibrio vulnificus*. *Cell Host Microbe* (2015) 17(1):47–57. doi: 10.1016/j.chom.2014.12.001
75. Ganz T, Nemeth E. Hepcidin and disorders of iron metabolism. *Annu Rev Med* (2011) 62:347–60. doi: 10.1146/annurev-med-050109-142444

Conflict of Interest: The authors declare that the research was conducted in the absence of any commercial or financial relationships that could be construed as a potential conflict of interest.

frontiers in Immunology

CASE REPORT
published: 03 November 2020
doi: 10.3389/fimmu.2020.601584

MPEG1/Perforin-2 Haploinsufficiency Associated Polymicrobial Skin Infections and Considerations for Interferon-γ Therapy

Leidy C. Merselis[1†], Shirley Y. Jiang[2†], on behalf of Undiagnosed Diseases Network, Stanley F. Nelson[3,4,5], Hane Lee[3,4], Kavitha K. Prabaker[6], Jennifer L. Baker[7], George P. Munson[2‡] and Manish J. Butte[1,5,8‡]*

[1] University of Miami Miller School of Medicine, Department of Microbiology and Immunology, Miami, FL, United States, [2] Division of Immunology, Allergy, and Rheumatology, Department of Pediatrics, University of California Los Angeles, Los Angeles, CA, United States, [3] Department of Human Genetics, University of California Los Angeles, Los Angeles CA, United States, [4] Department of Pathology and Laboratory Medicine, University of California Los Angeles, Los Angeles, CA, United States, [5] California Center for Rare Diseases, Institute for Precision Health, University of California Los Angeles, Los Angeles, CA, United States, [6] Division of Infectious Diseases, Department of Medicine, University of California Los Angeles, Los Angeles, CA, United States, [7] Department of Surgery, University of California Los Angeles, Los Angeles, CA, United States, [8] Department of Microbiology, Immunology, and Molecular Genetics, University of California Los Angeles, Los Angeles, CA, United States

OPEN ACCESS

Edited by:
Junji Xing,
Houston Methodist Research Institute, United States

Reviewed by:
Xiaocui He,
La Jolla Institute for Immunology (LJI), United States
Nithyananda Thorenoor,
Pennsylvania State University, United States

***Correspondence:**
Manish J. Butte
mbutte@mednet.ucla.edu
orcid.org/0000-0002-4490-5595

[†]These authors have contributed equally to this work

[‡]These authors share senior authorship

Specialty section:
This article was submitted to Molecular Innate Immunity, a section of the journal Frontiers in Immunology

Received: 01 September 2020
Accepted: 12 October 2020
Published: 03 November 2020

Citation:
Merselis LC, Jiang SY, Nelson SF, Lee H, Prabaker KK, Baker JL, Munson GP and Butte MJ (2020) MPEG1/Perforin-2 Haploinsufficiency Associated Polymicrobial Skin Infections and Considerations for Interferon-γ Therapy. Front. Immunol. 11:601584. doi: 10.3389/fimmu.2020.601584

Introduction: Macrophage expressed gene 1 (*MPEG1*) is highly expressed in macrophages and other phagocytes. The gene encodes a bactericidal pore-forming protein, dubbed Perforin-2. Structural-, animal-, and cell-based studies have established that perforin-2 facilitates the destruction of phagocytosed microbes upon its activation within acidic phagosomes. Relative to wild-type controls, *Mpeg1* knockout mice suffer significantly higher mortality rates when challenged with gram-negative or -positive pathogens. Only four variants of *MPEG1* have been functionally characterized, each in association with pulmonary infections. Here we report a new *MPEG1* non-sense variant in a patient with the a newly described association with persistent polymicrobial infections of the skin and soft tissue.

Case Description: A young adult female patient was evaluated for recurrent abscesses and cellulitis of the breast and demonstrated a heterozygous, rare variant in *MPEG1* p.Tyr430*. Multiple courses of broad-spectrum antimicrobials and surgical incision and drainage failed to resolve the infection. Functional studies revealed that the truncation variant resulted in significantly reduced capacity of the patient's phagocytes to kill intracellular bacteria. Patient-derived macrophages responded to interferon gamma (IFN-γ) by significantly increasing the expression of *MPEG1*. IFN-γ treatment supported perforin-2 dependent bactericidal activity and wound healing.

Conclusions: This case expands the phenotype of *MPEG1* deficiency to include severe skin and soft tissue infection. We showed that haploinsufficiency of perforin-2 reduced the

bactericidal capacity of human phagocytes. Interferon-gamma therapy increases expression of perforin-2, which may compensate for such variants. Thus, treatment with IFN-γ could help prevent infections.

Keywords: MPEG1 p.Tyr430*, perforin-2, primary immunodeficiency, membrane attack complex, interferon gamma, case report

INTRODUCTION

MPEG1 expression is constitutive in phagocytes and inducible in parenchymal cell lines by interferons or bacterial infection (1, 2). Its function in innate immunity is vital for intracellular pathogen elimination such that *Mpeg1* knockout mice exhibit increased susceptibility to infections (2–5). *MPEG1* variants can confer an immunodeficiency hallmarked by polymicrobial infections (1).

Until now, *MPEG1* mutations have been primarily studied *in vivo* in non-human subjects, with the exception of a study by McCormack *et al.* that describes the first four clinical cases of heterozygous *MPEG1* mutations in human disease, which notably involved pulmonary infections with a preponderance of non-tuberculous *Mycobacteria* (1). Skin and soft tissue infections were not described. Here we expand the phenotype of *MPEG1* haploinsufficiency by describing a patient with polymicrobial skin and soft tissue infections bearing a heterozygous nonsense variant of *MPEG1*. We offer considerations for treating this condition with interferon gamma (IFN-γ).

Case Description

The patient reported is a 23-year-old adopted woman with a limited history of early childhood. She has a complex medical history including bilateral sensorineural hearing loss and non-anatomic gastroparesis requiring feeds by jejunal tube. She also carries the heterozygous, pathogenic Factor V "Leiden" variant discovered after suffering multiple deep vein thromboses and pulmonary emboli, now on lifelong anticoagulation. The patient experienced numerous infections throughout adolescence and young adulthood including repeated facial impetigo, recurrent tonsillitis requiring tonsillectomy and adenoidectomy, skin abscesses, recurrent central line-associated blood stream infections (*Enterobacter cloacae*), and infections of the central line site (*Staphylococcus aureus*). Because of a concern for a primary immunodeficiency, she had been treated empirically with immune globulin, without evidence of hypogammaglobulinemia or specific antibody deficiency. At age 22, she presented with a breast abscess and cellulitis requiring incision and drainage (I&D). Over the next several months, she suffered recurrent abscesses despite serial debridement and intravenous antibiotics. During a prolonged inpatient stay for treatment of recurrent breast abscess at her local hospital, she was transferred to our institution for further evaluation and treatment. Her initial diagnostic work-up included laboratory studies that demonstrated a normal leukocyte count, mild anemia, overall normal lymphocyte counts, and a mild thrombocytosis, likely reactive to an acute infection (**Table 1**). An ultrasound of the right breast found complex fluid collections, of which the largest region measured 16 x 5 x 14 mm. A biopsy of the tissue supported a picture of acute on chronic inflammation without atypical hyperplasia or malignancy. Cultures obtained at different time points during her clinical course grew numerous organisms including *Staphylococcus pseudintermedius, Enterobacter cloacae, Klebsiella pneumoniae, Serratia marcescens, Veillonella parvula*, and *Candida* spp. (*glabrata, albicans*, and *lusitaniae*). Despite completing an extended course of appropriate antimicrobial coverage along with multiple I&D procedures, the infections did not resolve.

DIAGNOSTIC ASSESSMENT

A polymicrobial breast infection in a young woman persisting over several months despite treatment with multiple

TABLE 1 | Laboratory Results.

Complete blood count (CBC)	**Result**	**Units**	**Reference range**
WBC	8.00	1,000/μl	4.16–9.95
Hemoglobin	11.3	Gram/dl	11.6–15.2
Platelet	459	1,000/μl	143–398
Neutrophil	56.8	%	
Lymphocyte	33.3	%	
Monocyte	7.5	%	
Eosinophil	1.6	%	
Basophil	0.5	%	
Inflammatory markers	**Result**	**Units**	**Reference range**
C-reactive protein	0.3	mg/dl	<0.8
Erythrocyte sedimentation rate	16	mm/h	≤25
Immunoglobulins	**Result**	**Units**	**Reference range**
IgA, serum	170	mg/dl	87–426
IgG, serum	1,200	mg/dl	726–1521
IgM, serum	144	mg/dl	44–277
Lymphocyte counts	**Cell type**	**Result (/μl)**	**Reference range(/μl)**
CD3+	T cells	1,634	803–2,990
CD4+	Helper T cells	725	441–2,156
CD8+	Cytotoxic T cells	718	125–1,312
CD19+	B cells	441	107–698
CD56+/CD16+	NK cells	58	95–640
CD19+CD27+	Memory B cells	26.5	18–145
CD19+CD27+IgM+IgD-	IgM memory B cells	0	0–12
CD19+CD27+IgM+IgD+	Unswitched memory B cells	13.2	4–85
CD19+CD27+IgM-IgD-	Switched memory B cells	13.2	7–61
CD19+CD21low	Immature B cells	8.8	0.3–22
Other	**Interpretation**		
HIV-1/2 Ag/Ab screen fourth generation	Nonreactive		

antimicrobials was suspicious for primary immunodeficiency. Flow cytometric analysis of peripheral blood lymphocytes showed mild NK cell lymphopenia, which was normal in prior and subsequent tests. Whole genome sequencing revealed a few, rare genetic variants including a nonsense variant in *MPEG1* NM_001039396.1:c.1290C>A, resulting in p.Tyr430* (dbSNP rs773347395) (**Figure 1A**), which codes for the perforin-2 protein. The CADD phred score of this variant was 36. This variant is rare, occurring in only 1 of 124,579 individuals in the Genome Aggregation Database (gnomAD) and not in homozygous form (7). A heterozygous p.D113N variant of *IKBKG* was identified as well, but because of its commonness (found in ~3% of alleles of Europeans in gnomAD), this variant was felt unlikely to be the cause of her immunodeficiency.

Given the known bactericidal function of perforin-2 and the location of this variant in the P2 domain and eliminating the C-terminal transmembrane domain, the *MPEG1* variant was suspected to be pathogenic (**Figure 1B**). If the Tyr430* truncated protein product were stably expressed it would likely be secreted rather than delivered to endophagosomes as its transmembrane domain is essential for the intracellular retention of perforin-2 (6, 8). Immunologic assays demonstrated normal neutrophil chemotaxis and extracellular bactericidal activity against *Staphylococcus aureus* (**Table 2**). However, the latter laboratory assay did not differentiate between extracellular and intracellular killing. Thus, it may not

TABLE 2 | Clinical Neutrophil Assays.

Neutrophil chemotaxis assay before → after exposure to zymosan-activated serum

Sample	Migration (μm)	Reference range
Control	52 → 109	24–54 μm (before) → 68–114 μm (after)
Patient	52 → 100	

Bactericidal assay (*Staphylococcus aureus*, killing at 120 min)

Sample	Percent dead (%)	Reference range (%)
Control	87	>71
Patient	86	>71

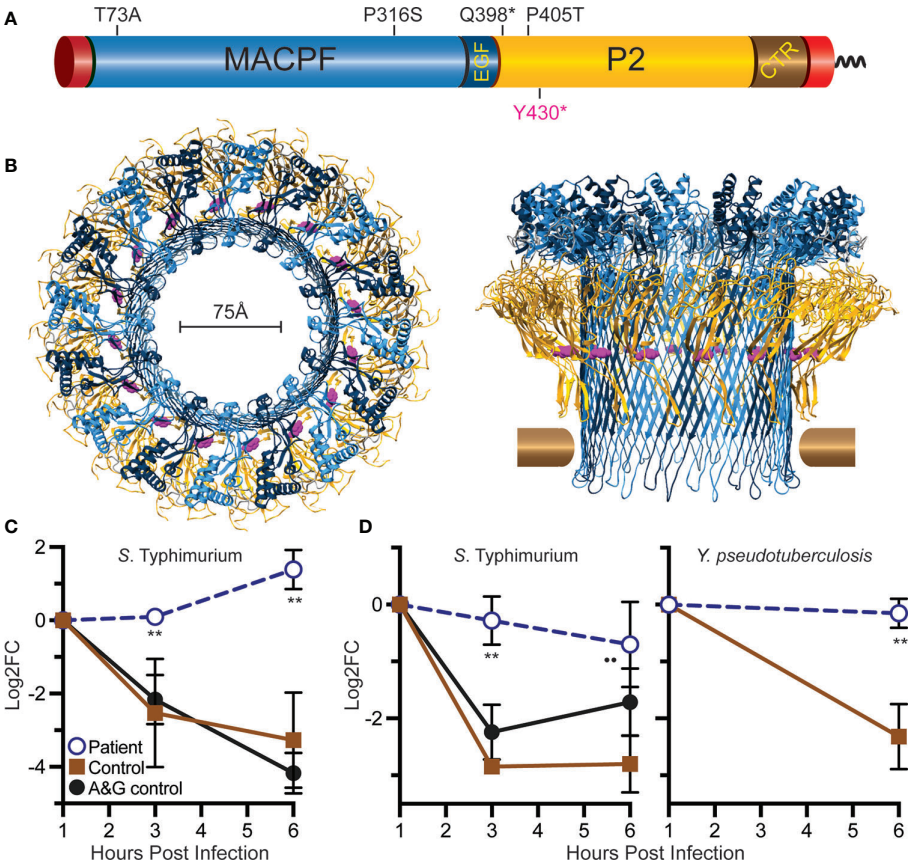

FIGURE 1 | Relative location of Tyr430 within perforin-2 and demonstration of reduced killing capacity of the patient's phagocytes. **(A)** Domain organization of perforin-2 with its signal peptide, membrane-attack-complex-perforin (MACPF) domain (blue), EGF-like domain (dark blue), perforin-2 domain (yellow), and carboxy-terminal transmembrane domain (brown, red). **(B)** Top and side view of the acid-dependent perforin-2 pore (6). Each polymer comprises 16 subunits with MACPF and P2 domains lining the interior and exterior of the polymer. Tyr430 is depicted as magenta spheres within the P2 domain. Horizontal bars represent the approximate location of the target lipid bilayer. **(C)** Neutrophil killing assay showing fold change over time of intracellular bacterial colony forming units. **(D)** Macrophage killing assay showing fold change over time of intracellular bacterial colony forming units. $\log_2$FC = $\log_2$(CFU at time X) – $\log_2$(CFU at time initial). $^{**}P < 0.04$ to age and gender (A&G) shipping control, and $P < 0.02$ to non-matched, unrelated control.

be sensitive enough to detect reduced Perforin-2 activity within phagosomes.

To assess the impact of the *MPEG1* variant, the subject's neutrophils and macrophages were tested for intracellular killing. These cells were purified from anticoagulated whole blood and allowed to phagocytose *Salmonella enterica* serovar Typhimurium (*S.* Typhimurium) or *Yersinia pseudotuberculosis*. The phagocytes were then treated with membrane impermeable gentamicin to eliminate the extracellular population of bacteria prior to enumeration of intracellular bacteria. This assay, commonly referred to as a gentamicin protection assay, revealed that the patient's neutrophils were unable to suppress the intracellular replication of *S.* Typhimurium (**Figure 1C**). As expected, cells from healthy controls were more effective at eliminating the intracellular pathogens. This defect was also observed with patient-derived macrophages infected with *S.* Typhimurium or *Y. pseudotuberculosis* (**Figure 1D**).

During the patient's admission, she was again treated with broad spectrum antimicrobials and multiple I&D's, however her hospital course was complicated by incomplete resolution and development of new abscesses in the right breast. Physical exam revealed multiple, tender, deep painful regions around the breast with corresponding regions of erythema (**Figure 2A**). Breast cultures during this admission again grew organisms previously present including *K. pneumoniae, S. marcescens*, and *C. glabrata*, as well as *Enterococcus faecalis* and Lactobacillus species. The patient became frustrated with months of inpatient treatments. Due to prolonged and inadequate resolution of the abscess despite multiple antibiotics and antifungals, she underwent surgical placement of antibiotic- and antifungal-impregnated calcium sulfate beads (9) and treatment with three injections of intralesional GM-CSF to promote wound healing and phagocytosis (10).

Adjuvant therapy with IFN-γ was considered next. To determine if the patient's phagocytes were responsive to interferons, macrophages differentiated from the patient's blood monocytes were treated with IFN-γ. Relative to untreated control, IFN-γ increased *MPEG1* expression by eight-fold (**Figure 2B**). Such upregulation may compensate for *MPEG1* haploinsufficiency by increasing perforin-2 expression from the normal allele. Facing steady worsening of the patient's condition, we treated her with IFN-γ at a dose of 50 $\mu g/m^2$ three times weekly for 3 weeks. The patient experienced initial improvement of symptoms with the adjuvant therapy, however she also experienced malaise, body aches, and low-grade fevers known to accompany IFN-γ therapy. Due to chronic pain and redeveloping abscesses, the patient underwent a unilateral total mastectomy using tumescent and scissor dissection, given the contraindication of cautery in the setting of her cochlear implants. Surgical pathology found inflamed granulation tissue with multiple micro-abscesses and periductal inflammation. Post-operatively she had clinical cure of infection and complete wound healing. IFN-γ therapy was continued in the outpatient setting as prophylaxis, but there have been difficulties tolerating side effects, including fever. There were no further infections in the 3 months following mastectomy.

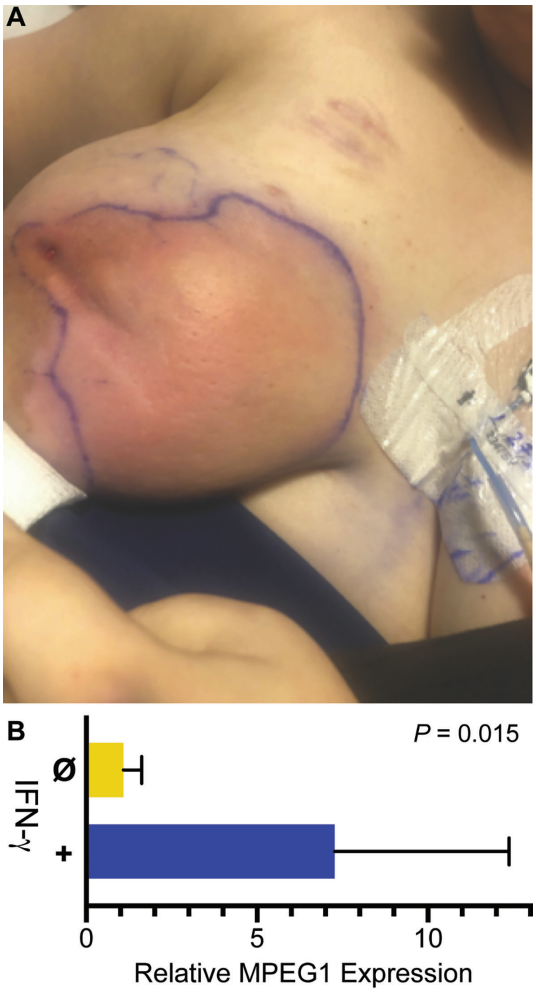

FIGURE 2 | Infection and IFN-γ induction of *MPEG1*. **(A)** Purulent abscesses in the right breast. **(B)** *MPEG1* transcripts are induced after treatment *in vitro* with IFN-γ.

DISCUSSION

This case illustrates the innate immune dysfunction in a young woman carrying a *MPEG1* genomic loss-of-function variant, presenting as difficult-to-manage skin and soft tissue infections. Perforin-2 is a member of the membrane attack complex/perforin (MACPF) family, which includes the terminal components of complement (C9) responsible for pore-forming membrane disruption to eradicate microbial invaders (6, 8). Expression of perforin-2 is upregulated by IFNs in primary fibroblasts and epithelial cell lines (11). Although the precise details are under investigation, perforin-2 is trafficked to endo/phagosomes where it polymerizes into a pre-pore structure that subsequently transitions to a pore conformation upon phagosome acidification (2, 4, 8). These pores perforate the envelope of phagocytosed pathogens, rendering them more susceptible to antimicrobial effector such as proteases, other hydrolases, and reactive oxygen and nitrogen

species (2, 5). Studies of *Mpeg1* knockout mice have shown that deficiencies in this protein lead to uncontrolled, disseminated infection from the gut and skin, as well as a host of other immunologic consequences (2–4). Pathogenic variants have been reported in patients with both intracellular and extracellular pulmonary infections with *Mycobacterium, Pseudomonas, Achromobacter, Bordetella, Pneumocystis*, and *Aspergillus* species (1), suggesting that this immunodeficiency extends beyond control of intracellular organisms. An important feature of this patient's disease is the location of the infection: the skin. Studies *in vitro* in human skin found that perforin-2 is induced during wound healing in the skin and is necessary for intracellular killing of Staphylococcus (12).

IFN-γ is a naturally occurring, pleotropic cytokine central to type-1 immunity and, as a medication, is approved for the prophylaxis of infections in the context of chronic granulomatous disease. *In vitro* studies have shown that IFN-γ induces *MPEG1* expression in an array of murine and human cell lines as well as primary cells (2, 11). Consistent with that work we found that IFN-γ significantly increased expression of *MPEG1* in patient-derived macrophages. Despite some improvement in clinical status, the widespread infection required mastectomy for resolution. The benefits of IFN-γ could thus not be fully determined. Further investigation will be required to assess if treatment with IFN-γ promotes perforin-2-mediated bactericidal activity and reduces infections in *MPEG1* deficiency.

CONCLUSIONS

Perforin-2 plays important roles in the ability of innate immune cells to kill intracellular pathogens. We present a single case demonstrating haploinsufficiency of perforin-2 with severe, bacterial, and fungal soft tissue infections. IFN-γ therapy may be used as a potential prophylaxis for inducing the expression of the functional allele.

MATERIALS AND METHODS

Structural Model

The structural model of perforin-2 comes from RCSB entry 6SB5.

Killing Assays

For neutrophil killing, polymorphonuclear neutrophils (PMNs) were isolated from whole blood by Ficoll-Paque centrifugation then seeded onto tissue culture plates for 2 h. Adherent cells were subsequently infected for 45 min with *S.* Typhimurium (strain SL1344); the multiplicity of infection (MOI) was 50. Extracellular bacteria were eliminated with 50 μg/ml gentamicin. PMNs were lysed with 0.1% Triton X-100 at the specified times. Released bacteria were serially diluted for enumeration of colony forming units (CFUs) on LB agar plates supplemented with 50 μg/ml of the appropriate antibiotic.

For macrophage killing, PBMCs isolated from whole blood by Ficoll-Paque centrifugation were seeded onto tissue culture treated 100 mm petri plates in IMDM + 10% FBS media supplemented with 50 ng/ml rh-MCSF (BioLegend cat #570206). Monocytes were allowed to adhere and differentiate over 7 days with media changes every 2 days. Following differentiation macrophages were infected with the indicated pathogens; MOI 50. Gentamicin protection assays were conducted as above.

Transcript Comparison

$1x10^6$ differentiated patient macrophages were stimulated for 14 h with 100 ng/ml of human recombinant IFN-γ and subsequently lysed in RLT buffer + 1% BME. Whole culture RNA was extracted with RNeasy columns and converted to cDNA using QuantiTec Reverse Transcription Kit. Samples were run in triplicate using TaqMan probes specific for human MPEG1. Results were normalized to expression of GAPDH and presented relative to untreated macrophages. *P* value as determined by unpaired *t* test.

DATA AVAILABILITY STATEMENT

Data for **Figures 1C, D** and **2B** have been deposited in FigShare; doi.org/10.6084/m9.figshare.13122821. Further inquiries can be directed to the corresponding author.

ETHICS STATEMENT

The studies involving human participants were reviewed and approved by UCLA IRB. The patients/participants provided their written informed consent to participate in this study. Written informed consent was obtained from the individual(s) for the publication of any potentially identifiable images or data included in this article.

UNDIAGNOSED DISEASES NETWORK

Maria T. Acosta; Margaret Adam; David R. Adams; Pankaj B. Agrawal; Mercedes E. Alejandro; Justin Alvey; Laura Amendola; Ashley Andrews; Euan A. Ashley; Mahshid S. Azamian; Carlos A. Bacino; Guney Bademci; Eva Baker; Ashok Balasubramanyam; Dustin Baldridge; Jim Bale; Michael Bamshad; Deborah Barbouth; Pinar Bayrak-Toydemir; Anita Beck; Alan H. Beggs; Edward Behrens; Gill Bejerano; Jimmy Bennet; Beverly Berg-Rood; Jonathan A. Bernstein; Gerard T. Berry; Anna Bican; Stephanie Bivona; Elizabeth Blue; John Bohnsack; Carsten Bonnenmann; Devon Bonner; Lorenzo Botto; Brenna Boyd; Lauren C. Briere; Elly Brokamp; Gabrielle Brown; Elizabeth A. Burke; Lindsay C. Burrage; Manish J. Butte; Peter Byers; William E. Byrd; John Carey; Olveen Carrasquillo; Ta Chen Peter Chang; Sirisak Chanprasert; Hsiao-Tuan Chao; Gary D. Clark; Terra R. Coakley; Laurel A. Cobban; Joy D. Cogan; Matthew Coggins;

F. Sessions Cole; Heather A. Colley; Cynthia M. Cooper; Heidi Cope; William J. Craigen; Andrew B. Crouse; Michael Cunningham; Precilla D'Souza; Hongzheng Dai; Surendra Dasari; Joie Davis; Jyoti G. Dayal; Matthew Deardorff; Esteban C. Dell'Angelica; Shweta U. Dhar; Katrina Dipple; Daniel Doherty; Naghmeh Dorrani; Argenia L. Doss; Emilie D. Douine; David D. Draper; Laura Duncan; Dawn Earl; David J. Eckstein; Lisa T. Emrick; Christine M. Eng; Cecilia Esteves; Marni Falk; Liliana Fernandez; Carlos Ferreira; Elizabeth L. Fieg; Laurie C. Findley; Paul G. Fisher; Brent L. Fogel; Irman Forghani; Laure Fresard; William A. Gahl; Ian Glass; Bernadette Gochuico; Rena A. Godfrey; Katie Golden-Grant; Alica M. Goldman; Madison P. Goldrich; David B. Goldstein; Alana Grajewski; Catherine A. Groden; Irma Gutierrez; Sihoun Hahn; Rizwan Hamid; Neil A. Hanchard; Kelly Hassey; Nichole Hayes; Frances High; Anne Hing; Fuki M. Hisama; Ingrid A. Holm; Jason Hom; Martha Horike-Pyne; Alden Huang; Yong Huang; Laryssa Huryn; Rosario Isasi; Fariha Jamal; Gail P. Jarvik; Jeffrey Jarvik; Suman Jayadev; Lefkothea Karaviti; Emily G. Kelley; Jennifer Kennedy; Dana Kiley; Isaac S. Kohane; Jennefer N. Kohler; Deborah Krakow; Donna M. Krasnewich; Elijah Kravets; Susan Korrick; Mary Koziura; Joel B. Krier; Seema R. Lalani; Byron Lam; Christina Lam; Grace L. LaMoure; Brendan C. Lanpher; Ian R. Lanza; Lea Latham; Kimberly LeBlanc; Brendan H. Lee; Hane Lee; Roy Levitt; Richard A. Lewis; Sharyn A. Lincoln; Pengfei Liu; Xue; Zhong Liu; Nicola Longo; Sandra K. Loo; Joseph Loscalzo; Richard L. Maas; John MacDowall; Ellen F. Macnamara; Calum A. MacRae; Valerie V. Maduro; Marta M. Majcherska; Bryan C. Mak; May Christine V. Malicdan; Laura A. Mamounas; Teri A. Manolio; Rong Mao; Kenneth Maravilla; Thomas C. Markello; Ronit Marom; Gabor Marth; Beth A. Martin; Martin G. MartinJulian A. Martínez-Agosto; Shruti Marwaha; Jacob McCauley; Allyn McConkie-Rosell; Colleen E. McCormack; Alexa T. McCray; Elisabeth McGee; Heather Mefford; J. Lawrence Merritt; Matthew Might; Ghayda Mirzaa; Eva Morava; Paolo M. Moretti; Deborah Mosbrook-Davis; John J. Mulvihill; David R. Murdock; Anna Nagy; Mariko Nakano-Okuno; Avi Nath; Stan F. Nelson; John H. Newman; Sarah K. Nicholas; Deborah Nickerson; Shirley Nieves-Rodriguez; Donna Novacic; Devin Oglesbee; James P. Orengo; Laura Pace; Stephen Pak; J. Carl Pallais; Christina GS. Palmer; Jeanette C. Papp; Neil H. Parker; John A. Phillips III; Jennifer E. Posey; Lorraine Potocki; Bradley Power; Barbara N. Pusey; Aaron Quinlan; Wendy Raskind; Archana N. Raja; Deepak A. Rao; Genecee Renteria; Chloe M. Reuter; Lynette Rives; Amy K. Robertson; Lance H. Rodan; Jill A. Rosenfeld; Natalie Rosenwasser; Francis Rossignol; Maura Ruzhnikov; Ralph Sacco; Jacinda B. Sampson; Susan L. Samson; Mario Saporta; C. Ron Scott; Judy Schaechter; Timothy Schedl; Kelly Schoch; Daryl A. Scott; Vandana Shashi; Jimann Shin; Rebecca Signer; Edwin K. Silverman; Janet S. Sinsheimer; Kathy Sisco; Edward C. Smith; Kevin S. Smith; Emily Solem; Lilianna Solnica-Krezel; Ben Solomon; Rebecca C. Spillmann; Joan M. Stoler; Jennifer A. Sullivan; Kathleen Sullivan; Angela Sun; Shirley Sutton; David A. Sweetser; Virginia Sybert; Holly K. Tabor; Queenie K.-G. Tan; Mustafa Tekin; Fred Telischi; Willa Thorson; Audrey Thurm; Cynthia J. Tifft; Camilo Toro; Alyssa A. Tran; Brianna M. Tucker; Tiina K. Urv; Adeline Vanderver; Matt Velinder; Dave Viskochil; Tiphanie P. Vogel; Colleen E. Wahl; Stephanie Wallace; Nicole M. Walley; Chris A. Walsh; Melissa Walker; Jennifer Wambach; Jijun Wan; Lee-kai Wang; Michael F. Wangler; Patricia A. Ward; Daniel Wegner; Mark Wener; Tara Wenger; Katherine Wesseling Perry; Monte Westerfield; Matthew T. Wheeler; Jordan Whitlock; Lynne A. Wolfe; Jeremy D. Woods; Shinya Yamamoto; John Yang; Muhammad Yousef; Diane B. Zastrow; Wadih Zein; Chunli Zhao; Stephan Zuchner.

AUTHOR CONTRIBUTIONS

MJB, GPM, and LCM developed the approach for cell based killing assays and MPEG1 quantification. LCM conducted the experiments, analyzed and visualized data. KKP, JLB, and MJB provided clinical care. HL and SFN performed sequencing data analysis. SYJ organized data and wrote the first draft. All authors participated in manuscript editing. All authors have read and approved the submitted version.

FUNDING

Perforin-2 research in the laboratory of GPM is supported by the National Institute of Allergy and Infectious Diseases of the National Institutes of Health under award number R01AI110810. MJB is supported by National Institutes of Health under R01 GM110482 and by the Jeffrey Modell Foundation. Sequencing and data analysis were supported by awards from the National Institutes of Health (NIH) Common Fund, U01HG007703 and the UCLA California Center for Rare Diseases of the Institute for Precision Health.

ACKNOWLEDGMENTS

Molecular graphics were rendered with UCSF Chimera, developed by the Resource for Biocomputing, Visualization, and Informatics at the University of California, San Francisco, with support from NIH P41GM103311 (13).

REFERENCES

1. Mccormack RM, Szymanski EP, Hsu AP, Perez E, Olivier KN, Goodhew EB, et al. MPEG1 / perforin-2 mutations in human pulmonary nontuberculous mycobacterial infections. *JCI Insight* (2017) 2:1–8. doi: 10.1172/jci.insight.89635.Research
2. McCormack RM, de Armas LR, Shiratsuchi M, Fiorentino DG, Olsson ML, Lichtenheld MG, et al. Perforin-2 is essential for intracellular defense of parenchymal cells and phagocytes against pathogenic bacteria. *Elife* (2015) 4:1–29. doi: 10.7554/eLife.06508
3. McCormack R, Bahnan W, Shrestha N, Boucher J, Barreto M, Barrera CM, et al. Perforin-2 protects host cells and mice by restricting the vacuole to

cytosol transitioning of a bacterial pathogen. *Infect Immun* (2016) 84:1083–91. doi: 10.1128/IAI.01434-15
4. McCormack RM, Lyapichev K, Olsson ML, Podack ER, Munson GP. Enteric pathogens deploy cell cycle inhibiting factors to block the bactericidal activity of Perforin-2. *Elife* (2015) 4:1–22. doi: 10.7554/eLife.06505
5. Bai F, McCormack RM, Hower S, Plano GV, Lichtenheld MG, Munson GP. Perforin-2 Breaches the Envelope of Phagocytosed Bacteria Allowing Antimicrobial Effectors Access to Intracellular Targets. *J Immunol* (2018) 201:2710–20. doi: 10.4049/jimmunol.1800365
6. Ni T, Jiao F, Yu X, Aden S, Ginger L, Williams SI, et al. Structure and mechanism of bactericidal mammalian perforin-2, an ancient agent of innate immunity. *Sci Adv* (2020) 6:1–13. doi: 10.1126/sciadv.aax8286
7. Karczewski KJ, Francioli LC, Tiao G, Cummings BB, Alföldi J, Wang Q, et al. The mutational constraint spectrum quantified from variation in 141,456 humans. *Nature* (2020) 581:434–43. doi: 10.1038/s41586-020-2308-7
8. Pang SS, Bayly-Jones C, Radjainia M, Spicer BA, Law RHP, Hodel AW, et al. The cryo-EM structure of the acid activatable pore-forming immune effector Macrophage-expressed gene 1. *Nat Commun* (2019) 10:1–9. doi: 10.1038/s41467-019-12279-2
9. Sherif RD, Ingargiola M, Sanati-Mehrizy P, Torina PJ, Harmaty MA. Use of antibiotic beads to salvage infected breast implants. *J Plast Reconstr Aesthet Surg* (2017) 70:1386–90. doi: 10.1016/j.bjps.2017.05.023
10. De Ugarte DA, Roberts RL, Lerdluedeeporn P, Stiehm ER, Atkinson JB. Treatment of chronic wounds by local delivery of granulocyte-macrophage colony-stimulating factor in patients with neutrophil dysfunction. *Pediatr Surg Int* (2002) 18:517–20. doi: 10.1007/s00383-002-0733-3
11. McCormack R, De Armas LR, Shiratsuchi M, Ramos JE, Podack ER. Inhibition of intracellular bacterial replication in fibroblasts is dependent on the perforin-like protein (Perforin-2) encoded by macrophage-expressed gene 1. *J Innate Immun* (2013) 5:185–94. doi: 10.1159/000345249
12. Strbo N, Pastar I, Romero L, Chen V, Vujanac M, Sawaya AP, et al. Single cell analyses reveal specific distribution of anti-bacterial molecule Perforin-2 in human skin and its modulation by wounding and Staphylococcus aureus infection. *Exp Dermatol* (2019) 28:225–32. doi: 10.1111/exd.13870
13. Pettersen EF, Goddard TD, Huang CC, Couch GS, Greenblatt DM, Meng EC, et al. UCSF Chimera—a visualization system for exploratory research and analysis.. *J Comput Chem* (2004) 25.13:1605–12. doi: 10.1002/jcc.20084

Conflict of Interest: The authors declare that the research was conducted in the absence of any commercial or financial relationships that could be construed as a potential conflict of interest.

frontiers in Immunology

REVIEW
published: 10 November 2020
doi: 10.3389/fimmu.2020.585108

Soluble Membrane Attack Complex: Biochemistry and Immunobiology

Scott R. Barnum[1]*, *Doryen Bubeck*[2] and *Theresa N. Schein*[1]

[1] CNine Biosolutions, LLC, Birmingham, AL, United States, [2] Department of Life Sciences, Imperial College London, London, United Kingdom

The soluble membrane attack complex (sMAC, a.k.a., sC5b-9 or TCC) is generated on activation of complement and contains the complement proteins C5b, C6, C7, C8, C9 together with the regulatory proteins clusterin and/or vitronectin. sMAC is a member of the MACPF/cholesterol-dependent-cytolysin superfamily of pore-forming molecules that insert into lipid bilayers and disrupt cellular integrity and function. sMAC is a unique complement activation macromolecule as it is comprised of several different subunits. To date no complement-mediated function has been identified for sMAC. sMAC is present in blood and other body fluids under homeostatic conditions and there is abundant evidence documenting changes in sMAC levels during infection, autoimmune disease and trauma. Despite decades of scientific interest in sMAC, the mechanisms regulating its formation in healthy individuals and its biological functions in both health and disease remain poorly understood. Here, we review the structural differences between sMAC and its membrane counterpart, MAC, and examine sMAC immunobiology with respect to its presence in body fluids in health and disease. Finally, we discuss the diagnostic potential of sMAC for diagnostic and prognostic applications and potential utility as a companion diagnostic.

Keywords: complement, soluble membrane attack complex, sC5b-9, cholesterol-dependent cytolysins, MAC, diagnostics, sMAC

OPEN ACCESS

Edited by:
Robert John Crispin Gilbert, University of Oxford, United Kingdom

Reviewed by:
Marjetka Podobnik, National Institute of Chemistry Slovenia, Slovenia
Peter Kraiczy, Goethe University Frankfurt, Germany

***Correspondence:**
Scott R. Barnum
sbarnum@cninebio.com

Specialty section:
This article was submitted to Molecular Innate Immunity, a section of the journal Frontiers in Immunology

Received: *19 July 2020*
Accepted: *14 October 2020*
Published: *10 November 2020*

Citation:
Barnum SR, Bubeck D and Schein TN (2020) Soluble Membrane Attack Complex: Biochemistry and Immunobiology. Front. Immunol. 11:585108. doi: 10.3389/fimmu.2020.585108

INTRODUCTION

The complement system is the most complex of the immunological and hematological pathways in human biology. Composed of ~50 proteins, four activation pathways (classical, lectin, alternative, and extrinsic) and a terminal lytic pathway, it is an important part of both innate and adaptive immune responses (1–3). Complement-mediated immune effector functions include chemoattraction of immune cells, activation of leukocytes, platelets and essentially all cell types proximal to complement activation, opsonization of invading pathogens, enhancement of the acute-phase response, lysis of susceptible pathogens and modulation of lymphocyte-mediated immune responses (1, 2, 4–6). Complement also serves to help in controlling T and B cell activation and function, stem cells and developmental processes, modulate basic cellular processes in intracellular sensing and cellular metabolism as it relates to immune responses (7–15), synaptic pruning (16, 17), modulation of the circadian clock (18), and possible contributions to schizophrenia (19, 20). Effector functions mediated by complement are driven by the proteolytic generation of activation fragments that either 1) bind to receptors expressed on both immune and non-immune cells, or 2) covalently attach to cell surfaces adjacent to sites of complement activation (1–3). These activities

are tightly controlled by more than a dozen fluid-phase and membrane-bound regulatory molecules whose function is to keep complement activation in proportion to the amount of activator present and to limit damage to host tissues (1, 21, 22). Additional non-canonical roles of complement are discussed in a series published in Seminars in Immunology (23).

sMAC: A Unique Activation Fragment

Activation of complement liberates more functional polypeptide fragments of various molecular species than any other immunological or hematological pathway. For example, activation of factor B releases Bb, a serine protease and key component of the alternative pathway C3 and C5 convertases, and Ba, a small polypeptide composed of three shushi domains with no known biological function. In contrast, cleavage of C3 and C4 generates C3a and C4a, respectively, which are small (~10 kDa) fragments that possess a wide range of functions including chemoattraction, antimicrobial activity, and modulation of T cell responses [reviewed in (6, 24)]. In addition, C3 and C4 cleavage produces multiple polypeptides from the larger 'b' fragments which are equally diverse in function (1, 2, 25). Enzymatic activity of complement serine proteases is responsible for production of at least a dozen activation fragments. The soluble membrane attack complex (sMAC) is an exception to the production of functionally-active polypeptide fragments. Generated by activation of the complement pathways, the formation of sMAC in the fluid-phase starts with the cleavage of C5 by C5 convertases, to C5a and C5b (**Figure 1A**). The addition of C6, C7, C8, C9 to C5b forms a basic MAC structure, which associates with the regulatory proteins clusterin and/or vitronectin, to form a soluble MAC complex inhibited from inserting into lipid bilayers (26–33). sMAC may have one to three C9 molecules and can bind one to two clusterin or vitronectin molecules, or a combination of clusterin and vitronectin molecules (**Figure 1B**). Thus, sMAC is not a single molecular species, but a family of closely related multi-molecular complexes. Based on this stoichiometry, at least fifteen different sMAC complexes are possible. Since each of the protein subunits in sMAC have polymorphic variants (34–43), there are many sMAC variants at the population level (similar to polymorphism at the population level for MHC molecules). The biological roles of

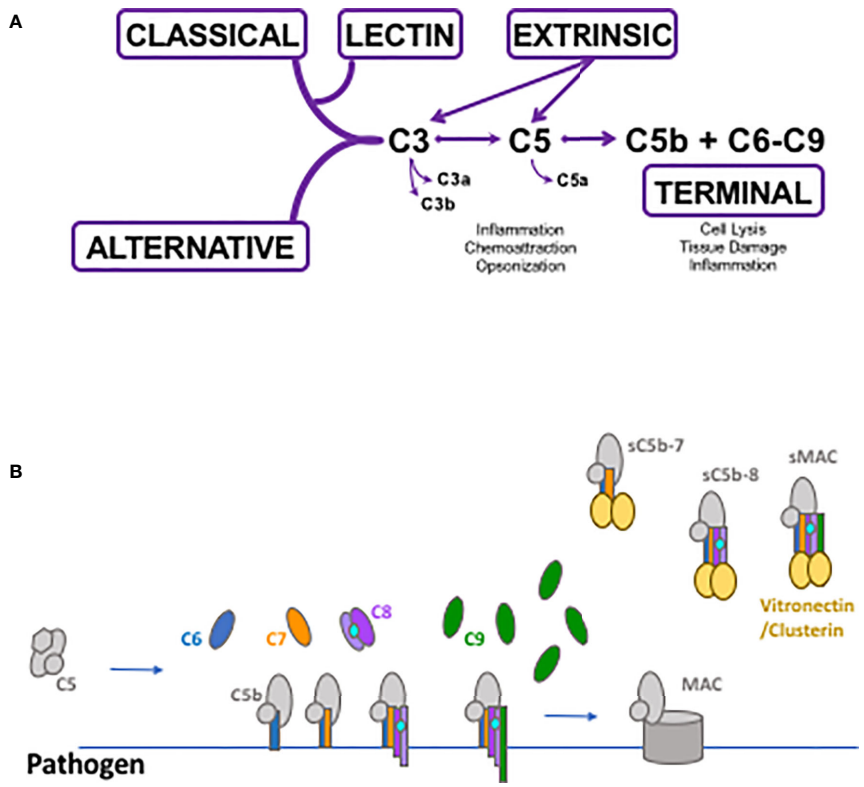

FIGURE 1 | Schematic depicting complement activation and soluble membrane attack complex (sMAC) and MAC formation. **(A)** The classical, lectin and alternative pathways generate C3 and C5 convertases that cleave C3 and C5 into their biologically active fragments. Direct cleavage of C3 and C5 occurs through the extrinsic protease pathway which utilizes several enzymes of the coagulation system such as activated thrombin and plasmin and others. Activation through any of the pathways can generate C5b which initiates the formation of MAC and sMAC through the terminal pathway. **(B)** Schematic of MAC formation on a pathogen surface. Generation of C5b as a result of complement activation allows the non-covalent association of C6 through C9 and the production of the pore-forming membrane attack complex. Simultaneously with MAC formation, C5b in the fluid-phase can associate with C6 through C9 forming soluble intermediates leading to sMAC generation. All of the soluble intermediates and sMAC associate with vitronectin and/or clusterin preventing their insertion into pathogen or human cell membranes.

these sMAC species in homeostatic conditions and disease pathophysiology are undefined. In contrast, studies in recent years have demonstrated that the MAC contributes to intracellular signaling, inflammation, and other functions (44–47).

Several intermediates leading to the formation of sMAC and MAC have been well characterized biochemically (**Table 1**). Cryo electron microscopy structures of sMAC (33) and MAC (33, 52, 53) suggests a similar overall arrangement of complement proteins within the complex (**Figure 2A**). In both complexes, C5b serves as a structural scaffold that organizes C6, C7, C8 and C9 into an arc through their pore-forming membrane attack complex perforin (MACPF) domains. During MAC formation, the core MACPF domains of C6, C7 C8 and C9 undergo a dramatic structural rearrangement in which two helical bundles unfurl to form a pair of β-hairpins that insert into the lipid bilayer. While it remains unclear from the low-resolution sMAC structure if these transmembrane-hairpins domains have unfurled, both complexes are of a similar length suggesting that at least some of sMAC β-hairpins maybe extended (**Figure 2B**). Negative stain electron microscopy images of vitronectin-labeled sMAC suggest that

TABLE 1 | Physicochemical parameters of soluble membrane attack complex (sMAC) and related complexes.

sMAC complex	Subunit composition	Mol. Wt.	Sedimentation coefficient (S)	Reference
sC5b-9	C5b C6, C7, C8, C9 (1 each), clusterin and/or vitronectrin	~1 MDa	23	(29)
C5b-6	C5b, C6*	328 kDa	11.5	(48)
sC5b-7	C5b, C6, C7, vitronectin or clusterin**	668 kDa	18.5–20	(49)
sC5b-8	C5b, C6, C7, C8, vitronectin, and/or clusterin**	800–850 kDa	19 – 21	(50)
MAC	C5b C6 C7 C8 (1 each), C9 (up to 18), vitronectin and/or clusterin	1.6 MDa	33	(26, 51)

*Studies have shown that vitronectin inhibits lytic activity of C5b,6, but no tri-molecular complex containing vitronectin has been characterized.
**The precise number of clusterin or vitronectin subunits binding to sC5b-6, sC5b-7, and sC5b-8 is currently unknown.

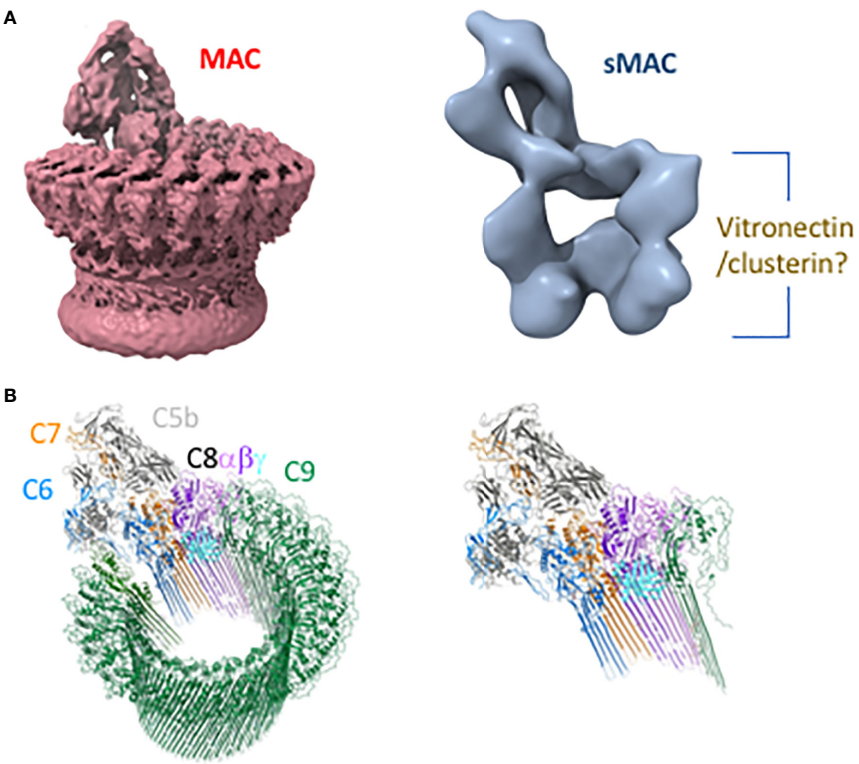

FIGURE 2 | Structures of membrane attack complex (MAC) and soluble MAC (sMAC). **(A)** CryoEM reconstruction of MAC at 4.9 Å resolution (EMD-0110) (53) shows a ring-like arrangement of complement proteins that comprise MAC (left). By contrast, the cryoEM reconstruction of sMAC at 24 Å resolution (EMD-1991) (33) reveals that the ring is stopped short by chaperones vitronectin and clusterin to form an arc (right). Vitronectin and clusterin may act to cap the arc and/or bind exposed hydrophobic residues of unfurled beta-hairpins. **(B)** The left depicts the MAC (PDB-6H04) as a ribbon diagram in which complement proteins are colored: C5b (gray), C6 (blue), C7 (orange), C8β (dark purple), C8α (light purple), C8γ (cyan), and C9 oligomer (green). On the right is a single copy of each protein that may fill the arc of density depicted in the low-resolution sMAC structure.

chaperones may bind to exposed hydrophobic hairpins (29), however, the molecular details of how clusterin and vitronectin prevent membrane insertion of sMAC are still unresolved. In MAC, the helix-to-hairpin transition of membrane-interacting residues exposes a charged surface of the MACPF. Charge complementarity between MACPF-MACPF interfaces is one of main factors that determines the direction of MAC assembly, and likely plays a similar role in formation of sMAC (53). The non-pore forming domains of complement proteins act as regulatory auxiliary modules, preventing the premature release of transmembrane β-hairpins during MAC assembly. How these regulatory domains are oriented in sMAC remains to be seen. High resolution structures of inhibited MAC complexes will be necessary to understand how regulators, such as vitronectin and clusterin, block membrane association of MAC.

sMAC in Biological Fluids in Normal and Disease States

sMAC was first quantitated in plasma in healthy individuals almost 50 years ago (54). Numerous studies since that time have documented the presence of sMAC in most body fluids as discussed below. Although sMAC is present in many of these fluids, the mechanism(s) that generate tissue-specific, basal sMAC levels have received little attention. The continuous activation of complement at low levels through C3 tickover, first described in the early 1970s (55, 56), likely contributes to sMAC generation. In addition to tickover, it is well established that the coagulation system, like complement, is continuously active at a basal level, and thus basal activation of the coagulation and fibrinolytic systems may also contribute to sMAC generation (57–61). This mechanism of complement activation is known as the extrinsic pathway, and it bypasses convertase formation and directly activates C3 and C5 [reviewed in (62, 63)]. The relative contribution of each of these mechanisms and any others that may be involved in basal sMAC generation remains to be established. Once complement is activated however, the high plasma concentration of vitronectin (200–400 μg/ml, (64) and clusterin [150–540 μg/ml, (65)] relative to C9 [~50–60 μg/ml, (66)] suggests formation of sMAC is favored, particularly since both regulatory proteins are elevated in concentration in the acute phase response (67, 68). Mathematical modeling supports this possibility revealing that sMAC is generated rapidly on activation of the classical and alternative pathways reaching peak concentration within 15 min (69). In contrast, MAC production and deposition on pathogens surfaces is characterized by a lag phase of ~20 min, followed by rapid production and deposition that peaks after 50 min (70).

Timing is important for the formation of functional MAC pores and could tip the balance to sMAC production. Rapid over-activation of the complement terminal pathway may overwhelm the C5 convertase. In addition to the proteolytic cleavage of C5, the C5 convertase also plays an important role in orienting MAC assembly precursors at the membrane (71). Improperly inserted precursors could then be scavenged by fluid-phase vitronectin and clusterin, to produce sMAC. On a bacterial surface, convertase generated C5b6 must rapidly recruit C7 to form functional MAC (72). If there is a delay in availability of C7, the inert C5b7 complex could be scavenged by clusterin and vitronectin. Indeed, C5b7 is the first MAC intermediate to bind these two chaperones.

Plasma and Serum

Although sMAC was detected in plasma several decades ago (54), the first quantitative assays based on sMAC neo-epitopes were not developed until the mid-1980's (73, 74). sMAC levels of plasma or serum were frequently measured with in-house assays using serum activated zymosan or inulin as a standard control. These standards and assays were not well characterized and interpretation of the results were complicated by variable assay sensitivity, sample handling, and sample storage (73–77) as highlighted in recent study by Yang and colleagues (78). The International Complement Standardization Committee has since defined an activation standard for quantitation of complement activation products, including sMAC, termed International complement standard #2 (79). International complement standard #2 was derived from healthy donor-derived pooled serum activated with heat-aggregated IgG and zymosan. The utility of this standard (defined as complement activation units, CAU) is limited by variability in pooled serum between different donor cohorts and the reagents used to activate complement. The relationship of CAU to standard measures of protein concentration remains poorly defined. However, immunoassays using purified sMAC as a reagent for generating quantitative standard curves overcomes these limitations.

A recent study using a sMAC ELISA (Quidel, Corp., San Diego, CA) reported mean plasma and serum levels of sMAC of 121 ± 3.7 ng/ml (n=199) and 175 ± 8.1 ng/ml (n=49) respectively, in healthy adult donors (80). Plasma sMAC levels were similar between African-Americans and Caucasians and between males and females. Interestingly, plasma sMAC levels in individuals above 50 years of age were significantly higher than those in their 40's and younger. The levels of sMAC in neonates have been measured in cord blood plasma samples obtained immediately after birth and were markedly lower than adult levels (81). This study, and a number of others, have shown that terminal pathway proteins comprising the MAC (C6-C9) are significantly lower in pre-term and full term infants, as are proteins of the classical and alterative pathways [reviewed in (82)]. In addition, a recent study determined that the blood levels of C9 in children less than one year of age were significantly lower compared to adults, and adult levels were reached between two and eighteen years of age (83). These studies indicate that sMAC levels in are lower in children, in part, because the concentration of proteins that compose the MAC are lower. Nonetheless, sMAC levels in children increase during infection, and activation of complement in neonatal serum by cobra venom factor also increased sMAC levels (81). Additional studies to determine sMAC blood levels in healthy adults and children are warranted to determine the value of sMAC as a diagnostic and prognostic tool in disease settings.

The sMAC in plasma and serum has been measured in many clinical settings including infectious and autoimmune disease, transplantation, trauma, and complement deficiencies (**Table 2**).

TABLE 2 | Soluble membrane attack complex (sMAC) changes in blood, plasma, and serum in various clinical conditions.

Body fluid	Clinical setting	Reference
Blood	Infectious disease:	(80, 84–90)
	Pneumoniae	
	HIV	
	Systemic meningococcal infection	
	Sepsis	
	Dengue shock syndrome	
	Malaria	
	Autoimmune disease:	(91–105)
	Arthritis	
	Lupus	
	ANCA-associated vasculitis	
	Anti-phospholipid syndrome	
	Multiple sclerosis	
	Neuromyelitis optica	
	Myasthenia gravis	
	C3 nephritic factors (immune complex-membranoproliferative glomerulonephritis)	
	Complement deficiency/mutations:	(106–112)
	PNH	
	aHUS	
	CFHR3/1	
	AMD	
	TTP	
	Transplantation/ECMO:	(113–118)
	Heart	
	Lung	
	Kidney/dialysis	
	Autologous stem cells	
	Red blood cells	
	Transplant-associated thrombotic Microangiopathy	
	Trauma	(119, 120)
	Dialysis & related treatments:	(121–125)
	Hemodialysis	
	Peritoneal dialysis	
	Intravenous iron treatment	
	Cardiac failure/disease	(126–128)
	Psychiatric disorders:	(129)
	Bipolar disorder	

TABLE 3 | Soluble membrane attack complex (sMAC) changes in cerebrospinal fluid (CSF) in various clinical conditions.

Body fluid	Clinical setting	Reference
CSF	Infectious disease:	(80, 130–134)
	Bacterial/cryptococcal meningitis	
	Intraventricular shunt infections	
	Autoimmune disease:	(91, 135–141)
	Multiple sclerosis	
	Neuromyelitis optica	
	Clinically Isolated syndrome	
	Guillain–Barré syndrome	
	Sjogren's syndrome	
	Systemic lupus erythematosus	
	Traumatic brain injury	(142, 143)
	Subarachnoid hemorrhage	(144)
	Alzheimer's disease	(145)

TABLE 4 | Mucosal and synovial soluble membrane attack complex (sMAC) changes in various clinical conditions.

Body fluid	Clinical setting	Reference
Urine	Autoimmune disease:	(146)
	Diabetic nephropathy	
	ANCA-associated glomerulonephritis	
	Kidney disease:	(147–152)
	Membranous nephropathy	
	Acute tubulointerstitial nephritis	
	Diabetic nephropathy	
	Focal segmental Glomerulosclerosis	
	Acute post-streptococcal Glomerulonephritis	
	Transplantation	(153–155)
	Preeclampsia	(156)
Synovial Fluid	Arthritis	(92, 94, 157)
Pleural Fluid	Tuberculosis	(88, 158–163)
	Rheumatic disease	
	Malignancy	
	Dengue shock syndrome	
Peritoneal Fluid/ Ascites	Endometriosis acute pancreatitis	(158, 164–166)
Pericardial Fluid	Pericarditis	(158)
Burn Bullae (Blister) Fluid	Burn injury	(158)
Ovarian Follicular Fluid	Infertility	(167)
Seminal Plasma	Infertility	(168)
Aqueous Humor	Glaucoma	(169)

The level of sMAC increases in these conditions in a disease-dependent fashion. However, an encompassing generalization regarding the magnitude and kinetics of the responses is not possible due to the variability in assay types used to quantify sMAC, and the baseline differences of sMAC concentration between serum and plasma. For this reason, we have not included the level of sMAC for the diseases and conditions listed in **Tables 2–4**. *In vivo* studies in rabbits have demonstrated that sMAC is eliminated with a half-life of 30–50 min (170), but no half-life studies have been reported for human sMAC. It is clear the diagnostic and prognostic value of sMAC in blood requires assay and sample handling standardization, particularly as complement therapeutics move into the clinical treatment repertoire (171).

Cerebrospinal Fluid

The normal range of sMAC concentration in cerebrospinal fluid (CSF) of healthy individuals has not been established, in part, because of the clinical risk and discomfort surrounding procuring CSF *via* lumbar puncture. As a result, normal levels of sMAC in CSF have frequently been derived from cohorts with "other neurological diseases" or from patients who underwent lumbar puncture as a part of standard clinical care and had negative bacterial cultures. In most studies using the Quidel sC5b-9 ELISA, CSF sMAC levels range from undetectable to the low nanogram/ml range (10–20 ng/ml) (130, 142, 144, 172, 173). Studies analyzing the sMAC CSF/serum quotient using Reiber–Felgenhauer nomograms of IgM suggest that sMAC is intrathecally produced rather than diffusing across the blood brain barrier (BBB) as has been shown for C9 (173, 174). There are exceptions to this low normal range. For example, Aly and colleagues reported mean levels of sMAC CSF to be ~50 ng/ml in

neonates with hypoxic-ischemic encephalopathy (175). The reasons for this higher level are unclear, but may be due to developmentally-reduced integrity of the BBB shortly after birth, to the elevated level of plasma proteins found in neonatal CSF compared to adults, or to the transport of plasma proteins across choroid plexus epithelial cells in fetal and neonatal brain [reviewed in (176)]. It is also possible that CSF sMAC in neonates is generated as a result of complement-mediated synaptic pruning (16) during neurodevelopment, which is subsequently cleared postnatally. Other studies have reported sMAC concentrations in control groups range from high ng/ml to low μg/ml levels (131, 135, 136). Although non-standardized, in-house sMAC assays were used many of these studies, one likely reason for the high sMAC levels in the control groups was the inclusion of patients with tumors, Huntington's disease, stroke, seizure disorder, cerebellar degeneration, progressive supranuclear palsy, or undetermined infections, which are, at least in part, inflammatory in nature.

Despite the contrasting reports on the levels of CSF sMAC in healthy individuals, it is clear the levels increase in a number of pathological conditions. **Table 3** lists a number of neurological diseases in which sMAC increases relative to levels in other neurological diseases. In bacterial meningitis and shunt infections, sMAC levels have been reported to increase compared to uninfected controls (130, 132–134). In shunt infections, the increase in sMAC was remarkably high (over 100-fold) compared to control CSF (130). Similar dramatic changes in sMAC levels have been reported for traumatic brain injury (as high as 1,800-fold) and subarachnoid hemorrhage (~200-fold) compared to control CSF (142–144). sMAC concentration of this magnitude in CSF suggests its production is derived through multiple mechanisms and sources including: 1) increased intrathecal complement production and activation, 2) blood-derived sMAC leaking across a compromised BBB, and 3) *in situ* generation of sMAC at injury site(s). Interestingly, admixture experiments using human CSF and serum demonstrated that sMAC could be generated in a dose-dependent fashion (up to 5-fold over CSF alone) (144). However, there are cases where sMAC levels are not elevated in infectious or other pathological conditions. For example, in viral and fungal infections, CSF sMAC levels do not increase or increase minimally (131). In idiopathic normal pressure hydrocephalus, a disorder characterized by faulty CSF mechanical dynamics and associated neurodegeneration and inflammation (177), median sMAC levels were a low ~13 ng/ml (173). The reason for the differences in sMAC levels in these latter pathological conditions is unclear, but if verified by additional studies, they could provide differential diagnostic opportunities.

In central nervous system, autoimmune diseases such as multiple sclerosis (MS), Guillain-Barre syndrome, Sjogren's syndrome and systemic lupus erythematosus, there have been reports of increased levels of sMAC (91, 135–138). However, other MS studies have reported no increases in sMAC (139, 178). Studies also present conflicting findings for sMAC levels in neuromyelitis optica (91, 139, 178). Clinically isolated syndrome, a neurodegenerative disease reminiscent of MS (179), has also been examined for changes in CSF sMAC levels. Although sMAC has been detected, the levels do not appear to increase in a clinically meaningful way, but the number of studies is limited (140, 141). There are several other central nervous system diseases where the MAC contributes to disease pathogenesis and, by extension, sMAC levels may change during the course of disease progression. These include epilepsy (180), Parkinson's disease (181) amyotrophic lateral sclerosis (182), Alzheimer's disease (183), various psychiatric conditions (20, 184) and possibly autoimmune encephalitis (185, 186). The inconsistencies noted in some of the above-mentioned studies most likely stem from the use of different sMAC assays, differential sample handling and storage, and the rarity of healthy patient CSF as a negative control. Going forward it would be important to agree on a standard assay for quantitating sMAC and to adopt standardized protocols for handling CSF samples such as that employed by the BioMS-eu network (187, 188).

Urine

Most complement proteins are too large to be excreted in urine. Even factor D, the smallest of the complement proteins (~ 24 Kd), does not pass through the tubular epithelium unless there is a kidney defect (189, 190). With a molecular weight approaching 1 MDa (29), studies have suggested that urinary sMAC is most likely locally generated rather than transported from blood into urine (147, 148, 153, 191). A number of factors may contribute to local sMAC generation in the kidney including high levels of proteinuria, cellular debris, urinary ammonia, and low urinary pH (153). In healthy individuals, sMAC is generally undetectable in urine regardless of the type of assay employed. The kidney appears particularly susceptible to complement-mediated damage for a variety of reasons [reviewed in (192)]. Not surprisingly then, nearly all studies examining for sMAC in urine are derived from patients with a variety of acute and chronic kidney diseases or post-kidney transplantation (147–155) (**Table 4**). A number of urinary biomarkers have been identified for acute kidney injury including kidney injury molecule-1 (KIM-1), IL-18, and others (193). Recent studies suggest that sMAC urinary levels are diagnostic for interstitial inflammation in acute kidney injury associated with nephritis (150) and severe preeclampsia (156) particularly in combination with KIM-1.

Surprisingly there is little known regarding sMAC and urinary tract infections (UTI). It has been shown that C3 promotes colonization of the upper urinary tract by *E. coli* and that C3- and C4-deficent mice develop fewer renal infections (194). Furthermore, in animal studies, C5a appears to exacerbate UTI through enhancing inflammation and recruitment of leukocytes as C5aR-deficient mice had less renal injury and reduced bacterial load compared to wild type mice (195). These studies indicate that complement contributes to UTI, at least for some pathogens, and that the terminal pathway could be involved since C5a is generated. It would be worth determining baseline levels of sMAC (once assays with higher sensitivity have been developed) in the urine of healthy individuals and comparing

it to the levels in UTI patients. sMAC might be an easy biomarker to monitor in UTI, especially in chronic pyelonephritis.

Synovial and Mucosal Fluids

In addition to blood, CSF, and urine, sMAC is found in synovial, pleural, pericardial and peritoneal fluid under conditions of infection, malignancy, or autoimmune disease (listed in **Table 4**). These fluids are routinely collected for diagnostic purposes, primarily to identify bacterial or viral infections, as well as other medical conditions (196–201). Less commonly analyzed is blister fluid from burn patients. Blister fluid is receiving more attention as a possible diagnostic tool based on recent biochemical and proteomic studies [reviewed in (202, 203)]. sMAC and other complement activation proteins have been detected in blister fluid, however their diagnostic utility remains to be determined (158). Complement components are present in male and female reproductive systems and play a role in both fertility and infertility (204, 205). The presence of sMAC in ovarian follicular fluid and seminal plasma not only indicates complement activation, but suggests possible complement-mediated contributions to infertility (204). This remains an understudied topic and is worth pursuing given the general worldwide decline in fertility (206). sMAC has also been detected in aqueous humor of patients with exfoliating glaucoma (169), but not in patients with neovascular age-related macular degeneration (207). sMAC may be present in other body fluids such as tears, nasopharynx secretions, intestinal secretions, and gingival crevicular fluid, but these have not yet been reported. Support for this possibility comes from studies demonstrating the presence of C5a in normal tears and aqueous humor from patients with cataracts, glaucoma, anterior uveitis, or gingival crevicular fluid (208–210).

sMAC in Complement Diagnostics

Changes in the blood levels of either complement proteins or complement functional activity have served as a valuable diagnostic tool for autoimmune diseases, syndromes, and complement deficiencies for over 60 years [initially reviewed in (211)]. Since then our understanding of the complement system and its relationship to the pathophysiology of infectious and autoimmune disease has increased significantly, and most clinical laboratories routinely run at least some complement-related diagnostic assays (212–214). In addition, commercial diagnostic laboratories offer an extensive array of assays to quantitate blood levels of many complement proteins, measure overall complement function, assess pathway- and protein-specific function and identify auto-antibodies to complement proteins. Identifying complement genetic mutations that contribute to syndromes such as hereditary angioedema, hemolytic uremic syndrome, and rare variants that contribute to deficiency or dysfunction [reviewed in (215)], is now offered by some diagnostic laboratories. The value of complement diagnostics will continue to grow as understanding of the role of complement in autoimmune, infectious, psychiatric diseases, and malignancies expands in the coming years (17, 216–218).

Although sMAC levels in blood, CSF, and other body fluids have been studied as a possible biomarker for diseases and inflammatory conditions (**Tables 2–4**), those studies have not translated into common use of sMAC as a clinical diagnostic tool. The literature provides numerous examples of the utility of sMAC as a diagnostic biomarker, but the lack of comprehensive reviews on this topic may be one contributing factor to the under-appreciation of its potential. There is no evidence to suggest that intermediates on the way to sMAC formation (sC5b-7 and sC5b-8) have any diagnostic value and there are currently no assays to specifically measure these MAC-related complexes. The advent of complement therapeutics may, however, be a game-changer for sMAC as a diagnostic tool. The anti-C5 antibody eculizumab prevents MAC and sMAC formation by blocking the cleavage of C5 into C5a and C5b, thereby inhibiting the terminal pathway (219). Initially used for treatment of patients with paroxysmal nocturnal hemoglobinuria and atypical hemolytic uremic syndrome, eculizumab has more recently been used in the management of myasthenia gravis, antibody-mediated graft rejection, neuromyelitis optica, and other conditions (220). Several studies have demonstrated that sMAC levels correlate well with eculizumab dosing further indicating that sMAC may be a useful biomarker for monitoring dosing and also aid in developing personalized patient treatment plans. This would usher in a new era in complement diagnostics particularly if patients could measure sMAC (and/or other complement fragments) at home and relay the information directly to their physician or clinic. This could include patients being treated for paroxysmal nocturnal hemoglobinuria and atypical hemolytic uremic syndrome (106, 221, 222), age-related macular degeneration (107), glomerulonephritis (223), hematopoietic stem cell transplantation (transplant associated thrombotic microangiopathy) (224), thrombotic thrombocytopenia purpura (108, 225), and acute post-infectious glomerulonephritis (226). sMAC monitoring may also have diagnostic value in anti-TNF-α treatment of spondylarthropathies (227), indicating the diagnostic value of sMAC exists beyond complement-specific therapeutics. By extension, sMAC may have diagnostic value in monitoring treatment in rheumatoid, psoriatic arthritis, and other autoimmune diseases given the findings in spondylarthropathies. Complement therapeutic drugs that target the terminal pathway directly or that inhibit the alternative pathway [through which most MAC/sMAC is generated (228)] are currently in development, and it may be beneficial to use sMAC as a biomarker in companion diagnostics to monitor drug efficacy and help manage patient dosing.

CONCLUSION

The terminal complement pathway gives rise to the MAC and multiple sMAC isoforms. Although multiple immunological roles have been identified for the MAC, little is known regarding the immunobiology of sMAC and intermediates generated during the formation of sMAC. There is, however, a large body of preclinical and clinical studies suggesting that sMAC may be a valuable diagnostic tool in multiple disease settings. In order to fully

appreciate the diagnostic potential of sMAC, a number of points should be addressed going forward. These include:

- Assay standardization for quantitating sMAC to allow comparison between datasets and disease settings
- Sample handling and storage standardization to maximize sample stability
- Increased reliance on true healthy controls instead of "non-inflammatory" or "other disease" control sample sets
- Studies to determine basal sMAC fluid levels across multiple demographics

In addition to formalized standardization, there is still much we do not know regarding sMAC with respect to basic physiology and biology. For instance, does sMAC containing vitronectin mediate unknown complement functions or contribute to hematological or cancer-related functions? The multi-functional roles of clusterin and vitronectin may provide insight into sMAC immunobiology, including identification of receptors used in the course of sMAC turnover. These would further aid in the use of sMAC as a biomarker for disease.

AUTHOR CONTRIBUTIONS

Conception and design was by TS and SB. Writing, review, and revision of the manuscript was performed by TS, DB, and SB. All authors contributed to the article and approved the submitted version.

FUNDING

This work was supported in part by a grant from the National Institutes of Health (R43-AI132038) to TS and SB. This project received funding from the European Research Council (ERC) under the European Union's Horizon 2020 research and innovation programme (grant agreement No. 864751 to DB).

ACKNOWLEDGMENTS

We thank Dr. Philip Stahel for critical reading of the manuscript.

REFERENCES

1. Merle NS, Church SE, Fremeaux-Bacchi V, Roumenina LT. Complement System Part I - Molecular Mechanisms of Activation and Regulation. *Front Immunol* (2015) 6:262. doi: 10.3389/fimmu.2015.00262
2. Merle NS, Church SE, Noe R, Halbwachs-Mecarell L, Roumenina LT . Complement System Part II: Role in Immunity. *Front Immunol* (2015) 6:257. doi: 10.3389/fimmu.2015.00257?
3. *The Complement Factsbook. 2nd ed*. SR Barnum, TN Schein eds. London: Academic Press (2018). p. 480.
4. Freeley S, Kemper C, Le Friec G. The "ins and outs" of complement-driven immune responses. *Immunol Rev* (2016) 274(1):16–32. doi: 10.1111/imr.12472
5. Erdei A, Sandor N, Macsik-Valent B, Lukacsi S, Kremlitzka M, Bajtay Z. The versatile functions of complement C3-derived ligands. *Immunol Rev* (2016) 274(1):127–40. doi: 10.1111/imr.12498
6. West EE, Kolev M, Kemper C. Complement and the Regulation of T Cell Responses. *Annu Rev Immunol* (2018) 36:309–38. doi: 10.1146/annurev-immunol-042617-053245
7. Hajishengallis G, Lambris JD. More than complementing Tolls: complement-Toll-like receptor synergy and crosstalk in innate immunity and inflammation. *Immunol Rev* (2016) 274(1):233–44. doi: 10.1111/imr.12467
8. Hajishengallis G, Reis ES, Mastellos DC, Ricklin D, Lambris JD. Novel mechanisms and functions of complement. *Nat Immunol* (2017) 18 (12):1288–98. doi: 10.1038/ni.3858
9. Hawksworth OA, Coulthard LG, Mantovani S. Complement in stem cells and development. *Semin Immunol* (2018) 37:74–84. doi: 10.1016/j.smim.2018.02.009
10. Tam JC, Bidgood SR, McEwan WA. Intracellular sensing of complement C3 activates cell autonomous immunity. *Science* (2014) 345(6201):1256070. doi: 10.1126/science.1256070
11. Barbu A, Hamad OA, Lind L, Ekdahl KN, Nilsson B. The role of complement factor C3 in lipid metabolism. *Mol Immunol* (2015) 67 (1):101–7. doi: 10.1016/j.molimm.2015.02.027
12. Hess C, Kemper C. Complement-mediated regulation of metabolism and basic cellular process. *Immunity* (2016) 45(2):240–54. doi: 10.1016/j.immuni.2016.08.003
13. Liszewski MK, Elvington M, Kulkarni HS, Atkinson JP. Complement's hidden arsenal: New insights and novel functions inside the cell. *Mol Immunol* (2017) 84:2–9. doi: 10.1016/j.molimm.2017.01.004
14. Arbore G, Kemper C, Kolev M. Intracellular complement - the complosome - in immune cell regulation. *Mol Immunol* (2017) 89:2–9. doi: 10.1016/j.molimm.2017.05.012
15. Kolev M, Kemper C. Keeping It All Going-Complement Meets Metabolism. *Front Immunol* (2017) 8:1. doi: 10.3389/fimmu.2017.00001
16. Stephan AH, Barres BA, Stevens B. The complement system: an unexpected role in synaptic pruning during development and disease. *Annu Rev Neurosci* (2012) 35:369–89. doi: 10.1146/annurev-neuro-061010-113810
17. Presumey J, Bialas AR, Carroll MC. Complement System in Neural Synapse Elimination in Development and Disease. *Adv Immunol* (2017) 135:53–79. doi: 10.1016/bs.ai.2017.06.004
18. Shivshankar P, Fekry B, Eckel-Mahan K, Wetsel RA. Circadian clock and complement immune system - complementary control of physiology and pathology? *Front Cell Infect Microbiol* (2020). doi: 10.3389/fcimb.2020.00418
19. Laskaris L, Zalesky A, Weickert CS, Di Biase MA, Chana G, Baune BT. Investigation of peripheral complement factors across stages of psychosis. *Schizophr Res* (2019) 204:30–7. doi: 10.1016/j.schres.2018.11.035
20. Kopczynska M, Zelek W, Touchard S, Gaughran F, Di Forti M, Mondelli V. Complement system biomarkers in first episode psychosis. *Schizophr Res* (2019) 204:16–22. doi: 10.1016/j.schres.2017.12.012
21. Schatz-Jakobsen JA, Pedersen DV, Andersen GR. Structural insight into proteolytic activation and regulation of the complement system. *Immunol Rev* (2016) 274(1):59–73. doi: 10.1111/imr.12465
22. Cserhalmi M, Papp A, Brandus B, Uzonyi B, Jozsi M. Regulation of regulators: Role of the complement factor H-related proteins. *Semin Immunol* (2019) 45:101341. doi: 10.1016/j.smim.2019.101341
23. Kemper C, Kohl J. Back to the future - non-canonical functions of complement. *Semin Immunol* (2018) 37:1–3. doi: 10.1016/j.smim.2018.05.002
24. Barnum SR. C4a: An Anaphylatoxin in Name Only. *J Innate Immun* (2015) 7(4):333–9. doi: 10.1159/000371423
25. Barnum SR. Complement: A primer for the coming therapeutic revolution. *Pharmacol Ther* (2017) 172:63–72. doi: 10.1016/j.pharmthera.2016.11.014
26. Podack ER, Esser AF, Biesecker G, Muller-Eberhard HJ. Membrane attack complex of complement: a structural analysis of its assembly. *J Exp Med* (1980) 151(2):301–13. doi: 10.1084/jem.151.2.301
27. Bhakdi S, Tranum-Jensen J. Terminal membrane C5b-9 complex of human complement: transition from an amphiphilic to a hydrophilic state through binding of the S protein from serum. *J Cell Biol* (1982) 94(3):755–9. doi: 10.1083/jcb.94.3.755
28. Murphy BF, Kirszbaum L, Walker ID, d'Apice AJ. SP-40,40, a newly identified normal human serum protein found in the SC5b-9 complex of

complement and in the immune deposits in glomerulonephritis. *J Clin Invest* (1988) 81(6):1858–64. doi: 10.1172/JCI113531
29. Preissner KP, Podack ER, Muller-Eberhard HJ. SC5b-7, SC5b-8 and SC5b-9 complexes of complement: ultrastructure and localization of the S-protein (vitronectin) within the macromolecules. *Eur J Immunol* (1989) 19(1):69–75. doi: 10.1002/eji.1830190112
30. Milis L, Morris CA, Sheehan MC, Charlesworth JA, Pussell BA. Vitronectin-mediated inhibition of complement: evidence for different binding sites for C5b-7 and C9. *Clin Exp Immunol* (1993) 92(1):114–9. doi: 10.1111/j.1365-2249.1993.tb05956.x
31. Tschopp J, Chonn A, Hertig S, French LE. Clusterin, the human apolipoprotein and complement inhibitor, binds to complement C7, C8 beta, and the b domain of C9. *J Immunol* (1993) 151(4):2159–65.
32. McDonald JF, Nelsestuen GL. Potent inhibition of terminal complement assembly by clusterin: characterization of its impact on C9 polymerization. *Biochemistry* (1997) 36(24):7464–73. doi: 10.1021/bi962895r
33. Hadders MA, Bubeck D, Roversi P, Hakobyan S, Forneris F, Morgan BP, et al. Assembly and regulation of the membrane attack complex based on structures of C5b6 and sC5b9. *Cell Rep* (2012) 1(3):200–7. doi: 10.1016/j.celrep.2012.02.003
34. Nishimura J, Yamamoto M, Hayashi S, Ohyashiki K, Ando K, Brodsky AL, et al. Genetic variants in C5 and poor response to eculizumab. *N Engl J Med* (2014) 370(7):632–9. doi: 10.1056/NEJMoa1311084
35. Giles JL, Choy E, van den Berg C, Morgan BP, Harris CL. Response to Comment on "Functional Analysis of a Complement Polymorphism (rs17611) Associated with Rheumatoid Arthritis". *J Immunol* (2015) 195 (1):4. doi: 10.4049/jimmunol.1500822
36. Fernie BA, Wurzner R, Unsworth DJ, Tuxworth RI, Hobart MJ. DNA polymorphisms of the complement C6 and C7 genes. *Ann Hum Genet* (1995) 59(Pt 2):163–81. doi: 10.1111/j.1469-1809.1995.tb00739.x
37. Fernie BA, Hobart MJ. Complement C7 deficiency: seven further molecular defects and their associated marker haplotypes. *Hum Genet* (1998) 103 (4):513–9. doi: 10.1007/s004390050859
38. Rittner C, Stradmann-Bellinghausen B. Human complement C81 (C8 A) polymorphism: detection and segregation of new variants. *Hum Genet* (1993) 92(4):413–6. doi: 10.1007/BF01247347
39. Dewald G, Hemmer S, Nothen MM. Human complement component C8. Molecular basis of the beta-chain polymorphism. *FEBS Lett* (1994) 340 (3):211–5. doi: 10.1016/0014-5793(94)80140-1
40. Dewald G, Cichon S, Bryant SP, Hemmer S, Nothen MM, Spurr NK. The human complement C8G gene, a member of the lipocalin gene family: polymorphisms and mapping to chromosome 9q34.3. *Ann Hum Genet* (1996) 60(4):281–91. doi: 10.1111/j.1469-1809.1996.tb01192.x
41. Bae JS, Pasaje CF, Park BL, Cheong HS, Kim JH, Park TJ, et al. Genetic analysis of complement component 9 (C9) polymorphisms with clearance of hepatitis B virus infection. *Dig Dis Sci* (2011) 56(9):2735–41. doi: 10.1007/s10620-011-1657-3
42. Kremlitzka M, Geerlings MJ, de Jong S, Bakker B, Nilsson SC, Fauser S, et al. Functional analyses of rare genetic variants in complement component C9 identified in patients with age-related macular degeneration. *Hum Mol Genet* (2018) 27(15):2678–88. doi: 10.1093/hmg/ddy178
43. Bumiller-Bini V, Cipolla GA, de Almeida RC, Petzl-Erler ML, Augusto DG, Boldt A. Sparking Fire Under the Skin? Answers From the Association of Complement Genes With Pemphigus Foliaceus. *Front Immunol* (2018) 9:695. doi: 10.3389/fimmu.2018.00695
44. Morgan BP. The membrane attack complex as an inflammatory trigger. *Immunobiology* (2016) 221(6):747–51. doi: 10.1016/j.imbio.2015.04.006
45. Morgan BP, Walters D, Serna M, Bubeck D. Terminal complexes of the complement system: new structural insights and their relevance to function. *Immunol Rev* (2016) 274(1):141–51. doi: 10.1111/imr.12461
46. Triantafilou M, Hughes TR, Morgan BP, Triantafilou K. Complementing the inflammasome. *Immunology* (2016) 147(2):152–64. doi: 10.1111/imm.12556
47. Morgan BP, Boyd C, Bubeck D. Molecular cell biology of complement membrane attack. *Semin Cell Dev Biol* (2017) 72:124–32. doi: 10.1016/j.semcdb.2017.06.009
48. Podack ER, Kolb WP, Muller-Eberhard HJ. The C5b-6 complex: formation, isolation, and inhibition of its activity by lipoprotein and the S-protein of human serum. *J Immunol* (1978) 120(6):1841–8.
49. Podack ER, Kolb WP, Muller-Eberhard HJ. The SC5b-7 complex: formation, isolation, properties, and subunit composition. *J Immunol* (1977) 119 (6):2024–9.
50. Bhakdi S, Roth M. Fluid-phase SC5b-8 complex of human complement: generation and isolation from serum. *J Immunol* (1981) 127(2):576–80.
51. Tschopp J, Engel A, Podack ER. Molecular weight of poly(C9). 12 to 18 C9 molecules form the transmembrane channel of complement. *J Biol Chem* (1984) 259(3):1922–8.
52. Serna M, Giles JL, Morgan BP, Bubeck D. Structural basis of complement membrane attack complex formation. *Nat Commun* (2016) 7:10587. doi: 10.1038/ncomms10587
53. Menny A, Serna M, Boyd CM, Gardner S, Joseph AP, Morgan BP, et al. CryoEM reveals how the complement membrane attack complex ruptures lipid bilayers. *Nat Commun* (2018) 9(1):5316. doi: 10.1038/s41467-018-07653-5
54. Kolb WP, Muller-Eberhard HJ. The membrane attack mechanism of complement. Verification of a stable C5-9 complex in free solution. *J Exp Med* (1973) 138(2):438–51. doi: 10.1084/jem.138.2.438
55. Abramson N, Lachmann PJ, Rosen FS, Jandl JH. Deficiency of C3 inactivator in man. *J Immunol* (1971) 107(1):19–27.
56. Alper CA, Abramson N, Johnston RB Jr., Jandl JH, Rosen FS. Studies in vivo and in vitro on an abnormality in the metabolism of C3 in a patient with increased susceptibility to infection. *J Clin Invest* (1970) 49(11):1975–85. doi: 10.1172/JCI106417
57. Nossel HL, Ti M, Kaplan KL, Spanondis K, Soland T, Butler VP Jr. The generation of fibrinopeptide A in clinical blood samples: evidence for thrombin activity. *J Clin Invest* (1976) 58(5):1136–44. doi: 10.1172/JCI108566
58. Nossel HL, Yudelman I, Canfield RE, Butler VP Jr., Spanondis K, Wilner GD, et al. Measurement of fibrinopeptide A in human blood. *J Clin Invest* (1974) 54(1):43–53. doi: 10.1172/JCI107749
59. Bauer KA, Rosenberger RD. The pathophysiology of the prethrombotic state in humans: Insights gained from studies using markers of hemostatic system activation. *Blood* (1987) 70:343–50. doi: 10.1182/blood.V70.2.343.bloodjournal702343
60. Bauer KA, Kass BL, ten Cate H, Hawiger JJ. Factor IX is activated in vivo by the tissue factor mechanism. *Blood* (1990) 76:731–6. doi: 10.1182/blood.V76.4.731.bloodjournal764731
61. Bauer KA, Kass BL, ten Cate H, Bednarek MA, Hawiger JJ, Rosenberger RD. Detection of factor X activation in humans. *Blood* (1989) 74(2007-2015). doi: 10.1182/blood.V74.6.2007.2007
62. Conway EM. Complement-coagulation connections. *Coagulation Fibrinol* (2018) 29:243–51. doi: 10.1097/MBC.0000000000000720
63. D'zik S. Complement and coagulation: Cross talk through time. *Transfusion Med Rev* (2019) 33:199–206. doi: 10.1016/j.tmrv.2019.08.004
64. Izumi M, Yamada KM, Hayashi M. Vitronectin exists in two structurally and functionally distinct forms in human plasma. *Biochim Biophys Acta* (1989) 990(2):101–8. doi: 10.1016/S0304-4165(89)80019-4
65. Trougakos IP, Poulakou M, Stathatos M, Chalikia A, Melidonis A, Gonos ES. Serum levels of the senescence biomarker clusterin/apolipoprotein J increase significantly in diabetes type II and during development of coronary heart disease or at myocardial infarction. *Exp Gerontol* (2002) 37(10-11):1175–87. doi: 10.1016/S0531-5565(02)00139-0
66. Biesecker G, Muller-Eberhard HJ. The ninth component of human complement: purification and physicochemical characterization. *J Immunol* (1980) 124(3):1291–6.
67. Falgarone G, Chiocchia G. Chapter 8: Clusterin: A multifacet protein at the crossroad of inflammation and autoimmunity. *Adv Cancer Res* (2009) 104:139–70. doi: 10.1016/S0065-230X(09)04008-1
68. Seiffert D. Constitutive and regulated expression of vitronectin. *Histol Histopathol* (1997) 12(3):787–97.
69. Zewde N, Morikis D. A computational model for the evaluation of complement system regulation under homeostasis, disease, and drug intervention. *PLoS One* (2018) 13(6):e0198644. doi: 10.1371/journal.pone.0198644
70. Zewde N, Gorham RD Jr., Dorado A, Morikis D. Quantitative Modeling of the Alternative Pathway of the Complement System. *PLoS One* (2016) 11(3): e0152337. doi: 10.1371/journal.pone.0152337

71. Heesterbeek DA, Bardoel BW, Parsons ES, Bennett I, Ruyken M, Doorduijn DJ, et al. Bacterial killing by complement requires membrane attack complex formation via surface-bound C5 convertases. *EMBO J* (2019) 38(4). doi: 10.15252/embj.201899852
72. Doorduijn DJ, Bardoel BW, Heesterbeek DAC, Ruyken M, Benn G, Parsons ES, et al. Bacterial killing by complement requires direct anchoring of membrane attack complex precursor C5b-7. *PLoS Pathog* (2020) 16(6): e1008606. doi: 10.1371/journal.ppat.1008606
73. Mollnes TE, Lea T, Froland SS, Harboe M. Quantification of the terminal complement complex in human plasma by an enzyme-linked immunosorbent assay based on monoclonal antibodies against a neoantigen of the complex. *Scand J Immunol* (1985) 22(2):197–202. doi: 10.1111/j.1365-3083.1985.tb01871.x
74. Mollnes TE, Lea T, Harboe M, Tschopp J. Monoclonal antibodies recognizing a neoantigen of poly(C9) detect the human terminal complement complex in tissue and plasma. *Scand J Immunol* (1985) 22(2):183–95. doi: 10.1111/j.1365-3083.1985.tb01870.x
75. Bhakdi S, Muhly M. A simple immunoradiometric assay for the terminal SC5b-9 complex of human complement. *J Immunol Methods* (1983) 57(1-3):283–9. doi: 10.1016/0022-1759(83)90088-1
76. Hugo F, Kramer S, Bhakdi S. Sensitive ELISA for quantitating the terminal membrane C5b-9 and fluid-phase SC5b-9 complex of human complement. *J Immunol Methods* (1987) 99(2):243–51. doi: 10.1016/0022-1759(87)90134-7
77. Haahr-Pedersen S, Bjerre M, Flyvbjerg A, Mogelvang R, Dominquez H, Hansen TK, et al. Level of complement activity predicts cardiac dysfunction after acute myocardial infarction treated with primary percutaneous coronary intervention. *J Invasive Cardiol* (2009) 21(1):13–9.
78. Yang S, McGookey M, Wang Y, Cataland SR, Wu HM. Effect of blood sampling, processing, and storage on the measurement of complement activation biomarkers. *Am J Clin Pathol* (2015) 143(4):558–65. doi: 10.1309/AJCPXPD7ZQXNTIAL
79. Bergseth G, Kirschfink M, Giclas PC, Nilsson B, Mollnes TE. An international serum standard for application in assays to detect human complement activation products. *Mol Immunol* (2013) 56(3):232–9. doi: 10.1016/j.molimm.2013.05.221
80. Schein TN, Blackburn TE, Heath SL, Barnum SR. Plasma levels of soluble membrane attack complex are elevated despite viral suppression in HIV patients with poor immune reconstitution. *Clin Exp Immunol* (2019) 198 (3):359–66. doi: 10.1111/cei.13366
81. Hogasen AK, Overlie I, Hansen TW, Abrahamsen TG, Finne PH, Hogasen K. The analysis of the complement activation product SC5 b-9 is applicable in neonates in spite of their profound C9 deficiency. *J Perinat Med* (2000) 28 (1):39–48. doi: 10.1515/JPM.2000.006
82. McGreal EP, Hearne K, Spiller OB. Off to a slow start: under-development of the complement system in term newborns is more substantial following premature birth. *Immunobiology* (2012) 217(2):176–86. doi: 10.1016/j.imbio.2011.07.027
83. Willems E, Alkema W, Keizer-Garritsen J, Suppers A, van der Flier M, Philipsen R, et al. Biosynthetic homeostasis and resilience of the complement system in health and infectious disease. *EBioMedicine* (2019) 45:303–13. doi: 10.1016/j.ebiom.2019.06.008
84. Tjernberg AR, Woksepp H, Sandholm K, Johansson M, Dahle C, Ludvigsson JF, et al. Celiac disease and complement activation in response to Streptococcus pneumoniae. *Eur J Pediatr* (2020) 179(1):133–40. doi: 10.1007/s00431-019-03490-w
85. Lin RY, Astiz ME, Saxon JC, Saha DC, Rackow EC. Alterations in C3, C4, factor B and related metabolites in septic shock. *Clin Immunol Immunopathol* (1993) 69:136–42. doi: 10.1006/clin.1993.1161
86. Brandtzaeg P, Mollnes TE, Kierulf P. Complement activation and endotoxin levels in systemic meningococcal disease. *J Infect Dis* (1989) 160(1):58–65. doi: 10.1093/infdis/160.1.58
87. Segura-Cervantes E, Mancilla-Ramirez J, Gonzalez-Canudas J, Alba E, Santillan-Ballesteros R, Morales-Barquet D, et al. Inflammatory Response in Preterm and Very Preterm Newborns with Sepsis. *Mediators Inflamm* (2016) 2016:6740827. doi: 10.1155/2016/6740827
88. Avirutnan P, Punyadee N, Noisakran S, Komoltri C, Thiemmeca S. Vascular leakage in severe dengue virus infections: a potential role for the nonstructural viral protein NS1 and complement. *J Infect Dis* (2006) 193 (8):1078–88. doi: 10.1086/500949
89. Schein TN, Barnum SR. "Role of complement in cerebral malaria". In: JA Stoute, editor. *Complement Activation in Malaria Immunity and Pathogenesis*. Berlin: Springer-Verlag (2018). p. 65–90.
90. Taylor RP, Stoute JA, Lindorfer MA. "Mechanisms of complement activation in malaria". In: JA Stoute, editor. *Compement Activation in Malaria Immunity and Pathogenesis*. Berlin: Springer-Verlag (2018). p. 31–49.
91. Wang H, Wang K, Wang C, Qui W, Lu Z, Hu X, et al. Increased soluble C5b-9 in CSF of neuromyelitis optica. *Scand J Immunol* (2014) 79:127–30. doi: 10.1111/sji.12132
92. Morgan BP, Daniels RH, Williams BD. Measurement of terminal complement complexes in rheumatoid arthritis. *Clin Exp Immunol* (1988) 73(3):473–8.
93. Dalmasso AP, Falk RJ, Raij L. The pathobiology of the terminal complement complexes. *Complement Inflammation* (1989) 6(1):36–48. doi: 10.1159/000463070
94. Rus V, Malide D, Bolosiu HD, Parasca I, Dutu AL. Levels of SC5b–9 complement complex in plasma and synovial fluid of patients with rheumatic disease. *Med Internet* (1990) 28(4):305–10.
95. Buyon JP, Tamerius J, Belmont HM, Abramson SB. Assessment of disease activity and impending flare in patients with systemic lupus erythematosus. Comparison of the use of complement split products and conventional measurements of complement. *Arthritis Rheum* (1992) 35(9):1028–37. doi: 10.1002/art.1780350907
96. Horigome I, Seino J, Sudo K, Kinoshita Y, Saito T, Yoshinaga K. Terminal complement complex in plasma from patients with systemic lupus erythematosus and other glomerular diseases. *Clin Exp Immunol* (1987) 70(2):417–24.
97. Mollnes TE, Haga HJ, Brun JG, Nielsen EW, Sjoholm A, Sturfeldt G, et al. Complement activation in patients with systemic lupus erythematosus without nephritis. *Rheumatol (Oxford)* (1999) 38(10):933–40. doi: 10.1093/rheumatology/38.10.933
98. Nagy G, Li DY, Chen M, Zhao MH. Usefulness of detection of complement activation products in evaluating SLE activity. *Lupus* (2000) 9(1):19–25. doi: 10.1177/096120330000900105
99. Nytrova P, Potlukova E, Kemlink D, Woodhall M, Horakova D, Waters P, et al. Complement activation in patients with neuromyelitis optica. *J Neuroimmunol* (2014) 274(1-2):185–91. doi: 10.1016/j.jneuroim.2014.07.001
100. Hakobyan S, Luppe S, Evans DR, Harding K, Loveless S, Robertson NP, et al. Plasma complement biomarkers distinguish multiple sclerosis and neuromyelitis optica spectrum disorder. *Mult Scler* (2017) 23(7):946–55. doi: 10.1177/1352458516669002
101. Miao D, Li DY, Chen M, Zhao MH. Platelets are activated in ANCA-associated vasculitis via thrombin-PARs pathway and can activate the alternative complement pathway. *Arthritis Res Ther* (2017) 19(1):252. doi: 10.1186/s13075-017-1458-y
102. Kim MY, Guerra MM, Kaplowitz E, Laskin CA, Petri M, Branch DW, et al. Complement activation predicts adverse pregnancy outcome in patients with systemic lupus erythematosus and/or antiphospholipid antibodies. *Ann Rheum Dis* (2018) 77(4):549–55. doi: 10.1136/annrheumdis-2017-212224
103. Wu EY, McInnis EA, Boyer-Suavet S, Mendoza CE, Aybar LT, Kennedy KB, et al. Measuring Circulating Complement Activation Products in Myeloperoxidase- and Proteinase 3-Antineutrophil Cytoplasmic Antibody-Associated Vasculitis. *Arthritis Rheumatol* (2019) 71(11):1894–903. doi: 10.1002/art.41011
104. Barohn RJ, Brey RL. Soluble terminal complement components in human myasthenia gravis. *Clin Neurol Neurosurg* (1993) 95(4):285–90. doi: 10.1016/0303-8467(93)90103-N
105. Donadelli R, Pulieri P, Piras R, Iatropoulos P, Valoti E, Benigni A, et al. Unraveling the Molecular Mechanisms Underlying Complement Dysregulation by Nephritic Factors in C3G and IC-MPGN. *Front Immunol* (2018) 9:2329. doi: 10.3389/fimmu.2018.02329
106. Wehling C, Amon O, Bommer M, Hoppe B, Kentouche K, Schalk G, et al. Monitoring of complement activation biomarkers and eculizumab in complement-mediated renal disorders. *Clin Exp Immunol* (2017) 187 (2):304–15. doi: 10.1111/cei.12890

107. Tian Y, Kijlstra A, van der Veen RL, Makridaki M, Murray IJ, Berendschot TT. Lutein supplementation leads to decreased soluble complement membrane attack complex sC5b-9 plasma levels. *Acta Ophthalmol* (2015) 93(2):141–5. doi: 10.1111/aos.12535
108. Bitzan M, Hammad RM, Bonnefoy A, Al Dhaheri WS Vezina C, Rivard GE. Acquired thrombotic thrombocytopenic purpura with isolated CFHR3/1 deletion-rapid remission following complement blockade. *Pediatr Nephrol* (2018) 33(8):1437–42. doi: 10.1007/s00467-018-3957-8
109. Omine M, Kinoshita T, Nakakuma H, Maciejewski JP, Parker CJ, Socie G. Paroxysmal nocturnal hemoglobinuria. *Int J Hematol* (2005) 82(5):417–21. doi: 10.1532/IJH97.05140
110. Parker C, Omine M, Richards S, Nishimura J, Bessler M, Ware R, et al. Diagnosis and management of paroxysmal nocturnal hemoglobinuria. *Blood* (2005) 106(12):3699–709. doi: 10.1182/blood-2005-04-1717
111. Noris M, Galbusera M, Gastoldi S, Macor P, Banterla F, Bresin E, et al. Dynamics of complement activation in aHUS and how to monitor eculizumab therapy. *Blood* (2014) 124(11):1715–26. doi: 10.1182/blood-2014-02-558296
112. Scholl HP, Charbel I, Walier M, Janzer S, Pollok-Kopp B, Borncke F, et al. Systemic complement activation in age-related macular degeneration. *PLoS One* (2008) 3(7):e2593. doi: 10.1371/journal.pone.0002593
113. Vallhonrat H, Williams WW, Dec GW, Keck S, Schoenfeld D, Cosimi AB, et al. Complement activation products in plasma after heart transplantation in humans. *Transplantation* (2001) 71(9):1308–11. doi: 10.1097/00007890-200105150-00022
114. Vallhonrat H, Williams WW, Cosimi AB, Tolkoff-Rubin N, Ginns LC, Wain JC, et al. In vivo generation of C4d, Bb, iC3b, and SC5b-9 after OKT3 administration in kidney and lung transplant recipients. *Transplantation* (1999) 67(2):253–8. doi: 10.1097/00007890-199901270-00011
115. Vallhonrat H, Swinford RD, Ingelfinger JR, Williams WW, Ryan DP, Tolkoff-Rubin N, et al. Rapid activation of the alternative pathway of complement by extracorporeal membrane oxygenation. *ASAIO J* (1999) 45 (1):113–4. doi: 10.1097/00002480-199901000-00025
116. Horvath O, Kallay K, Csuka D, Mezo B, Sinkovits G, Kassa C, et al. Early Increase in Complement Terminal Pathway Activation Marker sC5b-9 Is Predictive for the Development of Thrombotic Microangiopathy after Stem Cell Transplantation. *Biol Blood Marrow Transplant* (2018) 24(5):989–96. doi: 10.1016/j.bbmt.2018.01.009
117. Roumenina LT, Bartolucci P, Pirenne F. The role of Complement in Post-Transfusion Hemolysis and Hyperhemolysis Reaction. *Transfus Med Rev* (2019) 33(4):225–30. doi: 10.1016/j.tmrv.2019.09.007
118. Jodele S, Davies SM, Lane A, Khoury J, Dandoy C, Goebel J, et al. Diagnostic and risk criteria for HSCT-associated thrombotic microangiopathy: a study in children and young adults. *Blood* (2014) 124(4):645–53. doi: 10.1182/blood-2014-03-564997
119. Burk AM, Martin M, Flierl MA, Rittirsch D, Helm M, Lampl L, et al. Early complementopathy after multiple injuries in humans. *Shock* (2012) 37 (4):348–54. doi: 10.1097/SHK.0b013e3182471795
120. Li Y, Zhao Q, Liu B, Dixon A, Cancio L, Dubick M, et al. Early complementopathy predicts the outcomes of patients with trauma. *Trauma Surg Acute Care Open* (2019) 4(1):e000217. doi: 10.1136/tsaco-2018-000217
121. Deppisch R, Schmitt V, Bommer J, Hansch GM, Ritz E. Fluid phase generation of terminal complement complex as a novel index of bioincompatibility. *Kidney Int* (1990) 37(2):696–706. doi: 10.1038/ki.1990.36
122. Mizuno M, Suzuki Y, Higashide K, Sei Y, Iguchi D, Sakata F, et al. High Levels of Soluble C5b-9 Complex in Dialysis Fluid May Predict Poor Prognosis in Peritonitis in Peritoneal Dialysis Patients. *PLoS One* (2017) 12(1):e0169111. doi: 10.1371/journal.pone.0169111
123. Poppelaars F, Faria B, Gaya da Costa M, Franssen CFM, van Son WJ, Berger SP, et al. The Complement System in Dialysis: A Forgotten Story? *Front Immunol* (2018) 9:71. doi: 10.3389/fimmu.2018.00071
124. Faria B, Gaya da Costa M, Poppelaars F, Franssen CFM, Pestana M, Berger SP, et al. Administration of Intravenous Iron Formulations Induces Complement Activation in-vivo. *Front Immunol* (2019) 10:1885. doi: 10.3389/fimmu.2019.01885
125. Lines SW, Richardson VR, Thomas B, Dunn EJ, Wright MJ, Carter AM. Complement and Cardiovascular Disease–The Missing Link in Haemodialysis Patients. *Nephron* (2016) 132(1):5–14. doi: 10.1159/000442426
126. Yasuda M, Takeuchi K, Hiruma M, Iida H, Tahara A, Itagane H, et al. The complement system in ischemic heart disease. *Circulation* (1990) 81(1):156–63. doi: 10.1161/01.CIR.81.1.156
127. Trendelenburg M, Stallone F, Pershyna K, Eisenhut T, Twerenbold R, Wildi K, et al. Complement activation products in acute heart failure: Potential role in pathophysiology, responses to treatment and impacts on long-term survival. *Eur Heart J Acute Cardiovasc Care* (2018) 7(4):348–57. doi: 10.1177/2048872617694674
128. Orrem HL, Nilsson PH, Pischke SE, Grindheim G, Garred P, Seljeflot I, et al. Acute heart failure following myocardial infarction: complement activation correlates with the severity of heart failure in patients developing cardiogenic shock. *ESC Heart Fail* (2018) 5(3):292–301. doi: 10.1002/ehf2.12266
129. Akcan U, Karabulut S, Ismail Kucukali C, Cakir S, Tuzun E. Bipolar disorder patients display reduced serum complement levels and elevated peripheral blood complement expression levels. *Acta Neuropsychiatr* (2018) 30(2):70–8. doi: 10.1017/neu.2017.10
130. Ramos TN, Arynchyna AA, Blackburn TE, Barnum SR, Johnston JM. Soluble membrane attack complex is diagnostic for intraventricular shunt infection in children. *JCI Insight* (2016) 1(10):e87919. doi: 10.1172/jci.insight.87919
131. Shen L, Zheng J, Wang Y, Zhu M, Zhu H, Cheng Q, et al. Increased activity of the complement system in cerebrospinal fluid of the patients with Non-HIV cryptococcal meningitis. *BMC Infect Dis* (2017) 17. doi: 10.1186/s12879-016-2107-9
132. Woehrl B, Brouwer MC, Murr C, Heckenberg SG, Baas F, Pfister HW, et al. Complement component 5 contributes to poor disease outcome in humans and mice with pneumococcal meningitis. *J Clin Invest* (2011) 121(10):3943–53. doi: 10.1172/JCI57522
133. Brouwer MC, Baas F, van der Ende A, van de Beek D. Genetic variation and cerebrospinal fluid levels of mannose binding lectin in pneumococcal meningitis patients. *PLoS One* (2013) 8(5):e65151. doi: 10.1371/journal.pone.0065151
134. Mook-Kanamori BB, Brouwer MC, Geldhoff M, Ende AV, van de Beek D. Cerebrospinal fluid complement activation in patients with pneumococcal and meningococcal meningitis. *J Infect* (2014) 68(6):542–7. doi: 10.1016/j.jinf.2013.12.016
135. Sanders ME, Koski CL, Robbins D, Shin ML, Frank MM, Joiner KA. Activated terminal complement in cerebrospinal fluid in Guillain-Barre syndrome and multiple sclerosis. *J Immunol* (1986) 136(12):4456–9.
136. Sanders ME, Alexander EL, Koski CL, Frank MM, Joiner KA. Detection of activated terminal complement (C5b-9) in cerebrospinal fluid from patients with central nervous system involvement of primary Sjogren's syndrome or systemic lupus erythematosus. *J Immunol* (1987) 138(7):2095–9.
137. Sellebjerg F, Jaliashvili I, Christiansen M, Garred P. Intrathecal activation of the complement system and disability in multiple sclerosis. *J Neurol Sci* (1998) 157(2):168–74. doi: 10.1016/S0022-510X(98)00086-0
138. Jonsen A, Bengtsson AA, Nived O, Ryberg B, Truedsson L, Ronnblom L, et al. The heterogeneity of neuropsychiatric systemic lupus erythematosus is reflected in lack of association with cerebrospinal fluid cytokine profiles. *Lupus* (2003) 12(11):846–50. doi: 10.1191/0961203303lu472sr
139. Zelek WM, Fathalla D, Morgan A, Touchard S, Loveless S, Tallantyre E, et al. Cerebrospinal fluid complement system biomarkers in demyelinating disease. *Mult Scler* (2019) 1352458519887905. doi: 10.1177/1352458519887905
140. Ingram G, Hakobyan S, Hirst CL, Harris CL, Loveless S, Mitchell JP, et al. Systemic complement profiling in multiple sclerosis as a biomarker of disease state. *Mult Scler* (2012) 18(10):1401–11. doi: 10.1177/1352458512438238
141. Hakansson I, Vrethem M, Dahle C, Ekdahl KN. Complement activation in cerebrospinal fluid in clinically isolated syndrome and early stages of relapsing remitting multiple sclerosis. *J Neuroimmunol* (2020) 340:577147. doi: 10.1016/j.jneuroim.2020.577147
142. Stahel PF, Morganti-Kossmann MC, Perez D, Redaelli C, Gloor B, Trentz O, et al. Intrathecal levels of complement-derived soluble membrane attack complex (sC5b-9) correlate with blood-brain barrier dysfunction in patients with traumatic brain injury. *J Neurotrauma* (2001) 18(8):773–81. doi: 10.1089/089771501316919139
143. Parry J, Hwang J, Stahel CF, Henderson C, Nadeau J, Stacey S, et al. Soluble terminal complement activation fragment sC5b-9: a new serum biomarker

for traumatic brain injury? *Eur J Trauma Emerg Surg* (2020). doi: 10.1007/s00068-020-01407-z
144. Lindsberg PJ, Ohman J, Lehto T, Wuorimaa T, et al. Complement activation in the central nervous system following blood-brain barrier damage in man. *Ann Neurol* (1996) 40(4):587–96. doi: 10.1002/ana.410400408
145. Loeffler DA, Brickman CM, Juneau PL, Perry MF, Pomara N, Lewitt PA. Cerebrospinal fluid C3a increases with age, but does not increase further in Alzheimer's disease. *Neurobiol Aging* (1997) 18(5):555–7. doi: 10.1016/S0197-4580(97)00110-3
146. Pelletier K, Bonnefoy A, Chapdelaine H, Pichette V, Lejars M, Madore F, et al. Clinical Value of Complement Activation Biomarkers in Overt Diabetic Nephropathy. *Kidney Int Rep* (2019) 4(6):797–805. doi: 10.1016/j.ekir.2019.03.004
147. Matsell DG, Wyatt RJ, Gaber LW. Terminal complement complexes in acute poststreptococcal glomerulonephritis. *Pediatr Nephrol* (1994) 8(6):671–6. doi: 10.1007/BF00869086
148. Kusunoki Y, Akutsu Y, Itami N, Tochimaru H, Nagata Y, Takekoshi Y, et al. Urinary excretion of terminal complement complexes in glomerular disease. *Nephron* (1991) 59(1):27–32. doi: 10.1159/000186513
149. Zhang MF, Huang J, Zhang YM, Qu Z, Wang X, Wang F, et al. Complement activation products in the circulation and urine of primary membranous nephropathy. *BMC Nephrol* (2019) 20(1):313. doi: 10.1186/s12882-019-1509-5
150. Zhao WT, Huang JW, Sun PP, Su T, Tang JW, Wang SX, et al. Diagnostic roles of urinary kidney injury molecule 1 and soluble C5b-9 in acute tubulointerstitial nephritis. *Am J Physiol Renal Physiol* (2019) 317(3):F584–92. doi: 10.1152/ajprenal.00176.2019
151. Huang H, Li D, Huang X, Wang Y, Wang S, Wang X, et al. Association of Complement and Inflammatory Biomarkers with Diabetic Nephropathy. *Ann Clin Lab Sci* (2019) 49(4):488–95.
152. Thurman JM, Wong M, Renner B, Frazer-Abel A, Giclas PC, Joy MS, et al. Complement Activation in Patients with Focal Segmental Glomerulosclerosis. *PLoS One* (2015) 10(9):e0136558. doi: 10.1371/journal.pone.0136558
153. van der Pol P, de Vries DK, van Gijlswijk DJ, van Anken GE, Schlagwein N, Daha MR, et al. Pitfalls in urinary complement measurements. *Transpl Immunol* (2012) 27(1):55–8. doi: 10.1016/j.trim.2012.06.001
154. Biglarnia AR, Huber-Lang M, Mohlin C, Ekdahl KN, Nilsson B, et al. The multifaceted role of complement in kidney transplantation. *Nat Rev Nephrol* (2018) 14(12):767–81. doi: 10.1038/s41581-018-0071-x
155. Lammerts RGM, Eisenga MF, Alyami M, Daha MR, Seelen MA, Pol RA, et al. Urinary Properdin and sC5b-9 Are Independently Associated With Increased Risk for Graft Failure in Renal Transplant Recipients. *Front Immunol* (2019) 10:2511. doi: 10.3389/fimmu.2019.02511
156. Burwick RM, Easter SR, Dawood HY, Yamamoto HS, Fichorova RN, Feinberg BB, et al. Complement activation and kidney injury molecule-1-associated proximal tubule injury in severe preeclampsia. *Hypertension* (2014) 64(4):833–8. doi: 10.1161/HYPERTENSIONAHA.114.03456
157. Brodeur JP, Ruddy S, Schwartz LB, Moxley G. Synovial fluid levels of complement SC5b-9 and fragment Bb are elevated in patients with rheumatoid arthritis. *Arthritis Rheum* (1991) 34(12):1531–7. doi: 10.1002/art.1780341209
158. Bengtsson A, Bengtson JP, Rydenhag A, Roxvall L, Heideman M. Accumulation of anaphylatoxins and terminal complement complexes in inflammatory fluids. *J Intern Med* (1990) 228(2):173–6. doi: 10.1111/j.1365-2796.1990.tb00212.x
159. Hara N, Abe M, Inuzuka S, Kawarada Y, Shigematsu N. Pleural SC5b-9 in differential diagnosis of tuberculous, malignant, and other effusions. *Chest* (1992) 102(4):1060–4. doi: 10.1378/chest.102.4.1060
160. Salomaa ER, Viander M, Saaresranta T, Terho EO. Complement components and their activation products in pleural fluid. *Chest* (1998) 114(3):723–30. doi: 10.1378/chest.114.3.723
161. Porcel JM, Vives M, Gazquez I, Vicente de Vera MC, Perez B, Rubio M. Usefulness of pleural complement activation products in differentiating tuberculosis and malignant effusions. *Int J Tuberc Lung Dis* (2000) 4(1):76–82.
162. Vives M, Porcel JM, Gazquez I, Perez B, Rubio M. Pleural SC5b-9: a test for identifying complicated parapneumonic effusions. *Respiration* (2000) 67(4):433–8. doi: 10.1159/000029543
163. Porcel JM. Pleural fluid tests to identify complicated parapneumonic effusions. *Curr Opin Pulm Med* (2010) 16(4):357–61. doi: 10.1097/MCP.0b013e328338a108
164. Kabut J, Kondera-Anasz Z, Sikora J, Mielczarek-Palacz A. Levels of complement components iC3b, C3c, C4, and SC5b-9 in peritoneal fluid and serum of infertile women with endometriosis. *Fertil Steril* (2007) 88(5):1298–303. doi: 10.1016/j.fertnstert.2006.12.061
165. Bjerre M, Holland-Fischer P, Gronbaek H, Frystyk J, Hansen TK, Vilstrup H, et al. Soluble membrane attack complex in ascites in patients with liver cirrhosis without infections. *World J Hepatol* (2010) 2(6):221–5. doi: 10.4254/wjh.v2.i6.221
166. Shigemoto E, Mizuno M, Suzuki Y, Kobayashi K, Sakata F, Kariya T, et al. Increase of Eosinophil in Dialysate During Induction of Peritoneal Dialysis. *Perit Dial Int* (2019) 39(1):90–2. doi: 10.3747/pdi.2017.00205
167. D'Cruz OJ, Haas GG Jr., Lambert H. Evaluation of antisperm complement-dependent immune mediators in human ovarian follicular fluid. *J Immunol* (1990) 144(10):3841–8.
168. D'Cruz OJ, Haas GG Jr. Lack of complement activation in the seminal plasma of men with antisperm antibodies associated in vivo on their sperm. *Am J Reprod Immunol* (1990) 24(2):51–7. doi: 10.1111/j.1600-0897.1990.tb01038.x
169. Doudevski I, Rostagno A, Cowman M, Liebmann J, Ritch R, Ghiso J. Clusterin and complement activation in exfoliation glaucoma. *Invest Ophthalmol Vis Sci* (2014) 55(4):2491–9. doi: 10.1167/iovs.13-12941
170. Hugo F, Berstecher C, Kramer S, Fassbender W, Bhakdi S. In vivo clearance studies of the terminal fluid-phase complement complex in rabbits. *Clin Exp Immunol* (1989) 77(1):112–6.
171. Zelek WM, Xie L, Morgan BP, Harris CL. Compendium of current complement therapeutics. *Mol Immunol* (2019) 114:341–52. doi: 10.1016/j.molimm.2019.07.030
172. Anderson AM, Schein TN, Kalapila A, Lai L, Waldrop-Valverde D, Moore RC, et al. Soluble membrane attcak complex in the blood and cerebrospinal fluid of HIV-infected individuals, relationship to HIV RNA, and comparison with HIV negatives. *J Neuroimmunol* (2017) 311:35–9. doi: 10.1016/j.jneuroim.2017.07.014
173. Seele J, Kirschfink M, Djukic M, Lange P, Gossner J, Bunkowski S, et al. Cisterno-lumbar gradient of complement fractions in geriatric patients with suspected normal pressure hydrocephalus. *Clin Chim Acta* (2018) 486:1–7. doi: 10.1016/j.cca.2018.07.008
174. Broadwell RD, Sofroniew MV. Serum proteins bypass the blood-brain fluid barriers for extracellular entry to the central nervous system. *Exp Neurol* (1993) 120(2):245–63. doi: 10.1006/exnr.1993.1059
175. Aly H, Khashaba MT, Nada A, Hasanen BM, McCarter R, Schultz SJ, et al. The role of complement in neurodevelopment impairment following neonatal hypoxic-ischemic encephalopathy. *Am J Perinatol* (2009) 26:659–65. doi: 10.1055/s-0029-1220793
176. Saunders NR, Dziegielewska KM, Mollgard K, Habgood MD. Physiology and molecular biology of barrier mechanisms in the fetal and neonatal brain. *J Physiol* (2018) 596(23):5723–56. doi: 10.1113/JP275376
177. Brautigam K, Vakis A, Tsitsipanis C. Pathogenesis of idiopathic Normal Pressure Hydrocephalus: A review of knowledge. *J Clin Neurosci* (2019) 61:10–3. doi: 10.1016/j.jocn.2018.10.147
178. Tuzun E, Kurtuncu M, Turkoglu R, Icoz S, Pehlivan M, Birisik O, et al. Enhanced complement consumption in neuromyelitis optica and Behcet's disease patients. *J Neuroimmunol* (2011) 233(1-2):211–5. doi: 10.1016/j.jneuroim.2010.11.010
179. Miller DH, Chard DT, Ciccarelli O. Clinically isolated syndromes. *Lancet Neurol* (2020) 11:157–69. doi: 10.1016/S1474-4422(11)70274-5
180. Buckingham SC, Ramos TN, Barnum SR. Complement C5-deficient mice are protected from seizures in experimental cerebral malaria. *Epilepsia* (2014) 55(12):e139–42. doi: 10.1111/epi.12858
181. Loeffler DA, Camp DM, Conant SB. Complement activation in the Parkinson's disease substantia nigra: an immunocytochemical study. *J Neuroinflamm* (2006) 3:29. doi: 10.1186/1742-2094-3-29
182. Kjaeldgaard AL, Pilely K, Olsen KS, Pedersen SW, Lauritsen AO, Moller K, et al. Amyotrophic lateral sclerosis: The complement and inflammatory hypothesis. *Mol Immunol* (2018) 102:14–25. doi: 10.1016/j.molimm.2018.06.007

183. Kolev MV, Ruseva MM, Harris CL, Morgan BP, Donev RM. Implication of complement system and its regulators in Alzheimer's disease. *Curr Neuropharmacol* (2009) 7(1):1–8. doi: 10.2174/157015909787602805
184. Ishii T, Hattori K, Miyakawa T, Watanabe K, Hidese S, Sasayama D, et al. Increased cerebrospinal fluid complement C5 levels in major depressive disorder and schizophrenia. *Biochem Biophys Res Commun* (2018) 497 (2):683–8. doi: 10.1016/j.bbrc.2018.02.131
185. Dalmau J, Graus F. Antibody-Mediated Encephalitis. *N Engl J Med* (2018) 378(9):840–51. doi: 10.1056/NEJMra1708712
186. Lungen EM, Maier V, Venhoff N, Salzer U, Dersch R, Berger B, et al. Systemic Lupus Erythematosus With Isolated Psychiatric Symptoms and Antinuclear Antibody Detection in the Cerebrospinal Fluid. *Front Psychiatry* (2019) 10:226. doi: 10.3389/fpsyt.2019.00226
187. Teunissen CE, Petzold A, Bennett JL, Berven FS, Brundin L, Comabella M, et al. A consensus protocol for the standardization of cerebrospinal fluid collection and biobanking. *Neurology* (2009) 73(22):1914–22. doi: 10.1212/WNL.0b013e3181c47cc2
188. Teunissen CE, Tumani H, Engelborghs S, Mollenhauer B. Biobanking of CSF: international standardization to optimize biomarker development. *Clin Biochem* (2014) 47(4-5):288–92. doi: 10.1016/j.clinbiochem.2013.12.024
189. Volanakis JE, Barnum SR, Kilpatrick JM. Purification and properties of human factor D. *Methods Enzymol* (1993) 223:82–97. doi: 10.1016/0076-6879(93)23039-P
190. Volanakis JE, Barnum SR, Kilpatrick JM. Renal filtration and catabolism of complement protein D. *N Engl J Med* (1985) 312(7):395–9. doi: 10.1056/NEJM198502143120702
191. Thurman JM, Nester CM. All Things Complement. *Clin J Am Soc Nephrol* (2016) 11(10):1856–66. doi: 10.2215/CJN.01710216
192. Ricklin D, Reis ES, Lambris JD. Complement in disease: a defence system turning offensive. *Nat Rev Nephrol* (2016) 12(7):383–401. doi: 10.1038/nrneph.2016.70
193. Desanti De Oliveira B, Xu K, Shen TH, Callahan M, Kiryluk K, D'Agati VD, et al. Molecular nephrology: types of acute tubular injury. *Nat Rev Nephrol* (2019) 15(10):599–612. doi: 10.1038/s41581-019-0184-x
194. Springall T, Sheerin NS, Abe K, Holers VM, Wan H, Sacks SH. Epithelial secretion of C3 promotes colonization of the upper urinary tract by Escherichia coli. *Nat Med* (2001) 7(7):801–6. doi: 10.1038/89923
195. Choudhry N, Li K, KY Wu, Song Y, Farrar CA, et al. The complement factor 5a receptor 1 has a pathogenic role in chronic inflammation and renal fibrosis in a murine model of chronic pyelonephritis. *Kidney Int* (2016) 90 (3):540–54. doi: 10.1016/j.kint.2016.04.023
196. Oliviero F, Galozzi P, Ramonda R, de Oliveira FL, Schiavon F, Scanu A, et al. Unusual Findings in Synovial Fluid Analysis: A Review. *Ann Clin Lab Sci* (2017) 47(3):253–9.
197. Seidman AJ, Limaiem F. "Synovial Fluid Analysis". In: *StatPearls*. (Treasure Island (FL): Stat Pearls Publishing (2020).
198. Mercer RM, Corcoran JP, Porcel JM, Rahman NM, Psallidas I. Interpreting pleural fluid results. *Clin Med (Lond)* (2019) 19(3):213–7. doi: 10.7861/clinmedicine.19-3-213
199. Hou W, Sanyal AJ. Ascites: diagnosis and management. *Med Clin North Am* (2009) 93(4):801–17, vii. doi: 10.1016/j.mcna.2009.03.007
200. Oey RC, van Buuren HR, de Man RA. The diagnostic work-up in patients with ascites: current guidelines and future prospects. *Neth J Med* (2016) 74 (8):330–5.
201. Trindade F, Vitorino R, Leite-Moreira A, Falcao-Pires I. Pericardial fluid: an underrated molecular library of heart conditions and a potential vehicle for cardiac therapy. *Basic Res Cardiol* (2019) 114(2):10. doi: 10.1007/s00395-019-0716-3
202. Widgerow AD, King K, Tocco-Tussardi I, Banyard DA, Chiang R, Awad A, et al. The burn wound exudate-an under-utilized resource. *Burns* (2015) 41 (1):11–7. doi: 10.1016/j.burns.2014.06.002
203. Zang T, Broszczak DA, Broadbent JA, Cuttle L, Lu H, Parker TJ. The biochemistry of blister fluid from pediatric burn injuries: proteomics and metabolomics aspects. *Expert Rev Proteomics* (2016) 13(1):35–53. doi: 10.1586/14789450.2016.1122528
204. Rooney IA, Oglesby TJ, Atkinson JP. Complement in human reproduction: activation and control. *Immunol Res* (1993) 12(3):276–94. doi: 10.1007/BF02918258
205. Harris CL, Mizuno M, Morgan BP. Complement and complement regulators in the male reproductive system. *Mol Immunol* (2006) 43(1-2):57–67. doi: 10.1016/j.molimm.2005.06.026
206. Vander Borght M, Wyns C. Fertility and infertility: Definition and epidemiology. *Clin Biochem* (2018) 62:2–10. doi: 10.1016/j.clinbiochem.2018.03.012
207. Schick T, Steinhauer M, Aslanidis A, Altay L, Karlstetter M, Langmann T, et al. Local complement activation in aqueous humor in patients with age-related macular degeneration. *Eye (Lond)* (2017) 31(5):810–3. doi: 10.1038/eye.2016.328
208. Mondino BJ, Sumner H. Anaphylatoxin levels in human aqueous humor. *Invest Ophthalmol Vis Sci* (1986) 27(8):1288–92.
209. Gallenkamp J, Spanier G, Worle E, Englbrecht M, Kirschfink M, Greslechner R, et al. A novel multiplex detection array revealed systemic complement activation in oral squamous cell carcinoma. *Oncotarget* (2018) 9(3):3001–13. doi: 10.18632/oncotarget.22963
210. Hajishengallis G, Kajikawa T, Hajishengallis E, Maekawa T, Reis ES, Mastellos DC, et al. Complement-Dependent Mechanisms and Interventions in Periodontal Disease. *Front Immunol* (2019) 10:406. doi: 10.3389/fimmu.2019.00406
211. Schur PH, Austen KF. Complement in human disease. *Annu Rev Med* (1968) 19:1–24. doi: 10.1146/annurev.me.19.020168.000245
212. Lopez-Lera A, Corvillo F, Nozal P, Regueiro JR, Sanchez-Corral P, Lopez-Trascasa M. Complement as a diagnostic tool in immunopathology. *Semin Cell Dev Biol* (2019) 85:86–97. doi: 10.1016/j.semcdb.2017.12.017
213. Ekdahl KN, Persson B, Mohlin C, Sandholm K, Skattum L, Nilsson B. Interpretation of Serological Complement Biomarkers in Disease. *Front Immunol* (2018) 9:2237. doi: 10.3389/fimmu.2018.02237
214. Prohaszka Z, Kirschfink M, Frazer-Abel A. Complement analysis in the era of targeted therapeutics. *Mol Immunol* (2018) 102:84–8. doi: 10.1016/j.molimm.2018.06.001
215. Goicoechea de Jorge E, Lopez Lera A, Bayarri-Olmos R, Yebenes H, Lopez-Trascasa M, Rodriguez de Cordoba S. Common and rare genetic variants of complement components in human disease. *Mol Immunol* (2018) 102:42–57. doi: 10.1016/j.molimm.2018.06.011
216. Nimgaonkar VL, Prasad KM, Chowdari KV, Severance EG, Yolken RH. The complement system: a gateway to gene-environment interactions in schizophrenia pathogenesis. *Mol Psychiatry* (2017) 22(11):1554–61. doi: 10.1038/mp.2017.151
217. Afshar-Kharghan V. The role of the complement system in cancer. *J Clin Invest* (2017) 127(3):780–9. doi: 10.1172/JCI90962
218. Mamidi S, Hone S, Kirschfink M. The complement system in cancer: Ambivalence between tumour destruction and promotion. *Immunobiology* (2017) 222(1):45–54. doi: 10.1016/j.imbio.2015.11.008
219. Rother RP, Rollins SA, Mojcik CF, Brodsky RA, Bell L. Discovery and development of the complement inhibitor eculizumab for the treatment of paroxysmal nocturnal hemoglobinuria. *Nat Biotechnol* (2007) 25(11):1256–64. doi: 10.1038/nbt1344
220. Patriquin CJ, Kuo KHM. Eculizumab and Beyond: The Past, Present, and Future of Complement Therapeutics. *Transfus Med Rev* (2019) 33(4):256–65. doi: 10.1016/j.tmrv.2019.09.004
221. Cofiell R, Kukreja A, Bedard K, Yan Y, Mickle AP Ogawa M, et al. Eculizumab reduces complement activation, inflammation, endothelial damage, thrombosis, and renal injury markers in aHUS. *Blood* (2015) 125 (21):3253–62. doi: 10.1182/blood-2014-09-600411
222. Subias Hidalgo M, Martin Merinero H, Lopez A, Anter J, Garcia SP, Ataulfo Gonzalez-Fernandez F, et al. Extravascular hemolysis and complement consumption in Paroxysmal Nocturnal Hemoglobinuria patients undergoing eculizumab treatment. *Immunobiology* (2017) 222(2):363–71. doi: 10.1016/j.imbio.2016.09.002
223. Ruggenenti P, Daina E, Gennarini A, Carrara C, Gamba S, Noris M, et al. C5 Convertase Blockade in Membranoproliferative Glomerulonephritis: A Single-Arm Clinical Trial. *Am J Kidney Dis* (2019) 74(2):224–38. doi: 10.1053/j.ajkd.2018.12.046
224. Jodele S, Fukuda T, Mizuno K, Vinks AA, Laskin BL, Goebel J, et al. Variable Eculizumab Clearance Requires Pharmacodynamic Monitoring to Optimize Therapy for Thrombotic Microangiopathy after Hematopoietic Stem Cell Transplantation. *Biol Blood Marrow Transplant* (2016) 22(2):307–15. doi: 10.1016/j.bbmt.2015.10.002

225. Pecoraro C, Ferretti AV, Rurali E, Galbusera M, Noris M, Remuzzi G. Treatment of Congenital Thrombotic Thrombocytopenic Purpura With Eculizumab. *Am J Kidney Dis* (2015) 66(6):1067–70. doi: 10.1053/j.ajkd.2015.06.032

226. Chehade H, Rotman S, Fremeaux-Bacchi V, Aubert V, Sadallah S, Sifaki L, et al. Blockade of C5 in Severe Acute Postinfectious Glomerulonephritis Associated With Anti-Factor H Autoantibody. *Am J Kidney Dis* (2016) 68 (6):944–8. doi: 10.1053/j.ajkd.2016.06.026

227. Hokstad I, Deyab G, Wang Fagerland M, Lyberg T, Hjeltnes G, Forre O, et al. Tumor necrosis factor inhibitors are associated with reduced complement activation in spondylarthropathies: An observational study. *PLoS One* (2019) 14(7):e0220079. doi: 10.1371/journal.pone.0220079

228. Harboe M, Ulvund G, Vien L, Mollnes TE. The quantitative role of alternative pathway amplification in classical pathway induced terminal complement activation. *Clin Exp Immunol* (2004) 138(3):439–46. doi: 10.1111/j.1365-2249.2004.02627.x

Conflict of Interest: SB and TS are co-founders of CNine Biosolutions, LLC, a biotech company developing complement diagnostics and co-inventors on United States patents # 10,535,004 and 10,630,774 and European Union patent # 3137908, both entitled, *Methods and Compositions for Diagnosis and Treatment of Meningitis.*

The remaining author declares that the research was conducted in the absence of any commercial or financial relationships that could be construed as a potential conflict of interest.

frontiers in Immunology

REVIEW
published: 13 November 2020
doi: 10.3389/fimmu.2020.601405

To Kill But Not Be Killed: Controlling the Activity of Mammalian Pore-Forming Proteins

Patrycja A. Krawczyk[†], *Marco Laub*[†] *and Patrycja Kozik*[*]

MRC Laboratory of Molecular Biology, Protein and Nucleic Acid Chemistry Division, Cambridge Biomedical Campus, Cambridge, United Kingdom

Pore-forming proteins (PFPs) are present in all domains of life, and play an important role in host-pathogen warfare and in the elimination of cancers. They can be employed to deliver specific effectors across membranes, to disrupt membrane integrity interfering with cell homeostasis, and to lyse membranes either destroying intracellular organelles or entire cells. Considering the destructive potential of PFPs, it is perhaps not surprising that mechanisms controlling their activity are remarkably complex, especially in multicellular organisms. Mammalian PFPs discovered to date include the complement membrane attack complex (MAC), perforins, as well as gasdermins. While the primary function of perforin-1 and gasdermins is to eliminate infected or cancerous host cells, perforin-2 and MAC can target pathogens directly. Yet, all mammalian PFPs are in principle capable of generating pores in membranes of healthy host cells which—if uncontrolled—could have dire, and potentially lethal consequences. In this review, we will highlight the strategies employed to protect the host from destruction by endogenous PFPs, while enabling timely and efficient elimination of target cells.

Keywords: immunity, pore-forming proteins, membrane attack complex, perforins, gasdermins, membrane integrity

OPEN ACCESS

Edited by:
George P. Munson, University of Miami, United States

Reviewed by:
Ilia Voskoboinik, Peter MacCallum Cancer Centre, Australia
Tsan Sam Xiao, Case Western Reserve University, United States

***Correspondence:**
Patrycja Kozik
pkozik@mrc-lmb.cam.ac.uk

[†]*These authors have contributed equally to this work*

Specialty section:
This article was submitted to Molecular Innate Immunity, a section of the journal Frontiers in Immunology

Received: *31 August 2020*
Accepted: *20 October 2020*
Published: *13 November 2020*

Citation:
Krawczyk PA, Laub M and Kozik P (2020) To Kill But Not Be Killed: Controlling the Activity of Mammalian Pore-Forming Proteins. Front. Immunol. 11:601405. doi: 10.3389/fimmu.2020.601405

INTRODUCTION AND OVERVIEW

The emergence of cell membranes was critical for the evolution of all modern organisms. They provide a physical barrier to separate an organism from its environment and enable compartmentalization of biochemical processes inside cells. In modern multicellular organisms, interfering with membrane integrity is one the most effective strategies employed in immune defense, and membrane disrupting pore-forming proteins (PFPs) have evolved as key effectors in both innate and adaptive immune responses.

PFPs can be found in all kingdoms of life. Bacteria use them to facilitate their entry into cells (e.g., listeriolysin), to aid in the delivery of effector molecules across membranes (e.g., streptolysin O) or as toxic agents (e.g., diphtheria or anthrax toxins) (1). Eukaryotic multicellular organisms, including mammals, use PFPs as either membranolytic pores assembled directly on the surface of invading pathogens or as effectors to selectively eliminate infected or cancerous host cells (2, 3). While bacteria can specifically target eukaryotic membranes through recognition of host-specific molecules, mammals are faced with the more challenging task of eliminating unwanted cells

without accidentally damaging surrounding healthy tissues. In fact, mammalian PFPs evolved to show limited target membrane specificity in isolation and therefore depend on other proteins of the immune system to safely guide their activity.

In this review, we discuss how mammalian PFPs are controlled by both the innate and adaptive arms of the immune system. Our goal is to provide a comprehensive overview of the variety of mechanisms, ranging from inducible expression and regulated trafficking to post-translational modifications and proteolytic processing, that collectively ensure tight spatial and temporal regulation of pore formation during immune responses.

Mammalian PFPs in Innate and Adaptive Immunity

Toward the end of the 19th century, George Nuttall and Hans Ernst August Buchner noted that blood contains a heat-sensitive component with killing activity against bacteria (4, 5). The proteins responsible were later named membrane attack complex (MAC) or terminal complement complex. Today we know, that the soluble MAC components C5, C6, C7, C8 (comprising C8α, C8β, and C8γ), and C9 (**Figure 1**) present in the serum assemble to form membranolytic pores on the surface of Gram-negative bacteria, enveloped viruses, parasites, and host cells (6–10). The mediators that initiate the assembly of MAC pores include components of both the innate and adaptive arms of the immune system. Specific receptors of the complement system are able to recognize a wide range of structures including unique pathogen-associated molecular patterns (PAMPs) and microbes opsonized with antibodies (key components of the humoral adaptive immune system) such that MAC can in principle assemble in response to any antigen. Both, the important contribution of MAC to anti-bacterial immunity as well as its potential toxicity are reflected in population genetics. On the one hand, genetic deficiencies in MAC components are associated with susceptibility to neisserial disease including endemic meningococcal infections (11, 12), on the other hand, these deficiencies can also confer a selective advantage (13).

Five of the seven MAC subunits (the exceptions being C5 and C8γ) are evolutionarily related and, together with two perforins, they belong to the membrane attack complex/perforin (MACPF) superfamily of PFPs. Perforin-1 (**Figure 1**) is stored together with pro-apoptotic effectors, granzyme A and B, in specialized secretory granules of natural killer (NK) cells and cytotoxic T cells (CTLs). When released into the immune synapse formed between the cytotoxic lymphocyte and an infected or cancerous cell, it rapidly assembles into homo-oligomeric pores on the target membrane (14). The pores can be lytic at high concentration (15–17), but their primary function is to facilitate entry of granzymes into target cells inducing apoptosis (18). NK cells belong to the innate arm of the immune response and recognize a variety of stress signals

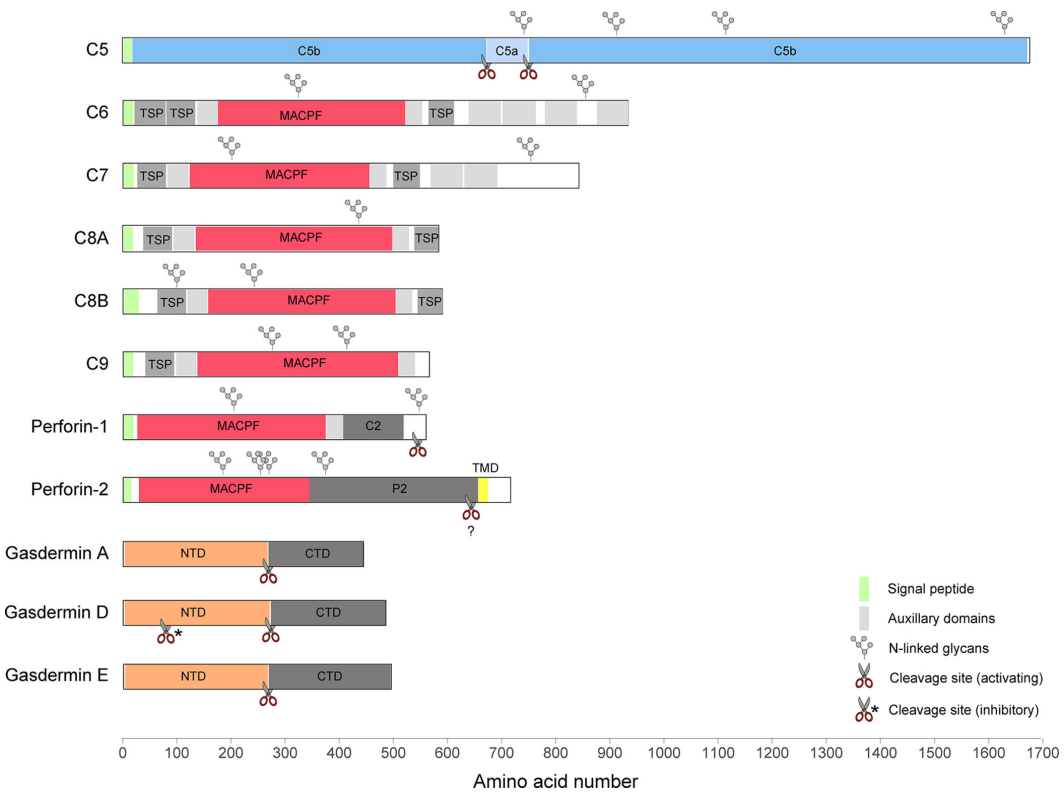

FIGURE 1 | A diagram illustrating the domain structures and selected regulatory features of mammalian PFPs.

presented on the cell surface. In CTLs, key effectors of adaptive immunity, the specificity during immune synapse formation relies on the interaction between the T cell receptor (TCR) and MHC class I complexed with a foreign or a mutated peptide. In line with the fundamental function of perforin-1 in immunity, deleterious variants in the *PRF1* gene in humans lead to an aggressive immunoregulatory disorder called familial hemophagocytic lymphohistiocytosis (FHL, which can be fatal without bone-marrow transplantation) (19, 20), as well as hematological malignancies (21–23). Perforin-1$^{-/-}$ mice exhibit an increased mortality in response to viral infections (24), fail to control tumor growth (25), and are highly prone to the development of spontaneous lymphomas (26).

Perforin-2 (also known as macrophage-expressed gene 1, MPEG1, **Figure 1**) has been discovered only recently (27), but appears to be the most ancient member of the MACPF family. It is encoded by the intronless *MPEG1* gene which is found already in some of the earliest multicellular organisms, such as sponges (28). In mammals, perforin-2 is predominantly expressed in cells of monocytic origin, such as macrophages. During bacterial infection, it is recruited to pathogen-containing vacuoles where it damages membranes of diverse bacterial species limiting their proliferation (29–34). Consistent with its proposed function in antimicrobial defense, four deleterious *MPEG1* variants have recently been identified through whole exome sequencing of patients with pulmonary non-tuberculous mycobacterial infection (35).

The second family of mammalian PFPs, gasdermins (**Figure 1**), has been discovered while searching for molecular mechanisms involved in an inflammatory cell death pathway termed pyroptosis (36, 37). Gasdermins are employed during both innate and adaptive immune responses, for example, in response to inflammasome assembly or following CTL-mediated delivery of granzymes into the cytosol. The best characterized member of this family, gasdermin D (GSDMD), is stored in the cytosol, and when activated, assembles into pores on the plasma membrane. The pores initially facilitate the secretion of cytosolic pro-inflammatory cytokines, such as IL-1β and IL-18, but if they persist unrepaired, the cell undergoes pyroptosis (38–40). In neutrophils, GSDMD pores contribute to the generation of neutrophil extracellular traps (NETs), secreted chromatin structures which capture extracellular pathogens (41). *In vitro*, GSDMD has also been shown to target cytosolic bacteria directly (38, 42).

In total there are six gasdermin paralogues in humans (*GSDMA*, *GSDMB*, *GSDMC*, *GSDMD*, *GSDME*/*DFNA5*, and *PJVK*/*DFNB59*) and 10 in mice (*Gsdma1*-3, *Gsdmc1*-4, *Gsdmd*, *Gsdme*, and *Pjvk*). Notably, gasdermin orthologues are also found in lower vertebrates, such as zebrafish (43), and more distant homologues are present in fungi (44). Mutations in gasdermin genes have been associated with a variety of disease phenotypes including skin and developmental defects (*GSDMA3*), susceptibility to asthma (*GSDMA3* and GSDMB) (45–47), and autosomal dominant and recessive hearing loss (*GSDME* and *DFNB59*) (48, 49). The precise functions, mechanisms of activation, and physiological relevance for the majority of the gasdermins remain to be uncovered.

General Mechanism of Pore Formation

Mammalian PFPs are synthesized and stored in an inactive conformation as monomeric, usually soluble proteins. Structural studies revealed that the pore-forming fold of the MACPF proteins is highly similar to the pore-forming domain of bacterial cholesterol-dependent cytolysins (CDC) (50–52). In contrast, the pore-forming N-terminal domain of gasdermins is structurally distinct from the MACPF/CDC fold and is thought to have evolved independently (53, 54). Nevertheless, the MACPF/CDC and gasdermin family members follow a broadly similar mechanism of pore formation which can be roughly divided into three stages: membrane binding, oligomerization, and membrane insertion (55, 56). Membrane insertion is accompanied by dramatic structural rearrangements that include refolding of α-helical regions into transmembrane β-hairpins, termed TMH1 and TMH2 in MACPF/CDC proteins, and HP1 and HP2 in gasdermins. In the resulting β-barrel pores, each monomer typically contributes one four-stranded lipid-embedded β-sheet.

Challenges in Storing and Targeting of Mammalian PFPs

Despite considerable similarity in the pore assembly process, the mechanisms involved in selecting target membranes differ strikingly between bacterial CDCs and mammalian MACPF proteins and gasdermins. For bacterial PFPs, the transition between soluble monomer and membrane pore is initiated by binding of the PFP to proteins, sugars, or lipids unique to the host. Thus, CDCs form pores preferentially on membranes with 25–35% cholesterol content, a lipid present only in eukaryotic cells (57). As mammalian PFPs themselves show limited target membrane selectivity, additional mechanisms need to be in place to enable spatiotemporal control of pore formation and to limit damage to both PFP-producing cells and surrounding tissues.

TRANSCRIPTIONAL CONTROL OF PFP EXPRESSION

While some PFPs can be safely expressed in the majority of cells (e.g., gasdermins), others (e.g., perforins) can be toxic soon after translation and are only produced by specialized cells of the immune system (**Figure 2A**).

MAC Components Are Produced in the Liver

The majority of the MAC components, similar to other serum proteins, are produced by hepatocytes in the liver (58). The exception is C7, which is expressed primarily extrahepatically as shown by the fact that, in liver transplant patients, as little as 10% of plasma C7 originated from the donor cells (59), compared to nearly 100% for C6 and C9 (60, 61). It has been proposed that local synthesis of C7 might be important for modulation of MAC activity (62), but this hypothesis has not yet been verified with tissue- or cell type-specific C7 knockouts. Intriguingly, liver-

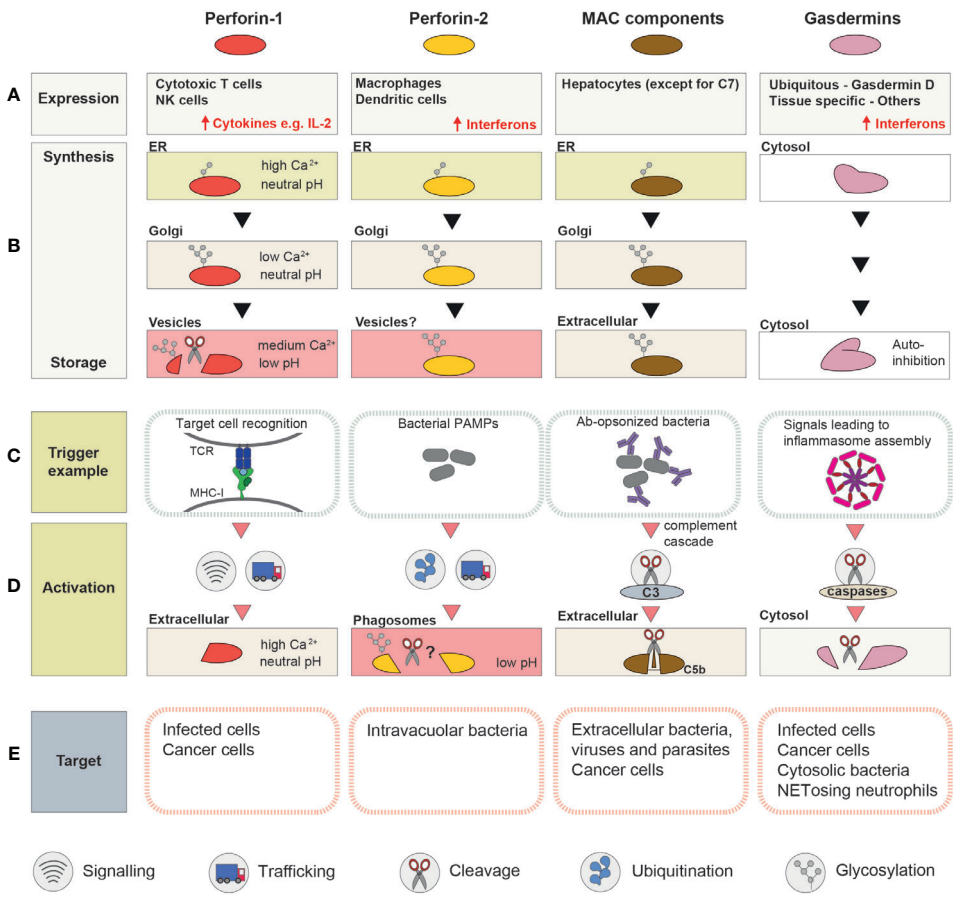

FIGURE 2 | A schematic summary of the mechanisms involved in regulation and activation of perforin-1, perforin-2, MAC, and gasdermins. **(A)** Cell types or tissues in which the PFP is constitutively expressed (inducible expression is highlighted with ↑). **(B)** Processing and trafficking steps involved in synthesis of the "stored" form of the PFP. The last row corresponds to the storage compartment. **(C)** Immune system components which initiate pore formation, and ligands they recognize. **(D)** A schematic representation of the events that precede pore assembly. **(E)** Targeted membranes.

derived C7 is actually not produced by hepatocytes, but by endothelial and stellate cells (63, 64), raising the question whether co-expression of C7 with the remaining MAC components might be toxic for the cells.

Gasdermins Can Be Expressed Ubiquitously or in a Tissue-Specific Manner

Members of the gasdermin family employ a wide range of different transcription factors to regulate their constitutive and inducible expression, and as a result, they all display different expression patterns [summarized in a recent review by Broz et al. (65)]. GSDMD and GMDMB are the most abundant and ubiquitous family members, while expression of the remaining gasdermins is more restricted. GSDMA, for example, is predominantly expressed in the skin, while GSDME is mainly present in the blood, spinal cord and uterus (58). Expression of gasdermins can be further regulated during a variety of pathological conditions, such as infection (66), cancer (67, 68), or in response to DNA damage (69). For example, GSDMD expression is strongly upregulated during bacterial, viral, and parasitic infections by interferon-γ-dependent signaling pathways (66).

Perforin-1—an Effector Restricted to Killer Lymphocytes

In contrast to MAC components and gasdermins, perforins are primarily expressed in immune cells. *PRF1* promoter activity is restricted to the T and NK cell lineages during development (70). In T cells, *PRF1* expression is induced upon maturation of naïve T cells into CTLs during an active immune response [reviewed in (71)]. T cell activation requires three distinct signals delivered by dendritic cells: signal 1—MHC class I-bound peptides, identical to those present in target cells (recognized by TCR); signal 2—cell surface molecules that act as stimulatory or inhibitory co-receptors, and signal 3—chemokines and cytokines that modulate T cell proliferation and differentiation. These requirements ensure that only T cells with relevant TCRs are activated, expanded, and upregulate perforin-1 (72).

Mechanistically, regulation of perforin-1 transcription is a complex process controlled by a 150 kb territory surrounding the *PRF1* gene (70) and several transcription factors (Sp-1, AP-1, MEF, MITF, T-bet, and EOMES) [reviewed in (73, 74)].

NK cells upregulate *Prf1* expression early during their development (75, 76). Yet, resting NK cells isolated from mice bred under pathogen-free conditions are only minimally cytotoxic and they contain only a small amount of perforin-1 protein (77). Instead, they store large quantities of *Prf1* mRNA, which is only translated upon NK cell activation (e.g., by cytokines IL-15 or IL-2). How mRNA translation is regulated in NK cells is not fully understood. The lymphocyte specific miRNA, miR-150, has been shown to target *Prf1* mRNA and downregulate its translation in resting NK cells (78), but additional mechanisms involving cytoplasmic mRNA-binding proteins and mRNA modifications are likely to be involved (79, 80).

MPEG1 Is Expressed Predominantly in Antigen-Presenting Cells

MPEG1 is constitutively expressed in macrophages, dendritic cells, monocytes, and granulocytes (81), but interferon-inducible expression has been observed in other cells types, e.g., fibroblasts and neurons (32, 82). Thus, *MPEG1* is strongly upregulated during bacterial, viral, and parasitic infections. For example, in the lungs of mice infected with influenza virus, it is among the top 30 genes with highest expression (66). Interestingly, pathogens that disrupt interferon signaling during infection have been reported to escape perforin-2-mediated killing. This has been demonstrated for *Chlamydia trachomatis*, which prevents interferon-dependent translocation of the STAT1 transcription factor into the nucleus (83). While ectopic expression of *MPEG1* in HeLa cells suppresses chlamydial growth, *MPEG1* is upregulated only in cells exposed to heat-killed *Chlamydiae*, but not live bacteria (29).

MATURATION AND STORAGE

Newly synthesized PFPs are rarely immediately activated. Instead, they are stored as inactive monomers that can be rapidly deployed in response to the appropriate signals (**Figure 2B**). These nascent PFP are unable to bind membranes as monomers, are synthesized as inactive immature propeptides, and/or are stored in a compartment where the ionic environment is incompatible with pore formation.

MAC Components Are Abundant in the Plasma

All seven MAC subunits are secreted into the plasma and circulate the body through the blood vessels. C8 isolated from plasma is a stable heterotrimer of C8α, C8β, and C8γ (with C8α covalently bound to C8γ *via* a disulfide bridge) (84), but the remaining subunits are monomeric. *In vitro*, C9 can be forced to form homooligomeric pores (85, 86) but the poly-C9 complex is unable to insert into cell membranes (85), and under physiological conditions, the TMH1 domain of C9 precludes polymerization in the absence of other MAC components (87). The secreted MAC components do not bind membranes efficiently on their own and as a consequence they are non-lytic at steady-state. C5 is the only MAC subunit which is proteolytically processed prior to pore formation, and this cleavage event is what initiates a cascade of conformational changes that drives MAC assembly.

Gasdermins Are Stored as Immature Propeptides in the Cytosol

In contrast to MAC components, gasdermins are synthesized and stored as immature cytosolic propeptides, which adopt an auto-inhibited state immediately after folding (38, 54, 88). Gasdermins contain an N-terminal pore-forming domain (NTD) connected to an inhibitory C-terminal domain (CTD) by a flexible linker (with the exception of PJVK/DFNB59 which has a truncated C-terminus). Proteolytic cleavage at the linker region destabilizes the NTD-CTD intramolecular interaction releasing the NTD to assemble into pores (36, 37). Indeed, ectopic expression of the NTD alone is sufficient to trigger pyroptotic cell death (42). It has been concluded that the CTD masks the lipid-binding motif of the NTD preventing membrane association of full-length gasdermins (54), but it does not sterically hinder pore formation. Mutations, including known disease variants, that weaken the NTD-CTD interdomain interactions are sufficient to expose the lipid binding motif and trigger constitutive gasdermin activity without cleavage (38) raising a possibility of alternative activation mechanisms.

Fully Processed Perforin-1 Is Stored in Cytotoxic Granules

Perforin-1 is also initially synthesized as an inactive propeptide but, in contrast to gasdermins, it is stored in a mature form. Besides the MACPF domain, immature perforin-1 consists of two additional domains: an epidermal growth factor (EGF) domain, and a C-terminal, Ca^{2+}-binding domain (C2) required for association with the membrane (89, 90). Perforin-1 maturation involves cleavage of a short (~2 kDa) fragment of the C-terminal domain which contains a bulky Asn549-glycan (91). The Asn549-glycan inhibits pore formation by steric hindrance interfering with oligomerization (92). Indeed, full length (uncleaved) perforin-1 purified from human NK KHYG1 cells does not form pores (92), while the full-length Asn549-glycosylation deficient mutant is lytic when purified and toxic when overexpressed (93). Intriguingly, full-length perforin-1 purified from insect cells is fully functional (52, 93), suggesting that the size of the glycan moiety is critical for inhibition of perforin-1 activity [N-glycoproteins produced in standard insect cell expression systems acquire simple side-chains instead of complex N-glycans found in mammalian proteins (94)]. Similarly, the unbranched N-glycans acquired initially in the ER offer only partial protection from unwanted lysis, and N-glycosylated perforin-1 is still toxic when ER exit is slow (e.g., in BFA-treated cells or upon fusion of an ER retention signal to perforin-1 C-terminus) (93).

Following further branching of glycans in the Golgi, perforin-1 is transported into lysosome-related organelles, called cytotoxic granules. Once in the granules, lysosomal proteases cleave the C-terminus, along with the inhibitory Asn549-glycan, to prime perforin-1 for activation upon secretion. *In vitro*, perforin-1 can be cleaved by cathepsins L or B (95, 96), but *Ctsl*$^{-/-}$ or *Ctsb*$^{-/-}$ mice do not show a defect in perforin-1-mediated killing (96, 97). In contrast, mice lacking asparaginyl endopeptidase (AEP) show degranulation defects, but the potential contribution of AEP to perforin-1 cleavage has not been addressed directly (98). Consistent with the potential involvement of multiple (or redundant) proteases, the cleavage site itself does not appear to be precise and mass spectrometry analysis of perforin-1 immunoprecipitated from KHYG1 cells identified fragments with multiple C-termini (92). In line with this observation, site-directed mutagenesis of the C-terminal region did not reveal any critical positions and cleavage occurred even when every residue from Gln540 through to Gly548 was replaced with a serine. Thus, perforin-1 proteolytic processing may be mediated by non-specific lysosomal proteases and the susceptibility of the region to cleavage is likely to be due to its disordered character.

Regardless of the exact nature of the protease, the cleavage takes place only after perforin-1 reaches a low pH compartment (91). This is critical, as acidic pH (~5.5 in the granules) prevents the fully processed perforin-1 from pore-formation (89). At pH < 6.2 the key acidic residues involved in ionic interactions between monomers are protonated preventing oligomerization (14). Furthermore, protonation of Ca^{2+}-binding Asp residues is expected to reduce Ca^{2+} binding to the C2 domain, which is critical for the association of perforin-1 with the target membrane (89, 90, 99). Ca^{2+} binding might be additionally prevented by granule-resident calreticulin, which sequesters free Ca^{2+} ions to further inhibit perforin-1 activity (100). Thus, cleavage only occurs when perforin-1 reaches a compartment with an environment incompatible with pore formation, providing an important safeguarding mechanism.

Where Is Perforin-2 Stored at Steady State?

Perforin-2 is a type I transmembrane protein comprising the MACPF domain, a unique membrane-binding P2 domain, a transmembrane domain, and a short cytosolic tail. The protective mechanisms involved in its biosynthesis and storage are not well characterized. In membrane-anchored perforin-2, the pore-forming TMH regions would face away from the membrane after unfurling (101, 102), suggesting that the transmembrane domain might be important for preventing perforin-2 assembly on host cell membranes. This unusual topological feature might therefore offer an elegant safeguard against accidental autolysis during biosynthesis and storage.

Overexpressed GFP- or RFP-tagged perforin-2 shows diffuse staining, which could correspond to small post-Golgi vesicles (29, 32). Hence, it appears that similar to perforin-1, perforin-2 might also be sorted into a specialized storage compartment. However, in contrast to perforin-1, the ectodomain of perforin-2 forms pores at low pH (101, 102), suggesting that the hypothetical storage compartment would have to have elevated rather than low luminal pH.

Intriguingly, overexpression of perforin-2 in HEK-293Ts is toxic (28, 103), yet in professional phagocytes it is one of the most abundant proteins. For example, in mouse dendritic cells, perforin-2 is ranked as the top 55th protein by abundance (104) with an estimated 3x10^6 copies safely stored within each cell (105). It appears likely, therefore, that antigen-presenting cells (APCs) employ specialized mechanisms to protect their intracellular membranes from perforin-2 mediated damage, but this has not been addressed to date. Considering that in non-immune cells, perforin-2 is expressed during infection or upon stimulation with interferons (30, 32), it is possible that interferons also facilitate expression of additional factors that control perforin-2 activity.

INITIATION OF PORE FORMATION

Despite broadly similar mechanisms of pore formation, the signals that trigger PFP activation and the events that precede pore formation are strikingly different between MAC, perforins, and gasdermins (**Figures 2C, D**).

MAC: Cleavage of C5 Triggers a Cascade of Conformational Changes

MAC assembly can be initiated by multiple enzymatic chain reactions known as the classical, lectin and alternative pathways [reviewed in (106)]. All three pathways converge on the formation of a C5 convertase, which catalyzes the cleavage of C5, the key event in initiation of MAC assembly. The activation of the classical pathway starts when the C1q component of the complement system binds to antigen-antibody complexes, e.g., IgM- or IgG-opsonized bacteria. The lectin pathway is initiated following the recognition of pathogen-specific carbohydrates on the bacterial surface (e.g., by mannose-binding lectins, collectins, or ficolins). Ligand-bound C1q or lectin receptors initiate distinct proteolytic cascades, but both lead to cleavage of C4 and C2. The resulting cleavage products, C4b and C2a, assemble into the C3 convertase, which then cleaves C3 to generate C3b. The C4bC2aC3b complex forms the classical C5 convertase. The alternative pathway starts with spontaneous C3 hydrolysis or by deposition of C3b directly on bacterial surface during ongoing complement activation. These events, in the presence of factors B and D, lead to formation of the alternative C5 convertase, C3bBbC3b.

The cleaved C5 initiates a cascade of conformational changes that lead to MAC assembly and unfurling of the TMH domains. Cleavage generates a small C5a fragment (74-77 residues in length) and a large 170 kDa C5b fragment formed by two peptide chains, β (residues 19–673) and α (residues 752–1676), linked by a disulfide bond. C5b is very labile and it decays (aggregates) within 2 min unless stabilized by binding of C6 (107). The C5bC6 associates weakly with the membrane but remains soluble as the TMHs of C6 are not yet deployed in the dimer (108). Membrane binding interfaces may instead be

provided by auxiliary domains such as C6 thrombospondin-like domain which has amphipathic properties at its base (109). The C5bC6 complex recruits C7 driving a cascade of conformational changes within auxiliary domains of C6 and C7 that ultimately trigger unfurling of TMHs in both C6 and C7 and membrane anchoring (110–113). The C6 and C7 β-hairpins, however, do not fully penetrate the membrane. Instead, recruitment and irreversible binding of the C8 trimer and unfurling of the four additional β-hairpins (in C8α/C8β) leads to formation of a stable C5bC6C7C8 complex that can no longer be removed from the membrane by washing (114, 115). The C5b-C8 complex initiates polymerization and membrane insertion of up to 18 copies of C9, recruited directly from solution to the growing pore (111). Notably, MAC pores are the only known PFPs that form hetero-oligomeric, asymmetric pores.

Gasdermins Are Cleaved to Release a Pore-Forming Domain

Gasdermin pores are formed following a regulated cleavage event of the immature propeptide. This cleavage is primarily executed by caspases, which themselves are stored as inactive propeptides that require proteolytic processing for activation.

GSDMD is primarily cleaved by caspases-1 and -4/5/11 (36, 37). Caspase-1 is activated by so-called canonical inflammasomes, a group of large multiprotein complexes composed of distinct pattern recognition receptors (LRP1, NLRP3, NLRC4, AIM2, and pyrin). Canonical inflammasomes assemble in response to a wide range of PAMPs and damage-associated molecular patterns (DAMPs), including bacterial flagellin, cytosolic dsDNA, ROS, ionic imbalances, and many others [reviewed in (116)]. By contrast, caspases-4 and -5 (and caspase-11 in mice) are activated within non-canonical inflammasomes by directly binding to bacterial lipopolysaccharides (LPS) (117). Activated, proteolytically processed caspases-1/4/5/11 bind to the GSDMD C-terminal domain executing cleavage within the GSDMD linker region at position Asp276, in the Phe-Leu-Thr-Asp (humans) or Leu-Leu-Ser-Asp (mice) tetrapeptide (118, 119). In *Yersinia*-infected cells, a caspase-8-dependent processing of GSDMD has also been reported (120, 121). However, considering the low efficiency with which caspase-8 cleaves GSDMD *in vitro*, it is unclear whether the observed effect was specifically due to cleavage of GSDMD or other co-factors (121, 122). Other proteases implicated in GSDMD activation include neutrophil elastase (released from cytoplasmic granules) (123, 124) and cathepsin G (released from lysosomes) (125), but the physiological relevance of these pathways remains to be addressed.

Non-inflammatory signals might also regulate the activity of gasdermins. For example, GSDME can be cleaved and activated by caspase-3, an executioner of canonical apoptosis. While this cleavage results in conversion of apoptotic cell death into pyroptosis (39, 40), intriguingly, caspase-3-mediated cleavage of GSDMD at position Asp87 inhibits pore formation, and as a result inhibits pyroptosis (40, 122, 126). Furthermore, two recent studies suggested that granzymes B and A, delivered by CTLs/NKs through perforin-1 pores, can cleave gasdermins E and B, respectively, and promote pyroptotic rather than apoptotic death of cancer cells (127–129). Hence, unexpectedly, gasdermin-mediated pyroptosis might also contribute to CTL-mediated killing during adaptive immune responses. These findings reveal an intriguing cooperation between mammalian PFPs and further strengthen the notion of plasticity between cell death pathways.

Perforin-1 Is Released From Cytotoxic Granules Into a Neutral pH Environment

The key event that triggers the assembly of perforin-1 pores involves the formation of an immune synapse between a CTL/NK cell and the target cell, followed by fusion of the lytic granules with the plasma membrane and secretion of their contents into the synaptic space.

For CTLs, secretion of the cytotoxic granules is triggered by the association of antigen-specific TCR with MHC I loaded with a foreign or a mutated peptide. Exocytosis of NK granules is controlled by integration of signals delivered from activating and inhibitory cell surface receptors [reviewed in (130)]. The best characterized inhibitory receptors, killer immunoglobulin-like receptors (KIRs) in humans (Ly49 in mice), also bind MHC I and are maximally engaged at the MHC I density found on healthy host cells (131). This, therefore, provides a mechanism to specifically target cells that escape CTL killing by downregulating MHC I—an evasion mechanisms employed by both viruses (132) and cancers [reviewed in (133)]. The NK activating receptors recognize either host proteins upregulated in response to cellular stress (134, 135) or viral proteins expressed on the cell (e.g., viral hemagglutinins bound by receptors NKp46 and NKp44).

The precision in killing is ensured by polarized secretion of the cytotoxic granules toward the immune synapse [reviewed in (136–139)]. The polarization depends on the phospholipase C-γ and Ca^{2+}-dependent signaling of the TCR or NK activating receptors and is followed by dynein-dependent movement and docking of the microtubule organizing center at the synapse. Subsequent microtubule-dependent transport and exocytosis of the granules release perforin-1 from its inhibitory storage compartment into an environment highly favorable for pore formation. The high extracellular Ca^{2+} concentration (~1–1.3 mM) stabilizes the perforin-1 C2 domain and induces a conformational change that permits four key hydrophobic residues to anchor perforin-1 to the plasma membrane of the target cell (99). The neutral pH further facilitates ionic intermolecular interactions of perforin-1 monomers driving their oligomerization into ring- and arc-shaped pores (14, 140, 141).

Perforin-2 Pores Are Assembled at Low pH

Perforin-2 activity has been observed only at low pH *in vitro* and is likely controlled by regulated trafficking to an acidic compartment. Indeed, RFP-tagged perforin-2 redistributes to bacteria-containing phagosomes during infection with *Escherichia coli* or *Salmonella typhimurium* (32). In cells infected with enteropathogenic *E. coli* strain E2348/69 or treated with LPS, the C-terminal cytosolic tail of perforin-2 is

monoubiquitinated by a cullin-RING E3 ubiquitin ligase (CRL) complex and mutation of the lysines in the cytosolic tails of perforin-2 prevents its recruitment to phagosomes and bactericidal activity (31). Yet, the signaling pathways that promote ubiquitination, the mechanisms involved in trafficking of ubiquitinated perforin-2 or whether ubiquitination is indeed required for perforin-2 recruitment to pathogen-containing vacuoles remain to be carefully addressed.

Several lines of evidence suggest that the activation of perforin-2 in acidic compartments might involve cleavage of its ectodomain from the transmembrane domain. Firstly, the ectodomain alone assembles into pre-pores and pores on liposomes *in vitro* (101, 102). Secondly, in HEK-293 cells perforin-2 was able to form ring-like structures only following trypsin treatment (32). Finally, perforin-2 that was present on bacteria isolated from MEFs expressing perforin-2-GFP was recognized by antibodies specific to MACPF and P2 domains but not to the cytosolic tail (32). Nevertheless, neither the cleavage site nor the relevant proteases have been identified to date and future work will need to address whether ectodomain release is indeed physiologically relevant.

Intriguingly, perforin-2 does not restrict bacterial growth without pre-stimulation of cells with IFN or LPS (32). It is not known, however, whether pre-stimulation is required for processing/trafficking of perforin-2 itself, whether it stimulates expression of co-factors required to trigger pore formation, or whether the pore forming ability of perforin-2 is insufficient to restrict bacterial growth in the absence of additional interferon-stimulated genes that facilitate killing of pathogens.

SAFETY MECHANISMS FOR PROTECTION OF BYSTANDER MEMBRANES

After the appropriate trigger signals have been received, the newly unleashed lytic activity of PFPs requires continuous control as unrestrained pore formation would not only be highly damaging to bystander membranes but would also reduce the availability of monomers for a productive lytic response at the target membrane (**Figure 2E**).

Lipid-Binding Selectivity of Gasdermins Prevents Bystander Cell Lysis

Gasdermins preferentially bind to negatively charged lipid species [cardiolipin, phosphatidylinositol phosphates (PIPs), phosphatidic acid (PA), and phosphatidylserine (PS)] which are found on the inner leaflet of the plasma membrane but are absent from its extracellular leaflet (38, 39, 42). This lipid-binding preference therefore appears to be sufficient to protect bystander cells from activated gasdermins released during pyroptosis (142). Given that the cytosolic leaflets of endosomes and phagosomes contain the same lipid species as the inner leaflet of the plasma membrane, it is likely that gasdermins pores are not restricted to the plasma membrane. Whether intracellular membranes [other than the mitochondrial membrane (143)] are indeed disrupted by gasdermins and, if not, how they are protected remains to be investigated.

Inactivation of MAC Assembly

The soluble C5bC6 complex can in principle diffuse away from the target membrane and initiate pore assembly on bystander cells. MAC formation, however, can be inhibited at multiple stages during pore formation, even after proteolysis of C5. The key factors that disarm MAC pores include CD59, clusterin, and vitronectin.

CD59 is a small GPI-anchored glycoprotein widely expressed on the surface of mammalian cells (58). CD59 inhibits MAC formation by binding to C8 in the C5b-8 complex thus preventing C9 incorporation, as well as by binding to C9 in the preformed C5b-9 complex suppressing further polymerization (144). Specifically, CD59 interacts with C8α and C9b in regions exposed during MAC formation (114, 145). The protective role of CD59 is most evident when its levels are pathologically low. Deficiencies in CD59 or in proteins required for biosynthesis of its GPI anchor result in inflammatory neuropathy, recurrent strokes, and chronic hemolysis (146–148).

In contrast to CD59, clusterin and vitronectin are soluble glycoproteins found in plasma (149). Clusterin can inhibit the lytic activity of C5b-7, C5b-8, and C5b-9 subcomplexes by interacting with C7, C8β, and C9 through binding sites exposed during pore formation (150). Vitronectin, also known as S-protein, has been reported to inhibit MAC insertion at two stages: either by binding to the nascent C5b-7, rendering the complex soluble (151) or by inhibiting polymerization of the C9 subunits (152). Interestingly, some Gram-negative bacteria including *Moraxella catarrhalis*, *Haemophilus influenzae*, and *Neisseria gonorrhoeae* recruit vitronectin to prevent MAC deposition on their surface and escape MAC-mediated killing [reviewed in (153)].

How Are Cytotoxic Lymphocytes Protected From Perforin-1 at the Immune Synapse?

Both CTL and NK cells can sequentially kill several target cells suggesting that the killing cell itself does not undergo a bystander death (154–157). Indeed, several studies have demonstrated that various T cell lines as well as primary T cells are more resistant to killing by other CTLs compared to, for example, cancer cell lines (158–160). A similar increased resistance was demonstrated to granule extracts and purified perforin-1 alone (158, 161, 162). Nevertheless, lymphocytes are not invulnerable to CTLs, especially when the attack is directed against them (160, 163, 164). This so-called fratricide (i.e., killing of CTLs by CTLs) might not only be crucial to eliminate CTLs that have been infected or accumulated mutations, but could also help to dampen an excessive immune response (165). Importantly, when an immune synapse between two CTLs is formed, only one cell gets polarized to inflict cell death and the killer always survives (166). Moreover, while a CTL engaged with the target cell avoids destruction by their own lytic mediators, it is not refractory to bystander lysis when induced by neighboring CTLs

(167). This apparent paradox suggests that cytotoxic lymphocytes acquire additional resistance to perforin-1 primarily within the immune synapse following degranulation.

Several models were proposed to explain why the degranulating lymphocyte might be resistant to perforin-1, but none has been widely accepted to date. Earlier studies suggested that other proteins contained within the granules might have protective functions during degranulation. For example, Balaji et al. (95) observed that CTLs are more prone to death in the presence of membrane impermeable cathepsin B inhibitors and proposed that secreted cathepsin B cleaves perforin-1 on the surface of degranulating CTLs to protect them. More recent work, however, revealed that CTLs of cathepsin B-null mice survive their encounter with target cells normally (97). Jiang et al. (168) suggested in turn that glycosylation and sialylation of membrane protein(s) on the CTL surface might provide negative charges that repel perforin-1 and in later work by Cohnen et al. (169), LAMP1/CD107a was implicated as a key O-glycosylated and sialylated protein involved. In line with this model, LAMP1 deficient NK cells were more susceptible to apoptosis after an encounter with the target and overexpression of truncated LAMP1 (targeted directly to the cell surface) reduced apoptosis caused by cytotoxic granules. A separate study, however, did not report a reduction in perforin-1 binding to the surface of primary mouse T cells that overexpress LAMP1 (162). Considering the putative role of LAMP1 in trafficking perforin-1 toward cytotoxic granules (170), the exact contribution of LAMP1 to preventing perforin-1 mediated damage might be difficult to decipher.

Alternatively, perforin-1 resistance could be conferred by local changes in lipid composition that follow degranulation. This model is supported by the observations that perforin-1 preferentially forms pores on phosphatidylcholine-rich, disordered lipid phases, avoiding sphingomyelin/cholesterol-rich ordered domains abundant within the immune synapse (162, 171–173). Furthermore, degranulation is associated with a transient increase of surface exposed PS which is also believed to provide a membrane composition unfavorable for pore assembly (174, 175). On the one hand, the presence of PS could simply interfere with perforin-1 membrane binding (42). On the other hand, PS might act as a negatively charged sink that binds perforin-1 in a conformation incompatible with pore assembly (162).

Finally, unidirectional killing might be facilitated by mechanopotentiation, the process of increasing membrane tension on the target cell *via* the exertion of synaptic forces (176). The forces at the immune synapse are generated by the concerted action of cytosolic proteins that regulate actin dynamics, myosin II, and integrins (177–179). A resulting increase in membrane tension on the target cell was proposed to lower the necessary concentration of perforin-1 required for pore assembly (176). This discovery implies an additional function of the immune synapse in protecting from perforin-1-mediated damage: not only does it protect bystander cells by limiting perforin-1 diffusion, but also the cytotoxic cells themselves, by lowering the effective concentration of perforin-1 required for pore assembly on the target membrane.

(How) Are Phagosomal Membranes Protected From Perforin-2 Activity?

Little is known about the mechanisms involved in the protection of host cells from perforin-2 pores formed in phagosomes. *In vitro*, perforin-2 displays preference for negatively charged lipids including PS, PIPs as well as cardiolipin, which is found in the membranes of most bacteria (101, 102). However, considering that overexpressed perforin-2 can be toxic (103) and that perforin-2 pores have been observed also on mammalian membranes (32), it is unclear whether in infected cells the pores are solely formed on the pathogen surface.

Pore Insertion and Membrane Repair Pathways

Even a small injury to the plasma membrane can lead to local spikes in cytosolic Ca^{2+} and trigger membrane repair pathways in the affected cell. In general, these repair pathways involve endocytosis to internalize damaged membranes, exocytosis to shed damaged membranes, and membrane patching to reseal any damage using internal endolysosome-derived donor membranes (180).

Perforin-1 insertion primarily triggers membrane patching using lysosomal and endosomal donor membranes (140, 181–183). It has also been observed that, in addition to patching, perforin-1-mediated membrane destabilization promotes clathrin- and dynamin-dependent endocytosis resulting in the internalization of both perforin-1 and granzymes (183–185). These data led to the hypothesis that endolysosomal compartments (gigantosomes) rather than the plasma membrane are the primary site of perforin-1 pore assembly and granzyme entry into the cytosol. Later studies, however, did not support this model. Firstly, it remains controversial whether the luminal pH and Ca^{2+} concentration in gigantosomes are permissive for assembly of perforin-1 pores (140, 186). Secondly, the relatively slow kinetics of granzyme endocytosis and release (~ 15 min) are inconsistent with the rapid (~ 2 min) induction of Bid cleavage reported in cells exposed to granzyme B and sublytic amounts of perforin-1 (140). Hence, Lopez et al. proposed that, while membrane repair pathways do indeed negatively regulate perforin-1 activity at the plasma membrane, they allow the formation of transient pores that persist for 20–80 s providing sufficient permeability to deliver granzymes into the cytosol of the target cell and to initiate apoptosis (140). Future work involving high-resolution electron tomography might be necessary to resolve the controversy surrounding the primary location of functional perforin-1 pores, but what remains clear is that membrane repair pathways are important to prevent uncontrolled perforin-1 mediated lysis of the target cells.

Ca^{2+} influx and membrane repair have also been reported upon membrane insertion of gasdermins (187). Gasdermin pores trigger recruitment of endosomal sorting complexes required for transport (ESCRTs) which mediate repair of damaged membranes through exocytosis (188). ESCRT-mediated membrane repair negatively regulates GSDMD-induced pyroptotic death as well as the release of IL-1β and IL-18 from

infected cells (187). Considering ESCRTs are also recruited to membranes exposed to CDCs such as streptolysin O and listeriolysin O (188), it appears likely that they may contribute to the removal of perforin-1 pores as well. Interestingly, ESCRTs are also involved in repair of small perforations in endolysosomes to facilitate recovery of damaged intracellular membranes (189). This pathway might provide a safety mechanism against possible accidental damage of PFP storage compartments and an additional layer of protection for PFP-producing cells.

CONCLUDING REMARKS

It is striking how both innate and adaptive immune systems employ PFPs as their key effectors. In this review, we aimed to provide an overview of the pathways and immune system components involved in controlling the activity of these membrane-disrupting molecules. However, it is important to recognize that PFP biology is tightly linked to fundamental processes that go well beyond what we discussed here including positive and negative T cell selection, antibody affinity maturation as well as signaling pathways associated with different types of cell death, all of which ultimately contribute to the regulation of PFP activity.

Despite the century of research since the discovery of MAC, many questions regarding PFPs remain unanswered. Is extrahepatic production of MAC components physiologically relevant during infections? What are the precise conformational changes that govern the initial membrane insertion of MAC and the final pore closure? Is mechanopotentiation involved in protecting degranulating CTLs and NKs cells from perforin-1 activity *in vivo*? How is translation of perforin-1 and other NK effectors suppressed in resting cells?

The recent discovery of perforin-2 and gasdermins has also opened new avenues to explore. What are the physiological functions of all gasdermins? Are they able to assemble on endolysosomal membranes and if so, what are the consequences of the potential damage? Is perforin-2 released from the phagosomal membrane to form pores on intravacuolar pathogens and if so, by which proteases? Does perforin-2 damage phagosomes or does it assemble exclusively on bacterial membranes?

The latest advances in the PFP field have uncovered an unexpected link between perforin-1-mediated granzyme delivery and gasdermin activation, and future work is likely to reveal other examples of such cooperativity. We now also only begin to appreciate the different mechanisms involved in the sensing and repair of damaged membranes and how they can affect the consequences of pore formation. Finally, many of the regulatory pathways discussed in this review can be disrupted by pathogens, and the full picture of the mechanisms involved in evasion of PFP-mediated immunity is yet to emerge.

There is no doubt that the PFP field continues to rapidly expand. Following the recent advances in cryo-electron microscopy, the structures of MAC, perforin-1/2, and gasdermin pores are now available shedding some light on the conformational changes involved in pore assembly. Whole exome sequencing data from immunodeficient patients is helping to uncover novel disease-associated variants both in PFPs themselves and in their regulators. Finally, CRISPR-Cas9 technology is facilitating the generation of cell-type specific knockouts to address the contribution of candidate proteins in PFP biology using primary cells and animal models of disease. Novel scalable assays to study PFPs *in vitro*, identification of co-regulators through genetic screens in the relevant primary cell types, and structural insights into pre-pore and pore intermediates should provide us with a more complete picture of the mechanisms involved in the regulation of these powerful effectors and facilitate development of targeted immunomodulatory therapeutics.

AUTHOR CONTRIBUTIONS

All authors listed have made a substantial, direct, and intellectual contribution to the work and approved it for publication.

FUNDING

We would like to thank Dr. Greg Slodkowicz for comments on the manuscript. The authors were supported by the MRC grant MC_UP_1201/26. PAK was also supported by a Boehringer Ingelheim Fonds PhD Fellowship and the Cambridge Trust.

REFERENCES

1. Peraro MD, van der Goot FG. Pore-forming toxins: ancient, but never really out of fashion. *Nat Rev Microbiol* (2016) 14(2):77–92. doi: 10.1038/nrmicro.2015.3
2. Anderluh G, Kisovec M, Kraševec N, Gilbert RJC. Distribution of MACPF/CDC Proteins. In: G Anderluh and R Gilbert, editors. *MACPF/CDC Proteins - Agents of Defence, Attack and Invasion*. Dordrecht: Springer Netherlands (2014). doi: 10.1007/978-94-017-8881-6_2
3. Liu X, Lieberman J. Knocking 'em dead: pore-forming proteins in immune defense. *Annu Rev Immunol* (2020) 38(1):455–85. doi: 10.1146/annurev-immunol-111319-023800
4. Nuttall G. Experimente über die bacterienfeindlichen Einflüsse des thierischen Körpers. *Z Hyg Infektionskr* (1888) 4(1):353–94. doi: 10.1007/BF02188097
5. Buchner HEA. Über die bakterientötende Wirkung des Zellfreien Blutserums. I and II. *Zentralbl Bakteriol* (1889) 5:817–23.
6. Tomlinson S, Taylor PW, Morgan BP, Luzio JP. Killing of gram-negative bacteria by complement. Fractionation of cell membranes after complement C5b-9 deposition on to the surface of Salmonella minnesota Re595. *Biochem J* (1989) 263(2):505–11. doi: 10.1042/bj2630505
7. Nakamura M, Okada H, Sasaki H, Yoshida K, Kamada M, Okada N, et al. Quantification of the CD55 and CD59, membrane inhibitors of complement on HIV-1 particles as a function of complement-mediated virolysis. *Microbiol Immunol* (1996) 40(8):561–7. doi: 10.1111/j.1348-0421.1996.tb01109.x
8. Hoover DL, Berger M, Nacy CA, Hockmeyer WT, Meltzer MS. Killing of Leishmania tropica amastigotes by factors in normal human serum. *J Immunol* (1984) 132(2):893.

9. Koski CL, Ramm LE, Hammer CH, Mayer MM, Shin ML. Cytolysis of nucleated cells by complement: cell death displays multi-hit characteristics. *Proc Natl Acad Sci U S A* (1983) 80(12):3816–20. doi: 10.1073/pnas.80.12.3816
10. Morgan BP. The membrane attack complex as an inflammatory trigger. *Immunobiology* (2016) 221(6):747–51. doi: 10.1016/j.imbio.2015.04.006
11. Ross SC, Densen P. Complement deficiency states and infection: epidemiology, pathogenesis and consequences of neisserial and other infections in an immune deficiency. *Medicine (Baltimore)* (1984) 63 (5):243–73. doi: 10.1097/00005792-198409000-00001
12. Orren A, Potter PC, Cooper RC, du Toit E. Deficiency of the sixth component of complement and susceptibility to Neisseria meningitidis infections: studies in 10 families and five isolated cases. *Immunology* (1987) 62(2):249–53.
13. Khajoee V, Ihara K, Kira R, Takemoto M, Torisu H, Sakai Y, et al. Founder effect of the C9 R95X mutation in Orientals. *Hum Genet* (2003) 112(3):244–8. doi: 10.1007/s00439-002-0870-8
14. Baran K, Dunstone M, Chia J, Ciccone A, Browne KA, Clarke CJP, et al. The molecular basis for perforin oligomerization and transmembrane pore assembly. *Immunity* (2009) 30(5):684–95. doi: 10.1016/j.immuni.2009.03.016
15. Zychlinsky A, Zheng LM, Liu CC, Young JD. Cytolytic lymphocytes induce both apoptosis and necrosis in target cells. *J Immunol* (1991) 146(1):393.
16. Waterhouse NJ, Sutton VR, Sedelies KA, Ciccone A, Jenkins M, Turner SJ, et al. Cytotoxic T lymphocyte-induced killing in the absence of granzymes A and B is unique and distinct from both apoptosis and perforin-dependent lysis. *J Cell Biol* (2006) 173(1):133–44. doi: 10.1083/jcb.200510072
17. Oshimi Y, Oshimi K, Miyazaki S. Necrosis and apoptosis associated with distinct Ca2+ response patterns in target cells attacked by human natural killer cells. *J Physiol* (1996) 495(Pt 2):319–29. doi: 10.1113/jphysiol.1996.sp021596
18. Voskoboinik I, Smyth MJ, Trapani JA. Perforin-mediated target-cell death and immune homeostasis. *Nat Rev Immunol* (2006) 6(12):940–52. doi: 10.1038/nri1983
19. Stepp SE, Dufourcq-Lagelouse R, Le Deist F, Bhawan S, Certain S, Mathew PA, et al. Perforin gene defects in familial hemophagocytic lymphohistiocytosis. *Science* (1999) 286(5446):1957–9. doi: 10.1126/science.286.5446.1957
20. Baker KS, DeLaat CA, Steinbuch M, Gross TG, Shapiro RS, Loechelt B, et al. Successful correction of hemophagocytic lymphohistiocytosis with related or unrelated bone marrow transplantation. *Blood* (1997) 89(10):3857–63. doi: 10.1182/blood.V89.10.3857.3857_3857_3863
21. Brennan AJ, Chia J, Trapani JA, Voskoboinik I. Perforin deficiency and susceptibility to cancer. *Cell Death Differ* (2010) 17(4):607–15. doi: 10.1038/cdd.2009.212
22. Clementi R, Locatelli F, Dupre L, Garaventa A, Emmi L, Bregni M, et al. A proportion of patients with lymphoma may harbor mutations of the perforin gene. *Blood* (2005) 105(11):4424–8. doi: 10.1182/blood-2004-04-1477
23. Chia J, Yeo KP, Whisstock JC, Dunstone MA, Trapani JA, Voskoboinik I. Temperature sensitivity of human perforin mutants unmasks subtotal loss of cytotoxicity, delayed FHL, and a predisposition to cancer. *Proc Natl Acad Sci U S A* (2009) 106(24):9809–14. doi: 10.1073/pnas.0903815106
24. Badovinac VP, Hamilton SE, Harty JT. Viral infection results in massive CD8+ T cell expansion and mortality in vaccinated perforin-deficient mice. *Immunity* (2003) 18(4):463–74. doi: 10.1016/s1074-7613(03)00079-7
25. van den Broek ME, Kägi D, Ossendorp F, Toes R, Vamvakas S, Lutz WK, et al. Decreased tumor surveillance in perforin-deficient mice. *J Exp Med* (1996) 184(5):1781–90. doi: 10.1084/jem.184.5.1781
26. Smyth MJ, Thia KY, Street SE, MacGregor D, Godfrey DII, Trapani JA. Perforin-mediated cytotoxicity is critical for surveillance of spontaneous lymphoma. *J Exp Med* (2000) 192(5):755–60. doi: 10.1084/jem.192.5.755
27. Spilsbury K, O'Mara MA, Wu W, Rowe PB, Symonds G, Takayama. Y. Isolation of a novel macrophage-specific gene by differential cDNA analysis. *Blood* (1995) 85(6):1620–9. doi: 10.1182/blood.V85.6.1620.bloodjournal8561620
28. McCormack R, Podack ER. Perforin-2/Mpeg1 and other pore-forming proteins throughout evolution. *J Leukoc Biol* (2015) 98(5):761–8. doi: 10.1189/jlb.4MR1114-523RR
29. Fields KA, McCormack R, de Armas LR, Podack ER. Perforin-2 restricts growth of Chlamydia trachomatis in macrophages. *Infect Immun* (2013) 81 (8):3045–54. doi: 10.1128/IAI.00497-13
30. McCormack R, de Armas LR, Shiratsuchi M, Ramos JE, Podack ER. Inhibition of intracellular bacterial replication in fibroblasts is dependent on the perforin-like protein (perforin-2) encoded by macrophage-expressed gene 1. *J innate Immun* (2013) 5(2):185–94. doi: 10.1159/000345249
31. McCormack RM, Lyapichev K, Olsson ML, Podack ER, Munson GP. Enteric pathogens deploy cell cycle inhibiting factors to block the bactericidal activity of Perforin-2. *Elife* (2015) 4:e06505. doi: 10.7554/eLife.06505
32. McCormack RM, de Armas LR, Shiratsuchi M, Fiorentino DG, Olsson ML, Lichtenheld MG, et al. Perforin-2 is essential for intracellular defense of parenchymal cells and phagocytes against pathogenic bacteria. *Elife* (2015) 4: e06508. doi: 10.7554/eLife.06508
33. McCormack R, Bahnan W, Shrestha N, Boucher J, Barreto M, Barrera CM, et al. Perforin-2 protects host cells and mice by restricting the vacuole to cytosol transitioning of a bacterial pathogen. *Infect Immun* (2016) 84 (4):1083–91. doi: 10.1128/IAI.01434-15
34. Bai F, McCormack RM, Hower S, Plano GV, Lichtenheld MG, Munson GP. Perforin-2 breaches the envelope of phagocytosed bacteria allowing antimicrobial effectors access to intracellular targets. *J Immunol* (2018) 201(9):2710–20. doi: 10.4049/jimmunol.1800365
35. McCormack RM, Szymanski EP, Hsu AP, Perez E, Olivier KN, Fisher E, et al. MPEG1/perforin-2 mutations in human pulmonary nontuberculous mycobacterial infections. *JCI Insight* (2017) 2(8):e89635. doi: 10.1172/jci.insight.89635
36. Kayagaki N, Stowe IB, Lee BL, O'Rourke K, Anderson K, Warming S, et al. Caspase-11 cleaves gasdermin D for non-canonical inflammasome signalling. *Nature* (2015) 526(7575):666–71. doi: 10.1038/nature15541
37. Shi J, Zhao Y, Wang K, Shi X, Wang Y, Huang H, et al. Cleavage of GSDMD by inflammatory caspases determines pyroptotic cell death. *Nature* (2015) 526(7575):660–5. doi: 10.1038/nature15514
38. Ding J, Wang K, Liu W, She Y, Sun Q, Shi J, et al. Pore-forming activity and structural autoinhibition of the gasdermin family. *Nature* (2016) 535 (7610):111–6. doi: 10.1038/nature18590
39. Wang Y, Gao W, Shi X, Ding J, Liu W, He H, et al. Chemotherapy drugs induce pyroptosis through caspase-3 cleavage of a gasdermin. *Nature* (2017) 547(7661):99–103. doi: 10.1038/nature22393
40. Rogers C, Fernandes-Alnemri T, Mayes L, Alnemri D, Cingolani G, Alnemri ES. Cleavage of DFNA5 by caspase-3 during apoptosis mediates progression to secondary necrotic/pyroptotic cell death. *Nat Commun* (2017) 8(1):14128. doi: 10.1038/ncomms14128
41. Chen KW, Monteleone M, Boucher D, Sollberger G, Ramnath D, Condon ND, et al. Noncanonical inflammasome signaling elicits gasdermin D-dependent neutrophil extracellular traps. *Sci Immunol* (2018) 3(26): eaar6676. doi: 10.1126/sciimmunol.aar6676
42. Liu X, Zhang Z, Ruan J, Pan Y, Magupalli VG, Wu H, et al. Inflammasome-activated gasdermin D causes pyroptosis by forming membrane pores. *Nature* (2016) 535(7610):153–8. doi: 10.1038/nature18629
43. Li JY, Wang YY, Shao T, Fan DD, Lin AF, Xiang LX, et al. The zebrafish NLRP3 inflammasome has functional roles in ASC-dependent interleukin-1beta maturation and gasdermin E-mediated pyroptosis. *J Biol Chem* (2020) 295(4):1120–41. doi: 10.1074/jbc.RA119.011751
44. Daskalov A, Mitchell PS, Sandstrom A, Vance RE, Glass NL. Molecular characterization of a fungal gasdermin-like protein. *Proc Natl Acad Sci U S A* (2020) 117(31):18600–7. doi: 10.1073/pnas.2004876117
45. Runkel F, Marquardt A, Stoeger C, Kochmann E, Simon D, Kohnke B, et al. The dominant alopecia phenotypes Bareskin, Rex-denuded, and Reduced Coat 2 are caused by mutations in gasdermin 3. *Genomics* (2004) 84(5):824–35. doi: 10.1016/j.ygeno.2004.07.003
46. Lunny DP, Weed E, Nolan PM, Marquardt A, Augustin M, Porter RM. Mutations in gasdermin 3 cause aberrant differentiation of the hair follicle and sebaceous gland. *J Invest Dermatol* (2005) 124(3):615–21. doi: 10.1111/j.0022-202X.2005.23623.x
47. Yu J, Kang M-J, Kim B-J, Kwon J-W, Song Y-H, Choi W-A, et al. Polymorphisms in GSDMA and GSDMB are associated with asthma susceptibility, atopy and BHR. *Pediatr Pulmonol* (2011) 46(7):701–8. doi: 10.1002/ppul.21424
48. Laer LV, Huizing EH, Verstreken M, v. Zuijlen D, Wauters JG, Bossuyt PJ, et al. Nonsyndromic hearing impairment is associated with a mutation in DFNA5. *Nat Genet* (1998) 20(2):194–7. doi: 10.1038/2503

49. Delmaghani S, del Castillo FJ, Michel V, Leibovici M, Aghaie A, Ron U, et al. Mutations in the gene encoding pejvakin, a newly identified protein of the afferent auditory pathway, cause DFNB59 auditory neuropathy. *Nat Genet* (2006) 38(7):770–8. doi: 10.1038/ng1829
50. Hadders MA, Beringer DX, Gros P. Structure of C8 -MACPF Reveals Mechanism of membrane attack in complement immune defense. *Science* (2007) 317(5844):1552–4. doi: 10.1126/science.1147103
51. Rosado CJ, Buckle AM, Law RHP, Butcher RE, Kan W-T, Bird CH, et al. A Common fold mediates vertebrate defense and bacterial attack. *Science* (2007) 317(5844):1548. doi: 10.1126/science.1144706
52. Law RHP, Lukoyanova N, Voskoboinik I, Caradoc-Davies TT, Baran K, Dunstone MA, et al. The structural basis for membrane binding and pore formation by lymphocyte perforin. *Nature* (2010) 468(7322):447–51. doi: 10.1038/nature09518PMID-21037563
53. Ruan J, Xia S, Liu X, Lieberman J, Wu H. Cryo-EM structure of the gasdermin A3 membrane pore. *Nature* (2018) 557(7703):62–7. doi: 10.1038/s41586-018-0058-6
54. Liu Z, Wang C, Yang J, Zhou B, Yang R, Ramachandran R, et al. Crystal structures of the full-length murine and human gasdermin D reveal mechanisms of autoinhibition, lipid binding, and oligomerization. *Immunity* (2019) 51(1):43–49.e4. doi: 10.1016/j.immuni.2019.04.017
55. Dunstone MA, Tweten RK. Packing a punch: the mechanism of pore formation by cholesterol dependent cytolysins and membrane attack complex/perforin-like proteins. *Curr Opin Struct Biol* (2012) 22(3):342–9. doi: 10.1016/j.sbi.2012.04.008
56. Mulvihill E, Sborgi L, Mari SA, Pfreundschuh M, Hiller S, Müller DJ. Mechanism of membrane pore formation by human gasdermin-D. *EMBO J* (2018) 37(14):e98321. doi: 10.15252/embj.201798321
57. Johnson BB, Moe PC, Wang D, Rossi K, Trigatti BL, Heuck AP. Modifications in perfringolysin O domain 4 alter the cholesterol concentration threshold required for binding. *Biochemistry* (2012) 51 (16):3373–82. doi: 10.1021/bi3003132
58. G. T. Consortium. The GTEx Consortium atlas of genetic regulatory effects across human tissues. *Science* (2020) 369(6509):1318–30. doi: 10.1126/science.aaz1776
59. Würzner R, Joysey VC, Lachmann PJ. Complement component C7. Assessment of in vivo synthesis after liver transplantation reveals that hepatocytes do not synthesize the majority of human C7. *J Immunol* (1994) 152(9):4624–9.
60. Hobart MJ, Lachmann PJ, Calne RY. C6: synthesis by the liver in vivo. *J Exp Med* (1977) 146(2):629–30. doi: 10.1084/jem.146.2.629
61. Alper CA, Raum D, Awdeh ZL, Petersen BH, Taylor PD, Starzl TE. Studies of hepatic synthesis in vivo of plasma proteins, including orosomucoid, transferrin, alpha 1-antitrypsin, C8, and factor B. *Clin Immunol Immunopathol* (1980) 16(1):84–9. doi: 10.1016/0090-1229(80)90169-5
62. Würzner R. Modulation of complement membrane attack by local C7 synthesis. *Clin Exp Immunol* (2000) 121(1):8–10. doi: 10.1046/j.1365-2249.2000.01263.x
63. Aizarani N, Saviano A, Sagar, Mailly L, Durand S, Herman JS, et al. A human liver cell atlas reveals heterogeneity and epithelial progenitors. *Nature* (2019) 572(7768):199–204. doi: 10.1038/s41586-019-1373-2
64. MacParland SA, Liu JC, Ma X-Z, Innes BT, Bartczak AM, Gage BK, et al. Single cell RNA sequencing of human liver reveals distinct intrahepatic macrophage populations. *Nat Commun* (2018) 9(1):4383–3. doi: 10.1038/s41467-018-06318-7
65. Broz P, Pelegrin P, Shao F. The gasdermins, a protein family executing cell death and inflammation. *Nat Rev Immunol* (2020) 20(3):143–57. doi: 10.1038/s41577-019-0228-2
66. Singhania A, Graham CM, Gabryšová L, Moreira-Teixeira L, Stavropoulos E, Pitt JM, et al. Transcriptional profiling unveils type I and II interferon networks in blood and tissues across diseases. *Nat Commun* (2019) 10 (1):2887. doi: 10.1038/s41467-019-10601-6
67. Saeki N, Usui T, Aoyagi K, Kim DH, Sato M, Mabuchi T, et al. Distinctive expression and function of four GSDM family genes (GSDMA-D) in normal and malignant upper gastrointestinal epithelium. *Genes Chromosomes Cancer* (2009) 48(3):261–71. doi: 10.1002/gcc.20636
68. Akino K, Toyota M, Suzuki H, Imai T, Maruyama R, Kusano M, et al. Identification of DFNA5 as a target of epigenetic inactivation in gastric cancer. *Cancer Sci* (2007) 98(1):88–95. doi: 10.1111/j.1349-7006.2006.00351.x
69. Masuda Y, Futamura M, Kamino H, Nakamura Y, Kitamura N, Ohnishi S, et al. The potential role of DFNA5, a hearing impairment gene, in p53-mediated cellular response to DNA damage. *J Hum Genet* (2006) 51(8):652–64. doi: 10.1007/s10038-006-0004-6
70. Pipkin ME, Ljutic B, Cruz-Guilloty F, Nouzova M, Rao A, Zúñiga-Pflücker JC, et al. Chromosome transfer activates and delineates a locus control region for perforin. *Immunity* (2007) 26(1):29–41. doi: 10.1016/j.immuni.2006.11.009
71. Podack ER, Hengartner H, Lichtenheld MG. A Central Role of Perforin in Cytolysis? *Annu Rev Immunol* (1991) 9(1):129–57. doi: 10.1146/annurev.iy.09.040191.001021PMID-1910674
72. Liu CC, Rafii S, Granelli-Piperno A, Trapani JA, Young JD. Perforin and serine esterase gene expression in stimulated human T cells. Kinetics, mitogen requirements, and effects of cyclosporin A. *J Exp Med* (1989) 170 (6):2105–18. doi: 10.1084/jem.170.6.2105
73. Glimcher LH, Townsend MJ, Sullivan BM, Lord GM. Recent developments in the transcriptional regulation of cytolytic effector cells. *Nat Rev Immunol* (2004) 4(11):900–11. doi: 10.1038/nri1490
74. Pipkin ME, Rao A, Lichtenheld MG. The transcriptional control of the perforin locus. *Immunol Rev* (2010) 235(1):55–72. doi: 10.1111/j.0105-2896.2010.00905.xPMID-20536555
75. Jacobs R, Hintzen G, Kemper A, Beul K, Kempf S, Behrens G, et al. CD56bright cells differ in their KIR repertoire and cytotoxic features from CD56dim NK cells. *Eur J Immunol* (2001) 31(10):3121–7. doi: 10.1002/1521-4141(2001010)31:10<3121::aid-immu3121>3.0.co;2-4
76. Lacorazza HD, Miyazaki Y, Di Cristofano A, Deblasio A, Hedvat C, Zhang J, et al. The ETS protein MEF plays a critical role in perforin gene expression and the development of natural killer and NK-T cells. *Immunity* (2002) 17 (4):437–49. doi: 10.1016/s1074-7613(02)00422-3
77. Fehniger TA, Cai SF, Cao X, Bredemeyer AJ, Presti RM, French AR, et al. Acquisition of murine NK cell cytotoxicity requires the translation of a pre-existing pool of granzyme B and perforin mRNAs. *Immunity* (2007) 26 (6):798–811. doi: 10.1016/j.immuni.2007.04.010
78. Kim N, Kim M, Yun S, Doh J, Greenberg PD, Kim TD, et al. MicroRNA-150 regulates the cytotoxicity of natural killers by targeting perforin-1. *J Allergy Clin Immunol* (2014) 134(1):195–203. doi: 10.1016/j.jaci.2014.02.018
79. Anderson P. Post-transcriptional regulons coordinate the initiation and resolution of inflammation. *Nat Rev Immunol* (2010) 10(1):24–35. doi: 10.1038/nri2685
80. Zhao BS, Roundtree IA, He C. Post-transcriptional gene regulation by mRNA modifications. *Nat Rev Mol Cell Biol* (2017) 18(1):31–42. doi: 10.1038/nrm.2016.132
81. Heng TS, Painter MW, Consortium IGP. The Immunological Genome Project: networks of gene expression in immune cells. *Nat Immunol* (2008) 9(10):1091–4. doi: 10.1038/ni1008-1091
82. Rusinova I, Forster S, Yu S, Kannan A, Masse M, Cumming H, et al. Interferome v2.0: an updated database of annotated interferon-regulated genes. *Nucleic Acids Res* (2013) 41(Database issue):D1040–6. doi: 10.1093/nar/gks1215
83. Ibana JA, Sherchand SP, Fontanilla FL, Nagamatsu T, Schust DJ, Quayle AJ, et al. Chlamydia trachomatis-infected cells and uninfected-bystander cells exhibit diametrically opposed responses to interferon gamma. *Sci Rep* (2018) 8(1):8476. doi: 10.1038/s41598-018-26765-y
84. Bubeck D, Roversi P, Donev R, Morgan BP, Llorca O, Lea SM. Structure of human complement C8, a precursor to membrane attack. *J Mol Biol* (2011) 405(2):325–30. doi: 10.1016/j.jmb.2010.10.031
85. Tschopp J, Müller-Eberhard HJ, Podack ER. Formation of transmembrane tubules by spontaneous polymerization of the hydrophilic complement protein C9. *Nature* (1982) 298(5874):534–8. doi: 10.1038/298534a0
86. Dudkina NV, Spicer BA, Reboul CF, Conroy PJ, Lukoyanova N, Elmlund H, et al. Structure of the poly-C9 component of the complement membrane attack complex. *Nat Commun* (2016) 7(1):10588. doi: 10.1038/ncomms10588PMID-26841934
87. Spicer BA, Law RHP, Caradoc-Davies TT, Ekkel SM, Bayly-Jones C, Pang S-S, et al. The first transmembrane region of complement component-9 acts as a brake on its self-assembly. *Nat Commun* (2018) 9(1):3266. doi: 10.1038/s41467-018-05717-0

88. Liu Z, Wang C, Rathkey JK, Yang J, Dubyak GR, Abbott DW, et al. Structures of the gasdermin D C-terminal domains reveal mechanisms of autoinhibition. *Structure (London Engl 1993)* (2018) 26(5):778–784.e3. doi: 10.1016/j.str.2018.03.002
89. Voskoboinik I, Thia M-C, Fletcher J, Ciccone A, Browne K, Smyth MJ, et al. Calcium-dependent plasma membrane binding and Cell Lysis by Perforin Are Mediated through Its C2 Domain A CRITICAL ROLE FOR ASPARTATE RESIDUES 429, 435, 483, AND 485 BUT NOT 491. *J Biol Chem* (2005) 280 (9):8426–34. doi: 10.1074/jbc.m413303200PMID-15576364
90. Tschopp J, Schäfer S, Masson D, Peitsch MC, Heusser C. Phosphorylcholine acts as a Ca2+-dependent receptor molecule for lymphocyte perforin. *Nature* (1989) 337(6204):272–4. doi: 10.1038/337272a0
91. Uellner R, Zvelebil MJ, Hopkins J, Jones J, MacDougall LK, Morgan BP, et al. Perforin is activated by a proteolytic cleavage during biosynthesis which reveals a phospholipid-binding C2 domain. *EMBO J* (1997) 16(24):7287–96. doi: 10.1093/emboj/16.24.7287
92. House IG, House CM, Brennan AJ, Gilan O, Dawson MA, Whisstock JC, et al. Regulation of perforin activation and pre-synaptic toxicity through C-terminal glycosylation. *EMBO Rep* (2017) 18(10):1775–85. doi: 10.15252/embr.201744351
93. Brennan AJ, Chia J, Browne KA, Ciccone A, Ellis S, Lopez JA, et al. Protection from endogenous perforin: glycans and the C terminus regulate exocytic trafficking in cytotoxic lymphocytes. *Immunity* (2011) 34(6):879–92. doi: 10.1016/j.immuni.2011.04.007
94. Shi X, Jarvis D. Protein N-glycosylation in the baculovirus-insect cell system. *Curr Drug Targets* (2007) 8(10):1116–25. doi: 10.2174/13894500 7782151360
95. Balaji KN, Schaschke N, Machleidt W, Catalfamo M, Henkart PA. Surface cathepsin b protects cytotoxic lymphocytes from self-destruction after degranulation. *J Exp Med* (2002) 196(4):493–503. doi: 10.1084/jem.20011836
96. Konjar Š., Sutton VR, Hoves S, Repnik U, Yagita H, Reinheckel T, et al. Human and mouse perforin are processed in part through cleavage by the lysosomal cysteine proteinase cathepsin L. *Immunology* (2010) 131(2):257–67. doi: 10.1111/j.1365-2567.2010.03299.x
97. Baran K, Ciccone A, Peters C, Yagita H, Bird PII, Villadangos JA, et al. Cytotoxic T lymphocytes from cathepsin B-deficient mice survive normally in vitro and in vivo after encountering and killing target cells. *J Biol Chem* (2006) 281(41):30485–91. doi: 10.1074/jbc.M602007200
98. Chan C-B, Abe M, Hashimoto N, Hao C, Williams IR, Liu X, et al. Mice lacking asparaginyl endopeptidase develop disorders resembling hemophagocytic syndrome. *Proc Natl Acad Sci U S A* (2009) 106(2):468–73. doi: 10.1073/pnas.0809824105
99. Traore DAK, Brennan AJ, Law RHP, Dogovski C, Perugini MA, Lukoyanova N, et al. Defining the interaction of perforin with calcium and the phospholipid membrane. *Biochem J* (2013) 456(3):323–35. doi: 10.1042/bj20130999
100. Dupuis M, Schaerer E, Krause KH, Tschopp J. The calcium-binding protein calreticulin is a major constituent of lytic granules in cytolytic T lymphocytes. *J Exp Med* (1993) 177(1):1–7. doi: 10.1084/jem.177.1.1
101. Pang SS, Bayly-Jones C, Radjainia M, Spicer BA, Law RHP, Hodel AW, et al. The cryo-EM structure of the acid activatable pore-forming immune effector Macrophage-expressed gene 1. *Nat Commun* (2019) 10(1):4288. doi: 10.1038/s41467-019-12279-2
102. Ni T, Jiao F, Yu X, Aden S, Ginger L, Williams SII, et al. Structure and mechanism of bactericidal mammalian perforin-2, an ancient agent of innate immunity. *Sci Adv* (2020) 6(5):eaax8286. doi: 10.1126/sciadv.aax8286
103. de Armas LR. *Characterization of Perforin-2, a Novel Anti-bacterial, Pore-forming Protein of the Innate Immune System*. (2013) University of Miami.
104. Luber CA, Cox J, Lauterbach H, Fancke B, Selbach M, Tschopp J, et al. Quantitative proteomics reveals subset-specific viral recognition in dendritic cells. *Immunity* (2010) 32(2):279–89. doi: 10.1016/j.immuni.2010.01.013
105. Kozik P, Gros M, Itzhak DN, Joannas L, Heurtebise-Chrétien S, Krawczyk PA, et al. Small Molecule Enhancers of Endosome-to-Cytosol Import Augment Anti-tumor Immunity. *Cell Rep* (2020) 32(2):107905. doi: 10.1016/j.celrep.2020.107905
106. Ricklin D, Hajishengallis G, Yang K, Lambris JD. Complement: a key system for immune surveillance and homeostasis. *Nat Immunol* (2010) 11(9):785–97. doi: 10.1038/ni.1923
107. DiScipio RG, Smith CA, Muller-Eberhard HJ, Hugli TE. The activation of human complement component C5 by a fluid phase C5 convertase. *J Biol Chem* (1983) 258(17):10629–36.
108. Hadders MA, Bubeck D, Roversi P, Hakobyan S, Forneris F, Morgan BP, et al. Assembly and Regulation of the Membrane Attack Complex Based on Structures of C5b6 and sC5b9. *Cell Rep* (2012) 1(3):200–7. doi: 10.1016/j.celrep.2012.02.003
109. Aleshin AE, Schraufstatter IU, Stec B, Bankston LA, Liddington RC, DiScipio RG. Structure of Complement C6 Suggests a Mechanism for Initiation and Unidirectional, Sequential Assembly of Membrane Attack Complex (MAC). *J Biol Chem* (2012) 287(13):10210–22. doi: 10.1074/jbc.m111.327809
110. Aleshin AE, DiScipio RG, Stec B, Liddington RC. Crystal Structure of C5b-6 Suggests Structural Basis for Priming Assembly of the Membrane Attack Complex. *J Biol Chem* (2012) 287(23):19642–52. doi: 10.1074/jbc.m112.361121
111. Parsons ES, Stanley GJ, Pyne ALB, Hodel AW, Nievergelt AP, Menny A, et al. Single-molecule kinetics of pore assembly by the membrane attack complex. *Nat Commun* (2019) 10(1):2066. doi: 10.1038/s41467-019-10058-7
112. Preissner KT, Podack ER, Müller-Eberhard HJ. The membrane attack complex of complement: relation of C7 to the metastable membrane binding site of the intermediate complex C5b-7. *J Immunol* (1985) 135 (1):445–51.
113. DiScipio RG, Chakravarti DN, Muller-Eberhard HJ, Fey GH. The structure of human complement component C7 and the C5b-7 complex. *J Biol Chem* (1988) 263(1):549–60.
114. Menny A, Serna M, Boyd CM, Gardner S, Joseph AP, Morgan BP, et al. CryoEM reveals how the complement membrane attack complex ruptures lipid bilayers. *Nat Commun* (2018) 9(1):5316. doi: 10.1038/s41467-018-07653-5
115. Steckel EW, Welbaum BE, Sodetz JM. Evidence of direct insertion of terminal complement proteins into cell membrane bilayers during cytolysis. Labeling by a photosensitive membrane probe reveals a major role for the eighth and ninth components. *J Biol Chem* (1983) 258(7):4318–24.
116. Broz P, Dixit VM. Inflammasomes: mechanism of assembly, regulation and signalling. *Nat Rev Immunol* (2016) 16(7):407–20. doi: 10.1038/nri.2016.58
117. Shi J, Zhao Y, Wang Y, Gao W, Ding J, Li P, et al. Inflammatory caspases are innate immune receptors for intracellular LPS. *Nature* (2014) 514 (7521):187–92. doi: 10.1038/nature13683
118. Wang K, Sun Q, Zhong X, Zeng M, Zeng H, Shi X, et al. Structural mechanism for GSDMD targeting by autoprocessed caspases in pyroptosis. *Cell* (2020) 180(5):941–955 e20. doi: 10.1016/j.cell.2020.02.002
119. Liu Z, Wang C, Yang J, Chen Y, Zhou B, Abbott DW, et al. Caspase-1 engages full-length gasdermin D through two distinct interfaces that mediate caspase recruitment and substrate cleavage. *Immunity* (2020) 53(1):106–114 e5. doi: 10.1016/j.immuni.2020.06.007
120. Sarhan J, Liu BC, Muendlein HII, Li P, Nilson R, Tang AY, et al. Caspase-8 induces cleavage of gasdermin D to elicit pyroptosis during. *Proc Natl Acad Sci U S A* (2018) 115(46):E10888–97. doi: 10.1073/pnas.1809548115
121. Orning P, Weng D, Starheim K, Ratner D, Best Z, Lee B, et al. Pathogen blockade of TAK1 triggers caspase-8-dependent cleavage of gasdermin D and cell death. *Science* (2018) 362(6418):1064–9. doi: 10.1126/science.aau2818
122. Chen KW, Demarco B, Heilig R, Shkarina K, Boettcher A, Farady CJ, et al. Extrinsic and intrinsic apoptosis activate pannexin-1 to drive NLRP3 inflammasome assembly. *EMBO J* (2019) 38(10):e101638. doi: 10.15252/embj.2019101638
123. Sollberger G, Choidas A, Burn GL, Habenberger P, Di Lucrezia R, Kordes S, et al. Gasdermin D plays a vital role in the generation of neutrophil extracellular traps. *Sci Immunol* (2018) 3(26):eaar6689. doi: 10.1126/sciimmunol.aar6689
124. Kambara H, Liu F, Zhang X, Liu P, Bajrami B, Teng Y, et al. Gasdermin D exerts anti-inflammatory effects by promoting neutrophil death. *Cell Rep* (2018) 22(11):2924–36. doi: 10.1016/j.celrep.2018.02.067
125. Burgener SS, Leborgne NGF, Snipas SJ, Salvesen GS, Bird PII, Benarafa C. Cathepsin G inhibition by Serpinb1 and Serpinb6 prevents programmed necrosis in neutrophils and monocytes and reduces GSDMD-driven inflammation. *Cell Rep* (2019) 27(12):3646–3656.e5. doi: 10.1016/j.celrep.2019.05.065

126. Taabazuing CY, Okondo MC, Bachovchin DA. Pyroptosis and apoptosis pathways engage in bidirectional crosstalk in monocytes and macrophages. *Cell Chem Biol* (2017) 24(4):507–514.e4. doi: 10.1016/j.chembiol.2017.03.009
127. Zhou Z, He H, Wang K, Shi X, Wang Y, Su Y, et al. Granzyme A from cytotoxic lymphocytes cleaves GSDMB to trigger pyroptosis in target cells. *Science* (2020) 368(6494):eaaz7548. doi: 10.1126/science.aaz7548
128. Zhang Z, Zhang Y, Xia S, Kong Q, Li S, Liu X, et al. Gasdermin E suppresses tumour growth by activating anti-tumour immunity. *Nature* (2020) 579 (7799):415–20. doi: 10.1038/s41586-020-2071-9
129. Liu Y, Fang Y, Chen X, Wang Z, Liang X, Zhang T, et al. Gasdermin E-mediated target cell pyroptosis by CAR T cells triggers cytokine release syndrome. *Sci Immunol* (2020) 5(43):eaax7969. doi: 10.1126/sciimmunol.aax7969
130. Lanier LL. NK CELL RECOGNITION. *Annu Rev Immunol* (2004) 23 (1):225–74. doi: 10.1146/annurev.immunol.23.021704.115526
131. Almeida CR, Davis DM. Segregation of HLA-C from ICAM-1 at NK cell immune synapses is controlled by its cell surface density. *J Immunol* (2006) 177(10):6904. doi: 10.4049/jimmunol.177.10.6904
132. Coscoy L, Ganem D. Kaposi's sarcoma-associated herpesvirus encodes two proteins that block cell surface display of MHC class I chains by enhancing their endocytosis. *Proc Natl Acad Sci U S A* (2000) 97(14):8051–6. doi: 10.1073/pnas.140129797
133. Garrido F, Aptsiauri N, Doorduijn EM, Garcia Lora AM, van Hall T. The urgent need to recover MHC class I in cancers for effective immunotherapy. *Curr Opin Immunol* (2016) 39:44–51. doi: 10.1016/j.coi.2015.12.007
134. Bauer S, Groh V, Wu J, Steinle A, Phillips JH, Lanier LL, et al. Activation of NK cells and T cells by NKG2D, a receptor for stress-inducible MICA. *Science* (1999) 285(5428):727. doi: 10.1126/science.285.5428.727
135. Cosman D, Müllberg J, Sutherland CL, Chin W, Armitage R, Fanslow W, et al. ULBPs, Novel MHC class I–related molecules, bind to CMV glycoprotein UL16 and stimulate NK cytotoxicity through the NKG2D receptor. *Immunity* (2001) 14(2):123–33. doi: 10.1016/S1074-7613(01)00095-4
136. Dieckmann NMG, Frazer GL, Asano Y, Stinchcombe JC, Griffiths GM. The cytotoxic T lymphocyte immune synapse at a glance. *J Cell Sci* (2016) 129 (15):2881. doi: 10.1242/jcs.186205
137. Kabanova A, Zurli V, Baldari CT. Signals controlling lytic granule polarization at the cytotoxic immune synapse. *Front Immunol* (2018) 9:307. doi: 10.3389/fimmu.2018.00307
138. Krzewski K, Coligan JE. Human NK cell lytic granules and regulation of their exocytosis. *Front Immunol* (2012) 3:335. doi: 10.3389/fimmu.2012.00335
139. Luzio JP, Hackmann Y, Dieckmann NMG, Griffiths GM. The biogenesis of lysosomes and lysosome-related organelles. *Cold Spring Harbor Perspect Biol* (2014) 6(9):a016840. doi: 10.1101/cshperspect.a016840PMID-25183830
140. Lopez JA, Susanto O, Jenkins MR, Lukoyanova N, Sutton VR, Law RH, et al. Perforin forms transient pores on the target cell plasma membrane to facilitate rapid access of granzymes during killer cell attack. *Blood* (2013) 121(14):2659–68. doi: 10.1182/blood-2012-07-446146
141. Leung C, Hodel AW, Brennan AJ, Lukoyanova N, Tran S, House CM, et al. Real-time visualization of perforin nanopore assembly. *Nat Nanotechnol* (2017) 12(5):467–73. doi: 10.1038/nnano.2016.303
142. Liu X, Lieberman J. A Mechanistic understanding of pyroptosis: the fiery death triggered by invasive infection. *Adv Immunol* (2017) 135:81–117. doi: 10.1016/bs.ai.2017.02.002
143. Rogers C, Erkes DA, Nardone A, Aplin AE, Fernandes-Alnemri T, Alnemri ES. Gasdermin pores permeabilize mitochondria to augment caspase-3 activation during apoptosis and inflammasome activation. *Nat Commun* (2019) 10(1):1689. doi: 10.1038/s41467-019-09397-2
144. Meri S, Morgan BP, Davies A, Daniels RH, Olavesen MG, Waldmann H, et al. Human protectin (CD59), an 18,000-20,000 MW complement lysis restricting factor, inhibits C5b-8 catalysed insertion of C9 into lipid bilayers. *Immunology* (1990) 71(1):1–9.
145. Ninomiya H, Sims PJ. The human complement regulatory protein CD59 binds to the alpha-chain of C8 and to the "b"domain of C9. *J Biol Chem* (1992) 267(19):13675–80.
146. Takeda J, Miyata T, Kawagoe K, Iida Y, Endo Y, Fujita T, et al. Deficiency of the GPI anchor caused by a somatic mutation of the PIG-A gene in paroxysmal nocturnal hemoglobinuria. *Cell* (1993) 73(4):703–11. doi: 10.1016/0092-8674(93)90250-t
147. Nevo Y, Ben-Zeev B, Tabib A, Straussberg R, Anikster Y, Shorer Z, et al. CD59 deficiency is associated with chronic hemolysis and childhood relapsing immune-mediated polyneuropathy. *Blood* (2013) 121(1):129–35. doi: 10.1182/blood-2012-07-441857
148. Haliloglu G, Maluenda J, Sayinbatur B, Aumont C, Temucin C, Tavil B, et al. Early-onset chronic axonal neuropathy, strokes, and hemolysis: inherited CD59 deficiency. *Neurology* (2015) 84(12):1220–4. doi: 10.1212/WNL.0000000000001391
149. Chauhan AK, Moore TL. Presence of plasma complement regulatory proteins clusterin (Apo J) and vitronectin (S40) on circulating immune complexes (CIC). *Clin Exp Immunol* (2006) 145(3):398–406. doi: 10.1111/j.1365-2249.2006.03135.x
150. Tschopp J, Chonn A, Hertig S, French LE. Clusterin, the human apolipoprotein and complement inhibitor, binds to complement C7, C8 beta, and the b domain of C9. *J Immunol* (1993) 151(4):2159–65.
151. Podack ER, Kolb WP, Müller-Eberhard HJ. The SC5b-7 complex: formation, isolation, properties, and subunit composition. *J Immunol* (1977) 119 (6):2024–9.
152. Podack ER, Preissner KT, Müller-Eberhard HJ. Inhibition of C9 polymerization within the SC5b-9 complex of complement by S-protein. *Acta Pathol Microbiol Immunol Scand Suppl* (1984) 284:89–96.
153. Singh B, Su YC, Riesbeck K. Vitronectin in bacterial pathogenesis: a host protein used in complement escape and cellular invasion. *Mol Microbiol* (2010) 78(3):545–60. doi: 10.1111/j.1365-2958.2010.07373.x
154. Rothstein TL, Mage M, Jones G, McHugh LL. Cytotoxic T lymphocyte sequential killing of immobilized allogeneic tumor target cells measured by time-lapse microcinematography. *J Immunol (Baltimore Md. 1950)* (1978) 121(5):1652–6.
155. Bhat R, Watzl C. Serial killing of tumor cells by human natural killer cells–enhancement by therapeutic antibodies. *PloS One* (2007) 2(3):e326. doi: 10.1371/journal.pone.0000326
156. Choi PJ, Mitchison TJ. Imaging burst kinetics and spatial coordination during serial killing by single natural killer cells. *Proc Natl Acad Sci U S A* (2013) 110(16):6488–93. doi: 10.1073/pnas.1221312110
157. Vanherberghen B, Olofsson PE, Forslund E, Sternberg-Simon M, Khorshidi MA, Pacouret S, et al. Classification of human natural killer cells based on migration behavior and cytotoxic response. *Blood* (2013) 121(8):1326–34. doi: 10.1182/blood-2012-06-439851
158. Blakely A, Gorman K, Ostergaard H, Svoboda K, Liu CC, Young JD, et al. Resistance of cloned cytotoxic T lymphocytes to cell-mediated cytotoxicity. *J Exp Med* (1987) 166(4):1070–83. doi: 10.1084/jem.166.4.1070
159. Kranz DM, Eisen HN. Resistance of cytotoxic T lymphocytes to lysis by a clone of cytotoxic T lymphocytes. *Proc Natl Acad Sci U S A* (1987) 84 (10):3375–9. doi: 10.1073/pnas.84.10.3375
160. Lopez JA, Jenkins MR, Rudd-Schmidt JA, Brennan AJ, Danne JC, Mannering SII, et al. Rapid and unidirectional perforin pore delivery at the cytotoxic immune synapse. *J Immunol* (2013) 191(5):2328–34. doi: 10.4049/jimmunol.1301205
161. Verret CR, Firmenich AA, Kranz DM, Eisen HN. Resistance of cytotoxic T lymphocytes to the lytic effects of their toxic granules. *J Exp Med* (1987) 166 (5):1536–47. doi: 10.1084/jem.166.5.1536
162. Rudd-Schmidt JA, Hodel AW, Noori T, Lopez JA, Cho HJ, Verschoor S, et al. Lipid order and charge protect killer T cells from accidental death. *Nat Commun* (2019) 10(1):5396. doi: 10.1038/s41467-019-13385-x
163. Golstein P. Sensitivity of cytotoxic T cells to T-cell mediated cytotoxicity. *Nature* (1974) 252(5478):81–3. doi: 10.1038/252081a0
164. Kuppers RC, Henney CS. Studies on the mechanism of lymphocyte-mediated cytolysis. IX. Relationships between antigen recognition and lytic expression in killer T cells. *J Immunol* (1977) 118(1):71–6.
165. Huang JF, Yang Y, Sepulveda H, Shi W, Hwang I, Peterson PA, et al. TCR-mediated internalization of peptide-MHC complexes acquired by T cells. *Science* (1999) 286(5441):952–4. doi: 10.1126/science.286.5441.952
166. Kupfer A, Singer SJ, Dennert G. On the mechanism of unidirectional killing in mixtures of two cytotoxic T lymphocytes. Unidirectional polarization of cytoplasmic organelles and the membrane-associated cytoskeleton in the effector cell. *J Exp Med* (1986) 163(3):489–98. doi: 10.1084/jem.163.3.489

167. Burrows SR, Fernan A, Argaet V, Suhrbier A. Bystander apoptosis induced by CD8+ cytotoxic T cell (CTL) clones: implications for CTL lytic mechanisms. *Int Immunol* (1993) 5(9):1049–58. doi: 10.1093/intimm/5.9.1049
168. Jiang SB, Ojcius DM, Persechini PM, Young JD. Resistance of cytolytic lymphocytes to perforin-mediated killing. Inhibition of perforin binding activity by surface membrane proteins. *J Immunol* (1990) 144(3):998–1003.
169. Cohnen A, Chiang SC, Stojanovic A, Schmidt H, Claus M, Saftig P, et al. Surface CD107a/LAMP-1 protects natural killer cells from degranulation-associated damage. *Blood* (2013) 122(8):1411–8. doi: 10.1182/blood-2012-07-441832
170. Krzewski K, Gil-Krzewska A, Nguyen V, Peruzzi G, Coligan JE. LAMP1/CD107a is required for efficient perforin delivery to lytic granules and NK-cell cytotoxicity. *Blood* (2013) 121(23):4672–83. doi: 10.1182/blood-2012-08-453738
171. Antia R, Schlegel RA, Williamson P. Binding of perforin to membranes is sensitive to lipid spacing and not headgroup. *Immunol Lett* (1992) 32 (2):153–7. doi: 10.1016/0165-2478(92)90108-z
172. Burack WR, Lee KH, Holdorf AD, Dustin ML, Shaw AS. Cutting edge: quantitative imaging of raft accumulation in the immunological synapse. *J Immunol* (2002) 169(6):2837–41. doi: 10.4049/jimmunol.169.6.2837
173. Gaus K, Chklovskaia E, Fazekas de St Groth B, Jessup W, Harder T. Condensation of the plasma membrane at the site of T lymphocyte activation. *J Cell Biol* (2005) 171(1):121–31. doi: 10.1083/jcb.200505047
174. Fischer K, Voelkl S, Berger J, Andreesen R, Pomorski T, Mackensen A. Antigen recognition induces phosphatidylserine exposure on the cell surface of human CD8+ T cells. *Blood* (2006) 108(13):4094–101. doi: 10.1182/blood-2006-03-011742
175. Zech T, Ejsing CS, Gaus K, de Wet B, Shevchenko A, Simons K, et al. Accumulation of raft lipids in T-cell plasma membrane domains engaged in TCR signalling. *EMBO J* (2009) 28(5):466–76. doi: 10.1038/emboj.2009.6
176. Basu R, Whitlock BM, Husson J, Le Floc'h A, Jin W, Oyler-Yaniv A, et al. Cytotoxic T cells use mechanical force to potentiate target cell killing. *Cell* (2016) 165(1):100–10. doi: 10.1016/j.cell.2016.01.021
177. Tamzalit F, Wang MS, Jin W, Tello-Lafoz M, Boyko V, Heddleston JM, et al. Interfacial actin protrusions mechanically enhance killing by cytotoxic T cells. *Sci Immunol* (2019) 4(33):eaav5445. doi: 10.1126/sciimmunol.aav5445
178. Tamzalit F, Tran D, Jin W, Boyko V, Bazzi H, Kepecs A, et al. Centrioles control the capacity, but not the specificity, of cytotoxic T cell killing. *Proc Natl Acad Sci U S A* (2020) 117(8):4310–9. doi: 10.1073/pnas.1913220117
179. Gawden-Bone CM, Griffiths GM. Phospholipids: pulling back the actin curtain for granule delivery to the immune synapse. *Front Immunol* (2019) 10:700. doi: 10.3389/fimmu.2019.00700
180. Andrews NW, Corrotte M. Plasma membrane repair. *Curr Biol* (2018) 28(8): R392–7. doi: 10.1016/j.cub.2017.12.034
181. Reddy A, Caler EV, Andrews NW. Plasma membrane repair is mediated by Ca(2+)-regulated exocytosis of lysosomes. *Cell* (2001) 106(2):157–69. doi: 10.1016/s0092-8674(01)00421-4
182. McNeil PL, Steinhardt RA. Plasma membrane disruption: repair, prevention, adaptation. *Annu Rev Cell Dev Biol* (2003) 19:697–731. doi: 10.1146/annurev.cellbio.19.111301.140101
183. Keefe D, Shi L, Feske S, Massol R, Navarro F, Kirchhausen T, et al. Perforin triggers a plasma membrane-repair response that facilitates CTL induction of apoptosis. *Immunity* (2005) 23(3):249–62. doi: 10.1016/j.immuni.2005.08.001
184. Thiery J, Keefe D, Saffarian S, Martinvalet D, Walch M, Boucrot E, et al. Perforin activates clathrin- and dynamin-dependent endocytosis, which is required for plasma membrane repair and delivery of granzyme B for granzyme-mediated apoptosis. *Blood* (2010) 115(8):1582–93. doi: 10.1182/blood-2009-10-246116
185. Thiery J, Keefe D, Boulant S, Boucrot E, Walch M, Martinvalet D, et al. Perforin pores in the endosomal membrane trigger the release of endocytosed granzyme B into the cytosol of target cells. *Nat Immunol* (2011) 12(8):770–7. doi: 10.1038/ni.2050
186. Voskoboinik I, Whisstock JC, Trapani JA. Perforin and granzymes: function, dysfunction and human pathology. *Nat Rev Immunol* (2015) 15(6):388–400. doi: 10.1038/nri3839
187. Rühl S, Shkarina K, Demarco B, Heilig R, Santos JC, Broz P. ESCRT-dependent membrane repair negatively regulates pyroptosis downstream of GSDMD activation. *Science* (2018) 362(6417):956. doi: 10.1126/science.aar7607
188. Jimenez AJ, Maiuri P, Lafaurie-Janvore J, Divoux S, Piel M, Perez F. ESCRT machinery is required for plasma membrane repair. *Science* (2014) 343 (6174):1247136. doi: 10.1126/science.1247136
189. Skowyra ML, Schlesinger PH, Naismith TV, Hanson PII. Triggered recruitment of ESCRT machinery promotes endolysosomal repair. *Science* (2018) 360(6384):eaar5078. doi: 10.1126/science.aar5078

Conflict of Interest: The authors declare that the research was conducted in the absence of any commercial or financial relationships that could be construed as a potential conflict of interest.

frontiers in Immunology

REVIEW
published: 22 February 2021
doi: 10.3389/fimmu.2021.597951

Breaching the Bacterial Envelope: The Pivotal Role of Perforin-2 (MPEG1) Within Phagocytes

Leidy C. Merselis[†], *Zachary P. Rivas*[†] *and George P. Munson*[*]

Department of Microbiology and Immunology, Leonard M. Miller School of Medicine, University of Miami, Miami, FL, United States

OPEN ACCESS

Edited by:
Cordula M. Stover, University of Leicester, United Kingdom

Reviewed by:
Ilia Voskoboinik, Peter MacCallum Cancer Centre, Australia
Doryen Bubeck, Imperial College London, United Kingdom

***Correspondence:**
George P. Munson
gmunson@miami.edu

[†]*These authors have contributed equally to this work*

Specialty section:
This article was submitted to Molecular Innate Immunity, a section of the journal Frontiers in Immunology

Received: *22 August 2020*
Accepted: *04 January 2021*
Published: *22 February 2021*

Citation:
Merselis LC, Rivas ZP and Munson GP (2021) Breaching the Bacterial Envelope: The Pivotal Role of Perforin-2 (MPEG1) Within Phagocytes. Front. Immunol. 12:597951. doi: 10.3389/fimmu.2021.597951

The membrane attack complex (MAC) of the complement system and Perforin-1 are well characterized innate immune effectors. MAC is composed of C9 and other complement proteins that target the envelope of gram-negative bacteria. Perforin-1 is deployed when killer lymphocytes degranulate to destroy virally infected or cancerous cells. These molecules polymerize with MAC-perforin/cholesterol-dependent cytolysin (MACPF/CDC) domains of each monomer deploying amphipathic β-strands to form pores through target lipid bilayers. In this review we discuss one of the most recently discovered members of this family; Perforin-2, the product of the *Mpeg1* gene. Since their initial description more than 100 years ago, innumerable studies have made macrophages and other phagocytes some of the best understood cells of the immune system. Yet remarkably it was only recently revealed that Perforin-2 underpins a pivotal function of phagocytes; the destruction of phagocytosed microbes. Several studies have established that phagocytosed bacteria persist and in some cases flourish within phagocytes that lack Perforin-2. When challenged with either gram-negative or gram-positive pathogens *Mpeg1* knockout mice succumb to infectious doses that the majority of wild-type mice survive. As expected by their immunocompromised phenotype, bacterial pathogens replicate and disseminate to deeper tissues of *Mpeg1* knockout mice. Thus, this evolutionarily ancient gene endows phagocytes with potent bactericidal capability across taxa spanning sponges to humans. The recently elucidated structures of mammalian Perforin-2 reveal it to be a homopolymer that depends upon low pH, such as within phagosomes, to transition to its membrane-spanning pore conformation. Clinical manifestations of *Mpeg1* missense mutations further highlight the pivotal role of Perforin-2 within phagocytes. Controversies and gaps within the field of Perforin-2 research are also discussed as well as animal models that may be used to resolve the outstanding issues. Our review concludes with a discussion of bacterial counter measures against Perforin-2.

Keywords: pore-forming protein, MACPF/CDC family proteins, innate immune effector, phagosome, phagocyte, perforin-2/MPEG1, macrophage

INTRODUCTION

Perforin-2 is a member of the Membrane Attack Complex, Perforin/Cholesterol-Dependent Cytolysin (MACPF/CDC) superfamily of proteins (1). Most, but not all, members of this family are pore-forming proteins (2–6). This includes lytic bacterial toxins such as pneumolysin and perfringolysin O, as well as innate immune effectors such as complement protein C9 and Perforin-1. In the blood C9, together with other complement proteins, forms the membrane attack complex (MAC) to perforate the envelope of gram-negative bacteria (7, 8). Perforin-1 is deployed when killer lymphocytes degranulate to destroy virally infected or cancerous cells (9, 10). These molecules polymerize into rings with inner diameters of 120–300 Å (7, 10–12). Pores are formed when each MACPF deploys four amphipathic β-strands through lipid bilayers to form the β-barrel of the pore.

The gene encoding Perforin-2, *Mpeg1*, was first described in 1995 as a highly expressed gene within macrophages (13). After noting the presence of a MACPF domain the authors proposed that Perforin-2 was likely another pore-forming protein. However, more than a decade would lapse before functional, mechanistic, and structural research would begin in earnest. It is now clear that *Mpeg1* is a primordial gene present in taxa spanning sponges to humans. Its domain organization has remained little changed by evolution except in cases of gene duplication. In such cases the paralog may diverge from *Mpeg1*. Indeed analyses across taxa and gene families suggest *Mpeg1* is the ancestor of Perforin-1 and MACPF-containing complement proteins (14). In this review we critically evaluate recent progress in the nascent but growing field of Perforin-2 research with an emphasis on its expression and function within phagocytic cells.

PERFORIN-2 STRUCTURE AND CELLULAR LOCATION

Unlike soluble Perforin-1 and C9, Perforin-2 is a type I transmembrane protein (**Figure 1**). In this orientation the MACPF of Perforin-2 resides within the lumen of vesicular structures. As determined by subcellular fractionation of human macrophages, endogenous Perforin-2 colocalizes with markers of the ER, Golgi, endosomes, and phagosomes (15). A proteomic study identified Perforin-2 (referred to as MPS1 in that study) in the phagolysosome compartment of activated murine macrophages (16). Another analyzed bone marrow derived dendritic cells and reported that Perforin-2 co-resides with subunits of the phagocytic NAPDH oxidase and other antimicrobial effectors of endo/phagosomes (17). Moreover, LPS stimulation increased the abundance of Perforin-2 within those vesicles. A third proteomic study found Perforin-2 within macrophage endo/phagosomes following phagocytosis of latex beads (18). Consistent with the studies above, a Perforin-2-RFP fusion protein was shown to co-localize with phagocytosed bacteria (15). This is unlikely to be an artefact because the fusion protein was also shown to be bactericidal against phagocytosed bacteria. In aggregate these studies provide compelling evidence that Perforin-2 is trafficked to endo/phagosomes.

The transmembrane domain of Perforin-2 is followed by a cytosolic tail; typically, of less than 40 residues. As discussed below this short cytosolic tail is involved in the intracellular trafficking of Perforin-2 (19). In addition to the loss of the transmembrane domain, Perforin-1 and C9 have also lost the P2 domain. This latter domain is conserved across taxa and to date has not been found in any gene other than *Mpeg1*. The function of the novel P2 domain was only recently investigated through structural and mechanistic studies (20, 21). Its most prominent feature is an extended β-hairpin—stiffened by inter-strand disulfide bonds—that culminates in a hydrophobic tip (**Figure 2**) (20). The extended β-hairpin is likely involved in the initial interactions with membranes as determined by liposome binding studies with the isolated P2 domain (20). As expected, liposome binding was abolished by deletion of the β-hairpin (20). Consistent with the composition of bacterial membranes, the P2 domain was also found to preferentially bind liposomes containing negatively charged lipids (20). Although more work is required these studies suggest that the P2 domain mediates

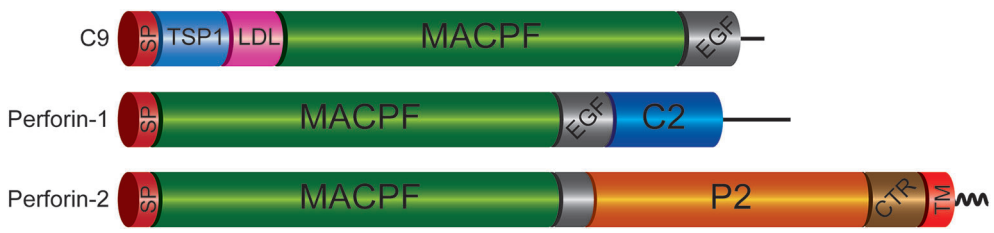

FIGURE 1 | Domain Organization of Mammalian C9 and Perforins. Each of the immune effectors contains a signal peptide (SP), membrane attack complex perforin (MACPF), and epidermal growth factor-like (EGF) domains. However, the latter is truncated in Perforin-2. The P2 domain is unique to Perforin-2 and has been evolutionarily conserved across taxa. Recent structural and functional studies suggest the P2 domain initiates contact with target membranes. However, this does not preclude other putative functions such oligomerization and/or ring stabilization. Another distinctive feature of Perforin-2 is a transmembrane domain (TM) near its carboxy terminus. Although Perforin-2 is initially a Type I transmembrane protein, it is likely cleaved from its TM domain as it is delivered to phagosomes to facilitate oligomerization and pore formation. The TM domain is followed by a short cytosolic tail that is involved in the intracellular trafficking of Perforin-2 to phagosomes. TSP1, thrombospondin type-1 repeat; LDL, low-density lipoprotein receptor class A repeat; C2, calcium-dependent phospholipid binding domain; CTR, carboxy-terminal region.

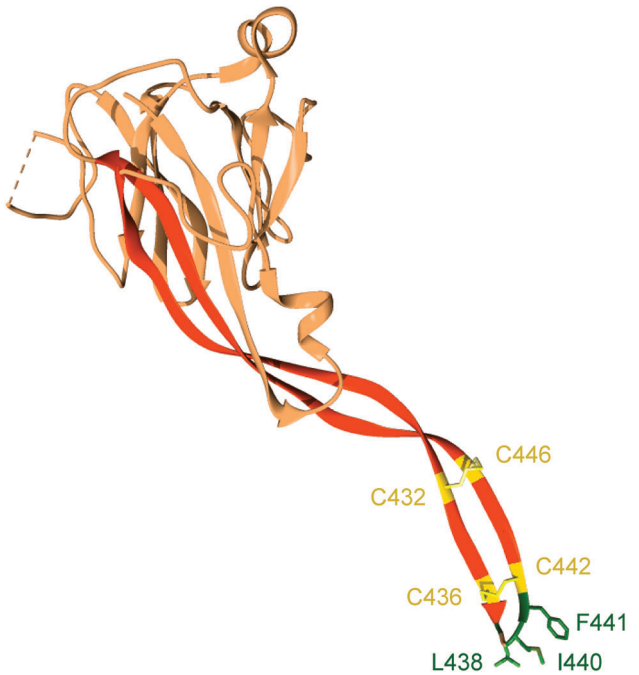

FIGURE 2 | The P2 domain of murine Perforin-2. The most prominent feature within the P2 domain is an extended β-hairpin; highlighted in dark orange. Two disulfide bonds stiffen the β-hairpin. Hydrophobic residues at the β-hairpin's tip are shown in dark green. These residues likely orient Perforin-2 on phagocytosed bacteria by initiating contact with target lipid bilayers. Numbering is relative to UniProt accession number A1L314. This graphic was rendered with UCSF Chimera from PDB file 6SB1 (http://www.rcsb.org/structure/6SB1) (20).

Perforin-2's initial interactions with target membranes. Moreover, its extended β-hairpin may be functionally analogous to domain 4 of cholesterol-dependent cytolysins. Domain 4 contains the cholesterol binding motif as well as a signature undecapeptide at the tip of the domain that anchors the cytolysins to the target membrane (22, 23).

In the recently determined structures of polymerized human and mouse Perforin-2 the P2 and MACPF domains form the exterior and interior rings of the polymer respectively (**Figure 3**) (20, 21). On average these rings are composed of 16 monomers with a height of 83 Å in the pre-pore conformation (20, 21). The pre-pore to pore transition is accompanied by a dramatic 170% increase in height as each monomer deploys its four amphipathic β-strands (**Figure 3**) (20). These β-strands align with each other and those of neighboring subunits to form the barrel of the pore. Acidic pH drives the pre-pore to pore transition (20, 21). This trigger is biologically relevant because it has long been established that phagosomes rapidly acidify and Perforin-2 has been shown to colocalize with phagocytosed bacteria such as *Salmonella enterica* serovar Typhimurium; hereafter *S.* Typhimurium (15, 24, 25). A separate study—graphically summarized in **Figure 4**—found that periplasmic proteins of *S.* Typhimurium were efficiently degraded within the phagosomes of wild-type macrophages and neutrophils (26). In contrast, the degradation of periplasmic proteins was delayed within the phagosomes of *Mpeg1*−/− phagocytes. This was not due to differences in phagosomal proteases because a surface marker (flagellin) was efficiently degraded in both wild-type and Perforin-2 deficient phagocytes. Thus, the *in situ* observations are consistent with Perforin-2 pores breaching the outer membrane of *S.* Typhimurium allowing the passage of phagosomal hydrolases to the periplasmic space.

PERFORIN-2 IN NON-MAMMALIAN SPECIES

Mpeg1 Expression in Invertebrates and Bony Fish

As in other animals the innate immune responses of invertebrates and bony fish provide protection against pathogenic threats. Some of those responses involve changes within the transcriptome and pathogen or PAMP induced expression can be indicative of a gene's immunological role. *Mpeg1* expression is upregulated in the sponge *Suberites domuncula* following LPS challenge relative to untreated animals (27). Similarly, LPS has been shown to induce the expression of *Mpeg1* in the stony coral *Pocillopora damicornis* (28). *Mpeg1* mRNA was significantly upregulated in the brain, head kidney, heart, liver, intestine, and spleen of the starry flounder *Platichthys stellatus* following infection with *Streptococcus parauberis* (29). Relative to untreated controls the expression of *Mpeg1* is significantly increased when the Mediterranean mussel *Mytilus galloprovincialis* is exposed to heat-killed *Vibrio anguillarum* (30). Likewise infection of the disk abalone *Haliotis discus discus* with either gram-negative *Vibrio parahaemolyticus* or gram-positive *Listeria monocytogenes* induces the expression of *Mpeg1* (31). Transcriptome analysis of the larvae of the eastern oyster *Crassostrea virginica* revealed that exposure to either the gram-negative *Phaeobacter inhibens* or gram-positive *Bacillus pumilus* induces expression of *Mpeg1* (32). Similar results were observed when another species of mollusk, *Haliotis midae*, was challenged with live *V. anguillarum* (33). In the latter study increased transcription of *Mpeg1* corresponded with elevated levels of Perforin-2. Of the studies discussed directly above the latter was the only one to evaluate expression at the protein level.

The genome of the orange spotted grouper, *Epinephelus coioides*, harbors two copies of *Mpeg1*. Relative to other organs both are constitutively expressed at high levels in the spleen and head kidney (34). Hematopoiesis occurs in the latter organ and it is analogous to mammalian bone marrow (35). Both copies were significantly upregulated in the spleen and gills following challenge with *Cryptocaryon irritans*, a protozoan parasite of significant concern to the aquaculture industry (34, 36). These results were subsequently confirmed by immunofluorescence with polyclonal antibodies that recognize both isoforms of *E. coiodes* Perforin-2 (37). In aggregate studies across species of invertebrates and bony fish have shown that infection and/or PAMPs induce the expression of *Mpeg1*.

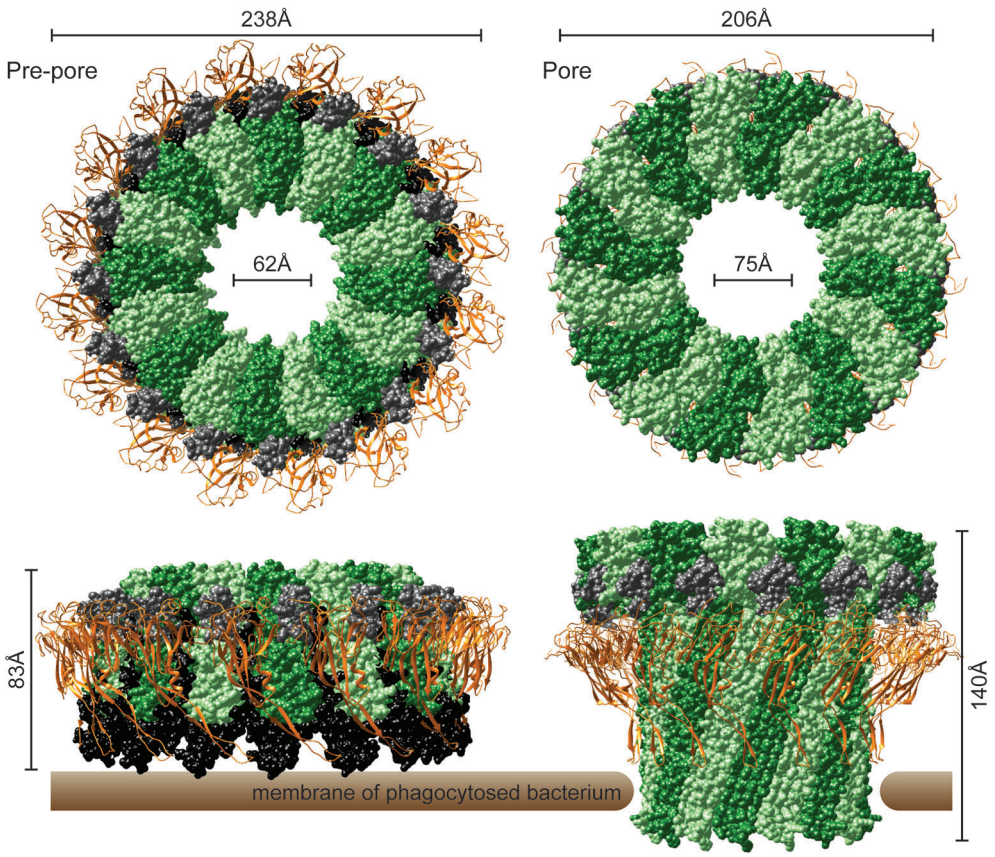

FIGURE 3 | The pre-pore and acid-dependent pore of murine Perforin-2 from top and side views. Each polymer is composed of 16 subunits. MACPF domains line the interior of each polymer and are depicted in alternating shades of green. P2 domains are depicted as orange ribbons that encircle the exterior of each polymer. A truncated EGF domain, light gray, links the MACPF and P2 domains. The carboxy-terminal region is shown in black. This region is visible in the pre-pore but was not resolved in the pore. Images were rendered with UCSF Chimera from PDB files 6SB3 (http://www.rcsb.org/structure/6SB3) and 6SB5 (http://www.rcsb.org/structure/6SB5) (20).

Although infection or PAMP induced expression of *Mpeg1* suggests Perforin-2 plays a role in host defense, *Mpeg1* downregulation following bacterial infection may be indicative of bacterial countermeasures. For example, in *S. domuncula* expression of *Mpeg1* is dampened by the bacterial sponge pathogen *Pseudoalteromonas* sp., but not the commensal bacterium *Endozoicomonas* sp.; species were indeterminate (38). This differential effect is suggestive of a pathogenic countermeasure deployed to defeat Perforin-2. Reduced *Mpeg1* expression has also been documented in the corals *Acropora cerviconis* and *Acropora palmata* when they present with white band disease (28, 39). Although the etiological agent of white band disease is currently unknown, it has been suggested to be bacterial (40). Although the number of studies is few and the data preliminary, they raise the possibility that certain species of pathogenic bacteria may suppress the expression of *Mpeg1* to promote colonization of invertebrates. Whether this is through stealth strategies, such as LPS modifications, or active counter measures, such as effector proteins and toxins, remains to be elucidated.

Analyses of Recombinant Perforin-2 From Invertebrates and Bony Fish

Seminal studies have reconstituted the activity of the complement membrane attack complex and Perforin-1 *in vitro* (7, 12, 41, 42). In recent years researchers have attempted to extend such analyses to Perforin-2. Although the P2 domain of Perforin-2 is evolutionarily conserved from sponges to humans, three studies dispensed with it to evaluate the activity of the MACPF domain from abalone, *H. discus discus*, oyster *Crassostrea gigas*, or flounder *Platichthys stellatus* (29, 31, 43). These studies reported at least some activity against gram-negative (*Edwardsiella piscicida, Escherichia coli*, *Vibrio anguillarum, Vibrio campbelli, Vibrio harveyi, Vibrio ordalii*, *Vibrio tapetis*, and *Vibrio alginolyticus*) and gram-positive (*Streptococcus iniae*, *Streptococcus parauberis*, *Staphylococcus aureus*, *Bacillus thuringiensis*, and *Bacillus subtilis*) bacteria. Others have examined the antibacterial effects of mostly full-length Perforin-2; minus signal peptides, transmembrane domains and carboxy terminal residues (27, 34). Recombinant Perforin-2 from sponge, *S. domuncula*, was reported to have a

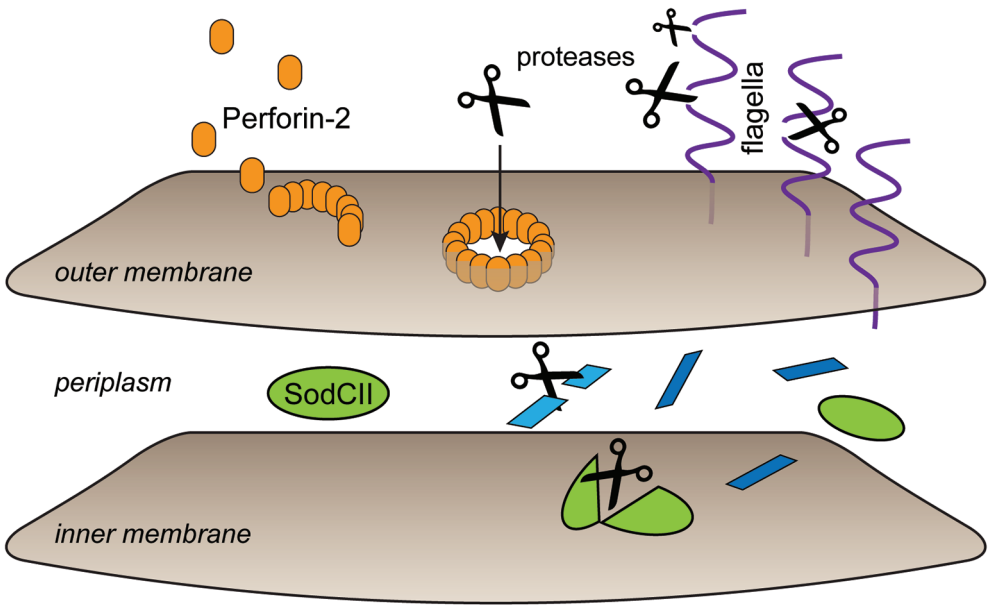

FIGURE 4 | Perforin-2 facilitates protease entry to the periplasmic space. Shortly after microbe phagocytosis Perforin-2 is delivered to the phagosome and deposits on the bacterial envelope. As the phagosome acidifies pre-pores transition to pores that breach the outer membrane. This allows proteases to enter the periplasmic space and begin the digestion of periplasmic and inner membrane proteins. In the absence of Perforin-2 phagosomal proteases are restricted to digestion of outer membrane proteins such as flagellin. This graphic is an adaptation from a previously published version (26).

negative effect upon *E. coli* K-12 and B; but not gram-positive *Staphylococcus aureus* (27). In contrast, Perforin-2a from orange spotted grouper, *E. coiodes*, was reported to inhibit the growth of both gram-negative and gram-positive bacteria (34). *E. coiodes* Perforin-2b was found to be active against only gram-positive bacteria (34). This difference is surprising because the two proteins have 90% overall identity. Nevertheless, differences were also observed when the two proteins were tested against parasitic *C. irritans*. Perforin-2b has no activity against *C. irritans*. In contrast Perforin-2a inhibited motility and caused rounding of theronts, the free-swimming infective form of the parasite. This rounding led the authors to speculate that Perforin-2a decreases *C. irritans* infectivity although this was not directly tested (34).

Although each of the above studies claim that recombinant Perforin-2, or its MACPF, has antimicrobial activity, each has methodological and analytical weaknesses. For example, each recombinant protein was expressed in *E. coli* and thus would lack their usual post-translational modifications. The MACPFs of complement protein C9 and Perforin-1 are known to be glycosylated (10, 44–49). Likewise, the MACPFs of Perforin-2 from sponges to humans are predicted to be N-glycosylated at two or more Asn residues (http://www.cbs.dtu.dk/services/NetNGlyc/). In the case of murine and human Perforin-2 these modifications have been confirmed and may play critical roles in folding and/or pore formation (20, 21, 50, 51). It is also important to point out that none of the four studies reported bacterial killing. Rather, three simply measured the optical absorbance of bacterial cultures (31, 34, 43). The fourth did quantify CFUs but only after overnight incubation with the protein (27). Thus, in all four cases it is unknown if the reported effects are due to bacterial death or growth inhibition.

Although it is impossible to discern the mechanism(s) of the reported effects, we can deduce that pore formation was probably not involved when only the MACPF domain of Perforin-2 was used (31, 43). Structural studies have shown that the P2 domain is likely intrinsic to polymerization and pore formation as it forms the outer ring of both pre-pores and pores with extensive surface area contacts between adjacent P2 domains and MACPFs (**Figure 3**) (20, 21). Phospholipid and liposome binding studies have also revealed that the P2 domain (**Figure 2**) is likely required for initiating interactions with the bacterial envelope (20, 21). The reported activity against gram-positive bacteria is also unexpected because they are surrounded by thick layers of peptidoglycan (27, 31, 34, 43). Although Perforin-2 does kill phagocytosed gram-positive bacteria, this likely requires the assistance of phagosomal hydrolases to degrade the peptidoglycan barrier (15, 52–54).

ANIMAL MODELS FOR PERFORIN-2 RESEARCH

Zebrafish

Zebrafish have three *Mpeg1* paralogs: *Mpeg1, Mpeg1.2, and Mpeg1.3* (55, 56). Both *Mpeg1* and *Mpeg1.2* are expressed in macrophages (57). In contrast, transcriptomic studies of both larval and adult zebrafish have determined that *Mpeg1.3* is a silent gene (57). *Mpeg1* is under the control of the spi/pu.1 transcription factor which also regulates the expression of genes associated with myeloid

differentiation (56). Thus, fluorescent reporters such as mCherry can be used to track macrophages *in situ* when the reporter is expressed from the *Mpeg1* promoter (56) (**Figure 5**). *Mpeg1.2* expression is upregulated during infection with mycobacteria, gram-negative and gram-positive bacteria (57). Curiously, the same bacterial infections inhibit *Mpeg1* expression (57). This expression pattern is unlikely the result of bacterial effectors or toxins, as *Mpeg1* downregulation was also observed when zebrafish were challenged with heat killed or avirulent bacteria.

Although *Mpeg1* and *Mpeg1.2* are inversely expressed during bacterial infections, both genes produce antibacterial responses (57). Zebrafish embryos treated with *Mpeg1* specific morpholinos have increased intracellular loads of *S.* Typhimurium and *Mycobacterium marinum* relative to control morpholinos. Likewise embryos treated with *Mpeg1.2* morpholinos succumb to bacterial infection significantly earlier than *Mpeg1* knockdowns and controls (57). It was also observed that *Mpeg1.2* has a greater antibacterial contribution than *Mpeg1* which is consistent with their expression patterns during infection (57). Curiously, *Mpeg1* knockdowns survive infections longer than control embryos despite greater bacterial burden. It has been proposed that *Mpeg1* is a broad regulator of innate immune responses that promotes survival by diminishing lethal inflammatory responses while *Mpeg1.2* is directly responsible for the bactericidal effects (57). This is surprising given that the two proteins share a common domain architecture and are 80%–90% identical. Additional experimentation is required to clarify the roles of *Mpeg1* and *Mpeg1.2* during infection.

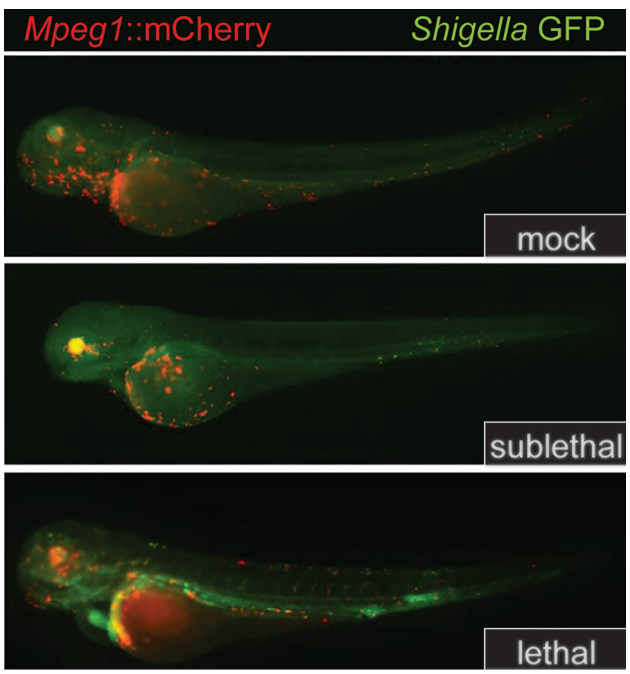

FIGURE 5 | *Mpeg1::mCherry* reporters facilitate the tracking of macrophages in larval zebrafish. Because the expression of Perforin-2 is largely restricted to macrophages in zebrafish, the insertion of *mCherry* into the *Mpeg1* locus allows localization of macrophages in both fixed and live animals. The transgenic animals above were infected with sublethal and lethal doses of *Shigella flexneri* and fixed 24 h post infection. The above images have been previously published (58) and are a composite of the red and green fluorescent channels. This figure was adapted from source images posted at https://doi.org/10.1371/journal.ppat.1003588.g002 under the CC BY 4.0 license.

Transgenic Mice

Eckhard R. Podack (1943–2015), in a remarkably productive collaboration with his trainee Dr. Ryan M. McCormack (59), was the first to demonstrate that mammalian Perforin-2 plays a pivotal role in the elimination of intracellular bacteria including MRSA, *Mycobacterium smegmatis*, and *S.* Typhimurium (15, 53). The Podack laboratory was also the first to report colocalization of Perforin-2 with phagocytosed bacteria (15), and interferon induced expression of *Mpeg1* in keratinocytes, fibroblast and a plethora of other cell types (15). Prof. Podack was also the first to demonstrate that bacterial challenge elicits the expression of *Mpeg1* in murine embryonic fibroblasts (53). Prof. Podack also coined the moniker "Perforin-2" and vigorously advocated for its usage because he understood that Perforin-2 is more descriptive of the protein's function than macrophage-expressed gene 1 protein (MPEG1) (60, 61). When coupled with his lifelong interest in MACPFs of the immune system (62–71), these and other foundational contributions to the field motivated Prof. Podack to commission the development of *Mpeg1* knockout mice at the University of Miami Miller School of Medicine, USA. When raised under specific pathogen-free conditions these knockout mice develop normally and are phenotypically indistinguishable from their wild-type counterparts. However, in another seminal publication—and his last as sole corresponding author — Prof. Podack reported that Perforin-2 deficient mice succumb to low dose bacterial infections that most wild-type mice survive (15). As described below these results are not limited to a particular route of infection or pathogen.

Orogastric Inoculation of Enteric, Gram-Negative Pathogens

Wild-type, *Mpeg1* +/– and –/– mice have been orogastrically challenged with the enteric pathogens *Yersinia pseudotuberculosis* and *S.* Typhimurium (15, 19). In both cases all *Mpeg1* –/– mice succumbed to infection within 15 days of inoculation (**Figure 6**). In contrast all wild-type mice survived sublethal challenges. Heterozygous mice revealed a gene dosage effect with survival profiles between wild-type and *Mpeg1* –/– mice. Perforin-2 deficiency also correlated with significantly higher loads of the pathogens in the intestines and dissemination to deeper tissues such as spleens and livers (**Figure 6**) (15, 19). Thus, two independent studies have demonstrated that Perforin-2 deficient mice are immunocompromised and unable to control infections that their wild-type cohorts survive (15, 19). These findings are further supported by *in vitro* studies which have demonstrated that Perforin-2 deficient phagocytes and fibroblasts are less efficient killers of intracellular bacteria than wild-type cells (15, 26, 52, 53, 72).

Chlamydia Intravaginal Infection

Because phagocytes limit chlamydiae infections, investigators evaluated the role of Perforin-2 in an intravaginal infection model with *Chlamydia muridarum*; a gram-negative, obligate

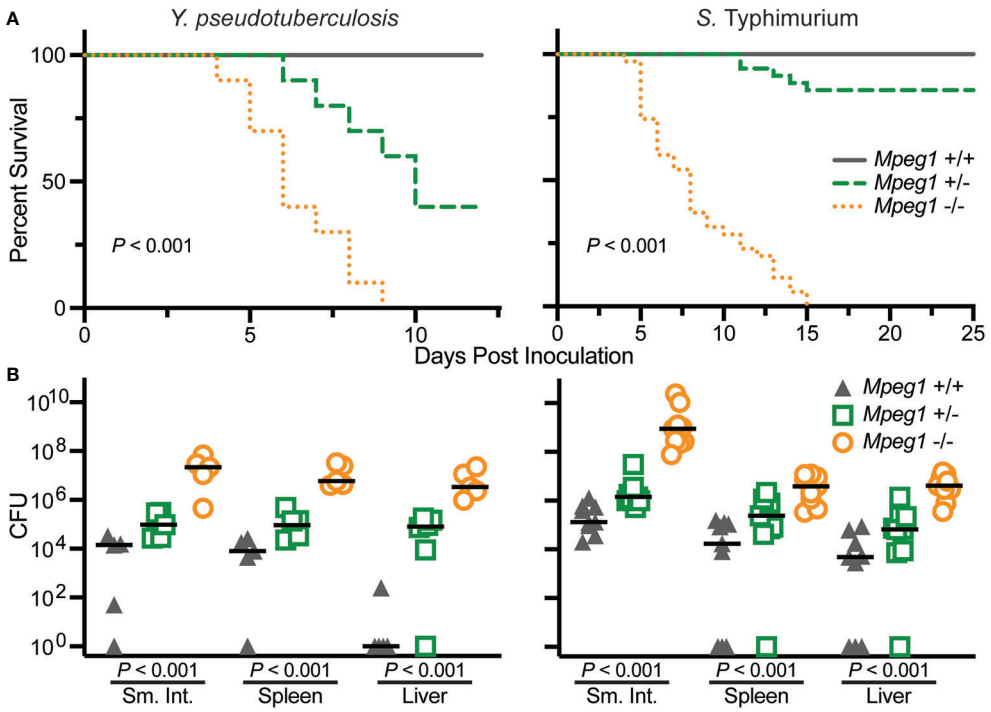

FIGURE 6 | Peforin-2 deficient mice are immunocompromised**. (A)** Survival curves of wild-type, *Mpeg1* +/–, and –/– C57Bl/6 x 129X1/SvJ mice after orogastric inoculation with 10^6 CFU *Y. pseudotuberculosis* or 10^5 CFU *S.* Typhimurium. *P* values determined by Log-rank (Mantel-Cox) test. **(B)** Organ loads of wild-type, *Mpeg1* +/–, and –/– C57Bl/6 x 129X1/SvJ mice after orogastric inoculation with 10^6 CFU *Y. pseudotuberculosis* or 10^5 CFU *S.* Typhimurium. The former group of animals were sacrificed 10 days post inoculation while the latter were sacrificed 5 days post inoculation. Horizontal bars denote the medians. *P* values were determined by non-parametric Kruskal-Wallis test. This figure was adapted from previously published work (15, 19) from source data posted at https://doi.org/10.35092/yhjc.12584993.v1 under the CC BY 4.0 license. Sm. Int., small intestine.

intracellular pathogen (73, 74). In addition, cell based assays had previously established that Perforin-2 limits the growth of chlamydiae in macrophages (72). In the intravaginal model *Mpeg1* –/– mice exhibited significantly greater weight loss than wild-type controls and displayed other signs of morbidity such as ruffled fur (74). Surprisingly, there was no difference in the time to resolution — as determined by shedding of inclusion forming units, a quantitative indicator of infectivity and/or transmissibility— between the two groups. However, the researchers also observed that Perforin-2 deficient mice shed less inclusion forming units; especially, at mid-time points of the infection. To explain this conundrum the researchers speculate that *C. muridarum* may more easily ascend the genital tract and disseminate in Perforin-2 deficient than wild-type mice (74). However the experiment was not designed to test that hypothesis. Therefore, it will be necessary to revisit this model and monitor dissemination to peripheral sites to determine whether or not *C. muridarum* does disseminate in Perforin-2 deficient mice.

Epicutaneous Infection With MRSA

S. aureus is a gram-positive bacterium often present on human skin as a part of the dermal microbiome. To evaluate the role of Perforin-2 at the dermal barrier investigators shaved mice then used tape to disrupt the epidermal barrier prior to administering methicillin resistant *S. aureus* (MRSA) (15). As with other infection modalities the vast majority of infected *Mpeg1* –/– mice perished; although, the time to death was significantly delayed compared to the orogastric models discussed above. In contrast, ca. 80%–100% of the heterozygous and wild-type mice survived MRSA challenge. In another experiment the skin of *Mpeg1* –/– mice contained 3 logs more MRSA than that of wild-type or heterozygous mice (15). As expected, Perforin-2 deficiency was accompanied by bacterial dissemination to the blood, spleen, and kidneys. MRSA may manipulate the transcriptome of host cells to promote its own survival because the pathogen was shown to decrease the expression of *Mpeg1* in human skin cells (75). However, pretreating human skin cells with the commensal bacterium *S. epidermidis* prior to MRSA infection led to increased *Mpeg1* expression and enhanced killing of intracellular bacteria.

Intravenous Delivery of *Listeria*

Perforin-2 has also been shown to aid in defense against another gram-positive bacterium, *Listeria monocytogenes*. Perforin-2 deficient mice infected intravenously with *L. monocytogenes* have significantly greater loads of the pathogen in their spleens and livers than wild-type mice (52). In a pregnancy model of infection Perforin-2 deficient mice had significantly higher loads of *L. monocytogenes* in both the placenta and fetuses (76). In these models injected bacteria are phagocytosed and killed by splenic and

liver macrophages (77). But some phagocytosed bacteria escape to the cytosol where they replicate and disseminate to other cells *via* actin polymerization (78). To escape the phagosomal vacuole *L. monocytogenes* deploys its own pore-forming protein, the cholesterol-dependent cytolysin listeriolysin O (79). Timing is likely critical: *L. monocytogenes* must escape the vacuole before Perforin-2 delivers its lethal blow. Consistent with this hypothesis significantly more bacteria escape to the cytosol of *Mpeg1* −/− than wild-type macrophages in cell based assays (52).

In the above experiments the authors also observed that phagocytosed *L. monocytogenes* were more likely to reside within acidic vacuoles of Perforin-2 deficient macrophages than wild-type macrophages (52). To explain this phenomenon the authors proposed that Perforin-2 limits vacuole acidification. This is controversial as to date there is no mechanistic evidence to support that hypothesis. Rather, the recent discovery that acid drives the Perforin-2 pre-pore to pore transition suggests an alternative hypothesis (20, 21). In our reinterpretation of the available data we propose that fewer *L. monocytogenes* reside within acidic vacuoles because acid activates Perforin-2 which then facilitates the destruction of vacuolar bacteria. In the absence of Perforin-2 bacteria are simply able to persist longer within acidic vacuoles. We also note that another study found that the acidification of *Salmonella* containing vacuoles was equivalent between wild-type and Perforin-2 deficient macrophages; see Bai et al., 2018, Supplementary Materials (26).

Contradictory Signals: Perforin-2 and Type I IFN Signaling

Although *Mpeg1* is an IFN stimulated gene (15, 53), it has also been reported that Perforin-2 is required for Type I IFN signaling by forming complexes with IFN receptors IFNAR1 and IFNAR2 (80). The impetus for that study was the observation that *Mpeg1* deficient mice are resistant to LPS induced septic shock; a model in which Type I IFNs play a central role in driving the cytokine storm. However other studies found that *Mpeg1* deficient mice, on either C57BL/6 or 129X1/SvJ backgrounds, are not more resistant to LPS induced septic shock than wild-type animals (81). As validation of the latter study's experimental design and outcome, both wild-type and knockout mice on the 129X1/SvJ genetic background were more resistant to LPS than C57BL/6 mice. This effect is consistent with previous studies and is due to the fact that 129X1/SvJ mice lack caspase-11 (82, 83).

Further contradicting Perforin-2's role in Type I IFN signaling, an RNAseq study found that Type I IFN signaling is functional in *Mpeg1* −/− murine phagocytes stimulated with IFN-β (84). It is also difficult to reconcile the proposed complexes with the structures of Perforin-2 and IFNARs (20, 21, 80, 85). For example, it was reported that binding to and signaling through IFNAR1 requires glycosylation of Perforin-2 residues Asn185 and Asn269; numbering relative to UniProt entry A1L314 (https://www.uniprot.org/uniprot/A1L314) (80). Although the structures of both mouse and human Perforin-2 confirm that both residues are glycosylated, Asn185 and Asn269 reside on opposite faces of the MACPF domain (**Figure 7**) (20, 21). Not surprisingly, docking simulations with the known structures of IFNAR1 and Perforin-2 monomers found no plausible pathway for simultaneous binding to Asn185 and Asn269 by IFNAR1 (86). Thus, it is not clear how IFNAR1 is able to contact both as has been proposed (80). Likewise, it has been reported that glycosylation of Asn375 in the P2 domain is essential for interactions with IFNAR2 (80). This residue is visible in all published structures of murine and human Perforin-2 but unlike Asn185 and Asn269, Asn375 is not glycosylated (**Figure 7**, middle image) (20, 21). Although it is possible that the glycosylation pattern of Perforin-2 differs

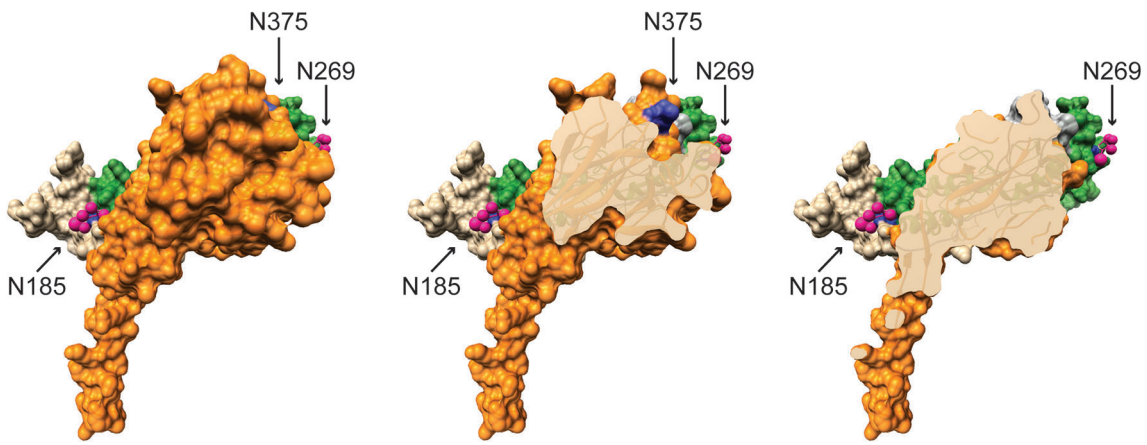

FIGURE 7 | Glycosylated Asn185 and Asn269 are located on opposite faces of the MACPF domain. A monomer of murine Perforin-2 shown in (Left) full view and (Middle & Right) progressive cross-sections into the molecule. The MACPF and P2 domains are shaded green and orange respectively. The truncated EGF domain, which connects the MACPF and P2 domains, is shaded grey and is partially visible in the upper right of the far right image. The extended carboxy terminal region is shown in tan. Asn185 and 269 are conserved and glycosylated in both murine and human Perforin-2 (20, 21). Their glycans are shown as pink spheres. In contrast to the MACPFs, the P2 domains of both species are devoid of glycosylation. This includes the absence of glycosylation of Asn375; shaded deep blue above and visible in the middle image. Images were rendered with UCSF Chimera from PDB file 6SB3 (http://www.rcsb.org/structure/6SB3) (20). Residue numbering is relative to UniProt entry A1L314 (https://www.uniprot.org/uniprot/A1L314).

between expression systems and cell lines, bioinformatics suggests otherwise. Like other servers, NetNGlyc identifies Asn-X-Ser/Thr sequons (http://www.cbs.dtu.dk/services/NetNGlyc/). However, its neural network also evaluates the surrounding sequences to predict the probability of glycosylation. In agreement with the structural studies (20, 21). NetNGlyc predicts glycosylation of Asn185 and Asn269 but not Asn375. In summary, the reported requirement for Perforin-2 in Type I IFN signaling and proposed mechanism (80) are challenged by transcriptomics, LPS induced sterile septic shock, and molecular analyses. Clearly additional studies are required to resolve these contradictions.

PfpL, A Paralog of Murine *Mpeg1*

Unlike humans, mice have a paralog of *Mpeg1* named Pore-Forming Protein Like (*PfpL*, UniProt entry Q5RKV8). Over their entire length PfpL and murine Perforin-2 are 65% identical. This suggest that PfpL could also function as an immune effector. However, to date there have been no functional studies of PfpL and expression of the *PfpL* transcript appears to be more limited than that of *Mpeg1* as determined by the murine gene expression database, GXD (87). Unlike *Mpeg1*, *PfpL* expression has only been observed in the context of murine development and in the adult mouse liver. Particularly high expression was also observed in a subset of trophoblast giant cells and the parietal yolk sac (88). Further experiments are needed to determine whether or not PfpL is a functional immune effector. In addition, greater clarity is required regarding the timing and location of its expression. However, the restricted expression of *PfpL* and the clear immunocompromised phenotype of *Mpeg1* knockout mice suggest *PfpL* is at best a minor player in host defense under most circumstances.

CLINICAL IMPACTS OF *MPEG1* MISSENSE AND NONSENSE MUTATIONS

The Genome Aggregation Database (gnomAD, https://gnomad.broadinstitute.org/) catalogs 432 missense (codon changes) and 23 nonsense (premature stop codon) mutations in human *Mpeg1* (89). With few exceptions these mutations are heterozygous and to date only five have been functionally evaluated (90, 91). In one study a young adult female with a history of recurrent polymicrobial skin infections was found to have a heterozygous nonsense mutation in codon Tyr430*; numbering relative to UniProt entry Q2M385 (https://www.uniprot.org/uniprot/Q2M385) (91). This nonsense mutation is within the extended β-hairpin of the P2 domain (**Figure 8A**). It is not known if this truncated protein is stably expressed. But even if it is, it is unlikely to reach endo/phagosomes because it lacks a transmembrane domain and cytosolic tail for retention and intracellular trafficking respectively. Thus, this mutation likely reduces the availability of Perforin-2 within endo/phagosomes. As expected, the ability of the patient's blood derived phagocytes to eliminate intracellular bacterial pathogens was found to be significantly impaired compared to phagocytes from healthy donors (**Figure 8B**) (91). This impairment is the likely cause of the patient's clinical presentations and is consistent with the gene dosage effects seen with Perforin-2 heterozygous mice after infection with a variety of pathogens (15, 19).

In another study three *Mpeg1* missense mutations and one nonsense mutation were identified within a cohort of patients with pulmonary nontuberculous mycobacterial infections (90). T73A and P316S are within the MACPF domain while Q398* and P405T reside within the P2 domain (**Figure 8A**). All are

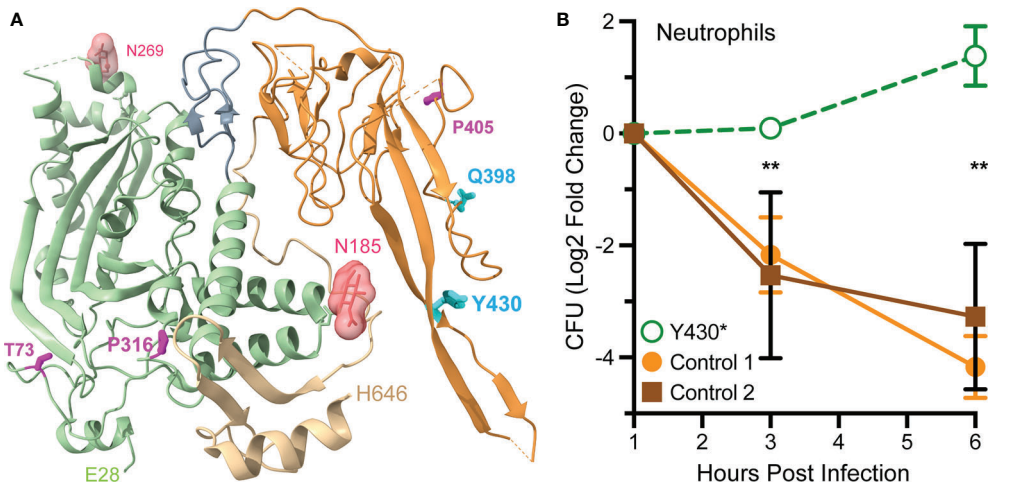

FIGURE 8 | Perforin-2 haploinsufficiency results in the reduced ability of human phagocytes to kill intracellular bacteria. **(A)** A monomer of human Perforin-2 in its pre-pore conformation. The MACPF and P2 domains are depicted in light green and orange respectively. The carboxy-terminal region is shown in tan. Glycans attached to N185 and N269 are shown as space filling models. Also shown are the positions of deleterious missense (magenta) and nonsense (cyan) mutations (90, 91). Residue numbering is relative to relative to UniProt entry Q2M385 (https://www.uniprot.org/uniprot/Q2M385). **(B)** Killing of intracellular *S.* Typhimurium by neutrophils isolated from the blood of a donor carrying a heterozygous Y430* nonsense mutation or healthy controls. Relative bacterial colony forming units are reported as Log2 Fold Change = log2(CFU at time X) – log2(CFU at time initial). $^{**}P < 0.01$ by 2way ANOVA. This figure was adapted from previously published work (91) under the CC BY 4.0 license. Molecular graphics were rendered with UCSF ChimeraX from PDB file 6U2J (http://www.rcsb.org/structure/6U2J) (21).

heterozygous and each patient presented with a history of pulmonary *Mycobacterium avium* complex as well as nonmycobacterial pulmonary infections. Each of the mutations are apparently deleterious because patient derived cells were less able to kill *M. avium* than cells from age matched controls (90). The researchers subsequently used CRISPR/Cas9 to introduce the mutations into THP-1 cells, a human macrophage-like cell line. As expected, THP-1 cells carrying the missense and nonsense mutations exhibited reduced killing capacity when infected with *M. smegmatis, S.* Typhimurium, and *S. aureus*. Based on their locations within the structures of Perforin-2 T73A and P316S may interfere with the deployment of the pore forming β-strands and pre-pore to pore transition respectively (20, 21). If it is stably expressed Q398* is likely secreted to the extracellular milieu because it lacks the transmembrane domain and cytosolic tail of full length Perforin-2. The impact of P405T is harder to predict as it lies in a more disordered region of the structure (21). However, it is also possible that the observed phenotypes are the result of low protein expression and/or instability since the researchers did not evaluate either (90). In the future higher resolution Perforin-2 structures and greater understanding of the mechanism of acid sensing, pre-pore to pore transition, and pore formation may facilitate testable hypotheses of the clinical impacts of *Mpeg1* missense mutations.

BACTERIAL DEFENSES AGAINST PERFORIN-2

In resting cells Perforin-2 has a diffuse, perinuclear dispersal. However, it is rapidly relocated to punctate bodies upon exposure to PAMPs or infection (19). Some of these punctate bodies are likely phagosomes because Perforin-2 has been shown to co-localize with phagocytosed bacteria (15). This is consistent with a proteomic study that found Perforin-2 co-resides with subunits of the phagocytic NAPDH oxidase, proton transporters, and many other antimicrobial effectors of phagosomes (17). Other punctate bodies may be sorting endosomes in the process of delivering Perforin-2 to phagosomes because another proteomic study found Perforin-2 in endosomes following phagocytosis of latex beads by macrophages (18). LPS stimulation of bone marrow derived macrophages has also been shown to increase the abundance of Perforin-2 in endo-lysosomes compared to untreated cells (17).

The intracellular trafficking of Perforin-2 is driven by PAMP-dependent ubiquitination — most likely monoubiquitination— of one or more conserved lysines in its short cytosolic tail (19). Mutagenesis of the three most conserved lysines abolished the formation of punctate bodies and Perforin-2 dependent killing of bacteria. Ubiquitination of Perforin-2's cytosolic tail was further shown to be dependent upon a cullin-RING E3 ubiquitin ligase (CRL) complex containing cullin-1 and βTrCP (**Figure 9**) (19). This led to the hypothesis that certain pathogens may deploy Cifs to block the intracellular trafficking of Perforin-2 because CRL activity is dependent upon the ubiquitin like molecule NEDD8 and Cifs are NEDD8 deamidases (92–96). As predicted, the researchers found that wild-type but not *cif* mutants of *Y. pseudotuberculosis* and enteropathogenic *E. coli* (EPEC) blocked the ubiquitination and intracellular trafficking of Perforin-2, as well as Perforin-2 dependent killing (19). In vivo ca. 80% of C57BL/6 mice infected with wild-type *Y. pseudotuberculosis* perished while all mice infected with a *cif* mutant survived (**Figure 10**). This difference was abolished when the two bacterial strains were used to infect *Mpeg1* −/− mice. Although Cif inactivation of CRLs has broad cellular consequences, the latter results suggest that inhibition of Perforin-2 is the primary objective and most consequential effect. While Cifs are just one example of anti-Perforin-2 effectors bacterial pathogens express a multitude of effectors aimed at promoting their survival; many of which have yet to be fully characterized (97). Given that Perforin-2 is a recently described immune effector, it is reasonable to predict that other anti-Perforin-2 effectors will be discovered as the field matures.

DISCUSSION

Relative to other MACPF proteins of innate immune systems, the field of Perforin-2 research is relatively new even though the gene that encodes Perforin-2, *Mpeg1*, is likely the most ancient of the MACPF encoding genes (14). Nevertheless in recent years vertebrate studies have established that Perforin-2 has broad spectrum bactericidal activity that significantly limits pathogen proliferation and dissemination *in vivo* (15, 19, 26, 52–54, 57, 72, 90). There is also evidence to suggest that Perforin-2 functions similarly in invertebrates; although, such studies are hampered by the lack of animal and tractable cell culture models (27, 28, 30, 31, 33, 38, 39). The recent structural determinations of both mouse and human Perforin-2 polymers have further provided significant insight with regards to the mechanism(s) of pore formation (20, 21). Eventually such high-resolution structures may afford greater understanding of the clinical impacts of *Mpeg1* missense mutations amongst the human population.

In vitro recombinant mammalian Perforin-2 spontaneously polymerizes and one of the most significant advancements from *in vitro* studies was the discovery that the pre-pore to pore transition is acid dependent (20, 21). In retrospect the fact that low pH drives pore formation seems intuitive given that Perforin-2 is deployed to acidic phagosomes. Acid dependency may also be a safety mechanism, ensuring that Perforin-2 remains in a latent state so as not to damage the vesicular and cellular membranes of the phagocyte. Acid dependency likely evolved very early as lower metazoans such as sponges, corals, and mollusks have been shown to express *Mpeg1* and have macrophage-like cells that phagocytose and eliminate foreign invaders through the use of lysosomal enzymes, reactive oxygen species, and cellular acidification (98–103). However, the exact mechanism of acid driven pore formation remains to be elucidated. One possibility is that acidification removes inhibitory inter- or intra-domain contacts that prevent pore formation. Clearly one of the most important objectives in this area will be to discover the acid-dependent trigger within Perforin-2.

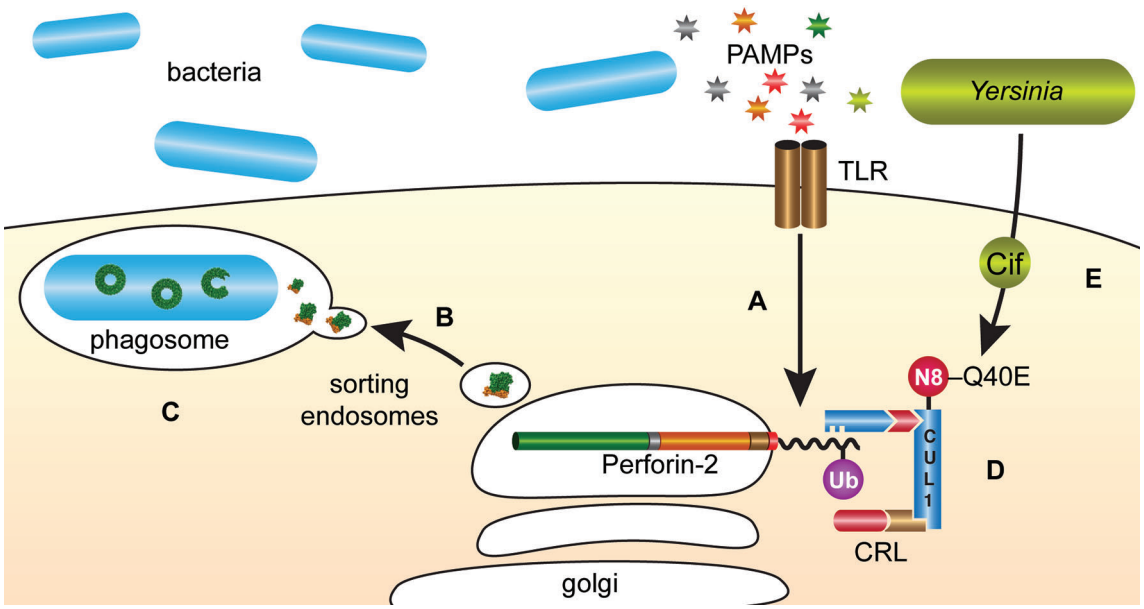

FIGURE 9 | *Y. pseudotuberculosis* and EPEC deploy Cifs to block the delivery of Perforin-2 to phagosomes. (A) The cytosolic tail of Perforin-2 is ubiquitinated in response to PAMPs such as LPS. (B) Ubiquitinated Perforin-2 is rapidly delivered to phagosomes where it oligomerizes and (C) phagosome acidification induces the pre-pore to pore transition. (D) The ligase responsible for conjugating ubiquitin to Perforin-2 is a multi-component cullin-RING E3 ubiquitin ligase (CRL) whose activity is itself dependent upon cullin neddylation. (E) Pathogenic *Y. pseudotuberculosis* and EPEC use Type III secretion systems to inject Cifs into the cytosol of host cells where they deamidate Gln40 of NEDD8. The enzymatic conversion of Gln to Glu inactivates the CRL and thus prevents ubiquitin dependent intracellular trafficking of Perforin-2. N8, NEDD8; Ub, ubiquitin; CUL1, cullin 1.

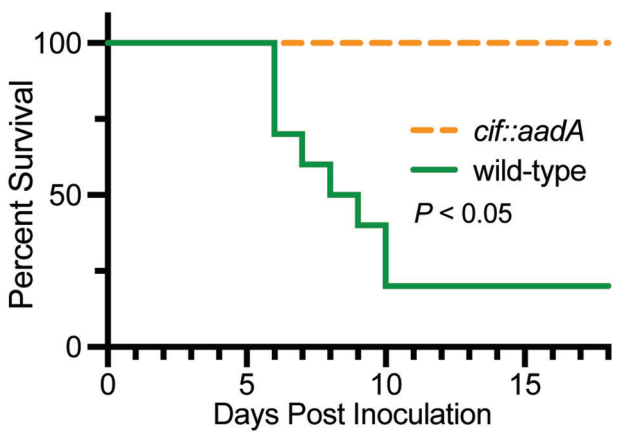

FIGURE 10 | Bacteria lacking the anti-Perforin-2 effector Cif are attenuated *in vivo*. Survival curves of C57BL/6 mice were orogastrically inoculated with 10^8 CFU wild-type *Y. pseudotuberculosis* or an isogenic *cif* mutant. Significance was calculated by log-rank (Mantel–Cox) test. This figure was adapted from work previously published under the CC BY 4.0 license (19).

It is also not yet known if Perforin-2 can breach bacterial membranes by itself or if it requires the assistance of other host proteins. Our review and evaluation of the *in vitro* systems reported to date raises significant doubts that Perforin-2 dependent killing was actually observed with recombinant protein (27, 29–31, 33, 34, 38, 39, 43). Our first major concern is that some researchers opted to purify the MACPF domain in the absence of the P2 domain (29, 31, 43). However, we now know that the P2 domain forms the outer ring of Perforin-2 polymers with extensive surface area packed between the two domains and neighboring subunits (**Figure 3**) (20, 21). Thus, it seems improbable that the MACPF domain of Perforin-2 would polymerize in the absence of the P2 domain. In addition, there is evidence that the extended β-hairpin of the P2 domain mediates the initial interactions with target membranes (**Figure 2**) (20). Therefore, even if the MACPF domain does polymerize it is unclear how it would target bacterial membranes. We also note that all studies with recombinant Perforin-2 did not convincingly demonstrate bacterial killing (27, 29, 31, 34, 43). Rather, most simply reported changes in the optical absorbance of bacterial cultures. As discussed below there is also the possibility that glycosylation is essential for Perforin-2 folding, polymerization, or pore formation/stabilization. These post-translational modifications would be absent in the studies that produced recombinant Perforin-2 or its MACPF in *E. coli* (27, 29, 31, 34, 43). Although claims of recombinant Perforin-2's bactericidal activity are to date unconvincing, the development of a technically sound *in vitro* bactericidal assay would be a substantial advance that would facilitate further mechanistic investigations.

Among other outstanding questions is the necessity of post-translational modifications; specifically, glycosylation. Two independent structural studies observed glycosylation of Asn185 and Asn269 (20, 21). These residues are conserved and glycosylated in both human and mouse Perforin-2. Despite their conservation it is not known if the glycans are required for protein stability/folding, oligomerization, or pore formation/stabilization. Elucidating the functional and mechanistic consequences of Perforin-2 glycosylation may have clinical implications because missense mutations of both Asn185 and Ans269 are present within the human population (gnomAD, https://gnomad.broadinstitute.org/).

There are also significant gaps in our understanding of the intracellular trafficking of Perforin-2. Although it has been shown that ubiquitination of Perforin-2's cytosolic tail drives trafficking (19), the mechanism(s) of intracellular trafficking and delivery to the phagosome is largely unknown. Likewise, the linkage between PAMP/TLR signaling and ubiquitination is unclear. This may involve the activation of a kinase that phosphorylates the cytosolic tail of Perforin-2 prior to CRL-dependent ubiquitination. However, this upstream pathway remains in the realm of the hypothetical.

Perforin-2 may also require proteolytic processing to release it from its transmembrane domain and facilitate subsequent polymerization. Indeed Perforin-2 fragments have been observed after cellular infection (15). Perhaps the cleavage products are relevant to polymerization and pore formation. Alternatively, they may be mechanistically insignificant degradation products. Although it is not yet known which of these two scenarios is correct, we and others suspect that tethering to a vacuolar membrane is inhibitory; preventing polymerization (20, 104, 105). In our "safety tether" hypothesis Perforin-2 is maintained as a monomer as long as it exists as a Type I transmembrane protein. However we also note that there is evidence for Perforin-2 dependent autolysis under certain circumstances. For example, Eckhard Podack used negative stain transmission electron microscopy to image apparent Perforin-2 polymers with membrane preparations of HEK-293 cells engineered to overexpress Perforin-2-GFP (15). Of potential relevance to our safety tether hypothesis, Perforin-2 polymers were only observed after partial trypsin digest. Polymers were not observed with undigested preparations. More recently Hung et al. have shown that Perforin-2 is required for the release of IL-33 from dendritic cells (106). Because IL-33 lacks a signal peptide, the authors propose that Perforin-2 forms pores in the plasma membrane to release cytosolic IL-33. Although the supporting data is quite convincing, the study raises many mechanistic questions. For example, does Perforin-2 attack the plasma membrane from the exterior or interior of the cell? In either case does pore formation involve proteolytic cleavage and/or low pH? In addition there is no known mechanism for the selective gating of Perforin-2 pores. Therefore, it seems likely that IL-33 secreting dendritic cells would also release a plethora of cytosolic molecules. Is Perforin-2 autolysis ultimately lethal or is autolysis somehow mitigated to prevent lethality? Addressing these and other questions will provide greater understanding of Perforin-2 functionality and may also identify novel clinical avenues that could be used to treat diseases associated with Perforin-2 deficiencies.

Although Perforin-2 research has made considerable progress from the perspective of the host, less is known about pathogen strategies to survive Perforin-2. To date, Cifs are the only class of anti-Perforin-2 effectors to be discovered. Given the persistence of Perforin-2 throughout diverse organisms, it is reasonable to expect that many other pathogenic countermeasures remain undiscovered. With sufficient interest progress in this area is possible and particularly suited to unbiased screens such as Tn-Seq. Once a candidate anti-Perforin-2 effector is identified, it can be thought of as a molecular probe that can elucidate the cellular and molecular mechanisms of Perforin-2 dependent killing. Of course, more passive survival strategies — such as alteration of the bacterial envelope or cell wall — are also possible. Despite numerous unknowns, it is clear that this field is poised for expansion and discovery.

AUTHOR CONTRIBUTIONS

LM, ZR, and GM developed the concept, critically reviewed the literature, and wrote various sections of the manuscript. GM was responsible for figure design and layout. All authors participated in the manuscript revision. All authors contributed to the article and approved the submitted version.

FUNDING

Perforin-2 research in the laboratory of GM is supported by the National Institute of Allergy and Infectious Diseases of the National Institutes of Health under award numbers R01AI110810 and R21AI156567. The content of this publication is solely the responsibility of the authors and does not necessarily represent the official views of the National Institutes of Health.

ACKNOWLEDGMENTS

The authors dedicate this publication to the memory of Eckhard R. Podack (1943–2015); the founder of Perforin-2 research and lead author of seminal studies in the field. Molecular graphics were rendered with UCSF Chimera or ChimeraX, developed by the Resource for Biocomputing, Visualization, and Informatics at the University of California, San Francisco, with support from the Office of Cyber Infrastructure and Computational Biology, National Institute of Allergy and Infectious Diseases, National Institutes of Health under award numbers P41GM103311 and R01GM129325 (107, 108). http://www.rbvi.ucsf.edu/chimera; https://www.cgl.ucsf.edu/chimerax

REFERENCES

1. Lukoyanova N, Hoogenboom BW, Saibil HR. The membrane attack complex, perforin and cholesterol-dependent cytolysin superfamily of pore-forming proteins. *J Cell Sci* (2016) 129:2125–33. doi: 10.1242/jcs.182741
2. Ni T, Gilbert RJC. Repurposing a pore: Highly conserved perforin-like proteins with alternative mechanisms. *Philos Trans R Soc B Biol Sci* (2017) 372. doi: 10.1098/rstb.2016.0212
3. Gilbert RJC. Pore-forming toxins. *Cell Mol Life Sci* (2002) 59:832–44. doi: 10.1007/s00018-002-8471-1
4. Anderluh G, Kisovec M, Kraševec N, Gilbert RJC. Distribution of MACPF/CDC proteins. *Subcell Biochem* (2014) 80:7–30. doi: 10.1007/978-94-017-8881-6_2
5. Yoshida A, Fukazawa M, Ushio H, Aiyoshi Y, Soeda S, Ito K. Study of cell kinetics in anaplastic thyroid carcinoma transplanted to nude mice. *J Surg Oncol* (1989) 41:1–4. doi: 10.1002/jso.2930410104
6. Gilbert RJC, Jiménez JL, Chen S, Tickle IJ, Rossjohn J, Parker M, et al. Two structural transitions in membrane pore formation by pneumolysin, the pore-forming toxin of Streptococcus pneumoniae. *Cell* (1999) 97:647–55. doi: 10.1016/S0092-8674(00)80775-8
7. Podack ER, Tschopp J. Polymerization of the ninth component of complement (C9): Formation of poly(C9) with a tubular ultrastructure resembling the membrane attack complex of complement. *Proc Natl Acad Sci USA* (1982) 79:574–8. doi: 10.1073/pnas.79.2.574
8. Morgan BP, Walters D, Serna M, Bubeck D. Terminal complexes of the complement system: new structural insights and their relevance to function. *Immunol Rev* (2016) 274:141–51. doi: 10.1111/imr.12461
9. Voskoboinik I, Whisstock JC, Trapani JA. Perforin and granzymes: Function, dysfunction and human pathology. *Nat Rev Immunol* (2015) 15:388–400. doi: 10.1038/nri3839
10. Law RHP, Lukoyanova N, Voskoboinik I, Caradoc-Davies TT, Baran K, Dunstone MA, et al. The structural basis for membrane binding and pore formation by lymphocyte perforin. *Nature* (2010) 468:447–51. doi: 10.1038/nature09518
11. Dudkina NV, Spicer BA, Reboul CF, Conroy PJ, Lukoyanova N, Elmlund H, et al. Structure of the poly-C9 component of the complement membrane attack complex. *Nat Commun* (2016) 7:10588. doi: 10.1038/ncomms10588
12. Podack ER, Tschopp J. Circular polymerization of the ninth component of complement. Ring closure of the tubular complex confers resistance to detergent dissociation and to proteolytic degradation. *J Biol Chem* (1982). doi: 10.1073/pnas.79.2.574
13. Spilsbury K, O'Mara MA, Wu WM, Rowe PB, Symonds G, Takayama Y. Isolation of a novel macrophage-specific gene by differential cDNA analysis. *Blood* (1995). doi: 10.1182/blood.v85.6.1620.bloodjournal8561620
14. Dangelo ME, Dunstone MA, Whisstock JC, Trapani JA, Bird PI. Perforin evolved from a gene duplication of MPEG1, followed by a complex pattern of gene gain and loss within Euteleostomi. *BMC Evol Biol* (2012) 12:59. doi: 10.1186/1471-2148-12-59
15. McCormack RM, de Armas LR, Shiratsuchi M, Fiorentino DG, Olsson ML, Lichtenheld MG, et al. Perforin-2 is essential for intracellular defense of parenchymal cells and phagocytes against pathogenic bacteria. *eLife* (2015) 4:1–29. doi: 10.7554/eLife.06508
16. Garin J, Diez R, Kieffer S, Dermine JF, Duclos S, Gagnon E, et al. The phagosome proteome: Insight into phagosome functions. *J Cell Biol* (2001) 4: e06508. doi: 10.1083/jcb.152.1.165
17. Nakamura N, Lill JR, Phung Q, Jiang Z, Bakalarski C, De Mazière A, et al. Endosomes are specialized platforms for bacterial sensing and NOD2 signalling. *Nature* (2014). doi: 10.1038/nature13133
18. Duclos S, Clavarino G, Rousserie G, Goyette G, Boulais J, Camossetto V, et al. The endosomal proteome of macrophage and dendritic cells. *Proteomics* (2011) 11:854–64. doi: 10.1002/pmic.201000577
19. McCormack RM, Lyapichev K, Olsson ML, Podack ER, Munson GP. Enteric pathogens deploy cell cycle inhibiting factors to block the bactericidal activity of Perforin-2. *eLife* (2015) 4:e06505. doi: 10.7554/eLife.06505
20. Ni T, Jiao F, Yu X, Aden S, Ginger L, Williams SI, et al. Structure and mechanism of bactericidal mammalian perforin-2, an ancient agent of innate immunity. *Sci Adv* (2020) 6:eaax8286. doi: 10.1126/sciadv.aax8286
21. Pang SS, Bayly-Jones C, Radjainia M, Spicer BA, Law RHP, Hodel AW, et al. The cryo-EM structure of the acid activatable pore-forming immune effector Macrophage-expressed gene 1. *Nat Commun* (2019). doi: 10.1038/s41467-019-12279-2
22. Christie MP, Johnstone BA, Tweten RK, Parker MW, Morton CJ. Cholesterol-dependent cytolysins: from water-soluble state to membrane pore. *Biophys Rev* (2018). doi: 10.1007/s12551-018-0448-x
23. Tweten RK. Cholesterol-dependent cytolysins, a family of versatile pore-forming toxins. *Infect Immun* (2005). doi: 10.1128/IAI.73.10.6199-6209.2005
24. Hackam DJ, Rotstein OD, Zhang WJ, Demaurex N, Woodside M, Tsai O, et al. Regulation of phagosomal acidification. Differential targeting of Na +/H + exchangers, Na +/K +-ATPases, and vacuolar-type H +-ATPases. *J Biol Chem* (1997). doi: 10.1074/jbc.272.47.29810
25. Beyenbach KW, Wieczorek H. The V-type H+ ATPase: Molecular structure and function, physiological roles and regulation. *J Exp Biol* (2006). doi: 10.1242/jeb.02014
26. Bai F, McCormack RM, Hower S, Plano GV, Lichtenheld MG, Munson GP. Perforin-2 Breaches the Envelope of Phagocytosed Bacteria Allowing Antimicrobial Effectors Access to Intracellular Targets. *J Immunol* (2018) 201:2710–20. doi: 10.4049/jimmunol.1800365
27. Wiens M, Korzhev M, Krasko A, Thakur NL, Perović-Ottstadt S, Breter HJ, et al. Innate immune defense of the sponge Suberites domuncula against bacteria involves a MyD88-dependent signaling pathway: Induction of a perforin-like molecule. *J Biol Chem* (2005) 280:27949–59. doi: 10.1074/jbc.M504049200
28. Walters BM, Connelly MT, Young B, Traylor-Knowles N. The Complicated Evolutionary Diversification of the Mpeg-1/Perforin-2 Family in Cnidarians. *Front Immunol* (2020) 11:1690. doi: 10.3389/fimmu.2020.01690
29. Choi KM, Cho DH, Joo MS, Choi HS, Kim MS, Han HJ, et al. Functional characterization and gene expression profile of perforin-2 in starry flounder (Platichthys stellatus). *Fish Shellfish Immunol* (2020) 107:511–8. doi: 10.1016/j.fsi.2020.11.011
30. Estévez-Calvar N, Romero A, Figueras A, Novoa B. Involvement of pore-forming molecules in immune defense and development of the Mediterranean mussel (Mytilus galloprovincialis). *Dev Comp Immunol* (2011) 35:1017–31. doi: 10.1016/j.dci.2011.03.023
31. Bathige SDNK, Umasuthan N, Whang I, Lim BS, Won SH, Lee J. Antibacterial activity and immune responses of a molluscan macrophage expressed gene-1 from disk abalone, Haliotis discus discus. *Fish Shellfish Immunol* (2014) 39:263–72. doi: 10.1016/j.fsi.2014.05.012
32. Modak TH, Gomez-Chiarri M. Contrasting immunomodulatory effects of probiotic and pathogenic bacteria on eastern oyster, crassostrea virginica, larvae. *Vaccines* (2020) 8:588. doi: 10.3390/vaccines8040588
33. Kemp IK, Coyne VE. Identification and characterisation of the Mpeg1 homologue in the South African abalone, Haliotis midae. *Fish Shellfish Immunol* (2011) 31:754–64. doi: 10.1016/j.fsi.2011.07.010
34. Ni L, Han Q, Chen H, Luo X, Li A, Dan X. Grouper (Epinephelus coioides) Mpeg1s : Molecular identification, expression analysis, and antimicrobial activity. *Fish Shellfish Immunol* (2019) 92:690–7. doi: 10.1016/j.fsi.2019.06.060
35. Jagannathan-Bogdan M, Zon LI. Hematopoiesis. *Dev* (2013) 140:2463–7. doi: 10.1242/dev.083147
36. Mo ZQ, Li YW, Wang HQ, Wang J, LY N, Yang M, et al. Comparative transcriptional profile of the fish parasite Cryptocaryon irritans. *Parasites Vectors* (2016) 9:1–12. doi: 10.1186/s13071-016-1919-1
37. Ni LY, Chen HP, Han R, Luo XC, Li AX, Li JZ, et al. Distribution of Mpeg1+ cells in healthy grouper (Epinephelus coioides) and after Cryptocaryon irritans infection. *Fish Shellfish Immunol* (2020) 104:222–7. doi: 10.1016/j.fsi.2020.06.018
38. Le Pennec G, Gardères J. The challenge of the sponge suberites domuncula (Olivi, 1792) in the presence of a symbiotic bacterium and a pathogen bacterium. *Genes (Basel)* (2019). doi: 10.3390/genes10070485
39. Libro S, Kaluziak ST, Vollmer SV. RNA-seq profiles of immune related genes in the staghorn coral Acropora cervicornis Infected with white band disease. *PLoS One* (2013). doi: 10.1371/journal.pone.0081821
40. Gignoux-Wolfsohn SA, Vollmer SV. Identification of candidate coral pathogens on white band disease-infected staghorn coral. *PLoS One* (2015). doi: 10.1371/journal.pone.0134416

41. Duke RC, Persechini PM, Chang S, Liu CC, Cohen JJ, Young JD. Purified perforin induces target cell lysis but not DNA fragmentation. *J Exp Med* (1989). doi: 10.1084/jem.170.4.1451
42. Masson D, Tschopp J. Isolation of a lytic, pore-forming protein (perforin) from cytolytic T-lymphocytes. *J Biol Chem* (1985) 260:9069–72.
43. He X, Zhang Y, Yu Z. An Mpeg (macrophage expressed gene) from the Pacific oyster Crassostrea gigas: Molecular characterization and gene expression. *Fish Shellfish Immunol* (2011) 30:870–6. doi: 10.1016/j.fsi.2011.01.009
44. Biesecker G, Muller-Eberhard HJ. The ninth component of human complement: Purification and physicochemical characterization. *J Immunol* (1980) 124:1291–6.
45. Biesecker G, Gerard C, Hugli TE. An amphiphilic structure of the ninth component of human complement. Evidence from analysis of fragments produced by α-thrombin. *J Biol Chem* (1982).
46. Kontermann R, Rauterberg EW. N-Deglycosylation of human complement component C9 reduces its hemolytic activity. *Mol Immunol* (1989). doi: 10.1016/0161-5890(89)90056-4
47. Franc V, Yang Y, Heck AJR. Proteoform Profile Mapping of the Human Serum Complement Component C9 Revealing Unexpected New Features of N-, O-, and C-Glycosylation. *Anal Chem* (2017). doi: 10.1021/acs.analchem.6b04527
48. Spicer BA, Law RHP, Caradoc-Davies TT, Ekkel SM, Bayly-Jones C, Pang SS, et al. The first transmembrane region of complement component-9 acts as a brake on its self-assembly. *Nat Commun* (2018). doi: 10.1038/s41467-018-05717-0
49. Chen R, Jiang X, Sun D, Han G, Wang F, Ye M, et al. Glycoproteomics analysis of human liver tissue by combination of multiple enzyme digestion and hydrazide chemistry. *J Proteome Res* (2009). doi: 10.1021/pr8008012
50. Shental-Bechor D, Levy Y. Effect of glycosylation on protein folding: A close look at thermodynamic stabilization. *Proc Natl Acad Sci U S A* (2008). doi: 10.1073/pnas.0801340105
51. Lee HS, Qi Y, Im W. Effects of N-glycosylation on protein conformation and dynamics: Protein Data Bank analysis and molecular dynamics simulation study. *Sci Rep* (2015) 5:8926. doi: 10.1038/srep08926
52. McCormack R, Bahnan W, Shrestha N, Boucher J, Barreto M, Barrera CM, et al. Perforin-2 Protects Host Cells and Mice by Restricting the Vacuole to Cytosol Transitioning of a Bacterial Pathogen. *Infect Immun* (2016) 84:1083–91. doi: 10.1128/iai.01434-15
53. McCormack R, De Armas LR, Shiratsuchi M, Ramos JE, Podack ER. Inhibition of intracellular bacterial replication in fibroblasts is dependent on the perforin-like protein (Perforin-2) encoded by macrophage-expressed gene 1. *J Innate Immun* (2013) 5:185–94. doi: 10.1159/000345249
54. Strbo N, Pastar I, Romero L, Chen V, Vujanac M, Sawaya AP, et al. Single cell analyses reveal specific distribution of anti-bacterial molecule Perforin-2 in human skin and its modulation by wounding and Staphylococcus aureus infection. *Exp Dermatol* (2019) 28:225–32. doi: 10.1111/exd.13870
55. Ellett F, Pase L, Hayman JW, Andrianopoulos A, Lieschke GJ. Phagocytes, Granulocytes, and Myelopoiesis mpeg1 promoter transgenes direct macrophage-lineage expression in zebrafish. *Blood* (2011) 27:e49–56. doi: 10.1182/blood-2010-10-314120
56. Zakrzewska A, Cui C, Stockhammer OW, Benard EL, Spaink HP, Meijer AH. Macrophage-specific gene functions in Spi1-directed innate immunity. *Blood* (2010) 116:1–12. doi: 10.1182/blood-2010-01-262873
57. Benard EL, Racz PI, Rougeot J, Nezhinsky AE, Verbeek FJ, Spaink HP, et al. Macrophage-expressed perforins Mpeg1 and Mpeg1.2 have an anti-bacterial function in zebrafish. *J Innate Immun* (2015) 7:136–52. doi: 10.1159/000366103
58. Mostowy S, Boucontet L, Mazon Moya MJ, Sirianni A, Boudinot P, Hollinshead M, et al. The Zebrafish as a New Model for the In Vivo Study of Shigella flexneri Interaction with Phagocytes and Bacterial Autophagy. *PLoS Pathog* (2013) 9:e81003588. doi: 10.1371/journal.ppat.1003588
59. McCormack RM. Elucidating Perforin-2 Mediated Killing Mechanisms Against Pathogenic Bacteria. (2017). Available at: https://scholarship.miami.edu/discovery/fulldisplay/alma991031447876202976/01UOML_INST:ResearchRepository?lang=en.
60. McCormack R, Podack ER. Perforin-2/Mpeg1 and other pore-forming proteins throughout evolution. *J Leukoc Biol* (2015) 98:761–8. doi: 10.1189/jlb.4MR1114-523RR
61. Podack ER, Munson GP. Killing of microbes and cancer by the immune system with three mammalian pore-forming killer proteins. *Front Immunol* (2016) 7:464. doi: 10.3389/fimmu.2016.00464
62. Podack ER, Kolb WP, Muller-Eberhard HJ. The SC5b-7 complex: Formation, isolation, properties, and subunit composition. *J Immunol* (1977).
63. Podack ER, Esser AF, Biesecker G, Muller-Eberhard HJ. Membrane attack complex of complement. A structural analysis of its assembly. *J Exp Med* (1980). doi: 10.1084/jem.151.2.301
64. Tschopp J, Podack ER. Membranolysis by the ninth component of human complement. *Biochem Biophys Res Commun* (1981). doi: 10.1016/0006-291X(81)91981-1
65. Tschopp J, Müller-Eberhard HJ, Podack ER. Formation of transmembrane tubules by spontaneous polymerization of the hydrophilic complement protein C9. *Nature* (1982). doi: 10.1038/298534a0
66. Podack ER, Dennert G. Assembly of two types of tubules with putative cytolytic function by cloned natural killer cells. *Nature* (1983). doi: 10.1038/302442a0
67. Podack ER, Konigsberg PJ, Acha-Orbea H, Pircher H, Hengartner H. Cytolytic T-cell granules: biochemical properties and functional specificity. *Adv Exp Med Biol* (1985). doi: 10.1007/978-1-4684-8326-0_8
68. Podack ER, Young JDE, Cohn ZA. Isolation and biochemical and functional characterization of perforin 1 from cytolytic T-cell granules. *Proc Natl Acad Sci U S A* (1985). doi: 10.1073/pnas.82.24.8629
69. Lichtenheld MG, Olsen KJ, Lu P, Lowrey DM, Hameed A, Hengartner H, et al. Structure and function of human perforin. *Nature* (1988). doi: 10.1038/335448a0
70. Podack ER, Hengartner H. Structure of perforin and its role in cytolysis. *Year Immunol* (1989).
71. McCormack R, De Armas L, Shiratsuchi M, Podack ER. Killing machines: Three pore-forming proteins of the immune system. *Immunol Res* (2013) 57:268–78. doi: 10.1007/s12026-013-8469-9
72. Fields KA, McCormack R, de Armas LR, Podack ER. Perforin-2 Restricts Growth of Chlamydia trachomatis in Macrophages. *Infect Immun* (2013) 81:3045–54. doi: 10.1128/iai.00497-13
73. Darville T, Hiltke TJ. Pathogenesis of genital tract disease due to Chlamydia trachomatis. *J Infect Dis* (2010) 201:114–25. doi: 10.1086/652397
74. Keb G, Fields KA. An Ancient Molecular Arms Race: Chlamydia vs. Membrane Attack Complex/Perforin (MACPF) Domain Proteins. *Front Immunol* (2020). doi: 10.3389/fimmu.2020.01490
75. Pastar I, O'Neill K, Padula L, Head CR, Burgess JL, Chen V, et al. Staphylococcus epidermidis Boosts Innate Immune Response by Activation of Gamma Delta T Cells and Induction of Perforin-2 in Human Skin. *Front Immunol* (2020) 11:550946. doi: 10.3389/fimmu.2020.550946
76. Gayle P, McGaughey V, Hernandez R, Wylie M, Colletti RC, Nguyen KL, et al. Maternal- and Fetal-Encoded Perforin-2 Limits Placental Infection by a Bloodborne Pathogen. *J Immunol* (2020) 205:1878–85. doi: 10.4049/jimmunol.2000615
77. Cheers C, Wood P. Listeriosis in beige mice and their heterozygous littermates. *Immunology* (1984) 51:711–7.
78. Portnoy DA, Auerbuch V, Glomski IJ. The cell biology of Listeria monocytogenes infection: The intersection of bacterial pathogenesis and cell-mediated immunity. *J Cell Biol* (2002). doi: 10.1083/jcb.200205009
79. Dramsi S, Cossart P. Listeriolysin O: A genuine cytolysin optimized for an intracellular parasite. *J Cell Biol* (2002). doi: 10.1083/jcb.200202121
80. McCormack R, Hunte R, Podack ER, Plano GV, Shembade N. An Essential Role for Perforin-2 in Type I IFN Signaling. *J Immunol* (2020). doi: 10.4049/jimmunol.1901013
81. Merselis LC, Munson GP. Perforin-2 (MPEG1) knockout mice are not resistant to LPS induced septic shock. *figshare* (2020). doi: 10.6084/m9.figshare.12652829.v2
82. Kayagaki N, Warming S, Lamkanfi M, Vande Walle L, Louie S, Dong J, et al. Non-canonical inflammasome activation targets caspase-11. *Nature* (2011). doi: 10.1038/nature10558
83. Kenneth NS, Younger JM, Hughes ED, Marcotte D, Barker PA, Saunders TL, et al. An inactivating caspase 11 passenger mutation originating from the

129 murine strain in mice targeted for c-IAP1. *Biochem J* (2012). doi: 10.1042/BJ20120249
84. McCormack RM, Munson GP. Perforin-2 (MPEG1) is not required for Type I Interferon signaling. *figshare* (2020). doi: 10.6084/m9.figshare.12654014.v1
85. Thomas C, Moraga I, Levin D, Krutzik PO, Podoplelova Y, Trejo A, et al. Structural linkage between ligand discrimination and receptor activation by Type I interferons. *Cell* (2011). doi: 10.1016/j.cell.2011.06.048
86. Weng G, Wang E, Wang Z, Liu H, Zhu F, Li D, et al. HawkDock: a web server to predict and analyze the protein-protein complex based on computational docking and MM/GBSA. *Nucleic Acids Res* (2019). doi: 10.1093/nar/gkz397
87. Ringwald M, Eppig JT, Kadin JA, Richardson JE, Begley DA, Corradi JP, et al. GXD: A gene expression database for the laboratory mouse: Current status and recent enhancements. *Nucleic Acids Res* (2000). doi: 10.1093/nar/28.1.115
88. Hemberger M, Himmelbauer H, Ruschmann J, Zeitz C, Fundele R. cDNA subtraction cloning reveals novel genes whose temporal and spatial expression indicates association with trophoblast invasion. *Dev Biol* (2000). doi: 10.1006/dbio.2000.9705
89. Karczewski KJ, Francioli LC, Tiao G, Cummings BB, Alföldi J, Wang Q, et al. The mutational constraint spectrum quantified from variation in 141,456 humans. *Nature* (2020) 581:434–43. doi: 10.1038/s41586-020-2308-7
90. McCormack RM, Szymanski EP, Hsu AP, Perez E, Olivier KN, Fisher E, et al. MPEG1/perforin-2 mutations in human pulmonary nontuberculous mycobacterial infections. *JCI Insight* (2017) 2:1–8. doi: 10.1172/jci.insight.89635
91. Merselis LC, Jiang SYUndiagnosed Diseases Network, , Nelson SF, Lee H, Prabaker KK, et al. MPEG1/Perforin-2 Haploinsufficiency Associated Polymicrobial Skin Infections and Considerations for Interferon-γ Therapy. *Front Immunol* (2020) 11:601584. doi: 10.3389/fimmu.2020.601584
92. Bosu DR, Kipreos ET. Cullin-RING ubiquitin ligases: Global regulation and activation cycles. *Cell Div* (2008). doi: 10.1186/1747-1028-3-7
93. Cardozo T, Pagano M. The SCF ubiquitin ligase: Insights into a molecular machine. *Nat Rev Mol Cell Biol* (2004). doi: 10.1038/nrm1471
94. Charpentier X, Oswald E. Identification of the secretion and translocation domain of the enteropathogenic and enterohemorrhagic Escherichia coli effector Cif, using TEM-1 β-lactamase as a new fluorescence-based reporter. *J Bacteriol* (2004). doi: 10.1128/JB.186.16.5486-5495.2004
95. Crow A, Hughes RK, Taieb F, Oswald E, Banfield MJ. The molecular basis of ubiquitin-like protein NEDD8 deamidation by the bacterial effector protein Cif. *Proc Natl Acad Sci U S A* (2012) 109:1830–8. doi: 10.1073/pnas.1112107109
96. Cui J, Yao Q, Li S, Ding X, Lu Q, Mao H, et al. Glutamine deamidation and dysfunction of ubiquitin/NEDD8 induced by a bacterial effector family. *Science* (2010) 80:1215–8. doi: 10.1126/science.1193844
97. Reddick LE, Alto NM. Bacteria fighting back: How pathogens target and subvert the host innate immune system. *Mol Cell* (2014) 54:321–8. doi: 10.1016/j.molcel.2014.03.010
98. Wilkinson CR, Garrone R, Vacelet J. Marine sponges discriminate between food bacteria and bacterial symbionts: Electron microscope radioautography and in situ evidence. *Proc R Soc London - Biol Sci* (1984). doi: 10.1098/rspb.1984.0018
99. Wehrl M, Steinert M, Hentschel U. Bacterial uptake by the marine sponge Aplysina aerophoba. *Microb Ecol* (2007). doi: 10.1007/s00248-006-9090-4
100. Olano CT, Bigger CH. Phagocytic activities of the gorgonian coral Swiftia exserta. *J Invertebr Pathol* (2000). doi: 10.1006/jipa.2000.4974
101. Adema CM, Vanderknaap WPW, Sminia T. Molluscan Hemocyte-Mediated Cytotoxicity - the Role of Reactive Oxygen Intermediates. *Rev Aquat Sci* (1991).
102. Mohandas A, Cheng TC, Cheng JB. Mechanism of lysosomal enzyme release from Mercenaria mercenaria granulocytes: A scanning electron microscope study. *J Invertebr Pathol* (1985). doi: 10.1016/0022-2011(85)90148-X
103. Willenz P, Van de Vyver G. Ultrastructural localization of lysosomal digestion in the fresh water sponge Ephydatia fluviatilis. *J Ultrasructure Res* (1984). doi: 10.1016/S0022-5320(84)90112-6
104. Krawczyk PA, Laub M, Kozik P. To Kill But Not Be Killed: Controlling the Activity of Mammalian Pore-Forming Proteins. *Front Immunol* (2020). doi: 10.3389/fimmu.2020.601405
105. Bayly-Jones C, Pang SS, Spicer BA, Whisstock JC, Dunstone MA. Ancient but Not Forgotten: New Insights Into MPEG1, a Macrophage Perforin-Like Immune Effector. *Front Immunol* (2020). doi: 10.3389/fimmu.2020.581906
106. Hung LY, Tanaka Y, Herbine K, Pastore C, Singh B, Ferguson A, et al. Cellular context of IL-33 expression dictates impact on anti-helminth immunity. *Sci Immunol* (2020). doi: 10.1126/sciimmunol.abc6259
107. Pettersen EF, Goddard TD, Huang CC, Couch GS, Greenblatt DM, Meng EC, et al. UCSF Chimera - A visualization system for exploratory research and analysis. *J Comput Chem* (2004). doi: 10.1002/jcc.20084
108. Pettersen EF, Goddard TD, Huang CC, Meng EC, Couch GS, Croll TI, et al. UCSF ChimeraX: Structure visualization for researchers, educators, and developers. *Protein Sci* (2020) 30:70–82. doi: 10.1002/pro.3943

Conflict of Interest: The authors declare that the research was conducted in the absence of any commercial or financial relationships that could be construed as a potential conflict of interest.

Advantages of publishing in Frontiers

OPEN ACCESS
Articles are free to read for greatest visibility and readership

FAST PUBLICATION
Around 90 days from submission to decision

HIGH QUALITY PEER-REVIEW
Rigorous, collaborative, and constructive peer-review

TRANSPARENT PEER-REVIEW
Editors and reviewers acknowledged by name on published articles

Frontiers
Avenue du Tribunal-Fédéral 34
1005 Lausanne | Switzerland

Visit us: www.frontiersin.org
Contact us: frontiersin.org/about/contact

REPRODUCIBILITY OF RESEARCH
Support open data and methods to enhance research reproducibility

DIGITAL PUBLISHING
Articles designed for optimal readership across devices

FOLLOW US
@frontiersin

IMPACT METRICS
Advanced article metrics track visibility across digital media

EXTENSIVE PROMOTION
Marketing and promotion of impactful research

LOOP RESEARCH NETWORK
Our network increases your article's readership